

AFIT/GSE/GSO/ENY/99M-1

SIMSAT: A SATELLITE SYSTEM SIMULATOR
AND EXPERIMENTAL TEST BED FOR
AIR FORCE RESEARCH

THESIS

GSE-99M AND GSO-99M
SYSTEMS ENGINEERING
DESIGN TEAM

AFIT/GSE/GSO/ENY/99M-1

Approved for public release; distribution unlimited

DTIC QUALITY INSPECTED 2

19990409 057

The views expressed in this thesis are those of the authors and do not reflect the official policy or position of the Department of Defense or the United States Government.

SIMSAT: A SATELLITE SYSTEM SIMULATOR AND
EXPERIMENTAL TEST BED FOR AIR FORCE RESEARCH

THESIS

Presented to the Faculty of the School of Engineering
of the Air Force Institute of Technology
Air University
In Partial Fulfillment of the
Requirements for the Degree of
Master of Science

James E. Colebank, B.S.
Captain, USAF

Robert D. Jones, B.S.
Captain, USAF

George R. Nagy, S.B., M.S.
Captain, USAF

Randall D. Pollak, B.S.
Captain, USAF

Donald R. Mannebach, B.S.
First Lieutenant, USAF

March, 1999

Approved for public release; distribution unlimited

SIMSAT: A SATELLITE SYSTEM SIMULATOR AND
EXPERIMENTAL TEST BED FOR AIR FORCE RESEARCH

James E. Colebank, B.S.
Captain, USAF


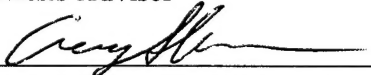
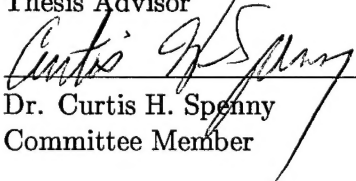
Robert D. Jones, B.S.
Captain, USAF

George R. Nagy, S.B., M.S.
Captain, USAF

Randall D. Pollak, B.S.
Captain, USAF

Donald R. Mannebach, B.S.
First Lieutenant, USAF

Approved:

	<u>8 MAR 99</u>
Lieutenant Colonel Stuart C. Kramer	Date
Thesis Advisor	
	<u>8 Mar 99</u>
Captain Gregory S. Agnes	Date
Thesis Advisor	
	<u>8 Mar 99</u>
Dr. Curtis H. Spenny	Date
Committee Member	

Acknowledgements

A project of the magnitude of *SIMSAT* would not be possible without a large number of individuals supporting the design team. For the first six months of the project, Mr. Mike Hanke was an integral member of the design team, and his AFIT thesis work directly contributed to the *SIMSAT* command and data handling architecture. Dr. Alan Heminger graciously allowed the design team use of his computer laboratory and issue-formulation software during the early stages of team building and *SIMSAT* concept exploration. Outstanding technical support was provided by the AFIT Aero/Astro Engineering department staff, including Mr. Jay Anderson, Mr. Bob Bacon, and Mr. Andy Pitts. From the AFIT Electrical Engineering department, Mr. Robert Conkle also contributed to the initial design of the *SIMSAT* power architecture. The AFIT Fabrication Shop, including Mr. Jan LeValley, Mr. Russ Hastings, and Mr. Condie Inman, provided incredible support related to the development and manufacture of the structural assembly. Throughout the design process, Dr. Curtis Spenny provided invaluable technical suggestions which were incorporated into the final design.

Outside of AFIT, Mr. Edmund Kong of Animatics, Inc., provided assistance with regard to motor selection and interface issues. Mr. Jim Werba of Servo Systems Co. was also noteworthy in this regard. Mr. Bob Jones provided technical support for understanding the Humphrey CF75 gyro. Mr. Ray Bzibziak of Moog, Inc., provided answers to detailed questions related to cold-gas thruster selection, and Mr. Bill Parker from Spec Air Specialty Gases assisted in the determination of gas bottle specifications. In addition, we would like to thank Mr. Don Neas of Digital Wireless Corporation for his assistance in wireless communications design and signal interfaces.

Finally, we would like to acknowledge the guidance provided by our advisors, Lt Col Stuart Kramer and Capt Greg Agnes. Their technical assistance, design inputs, and leadership directly influenced the success of our efforts.

James E. Colebank

Robert D. Jones

George R. Nagy

Randall D. Pollak

Donald R. Mannebach

Table of Contents

	Page
Acknowledgements	iii
List of Figures	xvi
List of Tables	xxiv
Abstract	xxviii
 I. Introduction	 1-1
1.1 Background	1-1
1.2 Design Requirements	1-2
1.3 Systems Engineering Approach	1-4
1.3.1 Systems Engineering Framework.	1-4
1.3.2 Systems Engineering Definition.	1-4
1.3.3 Systems Architecting vs. Systems Engineering.	1-6
1.3.4 Systems Engineering Dimensions.	1-7
1.4 Systems Engineering Process	1-8
1.4.1 Problem-Solving Methodology.	1-8
1.4.2 Issue Formulation.	1-10
1.4.3 Analysis.	1-11
1.4.4 Interpretation.	1-12
1.4.5 Other Problem-Solving Methods.	1-12
1.5 Design Lifecycle Description	1-14
1.5.1 Lifecycle Methodology.	1-14
1.5.2 Comparison of Various Lifecycle Models.	1-14
1.5.3 SIMSAT Lifecycle Model.	1-18
1.6 Document Format	1-20

	Page
II. Concept Exploration and Definition	2-1
2.1 Overview	2-1
2.2 Issue Formulation	2-2
2.2.1 Problem Statement	2-2
2.2.2 Problem Scope	2-2
2.2.3 Relevant Disciplines	2-3
2.2.4 Identification of Actors	2-3
2.2.5 Initial Needs	2-4
2.2.6 Problem Elements	2-5
2.2.7 Constraints and Alterables	2-6
2.2.8 Cost and Schedule Summary	2-6
2.2.9 Value System Design	2-7
2.2.10 System Architecture Development	2-9
2.2.11 System Decomposition	2-10
2.2.12 System Synthesis	2-11
2.3 Analysis	2-22
2.3.1 Analysis Methodology	2-22
2.3.2 Attitude Determination and Control	2-22
2.3.3 Power	2-24
2.3.4 Command and Data Handling.	2-25
2.3.5 Communications	2-28
2.3.6 Structures	2-31
2.4 Interpretation	2-31
2.4.1 General	2-31
2.4.2 Alternatives Summary	2-31

	Page
III. Preliminary Design	3-1
3.1 Overview	3-1
3.2 Issue Formulation	3-2
3.2.1 Problem Statement	3-2
3.2.2 Problem Scope	3-2
3.2.3 Requirements Refinement	3-2
3.2.4 System Functional Layout	3-3
3.2.5 Preliminary Design Issues	3-7
3.2.6 Additional Actors	3-9
3.2.7 Value System Design	3-10
3.2.8 Determination of C&DH Software	3-15
3.2.9 System Synthesis	3-16
3.3 Analysis	3-22
3.3.1 System Modeling	3-22
3.3.2 Preliminary Analysis	3-22
3.3.3 Remaining System Alternatives	3-27
3.3.4 Analysis Methodology	3-27
3.3.5 Raw Values	3-27
3.3.6 Utility Scale	3-38
3.4 Interpretation	3-39
3.4.1 Dominated Solutions	3-39
3.4.2 Worth Assessment Methodology	3-42
3.4.3 Weighting Factors	3-42
3.4.4 System Scoring	3-45
3.4.5 Sensitivity Analysis	3-45
3.4.6 Preferred Design	3-49

	Page
IV. Detailed Design	4-1
4.1 Overview	4-1
4.2 First-Iteration Issue Formulation	4-2
4.2.1 Problem Statement	4-2
4.2.2 Updated System Architecture	4-2
4.2.3 First-Iteration Design Issues	4-2
4.2.4 Value System Design	4-5
4.2.5 Equations-of-Motion (EOM) Modeling	4-8
4.2.6 System Synthesis	4-8
4.3 First-Iteration Analysis	4-16
4.3.1 System Modeling	4-16
4.3.2 Raw Values	4-19
4.3.3 Utility Scaling	4-19
4.4 First-Iteration Interpretation	4-19
4.4.1 Weighting Factors	4-19
4.4.2 System Ranking and Selection	4-21
4.4.3 Implementation	4-22
4.5 Command and Control Architecture	4-24
4.5.1 Problem Statement	4-24
4.5.2 Command and Control Issues	4-24
4.5.3 Value System Design	4-25
4.5.4 Development Approach	4-25
4.5.5 Plant Model	4-26
4.5.6 Controller Model	4-27
4.5.7 <i>SIMSAT</i> Control Options	4-33
4.5.8 MATLAB Simulation	4-39
4.5.9 SIMULINK Model Development	4-39

	Page
4.5.10 dSPACE Integration	4-51
4.5.11 User Interface Issues	4-52
4.5.12 Control Law/User Interface Software Integration . .	4-53
4.5.13 Ground Station Hardware Architecture	4-57
4.5.14 User Interface Summary	4-58
4.6 Structural Design	4-60
4.6.1 Problem Statement	4-60
4.6.2 Problem Scope	4-60
4.6.3 Structural Issues	4-61
4.6.4 Computer-Aided Design (CAD) Software	4-61
4.6.5 Initial Sizing	4-62
4.6.6 Structural Development	4-62
4.6.7 Structural Implementation	4-69
4.6.8 Baseline Structure Summary	4-69
4.7 Truss Design	4-70
4.7.1 Problem Statement	4-70
4.7.2 Problem Scope	4-71
4.7.3 Requirements	4-71
4.7.4 Value System Design	4-71
4.7.5 Development Approach	4-72
4.7.6 Finite-Element Model	4-73
4.7.7 Static Analysis	4-74
4.7.8 Payload-Side Dynamics	4-75
4.7.9 Wheel-Side Dynamics	4-76
4.7.10 Additional Truss Modeling	4-78
4.7.11 Truss Structure Summary	4-79
4.8 Wireless Communications Selection	4-80

	Page
4.8.1 Problem Statement	4-80
4.8.2 Problem Scope	4-80
4.8.3 Constraints	4-81
4.8.4 Value System Design	4-81
4.8.5 Wireless Background Sources	4-82
4.8.6 Wireless LAN Alternatives.	4-83
4.8.7 Wireless LAN Selection.	4-86
4.8.8 Wireless Modem Considerations	4-86
4.8.9 Wireless Modem Alternatives	4-87
4.8.10 Wireless Modem Selection	4-89
4.9 Subsystem Integration	4-90
4.9.1 Problem Statement	4-90
4.9.2 Problem Scope	4-90
4.9.3 Power Interface Issues	4-90
4.9.4 Signal Interface Issues	4-90
4.9.5 Power System Architecture	4-91
4.9.6 Communications Architecture	4-100
4.10 Safety System Design	4-108
4.10.1 Problem Statement	4-108
4.10.2 Problem Scope	4-108
4.10.3 Safety System Background	4-108
4.10.4 Safety Issues	4-109
4.10.5 Value System Design	4-110
4.10.6 Safety System Alternatives and Selection	4-110
4.10.7 Emergency Shutdown Considerations	4-113
4.10.8 Implementation	4-113
4.11 Thruster Integration	4-119

	Page
4.11.1 Problem Statement	4-119
4.11.2 Problem Scope	4-119
4.11.3 Value System Design	4-119
4.11.4 Thruster Selection	4-120
4.11.5 Thruster Interfaces	4-120
4.11.6 Initial Gas Bottle Sizing	4-122
4.11.7 Gas Bottle Selection	4-124
4.12 Detailed Design Summary	4-124
V. Final Design	5-1
5.1 Overview	5-1
5.2 Subsystem Components	5-1
5.2.1 Attitude Determination	5-1
5.2.2 Attitude Control	5-1
5.2.3 Command & Data Handling	5-6
5.2.4 Power System	5-12
5.3 Structural Layout	5-14
5.4 Support Assembly	5-30
5.5 Baseline <i>SIMSAT</i> Performance	5-30
5.6 Areas Requiring Further Integration	5-33
5.7 Recommended Future Design Activity	5-33
5.7.1 IPACS	5-34
5.7.2 CMGs	5-34
5.7.3 Thrusters	5-34
5.7.4 MicroAutoBox	5-34
5.7.5 Dual Spinner	5-35
5.8 Conclusions	5-36

	Page
Appendix A. Preliminary Design Measurables	A-1
A.1 Overview	A-1
A.2 Cost	A-2
A.2.1 Capital Cost	A-2
A.2.2 Operations and Maintenance Cost	A-3
A.3 Schedule	A-4
A.3.1 Total Delivery Weeks	A-4
A.4 Safety	A-5
A.4.1 Relative Damage Index	A-6
A.4.2 Relative Injury Index	A-7
A.5 Performance	A-8
A.5.1 Bandwidth Requirement	A-8
A.5.2 Command Capability	A-9
A.5.3 Communications Latency	A-10
A.5.4 Control Systems Analysis	A-11
A.5.5 Development Environment	A-12
A.5.6 Experiment Types	A-13
A.5.7 Interface Modularity	A-14
A.5.8 Maintenance and Test Time	A-15
A.5.9 Mass Margin	A-16
A.5.10 Motion Simulation	A-17
A.5.11 Rate Sensing Accuracy	A-18
A.5.12 Post-Mission Data Analysis	A-19
A.5.13 Power Margin	A-20
A.5.14 Processor Schedulability Analysis	A-21
A.5.15 Real-Time Data	A-22
A.5.16 Slew Capability	A-23

	Page
A.5.17 Slew Rate Sensing	A-24
A.5.18 Turn-Around Time	A-25
A.5.19 User Interface	A-26
Appendix B. Equations-of-Motion Development	B-1
B.1 Overview	B-1
B.2 Plant Model	B-1
B.3 Key Assumptions	B-1
B.4 Inertial Reference Frame, Inertial Basis, and Origin	B-2
B.5 <i>SIMSAT</i> Body Frame, Body Fixed Basis, and Reference Point	B-3
B.6 Identify Relevant Forces and Moments	B-4
B.7 Fundamental Equations	B-4
Appendix C. Momentum Wheel Sizing	C-1
C.1 Momentum Wheel Development	C-1
C.1.1 Location of Components	C-1
C.1.2 Estimating Motor Torque	C-4
C.1.3 Design Groundrules	C-8
C.1.4 Initial Wheel Analysis	C-9
C.1.5 Detailed Wheel Design	C-14
C.1.6 Final Momentum Wheel Design Alternatives	C-22
Appendix D. Gyro Range and Accuracy Analysis	D-1
D.1 Overview	D-1
D.2 Rate Determination	D-1
D.3 Range and Accuracy Analysis	D-6
D.4 Design Decisions	D-9

	Page
Appendix E. Gyro Calibration Curves	E-1
E.1 Overview	E-1
E.2 Pitch Axis Regression	E-2
E.3 Roll Axis Regression	E-4
E.4 Yaw Axis Regression	E-6
E.5 Fore/Aft Acceleration Regression	E-8
E.6 Lateral Acceleration Regression	E-10
E.7 Vertical Acceleration Regression	E-12
Appendix F. Detailed Design Raw Values & Scoring	F-1
F.1 Overview	F-1
F.2 Objective Measurables Raw Data	F-1
F.3 System Scoring	F-1
Appendix G. Initial Controller Design	G-1
G.1 Overview	G-1
G.2 Gain Settings Development	G-1
Appendix H. Model Transfer Procedures	H-1
H.1 Overview	H-1
H.2 Model Compilation and Transfer Procedures.	H-1
Appendix I. Designing the User Interface	I-1
I.1 Overview	I-1
I.2 TRACE.	I-1
I.3 COCKPIT.	I-4
Appendix J. Design and Operation of REALMOTION Interface	J-1
J.1 Overview	J-1
J.2 Software Links.	J-1
J.3 Scene Control.	J-2

	Page
Appendix K. Final Structural Design	K-1
K.1 Overview	K-1
K.2 Structural Design	K-1
K.3 Structure Summary	K-5
Appendix L. Finite-Element Modeling	L-1
L.1 Overview	L-1
L.2 CADRE Models	L-1
L.3 CADRE Pro Model	L-1
Appendix M. Final Controller Design	M-1
M.1 Overview	M-1
M.2 Gain Settings Development	M-1
Bibliography	BIB-1
Vita	VITA-1

List of Figures

Figure		Page
1.1.	Air Bearing Assembly	1-2
1.2.	Systems Engineering Dimensions [26]	1-8
1.3.	Sage's Lifecycle Model	1-16
1.4.	Lifecycle Models of Hall vs. Sage	1-17
1.5.	<i>SIMSAT</i> Lifecycle Model	1-19
1.6.	<i>SIMSAT</i> Summary of Design Activity	1-20
2.1.	Concept Exploration and Definition Design Activity	2-1
2.2.	Initial Value System Design (VSD)	2-8
2.3.	System and Environment Context Diagram	2-9
2.4.	Satellite Inertia and Stabilization Concepts	2-13
2.5.	Dual Spin Configuration	2-14
2.6.	Flight Test Telemetry System Schematic	2-21
3.1.	Preliminary Design Activity	3-1
3.2.	Preliminary Design Concept Map [26]	3-4
3.3.	Offboard Functional Layout	3-5
3.4.	Onboard Functional Layout	3-6
3.5.	Preliminary Design Objectives Hierarchy	3-11
3.6.	AutoBox DS400	3-18
3.7.	Real-Time Software Architecture [26]	3-19
3.8.	Preliminary Design Weighted Hierarchy	3-43
3.9.	Feasible Alternate-Result Weighting Factors	3-49
4.1.	Detailed Design Activity	4-1
4.2.	Detailed Design Objectives Hierarchy	4-6

Figure		Page
4.3.	Detailed Design Utility Scale	4-19
4.4.	Objectives Judgement Matrix	4-21
4.5.	Closed-Loop Feedback Control	4-28
4.6.	Motor Closed-Loop Feedback	4-30
4.7.	SIMULINK code for data input and output	4-42
4.8.	Controller Subsystem	4-43
4.9.	Comparison Subsystem, within the Controller	4-44
4.10.	Top-Level <i>SIMSAT</i> Plant Model	4-45
4.11.	Controller Gain Parameters	4-47
4.12.	Equation of Motion Parameters	4-48
4.13.	<i>SIMSAT</i> - Iteration 0	4-63
4.14.	<i>SIMSAT</i> - Iteration 1	4-64
4.15.	<i>SIMSAT</i> - Iteration 3	4-65
4.16.	<i>SIMSAT</i> - Iteration 4	4-66
4.17.	<i>SIMSAT</i> - Iteration 15	4-66
4.18.	<i>SIMSAT</i> - Iteration 23	4-68
4.19.	<i>SIMSAT</i> - Final Structural Iteration	4-70
4.20.	Linking of Truss Members	4-73
4.21.	Finite-Element Model (Payload Side)	4-75
4.22.	Truss Configurations (Payload Side)	4-76
4.23.	Truss Configurations (Momentum Wheel Side)	4-77
4.24.	Finite-Element Model Using Plates	4-79
4.25.	RadioLAN DockLINK Model 408 [45]	4-85
4.26.	Sonik Technologies Corporation's Skyline Modem [52]	4-88
4.27.	Digital Wireless Corporation's WIT2400E Modem [14]	4-89
4.28.	Initial Wiring Diagram	4-93
4.29.	Electrical Bus Design	4-97

Figure		Page
4.30.	Modified Wiring Diagram	4-99
4.31.	Signal Interface Architecture	4-103
4.32.	The "Cargo Net" Safety System	4-114
4.33.	The "Lion Trap" Safety System	4-115
4.34.	The "Trampoline" Safety System	4-116
4.35.	The "Catch Arms" Safety System	4-117
4.36.	The "Skullcap" Safety System	4-118
4.37.	Moog Model 50-820 Schematic [39]	4-121
4.38.	Moog Model 50-820 Cold Gas Thruster Triad [39]	4-121
5.1.	Momentum Wheel, Motor, and Amplifier	5-3
5.2.	Top-Level Software Architecture	5-5
5.3.	Input/Output Channel Interface	5-6
5.4.	COCKPIT Graphical User Interface	5-8
5.5.	TRACE Telemetry Display	5-9
5.6.	REALMOTION 3-D Animation Display	5-10
5.7.	Onboard Wireless Communications System	5-11
5.8.	System Wiring Diagram	5-12
5.9.	Power-Sonic PS-12180 Sealed Lead-Acid Battery	5-13
5.10.	Baseline <i>SIMSAT</i> Layout without Payload (support rods not shown for clarity)	5-19
5.11.	Partially-Assembled <i>SIMSAT</i> in the Laboratory	5-20
5.12.	Truss Attachment Collars	5-21
5.13.	Standard Plate	5-22
5.14.	Cross Member Attachment Using L-brackets	5-22
5.15.	Payload Mounting Plate	5-23
5.16.	Counterweight Mechanism	5-24
5.17.	Momentum Wheel Shelf Assembly	5-25

Figure		Page
5.18.	Lexan Box	5-26
5.19.	Battery Housing	5-27
5.20.	Batteries and Battery Housings on Mounting Plate	5-27
5.21.	Autobox Mounting	5-28
5.22.	Gyroscope, Battery, and Transceiver Mounting	5-28
5.23.	Rubber Vibration Control Mounts and Snubbing Washers	5-29
5.24.	Baseline <i>SIMSAT</i> Layout with Nominal Payload and Body-Fixed Axes	5-32
5.25.	The dSPACE MicroAutoBox [21]	5-35
A.1.	Capital Cost Value Function	A-2
A.2.	O&M Cost Value Function	A-3
A.3.	Total Delivery Weeks Value Function	A-4
A.4.	Hazard Index Table	A-5
A.5.	Relative Damage Index Value Function	A-6
A.6.	Relative Injury Index Value Function	A-7
A.7.	Bandwidth Requirement Value Function	A-8
A.8.	Command Capability Value Function	A-9
A.9.	Communications Latency Value Function	A-10
A.10.	Control Systems Analysis Value Function	A-11
A.11.	Development Environment Value Function	A-12
A.12.	Experiment Types Value Function	A-13
A.13.	Interface Modularity Value Function	A-14
A.14.	Maintenance & Test Time Value Function	A-15
A.15.	Mass Margin Value Function	A-16
A.16.	Motion Simulation Value Function	A-17
A.17.	Rate Sensing Accuracy Value Function	A-18
A.18.	Post-Mission Data Analysis Value Function	A-19
A.19.	Power Margin Value Function	A-20

Figure		Page
A.20.	Processor Schedulability Analysis Value Function	A-21
A.21.	Real-Time Data Value Function	A-22
A.22.	Slew Capability Value Function	A-23
A.23.	Slew Rate Sensing Value Function	A-24
A.24.	Turn-Around Time Value Function	A-25
A.25.	User Interface Value Function	A-26
B.1.	<i>SIMSAT</i> with Axes	B-4
B.2.	Geometric Shapes	B-10
B.3.	Center of Mass for Multiple Components	B-12
C.1.	Nominal Configuration Used for Momentum Wheel Design	C-2
C.2.	Animatics SmartMotor Torque vs. Motor Speed Curves	C-5
C.3.	48V Torque vs. Motor Speed Curve	C-6
C.4.	36V Torque vs. Motor Speed Curve	C-7
C.5.	24V Torque vs. Motor Speed Curve	C-7
C.6.	Momentum Wheel Shapes	C-12
C.7.	Momentum Wheel Speeds	C-12
C.8.	<i>SIMSAT</i> Angular Velocities	C-13
C.9.	<i>SIMSAT</i> Euler Angles	C-13
C.10.	Sizes of Final Wheel Alternatives	C-23
E.1.	Pitch Rate vs. Output Voltage	E-3
E.2.	Roll Rate vs. Output Voltage	E-5
E.3.	Yaw Rate vs. Output Voltage	E-7
E.4.	Fore/Aft Acceleration vs. Output Voltage	E-9
E.5.	Lateral Acceleration vs. Output Voltage	E-11
E.6.	Vertical Acceleration vs. Output Voltage	E-13
G.1.	Option 1 (Target Mode) - Maneuver 1	G-5

Figure		Page
G.2.	Option 1 (Target Mode) - Maneuver 2	G-6
G.3.	Option 1 (Target Mode) - Maneuver 3	G-7
G.4.	Option 1 (Target Mode) - Maneuver 4	G-8
G.5.	Option 1 (Target Mode) - Maneuver 5	G-9
G.6.	Option 2 (Target Mode with Roll Rate) - Maneuver 1	G-10
G.7.	Option 2 (Target Mode with Roll Rate) - Maneuver 2	G-11
G.8.	Option 2 (Target Mode with Roll Rate) - Maneuver 3	G-12
G.9.	Option 3 (Roll Spin Mode) - Maneuver 1	G-13
G.10.	Option 3 (Roll Spin Mode) - Maneuver 2	G-14
G.11.	Option 3 (Roll Spin Mode) - Maneuver 3	G-15
G.12.	Option 4 (Yaw Spin Mode) - Maneuver 1	G-16
G.13.	Option 4 (Yaw Spin Mode) - Maneuver 2	G-17
G.14.	Option 4 (Yaw Spin Mode) - Maneuver 3	G-18
G.15.	Option 4 (Yaw Spin Mode) - Maneuver 4	G-19
G.16.	Option 4 (Yaw Spin Mode) - Maneuver 5	G-20
G.17.	Option 4 (Yaw Spin Mode) - Maneuver 6	G-21
G.18.	Option 5 (Wheel RPM Mode) - Maneuver 1	G-22
G.19.	Option 5 (Wheel RPM Mode) - Maneuver 2	G-23
G.20.	Option 5 (Wheel RPM Mode) - Maneuver 3	G-24
G.21.	Option 5 (Wheel RPM Mode) - Maneuver 4	G-25
H.1.	Error Messages	H-3
H.2.	Successful Download Messages	H-4
K.1.	<i>SIMSAT</i> with Support Rods	K-6
K.2.	Baseline <i>SIMSAT</i> Layout (support rods not shown for clarity)	K-7
K.3.	Truss Attachment Collar - Front View	K-8
K.4.	Truss Attachment Collars - Side View	K-8

Figure		Page
K.5.	Payload Mounting Plate	K-9
K.6.	<i>SIMSAT</i> on Pedestal - Wireframe View	K-10
K.7.	<i>SIMSAT</i> on Pedestal - Wireframe Close-up View	K-11
K.8.	<i>SIMSAT</i> on Pedestal - Solid Form View	K-12
K.9.	Standard Mounting Plate Template	K-13
K.10.	Two-Battery Mounting Plate Template	K-14
K.11.	Battery Housing - 3D View	K-15
K.12.	Battery Mounting	K-16
K.13.	Battery Housing - Side View	K-17
K.14.	Battery Housing Pieces	K-18
K.15.	MathCad7 Counterweight Mass Calculations (page 1 of 5)	K-19
K.16.	Counterweight Fine-Tuning Mechanism with Weights	K-24
K.17.	Payload Plate with Weights	K-25
K.18.	Counterweight Fine-Tuning Balance Mechanism - Side view	K-26
K.19.	Counterweight Fine-Tuning Balance Mechanism - Perspective View	K-27
K.20.	Counterweight Fine-Tuning Mechanism - Pegboard Design	K-28
K.21.	Counterweight Mechanism with Dimensions - Right Side View	K-29
K.22.	Counterweight Mechanism with Dimensions (Pegboard Not Shown)	K-30
K.23.	Momentum Wheel Bay (Amplifiers Not Shown)	K-31
K.24.	Lexan Box (Momentum Wheels and Motors Not Shown)	K-32
K.25.	Amplifier Arrangement	K-33
K.26.	Gyroscope Housing for Attachment to Mounting Plate - Front View	K-34
K.27.	Gyroscope Housing - Side View	K-35
K.28.	Gyro, Battery, and Transceiver Mounting	K-36
K.29.	AutoBox U-clamp and Restraint L-brackets	K-37
K.30.	AutoBox Mounting	K-38
K.31.	Stanchion Restraint Collars - Side View	K-39

Figure		Page
K.32.	Stanchion Restraint Collars - Top View	K-40
L.1.	Finite-Element Models	L-2
M.1.	Option 1 (Target Mode) - Maneuver 1	M-4
M.2.	Option 1 (Target Mode) - Maneuver 2	M-5
M.3.	Option 1 (Target Mode) - Maneuver 3	M-6
M.4.	Option 1 (Target Mode) - Maneuver 4	M-7
M.5.	Option 1 (Target Mode) - Maneuver 5	M-8
M.6.	Option 2 (Target Mode with Roll Rate) - Maneuver 1	M-9
M.7.	Option 2 (Target Mode with Roll Rate) - Maneuver 2	M-10
M.8.	Option 3 (Roll Spin Mode) - Maneuver 1	M-11
M.9.	Option 3 (Roll Spin Mode) - Maneuver 2	M-12
M.10.	Option 3 (Roll Spin Mode) - Maneuver 3	M-13
M.11.	Option 4 (Yaw Spin Mode) - Maneuver 1	M-14
M.12.	Option 4 (Yaw Spin Mode) - Maneuver 2	M-15

List of Tables

Table	Page
1.1. Problem-Solving Processes of Sage vs. Hall	1-9
1.2. Problem-Solving Processes of Meredith, <i>et. al.</i> , vs. Hall	1-14
2.1. Concept Exploration and Definition Subsystem Alternatives	2-23
2.2. Concept Exploration and Definition Subsystems Summary	2-32
3.1. Preliminary Design Subsystem Alternatives	3-23
3.2. Chemical Battery Characteristics	3-26
3.3. Baseline Cost Breakdown	3-28
3.4. Raw Cost Data	3-28
3.5. Baseline Schedule Breakdown	3-29
3.6. Raw Schedule Data	3-30
3.7. Raw Safety Data	3-30
3.8. Raw Performance Data: Controllability	3-32
3.9. Raw Performance Data: Data Capability	3-32
3.10. Raw Performance Data: Satellite Movement	3-33
3.11. Raw Performance Data: Range of Experiments	3-35
3.12. Baseline Mass Breakdown	3-35
3.13. Raw Performance Data: Available Margins	3-36
3.14. Raw Performance Data: Ground Station Capability	3-37
3.15. Raw Performance Data: Command and Control	3-38
3.16. Raw Performance Data: O&M Time	3-39
3.17. Common Utility Scale	3-40
3.18. Scaled Scores Summary	3-41
3.19. Weighting Factors Vector	3-45

Table		Page
3.20.	System Scoring Results	3-46
3.21.	Utility of Each Performance Consideration	3-48
4.1.	Detailed Design Baseline Architecture	4-2
4.2.	SmartMotor Characteristics [51]	4-10
4.3.	"Dumb" Motor Characteristics [51]	4-11
4.4.	NEJ-3000 Characteristics	4-13
4.5.	Humphrey CF75 Characteristics	4-14
4.6.	Battery Configuration Alternatives	4-15
4.7.	Detailed Design Subsystem Alternatives	4-16
4.8.	Ranked Weighting Factors	4-20
4.9.	Detailed Design Resulting Architecture	4-23
4.10.	RadioLAN Product Data [45]	4-85
4.11.	Power Estimates Used for Wire Sizing	4-93
4.12.	Maximum 5min Rating (Amperes) for Aircraft-Grade Cables in Free Air	4-94
4.13.	Maximum 1min Rating (Amperes) for Aircraft-Grade Cables in Free Air	4-94
4.14.	Thruster (Moog Model 50-820) Specifications [39]	4-120
4.15.	Gas Bottle Specifications	4-123
5.1.	Humphrey CF75 Characteristics	5-2
5.2.	Animatics BL-3450 Motor Characteristics [51]	5-2
5.3.	Advanced Motion Control Amplifier Characteristics [51]	5-3
5.4.	Nominal Wire Gauges	5-14
5.5.	Baseline Components, Masses, and Positions	5-31
B.1.	<i>SIMSAT</i> Components	B-9
B.2.	Component Rotation Angles	B-11

Table		Page
C.1.	Nominal Configuration Component Properties	C-3
C.2.	Aluminum and Steel Solid Disk Wheels	C-10
C.3.	Aluminum and Steel Wheels with Six Holes	C-15
C.4.	Theoretical Aluminum and Steel Hoop Wheels	C-16
C.5.	Aluminum vs. Steel Hoops-Inertia Held Constant	C-17
C.6.	Aluminum vs. Steel Hoops-Width Variation of Steel Hoop	C-17
C.7.	Steel and Aluminum Wheel Optimization at 36V and 24V	C-21
C.8.	Final Wheel Alternatives for 36V and 24V Bus	C-22
D.1.	Roll Range Utility	D-7
D.2.	Pitch/Yaw Range Utility	D-8
E.1.	Pitch Axis Gyro Regression Analysis	E-2
E.2.	Roll Axis Gyro Regression Analysis	E-4
E.3.	Yaw Axis Gyro Regression Analysis	E-6
E.4.	Fore/Aft Acceleration Regression Analysis	E-8
E.5.	Lateral Acceleration Regression Analysis	E-10
E.6.	Vertical Acceleration Regression Analysis	E-12
F.1.	Detailed Design Raw Values	F-2
F.2.	Detailed Design Raw Values (continued)	F-3
F.3.	System Scoring and Ranking	F-4
G.1.	Options 1 and 2 - Gains	G-2
G.2.	Options 3 and 4 - Gains	G-3
G.3.	Option 5 - Gains	G-4
L.1.	Payload-Side Nodal Coordinates	L-3
L.2.	Payload-Side Element Specifications	L-4
L.3.	Payload-Side Nodal Mass Properties	L-5

Table		Page
L.4.	Payload-Side Displacements	L-6
L.5.	Wheel-Side Nodal Coordinates	L-7
L.6.	Wheel-Side Element Specifications	L-8
L.7.	Wheel-Side External Loading	L-9
L.8.	Wheel-Side Displacements	L-10
M.1.	Options 1 and 2 - Gains	M-2
M.2.	Options 3 and 4 - Gains	M-3

Abstract

This document describes the systematic development of the AFIT-sponsored program to develop a laboratory-based satellite simulator. The simulation satellite (*SIMSAT*) system supports experimentation in areas of attitude control, precision pointing, and vibration suppression. System development began with the purchase of the Tri-axis Gas Bearing from Space Electronics, Inc., which simulates a torque-free space environment using a low-friction air cushion. Researchers designed *SIMSAT* subsystems to provide power, attitude control, telemetry, and structural support to experimental payloads. Project challenges included integration of attitude control software/hardware, high-output power storage devices, remote communications, high-frequency data collection, structural design, and user-interface design.

SIMSAT: A SATELLITE SYSTEM SIMULATOR AND EXPERIMENTAL TEST BED FOR AIR FORCE RESEARCH

I. Introduction

1.1 Background

In recent years, the U.S. military has increasingly realized the significance of space as a strategic and tactical resource. Satellite imagery, GPS-guided munitions, missile warning, and global communications for deployed forces exemplify the importance of space assets in USAF planning. Recognizing the importance of space resources, the USAF has shifted its focus from being strictly an "air force" to becoming the premiere "space and air force" by the year 2025 [54]. Accordingly, the Air Force Institute of Technology (AFIT) has responded by developing curriculum and conducting research to support space operations and cutting-edge space technologies. Unfortunately, much of the space-related work at AFIT has been limited to computer simulation or stationary laboratory experiments due to a lack of representative space hardware. Consequently, AFIT desires to augment its laboratory facilities with a more realistic space-platform simulator. Development of a satellite simulator would allow implementation of practical experiments, demonstration of fundamental motion principles, and extension of Air Force research capabilities. Additionally, a satellite simulator would provide a hands-on learning tool to enhance the educational experience of AFIT students, particularly in the area of satellite attitude dynamics.

To initiate the development process of a satellite simulator, AFIT purchased a Tri-axis Air Bearing System from Space Electronics, Inc. of Berlin, Connecticut. The system consists of an air bearing (spherical rotor, hollow shaft, and mounting flanges), a pedestal, and an air compressor. Figure 1.1 shows the air bearing assembly. Compressed air (at

approximately 75 psi) flows inside the pedestal to six small jets in the air bearing cup; the spherical rotor floats above the cup on a gas film that is less than 0.0005 inch thick. The air bearing is capable of 360° of yaw (rotation about the vertical axis), 360° of roll (rotation about the horizontal axis), and $\pm 30^\circ$ of pitch (tilt in the vertical plane). The air bearing can support objects weighing up to 300 pounds [53]. Although not capable of independent pitch, roll, or yaw motion without attached components, the Tri-axis Air Bearing System served as the “backbone” for satellite simulator development.

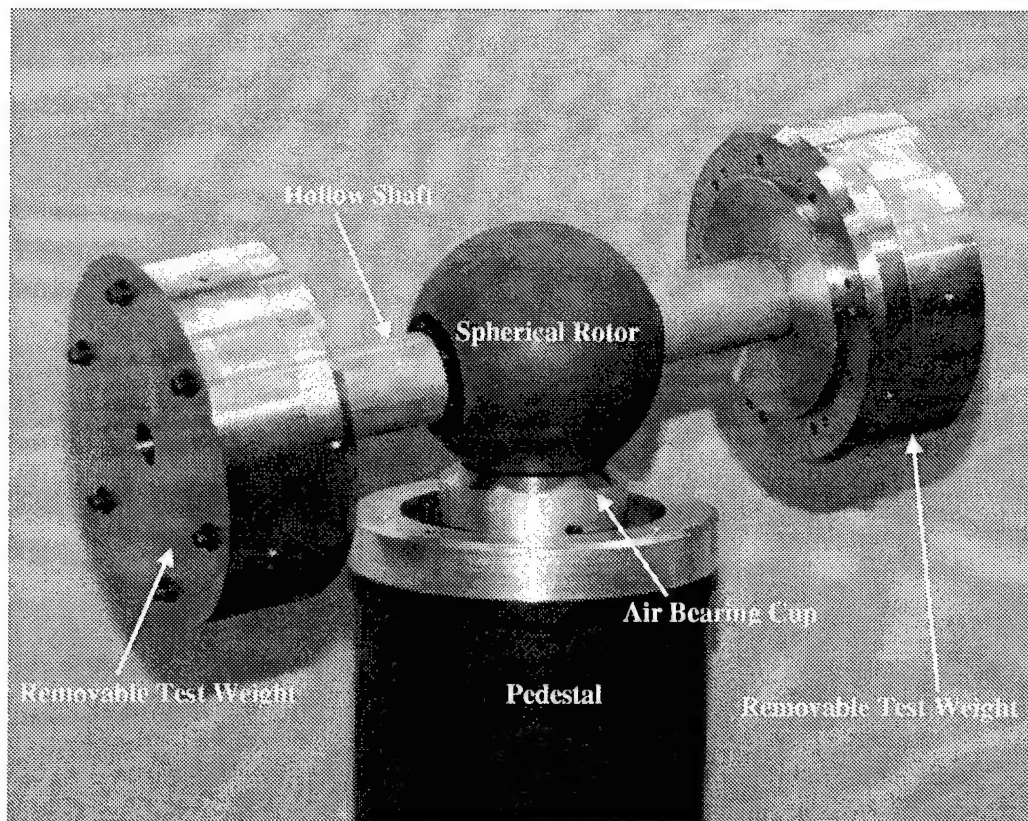


Figure 1.1 Air Bearing Assembly

1.2 Design Requirements

With the Tri-axis Air Bearing System in hand, AFIT faculty tasked the 1999 Graduate Systems Engineering Team to develop a satellite simulator for AFIT use. The team's

charter was to determine the customer requirements for the simulator, design a system to meet those requirements, order parts, and perform as much of the system integration/implementation as possible. As with any other development effort, this process began with a problem to be solved and a need to be fulfilled. To provide initial focus, the design team developed a “statement of need” as a one-line summary of the problem to be tackled in the design effort:

AFIT needs to simulate satellite behavior with as much fidelity as possible.

This needs statement served as a starting point from which the design team developed more-detailed design requirements. The team decided to name their overall design effort *SIMSAT*— the *SIM*ulation *SAT*ellite. The first meeting allowed the team to “sit down with the customers” and determine additional system details. The customers of the simulator (the team’s academic advisors) indicated *SIMSAT* should [32]:

- Support research and educational needs.
 - Pure and “dual” spin experiments.
 - 3-axis rigid and flexible structure experiments.
 - Host experimental payloads.
- Be simple to use.
 - Meaningful experiments setup and run by one researcher and one technician in less than a week.
 - Data intuitively displayed in real-time and easily stored for future replay and analysis.
- Be safe – as required, the following design techniques should be employed:
 - Highly reliable and/or redundant critical components.
 - Containment for components that could fail catastrophically.
- Stay within budgetary and scheduling constraints.
 - Total initial costs should remain under \$100K (additional funding may be possible, but will add to total development time).
 - The system should be ready to operate by FY 00.

1.3 Systems Engineering Approach

1.3.1 Systems Engineering Framework. Based on the identified top-level needs, it was clear the problem was multi-faceted. Given such a problem, how does one simultaneously evaluate all concerns that need to be considered? Given several alternative solutions, how is the “best” alternative selected? How can one make sure that no critical aspects of the system are overlooked? The ability to find answers to these questions, and others, forms the foundation of the field known as *systems engineering*. As an initial step in the design of AFIT’s satellite simulator, the design team researched several works on the theory and practice of systems design using the systems engineering approach. Study in the systems approach gave the team insight into multidiscipline design challenges, development of a structured problem-solving methodology, breakdown of lifecycle phases, and incorporation of systems engineering tools, modeling techniques, and decision making methods.

The *systems approach* “represents a broad-based systematic approach to problems that may be interdisciplinary. It is particularly useful when problems are complex and affected by many factors, and it entails the creation of a problem model that corresponds as closely as possible in some sense to reality. Its usefulness increases with problem complexity because it permits the engineer to take a broad overall view of the problem under consideration. Thus a clearer understanding of constraints, alternatives, and consequences that are associated with the problem may be attained.” [38:12] This summary of the systems approach clearly shows its relevance to the *SIMSAT* design problem, being interdisciplinary and complex in nature. This theme is further emphasized by Sage as he states, “The systems engineering approach to problem solving emphasizes interactions and interrelations among the diverse parts of a problem.” [49:*xi*]

1.3.2 Systems Engineering Definition. The top-down, interdisciplinary, and iterative aspects of systems design are evident in the following systems engineering definitions:

"Broadly defined, system engineering is 'the effective application of scientific and engineering efforts to transform an operational need into a defined system configuration through the top-down iterative process of requirements definition, functional analysis, synthesis, optimization, design, test, and evaluation.' The system engineering process, in its evolving of functional detail and design requirements, has at its goal the achievement of the proper balance between operational (i.e., performance), economic, and logistics factors." [8:12]

"Systems Engineering is an interdisciplinary approach and means to enable the realization of successful systems. It focuses on defining customer needs and required functionality early in the development cycle, documenting requirements, then proceeding with design synthesis and system validation while considering the complete problem: operations, performance, test, manufacturing, cost and schedule, training and support, and disposal. Systems Engineering integrates all the disciplines and specialty groups into a team effort forming a structured development process that proceeds from concept to production to operation. Systems Engineering considers both the business and the technical needs of all customers with the goal of providing a quality product that meets the user needs." (International Council on Systems Engineering) [29]

"Systems engineers are, of necessity, technical generalists. Systems engineering... is not intrinsically mathematical. Rather, it is organizational, judgmental, logical, goal-oriented, and admittedly must often be subjective." [5:x]

"Systems engineering is the systematic application of proven standards, procedures, and tools to the technical organization, control, and establishment of: system requirements, system design, system management, system fabrication, system integration, system testing, and system logistics support." [48:1-2]

"Systems engineering is a branch of engineering that 'concentrates on the design and application of the whole as distinct from the parts... looking at a problem in its entirety, taking into account all the facets and all the variables and relating the social to the technological aspects.' (Simon Ramo 1973)" [46:28]

Based on the previous definitions and others, the design team formulated its own systems engineering definition as follows:

"Systems engineering is not simply another engineering discipline, but a formal, multidisciplinary, iterative process to develop customer needs, possible solutions to those needs, and to determine which alternatives in that solution space would most effectively satisfy the customer."

1.3.3 Systems Architecting vs. Systems Engineering. What is *systems architecting* and how does it differ from *systems engineering*? As described previously, systems engineering encompasses the tools and methodology necessary to move from conceptualization to system implementation, with emphasis on the system as a whole and user needs. Indeed, systems architecting is also concerned with these same issues, and is occasionally used interchangeably with systems engineering. However, there are subtle, yet significant, differences between these systematic views of design.

Webster's Dictionary defines architecture as "the art or science of building." Traditionally, *architecture* refers to the planning and building of structures related to civil, military, or naval applications. In the last thirty years or so, the term has been applied to technical systems with increasing regularity, thus the common use of the terms *software architecture*, *computer architecture*, and the like. As stated by Rechtin [46:1], "The essence of architecting is structuring." Thus, the essence of systems architecting is structuring the system – "to bring structure in the form of systems to an inherently ill-structured unbounded world of human needs, technology, economics, politics, engineering, and industrial practice." [46:1] Clearly, this definition of architecting overlaps that of systems engineering. Rechtin identifies two areas in which distinctions are particularly important – function versus form and complexity versus specificity [46:12].

The guiding principle "form follows function" is basic to architecting, which focuses on the top-down design driven by *function* as opposed to *form*. Hillaker is quoted by Rechtin as stating [46:12], "System engineering is form-based and system architecting is function-based." With respect to complexity, the architect is "a specialist in reducing complexity, uncertainty and ambiguity to workable concepts. The systems engineer, in contrast, is the master of making feasible concepts work." [46:13] It follows that systems architecting "concentrate[s] on concepts, synthesis, top-level specifications, nontechnical as well as technical interfaces, and mission success", whereas systems engineering "concentrate[s] on defined subsystem interfaces, analysis, and performance to specification." [46:13]

The architect's role is most visible in the early stages of a design, when concepts are explored, both innovative and adaptive in nature. Beam describes architecture as "a matter

of repetition among members of the class, and often repetition within a single member” [46:1], illustrating the adaptive nature of architecting, wherein functions are addressed by exploring how other systems are designed regardless of their form. For example, a variable geometry wing designed to provide the lift function for an aircraft may incorporate techniques borrowed from biological systems, in which electrical impulses cause muscle contractions. Although a wing and a human muscle are very different in form, the function of altering physical characteristics may be similar. As the design progresses, the visibility of the systems engineer increases, as the proposed concepts are refined, detailed, and implemented. With a system concept already suggested, the tools of systems engineering can most efficiently be brought to bear.

Why are the distinctions between systems architecting and systems engineering relevant to the *SIMSAT* design? This design progressed from initial identification of needs and concept development, through the actual integration of subsystem components, necessitating an understanding of both systems architecting and systems engineering tools and techniques. Thus, the team performed both architecting as well as engineering roles. The line between these roles is indeed blurred, as the “architect hat” and “engineer hat” are sometimes worn simultaneously, especially during concept exploration and preliminary design. Once the design became more and more refined, systems engineering tools were more readily implemented.

1.3.4 Systems Engineering Dimensions. Hall divides the systems engineering approach into a three-axis morphological box, as shown in Figure 1.2 [25]. The *time* dimension of systems engineering refers to the system lifecycle – the sequences or phases that extend from initial conceptualization through system retirement. The *logic* dimension refers to the problem-solving process – the steps necessary to move the design from one lifecycle phase to the next. Finally, the *knowledge* dimension refers to the specialized knowledge from various fields necessary to address and solve the problems at hand.

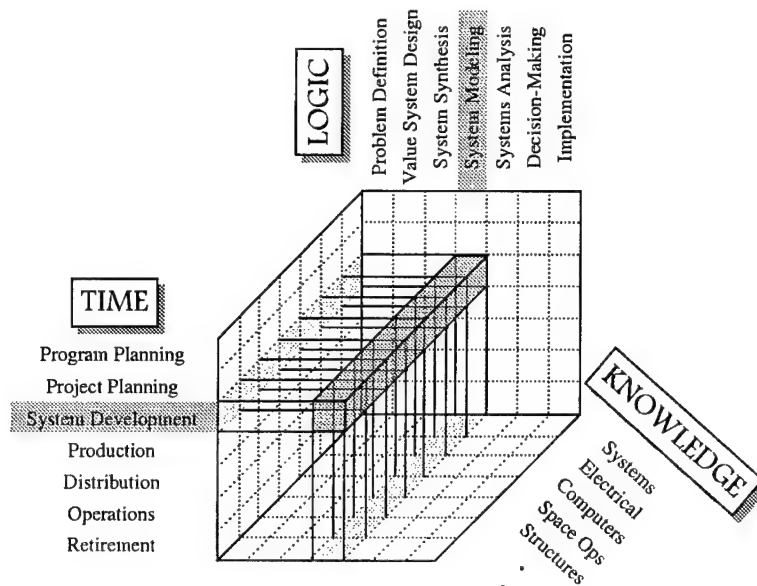


Figure 1.2 Systems Engineering Dimensions [26]

1.4 Systems Engineering Process

1.4.1 Problem-Solving Methodology. As described in Section 1.3, there is an underlying process in a well-planned design which facilitates the evolution of the design from a problem statement to conceptual alternative solutions, and finally to a resultant design ready for implementation. The design process by which this evolution occurs can be a considerable design problem in and of itself. A process which encumbers the design team and impedes conceptual evolution is not desirable. This situation can occur when a process is too rigid for the problem at hand. An overly rigid process can lead to overemphasis of process objectives at the expense of problem objectives. A simple test of a constraining design process is to ask whether the process steps are significantly contributing to a better final design. If process steps are being accomplished for their own sake, they are a waste of the design team's time and the client's resources. Conversely, a design process which is too flexible and unstructured provides inadequate methodology for the design team to conceptualize solutions, compare alternatives, and finally choose a "preferred" system. Existence of a formal process can be a significant driver in keeping

the design team on track and providing backbone to the seemingly unbounded world of systems design. Thus, the design process is a useful tool for the team in the management of complexity, which is inherent at some level in all design. The question therefore arises, what is the best design process for the problem at hand?

A significant objective identified by the customer in this project is the actual operation of the satellite simulator system. The design team was faced with a complex problem to be carried from the conceptualization stage of the lifecycle through to actual integration (and possible operation) of the system. A large portion of the system lifecycle development needed to be accomplished in a relatively short amount of time. The design team was required to make several iterations through the design process to move from initial conceptualization to detailed development. A flexible design process was used to handle this schedule-driven design problem.

The approach used by the team is outlined in Sage [50], who builds from the seven step process identified by Hall [25]. Table 1.1 illustrates the correspondence of the Sage method to the Hall method.

Table 1.1 Problem-Solving Processes of Sage vs. Hall

Sage	Hall
Issue Formulation	Problem Definition Value System Design System Synthesis
Analysis	System Modeling System Analysis
Interpretation	Decision-Making Implementation/Documentation

The key to Sage's structured process is that Hall's seven steps are aggregated into three fundamental steps: *issue formulation*, *analysis*, and *interpretation*. These three steps define the overall system design process; each iteration through the system or subsystem level design incorporates these steps. The tasks within each fundamental step may be over- or under-emphasized as necessary depending on the problem or subproblem. Thus, the design team is not encumbered by implementation and documentation of a formal seven-

step process for every problem or subproblem encountered. Sage's process accommodates the "time-to-market" approach which may require less emphasis on system synthesis and analysis for certain subproblems in favor of requirements satisfaction. It is important to note that although the process appears linear, there are feedback loops within every step and between steps. For example, during analysis it may be discovered that a significant objective was overlooked earlier, and this objective may then be incorporated into the value system design. Moreover, if requirements prove to be very difficult or costly to meet, they should be challenged and the problem redefined.

1.4.2 Issue Formulation. As a starting point for any design iteration, identification of problem characteristics and relevant issues must be accomplished. The following information should be considered by the design team at this stage: actors involved the design process, groups affected by the issues or proposed solutions, fields of knowledge required to solve the problem, specific needs addressed by the problem, design alterables, constraints imposed, and cost and schedule considerations. The problem itself is isolated, quantified, and clarified. The system (or subsystem) to be developed is delineated from its surrounding environment. This abstraction of the environment consists of those elements which significantly interact or affect the system (or subsystem), but are beyond the design team's sphere of control (at this stage). Determination of what is the system and what is the environment allows identification and classification of important external interfaces. These tasks correspond to Hall's "Problem Definition" step.

Once needs are identified, development of system objectives begins. This process, Hall's "Value System Design", is the selection of a set of objectives that will guide the search for alternatives and be used for comparisons. It is the formalization of what is important to the customer. Value system design itself can vary in form. For some problems or subproblems, value system design may be the enumeration of specific measurables by which all alternatives will be judged. Thus, the determination of a preferred solution can be accomplished quantitatively. At a top-level systems architecting perspective, it is highly desirable to create an objective hierarchy with associated measurables to comprise the value system design; these measurables will be weighted in the end to select a preferred

alternative ¹. This objective hierarchy approach to value system design can be carried over to each problem or subproblem encountered as the design evolves and goes through repeated iterations of the design process. In some instances, a formal objective hierarchy may not be needed. In these cases, alternatives which are feasible (within constraints) may be chosen without searching for the preferred alternative. This satisficing approach may be desired for various reasons: tight schedule constraints prevent detailed alternatives comparisons, lack of reliable modeling data prevents accurate comparisons, or the utility of a preferred solution is comparable to that of other feasible solutions.

The last phase of issue formulation corresponds to Hall's "System Synthesis" step. A set of alternative solutions is developed, through research, brainstorming, reverse engineering, heuristics, and other means. These alternatives should appear feasible, but need not fully comply with constraints at this stage (later investigation could reveal a feasible alternative was in fact infeasible; or conversely, a potentially infeasible solution may prove feasible). Determination of these alternatives is at the core of systems architecting.

1.4.3 Analysis. *Analysis* includes the necessary system modeling and evaluation to make decisions regarding which alternatives to pursue further. System modeling is the development of means to evaluate performance of each alternative. Models are system abstractions used to evaluate the measurables for each objective. The systems evaluation phase is the use of modeling to quantify these measurables. At this stage, alternatives may be refined as necessary to improve performance.

System analysis may take place in many different forms. Construction of simulations, itemization of costs, development of prototypes, and engineering estimates are just some of the modeling methods available to the design team to quantify performance measurables. The goal of system analysis is to provide data for the decision making phase. Therefore, modeling is only necessary to the level of fidelity allowing differentiation of system alternatives. For the satellite simulator design problem, significant use of mental

¹Depending on the fidelity necessary to make sound decisions, an objective hierarchy may include only qualitative "values". These values represent those aspects of the design important to the decision maker. Qualitative values are broken down into quantitative measurables as necessary to differentiate and rank alternative designs.

modeling, engineering estimates, and research allowed quantification of measurables to a level allowing decisions regarding alternatives.

1.4.4 Interpretation. *Interpretation* uses the information gained by analysis to make decisions and proceed to the next iteration of the design process. In the decision making phase, an alternative (or set of alternatives) is selected based on the analysis data and the value system identified earlier. There is an element of risk and uncertainty in the results obtained through analysis, and these uncertainties must be considered by the decision maker. Dominated solutions should be identified and discarded from consideration. Some alternatives may be better in certain aspects, but less preferred in other areas. Decision making tools, utility theory, and objectives weighting are needed to settle on a preferred solution set. Interaction with the customer and chief decision maker is critical during this stage.

Once this set of alternatives is identified, planning for action is necessary. The design process to this point should be communicated and documented. Looking ahead to the next iteration, the allocation of resources and development of another design schedule is performed. The design process then begins another iteration, in which the problem is recast given the current solution set. If this is the final iteration, the final design is documented and implemented.

1.4.5 Other Problem-Solving Methods. One major advantage of Hall's problem-solving process is its independence from the lifecycle phase. The iterative process can be applied at each stage of the design. Some proposed systems engineering processes overlap the problem-solving and lifecycle phases to the point that differentiating between the two can be difficult, and the iterative nature of design is not as apparent. The "systems approach" identified by Eisner is a broad overview of the major steps necessary to develop a system, implicitly defining an overlapping problem-solving process and design lifecycle². It was not used directly in the *SIMSAT* design due to the single-dimensionality of the

²Eisner did not recommend this "systems approach" to be used as a problem-solving process in itself. In fact, the seven-step process of Hall is referenced in Eisner's work.

process³, although Eisner's work provided additional systems perspective to be used by the team. The following list categorizes the steps of Eisner's "systems approach" [22:13-16]:

1. *Needs statement.*
2. *Goals and objectives.*
3. *System requirements.*
4. *Specifications.*
5. *Synthesis of alternatives.*
6. *Analysis of alternatives.*
7. *Formulation of evaluation criteria.*
8. *Update of specifications.*
9. *Building, testing, and acceptance of system.*
10. *Documentation and installation.*
11. *Operation of system.*
12. *Modification and upgrade of system.*

Another problem-solving process considered by the team was proposed by Meredith, Wong, Woodhead, and Wortman [38:13-15]. The process is similar in content to the seven-step process of Hall, but was deemed less effective than Hall's process for use in the *SIMSAT* design. This six-step process is compared to Hall's methodology in Table 1.2. Specifically, the design team favored an approach in which the synthesis of alternatives preceded the modeling and analysis step. Furthermore, the "allocate resources" step in this proposed process was considered extraneous by the design team since the team did not control the allocation of resources beyond team manpower. Thus, the team favored Sage's aggregated problem-solving process based on Hall's steps.

³The single-dimensionality of this "systems approach" refers to the overlap of problem-solving steps and lifecycle phases. It should be noted that Eisner included feedback loops and iteration within his "systems approach" steps.

Table 1.2 Problem-Solving Processes of Meredith, *et. al.*, vs. Hall

Meredith, <i>et. al.</i>	Hall
Problem Definition	Problem Definition
Plan Approach	Value System Design
Allocate Resources	System Synthesis
Model and Analyze	System Modeling
Design and Evaluate Alternatives	System Analysis
Select Preferred Alternative	Decision-Making
	Implementation/Documentation

1.5 Design Lifecycle Description

1.5.1 Lifecycle Methodology. The use of an appropriate lifecycle model as part of the systems engineering process allows the design to be effectively managed as it progresses from a concept to actual implementation, and beyond. As with the formal problem-solving process, the use of a specified systems engineering lifecycle has advantages and disadvantages when compared to another lifecycle model. Selection of an appropriate lifecycle model at the outset of design is an important decision which guides the ensuing design process. Several lifecycle models were considered for use in the *SIMSAT* design, with eventual selection of a tailored model specific to this design.

1.5.2 Comparison of Various Lifecycle Models. This section describes the advantages and disadvantages of several lifecycle models considered for use during the *SIMSAT* design.

1.5.2.1 Sage's Lifecycle Model. A relatively streamlined lifecycle model was proposed by Sage based on the three basic phases of design evolution [50:32-33]. The basic phases are the following ⁴:

- System definition.
- System design and development.
- System operation and maintenance.

⁴There exist feedback loops in this lifecycle model so that refinements can be made as the design evolves.

The activities within each phase of the three-phase model are generally obvious, but may be explicitly listed for larger system designs. Sage proposed a 22-phase model based on the three-phase model to be used for large systems [50:33-39]. This 22-phase model ensures certain objectives and design decisions are met before moving on to the next phase, thereby acting as both a system lifecycle and system management tool. Both the simplified three-phase model and expanded 22-phase model are shown in Figure 1.3. The advantage of Sage's simplified model is clear: it is easy to use and allows flexibility. The expanded model is more geared for large military/industrial projects and contains steps not applicable to this design. However, the simplified model had drawbacks with respect to the *SIMSAT* design. Aggregation of the majority of the design decisions into one "system design and development" phase made the natural course of design decisions and milestones less clear. This lack of explicit reference to the stages of design between identification of need and system implementation precluded use of this model by the design team.

1.5.2.2 Hall's Lifecycle Model. Hall proposed a seven-phase system lifecycle which covered the entire system life, to include system phase-out. Figure 1.4 shows how Hall's phases relate to those of Sage [50:42]. The individual phases of Hall's model are described below [25]:

Program planning. This phase results in formulation of activities and projects supportive of the overall system requirements. The system management plan is developed.

Project planning. Purpose is to configure a number of specific projects which together comprise the overall system program.

System development. This phase comprises the implementation of project plans through system design, resulting in preparation of architectures, specifications, diagrams, and other design material.

Production. This phase includes the activities necessary to physically realize the system.

Distribution. This phase results in the delivery of the system to the end user.

Operation. The ultimate goal of the system, this phase comprises use by the customer, to include maintenance and retrofit as necessary.

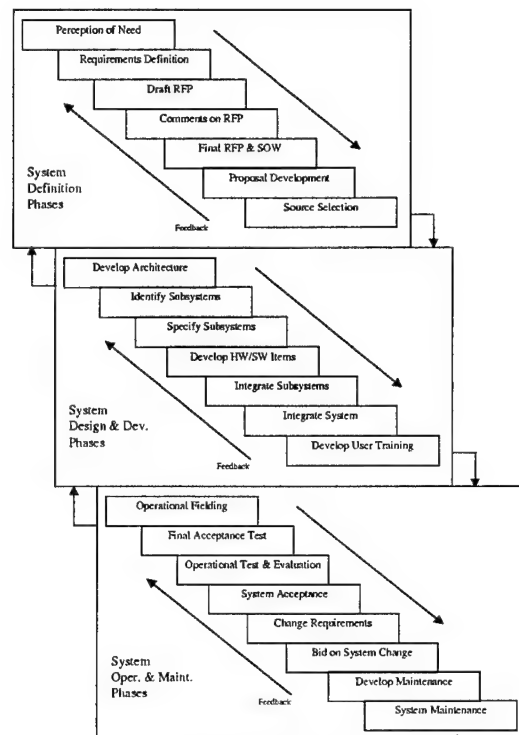


Figure 1.3 Sage's Lifecycle Model

Retirement. This phase, often overlooked in early planning, includes the phase-out and disposal of the system.

Although a comprehensive model, Hall's lifecycle was not used for this design for several reasons. Like Sage's three-phase model, the system development phase of Hall's model was not detailed enough to provide the design team with clear direction and objectives for this project. Furthermore, the system was designed and constructed in the same facility in which it would operate, making distribution an irrelevant step. As for the operations and retirement phases, they were not directly relevant to the design of this system, and were not addressed as separate lifecycle phases ⁵.

⁵ As needed, continuation of the current design team's efforts through system retrofits and modifications was accounted for. These upgrade programs would represent separate design problems and possibly separate thesis work, and thus were not included in the team's lifecycle model.

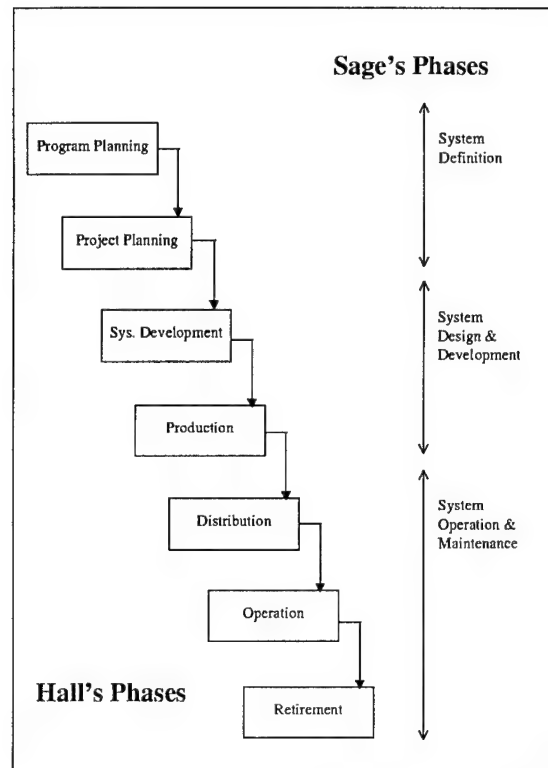


Figure 1.4 Lifecycle Models of Hall vs. Sage

1.5.2.3 Eisner's Lifecycle Model. Eisner presented a lifecycle model fairly similar to that of Hall. Despite more explicitly referencing concept exploration, this model still did not provide the design stage fidelity desired by the design team. Eisner's lifecycle consists of the following phases [22:37-39]:

- Need development.
- Concept definition.
- Concept validation.
- Engineering development.
- Production.
- Operations.

1.5.2.4 DoD Lifecycle Model. The Department of Defense acquisition model described in the Defense Acquisition Deskbook [13] was discounted for use in this design due to its relatively rigid review/milestone structure. As with the previous models discussed, the DoD lifecycle includes phases which were not relevant to the design team's academic charter. However, the DoD model provided useful guidance as to the delineation of design phases and use of design reviews.

1.5.3 SIMSAT Lifecycle Model. A system lifecycle tailored to the *SIMSAT* project was chosen to represent the design phases. The use of this model was driven by the following key factors used by the design team in their lifecycle modeling. The lifecycle should:

- Provide clear delineation of design progression.
- Allow natural breaks for important design decisions.
- Include only relevant lifecycle phases.
- Adequately accommodate a short design schedule.

The conceived lifecycle to meet these needs is shown in Figure 1.5. The following sections describe these lifecycle phases in detail.

1.5.3.1 Concept Exploration and Definition. Once a need has been identified and initial requirements have been defined, the system design process enters the first stage of the system lifecycle. This phase includes refinement of system requirements, along with exploration of various concepts which can be designed to meet identified requirements. Emphasis is on top-level system architectures, with detailed design decisions avoided at this point. The focus of this lifecycle phase is to identify and differentiate broad solution classes. Through initial modeling, research, trade studies, and decision maker inputs, a class (or classes) of solutions may be identified which stands out from the rest. This solution class (or classes) can then be further refined and investigated during the next lifecycle phase.

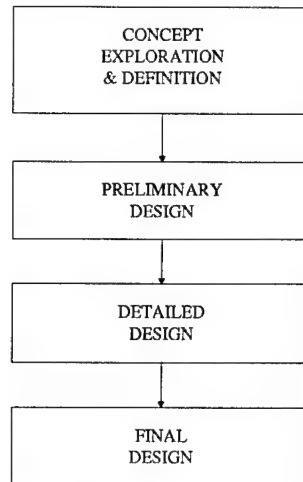


Figure 1.5 *SIMSAT* Lifecycle Model

1.5.3.2 Preliminary Design. In this lifecycle phase, the solution class(es) identified in Concept Exploration and Definition is (are) further refined. Subsystem level requirements are defined in this phase. Trade studies, research, and system modeling are used to determine which types of subsystems best meet the cost-effectiveness system goals. The output of this phase includes a system architecture complete with identified subsystem types, along with subsystem requirements and interface identification. In short, this phase translates system solution classes into subsystem solution classes, which are further defined and integrated in the next lifecycle phase.

1.5.3.3 Detailed Design. The subsystems are further designed in this phase. Detailed trade studies should be used to determine the exact subsystem architectures which make up the overall system. Integration and interface issues are resolved in this phase and the overall system is completely defined at this point, subject to change as system test and evaluation may require. The product of this lifecycle phase is a detailed functional system architecture with subsystems designed and integrated.

1.5.3.4 Final Design. The final product is described and documented for future users in this phase. Unresolved design issues are discussed. The design team makes recommendations and draws conclusions to aid future users and designers.

1.6 Document Format

The remainder of this document is structured to match the design activity shown in Figure 1.6. The following chapters correspond directly to each lifecycle phase. Within each chapter, the problem-solving process is described, with successive iterations within a phase detailed as necessary. Thus, each chapter documents the issue formulation, analysis, and interpretation activities relevant to the respective lifecycle phase. Background information on design decisions, applied theory, software development, and other pertinent areas is supplied in the appendices.

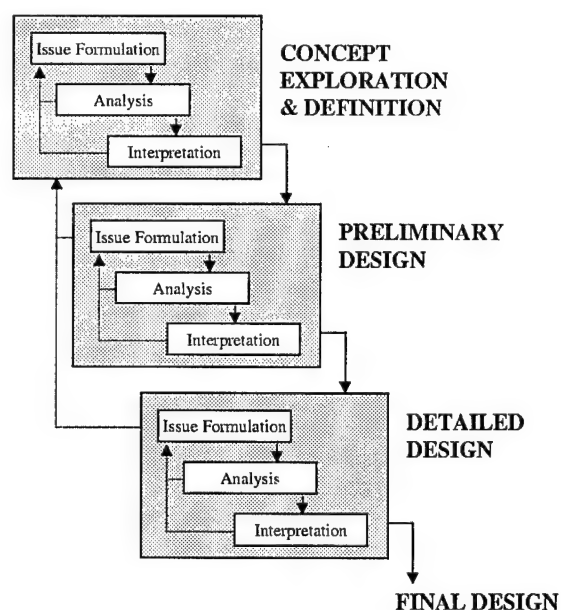


Figure 1.6 SIMSAT Summary of Design Activity

II. *Concept Exploration and Definition*

2.1 *Overview*

Once a need has been identified and initial requirements have been defined, the system design process entered the first stage of the system lifecycle. This phase included a formal definition of the user's needs and requirements, followed by an exploration into various concepts which can be designed to meet the identified requirements. To effectively manage the problem complexity, emphasis in this phase was on top-level system architecture issues, with detailed design decisions left for future phases. The focus of this lifecycle phase was to identify and differentiate broad solution classes. Through initial modeling, research, trade studies, and decision maker inputs, classes of solutions were identified which stand out from the rest. These solution classes can then be further refined and investigated in the next lifecycle phase. The waterfall design model in Figure 2.1 highlights the focus of this chapter.

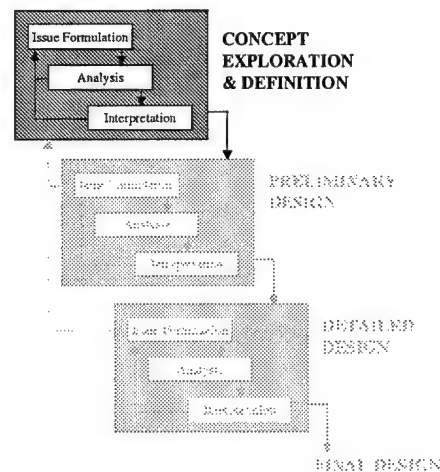


Figure 2.1 Concept Exploration and Definition Design Activity

2.2 Issue Formulation

2.2.1 Problem Statement. As a first step in the design process, a problem statement should be developed which captures the goals of the design in a clear and concise manner. The scope of this satellite simulator design was narrowed such that the needs of the direct customers were the primary design drivers, with the capability to meet outside agency needs retained, but not of primary concern. The problem statement was refined as follows:

Design a satellite system simulator for use as an experimental testbed for Air Force Institute of Technology (AFIT) and other Air Force/DoD research, and provide an instruction aid to AFIT instructors teaching satellite dynamics and control.

2.2.2 Problem Scope. The design study focused on developing a satellite simulator platform, and integrating the testbed hardware with a computer-based control system, hereafter referred to as the "ground station". The ground station must be capable of sending commands to and receiving data from the platform-based portion of the system, hereafter referred to as the "satellite". In addition, the ground station must support the development of the system control laws (including simulation of the proposed laws prior to actual satellite operation), provide a graphical representation of system controls and the satellite response to commands, and allow for collection and replay of satellite motion and experimental telemetry. The *SIMSAT* design should be robust such that a variety of experiments can be accomplished with minimal adjustments. Some experimental areas identified included investigation of control-moment gyros, optimal flywheel orientation design, flexible space structures behavior and vibration control, satellite attitude and tracking control, and ground station simulation of the satellite (including hardware-in-the-loop simulations, in-class presentations, and technology demonstrations). The project goal was to implement an operational *SIMSAT* design by March 1999.

This first iteration through the design process focused on refining requirements and exploration of concepts, and was not intended to result in design, implementation, or evaluation of an actual system. The goal of this phase was to understand the problem, gain knowledge in areas needed to attack the problem, develop objectives and enumerate

constraints, and then identify possible classes of solutions based on cost, performance, and other relevant criteria. This identification provided inputs into the Preliminary Design phase. This first iteration was completed by the end of June 1998.

2.2.3 Relevant Disciplines. The design team identified the following disciplines as relevant to solving this problem, incorporating knowledge from these disciplines as needed. These disciplines represent the *knowledge* dimension of the three-axis systems engineering morphology described by Hall [25].

- Systems engineering.
- Space operations.
- Orbital mechanics/satellite dynamics.
- Astronautical engineering.
- Mechanical engineering.
- Electrical engineering.
- Program management.
- Simulation/control theory.
- Software design and integration.
- Telemetry and data acquisition system design.
- Computer architecture design.

2.2.4 Identification of Actors. The major players in the design process and their contributing roles were identified to ensure success in the design effort through recognition of their concerns, needs, and limitations.

Lt Col Stuart Kramer and Capt Greg Agnes, USAF. These AFIT instructors were the direct customers of the *SIMSAT* design, thus their identified needs provided the

primary design drivers. As sponsors of the project, they also served as the chief decision making authority.¹

Systems Design Team. The team, comprised of AFIT Master's degree candidates in Space Operations and Systems Engineering, was responsible for the design and integration of the system, as well as final documentation and proposal.

Mr. Mike Hanke. A fellow AFIT Master's candidate in Systems Engineering, Mr. Hanke was responsible for the initial selection and integration of a computer-based architecture for the system. His thesis, "Design of the Computer Subsystem for the AFIT Simulation Satellite (*SIMSAT*)" [26], provides the principal documentation of the computer-based architecture decisions. His work was concurrent with the design team's work, and is considered a companion effort to the design.²

Mr. Jay Anderson. An AFIT civilian responsible for resource acquisition and laboratory support, Mr. Anderson was the focal point for facilities management, experimental support, logistics issues, hardware procurement, and safety-related issues.

Suppliers/Vendors. Commercial suppliers were the primary source for hardware and software used in the system design. An understanding of product availability, technological innovations, and customer support of these suppliers was critical to the design effort.

Indirect Customers. Some of the additional customers considered include other AFIT departments, other Air Force agencies, and joint Department of Defense agencies. These indirect considerations play a significant role in the need for a robust and timely design.

2.2.5 Initial Needs. At this stage of the design, needs were identified in general terms such that potential solution designs could be conceived and explored.

¹In addition to serving as both customers and chief decision makers, Lt Col Kramer and Capt Agnes were instrumental in providing direction to the design team. Their assistance in resolving technical issues and design trade-offs made this effort possible.

²Mr. Hanke was a member of the systems design team for much of the design process. His work was integral to the overall design, and does not represent a stand-alone effort. Many of the computer architecture decisions (specifically, the command and data handling issues) described in this document are a result of Mr. Hanke's work.

Actual subsystem requirements and quantitative system specifications were not considered this early in the design process. The following list summarizes the primary needs developed for *SIMSAT* at this level of detail:

- Support three-axis control for detailed experimentation. Three-axis stabilization is required for the primary experimental configuration.
- Support dual-spin demonstration experiments, which involve two sections of the satellite model to simultaneously rotate relative to one another.
- Support pure spinner demonstration experiments.
- System should be robust enough to support a multitude of experiments requiring different test bed configurations.
- Incorporate the air-bearing assembly (a piece of test equipment that allows the satellite to have full rotation in two axes and partial rotation on the third axis). This air-bearing mechanism was previously purchased expressly for this project.
- Provide unobstructed satellite model maneuvering; physical connections to the satellite should be minimized or eliminated.
- Develop a ground station to control and monitor the satellite and experimental hardware.
- Provide real-time data acquisition and command capability as necessary.
- Provide detailed data acquisition for post-test analysis, for both the satellite model and experimentation telemetry.
- Provide pre-test model simulation capability.
- Provide for real-time and post-test graphical representation of satellite motion. This need is highly desired, but not necessarily required.
- Allow emergency shutdown capability for the system.

2.2.6 Problem Elements. Once the needs were defined, the next step in the design process was to identify specific elements of the overall problem which must be addressed by the system architecture. These problem elements are summarized as follows:

- Rotating the satellite.
- Powering the satellite.
- Communicating with the satellite.
- Predicting satellite behavior.
- Commanding the satellite.
- Collecting and analyzing satellite telemetry and experimental data.
- Accommodating a variety of experiments.
- Providing emergency shutdown of the satellite.
- Representing the behavior of the satellite.

2.2.7 Constraints and Alterables. The only element of the design which is considered completely unalterable is the air-bearing model assembly. Within budget constraints and acceptability criteria, all other subsystems and components of the overall system are considered alterable, and the overall system architecture was left to the discretion of the design team. The physical location of the *SIMSAT* design is confined to the northwest corner of Room 146, Building 640, of the AFIT laboratories. This area is approximately 240 square feet. Laboratory lighting limits vertical height of any assembly to approximately 15 feet. The computer-based ground station should incorporate PC workstations, which can be networked to the AFIT system, allowing file transfer and use of AFIT software, such as MATLAB and SIMULINK. Compliance with AFIT, Wright-Patterson AFB, Air Force, and all other relevant agency policies is required. These policies pertain to safety, power, noise, pollution, radio frequency, and hazardous materials issues.

2.2.8 Cost and Schedule Summary. At this point in the design, specific cost allocations were not available, but a budget of approximately \$100,000 was considered an upper limit (although less expensive was preferred). A design timeline was formulated to provide a schedule at this stage. The significant events in the overall *SIMSAT* design timeline are summarized below.³

³Note that this schedule was constructed during the Concept Exploration and Definition stage, and was subject to subsequent change as later design issues may have dictated.

Apr 98. *Refine problem definition and attain initial needs and constraints.*

Apr 98. *Begin value system design and begin system synthesis.*

May 98. *Refine value system and further research.*

Jun 98. *Perform overall system evaluations.*

Jun 98. *Complete Concept Exploration and Definition phase.*

Sep 98. *Complete the Preliminary Design phase.*

Sep 98. *Order subsystem components which require long lead times.*

Dec 98. *Complete Detailed Design phase. Order remaining components.*

Feb 99. *Complete system integration; perform system test and evaluation.*

Mar 99. *Present final system design and associated documentation.*

2.2.9 Value System Design. At this stage of the design lifecycle, it was not considered productive to identify specific measurables within the value system to compare alternative solutions against. Because the classes of solutions may be very different, the solutions might not compare directly using detailed objective measurables. In addition, the top-level nature of solutions at this stage makes direct estimation of quantitative measurables difficult, if not impossible. Instead, the value system at this stage should provide a framework wherein each broad solution can be considered. If the value system without specific measurables allows differentiation of these solutions, then it serves the purpose of identifying the most promising class or classes of solutions at this stage. If no significant differentiation can be made between solution classes, further refinement of the value system design may be required, to include more specific measurables.

The primary system objectives were identified as cost minimization, performance maximization, and safety maximization. The top-level objective hierarchy is illustrated in Figure 2.2. Each objective is defined to allow a consistent and informative application of the value system against all potential solutions. The definitions which follow explain the intent of each objective within the value system at this level.

- **Total Cost.** System cost to bring the system on-line; consider the purchase and integration costs.

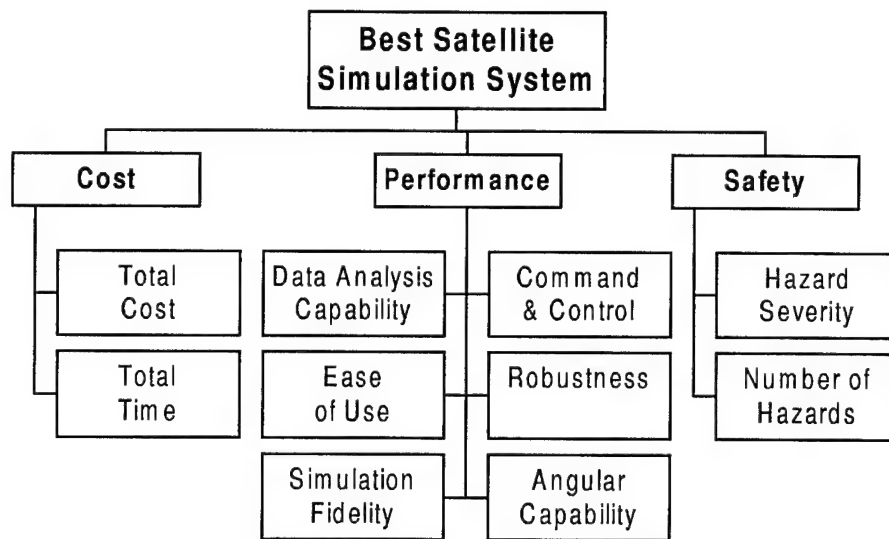


Figure 2.2 Initial Value System Design (VSD)

- *Total Time.* Total timeframe to bring the system on-line; consider the purchase and integration time requirements.
- *Data Capability.* Consider both data which can be displayed real-time, as well as the post-experiment data analysis capability.
- *Ease of Use.* Consider the user interface and how easy it is to switch components/experiments on the model.
- *Simulation Fidelity.* Consider how well a computer simulation model could represent the physical model's behavior, and consider how easy it is to develop the simulation model.
- *Command and Control.* Consider how well the system does what is desired, how responsive it is, and how autonomous it is.
- *Robustness.* Consider the range of experiments the system can support.

- *Angular Capability.* Consider the system's ability to move rapidly (high slew rate) to the desired position (high sensing accuracy) and stabilize.
- *Hazard Severity.* Estimate the system hazard severity in terms of potential damage to equipment or injury to personnel.
- *Number of Hazards.* Estimate the total number of significant hazards inherent to the system.

2.2.10 System Architecture Development. Using the problem elements discussed in Section 2.2.6, an initial system architecture was developed to meet the needs of the system and provide a basis for system synthesis (generation of alternatives). The initial system architecture also allowed identification of the system boundary and environment, and resulted in the system context diagram shown in Figure 2.3.

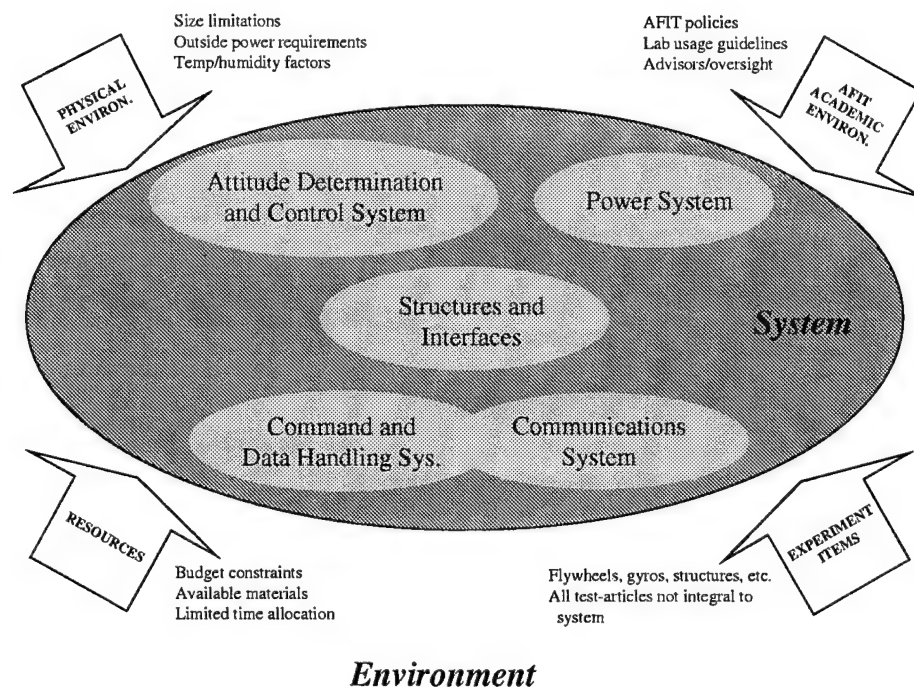


Figure 2.3 System and Environment Context Diagram

2.2.11 System Decomposition. The subsystems identified in Figure 2.3 resulted from analysis of the problem elements, and a functional approach to addressing these elements. Initial system decomposition into subsystems took several forms, with the subsystems shown in Figure 2.3 finally chosen as the preferred system decomposition.

A software/hardware breakdown was rejected due to the strong interdependencies of computer software and hardware solutions. Furthermore, this breakdown did not aid in development of solution alternatives since the specific problem elements are not addressed using this format. Similarly, a ground station/satellite breakdown was also rejected since functional divisions were overridden by physical divisions in this decomposition.

As stated above, the system decomposition of Figure 2.3 is based on functional breakdown, and was modeled after the spacecraft subsystem breakdown used in the Space Mission Analysis and Design (SMAD) textbook by Larsen and Wertz [33:287]. The "Guidance, Navigation, and Control" function identified in the SMAD text was ignored since the simulator model is fixed in the laboratory. Thus, guidance and navigation represent attitude positioning only, which is handled by the "Attitude Determination and Control System" (ADACS). The thermal subsystem identified by SMAD was eliminated from initial consideration as a separate subsystem because operating conditions were not expected to require dedicated thermal elements. If system operation required cooling of components, later stages of development could address environmental control mechanisms. The other subsystem divisions are very similar to the SMAD text definitions. The following list defines the system decomposition used in the *SIMSAT* design:

ADACS. The ADACS consists of three components: attitude determination equipment, attitude control equipment, and control software. The attitude determination equipment determines the system's actual position/orientation and provides information used to develop inputs for the attitude control mechanisms. The attitude control equipment provides the necessary forces and torques on the system based on information from the user or attitude determination and control software inputs. The control software element consists of software code incorporating control laws which provide the logic used to provide the proper inputs to the attitude control equipment. The ADACS

subsystem addresses the following problem elements identified in Section 2.2.6: "moving the satellite", "predicting satellite behavior", "and representing the behavior of the satellite".

Power System. The power subsystem includes elements associated with the supply, regulation, and distribution of necessary voltages and currents to operate all the onboard subsystems. This subsystem addresses the problem element "powering the satellite".

Command and Data Handling System. The C&DH subsystem receives, decodes, processes, and distributes all satellite commands. Moreover, it gathers, formats, stores, and transmits telemetry data from the onboard systems and experiments, as well as the ground station. This definition of the C&DH system is taken from the SMAD text [33:288]. Within the C&DH is the inherent computer architecture to perform these tasks, addressing the problem elements "commanding the satellite" and "collecting and analyzing satellite telemetry and experimental data".

Communications. The communications subsystem represents the interface between the satellite model and the ground station. The communications system is, in effect, an extension of the C&DH subsystem, linking the simulator C&DH elements with the ground station C&DH elements and thus performing the "communicating with the satellite" function listed in the problem elements. Thus, the communications and C&DH subsystems are shown in Figure 2.3 as slightly overlapped.

Structures and Interfaces. This subsystem represents the physical satellite model assembly, to include subsystem housing, structural supports, fasteners, and physical interfaces between the base model and experimental hardware. Although each subsystem must consider the following problem element, this subsystem addresses "accommodating a variety of experiments" most directly.

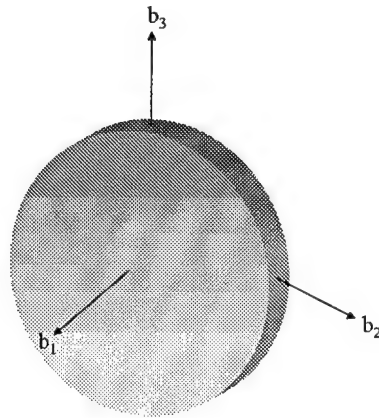
2.2.12 System Synthesis. Once a broad system architecture was conceived, the next task was the identification of feasible solutions through the development

of a list of potential subsystem alternatives, which can be integrated to create feasible system alternatives. These subsystem alternatives were the result of creative brainstorming and research into actual satellite systems, laboratory-based systems, flight test systems, and emerging technologies. Thus, a certain amount of knowledge must be first developed in order to generate solutions. Subsystem alternatives are described in the sections that follow.

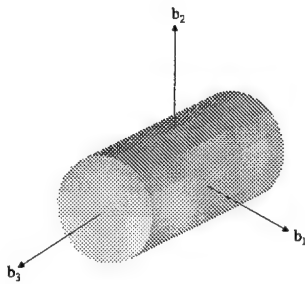
2.2.12.1 ADACS Background. As a first step in the synthesis of ADACS alternatives, further investigation into the methods of satellite stabilization was undertaken. From this point, alternatives can be conceived to apply the necessary stabilization techniques such that the needs of the user are satisfied. This section provides background on the methods of satellite stabilization requested by the user, which precedes the discussion of the various subsystem alternatives considered in this phase.

Spin stabilization generally involves a torque-free, axisymmetric body whose spinning motion about a given principal axis prevents small, external torques from perturbing the satellite's motion. "Axisymmetric" is defined as having two principal moments of inertia being equal. A general rigid body has three principle moments of inertia which are oriented about the body's principal axes. In Figure 2.4(a), the first moment of inertia, A, is oriented along the b1 axis. The second moment of inertia, B, rests along the b2 axis, and C rests along the b3 axis. In this case, A is the "major axis" of inertia (greatest moment of inertia).

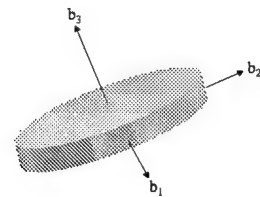
As requested by the customer, *SIMSAT* should provide examples of both prolate and oblate spinners. Prolate bodies, best described as cigar-shaped objects, have two identical moments of inertia with a third, smaller moment of inertia, as shown in Figure 2.4(b). With a prolate spinner, the satellite rotates about the b3 axis. Since this axis has the smallest moment of inertia, the body is said to spin about its minor axis. However, a body spinning about its minor inertia axis is naturally stable only in the case of a completely rigid body, which is not generally achievable in practice. Therefore, remaining stable with a prolate configuration requires the use of aggressive attitude control to maintain a constant angular velocity.



(a) Moments of Inertia



(b) A Prolate Body



(c) An Oblate Body

Figure 2.4 Satellite Inertia and Stabilization Concepts

An oblate body, the proverbial “tuna can” geometry, has a third moment of inertia which is larger than the other two moments of inertia. From Figure 2.4(c), the b_3 axis is the major inertia axis. Therefore, an oblate body spinning about the b_3 axis in a stable mode requires fewer, if any, attitude control inputs to maintain stability.

Dual spin stability involves two sections of a satellite which rotate relative to one another. The first (usually larger) section, the rotor, rotates at an angular velocity ω_r to maintain stability for the satellite. The second portion, the platform, rotates at a different rate ω_p . In this way, the platform section can be maintained at a constant orientation relative to the ground to maintain a constant pointing attitude for the payload⁴. Figure 2.5 illustrates the dual spin configuration.

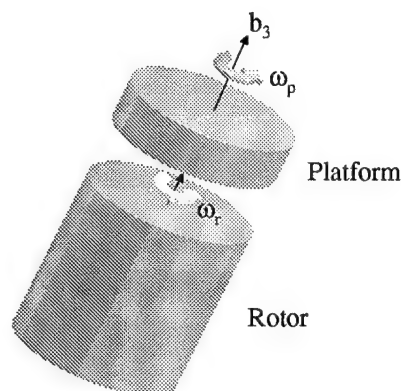


Figure 2.5 Dual Spin Configuration

Three axis stabilization is the most widely used method on modern day satellites. This stabilization technique requires the capability to produce torques in each axis using active control. Usually, an inertial platform is maintained onboard using a combination of software logic and hardware actuation systems. Compared to the previous two stabilization

⁴For example, this technique can be used to accommodate a communications link with degraded omnidirectional performance.

methods, three axis stabilization requires a greater combination of components. This method often utilizes determination and control hardware redundancy to ensure pointing accuracy.

2.2.12.2 ADACS - Attitude Determination. Having discussed the three types of stability which are necessary for the *SIMSAT* system, the next endeavor involved brainstorming ideas for attitude determination and attitude control components. For the attitude determination alternatives, there are two major classes of systems available for *SIMSAT*- passive and active. Passive systems are divided into inertial measurement units and IR/optical sensors. They are considered passive mechanisms since they detect changes through observation. Alternatively, active mechanisms emit energy to measure differences in position. Active systems include radio interferometers and laser grids. The following list summarizes the attitude determination alternatives conceived in this phase and identifies some of the feasibility considerations associated with their use:

Inertial Measurement Units. Inertial measurement units (IMUs) measure rotational motion through the use of gyroscopes (mechanically gimbaled systems) or high resolution software (strap down units). The IMU is first set to a zero point. Afterwards, whenever the satellite's orientation changes, the IMU measures its deflection from the initial point to determine by how much the orientation has changed. The main concern with IMUs is determining the drift rate of the sensors. For extended experiments, the drift rate could cause readings to be inaccurate. Typical drift rates are $0.005^\circ/\text{hr}$ and $3^\circ/\text{hr}$ [33:360].

Sun Sensor. Sun sensors are visible light detectors which are used to measure the relative angles between its mounting plate and incident sunlight. For the system design, this option involves mounting an external light source within the laboratory which acts as an artificial sun. The typical pointing accuracy for this option is between 0.005° and 3° [33:360].

Star Sensor. Star sensors use a variety of methods to determine vehicle attitude using the relative positions of stars. Based on fixed pointing accuracy,

the best candidate for the system design involves using a star tracker which "uses a wide field of view, scanning electronically until it locates and tracks a star of predetermined brightness." [33:361]. Following successful acquisition and tracking, any change in the apparent position of the star within the field of view corresponds to a change in vehicle orientation. Similar to the tracker, the star mapper uses several stars in its field of view. The typical attitude accuracy for this option is between 0.0003° and 0.01° [33:360]. An artificial "star" constellation within the laboratory would be required.

Horizon Sensor. Horizon sensors are infrared devices used by satellites which detect the "hot" surface of the earth compared to the "cold" vacuum of space. The system uses clear fields of view with various scan widths to determine its position relative to the body being scanned. For this design, a heated body in a fixed location within the design room would act as the Earth's surface. Typical accuracy for this alternative is between 0.1° and 1° [33:360].

Magnetometers. Magnetometers are used to measure the direction and size of the earth's magnetic field to determine satellite attitude and position. Attitude accuracy is between 0.5° and 3° . For *SIMSAT*, a contained, variable magnetic field would be needed for the magnetometers to monitor.

Radio Interferometers. Radio interferometers are used for distance determinations of celestial bodies in astronomical applications. Two parabolic dishes are set a fixed distance apart; returning radio waves are recorded with an amount of interference between them. The interference pattern is analyzed by software and determines the distance between the dish array and the emitting body.

Laser Grid. Use of an external laser, in conjunction with a finely etched grid upon the satellite assembly, could potentially allow position information to be calculated based on the number of grid lines which pass through the laser focus. This idea, borrowed from laser Doppler velocimetry techniques, was innovative but unproven.

2.2.12.3 ADACS - Attitude Control. For the attitude control components of ADACS, there are three major solution classes - momentum exchange systems, mass expulsion systems, and other external systems. These classes are discussed below:

Momentum Exchange Methods. *Reaction wheels* are essentially "high torque motors with high-inertia rotors." [33:352]. In cases where the satellite is disturbed by external forces, the reaction wheels spin in either direction to absorb the momentum imparted on the system. Eventually, the reaction wheels must perform momentum dumps to avoid saturation. It is necessary to have at least three reaction wheels for three-axis control. *Momentum wheels* differ from reaction wheels in that they have a nominal spin rate which provides a constant angular momentum to the system. By providing a constant angular momentum, this method provides "gyroscopic stiffness in two axes, while the motor torque is controlled to precisely point around the third axis." [33:352]. As with the reaction wheels, excess momentum must be dumped from the wheels to prevent saturation. It is also necessary to have at least three wheels for three-axis control. *Control moment gyros* are single or double-gimbaled wheels which spin at a constant speed. High output torques about the three body axes are created by moving about the gimbal axes. Control laws for this system are more complex than with reaction/momentum wheels.

Mass Expulsion Methods. Gas jets and/or thrusters are bipropellant, monopropellant, or cold gas systems which produce torque by expelling mass through a nozzle. The components for this alternative include a storage tank, feed lines, and a nozzle with a control valve.

External Methods. Magnetic torquers use electromagnets or magnetic coils to generate magnetic dipole moments to move a vehicle through an external magnetic field. Satellite applications include compensating for drift associated with minor disturbance torques, compensating for the vehicle's residual magnetic fields, and slowly desaturating momentum exchange systems [33:356]. As another option, external air currents applied by the *SIMSAT* operator to specific locations on the vehicle could be used

for initial spin stabilization. At this point, the attitude control element becomes more art than science.

2.2.12.4 ADACS - Control Laws. The control laws and logic within the software controllers are used to translate data received from the attitude determination components into input commands supplied to the applicable actuation mechanisms. At this point in the concept exploration phase, detailed discussions were not warranted. However, there are three alternatives for system design. First, the design team could have developed control laws using already existing software packages such as MATLAB/SIMULINK or computer code (such as C-code). Second, due to the fact that the system will be used for a variety of experiments, the control laws could be developed by the user. This option would require the system to be compatible with a multitude of software packages with proper interfaces. Finally, the control laws could be developed by a contractor.

2.2.12.5 Power. A primary concern for system operation was the provision for electrical power to various subsystems located onboard the satellite. The use of momentum exchange devices such as momentum wheels or control moment gyros requires substantial amounts of power for motor startup, changing torque outputs, and inherent frictional losses. Additionally, communication, C&DH, and other onboard subsystems require power for system operation.

During this phase of design, several methods of onboard energy production and storage were considered. A wide variety of potential energy sources were brainstormed, although most were deemed infeasible upon review. Potential energy sources included photovoltaic cells, fuel cells, thermal batteries, and chemical batteries. Other possible methods of energy production, such as directed energy transmission, radio-isotopic decay, or internal combustion, were immediately deemed unacceptable due to cost, weight, or safety considerations.

2.2.12.6 C&DH . The C&DH subsystem has two main purposes: interface with the user and, as required, execute the actual control laws determining how the effectors (devices that cause something to happen) are activated to respond to com-

mands. Theoretically, the control system could be as simple as a direct connection between the user controls and the effectors (similar to the mechanical control systems of early aircraft). Because this approach creates a tremendous workload for the operator, engineers have tried to find ways to improve the design of control systems. To determine the best C&DH design concept, some point solutions in the spectrum from simple, direct control systems to sophisticated computer control systems were considered. All these alternatives assume the other *SIMSAT* subsystems (ADACS, power, communications, and structures) will be sufficiently designed to allow for full subsystem capability. The C&DH subsystem technology alternatives include the following classes:

Direct Control. The direct, unassisted control option consisted of a user interface comprised of knobs, levers, switches, dials, display panels, and/or lights. The commands (from the knobs, levers, and/or switches) would be converted to a format that could be transmitted to the satellite, where they would be converted back to a format required by the effectors. The results of those commands would be sensed, converted to the transmission format, and then sent to the ground station where it would be converted to a format consistent with the dials, display panels, and/or lights. This functionality would require substantial research to locate compatible components, integrate them, and troubleshoot the system should problems arise.

Analog Control. The analog computer-assisted control option consisted of a user interface very similar to the "direct" system above. Control law implementation/adaptation would be handled by changing individual components. Before the recent advancements in digital computer hardware and software, analog computers were considered the preferred solution for real-time control due to reduced execution delay. Analog control box designs provide some flexibility by allowing "building block"-type implementations (reducing the likelihood of component incompatibilities), reducing research, implementation, and troubleshooting time. However, analog computer technology is not as well understood or supportable as digital technology.

Digital Control (Text). The digital computer-assisted control option was based on a command-line (or "text") user interface. Control law implementation and modification would be handled by well-defined software packages available for a number of different hardware platforms. Integrated subsystem implementation is similar to the analog computer approach, but more "building block" components are available. Expertise in these systems is more readily available as well.

Digital Control (Graphical). This solution class consisted of a digital computer-assisted control system, with a visual/graphically-based user interface. All the design advantages of the above classes of technologies exist with the added intuitiveness of the graphical development environment. Using the integrated hardware/software solution provided by dSPACE, Inc.⁵, reduces the testing and troubleshooting. Substantial in-house and proximate technical support exists for this system.

2.2.12.7 Communications. As stated previously, the communications subsystem provides the data link between the ground station and the satellite. Alternatives were generated by researching the data transfer systems used in satellite operations, flight test operations, and computer networks. These applications require wireless solutions, consistent with the needs of the *SIMSAT* design. The following list describes the classes of communication alternatives:

Flight Test Telemetry Systems. Flight test telemetry systems are used in many aircraft and missile testing applications. A typical setup includes a data bus monitoring unit to collect vehicle data, a multiplexer to format data for transmission, a transmitter antenna (typically S-band), a receiver unit to receive commands, and a decoder unit to interpret commands (sometimes integrated with the receivers). This type of system can be tailored to the problem at hand, but is mostly designed for long-range data transmission in open-air environments (unlike a laboratory). Figure 2.6 shows a typical flight test telemetry system schematic.

⁵A graphics-based data handling system developed by dSPACE, Inc., of Germany was already purchased for possible use in this project prior to actual system design. However, implementation of the dSPACE system was left as an option for the design team to consider.

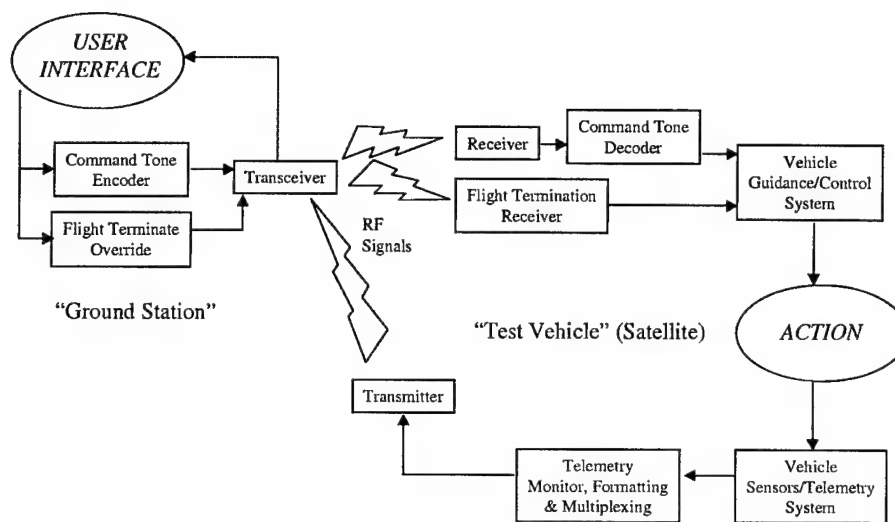


Figure 2.6 Flight Test Telemetry System Schematic

Satellite Relays. Also used in flight test applications, as well as many wireless telecommunication systems, satellite relay systems use existing satellites to link one user to another, such as a ground station to a test vehicle. These commercially-available solutions are impractical for a laboratory environment in which data transmission lengths are only several feet. Thus, this solution class was determined to be unrealistic prior to more formal analysis and modeling.

Wireless Modems. Wireless modem systems have been used in industrial applications for some time now. They are used in many radio control applications, ranging from remote sensing and control to telemetry data collection. The primary drawback of a wireless modem solution is the low data rates achievable using current technology.

Wireless Local Area Network (LAN). Wireless LANs are increasing in popularity and application. A wireless LAN system allows computers to network to each other via wireless technologies (typically IR/RF transmitters/receivers). Inherent in the wireless LAN concept is the need for a ground station computer as well as a sophisticated computer architecture onboard the satellite.

2.2.12.8 Structures. At this stage in the design, the structural configuration of the satellite was not well developed. Thus, the generation of different structural solutions was not practical at this point. For the most part, the structure of the satellite was driven by the choice of subsystems, the expertise of the fabrication shop, and stability/slewing requirements.

2.2.12.9 Subsystem Alternatives. The list of *SIMSAT* subsystem alternatives is summarized in Table 2.1. These subsystems represented the system synthesis step in the Concept Exploration and Definition phase.

2.3 Analysis

2.3.1 Analysis Methodology. A primary task of the Concept Exploration and Definition phase was to eliminate those subsystem alternatives which were determined to be infeasible, impractical, or relatively inferior to other alternatives. "Mental modeling" was the primary method for analyzing subsystem alternatives during this phase. Mental modeling relies on expert opinion, personal experience, research, and common sense rather than on sophisticated models or rigorous mathematical analysis. Mental modeling was an efficient tool for making a top level "first cut" between feasible and infeasible alternatives. In order to augment this mental modeling, the SMAD text was often used as a source for expert opinion or rudimentary math calculations. The following paragraphs document the mental modeling used to select a set of feasible solution classes through elimination of impractical alternatives.

2.3.2 Attitude Determination and Control. The main requirements for the system which pertain to ADACS were pointing accuracy, highest achievable slew

Table 2.1 Concept Exploration and Definition Subsystem Alternatives

Subsystem	Alternatives
Attitude Determination	IMUs Sun/Star/Horizon Sensors Magnetometers Radio Interferometers Laser Grid
Attitude Control	Momentum Exchange Mass Expulsion External Forces
Power Generation & Distribution	Photovoltaic Cells Fuel Cells Thermal Batteries Chemical Batteries
Command & Data Handling	Direct Control Analog Computer Digital Computer (Text) Digital Computer (Graphical)
Communications	Flight Test Telemetry Wireless Modem Wireless LAN
Structures	As Required

rate, and the capability to perform pure spin, dual spin, and three axis stabilization. During follow-on interviews with the customer, a pointing accuracy of 0.005° and slew rate minimum of $10^\circ/\text{sec}$ were identified as system requirements. Quantitative requirements at this stage were necessary in order to differentiate between solution classes, exemplifying the iterative nature of the systems engineering process.

Passive attitude determination methods via sun sensors, star sensors, horizon sensors, and magnetometers were eliminated from further consideration, as they did not meet these specifications in practical application. The sun and star sensors, although capable of meeting the pointing accuracy requirement, necessitated the design of an artificial star field or point light source within the laboratory, and would be of limited use for high slew maneuvers. Horizon sensors and magnetometers did not meet pointing and accuracy requirements, and would also be less precise during high slew maneuvers.

Instead of developing an in-house sun/star sensor system, the choice of IMUs for attitude determination allowed use of commercial off-the-shelf hardware. Since the use of IMUs is fairly standard for attitude determination systems, their choice allowed for confidence in achieving the pointing and attitude accuracy requirements.

Active attitude determination methods via radio interferometers/Doppler shift measurement or laser grid tracking were determined to be impractical. Again, these methods did not meet the pointing accuracy requirement and/or they required extensive manipulation of the environment. The use of the laser grid system also required expensive laser components and undesirable machining of the air bearing assembly.

For attitude control, the use of magnetic torquers or external air currents required extreme sophistication to meet the pointing accuracy requirement or the $10^\circ/\text{sec}$ slew rate requirement, and thus they were judged to be impractical. The use of momentum exchange methods, such as control-moment gyros (CMGs) or momentum wheels, appeared to meet the ADACS requirements. Mass expulsion methods, such as gas jets, were deemed to be impractical for fine attitude control due to the pointing accuracy required. However, this option had practical value as a secondary means to achieve higher slew rates or to dump momentum. Depending on the capacity/capability of a momentum exchange system, thrusters were considered to be of future value.

In summary, the general ADACS solution classes under consideration following Concept Exploration and Definition were IMUs for attitude determination and momentum exchange (with mass expulsion as necessary) for attitude control. Specific decisions on the software control laws were not made at this level.

2.3.3 Power. Microwave transmission and radio-isotopic power sources were eliminated because of safety risks. Fuel cells were also eliminated because of safety concerns related to their use of flammable and explosive materials. The use of a momentum wheel's kinetic energy as a power source was considered during analysis. This alternative could perhaps be explored as a future experiment to be tested on *SIMSAT*, but the idea was deemed too revolutionary to be used as a primary power source.

A photovoltaic power source (solar cell system) was also determined infeasible for *SIMSAT*. In order to analyze the solar cell alternative, a gross estimate of the final *SIMSAT* design was presumed and basic calculations were made. General characteristics for solar cell systems were extracted from SMAD [33:317]. For a *SIMSAT* device requiring 250 Watts of power (constant load), at least 10 kg of system mass would be required for a photovoltaic array. More importantly, the total surface area required to produce 250 Watts is between 2.5 and 10 square meters depending upon assumptions regarding the ambient lighting present in the experimental setup area. This large area requirement exceeds the reasonable bounds for *SIMSAT* overall size.

Although solar power is the preferred option in many space applications due to mission lifetime and relatively low power requirements, the need for *SIMSAT* to operate at high power levels for short experiment times suggests the use of chemical energy storage. In comparison to solar cells, a power system capable of providing 250 watts (constant load) for thirty minutes using nickel-cadmium batteries would require between 2.5 to 5.5 kg of system mass with significantly less volume. Based upon this top-level analysis, chemical batteries appeared to be a reasonable and effective power source, and they do not require extensive external lighting. The use of thermal batteries was less attractive than chemical batteries for two primary reasons: they generate intense heat, and they are non-rechargeable.

2.3.4 Command and Data Handling. ADACS, power, and communications subsystems were all dependent on the choice of C&DH architecture. Thus, an early choice for the C&DH architecture was critical to the overall system architecture. The VSD in Figure 2.2 represents the first step in conceptualizing what values were a part of the overall attempt to satisfy the customer. At this level of design abstraction, there was no point in determining the quantitative characteristics of each C&DH alternative – they have not been fully defined at this stage, making it impossible to establish actual measures of merit.

The qualitative assessment of the ability of each class of C&DH solutions to satisfy the objectives is discussed at length in the AFIT Master's thesis of Mr. Mike Hanke [26],

who worked in close cooperation with the design team throughout the design process. Mr. Hanke's thesis focused on the decisions regarding the C&DH subsystem and its initial development and integration. His work is considered a companion study to the *SIMSAT* design. The following paragraphs highlight the evaluation of each C&DH subsystem alternative against the values specified in the VSD.

Total Cost. While the direct control solution would have used simple components, the sunk costs of the dSPACE system meant the visual, digital computer solution can directly compete with the direct control solution. The analog computer solution was expected to be the most expensive due to the specialized nature of the technology. The digital (text) solution was moderately priced because the equivalent of the dSPACE hardware and software would have to be purchased; they are common, commercial off-the-shelf components, however.

Total Time. The digital solution was considered the best in this category because the parts were readily available and would take less time to arrive and be integrated into the system. The dSPACE system (graphical) required the least amount of time since most of the parts were already on hand at AFIT. The direct control solution was expected to take about as long as the digital (text) solution because both would require part selections, orders, and integration troubleshooting. The analog computer implementation would take the longest because it is unique, the order time would be considerable, and the integration would be difficult because of limited in-house expertise available for troubleshooting.

Number of Hazards. The digital computer solutions were ranked the highest because the assumption was that much of the implementation would be based upon previously tested "building block" solutions. Also, there are numerous sources for all components of a digital computer subsystem. This situation was not the case for the other technologies: the direct system would be nearly entirely fabricated at AFIT and would not be as "tight" as mass-produced commercial component solutions. The analog computer solution would have more commercial "building blocks" in its design, but would require

more fabricated portions than the digital systems. In-house fabrication could increase the potential for unforeseen hazards.

Hazard Severity. This category follows the same logic as the number of hazards – the more commercial building blocks used, the fewer things that can fail and the less severe the potential system failures.

Data Capability. The digital solutions assume the data can be viewed real-time and collected directly on the computer hard drive or use typical lab-quality data acquisition systems. The other two alternatives assume a totally independent data-logging system that would allow viewing any “user-friendly” data during the experiment; only oscilloscope traces or strip charts would be available real-time.

Ease of Use. The digital, graphical environment is generally the most intuitive for development and control. Digital computers are the most powerful due to the current tools available to users. Again, lack of expertise in analog computers would make system or payload changes a significant challenge; the possible user interfaces are likely to be similar to what can be used with the digital (text or graphical) class of alternatives. The interface and adaptation of the direct control would be the least favorable – the user would have to re-learn how to handle the system every time some change was made.

Simulation Fidelity. Obviously, the direct control system has no simulation capability in and of itself. How an analog computer-assisted system could be simulated (or how good the simulation would be) was unclear, but due to the lack of internal expertise, the difficulty of developing such a capability would be great. Digital simulations are well understood and supported with numerous software tools. A visual environment would make it easiest to build the model. Since dSPACE is an “integrated solution”, it would provide the highest fidelity model.

Command & Control. Any human-in-the-loop control system (i.e., the direct control system) is very difficult to deal with, and its responsiveness would be

user-dependent. The digital control systems allow the *SIMSAT* to perform commands easier (and convert to an autonomous system) due to the maturity and availability of development tools and supporting hardware. The dSPACE solution was determined to be best for command and control due to the integrated nature of the hardware and software.

Robustness. Scores in this category are correlated to the command and control measure. Again, graphical digital solutions appeared to handle the widest range of possible applications.

Angular Capability. Each technology has similar angular capabilities and scored the same. However, each technology has different drawbacks. The direct solution suffers from the requirement of the operator to know how to operate the controls to cause *SIMSAT* to move "fast" and stop "fast", then stay "on target." The computer solutions all suffer from the added weight and moment of inertia caused by onboard computer accessories.

2.3.5 Communications. Top-level investigation of wireless data transfer methods indicated that the wireless LAN option could achieve the necessary data transfer rates required by the *SIMSAT* design. Several vendors offered wireless LAN systems with advertised data rates up to 10Mbps for Ethernet and non-Ethernet connections, and even greater data rates for FastEthernet (or similar) solutions.

System modeling of the flight test telemetry system alternative was based on missile flight test systems, since these systems also require compact, lightweight components. Because these telemetry systems are generally designed for range applications; the transmission power, data rates, and environmental protection (such as "high-g" shock-proofing) were overdesigned for the *SIMSAT* laboratory environment. Furthermore, significant RF concerns existed with these alternatives since broadcast of such high-frequency data (typically UHF) in the laboratory environment at higher transmission powers could potentially cause interference with other electronic equipment, as well as endanger humans in the vicinity of the system. System evaluations for the flight test telemetry systems were based

on a baseline Aydin Vector ⁶ missile telemetry system [4]. The following paragraphs use the values identified in Section 2.2.9 to compare the flight test telemetry alternative to the wireless LAN alternative.

Total Cost. An integrated flight test telemetry system generally requires the use of a command encoder, command decoder, dual transmitters and receivers (or transceivers), telemetry bus monitoring equipment, and data formatting equipment. A typical system is generally in excess of \$10,000 as a minimum. These increased costs are due to the number of components, and the environmental protection necessary for range applications ⁷. Wireless LANs are relatively inexpensive, priced from \$400 to \$3000 depending on the network configuration and selected vendor.

Total Time. Wireless LANs are commercially available and built to "plug-and-play". Assuming a network-compatible data collection and formatting system is in place, the wireless LAN will not require the extensive integration efforts typical of a flight test telemetry system.

Number of Hazards. Typical operating voltages for a wireless LAN system are approximately 5V, with transmission powers on the order of 50mW. Conversely, the flight test systems are built to the aerospace standard of 28V, and incorporate transmission powers from 2W to 10W for range applications. The higher voltages and output powers of the flight test systems make them a more hazardous alternative.

Hazard Severity. Prolonged exposure to transmission powers in the 2W to 10W range may be dangerous for laboratory personnel, and are more likely to cause interference with other electronic laboratory equipment. Permission to use such systems may be difficult to obtain from the 88th Wing at Wright-Patterson AFB.

⁶Aydin Vector is one of four divisions of the Aydin Corporation, specializing in flight test instrumentation for the aerospace industry. Aydin Vector telemetry systems have been used extensively in missile flight test applications, to include the Sidewinder, Sparrow, AMRAAM, Air-Launched Cruise Missile, and Advanced Cruise Missile.

⁷Components are generally built to withstand 100-g shocks. These extremes will not be approached in the SIMSAT design.

Data Capability. The flight test systems have a robust data capability, and are designed for high data transfer rates. However, the digital, graphical control solution (such as dSPACE), generally requires a 10Mbps data rate, so that higher data rates provide no real performance advantage. Thus, the wireless LAN solution satisfies data requirements equally.

Ease of Use. Neither alternative appeared to have significant advantages in this category.

Simulation Fidelity. Again, neither alternative appeared to have significant advantages in this category.

Command & Control. A flight test vehicle is typically designed to operate under its own guidance and control system. Therefore, flight test telemetry systems use only a few commands to override this control; generally 20 command tones may be paired and transmitted to issue commands. These commands correspond to preset responses built into the vehicle software ⁸. The wireless LAN solution, coupled with the C&DH digital control, allows greater command and control flexibility by permitting the issuance of specific commands that need not be built into the onboard software.

Robustness. Scores in this category are correlated to the command and control measure. Again, a wireless LAN/digital control solution allows greater experimental flexibility.

Angular Capability. Neither solution appeared to have a marked effect on angular capability relative to one another.

Research of wireless modems showed that maximum data rates of 9600 bps are the typical industry standard at this time. This data rate would severely limit the real-time

⁸For example, a 10/13 tone pair may correspond to the command *Roll Clockwise*, wherein the satellite would perform a predetermined roll until a subsequent command is issued. The ability to roll at an arbitrary angular velocity or to an arbitrary angular position is not present.

data transfer between the ground station and the satellite. However, retention of the wireless modem alternative was practical since the possibility of a separate data link for remote control/spindown may be required in more detailed design. Furthermore, the dSPACE C&DH system, a digital computer with graphical interface, may require two data links, one for command/telemetry data and one for visualization of satellite motion (which may allow use of a wireless modem for this secondary data transfer).

2.3.6 Structures. At this stage of the design, no formal analysis into the structural support of the satellite subsystems was undertaken. However, the need to minimize the overall moment of inertia about body axes was recognized as a clear structural design goal. Moment of inertia is closely related to system torque requirements and satellite slewing performance. Once subsystem alternatives were chosen for further design, analysis of the structural configuration of the satellite would begin.

2.4 Interpretation

2.4.1 General. The Concept Exploration and Definition phase made several significant steps towards the design of an up-and-running satellite simulation system. The problem was refined, with an initial list of needs and top-level requirements generated. A top-level value system, complete with value hierarchy, was developed. The overall system architecture was framed, with potential subsystem classes considered and explored. Finally, these alternatives were compared and analyzed, with decisions made for each subsystem before progressing into the Preliminary Design phase.

2.4.2 Alternatives Summary. In general, only the C&DH setup significantly affected the overall system architecture once the infeasible and impractical subsystem alternatives were removed. As stated previously, choice of C&DH architecture was necessary to advance to the Preliminary Design phase. As the analysis showed, the dominant solution class for the C&DH was the digital computer with graphical interface. This solution was also favorable due to the sunk costs of the dSPACE system purchase.

For the ADACS alternatives, the choice of IMUs for attitude determination was made. Additionally, momentum exchange methods were chosen for further design of the attitude control system. These ADACS alternatives are proven methods and have fewer associated risks in terms of unforeseen problems, such as failure to meet requirements or difficulty in fabrication and integration. The use of gas jets (or other mass expulsion methods) was retained as a possible means for slewing/braking augmentation. However, gas jets alone were determined to be an impractical ADACS solution. The choice of chemical batteries for the power subsystem was also grounded in precedent. Through a range of available types and sizes, chemical batteries allow flexibility in meeting power requirements, quicker integration schedules, and confidence in proper operation.

The use of a wireless LAN/modem architecture was determined based on the use of a digital (graphical) computer C&DH subsystem. As described in Section 2.3.5, the wireless LAN solution dominated the flight test telemetry system for application in this design, thereby removing the choice of flight test telemetry systems from further consideration. The C&DH architecture, namely the use of dSPACE (or similar), suggested the use of a wireless network, and allowed for possible onboard computer processing. An in-depth investigation of onboard versus offboard data processing was left to the Preliminary Design phase.

Regarding the structures subsystem, refinement of the structural configuration was not made at this level of design. Table 2.2 summarizes the results of the Concept Exploration and Definition phase, and sets the stage for the beginning of Preliminary Design.

Table 2.2 Concept Exploration and Definition Subsystems Summary

Subsystem	Design Choice
ADACS	IMUs/Momentum Exchange
Power	Chemical Batteries
C&DH	Digital Computer (Graphical)
Communications	Wireless LAN/Modem
Structures	As Required

III. Preliminary Design

3.1 Overview

In this lifecycle phase, the solution classes identified in Concept Exploration and Definition were further refined. Trade studies, research, and system modeling were used to determine which types of subsystems best met the cost-effectiveness system goals. As the Preliminary Design phase progressed, several significant decision points became obvious before the design could progress into the Detailed Design phase. These decision points included selection of a C&DH architecture, as well as the momentum exchange method for ADACS. From that point, development of control laws, enumeration of communications interfaces, and evaluation of system power requirements could begin in more detail, allowing assessment and consideration of subsystem alternatives. The emphasis on this phase was to identify one solution class within each subsystem; the Detailed Design phase could then evaluate system alternatives using specific choices within each solution class. The waterfall design model in Figure 3.1 highlights the focus of this chapter.

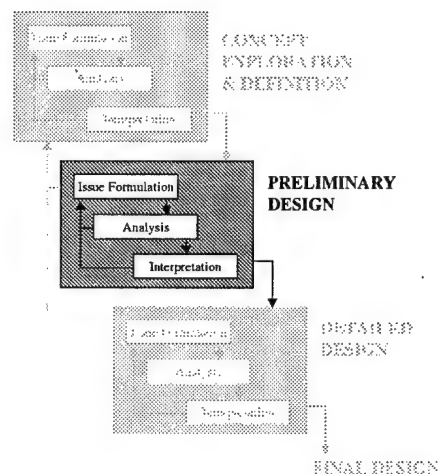


Figure 3.1 Preliminary Design Activity

3.2 Issue Formulation

3.2.1 Problem Statement. The problem statement was refined and narrowed to provide a more specific direction to the Preliminary Design phase. The problem statement was summarized as follows:

Incorporating the system architecture developed in the Concept Exploration and Definition phase, refine the subsystem alternatives within each solution class such that subsystem requirements are identified, subsystem interfaces are recognized, and the system architecture is developed to allow detailed design and system integration in the next phase.

3.2.2 Problem Scope. The output of the Concept Exploration and Definition phase was a general system architecture, to include individual subsystem classes within this architecture, as shown in Table 2.2. The goal of this phase was to determine the best subsystem choice within each subsystem class, and to investigate the subsystem interactions and develop subsystem requirements. As a first step in the accomplishment of these goals, the system architecture developed in Concept Exploration and Definition needed to be enhanced to include subsystem interactions. A determination of the most critical subsystem interactions could then be made. Based on these critical interactions, it could then be determined which subsystem choices had the greatest system impacts. These high-impact decisions could then be made at the system level, followed by determination of other subsystem alternatives as necessary. Decisions which need not, or could not, be made prior to Detailed Design were identified and left to be addressed in the Detailed Design phase. This complete iteration through the Preliminary Design phase was completed by mid-September 1998.

3.2.3 Requirements Refinement. The initial needs identified in the Concept Exploration and Definition phase (see Section 2.2.5) were further defined in this phase, as summarized below:

- System must support experiments of 30-60 minutes duration.
- Frequency of interest for vibration tests is approximately 250Hz.
- Sampling speed should be at least 500Hz (twice the frequency of interest).

- Data handling system should support 32 input and 32 output channels.
- Slew rate should be maximized within safety limits in the three-axis stabilized configuration.
- Nominal operating slew rate is $10^\circ/\text{sec}$.
- Pointing and attitude accuracy error should not exceed 0.005° .
- Payload weight is approximately 100-135 lb.
- Payload location is preferred on one side, with capability to accommodate two-sided experiments with minor adjustments.
- Pure and dual spin configurations are necessary for demonstration purposes only.
- Mass distribution calculations for simulator control laws will be handled by the experimenter, but the system should be user-friendly to accommodate inertial property inputs.
- Emergency shutdown of the system should allow a return to stable configuration before reserve air flow is depleted (approximately 5 minutes).

3.2.4 System Functional Layout. As a starting point in the Preliminary Design phase, the output of the Concept Exploration and Definition phase was summarized and refined. The construction of a concept map assisted in the identification of subsystem interactions, and aided in the framework of a functional layout. Figure 3.2 shows this concept map, including a preliminary delineation of onboard and offboard functions.

From this concept map and the system architecture developed in the Concept Exploration and Definition phase, the functional layout shown in Figure 3.3 and Figure 3.4 was developed. This functional breakdown allowed further insight into the subsystem interactions and flow of data. Implicit in this layout is the location of the controller assembly on the ground computer. Initially, the use of the digital, graphical C&DH subsystem was assumed to include ground processing using dSPACE (or similar) software loaded onto the ground computer. However, additional research revealed that the dSPACE AutoBox DS400 system may provide the capability for onboard processing while still using the

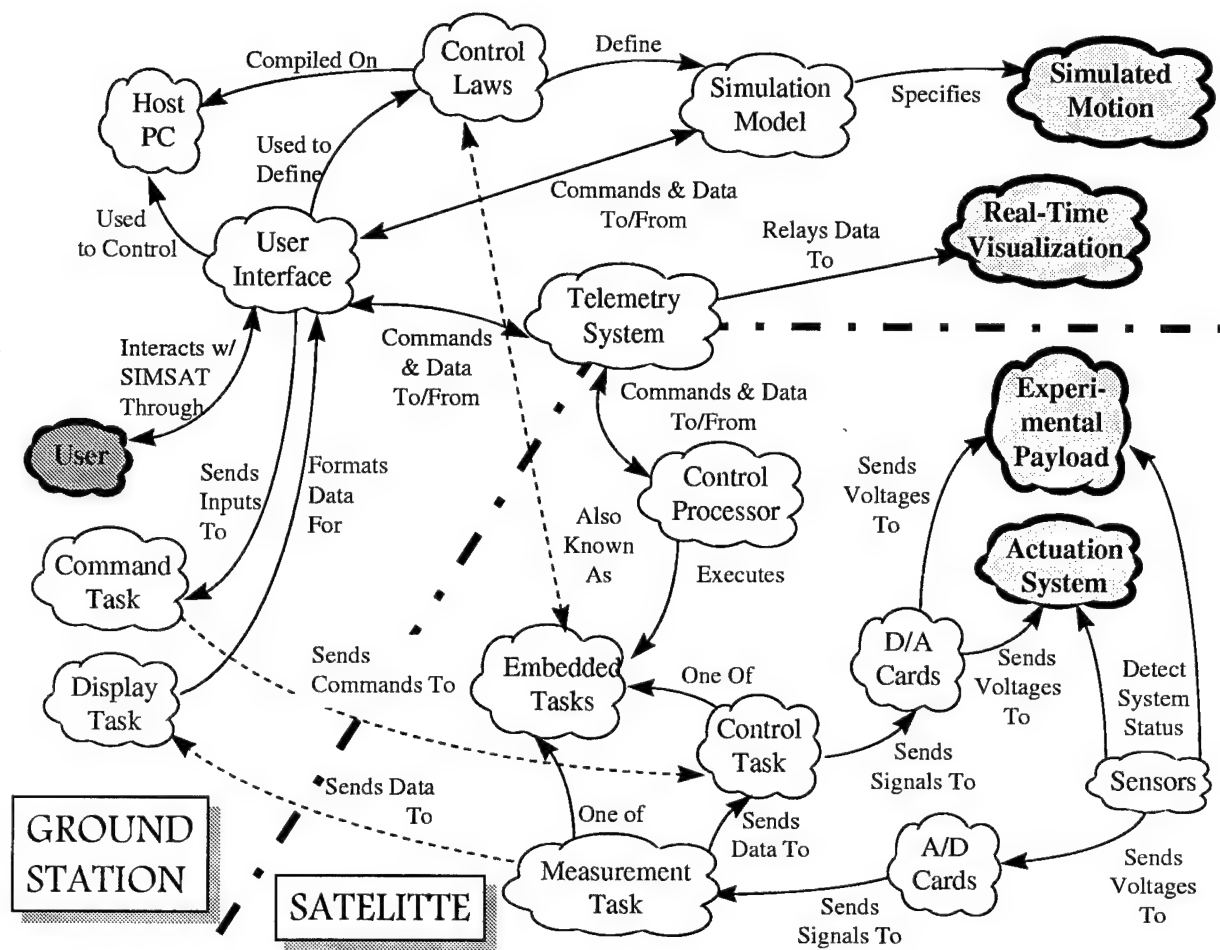


Figure 3.2 Preliminary Design Concept Map [26]

dSPACE graphical interface on the ground computer station¹. Other onboard processing alternatives may also be implemented should another digital, graphical C&DH subsystem have been used in favor of the dSPACE system. Thus, determination of onboard versus offboard processing (or a combination) was identified as an important system architecture decision to be made within this design phase.

¹The AutoBox was initially developed for use in automobile testing applications in a wired configuration with a personal computer loaded with dSPACE software, but was considered for use on *SIMSAT* in a wireless configuration.

“GROUND” FUNCTIONAL LAYOUT

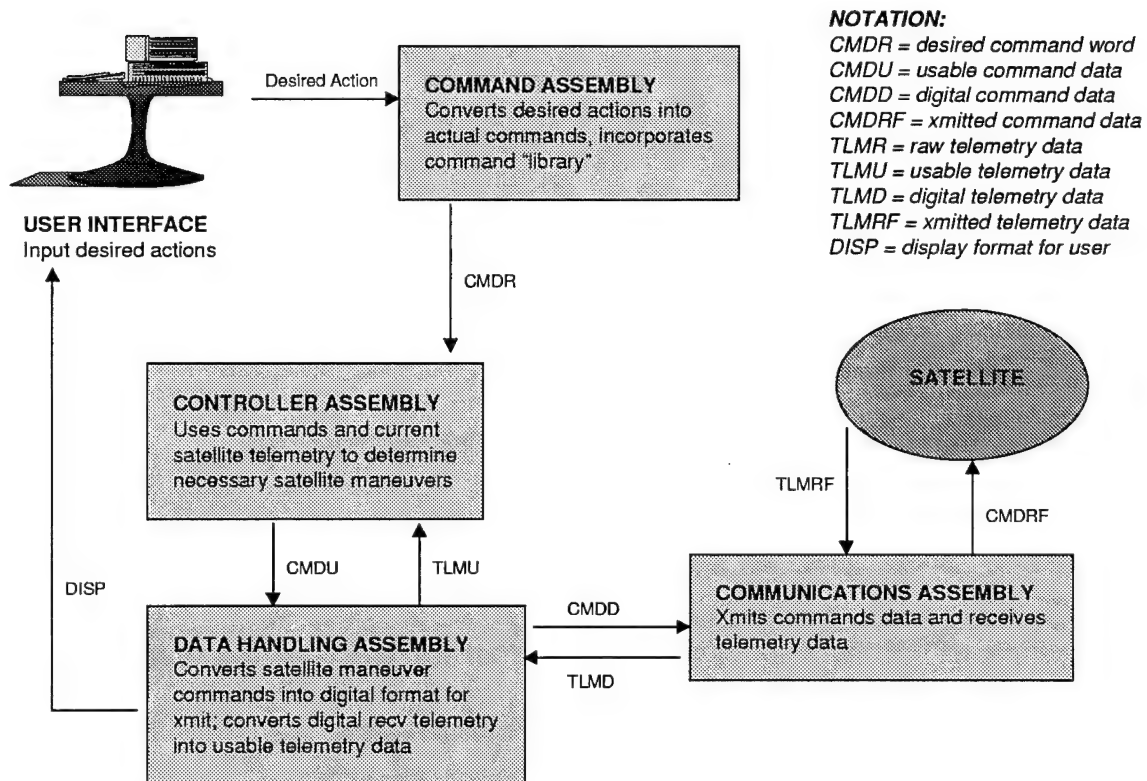


Figure 3.3 Offboard Functional Layout

"SATELLITE" FUNCTIONAL LAYOUT

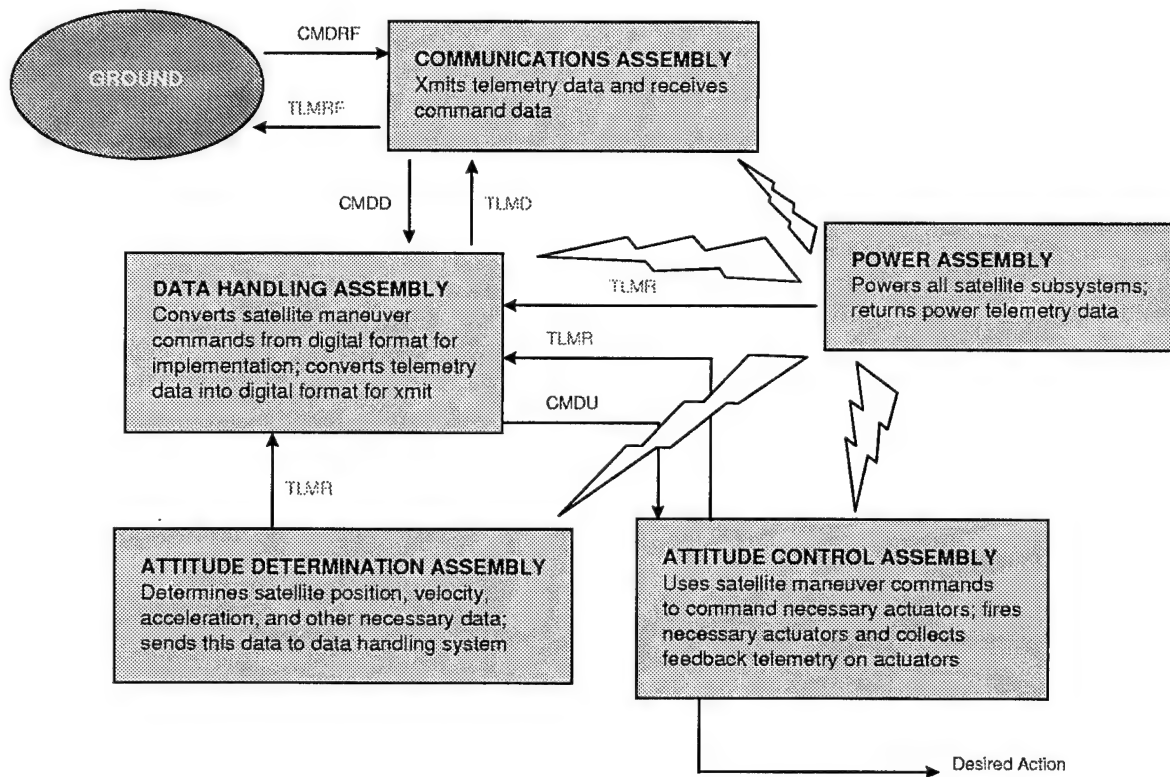


Figure 3.4 Onboard Functional Layout

3.2.5 Preliminary Design Issues. In order to take the design from the Concept Exploration and Definition phase into the Detailed Design phase, key issues needed to be identified and resolved within the Preliminary Design phase. The following system decisions were identified as critical to this stage of design:

- Specification of the digital, graphical C&DH software.
- Resolution of onboard versus offboard data processing and control.
- Selection of a momentum exchange method for the ADACS subsystem.
- Selection of a chemical battery type for the power subsystem.
- Determination of a wireless LAN development effort or commercial-off-the-shelf (COTS) procurement.
- Determination of the wireless transmission frequency ranges.
- Identification of structural considerations.

The following paragraphs describe why these design issues were important at this stage of system development.

3.2.5.1 C&DH Software. The C&DH architecture was a critical subsystem decision for the overall system design. Choice of a C&DH software solution determined the signal interfaces between all other subsystems, as well as the experimental payload. Since the C&DH subsystem is responsible for command entry and control law manipulation, it is also critical in defining the user interface. As stated in Section 2.2.11, the communications subsystem is highly dependent on the C&DH architecture, as it represents the bridge between onboard and offboard C&DH functions and components. Clearly, no subsystem design was immune to the choice of C&DH software. Furthermore, selection of a C&DH software package allowed the initiation of control law software development.

3.2.5.2 Onboard vs. Offboard Processing. The question of onboard versus offboard data processing and simulator control needed to be addressed before detailed subsystem design. In addition to the obvious impact on the communication system, the location of control law processing greatly influences the satellite's physical design.

Onboard processing would include the volumetric and weight penalties of the associated processing hardware, and also increase the power requirements onboard the vehicle. Volumetric and weight penalties not only impact the experimenter's usable payload margin, but also impact the requirements of the ADACS subsystem. Thus, the system architecture is highly dependent on location of the processing hardware, whether that be onboard, offboard, or a combination thereof.

3.2.5.3 Selection of Momentum Exchange Method. As described in Section 2.4.2, the attitude control function was narrowed down to momentum exchange methods in the Concept Exploration and Definition phase. Within the momentum exchange solution class, the CMGs alternative differed considerably from the momentum wheel alternative, therefore a decision between the two was critical to continued system design. Once this decision was made, the development of control laws, identification of ADACS signal specifications, estimation of onboard power requirements, and definition of the physical configuration could be accomplished in the next design phase.

3.2.5.4 Chemical Battery Types. Because some alternatives within the chemical battery solution class fall under strict hazardous material guidelines, identification of a preferred chemical battery type in this design phase would allow lead time to seek and acquire approval for use of hazardous materials as necessary. Furthermore, due to the wide variety of sizes, voltages, and discharge characteristics, the choice of a preferred battery type reduced the solution space and allowed more detailed comparisons in the next design phase.

3.2.5.5 Wireless LAN Design. The use of wireless LAN in the *SIM-SAT* design is a new, and relatively unique, application for wireless LAN technology. A custom-developed wireless LAN system using in-house or commercially-developed wireless technologies may encounter unforeseen challenges and become a significant and protracted design effort in and of itself. Therefore, determination of whether to pursue a custom-developed wireless LAN architecture or instead incorporate a COTS solution was important at this stage of the design.

3.2.5.6 Wireless Frequency Range. Since base approval is required for use of RF technologies on Wright-Patterson AFB, identification of the probable wireless frequency ranges was necessary to begin the process of acquiring this approval.

3.2.5.7 Structural Considerations. At this stage, detailed development of a structural subsystem was not necessary. Based on the other subsystem alternatives, investigation of the structural configuration on a system level could be accomplished within the Detailed Design phase. However, it was important to the continued design to ensure that structural considerations were addressed at this stage such that no critical structural issues were overlooked and the results of the Preliminary Design remained structurally feasible.

3.2.6 Additional Actors. In addition to the actors identified in the Concept Exploration and Definition phase, the following actors were identified as significant at this stage of design:

AFIT Computer Support. This office (AFIT/SC) provided technical support and expertise needed to upgrade, acquire, and install the computers needed to operate the *SIMSAT* system, as well as be used by the team in the design process. Furthermore, AFIT/SC provided the frequency management authority through which wireless communication issues must be coordinated.

AFIT Fabrication Shop. The fabrication shop was needed to discuss structural considerations, momentum wheel designs, and other construction issues. Although production specifications were not a goal of this design phase, the fabrication shop was involved early in the process to ensure that critical design issues were not overlooked.

Laboratory Technicians. The AFIT technicians were also included early in the design process to prevent overlook of critical issues, ensure they were familiarized with background design information, and gain design insights based on their laboratory expertise.

3.2.7 Value System Design. For this level of design, the value system constructed in the Concept Exploration and Definition phase was expanded to include quantitative measurables allowing more detailed system comparisons. The fundamental values identified in the initial VSD – cost, performance, and safety – were retained in this next iteration of the value system, except that the schedule-related measures under the cost heading were placed under the added system objective of schedule minimization. This division allowed cost and schedule to be traded and weighted more independently. Figure 3.5 shows the system-level objectives hierarchy. The fundamental values of cost, schedule, performance, and safety are divided into lower-level evaluation considerations, which are evaluated using associated measurables (also called *metrics*). The 24 metrics are described in the following sections corresponding to the fundamental values. Appendix A describes each metric in further detail.

3.2.7.1 Cost. This value was assessed based on both *Capital Costs* (the costs to get the system up and running) and *Operations and Maintenance (O&M) Costs* (the costs to keep the system up and running). Capital costs were measured in \$, whereas O&M costs were measured in \$/year.

3.2.7.2 Schedule. This value was assessed using the single metric of total delivery weeks. *Total Delivery Weeks* included the time required to order components, build components, deliver components, and integrate components into the system. Detailed testing and evaluation of components (beyond integration testing) was not included in this schedule metric.

3.2.7.3 Safety. Two evaluation considerations were assessed for this value: equipment damage and personnel risk. Equipment damage was quantified using a *Relative Damage Index*, which combined the probability of failures with the estimated damage due to failures. Likewise, personnel risk was quantified using a *Relative Injury Index*, which combined the probability of mishaps with the estimated injury due to mishaps. These indices are described more fully in Appendix A, page A-5.

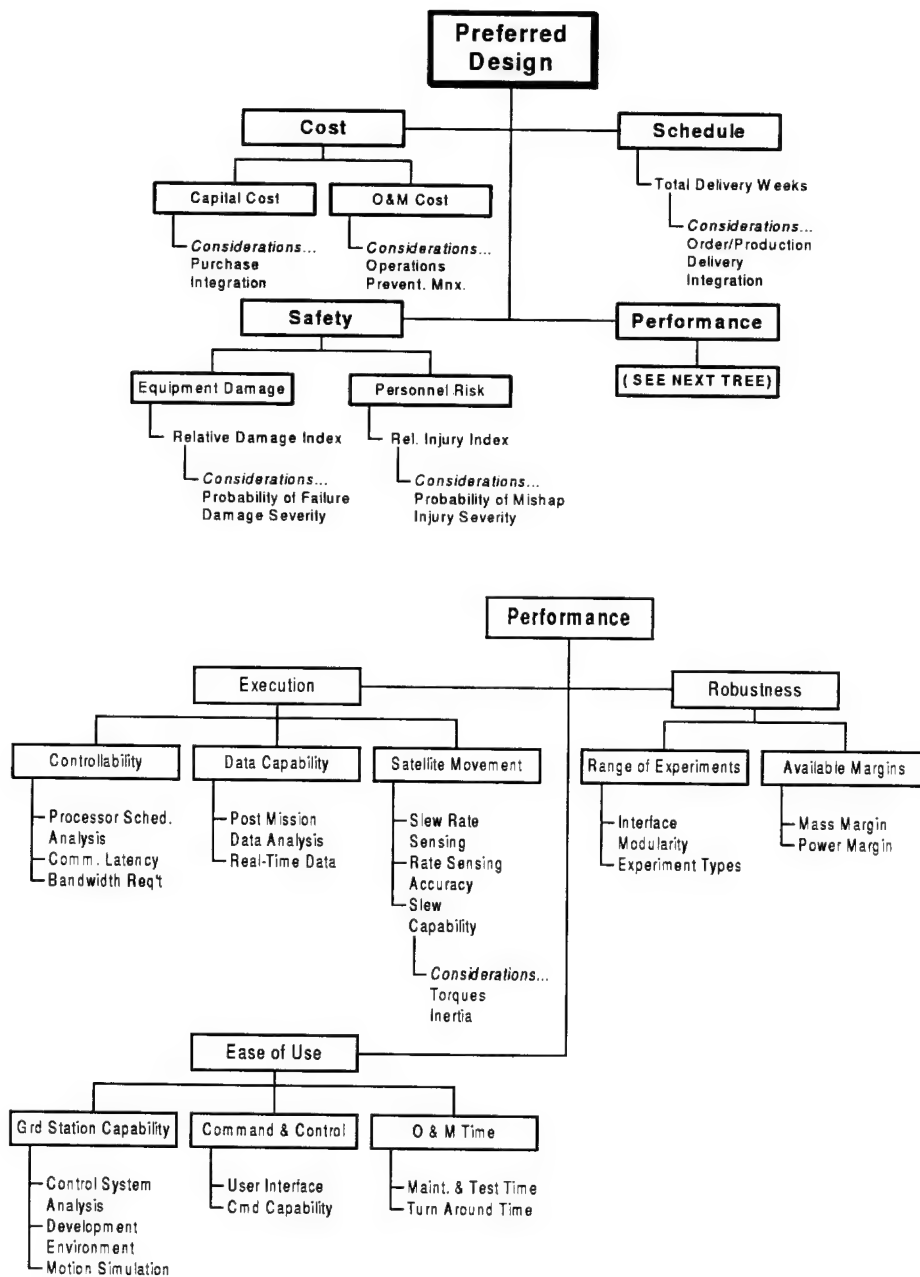


Figure 3.5 Preliminary Design Objectives Hierarchy

3.2.7.4 Performance. This category required the most elaboration in order to quantify all the values important to the overall system performance. The fundamental value of performance was divided into three second-tier values: *Execution*, *Robustness*, and *Ease of Use*. Evaluation considerations and associated measurables for each of these second-tier values are described in the following paragraphs.

Execution. *Execution* refers to the ability of the system to perform an experiment it has been fitted to accommodate. The following list of evaluation considerations and associated measurables was used to assess this value.

- **Controllability.** The communication and control aspects of performance were considered within this category.
 - *Processor Schedulability Analysis.* This measure quantified the support for Rate Monotonic Analysis (RMA) by the system. RMA and other schedulability techniques are described in detail in the companion thesis of Mr. Hanke [26:3-5-3-9]. RMA support was categorized by the following levels: none, unsupported, moderate, or full.
 - *Communications Latency.* This measure quantified the delay from sensor to processor to effector. This delay is the time involved in the gathering of telemetry, processing and transmission of telemetry, execution of control software, transmission of updated commands, and reception of these commands by control elements.
 - *Bandwidth Requirement.* The bandwidth required to maintain communication and control of the satellite was represented by this measure.
- **Data Capability.** Collection and real-time representation of data were considered within this category.
 - *Post-Mission Data Analysis.* This binary (yes/no) measure indicated whether data can be stored for post-mission playback.
 - *Real-Time Data.* This binary (yes/no) measure indicated whether data can be viewed real-time as an experiment is conducted.

- **Satellite Movement.** This category described the system's movement capabilities.

- *Slew Rate Sensing.* This measure referred to the slew rate range of the sensing equipment. Sensors are generally rated to be accurate only within a range of slew rates (for example, an IMU may be designed for accurate operation from $0^\circ/\text{sec}$ to $60^\circ/\text{sec}$).
- *Rate Sensing Accuracy.* The rate accuracy of the system's sensors (measured in deg/sec) was quantified.
- *Slew Capability.* This measure used the torque generation ability and moments of inertia of the system to determine slew capability, which is the degrees (or radians) of slew in a given amount of time.

Robustness. *Robustness* refers to the ability of the system to support a variety of experiments. The following list of evaluation considerations and associated measurables was used to assess this value.

- **Range of Experiments.** The interface capability to perform varied experiments was considered within this category.
 - *Interface Modularity.* This measure quantified the ease of installing and rearranging experimental hardware. This modularity was measured in terms of the percentage of components/subsystems that must be relocated or removed in order to accommodate a baseline experiment.
 - *Experiment Types.* The number of experiment types (requested by the customer) which are supported by the system were quantified by this measure.
- **Available Margins.** The system margins reserved for experiment payloads were considered within this category.
 - *Mass Margin.* The mass margin (measured in kg) is the additional mass the air-bearing/compressor assembly can support after accounting for the mass of the base system. Thus, this measure quantified the maximum payload mass supportable by the system.

- *Power Margin.* The power margin (measured in W) is the excess power provided by the onboard *SIMSAT* power supply after accounting for the base system power requirements. Thus, this measure quantified the maximum payload power consumption supportable by the system.

Ease of Use. *Ease of Use* refers to the ease with which the system can be operated. The following list of evaluation considerations and associated measurables was used to assess this value.

- **Ground Station Capability.** The capabilities and user-friendliness of the “ground station” environment were considered within this category.
 - *Control System Analysis.* This measure assessed the ability of the system to easily implement system changes (due to experimental configuration) and validate system control stability. The percentage of system components defined by the ground station control software (i.e., all control-related properties can be easily entered and evaluated for each component) was used as a quantitative measure.
 - *Development Environment.* This measure assessed the ease of programming system control laws based on the type of programming user interface: text, graphical, or object-oriented.
 - *Motion Simulation.* This binary (yes/no) measure indicated the capability of the system to model and predict satellite behavior before actual operation of an experiment.
- **Command and Control.** The ease with which the system can be controlled during operation was evaluated by this category.
 - *User Interface.* The intuitive nature of the user interface was measured as the percentage of the displays/controls presented in a graphical (visual) manner.

- *Command Capability.* The satellite/experiment activities controllable from the ground station were categorized by this measure as the following: experiment start/stop only, ADACS control, or ADACS and payload control.
- **O&M Time.** This category described the time required to configure, maintain, and alter the system in preparation for operation.
 - *Maintenance and Test Time.* This measure quantified the time required to install an experiment payload and validate the system for operation.
 - *Turn-Around Time.* Assuming an experiment has been installed and tested, the turn-around time between like experiments is quantified by this measure. In general, the turn-around time is reflected by the time spent changing batteries. Thus, the numbers of necessary battery swaps and spare batteries were considered by this measure.

3.2.8 Determination of C&DH Software. As described previously, determination of the C&DH software was a major design issue to be resolved within this lifecycle phase. The thesis work of Mr. Hanke specifically addressed this issue. Chapter III of his thesis evaluated candidate vendors of the digital control C&DH system, which was the solution class chosen in the Concept Exploration and Definition phase [26:3-1-3-18].

The same problem-solving process (i.e., issue formulation, analysis, and interpretation) was used to determine the best choice for the C&DH software. The value system shown in Figure 3.5 provided the objective hierarchy needed to choose amongst the C&DH candidates. Three candidate solutions were considered: the dSPACE software, as well as MATRIX_X² software and a “piece-part” solution. The “piece-part” solution involves searching for and acquiring the necessary components to develop a digital control C&DH package, to include software, electronic components, and other supporting hardware. [26:3-13]

²Integrated Systems, Inc., produces an entire range of products, including MATRIX_X, to support aerospace and automotive control applications.

Qualitative analysis between these three candidate solutions showed the dSPACE solution to be a clearly dominant choice [26:3-17]. As far as cost, the dSPACE solution was far superior, since the system was acquired before the *SIMSAT* design effort began and its associated costs were unrecoverable. Although an opportunity cost exists if the dSPACE system is not available for use on another AFIT project, its intended use was for this design and this opportunity cost was considered marginal. Even discounting this cost advantage of the dSPACE solution, it was still equal or better than the other two solutions in each value category. Thus, detailed quantitative analysis was unnecessary to distinguish amongst these C&DH candidates.

With the dSPACE solution chosen as the preferred C&DH software, further development of the C&DH architecture, namely onboard versus offboard processing, could be accomplished within this phase using dSPACE as a constraint.³

3.2.9 System Synthesis. Each subsystem solution class was expanded to narrow the design and address the Preliminary Design issues of Section 3.2.5.

3.2.9.1 ADACS. Within the solution class of momentum exchange methods for the attitude control function, there were two subsystem candidates: momentum wheels and control moment gyros (CMGs). The use of thrusters to augment these candidates was retained for further evaluation. For a three-axis stabilized configuration, if thrusters were needed to provide adequate slew rates, they would be accounted for in the system modeling. If thrusters were only needed for demonstration experiments, they would not be included in the system comparisons of this phase since demonstration experiments required less emphasis on slew performance. Regarding attitude determination, only rate gyros (with or without accelerometers, depending on the model) were considered for further investigation. Position sensors, whether onboard or external, were not considered at this stage of the design.

³The iterative nature of the systems engineering process is exemplified by the issue formulation, analysis, and interpretation steps of the C&DH software subproblem conducted within the issue formulation step of the Preliminary Design problem.

3.2.9.2 Power. The first decision regarding chemical batteries was whether to use primary or secondary battery types. Primary batteries are designed for long storage life and low power density, whereas secondary batteries are intended for multiple recharges, thereby reducing system lifecycle costs. Due to the repetitive nature of the experimentation intended for *SIMSAT*, secondary batteries were the preferred option. Thus, only rechargeable batteries were considered.

Several chemical battery classes were identified, to include lead acid, nickel cadmium, zinc/silver oxide, cadmium/silver oxide, manganese dioxide, and lithium. Adherence to AFIT hazardous material regulations⁴ prevented the use of lithium batteries, thus making that choice infeasible. Each of the other chemical battery classes was retained for system modeling and analysis.

In addition to the type of battery, the configuration of batteries was initially considered in this design phase. Battery configuration was divided into two classes: distributed power system and single-source power system. The rationale to divide the power configuration into these classes was that a single-source power system would require a less complicated electrical structure to provide the necessary bus operating voltage. However, it was determined that the single-source system was not significantly different than a distributed battery system. In fact, the simplicity of a single-source system would be compromised by the necessity to use voltage dividers to provide differing operating voltages for the various subsystems and payload. Furthermore, there was no need at this stage of design to specify the battery configuration since the choice of other subsystems would drive the amount of power required.

3.2.9.3 C&DH . Given that dSPACE software was the preferred C&DH solution class, determination of onboard versus offboard processing was the next major C&DH issue to be resolved within this phase. A top-level consideration of alternatives yielded two prominent solutions: (1) install an AutoBox on the satellite to house the processor and data acquisition boards in a self-contained, power-conditioned, shock-mounted

⁴AFIT hazardous material guidelines were identified as a constraint in the Concept Exploration and Definition phase.

enclosure, or (2) pass all signals (from sensors and effectors⁵ onboard the satellite, as well as commands from the ground) to and from the ground station. Shown in Figure 3.6, the AutoBox was designed with an integrated Ethernet card to send the 10Mbps data stream to a computer equipped with the dSPACE interface software. Within these two major classes, location of control law execution still needed to be designated.

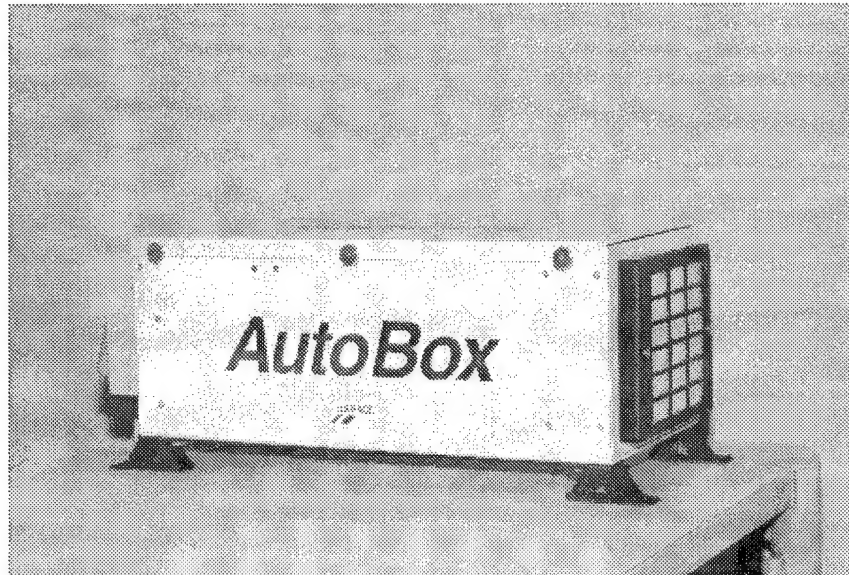


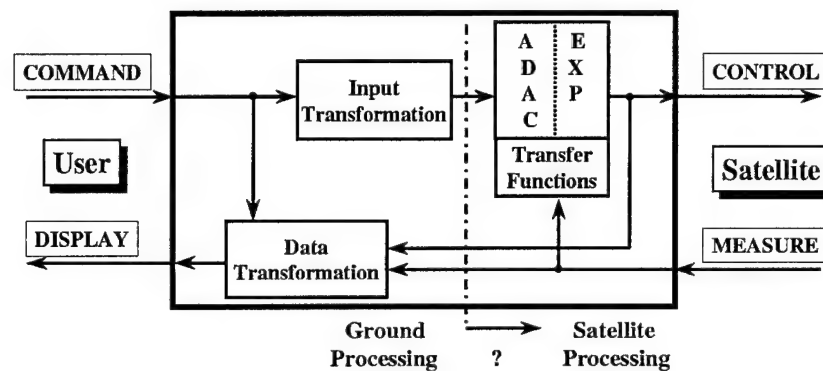
Figure 3.6 AutoBox DS400

Before more explicit definition of the C&DH alternatives could be made, the potential tasks required of the C&DH system needed to be further defined and categorized. These task sets are described in the following paragraphs and pictorially shown in Figure 3.7 [26].

- **Attitude Determination and Control.** This task set includes the evaluation of user commands, collection of satellite telemetry, determination of satellite status, and execution of satellite control laws. This task set is henceforth abbreviated as “ADAC”. Control of satellite functions outside of the ADACS function, but not a part of the experiment payload, is included in this task set.

⁵Those elements which cause an action are referred to as *effectors*.

- **Experiment Control.** This task set includes evaluation of user commands specific to the experiment payload, collection of experiment telemetry, determination of experiment status, and control of the experiment. This task set is labeled “EXP”.
- **User Interface.** This task set composes the capability to provide the command authority and display relevant information to the user.



ADAC and EXP tasks include the corresponding MEASUREMENT task

Figure 3.7 Real-Time Software Architecture [26]

The use of separate processors was considered for these task sets. Optimal control law execution requires minimization of the delay in measurement data induced by signal transmission. Thus, for control functions and measurement functions to be on separate processors, communications between these processors must be low delay, as well as able to handle large data volume. It was determined that a wireless solution may not adequately support control law execution using separate processors [26:4-17]. However, communications requirements between the experiment payload and the satellite ADACS were expected to be low enough that separation of these task sets on separate processors would be feasible [26:4-17].

The use of multiple processors for a given task set was also considered. However, the dSPACE system already included one processor board, and the purchase and integration of multiple processor boards was considered to provide little value for this design effort based on baseline data processing requirements. It was left to future design work to investigate and implement a multi-processor dSPACE solution if data processing needs should so require. As stated previously, the baseline design could be improved to better handle specific experiments once those experimental requirements are defined. The dSPACE software is designed to handle the addition of multiple processor boards, thereby allowing a multi-processing upgrade without extensive system reconfiguration.

An additional C&DH processing consideration needed to be addressed should a ground-based processing option be chosen: how to transmit sensor and effector signals to the ground. Two methods were considered to format data suitable to wireless transmission. Firstly, the AutoBox could be used strictly for signal consolidation (without onboard processing cards). Secondly, an alternative COTS solution could be designed/selected for signal consolidation. [26]

In summary, the following C&DH task allocations were defined and considered for modeling and analysis within this design phase:

- **All Onboard Processing.** This alternative includes all ADAC and EXP processing onboard the satellite using dSPACE's AutoBox solution.
- **Split Processing.** This alternative locates the ADAC processing on the ground computer using dSPACE software, with the EXP processing onboard using user-provided processing capability.
- **Offboard Processing with AutoBox.** All tasks using this alternative are executed on the ground computer using dSPACE software, with the AutoBox providing signal consolidation.
- **Offboard Processing without AutoBox.** All tasks using this alternative are executed on the ground computer using dSPACE software, with a COTS solution providing signal consolidation.

3.2.9.4 Communications. In order to provide the wireless link to the dSPACE software on the ground, several communications alternatives were considered. The first issue addressed was the overall degree of the communications design effort; in short, whether to develop a custom-designed wireless solution or procure a COTS solution. A custom system would require more expertise in the integration and testing phase, but may provide for more optimal performance. The second communications issue focused on the expected frequency ranges to be used in the *SIMSAT* design, such that base approval could be obtained in time to integrate the wireless communications system with the other subsystems. However, since the solution class was narrowed to wireless LAN/modem technologies, the AFIT frequency manager determined that base approval would not be difficult to obtain, so long as operating powers were restricted to common indoor ranges. Thus, identification of the communications frequency was not critical at this stage of design. The following two alternatives for communications were considered in this phase: custom-designed wireless LAN and COTS wireless LAN.

With the dSPACE software already selected, the use of a wireless modem to transfer REALMOTION data was retained. REALMOTION is a three-dimensional animation tool, provided by dSPACE, ideally suited to simulation applications. REALMOTION requires a separate station to view simulation animations in real-time (or offline), and also requires a separate data stream directly from the processor board controlling the simulation. At this stage of the design, a choice of wireless modem for this separate data stream was not necessary, but its incorporation into the design was accounted for.

3.2.9.5 Structures. Although a structural configuration was not chosen at this stage of the design, it was important to begin considering the system layout in order to ensure that subsystems remained feasible, to communicate the design to others, and to set the stage for detailed structural design in the next design phase. The following list of considerations, based on objectives already identified in the value system design, were identified as important in the structural design:

- Minimize moments of inertia to allow better slew rate performance.
- Minimize structural weight.

- Maximize structural rigidity to prevent resonant frequency oscillations.
- Maximize structural modularity to accommodate easy and quick configuration changes.
- Maximize safety by enclosing components which can cause serious injury or damage should they catastrophically fail.

Two structural alternatives were identified in this stage as baseline ideas for future structural development. These alternatives were classified as the "milkcrate" and "wedding cake" configurations⁶. The milkcrate configuration referred to a boxed truss structure on each side of the air bearing assembly. Within each box structure, components would be housed on shelves or using cross members. This concept differed from the wedding cake, which was named for its progressive layered structure. In this configuration, plates would be stacked on each side of the air bearing assembly (similar to a barbell with weight plates). Components would be affixed to these plates. The milkcrate and wedding cake structures were not directly evaluated at this stage of design, but were useful in later development of the structural design.

3.2.9.6 Alternatives Summary. The alternatives designated for further modeling and analysis in this design phase are shown in Table 3.1.

3.3 Analysis

3.3.1 System Modeling. At this stage of the design, significant use of mental modeling, background research, engineering estimates, and vendor specifications were used to evaluate the alternative system configurations.

3.3.2 Preliminary Analysis. Using the subsystem alternatives shown in Table 3.1, 80 system alternatives could be generated (using the full factorial breakdown of the subsystem combinations). Before analyzing each alternative on the system level, this number of alternatives was reduced through preliminary investigation which identified

⁶A third alternative, referred to as the "sombbrero", used a fixed structure joining the two sides of the air bearing assembly, but was rejected from consideration since it would prevent full freedom in the roll axis.

Table 3.1 Preliminary Design Subsystem Alternatives

Subsystem	Alternatives
Attitude Determination	Rate Gyros
Attitude Control	Momentum Wheels Control Moment Gyros
Power	Lead Acid Batteries Nickel Cadmium Batteries Zinc/Silver Oxide Batteries Cadmium/Silver Oxide Batteries Manganese Dioxide Batteries
Command & Data Handling	All Onboard Processing Split Processing Offboard Processing with AutoBox Offboard Processing without AutoBox
Communications	Custom-Designed Wireless LAN COTS Wireless LAN
Structures	As Required

infeasible or impractical alternatives, as well as combined alternatives which appeared similar on a system level into common alternative classes.

3.3.2.1 Control Moment Gyros. Alternatives incorporating CMGs were the first class of alternatives to be eliminated from consideration. Although CMGs were initially considered to be a possible solution for attitude control, in-depth research revealed that only space-rated CMGs were commercially available, which were on the order of hundreds of thousands of dollars to procure. These findings made space-rated CMGs economically infeasible. The possibility of using CMGs not intended for space application was also considered, but acquisition or development of this alternative was not practical in the time scheduled for initial *SIMSAT* design. Follow-on development of the baseline design could incorporate non-space CMGs through joint research efforts with a CMG manufacturer⁷ or a dedicated development effort.

⁷The use of *SIMSAT* in cooperation with industry was considered a future possibility. Discarded, or out-of-tolerance, CMGs could potentially be acquired through such an effort.

3.3.2.2 Wireless LAN Development. The practicality of a custom-designed wireless LAN system was considered before more formal system evaluations using this subsystem choice were made. Investigation into wireless LAN technologies showed two potentially promising research areas for wireless LAN applications: use of lossless data compression, and use of omnidirectional IR transceivers.

Lossless Data Compression. Lossless data compression could enhance a wireless LAN system with relatively low bandwidth capability to adequately handle higher communications traffic. Jung and Burleson presented a real-time, low-area, and low-power VLSI lossless data compressor which was claimed to provide "sufficient performance for all current and most foreseeable future wireless LANs" [30:27]. However, the use of such a system for this design was considered impractical for a number of reasons. For one, lossless data compression hardware/software solutions were not yet commercially available. Thus, in-house expertise would be required to develop and integrate such a system. This development effort was beyond the scope of this project, and beyond the design team's area of expertise. The benefit of such a system was determined to be relatively minor anyway, since wireless LAN systems were commercially available at 10Mbps data rates (required for a dSPACE/AutoBox link) with adequate bandwidth and comparable costs to lower data rate/bandwidth systems. Thus, the performance gains of lossless data compression were considered to be more than offset by the difficulty in developing and integrating such a system.

Omnidirectional IR. Omnidirectional IR transceivers were also considered for use on *SIMSAT*. The advantages of this alternative would be elimination of RF interference, no need for base RF approval, and most importantly, faster data rates offered by IR transmission. This technology was not well-developed and presented a high feasibility risk, and its application in a rotating body compounded this risk since omnidirectional IR depends on elimination of scatter and interference through software logic. If a transceiver is in motion (as it would be on the satellite), scatter and interference patterns would be unsteady and difficult, if not impossible, to manage. In short, this alternative was considered infeasible for this design.

COTS Wireless LAN. Because of the short design schedule and limited background of the design team, a custom-designed wireless LAN system was considered to be impractical in the *SIMSAT* design. With COTS wireless systems available, only the COTS wireless LAN alternative was considered in further Preliminary Design system evaluations.

3.3.2.3 Battery Types. The battery types identified in the system synthesis step all exhibited similar system-level interactions in terms of voltages and currents (which were driven by power requirements), regardless of the specific chemical used in the battery. Furthermore, delivery times were relatively similar for any battery type. It was in the areas of cost and battery characteristics where the different battery types were dissimilar. Table 3.2, from [34:13-10], lists some of the characteristics of the different chemical battery types compared for use in this design.

The first batteries eliminated from consideration were the NiCd vented plate batteries. Vented batteries are not designed for operation at arbitrary configurations, to include inverted; thus, only sealed batteries remained an option. A flat discharge profile was desired to ensure constant discharge from the batteries during operation, making the zinc/silver oxide and cadmium/silver oxide batteries less desirable due to their double plateau discharge profiles. These options also had a relatively short shelf life (1-3 years) and higher costs. Thus, these battery types offered no significant system advantages. Manganese dioxide batteries also displayed a non-constant discharge profile, as well as a low battery capacity per battery, measured in Amp-hours. Battery capacity is a measure of a battery's ability to meet system power requirements. The availability and price of manganese dioxide-based batteries were also drawbacks.

Both sealed lead acid and sealed NiCd batteries were readily available commercially, while generally satisfying system power requirements. Additionally, both types benefit from long cycle life spans, and offered numerous sizes and models. Sealed lead acid batteries, however, provided higher battery capacity per battery. On a system level, this higher battery capacity allowed smaller (or fewer) batteries, resulting in system mass and inertia savings. Furthermore, the lead acid batteries were less expensive. Thus, the NiCd sealed

Table 3.2 Chemical Battery Characteristics

	Lead Acid (stationary)	Lead Acid (portable)	NiCd (vented pocket plate)	NiCd (vented sintered plate)	NiCd (sealed)	Zinc/Silver Oxide	Cadmium/ Silver Oxide	MnO ₂
Nominal cell voltage	2.0	2.0	1.2	1.2	1.2	1.5	1.2	1.5
Energy density (Wh/kg)	10-20	30	20	37	30	90	55	30
Volume (Wh/L)	50-70	80	40	90	80	180	110	60
Discharge profile	Flat	Flat	Flat	Very Flat	Very Flat	Double Plateau	Double Plateau	Sloping
Power density	Moderately High	High	High	High	Moderate to High	High	Moderate to High	Low
Self-discharge rate (%/mo)	N/A	4-8	5	10	15-20	3	3	1
Calendar life (yrs)	18-25	2-8	8-25	3-10	2-5	1-3	2-3	20-50
Cycle life	N/A	250-500	500-1000	500-2000	300-700	100-150	150-600	20-50
High discharge rate	No	No	No	Yes	Yes	Yes	No	No
Battery capacity (Amp-hrs)	5-400	0.9-35	5-1300	10-100	0.5-10	1-800	1-500	0-5
Cost (\$/kWh)	100	200-500	400-1000	600-1000	1000-3000	800-1500	1000-2000	1000

battery offered no significant system advantages, and the sealed lead acid batteries were the sole remaining alternative.

3.3.3 Remaining System Alternatives. After the preliminary analysis, the only major subsystem decision at this stage left unanswered regarded the C&DH architecture. The momentum wheels, sealed lead acid batteries, and COTS wireless LAN were treated as system constraints for the next iteration of the design process within the Preliminary Design phase. Choice of C&DH architecture was made on the system level, comparing the following four alternatives: all onboard processing (with AutoBox), split (onboard/offboard) processing, offboard processing with AutoBox, and offboard processing without AutoBox. These alternative configurations were abbreviated as: *ALL-ON-SAT*, *SPLIT*, *GRD W/ ABX*, and *GRD W/O ABX*.

3.3.4 Analysis Methodology. The purpose of the following analysis was to determine actual measures (*raw values*) for the objectives identified in the objective hierarchy of Figure 3.5 for each remaining system alternative. Next, these raw values were converted into *scaled scores* using a standardized utility scale, based on decision maker/customer inputs. A confidence factor could then be applied to account for the level of confidence associated with the measurable raw values, resulting in *rated scores*. Because of the large degree of mental modeling and estimation used in this analysis, the use of confidence factors as derating multipliers needlessly narrowed the scoring differences since most all the raw values were considered to be of a similar level of confidence. Therefore, confidence factors were not used in this analysis, resulting in equivalency of rated scores and scaled scores. In the interpretation step, additional inputs from the decision makers were used to designate weighting factors to apply to the objective hierarchy, and a *system score* was thereby computed for each alternative, allowing ranking of alternatives and selection of a preferred alternative by the decision maker.

3.3.5 Raw Values. Each alternative was analyzed to determine a raw value for each measurable from the VSD. The resolution of a raw value was either binary (e.g., yes/no), a finite number of classes (e.g., low, medium, high), or continuous real numbers

(e.g., 29.5, 34.5). Resolution was dependent on the measurable considered⁸. A summary of the raw data collection was first published in Appendix B of Mr. Hanke's thesis [26].

3.3.5.1 Cost. *Capital Costs* and *O&M Costs* were determined through summation of the associated costs for each subsystem. These cost estimates were based on vendor research, as well as mental modeling of relative support and integration costs. The costs associated with the purchase of the air-bearing assembly and dSPACE ground station were not included, as these purchases were already completed at this stage of the design. Cost estimates are tabulated in Table 3.3 for the baseline configuration, *ALL-ON-SAT*. For the *SPLIT* and *GRD W/ ABX* configurations, capital costs were estimated to be \$5000 higher due to the need for ground processing equipment in addition to the AutoBox. The *GRD W/O ABX* option was also estimated to be more expensive due to the need for onboard signal consolidation equipment. This option also had higher estimated O&M costs because of the anticipated decreased reliability of a non-integrated solution, relative to the integrated⁹ solutions. Table 3.4 shows the cost data for each alternative.

Table 3.3 Baseline Cost Breakdown

Subsystem	Capital Costs	O&M Costs	Components
ADACS	\$17,000	\$5,000/yr	Motors, wheels, sensors, etc.
Power	\$5,000	\$2,000/yr	Batteries/chargers, dist./regulation
C&DH/Comm	\$7,000	\$1,000/yr	AutoBox, wireless LAN, cabling
Structures	\$500	\$0/yr	Materials and fabrication
TOTAL	\$29,500	\$8,000/yr	<i>ALL-ON-SAT</i> baseline

Table 3.4 Raw Cost Data

Alternative	Capital Costs	O&M Costs
<i>ALL-ON-SAT</i>	\$29,500	\$8,000/yr
<i>SPLIT</i>	\$34,500	\$8,000/yr
<i>GRD W/ ABX</i>	\$34,500	\$8,000/yr
<i>GRD W/O ABX</i>	\$34,500	\$8,500/yr

⁸See Section 3.2.7 for a description of each measurable within the VSD.

⁹"Integrated" refers to the use of dSPACE's AutoBox with the dSPACE ground station.

3.3.5.2 Schedule. To determine *Total Delivery Weeks*, estimates for the order¹⁰, delivery, and integration times for each subsystem were made. Several assumptions were made in this analysis. First, it was assumed that all order and delivery times of components would occur simultaneously. Thus, the system-level order and delivery time would be the maximum of the subsystem order and delivery times. Second, the integration of the system was assumed to begin once all subsystems were received. Moreover, the system integration time would be the summation of the individual subsystem integration times. The total delivery metric represented overall delivery time of the system to the customer, thus including both order/delivery and integration of subsystems. Table 3.5 lists the raw schedule estimates for each subsystem, using the *ALL-ON-SAT* baseline.¹¹

Table 3.5 Baseline Schedule Breakdown

Subsystem	Order	Delivery	Integration
ADACS	5 weeks	10 weeks	6 weeks
Power	8 weeks	4 weeks	4 weeks
C&DH/Comm	4 weeks	15 weeks	3 weeks
Structures	2 weeks	3 weeks	2 weeks
TOTAL <i>ALL-ON-SAT</i>	Order/Delivery 19 weeks	Integration 15 weeks	Total Delivery 34 weeks

For the *SPLIT* option, an additional week was added to the C&DH order and delivery time to account for the impact of selecting and ordering additional hardware and software. Similarly, the *GRD W/ ABX* option also includes this additional week, as well as an added 2 weeks to account for additional software integration. For the *GRD W/O ABX* option, more research would be required to determine the required signal consolidation equipment and select a preferred vendor, resulting in 2 weeks additional order time relative to the baseline. Furthermore, the integration time would also be longer to account for this non-integrated solution. Table 3.6 shows the raw schedule data for each system alternative.

¹⁰Order times included the selection of the components, granting of expenditure authority, and processing of all necessary paperwork.

¹¹These estimates were made in the summer of 1998, allowing for delivery of the system before March 1999.

Table 3.6 Raw Schedule Data

Alternative	Total Delivery Weeks	Comment
<i>ALL-ON-SAT</i>	34	Baseline
<i>SPLIT</i>	35	Additional processor
<i>GRD W/ ABX</i>	37	Software integration
<i>GRD W/O ABX</i>	40	Further integration

3.3.5.3 Safety. The *Relative Damage Index* and *Relative Injury Index* were difficult to accurately quantify at this point, but relative estimates were possible. The indices, which ranged from 1 (extremely dangerous and unacceptable) to 20 (no inherent danger), were estimated using mental modeling of possible dangers associated with the different alternatives. Because all the subsystems were to be commercially available or carefully designed products, they were expected to meet industry and military safety standards. Careful consideration of safety issues was stressed throughout the design process, as well. Thus, no anticipated substantial safety risks were identified. To provide for unanticipated system interactions, the damage and injury indices were conservatively estimated to be 18, which was an acceptable value. For the *GRD W/O ABX* option, these index estimates were reduced to 16; the decrease due to the required integration of a non-validated, piece-part design. Table 3.7 shows the raw values corresponding to the safety measurables.

Table 3.7 Raw Safety Data

Alternative	Relative Damage Index	Relative Injury Index
<i>ALL-ON-SAT</i>	18	18
<i>SPLIT</i>	18	18
<i>GRD W/ ABX</i>	18	18
<i>GRD W/O ABX</i>	16	16

3.3.5.4 Performance: Execution. System evaluations with respect to the *Execution* performance value are summarized below for each evaluation consideration and its associated measurables. Execution measurables were discussed in Section 3.2.7.4 and are shown in the objective hierarchy on page 3-11.

Controllability. *Processor Schedulability Analysis* quantified the support for RMA by the system. The *ALL-ON-SAT*, *SPLIT*, and *GRD W/ ABX* alternatives all offered "full" RMA support using the dSPACE system. However, the *GRD W/O ABX* option was rated as "moderate" support. Although also using the dSPACE ground software, additional hand-coded routines would likely be required to support schedulability analysis using the onboard non-dSPACE hardware in the *GRD W/O ABX* configuration [26:B-9].

Communications Latency was concerned with what part of the control system would be impacted by communications delays. The following scale was used to model this impact relative to the *ALL-ON-SAT* baseline: minimum, moderate, and significant. A rating of "minimum" would be used if communication delays were low, and had little impact. The *ALL-ON-SAT* option was rated as "minimum" because all processing would occur onboard the satellite, thereby incorporating the least signal delays between sensors, control elements, and effectors. Following this same reasoning, the *SPLIT* option was rated as "moderate", since some processing would be onboard. The offboard processing options both rated "significant" latency due to the impacts of offboard control law execution.

Bandwidth Requirement, although correlated with the communications latency, was a separate measure of communications data flow requirements. Mental modeling was used to estimate the bandwidth required for each alternative using the following resolution: low, moderate, and high. The *ALL-ON-SAT* alternative scored "low" because only command and display data need be transferred from the ground to the satellite. In the *SPLIT* configuration, additional telemetry data and effector commands would be required to execute offboard ADAC functions; thus, the "moderate" rating for this option. The high data requirements of the offboard processing options led to a rating of "high" for the bandwidth requirement.

Raw values for the *Controllability* measures are summarized in Table 3.8.

Data Capability. Initially, the binary measures of *Post-Mission Data Analysis* and *Real-Time Data* were expected to provide some differentiation of system alternatives. However, each alternative considered would support both real-time data

Table 3.8 Raw Performance Data: Controllability

Alternative	Processor Sched. Analysis	Communications Latency	Bandwidth Requirement
<i>ALL-ON-SAT</i>	Full	Minimum	Low
<i>SPLIT</i>	Full	Moderate	Moderate
<i>GRD W/ ABX</i>	Full	Significant	High
<i>GRD W/O ABX</i>	Moderate	Significant	High

display, as well as post-mission data playback and manipulation, as shown in Table 3.9. This result was due to the use of the dSPACE ground software in all configurations.

Table 3.9 Raw Performance Data: Data Capability

Alternative	Post-Mission Data Analysis	Real-Time Data
<i>ALL-ON-SAT</i>	Yes	Yes
<i>SPLIT</i>	Yes	Yes
<i>GRD W/ ABX</i>	Yes	Yes
<i>GRD W/O ABX</i>	Yes	Yes

Satellite Movement. At this stage of the design, a determination of specific rate gyros to be used for the attitude determination function was not made. Therefore, all of the alternatives incorporated a common baseline IMU. As stated previously, synthesis of specific rate gyro options was left to the Detailed Design phase. *Slew Rate Sensing*, therefore, did not offer differentiation of alternatives at this stage and need not be evaluated.

As with the slew rate sensing, *Rate Sensing Accuracy* did not differentiate solutions at this stage since each solution used a baseline IMU.

Slew Capability was defined as the maximum slew angle capable within a 10sec slew maneuver. Initial system estimates and mental modeling were used to analyze this measure. A baseline system comprising the AutoBox onboard was used, with an estimated slew capability of 60°/10sec. This baseline assumed momentum wheels/motors, two large batteries, and a generic payload would also be placed onboard, along with associated com-

munications and structural equipment. The *ALL-ON-SAT*, *SPLIT*, and *GRD W/ ABX* options all incorporated an onboard AutoBox, and their slew rates were estimated as 60°/10sec. The *GRD W/O ABX* alternative did not incorporate the AutoBox onboard, and allowed greater flexibility in the arrangement of components. Thus, this option could accommodate lower moment-of-inertia properties, and therefore higher slew rates. An estimate of 70°/10sec was used for the *GRD W/O ABX* slew capability. These estimates, although rough approximations, served the purpose of relative differentiation.

Table 3.10 summarizes the analysis data for the *Satellite Movement* measures.

Table 3.10 Raw Performance Data: Satellite Movement

Alternative	Slew Rate Sensing	Rate Sensing Accuracy	Slew Capability
<i>ALL-ON-SAT</i>	(not evaluated)	(not evaluated)	60°/10sec
<i>SPLIT</i>	(not evaluated)	(not evaluated)	60°/10sec
<i>GRD W/ ABX</i>	(not evaluated)	(not evaluated)	60°/10sec
<i>GRD W/O ABX</i>	(not evaluated)	(not evaluated)	70°/10sec

3.3.5.5 Performance: Robustness. System evaluations with respect to the *Robustness* performance value are summarized below for each evaluation consideration and its associated measurables. Robustness measurables were discussed in Section 3.2.7.4 and are shown in the objective hierarchy on page 3-11.

Range of Experiments. The *Interface Modularity* metric was measured in terms of the percentage of components that must be relocated or removed in order to accommodate an experiment. The following list describes the resolution used in the mental modeling of each configuration:

- **None.** Only complete subsystems can be replaced with payload parts; no component swapping is possible.
- **Some.** 10-50% of components can be relocated or substituted to accommodate an experimental payload.

- **Partial.** 50-75% of components can be relocated or substituted to accommodate an experimental payload.
- **Full.** All of the baseline components can be relocated or substituted to accommodate an experimental payload.

For the alternatives considered, it was assumed that use of the onboard AutoBox would make rearrangement of the onboard C&DH subsystem difficult due to the AutoBox's size and integrated hardware. Thus, the *ALL-ON-SAT*, *SPLIT*, and *GRD W/ ABX* configurations were all rated "partial" in terms of interface modularity. The "piece-part" nature of the *GRD W/O ABX* option would allow increased flexibility in accommodating experimental payloads, and was hence rated as "full" interface modularity.

Experiment Types measured the robustness of the system with respect to ability to support various experiments desired by the user. The resolution used in the modeling of each configuration is summarized by the following experimental support levels:

- **None.** No experimental support.
- **Educational.** Only spinner experimental support.
- **Rigid.** Spinner and 3-axis stabilized (rigid body) experimental support.
- **Full.** Full experimental support: spinner, 3-axis stabilized (rigid and flexible experiments).

The AutoBox options were assumed to handle all experimental types, based on the integrated dSPACE software and 32 in/32 out data channel capability. However, the non-Autobox option (*GRD W/O ABX*) may not be able to handle all the data requirements of a flexible experiment (e.g., vibration suppression). Thus, this option received a "rigid" rating for this measure.

Table 3.11 shows the scores for each configuration for the *Range of Experiments* measures.

Table 3.11 Raw Performance Data: Range of Experiments

Alternative	Interface Modularity	Experiment Types
<i>ALL-ON-SAT</i>	Partial	Full
<i>SPLIT</i>	Partial	Full
<i>GRD W/ ABX</i>	Partial	Full
<i>GRD W/O ABX</i>	Full	Rigid

Available Margins. The *Mass Margin* of each configuration was modeled through the summation of all onboard components. A baseline mass budget using an onboard AutoBox is shown in Table 3.12. These rough mass estimates were based on vendor research, and engineering approximations. Since the air-bearing supports approximately 150kg, the total system mass was subtracted from this value to calculate the mass margin (maximum payload weight). Thus, the AutoBox options offered 100kg mass margins. The non-AutoBox option was assumed to use lighter, more compact, signal consolidation equipment relative to the AutoBox. Furthermore, this would allow a tighter structure, reducing structural weight as well. Thus, a savings of 20kg was estimated for the *GRD W/O ABX* alternative, resulting in a 120kg mass margin.

Table 3.12 Baseline Mass Breakdown

Subsystem	Estimated Mass	Components
ADACS	18kg	Motors, wheels, sensors, etc.
Power	7kg	Batteries/chargers, dist./regulation
C&DH/Comm	10kg	AutoBox, wireless LAN, cabling
Structures	15kg	Materials and supports
TOTAL	50kg	<i>ALL-ON-SAT</i> baseline

The *Power Margin* estimates also required baseline system approximations. In order to account for experiment duration, it was decided that Amp-hours (A-hr) would be a better unit of measurement than total Watts. The ADACS subsystem was estimated to require 200W of power. The AutoBox 135W specification [19:121] was used to estimate C&DH power consumption for the *ALL-ON-SAT*, *SPLIT*, and *GRD W/ ABX* alternatives. An additional 10W was assumed for wireless communications and other onboard sensors. Assuming a nominal bus voltage of 24V and experiment duration of 60 minutes, the total

345W power demand resulted in 12.32 A-hr, which was rounded to 13 A-hr to account for line losses. The power system baseline was estimated to be two 10 A-hr batteries, thus providing 20 A-hr onboard. Thus, the baseline power margin was 7 A-hr. For the non-AutoBox solution, the signal consolidation equipment was assumed to use much less power than the AutoBox assembly, which was designed for much more than just signal processing. An estimate of 50W was used for the *GRD W/O ABX* C&DH power consumption, resulting in a 10 A-hr power margin.

Table 3.13 shows the mass and power margins for each configuration.

Table 3.13 Raw Performance Data: Available Margins

Alternative	Mass Margin (kg)	Power margin (A-hr)
<i>ALL-ON-SAT</i>	100	7
<i>SPLIT</i>	100	7
<i>GRD W/ ABX</i>	100	7
<i>GRD W/O ABX</i>	120	10

3.3.5.6 Performance: Ease of Use. System evaluations with respect to the *Ease of Use* performance value are summarized below for each evaluation consideration and its associated measurables. These measurables were discussed in Section 3.2.7.4 and are shown in the objective hierarchy on page 3-11.

Ground Station Capability. The *Control System Analysis* metric was defined as the percentage of system components readily defined by the ground station, in terms of geometric, mass, and inertial properties. The following resolution was used in this modeling: minimal (< 50% readily defined), partial (50 – 90% readily defined), and full (> 90% readily defined). The onboard AutoBox options were determined to have “full” capability, since the AutoBox could easily be modeled along with the other onboard systems. The *GRD W/O ABX* alternative made this analysis more difficult, due to the non-integrated onboard hardware. Because this solution was “piece-part” in nature, it was not as well defined ahead-of-time, relative to the AutoBox. Thus, this alternative was rated “partial” capability.

The *Development Environment* measure referred to the type of development interface: text, graphical, or object-oriented. The dSPACE ground station used a SIMULINK interface which can represent all input and output signals of the AutoBox. Thus, all AutoBox-based solutions were modeled as object-oriented development environments. The signal consolidation of a non-AutoBox solution would not be as easily handled within the dSPACE-SIMULINK model, and thus the *GRD W/O ABX* option was considered a graphical-only development environment.

Although the dSPACE simulation of the satellite motion may be more complex without the use of the AutoBox, all system alternatives would be capable of modeling satellite behavior prior to execution of an experiment. Thus, the *Motion Simulation* capability would exist for each option.

Table 3.14 consolidates the raw data for the *Ground Station Capability* measurables.

Table 3.14 Raw Performance Data: Ground Station Capability

Alternative	Control System Analysis	Development Environment	Motion Simulation
<i>ALL-ON-SAT</i>	Full	Object-Oriented	Yes
<i>SPLIT</i>	Full	Object-Oriented	Yes
<i>GRD W/ ABX</i>	Full	Object-Oriented	Yes
<i>GRD W/O ABX</i>	Partial	Graphical	Yes

Command and Control. The percentage of displays/controls presented graphically to the user was defined as the *User Interface* measure. Similar to *Control System Analysis*, the following resolution was used in the mental modeling of this measure: minimal (< 50% graphically displayed), partial (50 – 90% graphically displayed), and full (> 90% graphically displayed). Because the dSPACE environment allows easy graphical manipulation, all AutoBox-based solutions were rated “full” user interface capability. The *GRD W/O ABX* option may not incorporate as easy an interface due to non-dSPACE signal consolidation. If full capability could be achieved, it was expected to require much more development. Thus, this option was rated “partial” capability at this stage.

Command Capability used the following scale, increasing in command capability: only experiment start/stop commands, ADACS control, and ADACS/payload control. All alternatives provided for full ADACS/payload control. The relative ease of this control was reflected in other measurables.

Table 3.15 shows the *Command and Control* measurables data.

Table 3.15 Raw Performance Data: Command and Control

Alternative	User Interface	Command Capability
<i>ALL-ON-SAT</i>	Full	Full
<i>SPLIT</i>	Full	Full
<i>GRD W/ ABX</i>	Full	Full
<i>GRD W/O ABX</i>	Partial	Full

O&M Time. *Maintenance and Test Time* measured the time required to install a payload and validate the system for operation. As defined in Appendix A, this measure ranged from “very low” (under 15 minutes) to “very high” (more than 100 minutes). The AutoBox solutions allowed simple signal interfaces to the AutoBox, and would require less validation due to the integrated dSPACE hardware. Thus, a “very low” time was warranted for these alternatives. Because the *GRD W/O ABX* option made signal interfacing less straightforward, it was anticipated that configuring an experiment would require more time, and a rating of “low” (16-35 minutes) was given.

Turn-Around Time considered only the time required to reset the configuration for a like experiment. Since this time was most impacted by power (battery change-outs) and structures (accessibility) issues, the alternatives at this stage did not provide any differentiation. Thus, this measure need not be evaluated since it only considered baseline subsystems that were as yet not fully defined.

Table 3.16 shows the *O&M Time* measurable data.

3.3.6 Utility Scale. A utility scale, ranging from 0 (no utility) to 10 (highest utility), was used to scale each raw value. This common scale thereby allowed all the measurable data to be directly compared. The design team explicitly solicited utility

Table 3.16 Raw Performance Data: O&M Time

Alternative	Maintenance & Test Time	Turn-Around Time
<i>ALL-ON-SAT</i>	Very Low	(not evaluated)
<i>SPLIT</i>	Very Low	(not evaluated)
<i>GRD W/ ABX</i>	Very Low	(not evaluated)
<i>GRD W/O ABX</i>	Low	(not evaluated)

(preference) data from the decision makers/customers; this data was used to create utility curves for each measure, as shown in Appendix A. Table 3.17 is a tabular representation of these utility curves for each measure. The exact utility curves in Appendix A were used in actual scaled score calculations. These scaled scores are shown in Table 3.18 for each of the four system alternatives.

3.4 Interpretation

3.4.1 Dominated Solutions. As Table 3.18 shows, the *SPLIT* and *GRD W/ ABX* were *dominated solutions*. This term implies that another alternative was greater or equal in value for every measurable related to these options. Specifically, both the *ALL-ON-SAT* and *SPLIT* alternatives dominated the *GRD W/ ABX* alternative, and the *ALL-ON-SAT* alternative dominated the *SPLIT* alternative as well. This conclusion was logical since these two solutions were based on some offboard processing with an onboard AutoBox, thereby including the negative system impacts of offboard processing delays along with the negative system impacts of the large AutoBox assembly. Thus, the *SPLIT* and *GRD W/ ABX* options were not considered further in the decision-making process¹². The *GRD W/O ABX* option, however, was not dominated, since removal of the AutoBox gained certain advantages in terms of modularity, slew capability, and available mass and power margins. Thus, additional decision-making analysis was needed to resolve the preference of the *ALL-ON-SAT* versus *GRD W/O ABX* alternatives.

¹²The thesis of Mr. Hanke [26] included all four options for follow-on consideration. The decision-making techniques of this phase were similar, but not identical, to those employed by Mr. Hanke in his C&DH evaluations. The scaled scores, weighting factors, and resulting system scores were not identical.

Table 3.17 Common Utility Scale

Objective Measurable	Utility Scale				
	No utility	Little utility	Fair utility	Good utility	Excellent utility
	0	2	5	7	10
Capital costs	\$100,000	\$86,000	\$65,000	\$50,000	\$10,000
O&M costs (per year)	\$10,000	\$8,750	\$6,875	\$5,000	\$0
Total delivery weeks	56	53	48	43	24
Relative damage index	10	12	15	17	20
Relative injury index	10	12	15	17	20
Processor sched. analysis	None	Unsupported		Moderate	Full
Communications latency	Significant		Moderate		Minimal
Bandwidth requirement	High		Moderate		Low
Post-mission data analysis	No				Yes
Real-time data	No				Yes
Slew rate sensing	(not evaluated)				
Rate sensing accuracy	(not evaluated)				
Slew capability (deg/10sec)	30	38	50	60	100
Interface modularity	None	Some		Partial	Full
Experiment types	None	Educational		Rigid	Full
Mass margin (kg)	0	25	55	80	300
Power margin (A-hr)	0	1	2	4	15
Control system analysis	Minimal			Partial	Full
Development environment	Text			Graphical	Object-Oriented
Motion simulation	No				Yes
User interface	Minimal			Partial	Full
Command capability	Start/Stop-only			ADACS-only	ADACS/Payload
Maintenance & test time	Very High	High	Moderate	Low	Very Low
Turn-around time	(not evaluated)				

Table 3.18 Scaled Scores Summary

Objective Measurable	Scaled Scores (Common Units, 0 to 10)			
	<i>ALL-ON-SAT</i>	<i>SPLIT</i>	<i>GRD W/ ABX</i>	<i>GRD W/O ABX</i>
Capital costs	8.7	8.4	8.4	8.4
O&M costs	3.5	3.5	3.5	2.7
Total delivery weeks	8.9	8.7	8.4	7.7
Relative damage index	8	8	8	6
Relative injury index	8	8	8	6
Processor sched. analysis	10	10	10	7
Communications latency	10	5	0	0
Bandwidth requirement	10	5	0	0
Post-mission data analysis	10	10	10	10
Real-time data	10	10	10	10
Slew rate sensing	(not evaluated)			
Rate sensing accuracy	(not evaluated)			
Slew capability	7.0	7.0	7.0	8.2
Interface modularity	6	6	6	10
Experiment types	10	10	10	7
Mass margin	8.0	8.0	8.0	8.6
Power margin	9.1	9.1	9.1	9.7
Control system analysis	10	10	10	7
Development environment	10	10	10	7
Motion simulation	10	10	10	10
User interface	10	10	10	7
Command capability	10	10	10	10
Maintenance & test time	10	10	10	7
Turn-around time	(not evaluated)			

3.4.2 Worth Assessment Methodology. System ranking and selection were based on an overall worth assessment. This decision-making procedure was used to translate scaled utility scores for each measure into system scores for the remaining two alternatives. Sage described a six-step process in the overall assessment of system worth, as summarized below [49:356-358]:

- List the overall performance objectives or attributes.
- Construct a hierarchy of performance criteria.
- Select appropriate physical performance measures.
- Define the relationship between low-level criteria and physical performance measures; i.e., deal with the scoring problem.
- Establish relative importance within the subcriteria set.
- Adjust the weights to reflect confidence in the performance measures.

The first three steps in Sage's method were accomplished in the value system design, in which overall values were defined, and associated measurables were developed and arranged in the objective hierarchy. The fourth step corresponded to the development of a common utility scale, from which scaled scores were calculated. The fifth and sixth steps represented the development of weighting factors for each objective measure. This determination of weighting factors is summarized in Section 3.4.3.

3.4.3 Weighting Factors. Weighting factors were developed for each measure of the objective hierarchy through interactive discussion with the decision makers. These factors were assigned such that the multipliers for each level of the objective hierarchy summed to 1, as shown in Figure 3.8. The multipliers for each top level were then multiplied by the sublevel multipliers, all the way down to the objective measurables, to calculate a single weighting factor for each measurable. In this way, a weighting factors vector was created (with sum of components equal to 1), which was multiplied by the matrix of scaled scores (Figure 3.18) to determine a system score for each alternative.

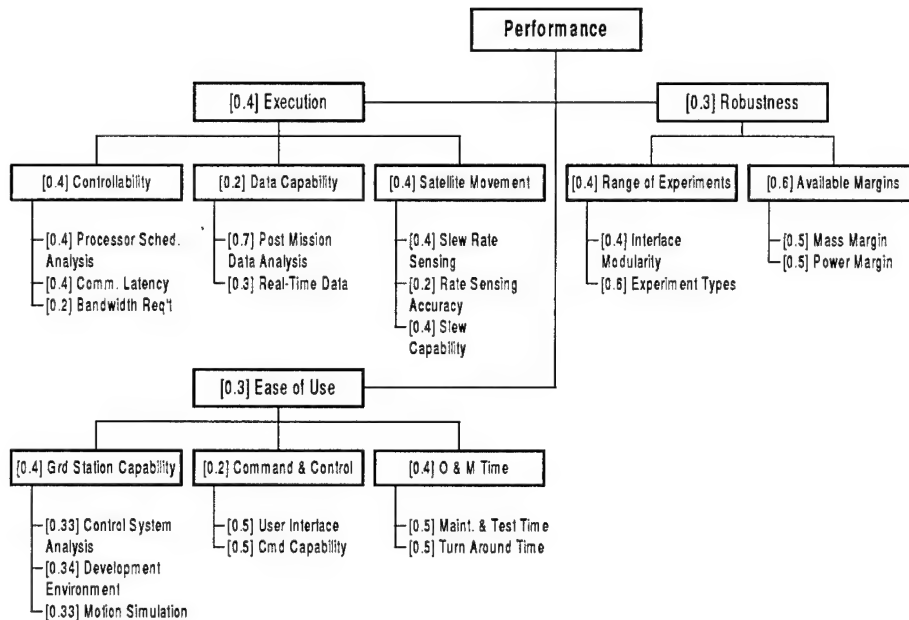
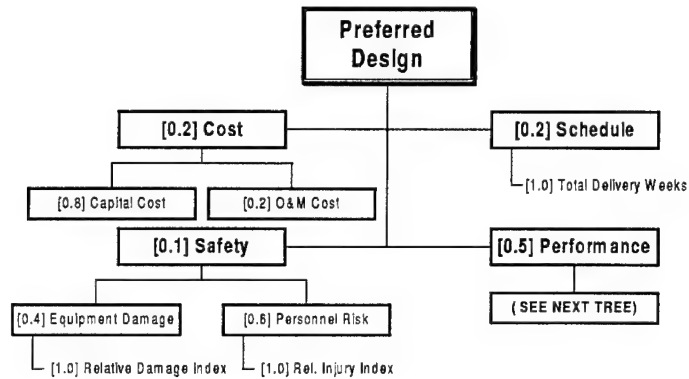


Figure 3.8 Preliminary Design Weighted Hierarchy

3.4.3.1 Adjustments. Because the *Data Capability* evaluation consideration revealed no system differentiation (all of the alternatives incorporated post-mission and real-time data analysis), the weighting factor for this branch was redistributed to the *Controllability* and *Satellite Movement* branches. Thus, their corresponding weights were increased from 0.4 to 0.5 to better provide system differentiation for the decision makers. Similarly, the weight corresponding to the *Turn-Around Time* was redistributed to the *Ground Station Capability* and *Command and Control* branches. The weight was not lumped with the *Maintenance and Test Time* because this action would have significantly increased the importance of this measure, whereas redistribution to the other branches was considered to aid in the system differentiation without inflating the importance of any specific measure. Thus, the *Ground Station Capability* branch was increased from 0.4 to 0.5, and the *Command and Control* was increased from 0.2 to 0.3.

Although *Slew Rate Sensing* and *Rate Sensing Accuracy* were not applicable to the solutions analyzed in this phase¹³, the weights of these measures were not redistributed, thus avoiding over-inflation of the *Slew Capability* measure. Instead, the two alternatives were considered of equal utility (an arbitrary value of 7) for these respective measures.

3.4.3.2 Confidence Factors. As stated previously, the level of confidence associated with the measurable data was considered equal at this stage of the design. Thus, no adjustments were made based on confidence factors.

3.4.3.3 Weighting Factors Vector. Weights for each measure were determined by multiplying the weighting factors from the bottom of the hierarchy (objective measures) to the top (top-level values). These weights provided a means of ranking the objective measures to ensure that important measures were weighted more heavily. The decision maker was able to adjust the branch and measure weights that resulted in the finalized weighting vector. This resulting weighting factors vector is shown in Table 3.19.

¹³The measurable weighting factors were developed before preliminary system analysis revealed the system configurations which would require detailed measurable data for comparison.

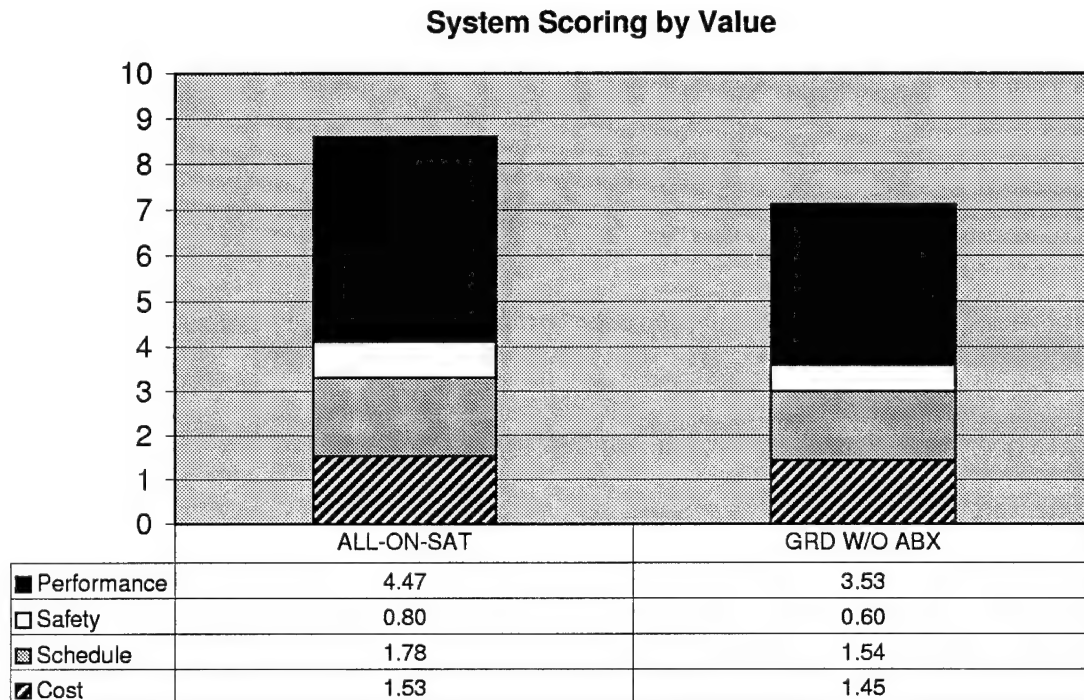
Table 3.19 Weighting Factors Vector

Measurable	Weighting Factor
Capital Cost	0.160
O&M Cost	0.040
Total Delivery Weeks	0.200
Relative Damage Index	0.040
Relative Injury Index	0.060
Processor Schedulability Analysis	0.040
Communications Latency	0.040
Bandwidth Requirement	0.020
Post-Mission Data Analysis	0.000
Real-Time Data	0.000
Slew Rate Sensing	0.040
Rate Sensing Accuracy	0.020
Slew Capability	0.040
Interface Modularity	0.024
Experiment Types	0.036
Mass Margin	0.045
Power Margin	0.045
Control System Analysis	0.025
Development Environment	0.025
Motion Simulation	0.025
User Interface	0.023
Command Capability	0.022
Maintenance & Test Time	0.030
Turn-Around Time	0.000
Components Sum	1.000

3.4.4 System Scoring. Since the system scores were determined by multiplying the scaled scores matrix by the weighting factors vector, the scoring range also varied from 0 (no utility) to 10 (excellent utility). The system scores for the *ALL-ON-SAT* and *GRD W/O ABX* alternatives are shown in Table 3.20. The *ALL-ON-SAT* alternative scored higher than the *GRD W/O ABX* alternative for each top-level value.

3.4.5 Sensitivity Analysis. Before selecting the *ALL-ON-SAT* alternative based on system scores, the ranking of alternatives was investigated to determine sensitivity to the weighting factors. This sensitivity analysis allowed understanding of how the system scores were dependent on the weighting factors used in the decision-making process.

Table 3.20 System Scoring Results



3.4.5.1 Cost, Schedule, and Safety. Because the *ALL-ON-SAT* alternative was rated superior to the *GRD W/O ABX* alternative in every cost, schedule, and safety measure, no alteration of lower-level weighting factors would allow the *GRD W/O ABX* option to show an advantage over the *ALL-ON-SAT* option for these values.

3.4.5.2 Performance. In the *Performance* hierarchy, the *ALL-ON-SAT* option was superior or equal in all *Ease of Use* measures. Moreover, the *ALL-ON-SAT* option was superior or equal in all *Execution* measures, except *Slew Rate Sensing*. Because of the dominance of the *ALL-ON-SAT* in most measures within the *Execution* branch, only extremely skewed weighting of the *Slew Rate Sensing* measure could possibly result

in the *GRD W/O ABX* option having greater *Execution* utility. Thus, the *ALL-ON-SAT* alternative was considered superior in both *Ease of Use* and *Execution* under any reasonable weighting scheme.

For the *Robustness* measures, however, the *GRD W/O ABX* option showed superiority in *Mass Margin*, *Power Margin*, and *Interface Modularity*, whereas the *ALL-ON-SAT* option was only superior in terms of *Experiment Types*. Thus, only by placing additional weight to the *Robustness* branch could the *GRD W/O ABX* option show an advantage over the *ALL-ON-SAT* option.

3.4.5.3 Worst-Case Weighting. Assuming the branch weights of cost, schedule, and safety were reduced to 0, the *ALL-ON-SAT* advantage due to these categories was thereby eliminated. Thus, only the performance measures were considered in the remaining worst-case sensitivity analysis. The challenge was then to determine the weighting scheme amongst the performance measures which would show the *GRD W/O ABX* option to be superior. If this weighting scheme was considered unreasonable, then the *ALL-ON-SAT* option would be superior under any reasonable weights breakdown.

To further simplify the vast solution space of weighting schemes, the relative weighting within *Execution* and *Ease of Use* were held constant. This assumption was reasonable in this situation because the *ALL-ON-SAT* option dominated all but one measure within these categories; varying the internal weights of these measures would not significantly change this *ALL-ON-SAT* scoring advantage. An additional assumption was that the *Interface Modularity* measure would receive all the weight within the *Range of Experiments* branch (*Experiment Types* equal to 0), thus giving advantage to the *GRD W/O ABX* option. With this weighting scheme, the relative weights of the *Execution*, *Robustness*, and *Ease of Use* performance considerations could be traded to determine favorable *GRD W/O ABX* situations. Multiplying the low-level weighting factors against the utility values corresponding to those measures, the results of Table 3.21 were obtained.

Table 3.21 Utility of Each Performance Consideration

Evaluation Consideration	<i>ALL-ON-SAT</i> Utility	<i>GRD W/O ABX</i> Utility
Execution	8.50	5.14
Robustness	7.53	9.49
Ease of Use	8.00	6.30

3.4.5.4 Varying the Performance Weights. Using the utility values for each branch, the following equations represent the sensitivity analysis solution space (where x , y , and z are the *Execution*, *Robustness*, and *Ease of Use* weights, respectively):

$$8.50 \cdot x + 7.53 \cdot y + 8.00 \cdot z = \text{ALL-ON-SAT Score}$$

$$5.14 \cdot x + 9.49 \cdot y + 6.30 \cdot z = \text{GRD W/O ABX Score}$$

$$x + y + z = 1$$

$$x, y, z > 0$$

$$x, y, z < 1$$

By setting the *ALL-ON-SAT* and *GRD W/O ABX* scores equal to determine the point where the *GRD W/O ABX* option becomes favorable under these worst-case weighting conditions, the weighting factors solution space is determined by two equations in three unknowns (the intersection of two planes being a line). Thus, only one weighting factor is an independent variable. For this analysis, the *Robustness* weight was varied, thereby determining the corresponding weights of the other two branches. These solutions are shown in Figure 3.9.

The *GRD W/O ABX* option was superior in terms of performance only when either the *Execution* or the *Ease of Use* considerations were weighted less than 0.22. It would require a considerable shift in the weighting of the performance branches, even in this worst-case scheme (discounting the *ALL-ON-SAT* advantages in terms of cost, schedule, and safety), to result in a favorable *GRD W/O ABX* scenario. For any weight distribution considered reasonable (i.e., not so skewed towards *Robustness*) by the team and decision maker, the *ALL-ON-SAT* alternative maintained its advantage in overall utility. Thus, this advantage was not very sensitive to the weighting factors.

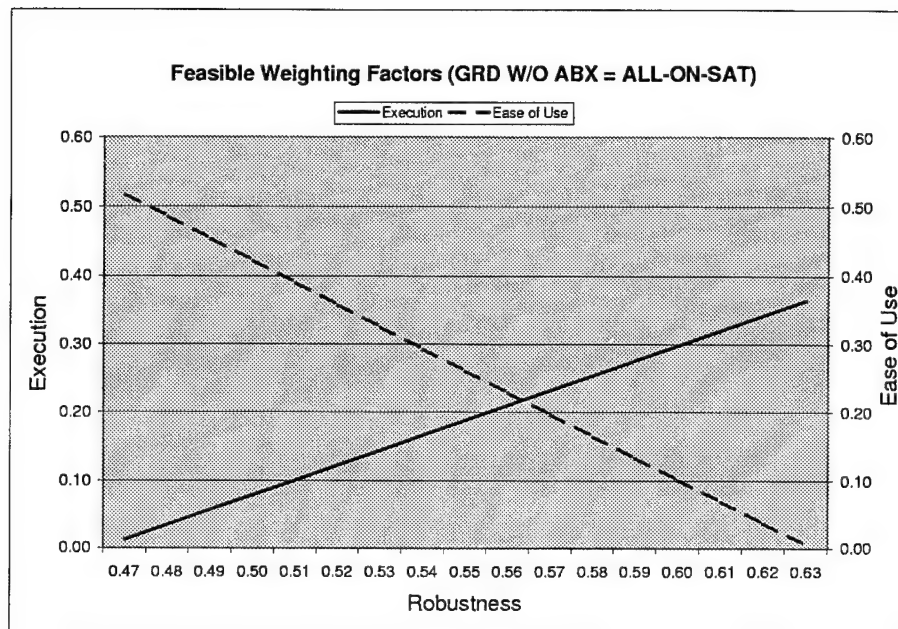


Figure 3.9 Feasible Alternate-Result Weighting Factors

3.4.6 Preferred Design. Based on the system scoring results and the sensitivity analysis, the *ALL-ON-SAT* option was selected as the preferred architecture for further design. The design resulting from the Preliminary Design phase included momentum wheels and rate gyros for the ADACS functions, full onboard processing capability for the C&DH system, lead acid batteries for power, and COTS wireless communications. This system architecture provided a baseline for more detailed development in the Detailed Design phase.

IV. Detailed Design

4.1 Overview

In this lifecycle phase, subsystem design began in detail. The subsystem architecture selected in the Preliminary Design phase was further refined, with emphasis on resolving system integration and interface issues. The phase began with a system-level investigation to determine the preferred battery configuration, momentum wheel sizes, momentum wheel motors, and rate gyros. Once these decisions were made, detailed subsystem design began in full. Research and system trade studies were used to select preferred subsystem configurations and vendors. The software control laws were developed and integrated into the C&DH architecture. Structural design and subsystem integration were accomplished using the systems approach. The final product of this phase was a detailed functional system architecture with subsystems designed and integrated to the maximum extent possible. This chapter documents the design iterations encountered in Detailed Design. The waterfall design model in Figure 4.1 highlights the focus of this chapter.

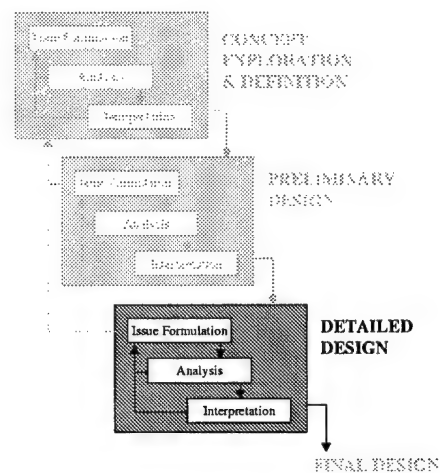


Figure 4.1 Detailed Design Activity

4.2 First-Iteration Issue Formulation

4.2.1 Problem Statement. This "first cut" through the Detailed Design phase addressed the following problem:

Based on the subsystem classes developed in the Preliminary Design phase, refine these subsystem alternatives such that control laws can be developed, simulation of SIMSAT behavior can be made, and structural design can be initiated in detail.

4.2.2 Updated System Architecture. As a starting point for the Detailed Design phase, the system architecture resulting from the Preliminary Design phase was summarized. The basic architecture is listed in Table 4.1.

Table 4.1 Detailed Design Baseline Architecture

Subsystem	Preliminary Design Decision
Attitude Determination	Rate Gyros
Attitude Control	Momentum Wheels
Power	Sealed Lead Acid Batteries
C&DH	All-Onboard AutoBox Processing
Communications	COTS Wireless LAN/Modem
Structures	As Required

4.2.3 First-Iteration Design Issues.

4.2.3.1 ADACS. The momentum wheel alternative, chosen in Preliminary Design, required the design of momentum wheels and the selection of motors to drive the wheels, to provide attitude control. Attitude determination was to be accomplished through the use of rate gyros. The following paragraphs highlight the ADACS issues to be addressed in this design iteration.

Momentum Wheels. Three momentum wheels were used to provide attitude control torques in the three axes – roll, pitch, and yaw. Determination of the size and inertial properties of the momentum wheels was required in order to begin wheel fabrication, as well as to be used in system modeling, controller development, and

structural design. Thus, the physical design of the momentum wheels was identified as a key design issue to be addressed in this first iteration of Detailed Design. In order to evaluate momentum wheel designs, an equations-of-motion (EOM) model first needed to be developed.

Motors. The type of motors used to rotate the momentum wheels needed to be understood at this stage to ensure compatibility with the dSPACE software, and to accommodate system modeling and momentum wheel sizing. Motor sizing was also necessary for structural development. Identification of motor types and selection of a preferred motor class were therefore identified as necessary in this iteration.

Rate Gyros. Regarding attitude determination, selection of a preferred rate gyro alternative was also identified as a critical system decision. The rate gyro determined much of the rate accuracy necessary for controller feedback in the execution of experiments. Furthermore, system-level development at this stage required narrowing the rate gyro solution class, which was far too broad for detailed design of C&DH interfaces and control laws.

Safety. Because of the high RPM momentum wheel design, a safety mechanism was required to prevent small, loose items onboard the satellite from ricocheting dangerously off the wheel. Catastrophic failure of a motor shaft needed to be contained, as well, to prevent extensive satellite damage and risk of injury. Thus, an enclosed box around the momentum wheels was also required as part of the momentum wheel assembly.

Thrusters. Regarding thruster augmentation, selection and incorporation of a thruster assembly was not made at this stage of the design. Thrusters were identified as non-critical items for baseline *SIMSAT* operation and were left for later design, after critical subsystems were addressed. Thrusters were, however, considered in the power requirements and mass/inertia estimates to ensure feasible implementation if thrusters were later added.

4.2.3.2 Power. The Preliminary Design decision to use sealed lead acid batteries did not specify the number or sizes of batteries to be considered. At this stage of the design, power requirements needed to be developed for each subsystem, battery configurations needed to be considered, and a preferred power architecture was required. The relatively heavy nature of the power system made choice of batteries crucial to accommodate structural development, and to necessitate the feasibility of subsystem power requirements before further design progression was made.

4.2.3.3 C&DH. The use of onboard processing through the dSPACE AutoBox was resolved in the Preliminary Design phase. At this stage, the AutoBox was ordered and delivered, and wired integration with the dSPACE ground software was accomplished by Mr. Hanke as part of his thesis. For the problem statement addressed in this iteration, no additional C&DH issues were identified as critical to continued design.

4.2.3.4 Communications. Research into commercially-available wireless LANs suitable for AutoBox/dSPACE connectivity indicated that the power requirements, mass properties, and associated costs of available systems were similar ¹. At the system level, the wireless LAN choice did not impact structural design, control law development, or power requirements. Therefore, selection of a preferred wireless LAN was left for a separate design subproblem.

Since integration of the REALMOTION software was not addressed at this stage of the design, selection of a wireless modem to provide the REALMOTION data link was also not addressed. Although desired, REALMOTION data was not critical to *SIMSAT* operation and experimental capability. With limited schedule available, integration of the wireless LAN (a critical link in system operation) proceeded the wireless modem development. As with the thruster augmentation, consideration of future wireless modem integration was made at this stage to ensure feasible implementation once the REALMOTION issues were fully addressed.

¹Section 4.2.6.6 describes these systems more fully.

4.2.3.5 Structures. From a structures standpoint, only a baseline concept was necessary at this stage of the design. Structural weight and inertia properties could thereby be used in system modeling and momentum wheel development. Detailed structural development was left for after this first iteration, following determination of sizes and shapes of the momentum wheels, motors, and batteries.

4.2.3.6 Issues Summary. The following list represents the key issues identified for address in this design iteration:

- Development of an EOM system model.
- Specification of a preferred momentum wheel design.
- Selection of a class of momentum wheel motors.
- Specification of rate gyros for attitude determination.
- Preliminary design of a momentum wheel casing.
- Determination of system power requirements.
- Selection of a preferred battery configuration.

4.2.4 Value System Design. The objectives hierarchy created in the Preliminary Design phase, shown in Figure 3.5, served as a starting point for a modified VSD for this design iteration. Values and measures which were determined to provide no system differentiation, with respect to the reduced subsystem solution spaces, were eliminated from the hierarchy. Furthermore, several measures were added in order to capture some of the system aspects compared in this iteration. The resulting objectives hierarchy is shown in Figure 4.2. This hierarchy was relatively streamlined and allowed direct comparison and weighting of all measurables without the need for branch weights. The top-level values were more specific than those addressed in Preliminary Design, corresponding to the increased specificity of the system architecture at this stage. Modifications from the Preliminary Design VSD, as well as description of the measurables for each top-level value, are described in the following paragraphs.

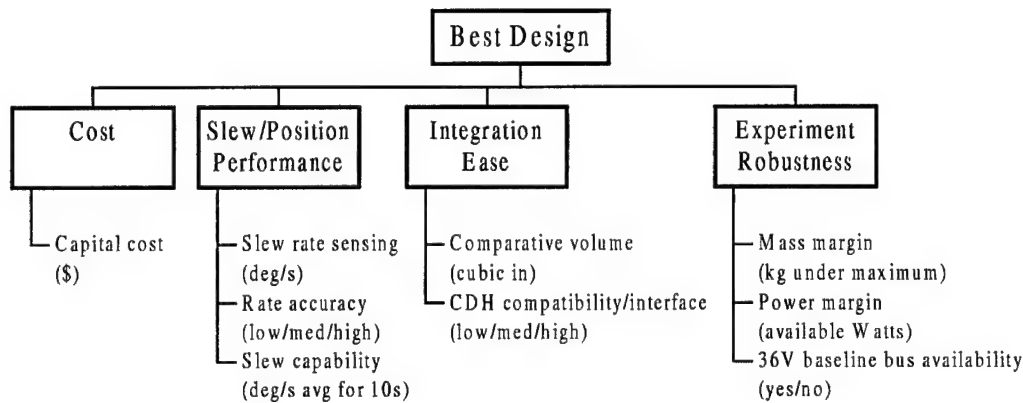


Figure 4.2 Detailed Design Objectives Hierarchy

4.2.4.1 VSD Modifications. The *Schedule* value identified in the Preliminary Design VSD was no longer appropriate at this stage because each subsystem class was reduced such that no significant differences in order, delivery, or integration times were identified. Thus, this value provided no tradable measures. Similarly, the *Safety* branch of the earlier VSD provided no identifiable system differentiation at this stage, and was likewise removed as a top-level value. *Cost* remained in the objective hierarchy.

The *Performance* value was also modified significantly. With the decision to use onboard AutoBox processing, the C&DH architecture was basically set. The communications link was thereby driven by the dSPACE/AutoBox requirements. Thus, the C&DH/communications architecture determined the measures related to data capability, command and control, communications requirements, and the ground station environment. These aspects of performance were no longer tradable.

Three performance areas were identified as top-level values: *Slew/Position Performance*, *Integration Ease*, and *Experiment Robustness*. The measures of *Slew/Position Performance* were taken from the *Satellite Movement* branch of the Preliminary Design VSD. These measures still allowed system differentiation and were considered important aspects of overall performance. The *Integration Ease* branch provided means to compare the technical integration aspects of the system alternatives. The *Experiment Robustness* branch again included mass and power margins, as well as the ability to readily support thruster integration.

4.2.4.2 Cost. The single measure of *Capital Cost*, expressed in dollars, was used at this stage. Significant differences in O&M costs were not identified within the reduced subsystem solution classes and were therefore not explicitly considered.

4.2.4.3 Slew/Position Performance. The three measures within this top-level value directly correspond to those of the *Satellite Movement* branch of the Preliminary Design VSD. *Slew Rate Sensing* measured the system's range of reliable slew rate data. *Rate Sensing Accuracy* measured the system's accuracy of slew rate data within the system's reliable data range. These two measures were determined by the choice of rate gyros used on the satellite. The last measure, *Slew Capability*, again was defined as the maximum slew capable within a 10sec maneuver.

4.2.4.4 Integration Ease. As a means of quantifying the ease of integration, *Comparative Volume* measured the relative volume of competing alternatives. This proxy measure was based on the assumption that larger volumes (all else equal) are more difficult to integrate due to their size and decreased modularity. The second integration measure, *C&DH Compatibility/Interface*, was a subjective measure to assess the compatibility of alternatives with the dSPACE/AutoBox architecture. This measure accounted for difficulties in communication and control of motor and rate gyro alternatives.

4.2.4.5 Experiment Robustness. Again, the *Mass Margin* and *Power Margin* were identified as important measures of SIMSAT performance. A third measure, *36V Baseline Bus Availability*, was a binary (yes/no) indicator of 36V capability. Use

of this indicator as a robustness metric was based on several assumptions: (1) thrusters would be more difficult to integrate using a 24V maximum capability, (2) a 36V bus would offer greater experimental robustness, and (3) a 36V bus would accommodate all baseline power requirements. Section 4.9.5.1, page 4-91, describes the 24V versus 36V power system rationale in detail.

4.2.5 Equations-of-Motion (EOM) Modeling. Before conceptualization of momentum wheel alternatives could be made, EOM modeling was required to provide a system model allowing exploration and understanding of momentum wheel performance. This model would be used to estimate slew rates of various system alternatives for analysis within this first Detailed Design iteration. In addition, an EOM model would be useful in later controller development and satellite simulation. Appendix B details the complete EOM development used in this design iteration.

4.2.6 System Synthesis. For the system synthesis step, system alternatives were generated to address the issues presented in Section 4.2.3.6. Subsystem alternatives within each respective solution class selected in Preliminary Design were first considered. These subsystem alternatives allowed selection on the system level of a preferred momentum wheel design, preferred motor type, preferred rate gyro assembly, and preferred battery configuration. The dSPACE/AutoBox C&DH architecture served as a constraint inherent in each system alternative. Additionally, since the wireless LAN alternatives at this stage were similar at the system level, a representative wireless LAN subsystem was used as a baseline for each alternative. Structural configurations were not addressed explicitly at this stage of the design. The following paragraphs describe the subsystem alternatives considered for analysis.

4.2.6.1 Momentum Wheels. The EOM modeling allowed comparison of various momentum wheel configurations. Appendix C describes the methodology and analysis of the momentum wheel sizing problem. The resulting configurations retained for system-level analysis are listed below. As described in Appendix C, these alternatives allowed distinct size versus slew performance tradeoffs.

- 12.5"-diameter wheels with an aluminum hoop affixed to an aluminum disk.
- 9"-diameter wheels with a steel hoop affixed to an aluminum disk.
- 8"-diameter wheels with a steel hoop affixed to an aluminum disk.

4.2.6.2 Motors. The motors were required to drive the momentum wheels. As a starting point in their selection, several desired characteristics were defined, as listed below:

- Control based on inputs from position (or rate) sensors.
- Controlled by either wheel speed or torque commands.
- Provide sufficient torque over the entire speed range of the motor.
- Use of a DC power supply.
- Based on initial figures, need a continuous torque of at least 150 oz-in.
- Maximize the peak torque.
- Minimize the motor's size and weight.

The first three characteristics were used to determine the required motor type for the *SIMSAT* application, using the Motor Selection Guide in the Oriental Motor General Catalog [41:12]. One solution class emerged: brushless DC motors. According to the manual, these motors provided sufficient torque across the entire speed range, could be operated by speed control, and could be controlled based on inputs from position (or rate) sensors.

While research indicated a wide variety of brushless DC motors were available, there were surprisingly few choices which met the general requirements of the design. Due to high power requirements, insufficient torque values, unacceptable physical dimensions, or excessive mass requirements (based on an initial 18kg mass budget for the ADACS subsystem), many alternatives were eliminated. Dr. Chris Hall, a noted specialist in the area of space systems design and spacecraft attitude and determination control, recommended the

Animatics SmartMotor series to the design team. Dr. Hall had used the SmartMotor series in his previous momentum wheel research due to their flexibility and programmability.

In addition to satisfying performance requirements, the SmartMotor has an internal memory chip within its controller which stores various control programs. Depending on the application, the program could be changed prior to an experiment to change the characteristics of the motor. This capability was initially determined to be of possible use in *SIMSAT* operation.

Based on the available information, one SmartMotor (model 3450) was purchased for research and testing through Servo Systems, Co., of Montville, NJ. With end-of-year funds available, this short-notice purchase would allow insight into the SmartMotor before ordering all three motors. Other laboratory uses of the motor were intended should the motor prove to be unacceptable or less desired for *SIMSAT* application. Table 4.2 shows some of the characteristics of the SmartMotor. The SmartMotor's parameters were used to provide a general motor model for the MATLAB code used in the EOM modeling (see Appendix B).

Table 4.2 SmartMotor Characteristics [51]

Parameter	Value
Peak Torque	750 oz-in
Continuous Torque	250 oz-in
Voltage Constant	13.7V/krpm
No Load Speed	3398 RPM
Torque Constant	18.5 oz-in/Amp
Rotor Inertia	0.025 oz-in-sec ²
Weight	3.47 kg
Number of Poles	4
Number of Slots	24
Length	6.088 in

Once the SmartMotor was delivered, more knowledge was gained on the interface issues between the AutoBox and the SmartMotor. It became apparent that intermediate components would be needed to allow the AutoBox to control the motor. In particular, the outgoing signal from the AutoBox was an analog signal. The SmartMotor was primarily

designed for a digital signal. To properly convert the signal, an Animatics I/O-116 analog card was needed to convert the $\pm 5V$ analog input signal to a 16-bit digital signal. Additionally, to read wheel speed information from the motor, a velocity reader chip attached to the SmartMotor's encoder was needed to provide an analog input to the Autobox. Due to these requirements, the complexity of the system was significantly greater than originally anticipated.

Since the SmartMotor was initially designed as a stand-alone system, it did not integrate well with other controllers performing the same function (such as the AutoBox processor). By purchasing I/O cards and velocity reader chips, the SmartMotor controller would essentially be bypassed.

Through discussions with Mr. Edmund Kong, a technical support representative at Animatics, an alternative solution appeared. A different motor, the BL-3450, did not use the integrated controller and amplifier of the SmartMotor, but provided similar performance. Its characteristics are shown in Table 4.3. This motor offered the simplicity of a direct connection to/from the AutoBox through an amplifier. Additionally, since the motor's parameters were identical to the SmartMotor, the MATLAB code used for EOM modeling required no modifications.

Table 4.3 "Dumb" Motor Characteristics [51]

Parameter	Value
Peak Torque	750 oz-in
Continuous Torque	250 oz-in
Voltage Constant	13.7V/kRPM
No Load Speed	3398 RPM
Torque Constant	18.5 oz-in/Amp
Rotor Inertia	0.025 oz-in-sec ²
Weight	3.27 kg
Number of Poles	4
Number of Slots	24
Length	6.088 in

Both the Animatics SmartMotor 3450 and Animatics BL-3450 (referred to as the "smart" motor and "dumb" motor, respectively) were considered in system-level analysis in this design iteration, as neither model was superior in all performance measures.

4.2.6.3 Momentum Wheel Safety. As described previously, enclosure of the momentum wheels was required to protect against equipment damage or personnel injury should a loose part contact a rotating wheel or a motor shaft catastrophically fail. It was desired that this enclosure be strong enough to provide safety benefits, yet light enough to minimize weight penalties. Furthermore, a clear enclosure would allow visual observation of the momentum wheels during operation, enhancing the teaching utility of the system and allowing for monitoring of the motors and wheels. It was decided that lexan would be a logical choice for such an application. This strong, clear material was readily available from a local supplier, Dayton Plastics of Dayton, OH. Further evaluation of the momentum wheel enclosure was determined to be of little value, as the lexan solution satisfied all requirements.

4.2.6.4 Rate Gyros. Internet resources, as well as discussions with Capt. Agnes and Mr. Anderson of AFIT/ENY, were used to research gyro alternatives. The main problem with finding an adequate gyro for *SIMSAT* was that most gyros are built for a specific application. Commercially-available gyros are often used for small applications such as model airplanes and model helicopters. While these alternatives were relatively inexpensive (under \$200 per gyro), the accuracy of these systems was unknown. At the other extreme, space-rated systems offered excellent accuracy capability with small drift rates. However, the cost of these systems was deemed infeasible. As a compromise, the gyros used with full-size aircraft (such as helicopters) provided a middle ground in both the cost and performance for this design application.

After researching the alternatives, two systems were identified and purchased with fallout money at the end of FY98. The NEJ-3000 Piezo Gyro, developed by JR Propo, fell within the model helicopter category. Based on information from model helicopter resources, this rate gyro was the best model helicopter gyro available with respect to drift rates and operating ranges. However, to integrate the gyro successfully, additional servos

were needed to provide the power and reference signal for the gyro (\$20-\$50 per servo). Since technical support was provided by the Horizon Service Center in Champaign, IL, this alternative was labeled the Horizon gyro within this design iteration. The Horizon gyro specifications, provided by the manufacturer, are shown in Table 4.4.

Table 4.4 NEJ-3000 Characteristics

Parameter	Value
Operating Voltage	4.8V
Operating Current	0.05A
Weight	0.037 kg
Slew Rate Range	± 720 deg/sec
Half Range Accuracy	7.2 deg/sec
Full Range Accuracy	28.8 deg/sec

The second alternative, the CF75 Series Axis rate gyro, was developed by Humphrey, Inc., located in San Diego, CA. In addition to being a three-axis rate gyro used on full-size helicopters, the CF75 also included linear accelerometers that could be used for more precise position measurements. Additionally, unlike the Horizon gyro, the rate ranges were not pre-determined and could be adjusted to fit the needs of *SIMSAT* during development². This alternative was also more expensive than the Horizon gyro. Table 4.5 lists the Humphrey gyro specifications provided by the manufacturer and the selected sensing ranges.

4.2.6.5 Battery Configurations. Using the sealed lead acid battery solution class, battery vendors were first considered. Based on technical data regarding specifications and performance, the Power-Sonic line of sealed lead acid batteries was chosen as the baseline for power subsystem development. Power-Sonic products were distinguished by their high discharge rate compared to other lead acid batteries; low internal resistance allows discharge currents of up to ten times the rated capacity of the battery. Additionally, the use of special separators, advanced plate composition, and a finely balanced electrolyte system greatly improves the ability of Power-Sonic batteries to recover

²See Appendix D for a description of the gyro range determination.

Table 4.5 Humphrey CF75 Characteristics

Parameter	Value
Operating Voltage	28±4V
Operating Current	0.58A
Weight	1.05 kg
Roll Rate Range	±120 deg/sec
Roll Accuracy (Half Range)	1.2 deg/sec
Roll Accuracy (Full Range)	4.8 deg/sec
Pitch/Yaw Rate Range	±40 deg/sec
Pitch/Yaw Accuracy (Half Range)	0.6 deg/sec
Pitch/Yaw Accuracy (Full Range)	2.4 deg/sec

from excessively deep discharge [43]. The availability and wide range of batteries also justified the decision to use Power-Sonic products.

The next step in determining battery alternatives was to select appropriately sized batteries. The capacity of a battery is the total amount of electrical energy available from the fully charged cell(s). Battery capacity depends on the discharge current, temperature during discharge, final cut-off voltage, and general battery history. Capacity, expressed in Ampere-hours (Ahr) is the product of the current discharged and the length of discharge time. The rated capacity of a battery is measured by its performance over 20 hours of constant current discharge at a temperature of 20 degrees Celsius to a cut-off voltage of 1.75 volts. For a battery discharging at a constant rate, its capacity changes according to the system load. Capacity increases when the discharge current is less than the 20 hour rate, and decreases when the current is higher.

To choose the appropriately sized battery capacity for *SIMSAT* use, a hypothetical power profile was established for basic sizing estimates. "Worst-case" values were obtained by assuming maximum power draw (full load on all components) for the longest possible experiment length. With the bus voltage specified as 24V or 36V, the required battery capacity was determined using logarithmic sizing graphs provided by Power-Sonic. For example, assuming a constant discharge current of 10A for one hour, an 18-Ahr battery provides the required power (rather than the 10-Ahr value suggested by strict dimensional analysis). In this way, various combinations of Power-Sonic batteries were selected, with

both 24V and 36V alternatives considered. These five battery alternatives are displayed in Table 4.6.

Table 4.6 Battery Configuration Alternatives

Alternative Designator	Battery Setup	Rated Capacity	Amps at 0.5C rate (1.3 hr)	Actual Capacity (1.3 hr)	Amps at 1.0C rate (33 min)	Actual Capacity (33 min)
3-batt-18	3 Batteries 18 Ahr	54 Ahr (36V)	27	35.1 Ahr	54	29.7 Ahr
3-batt-12	3 Batteries 12 Ahr	36 Ahr (36V)	18	23.4 Ahr	36	20.2 Ahr
3-batt-10	3 Batteries 10 Ahr	30 Ahr (36V)	15	19.5 Ahr	30	16.8 Ahr
2-batt-18	2 Batteries 18 Ahr	36 Ahr (24V)	18	23.4 Ahr	36	19.8 Ahr
2-batt-12	2 Batteries 12 Ahr	24 Ahr (24V)	12	15.6 Ahr	24	13.4 Ahr

4.2.6.6 Wireless LAN. As stated previously, a baseline wireless LAN system was used for each system alternative. Based on initial research³, only two COTS wireless LAN systems were available to meet the 10Mbps Ethernet specification required for dSPACE/AutoBox communications. Aironet Wireless Communications, Inc., of Akron, OH, offered the 11Mbps Aironet 4800 Turbo DS Series as of 1 December 1998 [2]. The AP4800 uses 2.4GHz RF transmission at 100mW transmission power, with a Type II PC-card interface. System-level specifications included a 12V power supply at 1.5A, 0.7kg mass, and dimensions of 20cm x 15cm x 5cm. The second alternative was produced by RadioLAN of Sunnyvale, CA [45]. RadioLAN's ISA CardLINK system offered 10Mbps Ethernet connectivity using 5.8GHz transmission at 50mW output. System-level specifications included 12V power supply at 50mA (or 5V at 500mA) for the ISA interface card, 0.5kg mass, and dimensions of 18cm x 7cm x 4cm. Thus, both systems offered comparable performance and physical specifications. As they were also similarly priced, they offered similar system-level interactions, justifying the selection of a wireless LAN model as a separate subproblem to be addressed in later design.

³Detailed wireless LAN specifications are described in Section 4.8, page 4-80.

For this design iteration, RadioLAN's ISA CardLINK was chosen as a baseline for all system alternatives. This model was available at the time this design iteration was accomplished (unlike the Aironet 4800 model), prompting its choice as a baseline.

4.2.6.7 Alternatives Summary. Table 4.7 shows the subsystem alternatives used to generate system alternatives for analysis in this phase. System alternatives were constructed using the full-factorial combinations of the subsystem alternatives. Thus, a total of 60 system alternatives were considered.

Table 4.7 Detailed Design Subsystem Alternatives

Subsystem	Alternatives
Attitude Determination	Humphrey Gyros Horizon Gyros
Attitude Control (Momentum Wheels)	Aluminum Hoop/Aluminum Disk (12.5"-dia.) Steel Hoop/Aluminum Disk (9"-dia.) Steel Hoop/Aluminum Disk (8"-dia.)
Attitude Control (Motors)	"Smart" Motors "Dumb" Motors
Power	3 Batteries (18 Ahr) 3 Batteries (12 Ahr) 3 Batteries (10 Ahr) 2 Batteries (18 Ahr) 2 Batteries (12 Ahr)
C&DH	Onboard AutoBox Processing
Communications	RadioLAN (Wireless Baseline)
Structures	As Required

4.3 First-Iteration Analysis

4.3.1 System Modeling. The following sections describe the system modeling used to evaluate each measurable of the objective hierarchy (Figure 4.2).

4.3.1.1 Capital Cost. This measurable was assessed through summation of the subsystem costs for each alternative. With the narrowed system configurations, integration costs were considered to be similar for each system alternative, and were thus not included in this measurable. Furthermore, costs associated with the in-house manu-

facturing of the momentum wheel designs, using the AFIT fabrication shop, were also not included. The baseline costs of the AutoBox and wireless communications were also not included, as these costs were common to all configurations. At this stage of the design, both rate gyro systems were purchased (using "fallout" funds from FY98). Rate gyro costs were therefore not included in the *Capital Cost* measure since these costs were considered unrecoverable for either gyro alternative. Thus, the motors and batteries comprised the *Capital Cost* measure.

4.3.1.2 Slew Rate Sensing. This measure was assessed using the slew rate ranges given by the rate gyro specifications, measured in deg/sec. Thus, this measure was gyro-dependent.

4.3.1.3 Rate Sensing Accuracy. Like *Slew Rate Sensing*, this measure was based on gyro capabilities. A resolution of low (poor sensing range), medium (adequate sensing range), and high (good sensing range) was used to model the relative accuracy of the gyro alternatives based on their intended applications and performance specifications.

4.3.1.4 Slew Capability. A MATLAB simulation, based on the EOM modeling of Appendix B, was used to estimate maximum slew maneuvers in a 10sec period. Since the motor alternatives had comparable weight and torque capabilities, this measure was considered independent of the motor selection. Moreover, the choice of battery size had negligible effects on slew performance since battery mass was a small percentage of total system weight. However, the choice between a two- or three-battery configuration significantly impacted slew maneuvers since motor outputs differed for a 24V system versus a 36V system. The choice of momentum wheel configuration also impacted this measure, as the momentum wheels provide the necessary slewing torques.

4.3.1.5 Comparative Volume. This proxy measure of structural modularity did not include the gyros or motors, as the relative volumes of alternatives were similar. Thus, volume differences between system configurations were dependent on the choice of battery configuration as well as the choice of momentum wheel design. The wheel

volumes assumed a 1/4" (thick) lexan box with 1/2" clearance on each side enclosing each momentum wheel.

4.3.1.6 C&DH Compatibility/Interface. This subjective measure was modeled using the assumption that non-dSPACE control software (inherent in the smart motors) would be difficult to circumvent. The experience with the smart motor showed that this condition was indeed the case⁴. The gyro compatibility with the AutoBox was also considered in the mental modeling of this measure. The following resolution was used in the evaluation of this measure:

- **Low.** Significant interface challenges (in number or magnitude) were anticipated.
- **Medium.** Some interface challenges were anticipated.
- **High.** Few, if any, significant interface challenges were anticipated.

4.3.1.7 Mass Margin. A maximum system weight of 300lb was used to determine this margin. The weight of all components, including representative thrusters, was subtracted from this 300lb. Thus, this measure represents the maximum payload mass supportable by the system. Because the structure was as yet undetermined, the mass of all components was increased 30% for each configuration to account for structural weight and cabling. Lexan boxes (1/4" thick) were included in the mass of the momentum wheels.

4.3.1.8 Power Margin. This measure was defined as available payload power, measured in Watts. The total power consumption of each alternative was subtracted from the total power output of each battery configuration. Power consumption was based on performance specifications, motor models, and, in the case of the AutoBox, actual experimental data⁵.

⁴The motor purchased in FY98 was controllable using the supplied PC-based control software, but integration with dSPACE would require this software to be bypassed. Conversation with Animatics engineers revealed that this design problem was not trivial.

⁵Using an external DC power source, the AutoBox was shown to draw approximately 60W in the laboratory, significantly less than the 135W peak power specification.

4.3.1.9 36V Baseline Bus Availability. This binary measure was modeled as "yes" for 36V battery configurations, and "no" for 24V configurations.

4.3.2 Raw Values. The raw values for all 60 system configurations are shown in Appendix F, Tables F.1 and F.2.

4.3.3 Utility Scaling. The next step in the system evaluation of these alternatives was to determine a common utility scale for each measure. As in the Preliminary Design phase, a scale ranging from 0 (no utility) to 10 (excellent utility) was used. Direct inputs from the decision maker were used to construct the utility scale for each measure. These inputs are summarized in Figure 4.3. For each system alternative, the raw values for each measurable were scaled using these utility functions.

Objective Measurable	Utility Scale										
	0	1	2	3	4	5	6	7	8	9	10
Capital Costs	\$7,400 -----> Linear Scale -----> \$5,400										
Slew Rate Sensing (deg/s range)	20 -----> 720										
Rate Sensing Accuracy	Low -----> High										
Slew Capability (deg/s avg - 10s)	5.98 6.38 -----> 7.00 -----> 9.06 9.69 10.77										
Comparative Volume (in ³)	> 900 800-900 -----> 700-800 -----> 600-700 -----> 500-600 -----> < 500										
CDH Compatibility/Interface	Low -----> Medium -----> High										
Mass Margin (kg)	58 -----> Linear Scale -----> 76										
Power Margin (W)	0 -----> Linear Scale -----> 550										
36V Bus Availability	No -----> Yes										

Figure 4.3 Detailed Design Utility Scale

4.4 First-Iteration Interpretation

4.4.1 Weighting Factors. In order to convert scaled scores into system scores, the measurables were weighted using inputs from the decision makers. A judgement

matrix approach was used to generate an initial weighting factors vector. From this resultant vector, the decision maker modified the weighting factors for use in system ranking and selection.

4.4.1.1 Judgement Matrix Approach. As described by Sage [49], weighting factors can be determined through a one-to-one comparison of importance for all measures. This comparison, made by the decision maker, results in a matrix of relative importance, referred to as a *judgement matrix*. For each measurable, a geometric mean of the relative importance “scores” across every other measurable can be computed. These geometric means are then normalized to produce initial weighting factors.

For this design iteration, the judgement matrix shown in Figure 4.4 was considered by the decision maker. This figure shows the scale used in importance estimation, the decision maker inputs, and the resulting weighting factors.

4.4.1.2 Weighting Factor Refinements. The decision maker refined the weighting factors developed in the judgement matrix approach to better reflect the level of importance of each measure. The weighting factors vector used in system scoring is listed in Table 4.8.

Table 4.8 Ranked Weighting Factors

Measurable	Weighting Factor
Mass Margin	0.20
Power Margin	0.20
Slew Capability	0.20
Slew Rate Sensing	0.10
Rate Sensing Accuracy	0.10
CDH Compatibility/Interface	0.08
Capital Cost	0.04
Comparative Volume	0.04
36V Baseline Bus Availability	0.04
Components Sum	1.000

JUDGEMENT MATRIX DETERMINATION OF WEIGHTING FACTORS

A \ B	Capital Cost	Slew Rate Sensing	Rate Sensing Acc.	Comp. Volume	CDH Compatibility	Slew Capability	Mass Margin	Power Margin	36V Bus Avail.	GEOMETRIC MEAN	NORMALIZED WTS
Capital Cost	1.000	0.200	0.200	0.333	0.333	0.143	0.143	0.143	1.000	0.2864	0.022
Slew Rate Sensing	5.000	1.000	1.000	5.000	3.000	0.333	0.333	0.333	7.000	1.3906	0.108
Rate Sensing Acc.	5.000	1.000	1.000	5.000	3.000	0.333	0.333	0.333	7.000	1.3906	0.108
Comp. Volume	3.000	0.200	0.200	1.000	1.000	0.200	0.200	0.200	3.000	0.5220	0.041
CDH Compatibility	3.000	0.333	0.333	1.000	1.000	0.200	0.200	0.200	0.200	0.4328	0.034
Slew Capability	7.000	3.000	3.000	5.000	5.000	1.000	1.000	1.000	7.000	2.8129	0.219
Mass Margin	7.000	3.000	3.000	5.000	5.000	1.000	1.000	1.000	7.000	2.8129	0.219
Power Margin	7.000	3.000	3.000	5.000	5.000	1.000	1.000	1.000	7.000	2.8129	0.219
36V Bus Avail.	1.000	0.143	0.143	0.333	0.333	0.143	0.143	0.143	1.000	0.3590	0.028

Relative importance evaluated by Lt Col Kramer, 13 Nov 98.

sum: 12.8202 1

Judgement matrix is "reciprocal-symmetric"

RELATIVE IMPORTANCE SCALE:

- 9 = A is so important that B has little, if any, relative value
- 7 = A substantially more important than B
- 5 = A significantly more important than B
- 3 = A slightly more important than B
- 1 = A and B are comparable
- 1/3 = B slightly more important than A
- 1/5 = B significantly more important than A
- 1/7 = B substantially more important than A
- 1/9 = B is so important that A has little, if any, relative value

Figure 4.4 Objectives Judgement Matrix

4.4.2 System Ranking and Selection. The scaled scores for each system alternative were normalized and multiplied by the weighting factors vector to determine system scores for each alternative. These system scores were ranked, as shown in Appendix F, Table F.3. Slight adjustments to the weighting factors did not alter the top choices significantly. With just nine measurables to consider, the decision maker was comfortable with the weighting factors (they were direct in that no branch weights diluted important measures); thus, an in-depth sensitivity analysis was deemed to provide little added value. From these system rankings, subsystem conclusions were made.

4.4.2.1 Motors. In general, "dumb" motor alternatives ranked over "smart" motor alternatives. This result was logical since both motors produced comparable

torques, yet the smart motors were more expensive and difficult to interface with the AutoBox solution. These drawbacks more than offset the weight savings⁶ of the smart motors. Dumb motors were chosen for continued design.

4.4.2.2 Momentum Wheels. The 9" momentum wheels scored higher for comparable alternatives. Based on the weighting factors, this result was due to the compromise of lower slew rates relative to the 12.5" wheels for less weight and volume penalties. Alternatively, the 9" wheels gave enough performance advantage to offset the increased weight and volume relative to the 8" wheels. Thus, a 9" momentum wheel design was considered for further development.

4.4.2.3 Rate Gyros. The rate gyros did not provide much scoring differentiation, with the Humphrey model scoring slightly higher than the Horizon model. Before a decision was made, the Horizon model, designed for radio-control helicopters with a radio-control interface, was hooked up to an oscilloscope within the laboratory to better determine its signal data. Without complete signal documentation, these rate gyros were difficult to analyze. Additional system description was sought from the manufacturer with little results. The Humphrey models provided more complete documentation and were considered less risky to integrate. Thus, the Humphrey models were chosen for continued design. Should future problems warrant, the Horizon models were still available for implementation.

4.4.2.4 Battery Configuration. The 3-battery alternative with 18-Ahr batteries ranked atop the system alternatives. This alternative provided the greatest power availability which, upon system-level analysis, more than offset the additional cost and mass. This alternative was selected for *SIMSAT* implementation.

4.4.3 Implementation. The resulting system architecture is described in Table 4.9. This architecture served as the baseline for the Detailed Design subproblems addressed further in this design phase.

⁶Smart motors included controller software whereas dumb motors required an additional amplifier interface.

Table 4.9 Detailed Design Resulting Architecture

Subsystem	Detailed Design Decision
Attitude Determination	Humphrey Rate Gyros
Attitude Control (Momentum Wheels)	Steel Hoop/Aluminum Disk (9" outer diameter)
Attitude Control (Motors)	"Dumb" Motors with Amplifiers
Power	3 Batteries (18 Ahr)
C&DH	Onboard AutoBox Processing
Communications	COTS Wireless LAN/Modem
Structures	As Required

The first step in the implementation of this architecture was to deliver momentum wheel designs to the AFIT fabrication shop. Based on the shop's on-hand supplies, the momentum wheel sizes were slightly adjusted to accommodate quicker manufacturing. With the selection of the dumb motor option, three Animatics BL-3450 motors and accompanying amplifiers were ordered for the momentum wheel assembly. Power-Sonic 18-Ahr batteries were also ready for order at this time. A total of six batteries were procured; three for operation and three as spares, allowing complete swapping of batteries during experimentation without any recharge downtime.

At this stage, further design issues were formulated to progress to a final design. With the narrowing of the system architecture, detailed subsystem design could be accomplished without the need to make complete system alternative comparisons, as done in the previous design iterations. Subsystem design was accomplished on a system-level through the consideration of subsystem interfaces, system impacts, and subsystem integration. The following list of subproblems was identified for further detailed design:

- Development of the controller and command interface.
- Development of a baseline structural design.
- Calculation of static and dynamic structural deflections under loading.
- Selection of wireless communications vendors.
- Subsystem integration, to include signals and power.

- Design of a safety system for *SIMSAT* operation.
- Consideration of thruster integration.

The remaining portion of the Detailed Design chapter specifically addresses the systems approach to these subproblems.

4.5 *Command and Control Architecture*

4.5.1 Problem Statement. In the preliminary design phase, several decisions were made that affected the direction of command and control development in the Detailed Design phase. Since dSPACE software was selected for C&DH functions, and the method of attitude determination and control was chosen, actual coding of *SIMSAT* control software could begin. The problem statement dealing specifically with the software architecture was:

Based on the ADACS and C&DH system architectures developed in the Preliminary Design phase, design the software control laws and user interface(s) to meet requirements for SIMSAT operations.

4.5.2 Command and Control Issues. From the Preliminary Design phase, the system architecture included an ADACS subsystem consisting of momentum wheels and rate gyros and a C&DH subsystem employing full onboard processing using the dSPACE AutoBox. This Detailed Design iteration concerns the process of developing control laws for integration with ADACS and C&DH.

Based on the system needs, the following issues involving command and control development needed to be addressed to design a final product:

- It was necessary to determine an appropriate method of providing control to the ADACS hardware in order to meet performance requirements.
- To safely test the control law design off-line, and allow off-line simulations of system performance, a model of the *SIMSAT* plant dynamics was needed.

- Development of a user interface was required to provide command and control inputs to *SIMSAT*.
- A method of displaying real-time and post-test data from *SIMSAT* operations was essential to provide user feedback and allow experiment analysis.
- While managing the above issues, maintaining ease-of-use and user-friendliness of the ground station architecture was also necessary.
- Finally, the software architecture needed to be robust to allow future modifications for yet undetermined experiments.

4.5.3 Value System Design. To address these design issues, the following list of objectives was used in the development of the user interface and control laws:

- Ensure control law compatibility with the dSPACE software.
- To enhance control law processing, minimize extraneous software coding.
- Minimize the text-based software coding required for control law development to allow easier and quicker development.
- Maximize user friendliness through graphical methods to enhance command capability and real-time data display.
- To allow control logic modifications, maximize robustness of the control law development.
- Minimize additional costs incurred in software architecture development.

4.5.4 Development Approach. Based on the objectives, several design decisions were immediately apparent. To start, MATLAB-based software was chosen as the primary control law development tool. This software was compatible with the dSPACE software (MATLAB/SIMULINK interfaces were inherent in the dSPACE control architecture) and incorporated built-in control toolboxes and optimization routines. MATLAB and SIMULINK were also readily available at AFIT, and the design team had significant programming

expertise with this software. Although C-coding could be used directly by dSPACE, MATLAB/SIMULINK was easier to use and compiled to C-code. The COCKPIT and TRACE software provided the primary command and data display capabilities. These software packages were also dSPACE-compatible and already available with the dSPACE system. Likewise, REALMOTION was the preferred animation software, as it was also provided with the dSPACE system and allowed excellent graphical animation capability.

The basic approach to developing the command and control software architecture involved the following steps. First, a satisfactory mathematical model was created to simulate *SIMSAT* behavior during off-line simulations. Next, the control laws needed to operate the system according to requirements were established. Once a simulation demonstrating desired *SIMSAT* performance was developed, it was converted for download to the AutoBox. Finally, the software links required to provide graphical command and control, telemetry analysis, and 3-D motion simulation were developed.

Specifically, mathematical models were developed for the *SIMSAT* "plant" and controllers. Once these dynamic models were understood, the equations were coded into MATLAB software. This MATLAB program was then used to simulate the control laws. For real-time applications, and off-line simulations using the AutoBox, these models were coded in SIMULINK (based on the MATLAB code), a part of the dSPACE software suite. The dSPACE software then compiled this code to a working application and downloaded it to AutoBox. The COCKPIT and TRACE applications within the dSPACE suite were then used to create the "virtual" ground station.

4.5.5 Plant Model. Equations of motion were developed to create a dynamic mathematical model of the *SIMSAT* plant (see Appendix B). Originally used in system modeling and momentum wheel sizing, these equations facilitated control law development, simulation, and operational software verification. Based on the MATLAB coding of the equations of motion⁷, a *SIMSAT* plant model was developed within the SIMULINK environment. This plant model was developed with the same assumptions made in the equations of motion development (see Appendix B). For the SIMULINK version, the plant

⁷MATLAB code is provided in the *SIMSAT* User's Manual.

model also included code to link the equations of motion with the controller in a realistic manner.

4.5.6 Controller Model. Having the equations of motion to serve as a model of the *SIMSAT* plant, the next step was to develop a controller that was capable of performing three-axis active control. For this initial controller, it was assumed that sensor noise from the gyros was negligible (in addition to the other assumptions made while developing the equations of motion). As shown in Appendix C (Momentum Wheel Sizing), the asymmetric nature of *SIMSAT* led to inertial coupling between the roll, yaw, and pitch axes. As a result, simple open-loop control would not successfully maintain *SIMSAT* stability. Instead, closed-loop feedback control was required.

Figure 4.5 demonstrates the baseline closed-loop control design. Since the gyros to be used onboard *SIMSAT* provide angular velocity signals, rate feedback was available to the controller. In addition, angular position feedback was available by numerically solving the Euler rate equations.

Explanation of Figure 4.5 is as follows:

- $\vec{\theta}_{com}$ = user command input vector representing desired attitude angles

$$\vec{\theta}_{com} = \begin{bmatrix} \theta_{1com} \\ \theta_{2com} \\ \theta_{3com} \end{bmatrix}$$

where

θ_{1com} = desired roll angle

θ_{2com} = desired yaw angle

θ_{3com} = desired pitch angle

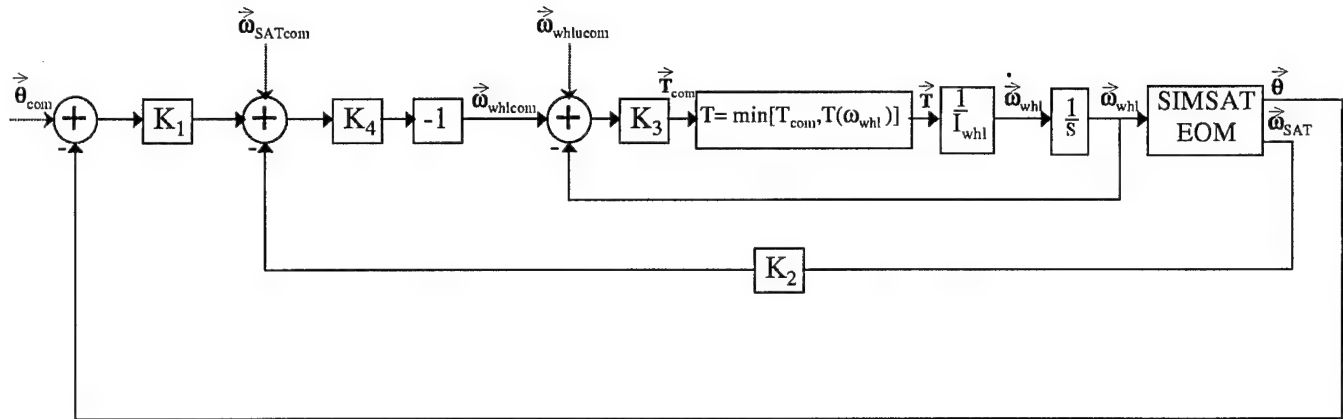


Figure 4.5 Closed-Loop Feedback Control

The user inputs all desired attitude angles in degrees, the computer simulation then converts these angles to radians.

- $K_1 = 3$ by 3 gain matrix of real numbers, baselined to be a diagonal matrix with off-diagonal terms equal to zero.
- $K_2 = 3$ by 3 gain matrix of real numbers, baselined to be a diagonal matrix with off-diagonal terms equal to zero.
- $K_4 = 3$ by 3 gain matrix of real numbers, baselined to be a diagonal matrix with off-diagonal terms equal to zero.
- $\vec{\omega}_{SATcom} = \underline{\text{user}}$ command input vector representing desired *SIMSAT* rotation rates

$$\vec{\omega}_{SATcom} = \begin{bmatrix} \text{desired roll rate} \\ \text{desired yaw rate} \\ \text{desired pitch rate} \end{bmatrix}$$

The user inputs these rates in degrees/second, the computer simulation then converts these to radians/second.

Note: $\vec{\omega}_{SATcom}$ does not represent desired Euler rates (defined as the time derivatives of the roll, yaw, and pitch angles). Instead, this vector represents the desired angular velocity of *SIMSAT*, written in the 'b' basis set (body-fixed reference frame), with respect to inertial space.

- '-1' block = scaling factor, needed because *SIMSAT* reacts (ideally) in the opposite direction from a commanded torque (according to the law of conservation of angular momentum for a rigid body).
- $\vec{\omega}_{whlcom} = \text{feedback control}$ vector of commanded momentum wheel/motor speeds (in radians/second), calculated from block diagram algebra

$$\vec{\omega}_{whlcom} = \begin{bmatrix} \text{wheel 1 commanded speed} \\ \text{wheel 2 commanded speed} \\ \text{wheel 3 commanded speed} \end{bmatrix}$$

Motor speed, rather than motor torque, was chosen as a control input because the Animatics BL-3450 motor was designed only for speed control. As a result, motor torque is indirectly controlled via motor speed.

Note: The Animatics motor speed controller (amplifier) is a separate item from the motor.

- $\vec{\omega}_{whlucm} = \text{user}$ command input vector of desired wheel speeds

$$\vec{\omega}_{whlucm} = \begin{bmatrix} \text{wheel 1 desired speed} \\ \text{wheel 2 desired speed} \\ \text{wheel 3 desired speed} \end{bmatrix}$$

The user inputs these desired wheel speeds in RPM, the computer simulation then converts these to radians/second.

- I_{whl} = moment of inertia of the wheel about an axis passing through its axle. This scalar quantity is the same for all three wheels since the wheels are identical in mass and shape. I_{whl} was calculated from the final momentum wheel design (i.e., the 8.625" outer diameter momentum wheels being produced by the AFIT fabrication shop) as:

$$I_{whl} = .0195 \text{ kg-m}^2$$

- K_3 = simple scalar gain representing the motor (and amplifier) transfer function. This gain roughly approximates the motor dynamics necessary for converting a wheel speed command input to a torque output. Since Animatics considered its motor and amplifier transfer function as "proprietary" information, a scalar gain was used to expedite *SIMSAT* closed-loop analysis. Experimental determination of the motor transfer function was not possible because of time limitations and because the motors had not been acquired yet.

Determination of K_3 : The motor/motor controller subsystem is represented by the inner-most feedback loop in Figure 4.5. For one motor/motor controller, this subsystem was simplified to be a scalar gain, K_{motor} , and an integrator as shown in Figure 4.6.

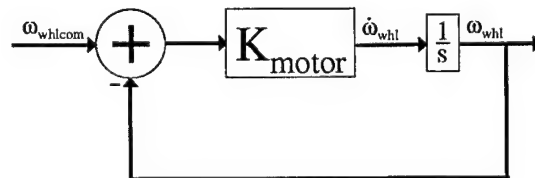


Figure 4.6 Motor Closed-Loop Feedback

The closed-loop transfer function of the motor/motor controller subsystem (in Laplace 's' domain) is:

$$\frac{\omega_{whl}(s)}{\omega_{whlcom}(s)} = \frac{K_{motor}}{s + K_{motor}}$$

where

$$K_{motor} = \frac{K_3}{I_{whl}}$$

Using this simple transfer function, a value of K_{motor} was sought to give a "reasonable" step response in the time domain. From the 36V Torque vs. Wheel Speed curve, the midrange speed of the motor is approximately 135 rad/sec (1300 RPM). Therefore, a 135 rad/sec step command for ω_{whlcom} was used as the input. Based on trial runs with the SmartMotor, it was known that the motor (starting from rest) took two to three seconds to reach its midrange speed after receiving a step command. It was also known that overshoot of a commanded speed was minimal. With this in mind, setting K_{motor} equal to 3 gave a reasonable response with no overshoot and approximately two seconds of settling time.

Note: For this analysis, it was assumed the dynamics of the BL-3450 motor were the same as the SmartMotor.

Solving for K_3 used in Figure 4.5:

$$K_3 = K_{motor}(I_{whl})$$

$$K_3 = 3(.0195)$$

$$K_3 = 0.0585$$

• \vec{T}_{com} = feedback control vector of commanded torques to each motor (in Newton-meters), calculated from block diagram algebra

$$\vec{T}_{com} = \begin{bmatrix} \text{motor 1 commanded torque} \\ \text{motor 2 commanded torque} \\ \text{motor 3 commanded torque} \end{bmatrix} = \begin{bmatrix} T_{com1} \\ T_{com2} \\ T_{com3} \end{bmatrix}$$

- $\vec{\omega}_{whl}$ = vector representing the measured speed of each momentum wheel in rad/sec. In the real world, $\vec{\omega}_{whl}$ will be provided by tachometer signals from the amplifiers.
- \vec{T} = vector of each motor's output torque (in N-m)

$$\vec{T} = \begin{bmatrix} \text{motor 1 output torque} \\ \text{motor 2 output torque} \\ \text{motor 3 output torque} \end{bmatrix} = \begin{bmatrix} \text{minimum}[|T_{com1}, T(\omega_{whl1})|] \\ \text{minimum}[|T_{com2}, T(\omega_{whl2})|] \\ \text{minimum}[|T_{com3}, T(\omega_{whl3})|] \end{bmatrix}$$

$T(\omega_{whl})$ is calculated from the 36V Torque vs. Wheel Speed curve described in the momentum wheel sizing problem of Appendix C.

Since the absolute value of T_{com1} , T_{com2} , or T_{com3} could be unrealistically large, the minimum operator is needed. This prevents the computer simulation from producing motor output torque (T_1 , T_2 , or T_3) that exceeds the motor's maximum continuous torque capabilities.

- $\dot{\vec{\omega}}_{whl}$ = vector of each wheel's angular acceleration in rad/sec²

$$\dot{\vec{\omega}}_{whl} = \vec{T}/I_{whl}$$

- $\frac{1}{s}$ block = represents integration with respect to time (in the "s" domain).
- *SIMSAT* EOM block = represents the *SIMSAT* equations of motion
- $\vec{\omega}_{SAT}$ = vector representing the angular velocity of *SIMSAT*, written in the 'b' basis set, with respect to inertial space. In the real world, $\vec{\omega}_{SAT}$ would be measured from the onboard gyros.

$$\vec{\omega}_{SAT} = \begin{bmatrix} \omega_{SAT1} \\ \omega_{SAT2} \\ \omega_{SAT3} \end{bmatrix} = \begin{bmatrix} \text{roll rate} \\ \text{yaw rate} \\ \text{pitch rate} \end{bmatrix}$$

Note again that the Euler rates are not contained in this vector

- $\vec{\theta}$ = vector of Euler angles (in radians) resulting from *SIMSAT* motion (angles are later converted to degrees for graphing purposes)

$$\vec{\theta} = \begin{bmatrix} \theta_1 \\ \theta_2 \\ \theta_3 \end{bmatrix} = \begin{bmatrix} \text{roll angle} \\ \text{yaw angle} \\ \text{pitch angle} \end{bmatrix}$$

As described in the equations of motion development (Appendix B), the Euler angles, $\vec{\theta}$, are calculated by numerically solving the Euler rate ($\dot{\vec{\theta}}$) equations. The Euler rate equations are written as a function of $\vec{\omega}_{SAT}$.

- For computational efficiency, a MATLAB variable time-step, Runge-Kutta numerical integration routine ('ODE 45') was used to solve for the system state. The state vector was defined as:

$$\vec{x} = \begin{bmatrix} \omega_{whl1} \\ \omega_{whl2} \\ \omega_{whl3} \\ \omega_{SAT1} \\ \omega_{SAT2} \\ \omega_{SAT3} \\ \theta_1 \\ \theta_2 \\ \theta_3 \end{bmatrix}$$

Specifically, Runge-Kutta integration was used to solve: $\dot{\vec{x}} = f(\vec{x})$

4.5.7 SIMSAT Control Options. At this point in the design process, the customers were interested in demonstrating basic feedback control of *SIMSAT*, not necessarily optimal control. The error signals (error = command signal - measured signal) were

manipulated through simple gain matrices to demonstrate closed-loop control. Although the *SIMSAT* equations of motion represent a nonlinear system, basic control was achieved by varying K_1 , K_2 and K_4 . Detailed linear control analysis methods, such as linearization of the equations of motion about certain operating points, closed-loop pole placement, and gain scheduling, were not attempted in this thesis. Since *SIMSAT* is an experimental test bed, other control approaches can be evaluated by future users.

The closed-loop control design shown in Figure 4.5 gives the user five control options. For all control options, it is assumed *SIMSAT* begins at a "base" configuration at time $t=0$. In the "base" configuration at $t=0$, the *SIMSAT* body-fixed axis system ('b₁', 'b₂' and 'b₃' basis set) described in Appendix B is aligned with the inertial axis system ('x', 'y' and 'z' basis set). The origin of the inertial axis system is located at the center of the central sphere and the 'y' inertial axis points directly at the laboratory ceiling. The 'x' inertial axis points at a pre-defined location in the laboratory, such as a painted mark on the north laboratory wall (or any other convenient wall). With the 'x' and 'y' inertial axes defined, the 'z' inertial axis can be deduced from right-handed orthogonality.

All *SIMSAT* maneuvers within the five control options are initiated by step-commands. Before a maneuver is initiated (at $t=0$), the *SIMSAT* state vector, \vec{x} , is assumed to be zero (i.e., $\vec{\omega}_{whl} = 0$, $\vec{\omega}_{SAT} = 0$ and $\vec{\theta} = 0$). For this thesis, sequential control maneuvers are not attempted. In other words, after one step-command maneuver is completed, the *SIMSAT* state vector is reset to zero in the computer simulation before the next maneuver is initiated.

The five control options are described below:

Option 1 (Target Mode):

The user enters a desired roll angle (range is ± 180 degrees), desired yaw angle (range is ± 360 degrees), and desired pitch angle (range is ± 25 degrees). For Target mode:

$$K_1 = \begin{bmatrix} k_{roll} & 0 & 0 \\ 0 & k_{yaw} & 0 \\ 0 & 0 & k_{pitch} \end{bmatrix} \text{ where } k_{roll}, k_{yaw} \text{ and } k_{pitch} \text{ are control design variables.}$$

$$K_2 = \begin{bmatrix} k_{rollrate} & 0 & 0 \\ 0 & k_{yawrate} & 0 \\ 0 & 0 & k_{pitchrate} \end{bmatrix}$$

where $k_{rollrate}$, $k_{yawrate}$ and $k_{pitchrate}$ are control design variables.

$$K_3 = .0585$$

$$K_4 = \begin{bmatrix} 1 & 0 & 0 \\ 0 & 1 & 0 \\ 0 & 0 & 1 \end{bmatrix}$$

$$\vec{\theta}_{com} = \begin{bmatrix} \text{desired roll angle} \\ \text{desired yaw angle} \\ \text{desired pitch angle} \end{bmatrix} \text{ (degrees)}$$

$$\vec{\omega}_{SATcom} = \vec{0}$$

$$\vec{\omega}_{whlucom} = \vec{0}$$

Option 2 (Target Mode with Roll Rate):

The user enters a desired yaw angle (range is ± 360 degrees) and desired pitch angle (range is ± 25 degrees). The user also enters a desired roll rate for *SIMSAT* (range is ± 9 RPM – without thrusters, *SIMSAT* cannot spin outside this range). The desired effect of this maneuver is for *SIMSAT* to point at a target while rolling. For this option:

$$K_1 = \begin{bmatrix} 0 & 0 & 0 \\ 0 & k_{yaw} & 0 \\ 0 & 0 & k_{pitch} \end{bmatrix} \text{ where } k_{yaw} \text{ and } k_{pitch} \text{ are control design variables.}$$

$$K_2 = \begin{bmatrix} 1 & 0 & 0 \\ 0 & k_{yawrate} & 0 \\ 0 & 0 & k_{pitchrate} \end{bmatrix} \text{ where } k_{yawrate} \text{ and } k_{pitchrate} \text{ are control design variables.}$$

$$K_3 = .0585$$

$$K_4 = \begin{bmatrix} k_{4rollrate} & 0 & 0 \\ 0 & 1 & 0 \\ 0 & 0 & 1 \end{bmatrix} \text{ where } k_{4rollrate} \text{ is a control design variable.}$$

$$\vec{\theta}_{com} = \begin{bmatrix} 0 \\ \text{desired yaw angle} \\ \text{desired pitch angle} \end{bmatrix} \text{ (degrees)}$$

$$\vec{\omega}_{SATcom} = \begin{bmatrix} \text{desired roll rate} \\ 0 \\ 0 \end{bmatrix} \text{ (rad/sec)}$$

$$\vec{\omega}_{whlucom} = \vec{0}$$

Option 3 (Roll Spin Mode):

The user enters a desired roll rate for *SIMSAT* (range is ± 9 RPM). The desired effect of this maneuver is for *SIMSAT* to spin about the roll axis while minimizing motion about the yaw and pitch axes. For this option:

$$K_1 = \begin{bmatrix} 0 & 0 & 0 \\ 0 & k_{yaw} & 0 \\ 0 & 0 & k_{pitch} \end{bmatrix} \text{ where } k_{yaw} \text{ and } k_{pitch} \text{ are control design variables.}$$

$$K_2 = \begin{bmatrix} 1 & 0 & 0 \\ 0 & k_{yawrate} & 0 \\ 0 & 0 & k_{pitchrate} \end{bmatrix} \text{ where } k_{yawrate} \text{ and } k_{pitchrate} \text{ are control design variables.}$$

$$K_3 = .0585$$

$$K_4 = \begin{bmatrix} k_{rollrate} & 0 & 0 \\ 0 & 1 & 0 \\ 0 & 0 & 1 \end{bmatrix} \text{ where } k_{rollrate} \text{ is a control design variable.}$$

$$\vec{\theta}_{com} = \vec{0}$$

$$\vec{\omega}_{SATcom} = \begin{bmatrix} \text{desired roll rate} \\ 0 \\ 0 \end{bmatrix} \text{ (rad/sec)}$$

$$\vec{\omega}_{whlucom} = \vec{0}$$

Option 4 (Yaw Spin Mode):

The user enters a desired yaw rate for *SIMSAT* (range is ± 2.6 RPM – without thrusters, *SIMSAT* cannot spin outside this range). The desired effect of this maneuver is for *SIMSAT* to spin about the yaw axis while minimizing motion about the roll and pitch axes. For this option:

$$K_1 = \begin{bmatrix} k_{roll} & 0 & 0 \\ 0 & 0 & 0 \\ 0 & 0 & k_{pitch} \end{bmatrix} \text{ where } k_{roll} \text{ and } k_{pitch} \text{ are control design variables.}$$

$$K_2 = \begin{bmatrix} k_{rollrate} & 0 & 0 \\ 0 & 1 & 0 \\ 0 & 0 & k_{pitchrate} \end{bmatrix} \text{ where } k_{rollrate} \text{ and } k_{pitchrate} \text{ are control design variables.}$$

$$K_3 = .0585$$

$$K_4 = \begin{bmatrix} 1 & 0 & 0 \\ 0 & k_{yawrate} & 0 \\ 0 & 0 & 1 \end{bmatrix} \text{ where } k_{yawrate} \text{ is a control design variable.}$$

$$\vec{\theta}_{com} = \vec{0}$$

$$\vec{\omega}_{SATcom} = \begin{bmatrix} 0 \\ \text{desired yaw rate} \\ 0 \end{bmatrix} \text{ (rad/sec)}$$

$$\vec{\omega}_{whlucom} = \vec{0}$$

Option 5 (Wheel RPM Mode):

The user enters desired speeds for each of the momentum wheels (user's range is ± 200 RPM). This mode will be rarely used because it is an open-loop *SIMSAT* control method. Since Euler angle and body rate feedback are not used, direct wheel speed control will quickly reveal the coupled inertia properties of *SIMSAT*. For this option:

$$K_1 = 0$$

$$K_2 = 0$$

$$K_3 = .0585$$

$$K_4 = \text{identity matrix}$$

$$\vec{\theta}_{com} = \vec{0}$$

$$\vec{\omega}_{SATcom} = \vec{0}$$

$$\vec{\omega}_{whlucom} = \begin{bmatrix} \text{desired wheel 1 speed} \\ \text{desired wheel 2 speed} \\ \text{desired wheel 3 speed} \end{bmatrix} \text{ (rad/sec)}$$

4.5.8 MATLAB Simulation. Once the basic closed-loop controller was developed, it was necessary to determine gain values that would provide adequate *SIMSAT* control for the five operational modes. A MATLAB simulation of the closed-loop controller was used as part of an iterative gain-determination process. Since *SIMSAT* is a non-linear system, gains developed for one maneuver could be inadequate for a different operating regime. Also, within each of the five operational modes, there are an infinite number of possible maneuvers. Therefore, a few nominal maneuvers within each operational mode were chosen for simulation in MATLAB.

Appendix G shows possible matrix gain values and MATLAB output graphs for these nominal maneuvers. As stated previously, these maneuvers are NOT performed sequentially and the *SIMSAT* state vector is set to zero before each maneuver. The gain values were chosen to reduce overshoot, avoid excessive oscillations, and track the command signal within a reasonable amount of time. However, certain *SIMSAT* maneuvers, such as spinning about the roll axis, are inherently unstable and control is difficult.

4.5.9 SIMULINK Model Development. Once the *SIMSAT* system dynamics were understood, as discussed above, SIMULINK was used to code the plant and controller equations for use with the dSPACE system and onboard AutoBox⁸. The MATLAB simulation was used as an independent verification of the SIMULINK coding and aided debugging efforts. Due to the graphical, block diagram nature of SIMULINK, the command and control process was broken into several segments linked by signal lines within the software code⁹. The top-level architecture contained the following categories of blocks:

⁸Reference the SIMULINK User's Guide [35] for more detailed SIMULINK development procedures.

⁹The "signal lines" simply defined what variables were passed from one block to another, in a graphical manner.

- Various input and output ports (for commanding *SIMSAT* and receiving telemetry data from its systems).
- The controller subsystem (containing gains for both *SIMSAT* motion and motor control feedback).
- The *SIMSAT* plant subsystem (including the equations of motion representing the plant in the off-line simulation code).
- An Euler transformation segment (to convert onboard rate gyro measurements to the inertial coordinate system).
- Miscellaneous blocks (for unit conversions, math operations, and signal flow).

4.5.9.1 General Topics. To begin coding the command and control software for *SIMSAT*, the SIMULINK model development application was started by either selecting the “Simulink” or “dSPACE Library” icons in the dSPACE window. SIMULINK is accessed from the MATLAB Command Window by selecting the “New Simulink Model” icon on the toolbar, or typing “simulink” at the MATLAB command prompt.

A few points must be stated in order to understand the architecture of the SIMULINK software code. The ability to create “masked” blocks within SIMULINK was used extensively to simplify the top-level code. For example, the controller subsystem, *SIMSAT* equations of motion, and Euler transformations mentioned above all appear as single blocks in the top-level architecture. However, with SIMULINK’s ability to “look under the mask,” the code required to accomplish the top-level function can be accessed¹⁰. Since SIMULINK’s pre-existing “block library” only contains a limited number of fundamental math functions, this capability allows the user to create a new library with self-developed, application specific, block functions.

In the development of the *SIMSAT* code, two other items were necessary to consider. It was important to keep short the lengths of names given to all components of the SIMULINK code, since descriptive names of excessive length caused problems with the

¹⁰All SIMULINK code is provided in the *SIMSAT* User’s Manual.

compilation of the code. Also, although the capability existed, external MATLAB functions were avoided since their use would result in slower processing speeds. This included not using the SIMULINK "MATLAB Fcn," "Memory," or "S-Function" blocks invoking M-files. In addition to the slower speeds resulting from use of these blocks, the software for download to AutoBox cannot automatically compile them. These and other limitations of SIMULINK are outlined in the SIMULINK User's Manual. Since this manual also provides descriptions of the existing SIMULINK blocks, it is recommended that future users have this source available as a guide while coding in SIMULINK.

In general terms, it was necessary to develop top-level code that could receive command inputs from the ground station, convert the input values into the appropriate units, and allow these values to be used by the controller. In addition, the controller needed the values of the current *SIMSAT* system state, including position, angular velocity, and momentum wheel rates. Therefore, the code had to provide for receiving these state values from the *SIMSAT* plant. Once all input values were available, the controller could then determine the necessary momentum wheel speeds to achieve the commanded orientation. In the case of the off-line simulation, these wheel speeds were input into the *SIMSAT* equations of motion subsystem. Based on the system dynamics, this block determined the resulting *SIMSAT* angular acceleration. An integrator within the code was used to find the angular velocity to use as simulated gyro measurements. For real-time applications, code allowing calculated wheel speeds to be sent to hardware components was required. The code also needed to accept inputs from the rate gyros and the wheel tachometers. A means for using Euler angles to transform gyro data into the inertial reference frame was coded, allowing the angular data to be routed back as necessary to the controller. Finally, the top-level code provided a means to output telemetry data to the ground station. The SIMULINK development of the above process is outlined in the following discussion.

4.5.9.2 SIMULINK Code Segments.

IO Ports. There were four main types of ports used within the SIMULINK code for passing variables in and out of the software. "Inports" were used to input user commands to the system, while "Outports" were used to output telemetry data

to ground station displays. A dSPACE DAC port was used to interface software with the appropriate DSP card in AutoBox, and a dSPACE ADC port was used for bringing data off the DSP card into the software. The inport/outport blocks were used since they provided interfaces that could be easily linked with external software, such as that used on the ground station. The dSPACE blocks were specially designed by dSPACE to allow for software interface with the AutoBox hardware. Since the inports and outports were generally used to input or output a single variable, it was necessary to use "Mux" and "Demux" blocks to combine single values into vectors or separate a vector into its components, respectively. See Figure 4.7 for an example of how these blocks were integrated together. All these blocks were available in the standard SIMULINK and dSPACE block libraries, so further details can be obtained from the SIMULINK User's Manual and dSPACE documentation.

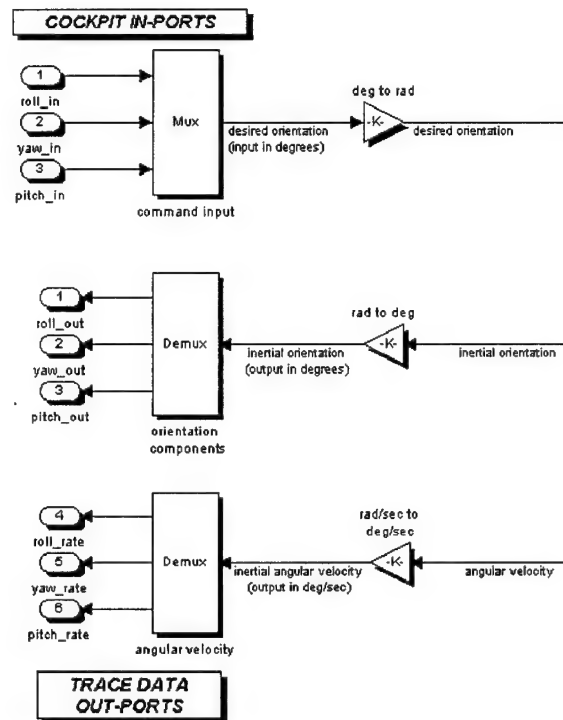


Figure 4.7 SIMULINK code for data input and output

Controller. This block was based on the controller model as developed in the discussion above (see Figure 4.8). The controller subsystem contained the

gains for both *SIMSAT* motion and motor control feedback and a block for comparing the desired torque with the available torque based on motor torque curve equation(s) and maximum wheel speed(s). After determining the torque command to supply to the motors, this command was converted to wheel acceleration and then integrated to wheel speed.

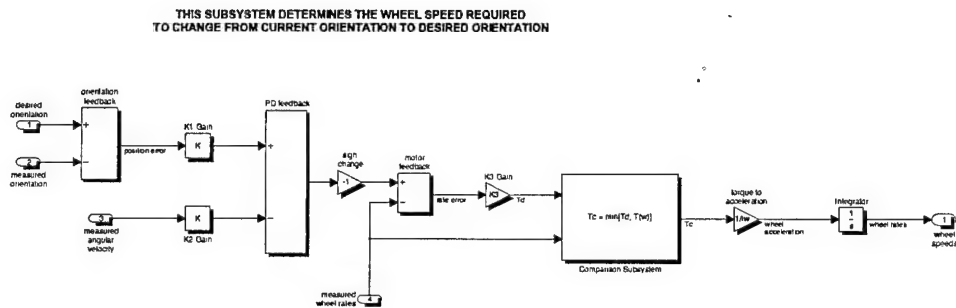


Figure 4.8 Controller Subsystem

Comparison Subsystem. Using SIMULINK relational operators, this block compares the desired torque to the available torque generating capability of the motors. The lesser of the two is passed on as the torque command to the system. To prevent momentum wheel saturation, this block also compares the measured wheel speed to the maximum wheel speed and uses the lesser of the two. See Figure 4.9 for an illustration of the SIMULINK code. In this way, the controller represents the physical capabilities of the motor-momentum wheel assembly.

SIMSAT Plant. This section of code represented the dynamics of how *SIMSAT* would react to the commanded wheel speed by returning simulated rate gyro

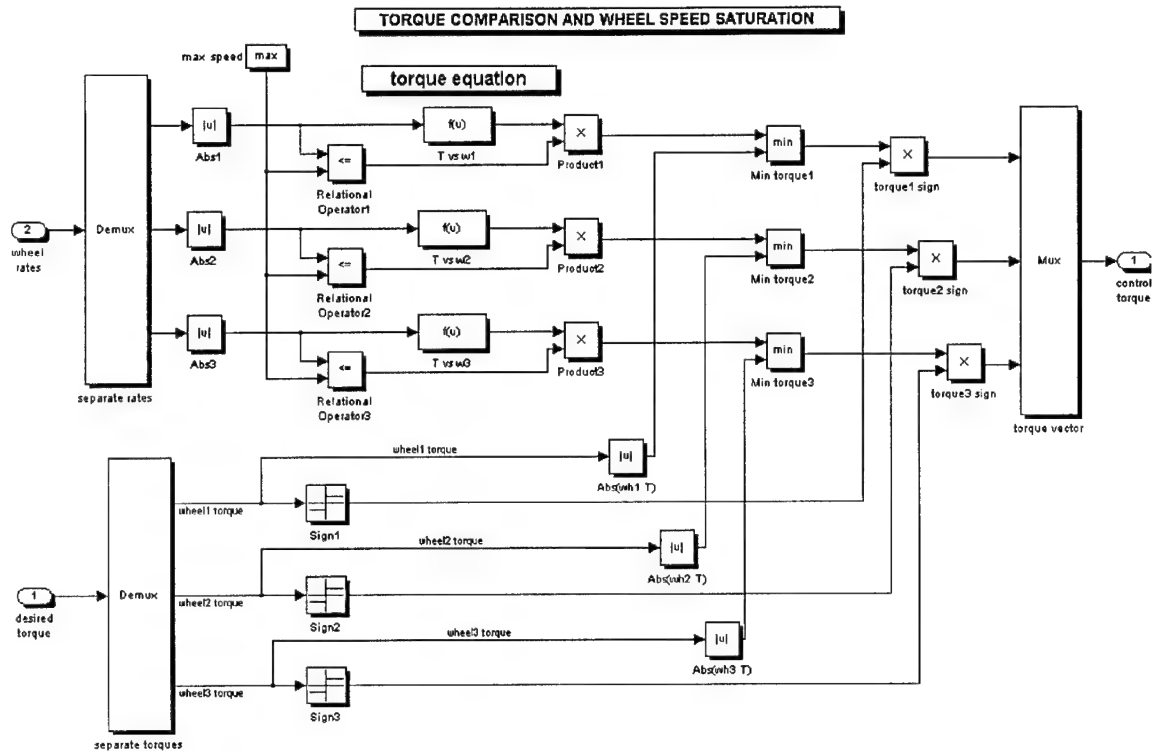


Figure 4.9 Comparison Subsystem, within the Controller

measurements. Within this section was the block containing the equations based on the EOM as derived in the above discussion. Just as the above EOM were complicated, this block also is complicated. However, it just contains a graphical representation of the same set of dynamic equations, simply replacing variables and operators with SIMULINK and “self-developed” (in the case of cross-products) blocks. This subsystem representing the *SIMSAT* plant was created for the off-line simulation code. In the real-time application this section is simply removed since the actual physical *SIMSAT* system takes its place. See Figure 4.10 for the top-level representation of the *SIMSAT* plant.

Euler Transformation. Although pictured as a single block, this subsystem was split into four sections functionally: (1) orientation input, (2) rate input, (3) Euler equations, and (4) rate output. Standard SIMULINK blocks, such as “Trigonometry” and “Product,” were used to build the Euler equations. “Goto” and “From” blocks were

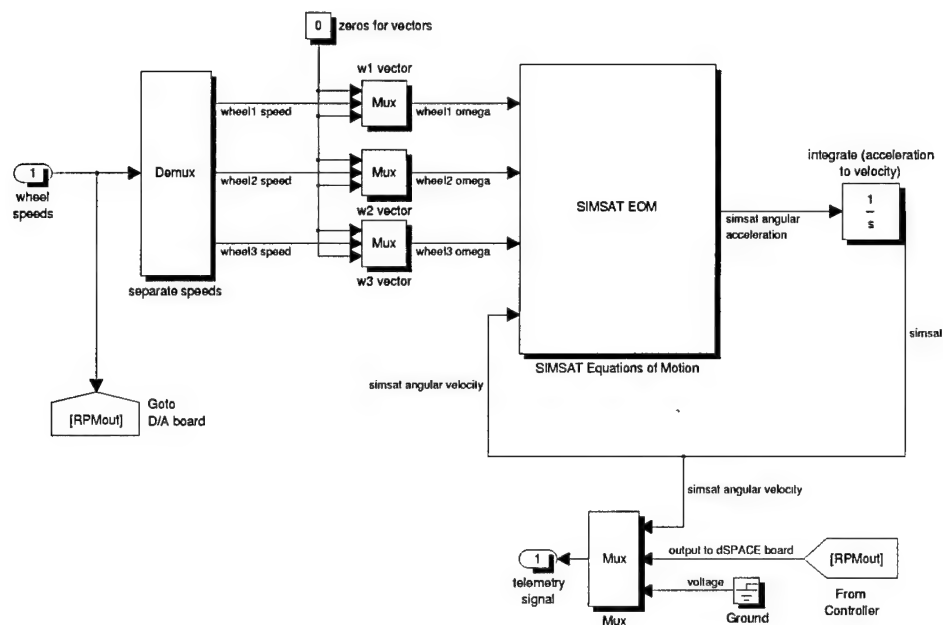


Figure 4.10 Top-Level *SIMSAT* Plant Model

used to connect input variable signals to the necessary equations to provide a clearer presentation than with direct signal lines.¹¹

Unit Conversions. As the ground station commands are input in degrees, it was necessary to convert to radians within the code. Likewise, the code converts from radians and rad/sec to degrees and deg/sec for *SIMSAT* motion data and rad/sec to RPM for wheel speed output to the ground station components. These conversions were accomplished within the code by using the standard SIMULINK linear “Gain” block.

Signal Flow. For proper signal flow in the off-line simulation code, “Goto” and “From” blocks were used to demonstrate where the DSP blocks were in the real-time application. It is very straightforward to see what variables are used by functions

¹¹No figures are presented for this, or following, categories since most SIMULINK blocks have already been illustrated.

within SIMULINK due to its graphical nature. Signal lines connect all blocks, with arrows indicating whether a variable passing over a line is an input or an output of a block.

Other. A built in "hook" for power signal monitoring (low voltage saturation) was placed within the code. Although currently not being used, it provides the capability of using voltage data within the code. This also was designed to illustrate an example for future experimental signals.

4.5.9.3 Constants and Variables. The following lists present the constants defined within the SIMULINK code and the variables linked with the graphical user interface. (NOTE: The constants are values that must be defined in the code before compiling, and may change based on *SIMSAT* configuration modifications. The variables are values that can be changed real-time during an experiment. Select the appropriate block within the SIMULINK code to open the dialog box for entering the necessary block parameters. See Figure 4.11 and Figure 4.12 for examples.)

Control Constants. These are the values defined in the Controller Subsystem (required for both simulations and real-time applications).

- Momentum Wheel Inertia (scalar value) - used within the controller block to calculate momentum wheel acceleration from the torque command.
- Maximum Wheel Speed (scalar value) - used within the comparison block of the controller subsystem to prevent momentum wheel saturation.
- K1 Gain Matrix (roll, yaw, pitch diagonal elements) - used within the controller subsystem as proportional gain on *SIMSAT* position error.
- K2 Gain Matrix (roll, yaw, and pitch diagonal elements - used within the controller subsystem as derivative gain on *SIMSAT* angular velocity.
- K3 Gain (scalar value) - used within the controller subsystem for motor control feedback.

Block Parameters: Controller Subsystem

CONTROLLER (mask)
Provides closed-loop PD feedback control and motor control.

Parameters

Enter Momentum Wheel Inertia:
0.0195

Enter Maximum Wheel Speed (in RPM):
2500

K1 roll element:
100

K1 yaw element:
200

K1 pitch element:
1000

K2 roll element:
-50

K2 yaw element:
-50

K2 pitch element:
-10

K3 Gain:
0.0585

Apply Reset Help Close

Figure 4.11 Controller Gain Parameters

Plant Constants. These constants are the values defined in the plant subsystem (only required for simulations).

- Momentum Wheel Inertia Matrices (J_1 , J_2 , J_3) - both about wheel center of mass, with respect to wheel reference frame and about *SIMSAT* center of mass, with respect to *SIMSAT* reference frame; based on the current configuration of the *SIMSAT* system.
- Composite *SIMSAT* Inertia Matrix (I_{comp}) - calculated as previously discussed; based on the current configuration of the *SIMSAT* system.
- Inverse Matrix from Sum of Inertia Matrices [$INV(I+J_1+J_2+J_3)$] - see above discussion for a definition.

Variables. These values are accessed from the user interface, and can be changed real-time.

Block Parameters: SIMSAT Equations of Motion

SIMSAT EDM (mask)

Simulation of SIMSAT dynamics:

Determines angular acceleration of SIMSAT based on momentum wheel speeds, SIMSAT's angular velocity, and inertia matrices of SIMSAT and momentum wheels.

Parameters:

Enter the temporary INVT(J1+J2+J3) Matrix:

210169433 0.00212579631833 -0.05330174420279

Inertia Matrix of Momentum Wheel 1 about its cm (wrt d-frame):

[0.00966328021014 0 0 0 0.01909883221232 0 0 0 0.0096632

Inertia Matrix of Momentum Wheel 2 about its cm (wrt f-frame):

[0.00966328021014 0 0 0 0.01909883221232 0 0 0 0.0096632

Inertia Matrix of Momentum Wheel 3 about its cm (wrt h-frame):

[0.00966328021014 0 0 0 0.01909883221232 0 0 0 0.0096632

Inertia Matrix of Composite SIMSAT System:

[4.48802735385669 2.30481534832553 -1.64315743439249;2.3

Inertia Matrix of Momentum Wheel 1 about SIMSAT cm (wrt b-basis):

[0.01909883221232 0 0 0 1.04137227842783 0 0 0 1.0413722

Inertia Matrix of Momentum Wheel 2 about SIMSAT cm (wrt b-basis):

[0.45095311414309 0 -0.41376853246186;0 0.84835227937832

Inertia Matrix of Momentum Wheel 3 about SIMSAT cm (wrt b-basis):

[0.41380905134934 -0.37780818155934 0;-0.37780818155934

OK Cancel Help Close

Figure 4.12 Equation of Motion Parameters

- Desired Roll Command - entered as degrees of desired roll using the graphical interface; converted to radians within the SIMULINK code.
- Desired Yaw Command - same as roll command.
- Desired Pitch Command - same as roll and yaw command.
- (Pitch Angle Limit) - to prevent commanding the system to a pitch angle beyond the system's physical limits; although not capable of preventing the system from attempting an impossible pitch angle due to coupling with roll and yaw, this prevents the ground operator from intentionally entering an unattainable pitch angle. (This was not a true variable used within the SIMULINK code, but a limitation on the range of user interface controls. Therefore, the ground station instruments can also be changed to reflect a "margin" for commanded pitch angle.)

4.5.9.4 Testing. The following steps were completed to test the control law software by running an off-line simulation. As an aid in debugging, there are a few tools available within the SIMULINK environment. Under "Format" on the toolbar, the user has options for the display of signal lines. By selecting "Wide Vector Lengths" the thickness of signal lines reflects the number of elements passing over it. For a scalar variable, the line width will remain the same. However, for vector variables, the line widths will become bold. Selecting "Line Widths" will display the exact number of values entering or leaving a block over an individual signal line. These options can be selected before, during, or after running a simulation, but results will not appear before a simulation has been started.

- Start the SIMULINK model development application by either selecting the icon in the dSPACE window, opening MATLAB and selecting the "New SIMULINK Model" icon on the toolbar, or typing "simulink" at the MATLAB command prompt.
- Open the desired *SIMSAT* model file (i.e. "SSMtest.mdl") from the appropriate directory.
- In the "Simulation, Parameters..." menu, make sure the desired solver options are selected. Although a fixed-step solver is necessary for real-time applications, the type of solver can be varied during off-line testing. (A fixed-step solver is not recommended for initial off-line testing, using only the PC, due to the extremely slow running speed.)
- Select "Start" from the "Simulation" menu, or click on the "play" icon, to begin running the model within the SIMULINK environment. If the model has been properly coded according to SIMULINK syntax rules, the time count will begin updating in the lower right of the screen to signify a running simulation.
- If errors exist in the code, use the displayed error messages and the user's manual to fix the problem(s). One of the most common problems involved incorrect signal widths, as when a block expected a scalar rather than a vector input, or vice versa. The debugging tools mentioned above helped in locating the source of this error. Other errors were caused by using incorrect SIMULINK blocks to perform certain functions. For example, although the SIMULINK "Product" block is "vectorized" to

accept and return vectors, it does not perform a cross-product operation. Therefore, it was necessary to develop a new SIMULINK block, by combining existing ones, to conduct cross-product operations.

- Once the coding errors had been debugged within SIMULINK, the software was ready to be integrated with dSPACE, as will be covered in a later section.

4.5.9.5 Summary. The following SIMULINK code was developed during the Detailed Design phase, and is currently available for use with *SIMSAT*.

- *SIMSAT* model block library (SSMlib.mdl): This is a file containing several of the SIMULINK blocks developed for use in the *SIMSAT* command and control software. The current version lists blocks with the dates they were last updated/modified. Besides providing a back up of essential components, it also allows future users to choose individual blocks from this library for use in new code, rather than breaking apart existing *SIMSAT* code.
- Test version (SSMtest.mdl): This code was used to conduct simulations of *SIMSAT* for testing the control laws, command and display capabilities, and integration with dSPACE. It has undergone all the testing and compiling described in this section.
- Real-time application (SSMreal.mdl): As yet untested, this code is the same as the test version except for the modifications required for hardware-in-the-loop applications. The blocks closing the loop in the test version were replaced by the dSPACE blocks designed to interface with the DSP cards in the onboard AutoBox. In addition, the subsystems used in the test version to simulate the physical *SIMSAT* system were removed (i.e. the equations of motion block).

Naturally, future coding changes will be necessary based on the characteristics of an experiment. The two main categories of coding alterations are additions to and modifications of the existing code. Any experiment added to the baseline *SIMSAT* will change the inertia of the system, requiring that the user enter the new inertia values in the Equations of Motion subsystem of the test version. The user can then use this code to generate

any necessary changes to the feedback gains for proper control. These new values should then be entered into the real-time application version of the software. Finally, any new SIMULINK blocks required for experimental use should be added and tested with the test version before adding to the real-time version. Modification of the existing code may be as simple as changing the inputs or outputs and removing unneeded blocks, or complex such as making major changes to the feedback control laws.

One future addition/modification already identified is the need for the software to simulate, and provide real-time control of, gas thrusters used for momentum dumping to avoid wheel saturation. Better off-line simulations could be accomplished by designing code to model sensor noise and disturbance torques. Another recommendation for possible future software revision is to develop a method for recognizing loss of signal with the ground station or motion instability and returning the system to a stable zero orientation. However, this would only work for a few emergency cases, not incidents such as loss of power, onboard computer problem, hardware failure, an already unstable system, etc., so an emergency “catch-all” safety system will always be required. This reality limited the usefulness of extensive time creating “emergency” code during early software development. Finally, adding a “power-off” capability to the code would be useful for sending a simple switch command to power down the batteries at the end of an experiment.

Before the developed SIMULINK code could be used for on-line/real-time operations, it had to be integrated with the dSPACE software. The next section outlines the process required to do this.

4.5.10 dSPACE Integration. In general, to integrate the code discussed above with dSPACE for compiling and downloading to AutoBox, the following steps were taken. (See Appendix H for detailed information.)

- Power up the AutoBox and ensure it is connected with the PC.
- Select “dSPACE Library” from the “dSPACE Files” window, or type “rtilib” within the MATLAB Command Window.

- From within SIMULINK, select "RTW Build" from the "Tools" menu, or press (Ctrl+B), to begin the compilation process (if the RTW Options have already been set correctly: dSPACE requires a fixed-step solver for real-time applications, a fixed step size of 0.001, using ode4 or ode5, is recommended).
- The Real Time Workshop (RTW) and Real Time Interface (RTI) will then compile the SIMULINK model into C-code, generate the associated files, start the DSP onboard AutoBox, and download the program to AutoBox.
- The application program would now be running onboard AutoBox, until the DSP is manually reset or a loss of power occurs.
- With a successful download, the previous process is not repeated to reload the compiled model after a DSP reset or power-down. Instead, after restarting AutoBox use the dSPACE MON40NET program to load the object module of the desired control software and restart the DSP.

4.5.11 User Interface Issues. At this stage, the software architecture included the user-created SIMULINK code and all the files created by the dSPACE software during compilation and download to the AutoBox. The next challenge was to integrate this onboard command and control software with the user interface software on the ground station computers.

To meet the user requirements for an easy-to-use interface providing command control and telemetry monitoring functions to an experimenter, the ground station was developed. This involved the following design issues.

- The ground station was required to provide real-time command and control of *SIMSAT* operations.
- To aid in providing the real-time command and control, real-time display of data during *SIMSAT* operations, with control feedback matching the actual system behavior, was necessary.

- A means for saving experimental data (and system motion data) for post-test analysis was required.
- User controls and displays should be easy-to-use and understand.
- Robust user interface software allowing simple modification based on future experimental use.

The development of the ground station software is described in the next section, while the hardware architecture of the ground station is discussed in Section 4.5.13.

4.5.12 Control Law/User Interface Software Integration. The following descriptions explain how the SIMULINK-developed command and control code was linked with the TRACE, COCKPIT, and REALMOTION applications¹². These tools were part of the graphical user interface software provided with the dSPACE system. They were designed to easily link with code developed in SIMULINK and compiled with RTW/RTI¹³. Using a wireless communication link, the user interface software running on the ground station computer can connect with the simulation software on the AutoBox, passing command and telemetry variables back and forth.

4.5.12.1 TRACE Telemetry Display. This plotting tool presents time histories of variables in the command and control software. The interval length of real-time data capture can be varied, allowing the user to view instantaneous variable updates, or a plot covering several seconds, such as 5, 10, or 30 seconds. These time history plots can be saved to a file following an experiment, allowing post-test analysis as required. After creating a properly working SIMULINK model, and successfully compiling and downloading it to the AutoBox, the following steps outline how the command and control code was linked with the TRACE tool. (See Appendix I for detailed information.)

¹²Reference the TRACE [17], COCKPIT [16], and REALMOTION [15] User's Guides for detailed description of the information presented in this section.

¹³Reference the RTW [37], RTI [18], and MATLAB Target Language Compiler [36] User's Guides for detailed description of the information presented in this section.

- The TRACE development environment consists of two windows, the "Trace Net Control Panel" and "Trace Plots." The Control Panel was used for the general process of linking a real-time application with TRACE, while the plotting window was where the graphs for signal plotting were developed.
- The initial step in the linking process was to load the TRACE file created during the RTW/RTW compilation process. Once loaded, this file provided a tree structure of the simulation program.
- Signals desired for plotting were selected from a variable list generated from the tree structure.
- After using the tree structure and variable list to establish the graphs for signal plotting, the TRACE "Template" was designed. Plotting options available included using grids on the graphs and scaling of axes.
- Of considerable utility was the "Reference..." option, which allowed the plotting of multiple signals on a single graph based on a reference signal selection. This capability was useful for direct comparison of related signals, such as the roll, yaw, and pitch angle variables.
- It was also determined that TRACE plot data can be saved to a MATLAB *.mat file following a simulation, and later used to graph the results of the experiment in MATLAB.

4.5.12.2 COCKPIT *Command and Control Suite*. This software tool provided input control and output display instruments that can be linked with variables in the command and control code. COCKPIT was designed to provide real-time command and control of *SIMSAT* operations with graphical user controls and displays. The robustness of this user interface software allows simple modifications for future experimental use.

The design of the COCKPIT user interface was accomplished in a similar manner to the TRACE development. Once again, the appropriate TRACE file was loaded, providing the same tree structure and variable list. Various COCKPIT control and display instruments were linked with variables to provide user control. Control parameters such as initial input

values and ranges were set, and the control panel design was saved for use in simulations and real-time applications. (See Appendix I for more information.) The following list describes the control instruments planned for the *SIMSAT* user interface.

- *Slider*. This instrument is a simple slide bar that can be used for basic roll, yaw, or pitch control. Although not very accurate, it provides a straightforward control for demonstration of general motion.
- *Knob*. An alternative for basic roll, yaw, or pitch control, this dial-like instrument would serve the same function as the slider. Just like the slider, it is also ineffective for precise motion control since a reasonably sized instrument does not provide for fine command inputs.
- *Incremental Input*. This instrument can be used for fine roll, yaw, or pitch control by allowing incremental commands above or below a set point. For example, use of the slider control can get the commanded angle near the desired one, and the incremental input control can move it closer. (The value of the increment is user-defined.)
- *Numeric Input*. This input provides for keyboard entry of the exact roll, yaw, or pitch commands.
- *Pushbutton*. This plain button can be used to command roll, yaw, or pitch to a pre-defined angle. For example, this is useful as a quick "return to zero" command.
- *Display*. Several digital-style numeric displays are used to indicate the current values of motion variables.
- *Gauge*. This instrument is used for output display of *SIMSAT* angular velocities and momentum wheel speeds. It is an intuitive display since the pointer can indicate the direction, as well as the rate, of the motion.
- *Alert*. This instrument only provides a visual and audible indication of the pitch angle reaching pre-set limits. (If power monitoring is included in a future design, an "alert" instrument can be used to indicate a low power level.)
- *Bar*. This instrument could be used for power monitoring by presenting the current power level.

- *On/Off Button.* This button may be designed to shut down *SIMSAT* power. Since the command and control software must be running on the AutoBox before the COCKPIT user interface can be started, this option only works for powering down after an experiment (or when appropriate in an emergency situation), not for turning *SIMSAT* on.

4.5.12.3 REALMOTION 3-D Animated Display. This software tool links a 3-D geometric model to orientation variable outputs, providing a real-time 3-D representation of *SIMSAT* motion. The following topics cover the design of the REALMOTION application.

A geometric model (an AutoCAD *.dxf file) and a scene control file (*.ctl) were created, and they defined different "members" of a baseline *SIMSAT* representation. This allowed for naming, coloring, and motion scaling of individual parts of the model. For example, this capability would allow a future experiment incorporating attached appendages (i.e. solar panels) to emphasize the motion of the payload over that of the support structure. Also, several observer points-of-view can be defined within the scene control file, as desired. Once the geometric model had been linked with a scene control file, the following animation options were available.

- Off-line simulation with the use of a motion data file (*.mdf).
- On-line simulation when the simulation program is running on a DSP board.
- Real-time animation when the command and control program is running on the onboard AutoBox, and motion data is being updated constantly. However, this option required additions to the software code, as described below.

The simulation's *.usr file, a part of the command and control software created during the dSPACE compilation process, was modified to create links between the *SIMSAT* C-code motion variables and the members of the REALMOTION model. If the names of the output motion variables are not changed within the original code, and the geometric model is kept the same, no further changes to any REALMOTION related files is required with

future revisions. However, if the code is modified by changing the names or adding new output variables, the *.ctl and *.usr files will also need modification. The *.ctl file must also be updated to reflect any additions to the geometric model. (See Appendix J for more detail on creating and modifying the files linked to REALMOTION.)

Upon opening REALMOTION, two windows will appear. The "Status Window" provides background details based on a loaded simulation program, scene control file, and geometric model. The REALMOTION Display Window portrays the 3-D representation of the model. The status window is for reference only, all REALMOTION manipulation must be done from the display window. The following are a few options regarding the display window set-up.

- Use "Load Scene..." under the "File" menu to open an existing scene control file. If the associated application program is not running on the DSP board, an error message will appear. This message can be ignored for off-line work.
- Most scene options can be changed from the default cases defined by "keywords" in the *.ctl file by using the display window menus. Keyword/menu selections allow the specification of the observer point-of-view, attributes of the model members, and qualities of the scene such as lighting conditions, background color, window size, etc. (It is suggested that the model be viewed in the large window.)
- The "Position Control Tools" toolbar (accessed from the "View" menu) allows translation and rotation of the model to demonstrate motion in off-line status.
- The "Light Tools" toolbar (accessed from the "View" menu) enables simple point-and-click control of the object lighting. Using Lights 3 and 8 is recommended for the best visibility of the model.

With a simulation running on the PC's DSP card, or the real-time application running on the AutoBox, the geometric model's orientation will update based on the current motion variables received from *SIMSAT*.

4.5.13 Ground Station Hardware Architecture. The ground station consisted of two computers, each with its own monitor and capability for wireless commu-

nication with *SIMSAT*. The physical arrangement was based on the design conclusions of Mr. Hanke's thesis, but just as the rest of the system it is flexible to allow future reconfiguration. After completing the initial software development using the existing systems, the following recommendations for future ground station development were made.

- Reconfiguring the lab arrangement (i.e. computer locations) is recommended to avoid the hazards of sitting too near an operational *SIMSAT* during an experiment. Also, the operator should face *SIMSAT*, so repositioning the computers farther from *SIMSAT* and giving the operator a clear line of view will aid the individual in matching ground displays with actual motion. This view will be especially important during initial test runs to determine if the controller works for the physical system as well as its software simulation.
- A better command and control station is possible with alternate computer components. Utilizing two screens with the ground control PC would allow the user to observe real-time updates of TRACE motion plotting on one screen, while operating the COCKPIT instrument panel on the other. This arrangement would provide greater control to the experimenter since switching between displays on a single monitor would not be necessary. Along the same lines, larger monitors would allow better display fidelity and easier access to more control instruments.

4.5.14 User Interface Summary. This section serves to encapsulate the design and development of the *SIMSAT* command and control software and ground station described above.

- *Dynamic Models of Equations of Motion and Controller.* The software architecture used in command and control and user interface development was based on the mathematical model created to represent the *SIMSAT* system. The controller design used within the software was developed and tested against these equations of motion, using closed-loop feedback.
- *MATLAB.* The MATLAB coding environment was used extensively to develop the software architecture. The equations of motion and controller were separately coded

in MATLAB to provide independent verification of the SIMULINK application software. MATLAB also served as an integral part of the final software architecture since it is the foundation of SIMULINK, and the TRACE application is designed to save plot data into *.mat files for later analysis using MATLAB.

- *SIMULINK*. This software served as the fundamental coding environment. Along with dSPACE compatibility, SIMULINK allowed easier software integration of the *SIMSAT* system, controller, and ground station.
- *dSPACE Library*. As an essential part of the dSPACE software suite, this library provided the SIMULINK code blocks for linking the software architecture with the AutoBox hardware.
- *RTW/RTI*. The Real Time Workshop and Real Time Interface applications were used to convert the graphical SIMULINK code into C-code, which was then compiled and downloaded to the AutoBox. They provided the link between a user-friendly coding environment and the AutoBox compatible code.
- *TRACE*. This application provided a real-time display for the time histories of motion variables. It also supplied the capability of saving test results to a *.mat file, for later analysis using MATLAB. The software development included the design of a template for the graphs of variable plots (SSMtrace.tpl) and a general experiment set-up file (SSM-trace.exp) used to define sample rate, plotting interval, and the file used to link TRACE with the AutoBox.
- *COCKPIT*. User-friendly ground control capabilities were developed using the COCKPIT application. The design included instruments such as simulated slide bars and buttons to send commands to *SIMSAT*, and gauges and numeric displays to provide instant feedback on the measured orientations and velocities. The graphical user-interface (Grnd-Ctrl.ccs) was designed for use with the existing system and ground station set-up, but its integration with the rest of the dSPACE software only requires simple modifications to meet future needs.
- *RealMotion*. 3-D animation of real-time *SIMSAT* motion is provided by REAL-MOTION. Developing this capability required the design of a geometric model to

represent *SIMSAT* and creating or modifying software code to provide the necessary links between programs. The geometric model (Simsat.dxf) was created in AutoCAD and defined for REALMOTION use in the scene control file (Simsat.ctl). Finally, C-code modifications made to the *.usr file created during compilation of the original SIMULINK code linked the orientation variables to the REALMOTION model.

- *Ground Station Configuration.* The arrangement of ground station computers during the software development process consisted of one PC with TRACE and COCKPIT, to be used later as the "mission operations" and ground control station, and another PC with REALMOTION, for display of the 3-D animation, both simulated and real-time. These two PCs were located near the air-bearing pedestal in the lab. Having the two PCs co-located during the detailed design phase was useful, and safety concerns were not significant. However, it is recommended that the current ground station configuration be altered for the final operational design to prevent safety hazards due to close proximity to *SIMSAT*.

4.6 Structural Design

4.6.1 Problem Statement. Structural design addressed the development of a mounting framework for attaching *SIMSAT* components to the central air-bearing assembly. The structural design problem was summarized as follows:

Using the selected components, design a structure which supports easy integration of these items onto SIMSAT, maximizes modularity, and minimizes mass and inertia.

4.6.2 Problem Scope. During the Concept Exploration and Definition phase, structural design began with general considerations of the classes of structural solutions deemed most likely for final implementation. Without knowledge of the masses and volumes of individual components, however, these efforts yielded few tangible results. During the Preliminary Design phase, however, subsystem decisions were made which allowed for the overall structural design to begin. Several structural alternatives were considered; but without specified subsystem components, detailed structural design was delayed until after the first iteration of the Detailed Design phase. Once subsystem classes were nar-

rowed, development of a logical support structure to enhance the overall performance of *SIMSAT* was initiated in detail. At this stage, only the baseline structural design was considered; detailed mounting of components, static and dynamic responses, and detailed structural specifications were investigated in later design. The structural design problem demonstrated the importance of systems integration to the *SIMSAT* design team, as the final design became more than just the sum of the characteristics of the individual parts.

4.6.3 Structural Issues. The following issues were identified as critical in the development of the baseline structural design:

- Develop a preferred *SIMSAT* configuration, to include relative arrangement of subsystems and structural members.
- Ensure the structural design is robust and modular to support subsystem reconfiguration.
- Incorporate a payload structural interface, to include adequate mass and volume margins.
- Allow 3-D visualization of the structure prior to fabrication to aid decision-making and ensure feasibility.
- As much as possible, minimize the mass and inertia penalties associated with the structural design.

4.6.4 Computer-Aided Design (CAD) Software. Nominal position vectors for the components used in the original MATLAB simulation were estimated from preliminary *SIMSAT* hand sketches. Although this approach provided a starting point for momentum wheel sizing, it was apparent that computer-aided design (CAD) would be needed. A CAD package would allow exploration of multiple *SIMSAT* configurations within the time constraints of the project. Therefore, the team actively pursued the purchase of a PC-based CAD system to support structural development. AutoCAD software (release 14), produced by Autodesk, Inc., was selected by the design team as the primary CAD package of the *SIMSAT* project. Additionally, 3D Studio VIZ (release 2), also

produced by Autodesk, Inc., was used for three-dimensional solid object visualization. AutoCAD software is an industry standard, and it produces drawing files compatible with the dSPACE REALMOTION display system. These two software packages, designed to be used together in concert, provided a powerful tool for on-screen manipulation of structural elements. Without these software packages, the *SIMSAT* design effort would have been impossible to achieve on schedule. Additionally, as the structural design continued to mature, cardboard mockups were constructed to verify computer drawings and provide a hands-on environment for making design decisions. Mockups also enhanced the ability of fabrication shop personnel to visualize the design and make valuable suggestions.

4.6.5 Initial Sizing. The generic MATLAB simulation used for momentum wheel sizing (reference Appendix C) provided a useful tool to begin formal structural design work. Although this simulation neglected structural mass, the simulation demonstrated the effect of component weights and positions on *SIMSAT* motion performance. The outputs from this simulation provided an initial "feel" for how the arrangement of structural components could affect the system. The *SIMSAT* configuration used for momentum wheel sizing was drawn using AutoCAD (reference Appendix B, Figure B.1) and then rendered (i.e., made into a solid or wireframe three-dimensional image) using the 3D Studio VIZ software. Figure 4.13¹⁴ shows this original configuration (referred to as *SIMSAT-0*). Readily apparent in the drawing is the excessive volume needed to enclose *SIMSAT* components. This unnecessary volume needed to be removed to reduce the system moment of inertia and improve axis symmetry.

4.6.6 Structural Development. Beginning with the next structural design iteration, every effort was made to reduce *SIMSAT* volume and position components as close to the central air-bearing as possible. Figure 4.14 shows the *SIMSAT-1* configuration, the first attempt at establishing a logical placement of components to support structural design. At this stage of development, component placement was accomplished without actually designing a supporting structure; structural design was not incorporated into the AutoCAD models until later in this design subproblem. *SIMSAT* structural de-

¹⁴Reference Appendix B, page B-4, for identification of components in this figure.

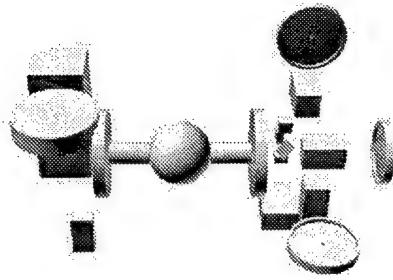


Figure 4.13 *SIMSAT*- Iteration 0

sign quickly became a highly integrated process where equipment constraints, placement considerations, and structural mass minimization were intertwined in a complex fashion. The classic role of a systems engineer as designer and integrator was never more apparent than during the *SIMSAT* structural design effort.

No attempt will be made to fully discuss every structural design iteration attempted by the systems engineering team; approximately 30 separate design drawings were produced as the structural design became more refined and system decisions were made. However, several major iterations are described below to illustrate important shifts in thinking with regard to component placement and system-level impacts.

4.6.6.1 Momentum Wheel Enclosure. As shown in the *SIMSAT*-1 configuration, the three momentum wheels were originally designed with separate lexan enclosures. This allowed for maximum modularity, as the momentum wheels could be separated and moved to opposite sides of the air-bearing assembly. Subsequent examination of this arrangement, however, indicated a substantial mass penalty was incurred (using separate boxes) without any significant performance improvements realized. Beginning with *SIMSAT*-3, all three momentum wheels were moved into a single enclosure, with the motors attached to a complex shelf support structure. This shelf support structure represented a design subproblem in which the momentum wheels, motors, and supporting

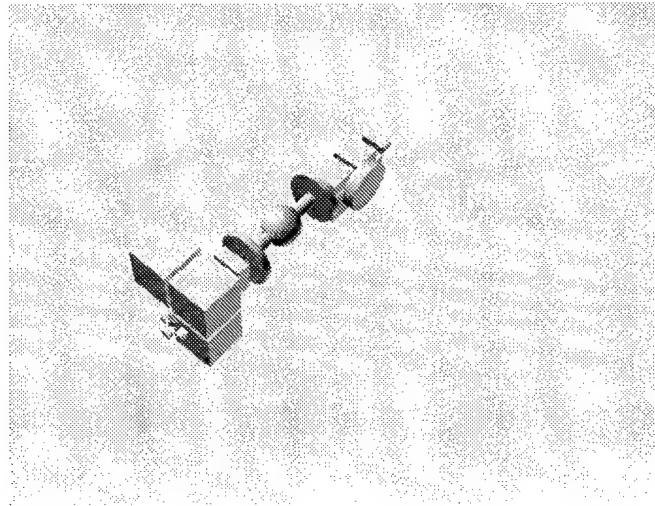


Figure 4.14 *SIMSAT*- Iteration 1

elements were housed in as tight a configuration as possible, while providing adequate rigidity to mount the high RPM wheels and motors. Figure 4.15 shows the *SIMSAT*-3 configuration in wireframe view. In addition to reducing mass, this decision also had the benefit of reducing total subsystem volume, although at the expense of lumping the volume into a single large space (impacting subsystem modularity).

4.6.6.2 AutoBox Orientation. Another major configuration decision involved the relative placement of the AutoBox with respect to the structure. As one of the largest subsystem components, the AutoBox's orientation would be a driver in the structural development. Because of the need to shock-mount AutoBox to minimize vibration, both horizontal and vertical AutoBox mounting schemes were examined. *SIMSAT*-4 modeled AutoBox in a horizontal¹⁵ fashion (see Figure 4.16). Attaching the AutoBox to the structure horizontally would allow the rubber shock-mounting feet supplied with the unit to be used. However, this approach suffered from several disadvantages. First, since *SIMSAT* has the ability to roll upside-down, an additional set of mounting feet would have to be added to the opposite side of AutoBox to reduce tension loads on the origi-

¹⁵ "Horizontal" implies parallel to the longitudinal (roll) axis of *SIMSAT*.



Figure 4.15 *SIMSAT*- Iteration 3

nal mounting feet, which were not strong enough to support the weight of the AutoBox. Second, mounting the AutoBox horizontally with respect to the long axis of *SIMSAT* interfered with the truss structure as it was then envisioned; a non-standard mounting plate placed orthogonal to all the other mounting plates would be needed. Finally (and most importantly), a moment of inertia penalty was incurred by mounting AutoBox horizontally rather than vertically. This fact drove the design decision to mount AutoBox vertically with respect to the *SIMSAT* long axis.

4.6.6.3 Structural Rod Arrangement. Both box (four mounting rods for each side) and prismatic (three rods) structures were examined for mounting *SIMSAT* components. Prismatic structures were quickly abandoned because of component mounting difficulties. The weight savings and torsional stiffness provided by a prismatic shape were outweighed by the problem of mounting rectangular subsystem components to non-rectangular surfaces. *SIMSAT*-15 (see Figure 4.17) represents a fairly mature structural design configuration. The size of the momentum wheel box dictated the overall structural dimensions, while the use of standard mounting plates for component attachment was an intuitive design decision.

4.6.6.4 Battery Arrangement. The three-battery power system offered several arrangement possibilities. Originally, two batteries were placed on the payload side, and one on the momentum wheel side. However, batteries were rearranged in this iteration, with one battery moved from the payload side to the momentum wheel side. This allowed

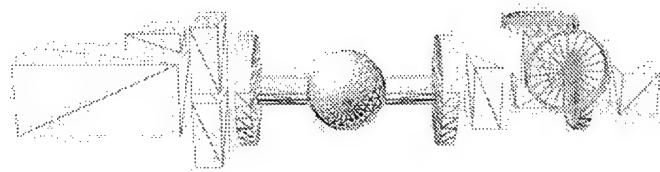


Figure 4.16 *SIMSAT*- Iteration 4

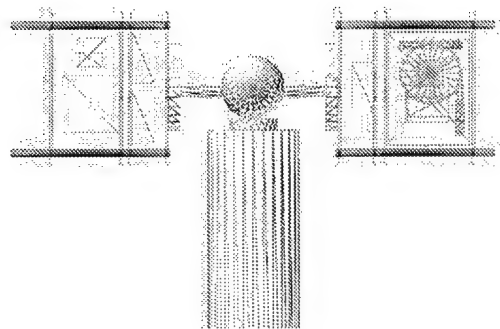


Figure 4.17 *SIMSAT*- Iteration 15

placement of the gyros and wireless communications equipment next to the AutoBox, reducing the length and complexity of system wiring. Also in this structural iteration, the AutoBox was reoriented to take advantage of the proposed mounting plate's rectangular shape to improve its shock-mounting system. Previously, the AutoBox had been drawn to extend past the structural envelope defined by the support rods. The reorientation of the AutoBox parallel to the long side of the mounting plate (while having negligible effect on inertia properties) allowed for the supplied shock-mount feet to once again be used (additional support such as U-clamps were still required).

4.6.6.5 Structural Mass Reduction. Using 1/4" aluminum mounting plates with 1/2" aluminum base plates rods resulted in a significantly heavier system structure than first anticipated. Some means of reducing the total weight was required. The first, and most easily implemented, weight-savings decision was to remove the air-bearing's mounting disks (supplied with the air-bearing system) which had been previously considered for structural attachment. Rather than mounting onto these disks, the *SIMSAT* structure would be attached directly to the mounting shafts extending from the central sphere. Removal of the circular mounting plates immediately reduced overall *SIMSAT* mass by 108lb (each disk weighed 54lb). This decision, however, reduced the available pitch clearance to under 20 degrees since removal of these mounting disks moved the base (innermost) plate inward towards the central sphere. Additionally, the fastener pattern of the air-bearing mounting shaft would be required to secure the base plate to the shaft. These screw holes were too close to the center of the base plate to adequately support the shear and bending loads from the structural mounting rods near the plate edge. A circular collar (redesigned on several occasions) was added to *SIMSAT* to increase the distance between the central sphere and the base plate and provided a pitch clearance of approximately 22 degrees, as shown in Figure 4.18. This collar also allowed a wider fastener pattern to the base plate, aiding in the load support of the plate. These circular mounting collars were later redesigned to include a recessed portion. This recession overlaps the mounting shaft and reduces the shear load experienced by the mounting shaft screws.

Another weight-savings measure was to re-examine the thickness of the mounting plates. Baseline structural estimates did not include holes cut into the mounting plates to save weight. It was decided that all mounting plate estimates would assume a solid plate, and these lightening holes could be added in later design as subsystems are fitted to the plates and testing of the system is underway¹⁶. Various plate thicknesses, ranging from 3/32" to 1/4" were ordered and submitted for mounting plate fabrication. The appropriately-sized plate could be determined should system testing prove a plate to be over- or under-designed. As a starting point, 1/8" plates were shown (through rough calculations) to provide adequate stiffness for the AutoBox and battery/gyro plates, resulting in system weight savings.

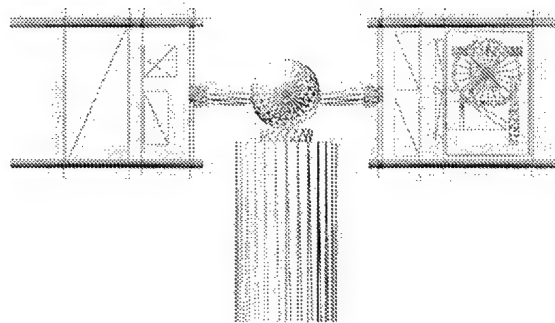


Figure 4.18 *SIMSAT- Iteration 23*

4.6.6.6 Momentum Wheel Bay Offset. Although most of the structural design was set by the *SIMSAT-23* configuration, several detailed refinements were added to improve overall performance. Prior to this stage of development, the center of

¹⁶Delaying this decision was obvious since cutting holes into the plates is an easy operation, whereas a redesign would be required if the plates were originally designed too optimistically (not strong or stiff enough).

mass of the momentum wheel bay was assumed to lie on the geometric center of the box. Detailed modeling of the momentum wheels, lexan box, and support structure refined this location, and the momentum wheel box was offset (in the z-direction) in order to place the momentum wheel bay center of mass on the *SIMSAT* roll axis (to aid in balancing *SIMSAT*).

4.6.7 Structural Implementation. At this stage, the arrangement of subsystem components was fairly complete and the baseline structural design was developed. Before fabrication of the *SIMSAT* structure could begin, however, several key issues still required resolution¹⁷. The remaining structural design issues are summarized in the following list:

- Specification of mounting rod/plate materials and dimensions, as well as mounting plate fasteners.
- Determination of structural responses to static and dynamic loading.
- Design of a supporting truss for rigidity to meet all static and dynamic requirements.
- Detailed design of the housing and mounting of all subsystem components, to include shock-mounting and vibration suppression for sensitive equipment.
- Design of a payload mounting plate.
- Design of a counterweight system to aid in system balancing.

4.6.8 Baseline Structure Summary. The evolution of the *SIMSAT* structural design represented an important milestone towards the goal of successful project completion. The use of CAD tools to manipulate component configurations was crucial in achieving this success. Figure 4.19 shows the final *SIMSAT* design as presented in this document. This baseline *SIMSAT* structural design represents a robust solution balancing performance needs against system modularity and ease of use. Chapter V and Appendix K further describe the final structural design.

¹⁷These issues are addressed in the truss design subproblem (Section 4.7), the final structural design appendix (Appendix K), and the presentation of the final design (Chapter V).

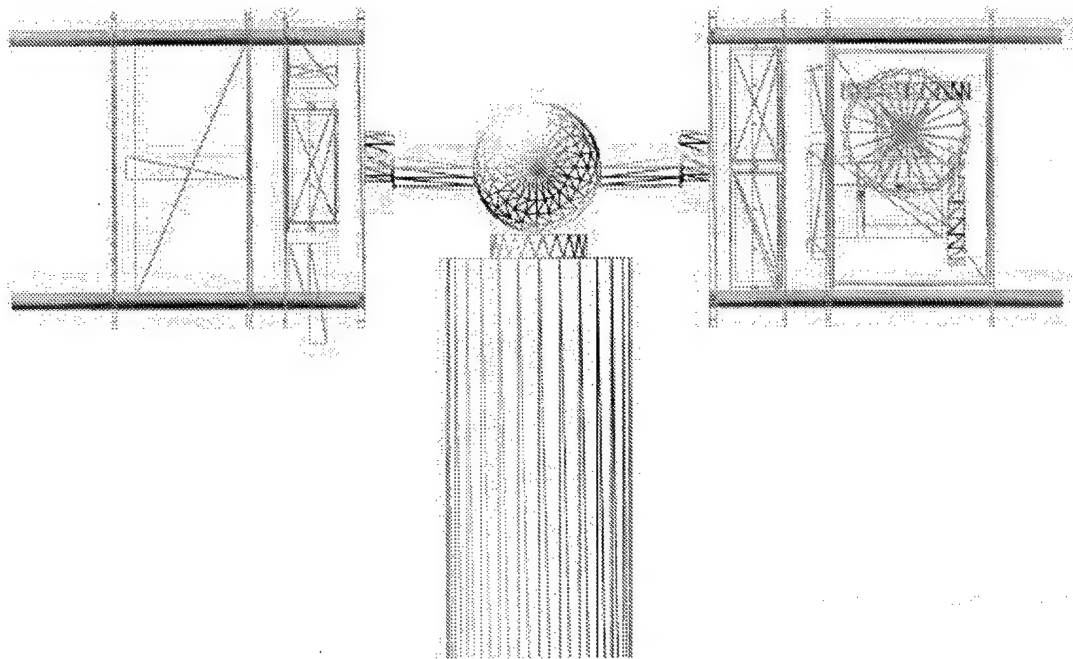


Figure 4.19 SIMSAT- Final Structural Iteration

4.7 Truss Design

4.7.1 Problem Statement. The truss design problem was summarized as follows:

Using the basic satellite structure, refine the structural design such that the structure meets static and dynamic requirements.

4.7.2 Problem Scope. At this stage of the design, the structure was shown to adequately support anticipated loads without approaching the yield strength of the main aluminum support rods. However, a static analysis to determine maximum tip deflections was desired to ensure that the structure would not significantly deform under loading, potentially creating undesirable stress concentrations. Furthermore, dynamic analysis was required to estimate natural frequencies of the structure. The structure can then be stiffened as necessary to ensure that its natural frequencies exceed the maximum frequency of the motors/momentum wheels. In this way, resonant coupling between the spinning momentum wheels and the structure can be avoided. Moreover, a more rigid structure would provide a better platform for use in vibration experiments and other experiments involving flexible-structure payloads.

4.7.3 Requirements. The following requirements were specified to ensure adequate static and dynamic structural performance:

- Maximum tip deflections should not exceed 10mm under static loading conditions.
- Natural frequencies of each side of the structure should be greater than maximum momentum wheel rotation rates (approximately 43Hz) to avoid resonant coupling. First-mode frequency should exceed 60Hz to account for approximations used in the dynamic analysis.
- Slew performance should not be compromised by the truss design.
- The truss should easily accommodate the addition of members to add stiffness should an experiment require improved rigidity.

4.7.4 Value System Design. For this portion of the design, a detailed objective hierarchy was considered to be of little added value in the design of the structural truss. Instead, objectives were identified to be used as qualitative evaluation considerations. Designs could then be developed and considered against these objectives, followed by a decision by the customer based on a presentation of the more favorable truss designs. The

following objectives, ranked by order of importance, were identified as important in this segment of the design:

- Meet tip deflection requirements.
- Maximize the first natural frequency.
- Minimize impacts on system modularity.
- Minimize added structural weight.
- Minimize impacts on the basic structural design.
- Minimize impacts on slew performance.
- Maximize higher-order natural frequencies.
- Minimize added cost.

4.7.5 Development Approach. The rod-and-plate structure provided a baseline configuration to begin the truss design. A worst-case bending deflection was modeled for each rod to provide initial estimates of the material and size of the rods. A finite-element analysis package, called *CADRE*¹⁸, was used in the static and dynamic analyses. Using *CADRE*, a structural model of each side of the *SIMSAT* was built using nodes and elements, along with associated loads and inertia properties. The software computed structural static and dynamic displacements, internal forces and moments, and displayed results using 3-D animation. Once the rod-and-plate structure was modeled, static displacements and natural frequencies were then determined for the baseline configuration. As needed, structural elements were added and the analyses repeated.

Unless absolutely needed, it was desired to provide structural stiffness without rearrangement of the mounting plates. This restriction was due to the balancing and arrangement of components on the mounting plates. The truss members were designed and modeled to link the outsides of the plate. In this way, interference with internal components and wiring paths was avoided, and the basic structural design was left intact. Each

¹⁸CADRE Analytic of Issaquah, WA, produces a shareware finite-element package called *CADRE*, as well as the professional version *CADRE Pro* [9].

mounting plate could be drilled with holes in which an L-bracket could be attached. A bolt through the L-bracket would be used as the cross-member attachment pin, as shown in Figure 4.20. This assembly allowed easy addition and removal of cross-member supports as necessary.

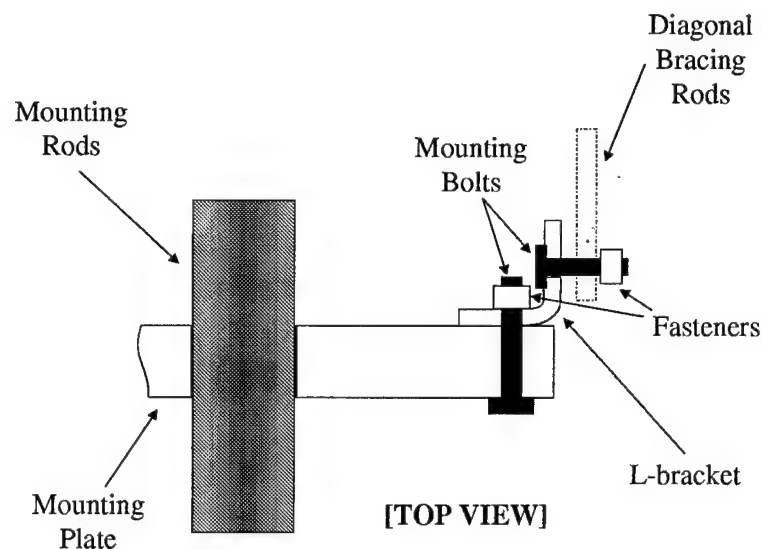


Figure 4.20 Linking of Truss Members

4.7.6 Finite-Element Model. A 49-node, 66-element baseline model was constructed for each side of the *SIMSAT*. The payload-side model is shown in Figure 4.21. The following assumptions were used in the finite-element analysis¹⁹. Although the *SIMSAT* final design differed slightly in element specifications, the results of this model were still applicable.

- Mounting rods are represented by hollow aluminum tubes of outer diameter 2.8cm and 0.5cm thickness.

¹⁹Appendix L lists the inputs and results of the finite-element modeling, to include nodal loads, element properties, and static deflections.

- Mounting plates are represented by eight 0.5cm diameter solid aluminum rods in a wire-frame configuration with cross members.
- Mounting rod mass is equally shared by rod nodes.
- Mounting plate mass is equally shared by plate nodes.
- Cross-member support elements are modeled as 1.0cm diameter solid aluminum rods.
- Cross-member support elements are considered massless.²⁰
- Cross-member support elements are drawn from the rod/plate juncture (neglecting the slight offset between the mounting rod and the end of the plate).
- All masses are modeled as point masses at a node, except for the component masses at the plate centers which are offset to the centers of gravity.
- Mounting rods are affixed cantilever to the base plates with one end clamped (no degrees of freedom at joint).
- All other truss joints are assumed to be free in translation and rotation (six degrees of freedom).
- An 18kg payload with center of gravity 12cm outside of the payload mounting plate is included.
- Static/vibratory response is modeled for each side of *SIMSAT* separately; no attempt is made to model the dynamics of the central sphere or the fully-joined *SIMSAT* structure.

4.7.7 Static Analysis. Both the payload-side²¹ and wheel-side²² structures exhibited tip deflections less than 2mm, under both y-loading (applied along the longer dimension [height] of the structure) and z-loading (applied along the shorter dimension [width]). These deflections, calculated using the *CADRE* shareware software, were for the

²⁰ A 55cm rod of 1.0cm diameter aluminum weighs 0.12kg, so that eight support rods measure less than 1kg total, which is considered negligible.

²¹ This side included the payload, AutoBox, battery, gyros, and wireless LAN.

²² This side included the momentum wheel/motor assembly with lexan box, along with two batteries.

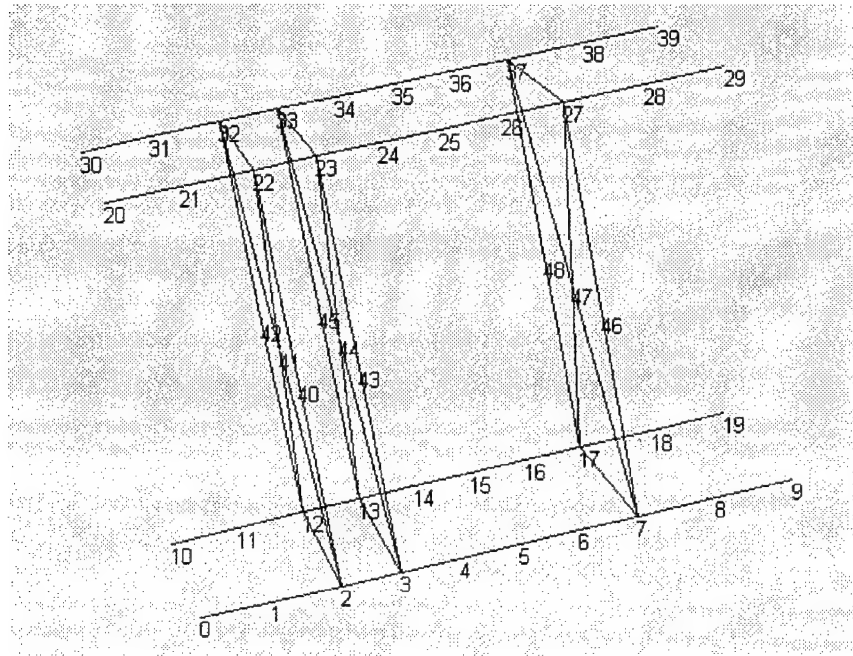







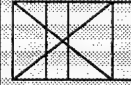


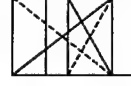
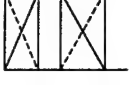






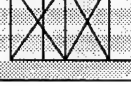

Figure 4.21 Finite-Element Model (Payload Side)

baseline configurations (no additional cross-members). Thus, no structural support was necessary to meet static deflection requirements.

4.7.8 Payload-Side Dynamics. Dynamic analysis of the baseline model indicated that, although the configuration was acceptable for static deflection, the frequencies of the lower modes were inadequate from the perspective of system vibratory response. The first three modes on the payload/AutoBox-side of the truss occurred at 16Hz (sinusoidal), 75Hz (torsional), and 98Hz (double-sinusoidal), respectively. These low frequencies demonstrated the need for diagonal cross-bracing along the exterior of the truss to increase structural stiffness and raise the system's natural frequencies.

Seventeen configurations of diagonal bracing were evaluated using the *CADRE* software package. Cross-member supports along the top of the structure were not explicitly considered because the lowest frequency responses were insignificantly affected by such bracing, and the AutoBox wiring would be impeded by such design. The various configuration models are displayed in Figure 4.22, along with the calculated modal responses.

The highest first-mode frequency configurations are shaded. In all cases, diagonal cross-member supports significantly improved the vibratory response of the truss. Based upon discussions with the decision makers, the “double-X” scheme (shaded as “1”) was selected as the preferred design solution for the payload-side structure.

Design	Mode 1/2/3 (Hz)	Design	Mode 1/2/3 (Hz)	Design	Mode 1/2/3 (Hz)
	16/75/98		85/158/187		74/99/185
	46/123/151		88/158/188		94/105/185 (2)
	53/147/187		69/139/187		79/128/186
	62/132/174		74/133/187		78/154/189
	56/138/164		85/152/188		71/143/188
	72/152/187		99/158/190 (1)		50/134/168

**2-D VIEW
LEGEND:**

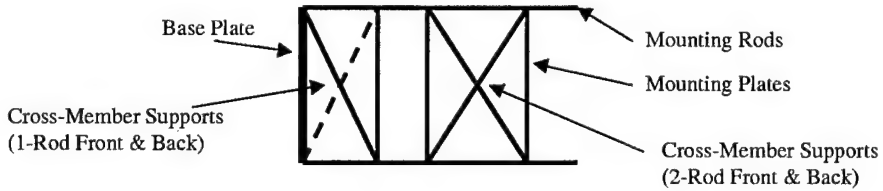


Figure 4.22 Truss Configurations (Payload Side)

4.7.9 Wheel-Side Dynamics. Development of the momentum wheel side of the *SIMSAT* truss proceeded initially in a similar manner to the development of the

Design Mode 1/2/3 (Hz)



20/66/72



38/95/105



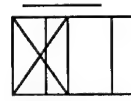
38/94/111



38/113/165

↑
Top and bottom cross-member supports

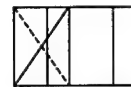
Design Mode 1/2/3 (Hz)



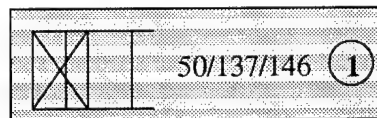
38/112/165



39/92/105

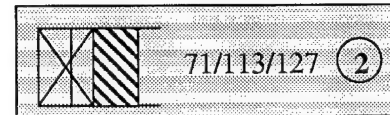


26/72/85



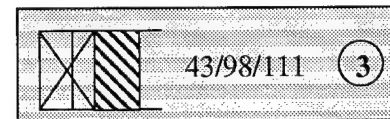
50/137/146 (1)

Design Mode 1/2/3 (Hz)



71/113/127 (2)

Lexan box modeled as two diagonal rods on each side of the truss structure.



43/98/111 (3)

Lexan box modeled as one diagonal rod on each side of the truss structure.

**2-D VIEW
LEGEND:**

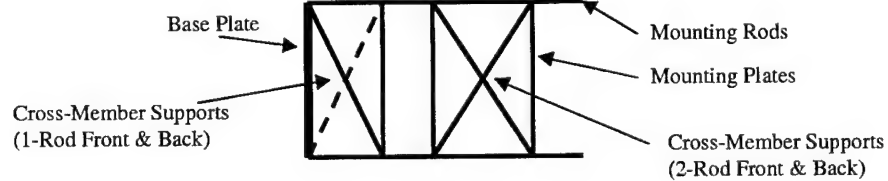


Figure 4.23 Truss Configurations (Momentum Wheel Side)

payload-side truss. Support elements were again modeled as 1.0cm diameter rods. The first three vibratory modes for the baseline truss (no bracing elements) were calculated to be 20Hz (sinusoidal), 66Hz (torsional), and 72Hz (double-sinusoidal), respectively. Further analysis indicated, however, that diagonal support elements would not be as effective on the momentum wheel side of the truss as compared to the payload side. Because the lexan box surrounding the momentum wheels extended beyond the truss exterior in the z-dimension (width), vertical cross-bracing was impeded for the momentum wheel bay. Therefore, cross-bracing was only possible along the interior bays of the truss, and along the top of the momentum wheel bay. Neither of these arrangements, however, significantly altered the first-mode response of the structure to meet the 60Hz minimum requirement, as shown in Figure 4.23. To illustrate this condition, a truss using support elements having a modulus of elasticity 1000 times greater than aluminum only yielded a first mode of 50Hz (shown as "1"). Even the modeling of much stiffer mounting rods resulted in negligible modal improvements. The momentum wheel model did not include the stiffness due to the lexan box itself, however. Inclusion of the lexan box, modeled to behave in a manner approximating diagonal supports, resulted in first modes of 71Hz and 43Hz for alternate models (shaded as "2" and "3").

4.7.10 Additional Truss Modeling. Because of the difficulty in modeling the plates and lexan box, the *CADRE Pro* professional version was procured to allow a more complete finite-element model to be developed. In addition to the basic beam modeling available in *CADRE*, *CADRE Pro* allows for modeling of flat plates, using 2-D triangular elements to build plates capable of carrying in-plane loads. A 686-element truss model was constructed using material properties of updated structural components, shown in Figure 4.24. Mounting rods were represented as 1" 304 stainless steel tubes of 0.065" wall thickness. The innermost mounting plate (attached to the air bearing collar) was modeled as 1/2" 2024 aluminum plate, with the remaining plates assumed to be made of 1/4" 2024 aluminum. The deadweight of truss elements was modeled at the nodes automatically by *CADRE Pro*. Additional *SIMSAT* components were modeled as point masses located at the centers (with longitudinal offset) of the appropriate mounting plates.

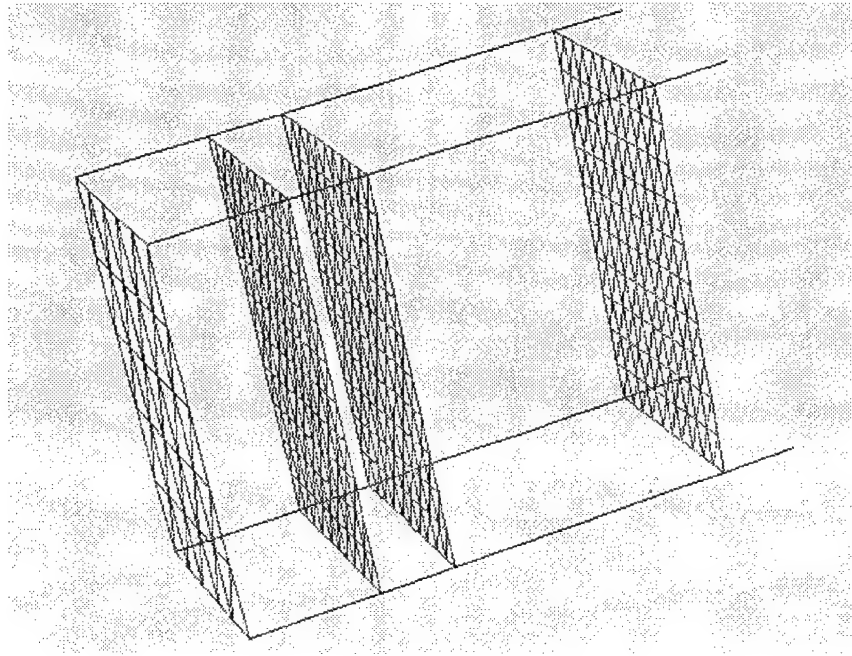


Figure 4.24 Finite-Element Model Using Plates

Analysis of this improved model indicated that static deflections were negligible (less than 0.1mm). Vibratory response was noticeably improved in comparison to the original beam element-only model. The first three modes of the new model were 94Hz, 144Hz, and 430Hz, respectively. The results indicated that modeling of 2-D plates, which are structurally stiffer than their beam analogs used in the *CADRE* model, provided a less conservative estimate of the lowest mode frequency. The absolute certainty of these values was still unknown, however, due to the inability of both *CADRE* and *CADRE Pro* to fully model the complete *SIMSAT* structure as designed. Discussions with the decision makers indicated their belief that vibration of individual components (most notably the AutoBox) separate from the truss itself may drive the determination of system natural frequencies. Therefore, additional finite-element modeling of the system was determined to be of limited value for further design decisions.

4.7.11 Truss Structure Summary. The results of the finite-element analyses directly impacted design decisions made regarding the truss structure. It was

decided that diagonal cross-bracing elements would be added to the design to ensure sufficient structural rigidity to prevent vibratory coupling and resonance. The models clearly supported the improved rigidity benefits of additional cross-member supports in this design. All mounting plates would, therefore, be drilled to fit L-bracket attachments so that cross-braces may be added or removed as necessary. Further discussions with the decision maker indicated a desire to make the structure as stiff as reasonably possible, aiming for a 100Hz minimum mode frequency rather than the 60Hz minimum initially required. To this end, multiple thicknesses of aluminum ($1/2''$, $1/4''$, $1/8''$, $3/16''$, and $3/32''$) were purchased as available sheet stock to be used as mounting plates. The final determination of which elements (plates and stiffeners) to use in the baseline configuration would be determined after experimentation and empirical testing. As a starting point, the "double-X" and "single-X" support schemes would be used for the payload-side and wheel-side structures, respectively. The modularity of the structural configuration would easily accommodate additional cross-members, use of other cross-member rods (such as hollow steel), or use of stiffer mounting plates.

4.8 Wireless Communications Selection

4.8.1 Problem Statement. The following design subproblem was the focus of this Detailed Design iteration:

Select a preferred commercial-off-the-shelf (COTS) wireless communications system, to include wireless LAN and wireless modem for transmission of command and telemetry data (COCKPIT, TRACE, and REALMOTION data).

4.8.2 Problem Scope. In the Preliminary Design phase, an all-onboard (using dSPACE's AutoBox) processing option was selected. This processor would collect and process sensor data, receive commands from the ground station, process control laws real-time, issue inputs to onboard systems, and transmit telemetry data to the ground station (Simulation PC). The wireless communications system to link the AutoBox with the ground station would be COTS-designed, as determined in the Preliminary Design phase. With this background, this design subproblem focused on identifying communica-

tions constraints, developing rationale for system selection, and finally selecting preferred wireless LAN and wireless modem systems for *SIMSAT* integration. Identification of specific vendors and model numbers was the final output of this subproblem.

4.8.3 Constraints. The 10Mbps Ethernet connection required for ground-station-to-AutoBox connectivity imposed several constraints on the wireless communications system. In addition, onboard power system constraints were specified to ensure feasibility. The following list identifies the wireless communications constraints used to narrow the communications solution space:

- Wireless systems must be commercially available.
- The wireless LAN must provide a 10Mbps Ethernet connection for COCKPIT and TRACE data.
- The wireless modem must provide serial data transmission at adequate transmission speed for REALMOTION data.²³
- The AutoBox requires ISA-compatible network cards.
- Wireless systems must operate using a DC power supply (36V maximum).
- As accounted for in power budgets, power consumption should not exceed 5W.
- For safety and RF interference considerations, only systems designed for indoor use will be implemented.
- RF transmission must use FCC-approved frequency bands.
- Because of the changing antenna orientation during *SIMSAT* operation, wireless systems must use omnidirectional antennas.

4.8.4 Value System Design. To provide a basis for the evaluation of communications system alternatives, the following system-level considerations were identified. These considerations are ranked by order of importance in system selection. A formal

²³Since the REALMOTION data is neither mission-critical nor high-volume, a specified connection speed was not a constraint.

objective hierarchy was not needed as these evaluation considerations provided sufficient direction for the wireless selections.

- *Integration.* Minimization of integration complexity is desired. Models offering AutoBox-compatible connections are preferred.
- *Weight and Volume.* Minimization of the weight and volume of the communications subsystem is desired.
- *Data Transmission.* Wireless LAN data rates exceeding the 10Mbps constraint provide no performance advantage, as the Ethernet data is sent at only 10Mbps by the AutoBox. Faster wireless modem speeds provide some performance advantage.
- *Cost and Delivery.* Minimization of communications subsystem cost is desired. Shorter delivery times are preferred.
- *Power Consumption.* Less power consumption is desired.
- *Vendor Reputation.* Research into a vendor's reputation, based on objective sources, can be used to differentiate wireless models, as necessary or applicable.
- *Warranty.* Longer system warranties are preferred.
- *Transmission Power.* All indoor wireless designs are considered safe for laboratory usage; thus, minimization of transmission power provides minimal safety and RF interference benefits.

4.8.5 Wireless Background Sources. The design team first contacted dSPACE, Inc., directly to inquire about dSPACE/AutoBox wireless applications by dSPACE customers. Apparently, only one other wireless AutoBox application had been accomplished to dSPACE's knowledge. Engineering students at the Ohio State University had linked several AutoBoxes using wireless modems to transfer low-speed serial data. Through contact with these engineers, it was learned that their application did not involve COCKPIT, TRACE, or REALMOTION data, and their laboratory had only one AutoBox remaining [47]. Thus, an existing wireless AutoBox solution comparable to the

SIMSAT application was not found, making the *SIMSAT* design somewhat of a pioneer in AutoBox wireless networking²⁴.

COTS wireless system alternatives were then explored using Internet searches and publications research²⁵. By applying the system constraints to this solution space, the number of alternatives was reduced from several hundred to only a handful.

4.8.6 Wireless LAN Alternatives. The major driver in reducing the wireless LAN solution space was the 10Mbps Ethernet capability. Six 10Mbps system vendors were discovered. Of these six, four vendors offered wireless LAN bridges primarily for outdoor use. Further research indicated that the transmission powers and RF interference for these outdoor designs did not pose as great a problem as first predicted. In fact, some of these outdoor designs were advertised for indoor use as well. Thus, more information on wireless bridge designs was required to determine their feasibility for *SIMSAT* use.

4.8.6.1 Wireless LAN Bridges. The *WaveSpan 5800*, offering 10Mbps connectivity for up to 5 miles, was considered a baseline wireless LAN bridge. Priced at \$23,950 per link [12:103], this system was considered far too expensive for *SIMSAT* integration. Furthermore, the wireless bridge solutions were designed to link one LAN to another LAN, instead of a peer-to-peer architecture desired between the ground station and the satellite. For these reasons, the wireless bridge solutions were no longer considered for the communications function.

4.8.6.2 Office-Use Wireless LANs. Two wireless LAN solutions remained: the Aironet 4800 Turbo DS Series (11Mbps) and the RadioLAN product series (10Mbps). As described in Section 4.2.6.6, page 4-15, the Aironet AP4800 and RadioLAN ISA CardLINK are very similar in transmission capability, mass, size, and power. However, additional research showed that the PC-card interface of the Aironet model would be

²⁴As an unproven technology application, the wireless LAN involved system risks which were conveyed to the decision makers.

²⁵An excellent source for wireless product information was the Ottawa Amateur Radio Club website [42], with specifications and company information for over 150 different wireless systems.

very difficult to integrate with the ISA-compatible design of the AutoBox. Therefore, the RadioLAN product series was selected over the Aironet model for continued investigation.

RadioLAN offers several wireless systems in its 10Mbps product series: *BackboneLINK 208*, *ISA CardLINK 101*, *PC CardLINK 130*, and *DockLINK 408*²⁶. All four options offer Ethernet connectivity through an omnidirectional radio transceiver unit, but each option was intended for a different network application. The BackboneLINK was designed as a stand-alone wireless hub for multi-user wireless networking, priced around \$1,000²⁷. The ISA CardLINK (\$349) is the standard user (desktop) access link, whereas the PC CardLINK (\$449) was designed for laptop users. Finally, the DockLINK (\$799) serves as a transparent bridge for Ethernet-enabled network devices, such as UNIX workstations, printers, and Macintosh workstations.

Initial analysis revealed that a BackboneLINK would not be required for the *SIMSAT* design ; a peer-to-peer link would suffice. As with the Aironet model, the PC CardLINK was ruled out due to the PC-card interface. Thus, only the ISA CardLINK and DockLINK alternatives remained for consideration – a CardLINK-CardLINK (ground-satellite) architecture versus a CardLINK-DockLINK architecture. The DockLINK is shown in Figure 4.25.

The ISA CardLINK included software required to install network drivers for wireless networking. Since the AutoBox does not contain a floppy-disk drive, further research was required to determine the feasibility of the CardLINK onboard the satellite. Initial conversation with dSPACE engineers indicated that a “burn-in” of these drivers could be made on the AutoBox, either at dSPACE’s facility or by the design team using a flashdrive configuration. However, the technical support representative at RadioLAN stated that although the network drivers could be loaded onto the AutoBox processing board, an operating system (Windows 95/98) was needed to actually enable the wireless network. His recommendation was that the DockLINK was better suited for onboard installation, providing a “dumb” network bridge. Since the DockLINK was intended for office use in a constant orientation, its application in the *SIMSAT* design presented risks, such as loss of

²⁶Each RadioLAN device is described on the RadioLAN website, www.radiolan.com.

²⁷Product prices according to PC Magazine, 1 September 1998 [57].



Figure 4.25 RadioLAN DockLINK Model 408 [45]

data or subsystem failure. With the omnidirectional antenna, the RadioLAN technician determined the risk of data dropout to be minimal at the very short ranges required by *SIMSAT* (approximately 10 ft). Shock-mounting of the transceiver onboard the satellite adequately negated the risk of system failure due to an unsteady environment. Table 4.10 describes the specifics for both the ISA CardLINK and the DockLINK.

Table 4.10 RadioLAN Product Data [45]

Parameter	ISA CardLINK	DockLINK
Purchase Cost	\$349	\$799
Radio Frequency	5.8GHz ISM band	5.8GHz ISM band
Transceiver Weight	9.8oz (278g)	7.4oz (206g)
Unit Weight	4.6oz (130g)	22.3oz (632g)
Input Power	5V/12V	12V (or 110VAC)
Transmission Power	50mW peak	50mW peak
Media Access Protocol	CSMA/CA	CSMA/CA
Network Interface	16-bit ISA	RJ-45 jack
Warranty	1 yr (parts & labor)	1 yr (parts & labor)

4.8.7 Wireless LAN Selection. Based on the wireless LAN research and analysis, the selected wireless LAN architecture included a ground-based ISA CardLINK with transceiver and a satellite-based DockLINK with transceiver. Because the wireless LAN is relatively inexpensive and a "tight" subsystem (in that its interfaces are few and well-defined) replacement of this RadioLAN architecture with a different model should not be significantly difficult. Thus, an alternative wireless LAN can be implemented without significant system impacts should the RadioLAN system prove to have unforeseen drawbacks, or a more-capable system becomes available at a later date. As the technology expands, the future of wireless LANs will certainly see more 10Mbps systems on the market, including the Bluetooth 2.4GHz model scheduled for release late in 1999 [27]. Thus, the risks associated with the implementation of this wireless LAN in an untested application were considered acceptable. The RadioLAN ISA CardLINK and DockLINK were approved and ordered.

4.8.8 Wireless Modem Considerations. As stated previously, the incorporation of the wireless modem was not critical to *SIMSAT* operation. The wireless modem was to provide the communications link for the REALMOTION data stream, which allowed 3-D animation capability but was not used for data collection or control processing. With the schedule constraints imposed on the baseline design, integration of the wireless modem for this function was determined to be of secondary priority. Wireless modems were investigated and a vendor (including model) was selected, but purchase and integration were delayed until after the wireless LAN was successfully integrated²⁸. This decision was based on several factors:

- Integration of the wireless LAN was critical to system operation, whereas integration of the REALMOTION communications link was not.
- Integration of the wireless LAN would provide greater knowledge of omnidirectional antenna capabilities on a rotating, laboratory-based satellite. This knowledge may

²⁸The wireless LAN system was received in late January, 1999. Integration of the LAN was not complete before this document went to print.

significantly impact the choice of wireless modem system as problems and solutions related to antenna interference are encountered.

- Being a COTS subsystem, order and delivery of a wireless modem would require minimal time, and relative to other subsystems, the costs of a wireless modem would not be great.
- Integration of the wireless LAN would set the data architecture, and a wireless modem could more easily be integrated as a "plug-and-play" component.
- As a general design rule, making system decisions before they are necessary often results in increased financial and technical risks.

4.8.9 Wireless Modem Alternatives. With a large number of wireless modem vendors available, certain criteria were required to reduce the number of subsystem alternatives. The first constraint used in selection was to only consider those models designed for telemetry data acquisition. This decision was based on the assumption that a modem developed for industrial/telemetry applications would be less risky to integrate into the *SIMSAT* design than a modem designed for office PC applications, such as wireless internet or wireless networking. Because of the team's limited knowledge of wireless applications, it was also desired to consider vendors who offered easy accessibility and quick response time to technical questions. This subjective measure was important because *SIMSAT* involved unique data transmission problems, as the onboard transceiver would be in motion. Thus, interaction with technical support was essential to identify and solve integration issues.

Based on these constraints, several wireless modem designs were available. One promising alternative was the SkyLine Wireless Modem of Sonik Technologies Corporation, San Marcos, CA. This model, designed for radio control and data acquisition applications, featured a sophisticated communications processor which uses a powerful and efficient communications protocol developed by Sonik to reduce multipath, RF interference, intermodulation, and signal fade problems. Operating at 9600 bps over the air, the modem uses an RS-232 interface which can be configured to connect to the AutoBox.

Specifications include 2W RF power output, a range of frequency bands (up to 512MHz), 12.5V DC power requirements, and a 3.0" x 3.0" x 1.5" size [52]. The quoted cost of this modem was \$599 each. Figure 4.26 shows the Sonik Skyline modem.



Figure 4.26 Sonik Technologies Corporation's Skyline Modem [52]

A second, more promising, alternative was the WIT2400M of Digital Wireless Corporation (DWC), Norcross, GA. This modem, operating in the 2.4GHz range, offered greater data throughput (up to 115 kbps) due to the higher transmission frequency²⁹. With a lower output power than the SkyLine modem, specified at 10mW or 100mW, less RF interference with the wireless LAN system was anticipated. The WIT2400M also incorporates an RS-232 interface to the AutoBox. The modem requires a 5.5V to 10V power supply, with operating currents up to 150mA (typical). Prices start at \$590 per modem. [14]

Conversation with the DWC technical support representative, Mr. Don Neas, revealed that a development kit was available from DWC which would suit the *SIMSAT* application quite well. The development kit (\$2250) included a pair of modems equipped with power supplies, battery packs, battery charger, flow control indicators, dipole anten-

²⁹Use of a 2.4GHz wireless LAN should not be used with this modem due to interference concerns.

nas, RS-232 interface, configuration software, and technical support. Figure 4.27 shows the packaged unit (called the WIT2400E). Small in size (4.5" x 6" x 1.5") and lightweight (approximately 1kg), this modem alternative could be integrated with minimal complexity as a stand-alone, self-powered subsystem. Experience with the DWC technical support showed that response to questions was quick and complete. With the short transmission ranges required by *SIMSAT* (approximately 10 ft), Mr. Neas believed that data dropouts due to polarization fading would be minimal as signal transmission via reflection at these short ranges was adequate. Thus, loss of signal due to *SIMSAT* motion was not anticipated.

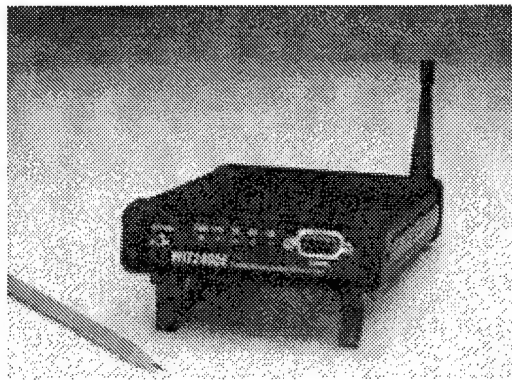


Figure 4.27 Digital Wireless Corporation's WIT2400E Modem [14]

4.8.10 Wireless Modem Selection. The WIT2400 Developer's Kit from Digital Wireless Corporation was selected for *SIMSAT* implementation. From an integration perspective, this option did not require incorporation of the wireless modem into the power architecture, and it incorporated an RS-232 interface to the AutoBox. Software could be used to adjust modem settings from a standard PC station before integration onboard the satellite. Thus, this alternative was determined to be easy to integrate into the system. With a next-day delivery time, acquisition of the kit was not time-critical. For

these reasons, the kit was selected for *SIMSAT* use, but was not ordered early in system integration.

4.9 Subsystem Integration

4.9.1 Problem Statement. The integration subproblem is summarized below:

Based on the selected subsystems and structural design, develop an integration strategy for the power and signal interfaces of each subsystem.

4.9.2 Problem Scope. Because of the limited design schedule and late delivery of some system components, full integration of the *SIMSAT* architecture was not possible before publication of this document. Thus, this design iteration focused on considering integration issues, identifying subsystem interfaces, and developing power and communications architectures. This section does not include actual system integration, test, or evaluation. At this stage, laboratory technicians, technical support representatives, and design advisors played a key role in system development.

4.9.3 Power Interface Issues. The following power-related tasks were identified for consideration in this design phase:

- Developing the overall electrical bus architecture.
- Determining wire gauges.
- Providing capability to monitor power usage.
- Providing payload power interfaces.
- Grounding the satellite.
- Reducing RF/electromagnetic interference (RFI/EMI).

4.9.4 Signal Interface Issues. The following signal-related tasks were identified for consideration in this design subproblem:

- Providing payload signal interfaces to the AutoBox.
- Momentum wheel assembly integration (to include connecting motors and amplifiers, and connections to the AutoBox).
- Calibrating the gyros.
- Receiving data from the gyros.
- Connecting the wireless LAN to the AutoBox.
- Connecting the wireless modem to the AutoBox.

4.9.5 Power System Architecture. Early in Detailed Design, it was decided to use the Power-Sonic line of sealed lead acid batteries to meet system power requirements. From this starting point, detailed design of the power subsystem began in earnest. Major integration issues involving operating voltages, current protection, wire gauge, power consumption, and other interfaces surfaced during this phase of design. The power subsystem changed several times during the course of detailed design as power requirements were added, modified, or deleted.

4.9.5.1 Bus Voltage Determination. At the beginning of power system development, the baseline *SIMSAT* operating voltage was initially set at 24V DC. This voltage provided acceptable operating conditions for the momentum wheel motors and AutoBox. The NEJ-3000 Piezo Electronic Gyro System (Horizon gyro) was originally determined to require a dedicated 4.8V/50mA dry cell power supply for optimum system performance; however, this item was subsequently deferred in favor of the Humphrey helicopter gyro package in the Detailed Design first iteration. Power requirements for the communications subsystem were estimated as 12V/50mA for a typical arrangement.

The 24V operating voltage allowed for two 12V batteries to be placed in series, achieving the required voltage to operate the momentum wheel motors. Minimum operating voltage for the motor was listed at 20V, although initial experimentation with a similar motor by the same manufacturer (the SmartMotor) indicated that a voltage slightly higher than this value was required for consistent operation. Experimentation with AutoBox con-

firmed 8 to 36V autoranging operation, although a minimum 15V for system startup was required prior to operation at lower voltages. AutoBox power draw remained a constant 60W throughout the range of operating voltages.

An additional factor considered during design of the power subsystem involved potential requirements of experimental systems not included in the baseline design. An example of this integration issue was the cold-gas thruster system planned for eventual implementation. The operating voltage range of the Moog Model 50-673 Cold Gas Thruster Triad is 24V to 32V; if SIMSAT were operating only at a maximum voltage of 24V, the system would not be robust enough to support thruster operation for more than the first few minutes of the experiment. This situation would occur as battery power was drawn down and the output voltage dropped below 24V³⁰.

Given these conflicting requirements, it was decided to consider both 24V and 36V operating bus voltages for the *SIMSAT* baseline. A system-level trade study conducted earlier in this phase of the design indicated a clear preference for a 36V bus voltage. This voltage alleviated any concerns regarding insufficient operating voltage for any hardware contemplated for eventual *SIMSAT* use. Additionally, a multiple power bus architecture was decided upon for the baseline power design. Since power would be supplied by 12V batteries, it would be possible to wire three batteries in series to provide a full 36V, or place components in series with only one or two batteries to obtain 12V or 24V power. This arrangement allowed the greatest flexibility in matching varying component interfaces. Figure 4.28 shows the original wiring diagram developed at this stage of the design.

4.9.5.2 Wire Gauge Selection. Standard electrical handbooks were consulted to determine the wire gauge needed for safe operation. The maximum current drawn by each component was estimated (shown in Table 4.11) and compared to data from the American Electrician's Handbook [10]. This reference indicated that 18 gauge wire would be sufficient for basic system wiring needs. The exception to this design would be motor/amplifier wiring due to the large currents anticipated. A minimum 12 gauge was

³⁰For this reason, the *36V Baseline Bus Availability* metric was used in the first Detailed Design system evaluations.

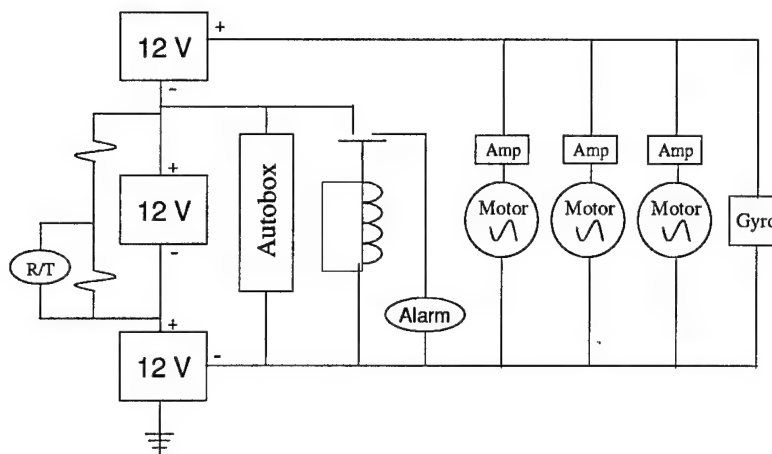


Figure 4.28 Initial Wiring Diagram

determined to be sufficient between the batteries and the amplifiers, while slightly lighter wire (14 gauge) would suffice between the amplifiers and the motors. This design decision reflected a tradeoff between a worst-case possibility and expected operating performance.

Table 4.11 Power Estimates Used for Wire Sizing

Component	Current (A)	Voltage (V)	Power (W)	Minimum Wire Gauge
AutoBox	2.5	24	60	18
Motor/Amplifier	20	36	720	12/14
Receiver/Transmitter	0.5	12	6	27
Gyro	1.78	28	50	18
Thrusters	0.75	32	24	18

Assuming the theoretical situation in which all three motors were simultaneously drawing maximum current, wiring extending from the battery terminals would need to be rated for a maximum 60A current. Such wiring would be unacceptable for *SIMSAT* use, due to its inherent bulk, thickness, inflexibility, and internal resistance. A more likely situation would be infrequent maximum power output to a single motor, with light to

moderate current supplied to the remaining motors. These power events would likely last for only a few seconds (perhaps up to 30 seconds), with maneuvers alternately led by different motors in an unpredictable fashion. This situation would effectively lead to pulses of current flowing through the motor/amplifier leads, allowing some time for heat dissipation. For this reason, motor/amplifier wire sizing is based upon a nominal 20A continuous current, thereby permitting the use of thinner wire compared to the worst-case situation.

Tables 4.12 and 4.13 provide representative values for short-time ratings of aircraft-grade cables [55]; these results support the system design decision. It should be noted, however, that bundling of cables reduces the maximum rating due to the decreased heat dissipation from shared surface areas.

Table 4.12 Maximum 5min Rating (Amperes) for Aircraft-Grade Cables in Free Air

AWG Size (approx.)	1 Cable	3 Cables	7 Cables	12 Cables
22	12	8	7	6
16	25	19	14	13
10	71	56	48	45

Table 4.13 Maximum 1min Rating (Amperes) for Aircraft-Grade Cables in Free Air

AWG Size (approx.)	1 Cable	3 Cables	7 Cables	12 Cables
22	15	12	9	9
16	33	28	26	25
10	110	107	104	101

4.9.5.3 Power Monitoring. It was recognized that some method of determining battery discharge levels would be required during experiments. This requirement was necessitated by the need to ensure the controlled termination of maneuvering prior to battery power falling below acceptable minimums. Premature shutdown due to inadequate power margins could prove catastrophic; the loss of motor torque might result in the uncontrolled dumping of system momentum, thereby manifesting itself in uncon-

trolled angular accelerations imparted to the satellite. For this reason, hardware to monitor available power was deemed a requirement.

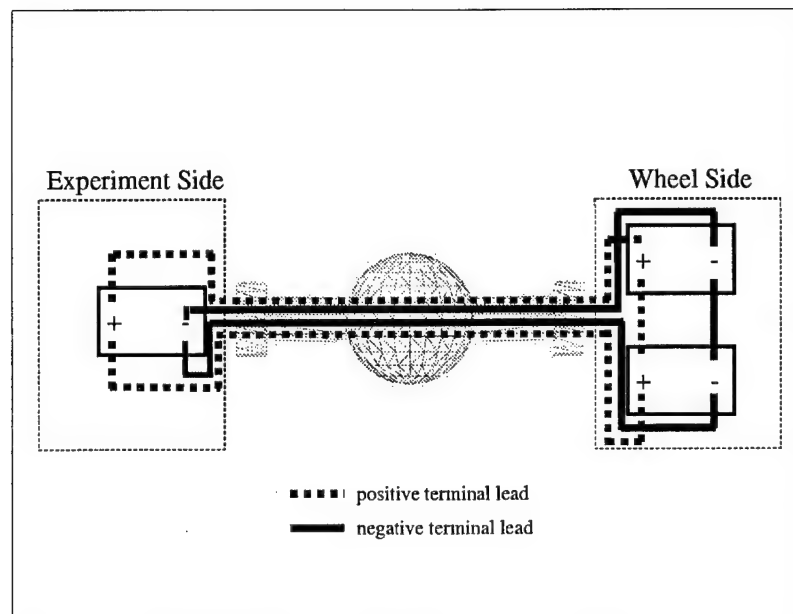
One possible method of implementing power monitoring capabilities would rely upon the data collection and telemetry subsystem already onboard *SIMSAT*. Voltage and current (across each of the batteries individually, or collectively) could be monitored using voltmeters and ammeters. Telemetry from these sensors would be collected using data input channels routed to AutoBox, which in turn would transmit the telemetry stream to the ground station. Outputs from these channels would be displayed for the experimenter. Although attractive in some respects, this method was not chosen for baseline system implementation. Concerns centered on system complexity, particularly with regard to the issue of data dropout during an experiment. This scheme also requires the allotment of AutoBox input channels, decreasing the available channels for an experimenter/user. Although battery telemetry remains a possibility for future system implementation, this option was not incorporated in the baseline *SIMSAT* design.

In lieu of battery telemetry, which resembles current satellite monitoring practices, a more prosaic option was selected. This system takes advantage of the fact that the satellite is not remotely located, but instead is in close proximity to the user. A voltage monitoring relay in series with a sonalarm (audible tone buzzer) provides a direct indication of system voltage falling below a specified level. Since the operating characteristic curve of a Power-Sonic PS-12180 is specified with reasonable certainty (from manufacturer specifications), a drop-out voltage can be selected corresponding to an acceptable power margin for immediate system shutdown. This electromechanical system would provide a straightforward approach to achieving the desired end result, while minimizing system hardware and integration impacts.

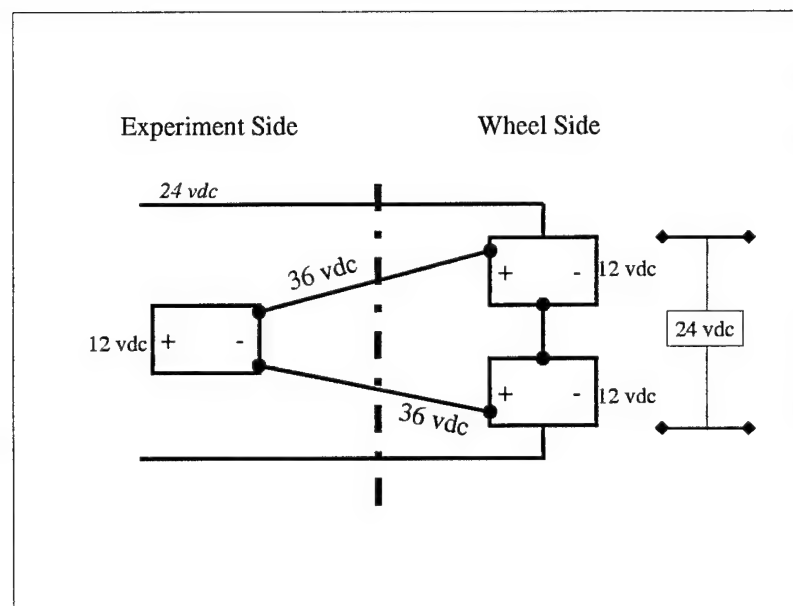
Catalog searches indicated that the Macromatic VMP024D voltage monitoring relay was suited to meet system requirements. This part was commercially available with minimum time delay. Voltage monitoring relays are not commonly found for voltages around 36V since this operating voltage is not typical for most applications. 24V systems, by comparison, are more common; therefore, the VMP024D was designed around a nominal 24V. Because of this constraint, the VMP024D was integrated to measure the voltage

drop across only two of the three onboard batteries. This voltage allows a proxy measure for the total system voltage, since the discharge across any one battery should remain fairly close to that of the other two. Since some batteries are "loaded" more heavily than others, however, the relay was wired across the two most heavily loaded batteries to ensure a conservative reading. Based upon characteristic curves for Power-Sonic batteries, a lowest allowable discharge voltage of 11.6V (for each battery) was desired. This voltage corresponds to a remaining battery capacity of approximately 10%. The VMP024D relay can be ordered with a pick-up voltage between 21-27V. The relay de-energizes when the monitored voltage is below the drop-out setting, set at 3% below the pick-up voltage. A VMP024D relay with pick-up voltage set at 24V would drop out near 23.3V, or 11.6V over each of two batteries; therefore, this setting was specified for purchase.

4.9.5.4 Bus Modularity. A major objective of the *SIMSAT* design effort was to maximize system modularity to the greatest extent possible. Modularity, particularly at the payload interface level, provides the experimenter with the most flexibility in obtaining the desired data set. From a power perspective, the decision to use 12V batteries allowed for the consideration of multiple power "buses", offering standard connections to 12, 24, and 36V DC supplies. Because of structural design constraints, however, implementation of all three buses on both sides of the truss presented some wiring challenges. Equipment separation (i.e., placement of hardware on both sides of the central sphere) implied the need for power cabling through the hollow center of the air-bearing assembly, as shown in Figure 4.29. Minimizing the amount of power cabling was highly desired, since the total volume available for all types of cable (power, communications, air, etc.) was limited. Although power from the 36V supply line could be easily tapped on both sides of the system, availability of 24V power was constrained by the arrangement of batteries onboard (see Figure 4.29). A decision to require 24V power connections on the experiment side of the truss required two extra cables run through the central sphere (a total of 6 wires compared to the minimum of 4). 12V power could be readily provided on both sides of the satellite, however, since at least one battery is present on either side of the air-bearing assembly. Further inputs from the decision makers were required to determine the payload power interfaces.



(a) Electrical Bus Configuration



(b) Detailed 24V and 36V View

Figure 4.29 Electrical Bus Design

4.9.5.5 Power Interfaces. Discussions with the decision makers identified their preferences in considering power connections to experimental payloads. The following characteristics were listed as important when designing the payload/component power interfaces:

- 12V/24V/36V bus capability required on both sides of the satellite.
- Power and data cable connections should be physically different to prevent improper connection.
- Positive latch mechanism required to ensure good physical connection is established and maintained.
- Single multi-pin plug with all three bus voltages should be available, or three separate plugs (one each for 12V, 24V, and 36V) providing a "single face" to the experimenter (multi-pin plug is preferred).
- In addition to supporting experimental hardware connections, components should be designed to interface with the appropriate voltage bus where possible, rather than directly hardwiring them to the battery terminals.
- Fiber-optic cable attachments were not deemed necessary for baseline system implementation.

Based upon these inputs, the original wiring diagram was modified to indicate the use of bus terminals as wiring junctions, as shown in Figure 4.30. Location of the buses was determined based upon the updated physical layout. On the payload side of *SIMSAT*, the bus bars were mounted on the reverse side of the gyro/battery/transceiver mounting plate, while on the momentum wheel side the buses were located on the reverse side of the primary battery mounting plate. Due to the heavy wire required between the batteries and amplifiers, these connections were not considered appropriate to place on the 36V bus. All other items (including all 12V and 24V connections) were deemed appropriate for inclusion on their respective buses. Additionally, a multi-strand power connector cable running from all three payload-side buses to the payload plate was required. The use of 18-gauge wire in the power connector cable allowed for power outputs of up to 60W, 120W, and 180W, for

experiments running at 12V, 24V, and 36V, respectively. A power connection cable was not included for the momentum wheel side in the baseline design, due to no foreseen need for such capability at this time (as decided by the decision makers). Should the need arise to provide power to momentum wheel-side experimental payloads, power connections from the momentum-wheel side buses could be implemented with relatively little effort.

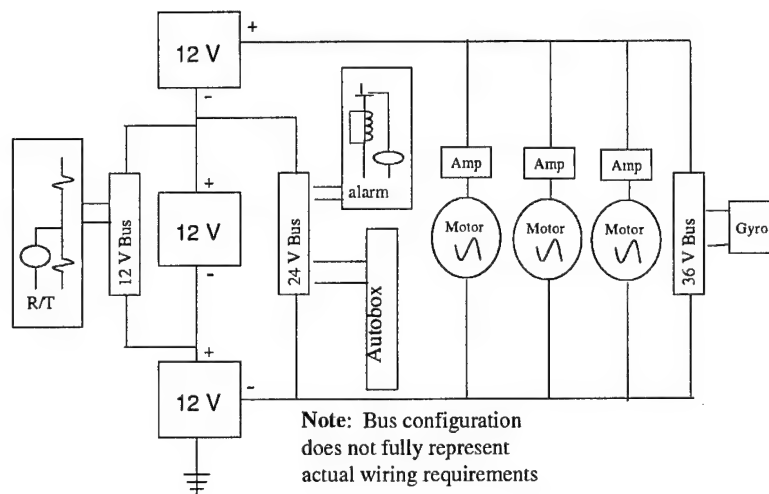


Figure 4.30 Modified Wiring Diagram

4.9.5.6 Electrical Grounding. Grounding (more generally, prevention of excessive static charge buildup) remains an issue subject to further design work as system integration and initial testing warrants. Because the air-bearing is a Teflon sphere physically separated from the pedestal on a cushion of air, it is very possible that the satellite will remain electrically isolated from its surroundings. The presence of rotating electromechanical devices (i.e., the momentum wheels and their associated motors) presents an opportunity for static charge creation and buildup on the surface. Even if this charge is not sufficient to present a safety hazard to laboratory personnel, the possibility of uncontrolled discharge or arcing presents the possibility for damage to sensitive electronic components. At this time, the problem of static charging has not been defined in quantifi-

able terms. Possible methods for mitigation may include static discharge probes mounted to *SIMSAT* in a manner similar to modern aircraft. Alternatively, periodic discharging using a brush or pole mechanism operated manually or automatically may be required. Finally, if the problem proves severe enough, a permanent grounding wire may need to be attached to satellite connecting it to "earth" ground. This solution would not only impede free motion of the satellite, but it would also add a permanent (albeit small) disturbance torque to the simulator which would need to be countered.

4.9.5.7 RFI/EMI Interference. Another related electrical issue was the possibility of radio frequency/electromagnetic interference (RFI/EMI) created by *SIMSAT* subsystems. The momentum wheel motors pose the greatest potential source of interference within the simulator, since rotating machinery is notorious for creating electrical noise. Additionally, the mere presence of passing electric current through wiring implies the creation of an antenna, with the potential of creating undesirable RFI. Use of wireless communications may provide some concern, as well. Again, the RFI issue has not been defined in quantifiable terms. It was hoped that experience gained during initial integration efforts would result in scoping of the problem and its overall relative importance. Potential mitigation techniques include shielding of cables and individual components, movement of components to induce shadowing effects, or line filters. Additionally, the use of optical signals (rather than electrical signals) would completely avoid the RFI issue, at least with regard to some channels (particularly data collection). Fiber optic cable assemblies can be purchased commercially in standard lengths with standard end connectors. However, system complexity and cost would be substantially increased.

4.9.6 Communications Architecture. Development of the communications architecture was an ongoing design process, which required modifications as subsystem components were selected and altered. For the most part, communications architecture decisions were driven by signal requirements of the various components. As the full integration of components was not possible as this document went to print, detailed signal requirements were left unspecified, but a general communications architecture was developed such that integration of components would be easily facilitated.

4.9.6.1 Payload Signal Interface Design. A primary driver in the overall communications architecture concerned the interface with the experimental payload. As a testbed for experimental research, a well-defined and easily adaptable communications interface was required to ensure adequate input/output data channels for experiment telemetry and command data. Signal interface design was initiated with an estimation of baseline system channel requirements. The dSPACE/AutoBox C&DH architecture provided up to 32 input and 32 output signals. Internal A/D and D/A cards (DS2003 and DS2103, respectively) allow analog voltage signals ($\pm 5V$ or $\pm 10V$) to interface with the dSPACE/AutoBox.

No telemetry data from the power system or the wireless systems was anticipated, but the gyros and amplifiers would require a number of input and output signals. For the Humphrey gyro system, initial signal estimates included ten inputs from the gyros, with four outputs to the gyros (may not be required in the final design). These estimates were considered conservative; laboratory evaluation of the gyros was in process at this stage which should indicate which signals were required and which were not. Similarly, six input and six output channels were estimated for the amplifiers. This estimate allowed two channels per motor. Using these estimates, 16 input channels were available to the experiment payload. Six output channels were reserved for thruster integration. The exact number of signals to the thrusters was not known at this time, but this estimate was considered reasonable. Thus, 16 output channels were also unused by the baseline system.

Early communications architecture design stressed full signal interface modularity. A proposed architecture included a full 32-input/32-output ("32/32") interface board on each side of the central sphere. This design would allow complete channel availability on either side, without the need to route additional wires through the sphere during an experiment. Basically, the design would incorporate two 32-wire lines permanently configured through the center, with a full 32/32 interface board on both base mounting plates, wherein all input/output connections would be made. The 32/32 interface board would be similar to

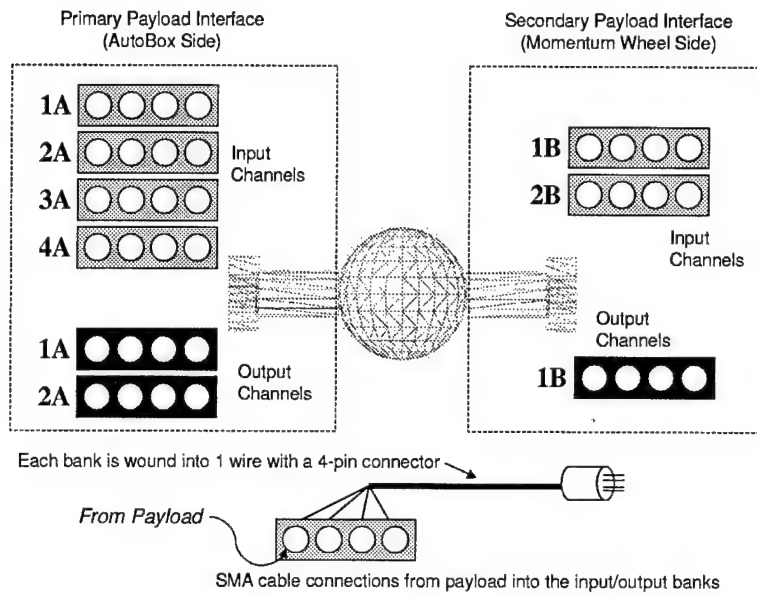
that used with the ground-based dSPACE system³¹. This proposed architecture was expanded further to allow full 32/32 channel availability at each mounting plate, wherein each plate would be connected using 32-wire lines and junction boxes would allow selection of which input/output channels were active. However, this architecture was considered overly modular since in no foreseeable instance would either side require all 32 channels. In short, the ADACS and payload hardware would never be both on the one side simultaneously. The benefits of a common 32-pin (maximum) connector for each subsystem interface (with inactive pins removed for each subsystem) were deemed marginal at best. This alternative also included the drawback of excess cabling/junction weight.

Conversation with the decision makers indicated that a 16-input and 8-output interface would meet foreseeable *SIMSAT* requirements for the primary payload side. For the momentum wheel side, an 8-input and 4-output capability would adequately allow mounting of payload hardware and collection of data on that side. This reduction in channel availability allowed savings in cabling weight and wiring complexity. Several interfacing techniques were considered. The preferred design included 4-channel banks which would take four channel signals from the payload and bundle them into one wire. Figure 4.31(a) shows the payload input/output interface architecture using the 4-channel banks. This wire would be permanently routed to the main AutoBox signal interface board which would be plugged into the AutoBox using 32-pin connectors, as shown in Figure 4.31(b). A physical constraint, the AutoBox required a 32-pin connector for both the input and output channels. This design allowed a reasonable compromise in the number of connection wires (minimum preferred) versus the number of available channel configurations (maximum preferred)³². Several details of this architecture still required definition.

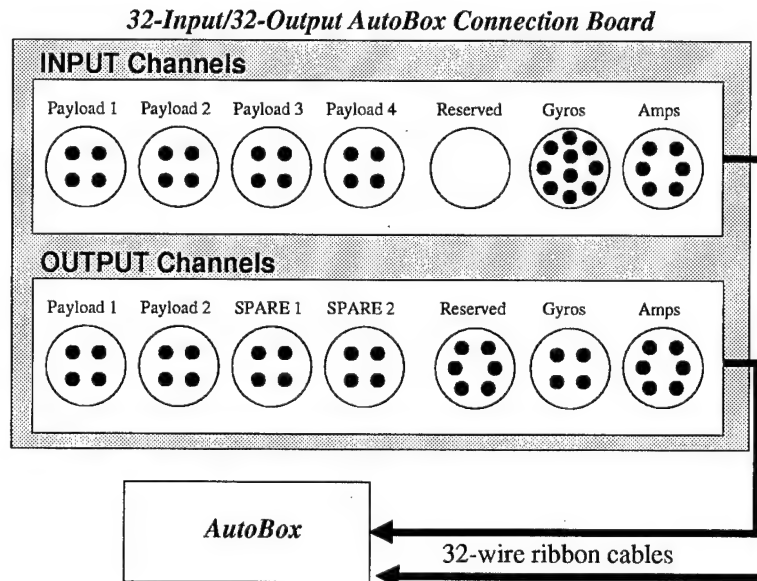
Channel Switching. To start, not all channels could simultaneously be used at once. Only 16 total inputs were available, so if a bank of four channels was being used on the momentum wheel side, only three banks of four would be available on the

³¹Rack-mounted 32-input/32-output connection panels were provided with the dSPACE system. These panels allow the development of a ground-based simulator which can be used without the air-bearing assembly and satellite power system.

³²For example, nine input channels on the primary payload side and seven input channels on the momentum wheel side would not be a feasible configuration using 4-channel banks.



(a) Payload Input/Output Channel Banks



(b) AutoBox Channel Interface Board

Figure 4.31 Signal Interface Architecture

primary payload side. Activating the necessary banks required either a switch or manually plugging the needed bank into the input/output interface board. It was determined that a switch would entail added complexity in the design for little benefit. It would be almost as easy to unplug one bank and plug in another. Thus, the final signal interface architecture required the experimenter to plug in the active channel banks. Three cables would be permanently routed through the center to provide the momentum wheel-side banks. At the input/output interface board (see Figure 4.31(b)), these channel bank wires would be permanently positioned, allowing active banks to be easily plugged in.

Interface Board Placement. The channel banks would be mounted on the payload interface mounting plates along with the power interface connections. The input/output interface board would be positioned near the AutoBox, allowing a very short distance between the board and the AutoBox 32-pin connectors. Preferably, the interface board would be mounted on one of the AutoBox mounting plates.

Wiring Identification. To ensure that wires are clearly defined, input wires would have black connections to the interface board, and output wires could have blue connections. This color-coding is consistent with the black/blue 32-wire ribbon cables used on the rack-mounted input/output boards³³. Similarly, black and blue ribbon cables could be used for the onboard AutoBox connections. To identify which side the bank wires connect to, all momentum wheel-side (secondary payload interface) banks could be marked with tape (or a similar marking).

Baseline Channel Requirements. The architecture allows each subsystem to interface to the AutoBox interface board with a single cable. This communications architecture is simple enough that modifications can easily be made. If more or less channels are required by the baseline subsystems, the number of pins used in their respective connector can be adjusted.

³³ Any color-coding protocol would suffice, but the design team recommended this scheme.

4.9.6.2 Momentum Wheel Integration. Integration of the momentum wheels with each subsystem was a phased approach. In the first phase, each momentum wheel was successfully mounted on the motor shaft. A primary concern during this phase was designing a mechanism to prevent disaster if the motor "locked up" during an experiment. It was unknown if the sudden loss of power to the motor would cause the momentum wheel to come to an abrupt halt. Therefore, to prevent total momentum transfer to the vehicle, a brass shear pin was inserted through the axle and the momentum wheel's mounting sleeve. In case of emergency, the brass pin would break and allow the momentum wheel to spin freely until it came to rest. This would still transfer momentum, but would occur at a gradual, not instantaneous, rate.

Following the successful mounting of the momentum wheel, the second phase was connecting the motor with the amplifier (amp). From a signal standpoint, wheel speed information is passed from the motor to the amp. Control inputs are sent from the amp to the motor.

On 2 February 1999, an amp was successfully connected to a momentum wheel. Using a 20VDC power supply, the momentum wheel achieved a top speed of 1050 RPM. This speed was measured using a timing gun provided by Mr. Jay Anderson.

The final phase (yet to be accomplished at the time of this printing) involves the integration of the amps with the AutoBox.

4.9.6.3 Rate Gyro Integration. Three integration issues existed for the Humphrey gyro. First, due to the sensitivity of the gyro, it was imperative that it be shock mounted. Natural rubber plate-form mounts from the McMaster-Carr Supply Company in Cleveland, OH, were ordered to be used to isolate the gyro components from the mounting plate.

Second, the gyro has to be integrated with the AutoBox to send *SIMSAT* rate and acceleration information. The output signal from each rate gyro and accelerometer is a 0-5V analog signal. For each rate gyro and accelerometer, 2.5V represents a null reading. Readings above 2.5V represent a clockwise rotation. Readings below 2.5V represent a counterclockwise movement.

This signal is sent to the AutoBox and is converted to a 16-bit digital signal through an A/D converter. At this point, the SIMULINK code receives the digital signal as the *SIMSAT* angular velocities and accelerations in terms of voltage. Using a calibration curve developed from data delivered by the manufacturer, the input voltage is converted to deg/sec or deg/sec² (see Appendix E for conversion details). The output of these conversions is then used by the for controlling *SIMSAT* motion. At the time of this printing, laboratory technicians were working on collecting and interpreting these gyro signals.

The last integration consideration was the input power specification. As stated before, the gyro uses an operating voltage of $28\pm V$ DC.

4.9.6.4 Wireless LAN Integration. Due to schedule constraints and the late acquisition of the wireless LAN system, the wireless integration was delayed. Integration procedures are described in this section, but actual integration and testing of the system was anticipated to begin in late February 1999. Integration was to proceed in several steps, described by the following paragraphs.

ISA CardLINK Connection. The following integration tasks provide a brief summary of the ISA CardLINK installation procedures. Detailed procedures are described in the user's guide provided with the ISA CardLINK.

- Mount the transceiver within the *SIMSAT* enclosed laboratory area.
- With PC power removed, install the Model 101c adapter card using an available ISA slot in the Simulation PC.
- Connect the transceiver to the Model 101c card using the supplied adapter cable.
- Power the PC; Windows operating system will detect the Model 101c card and prompt for software installation.
- Insert the RadioLAN Drivers disk and install the driver software.

DockLINK Integration. The DockLINK User Guide [44] provides detailed system installation procedures. This section identifies points to consider during the integration of the DockLINK system.

First, the radio transceiver is connected to the DockLINK using the supplied DB15 jack. The installation procedures indicate that the transceiver should be mounted parallel to the ground station transceiver. As *SIMSAT* will be in motion, this parallel alignment is not possible. Conversation with RadioLAN technical support confirmed that in a short-range application such as this design, a rotating transceiver should not be an issue. However, if this configuration results in high data dropout, the system should be returned to RadioLAN.

The supplied power adapter should be used to power the DockLINK during initial testing. Once initial checkout is accomplished and the power architecture is developed, use of *SIMSAT* battery power can be used.

The DockLINK RJ-45 jack will need to be connected to the AutoBox using a 10BaseT Network Interface Card. With the AutoBox Ethernet card, this connection should be provided already³⁴. An IP address is assigned to the DockLINK using procedures described in the user guide.

4.9.6.5 Wireless Modem Integration. As stated in Section 4.8.10, page 4-89, the wireless modem would not require significant integration effort. The WIT2400E unit includes its own power supply and connection cabling, and it is small enough to be mounted nearly anywhere convenient. Thus, power and physical integration issues were not of concern. A DB-25 data connector is supplied with the WIT2400 Developer's Kit. If individual signal pin-out information is required, the DWC website [14] provides all modem signal information. Once the modem is delivered, laboratory technicians would be required to connect the wireless modem using the RS-232 interface by configuring a suitable connection to the RS-422-A high density sub-D connector of the AutoBox. This connector can be in-house developed, or a COTS converter can be purchased. Black Box

³⁴Wired integration of the AutoBox to the Simulation PC was successfully accomplished. The wireless LAN should use the same connections.

Corporation produces a line of interface converters, to include RS-232 to RS-422, which may be used once wireless modem integration is underway [6].

4.10 Safety System Design

4.10.1 Problem Statement. This design iteration addressed the safety system subproblem, as summarized below:

Investigate the safety issues associated with SIMSAT operation, and recommend a preferred safety system (or systems) to mitigate the risks of personnel injury and equipment damage.

4.10.2 Problem Scope. The *SIMSAT* system was to be operated in a laboratory environment, wherein certain safety measures were desired to ensure that researchers, students, and observers could safely perform and monitor simulator-based experiments. Furthermore, the high costs associated with this project made the reduction of equipment damage due to mishaps or system failures a necessity. As a one-of-a-kind system, any significant damage to the *SIMSAT* software or hardware components may result in extensive research program setbacks. Enhanced safety measures would better accommodate sensitive and expensive experimental payloads as well, thereby encouraging more research and experimentation by outside agencies.

In order to provide this necessary level of safety, operational risks first needed to be identified. Based on these risks, techniques and mechanisms were formulated to minimize the system impacts associated with these risks. These safety measures were analyzed on a system level to allow selection of a preferred safety system which reduces risk while considering system impacts with respect to cost, schedule, and performance.

4.10.3 Safety System Background. Throughout the *SIMSAT* development, the importance of minimizing operational risks was recognized as fundamental to system design. From the first objective hierarchy of the Concept Exploration and Definition phase, personnel injury and equipment damage were addressed, through the identification of hazards and associated hazard severity of competing system architectures. The Pre-

liminary Design phase included estimations of relative safety indices to be used in system evaluation and selection. Moreover, in the first iteration of the Detailed Design phase, the need to contain the momentum wheel assembly was addressed to prevent loose objects from projecting off a rotating momentum wheel, as well as prevent significant damage in the event of a catastrophic motor shaft failure. A lexan box enclosure about the momentum wheels was selected to satisfy these safety concerns. Other safety measures considered in the Detailed Design phase included the following:

- Anti-tipping stanchion braces to prevent an unbalanced satellite from falling off the stanchion supports (while being configured).
- Incorporation of an alarm mechanism to detect low voltage conditions, thereby warning an experimenter when the system is running low on power.
- Use of a padded collar about the air bearing pedestal, minimizing structural damage to the satellite and pedestal if pitch limits are exceeded.
- Consideration of safe electrical design, to include grounding of the satellite to prevent a charge buildup.

At this stage, however, two remaining safety issues were yet to be examined through formal system analysis. This design subproblem addressed these issues.

4.10.4 Safety Issues. The first issue of concern at this stage of the design was how to minimize the damage should the satellite topple off the pedestal, due to a structural failure, seized motor, physical contact, or other means. Given the cost of the *SIMSAT* hardware, the system weight, a drop distance of approximately 4 ft, and the hard concrete floor of the lab environment, a safety system was deemed necessary to safeguard against the catastrophic loss of the satellite in such a falling accident. The second issue was related to the emergency shutdown of the system, which was an identified need in the Concept Exploration and Definition phase. The ability to prevent system damage in the event of a communications link failure, loss of power, control law error, or other emergency situation, was necessary in the overall system design. These two issues were interrelated

to a large degree, as an emergency situation could potentially induce the toppling of the satellite.

4.10.5 Value System Design. The following prioritized objectives were used in the evaluation of safety mechanisms:

- Minimize system damage (to include the satellite hardware, the air-bearing cup, the rotor, and the pedestal) in the event of an emergency shutdown or toppling condition.
- Minimize the system impacts, in terms of both performance and structural redesign, associated with the safety system implementation.
- Minimize environmental impacts due to implementation, such as laboratory construction or reconfiguration.
- To the maximum extent possible, allow system accessibility during operation.
- Minimize the cost and schedule of the safety system implementation.

4.10.6 Safety System Alternatives and Selection. Several safety system mechanisms were considered throughout the *SIMSAT* development. Each of these ideas suffered from potential drawbacks in addition to its merits. During this phase of design, these potential solutions were documented and analyzed, as described by the following paragraphs. A recommended safety system was selected for implementation.

4.10.6.1 Cargo Net. The first concept examined was a safety net suspended over the satellite which could be dropped on the device should it begin to gyrate in an unstable or uncontrollable fashion, as shown in Figure 4.32 (figures at the end of this section). This "cargo net" would slow down *SIMSAT* as the device became entangled within the net. Although inexpensive and easy to implement, this device would not prevent *SIMSAT* from bouncing out of the air-bearing pedestal cup, and might actually cause such a mishap depending upon the situation. Therefore, the cargo net option might slow down a tumbling system, but it could not protect against the more serious threat of *SIMSAT* falling onto the laboratory floor.

4.10.6.2 Lion Trap. The next concept that was considered had the cargo net arrangement reversed, with the net kept on the floor during normal operation. The "lion trap" scheme, shown in Figure 4.33, involved the hoisting of shroud lines should *SIMSAT* begin to tumble out of control. The cargo net would effectively ensnare *SIMSAT* as it was being hoisted towards the ceiling, thereby preventing it from falling to the floor. The lion trap option suffered from at least three problems. First, having the cargo net on the floor would create a safety hazard during day-to-day operations and impede access to the satellite during experiments. Second, the positioning of shroud lines on the cargo net presented an opportunity for interference with experimental payloads extending from the basic structure. Finally, it was unclear that the lion trap could be "sprung" with sufficient rapidity to prevent *SIMSAT* from hitting the floor first. During operation, an individual would be required to standby for actuation of the safety system at all times, and even then, a person may not be able to react fast enough under all scenarios. The limitations of the lion trap scheme suggested any safety mechanism would need to work without operator intervention.

4.10.6.3 Trampoline. The next alternative considered was the so-called "trampoline" consisting of a net suspended above the floor but below the satellite. Figure 4.34 shows this arrangement. The trampoline would be set prior to the beginning of an experiment. Should the satellite fall off the air-bearing pedestal, the trampoline would prevent contact with the floor. Again, this option suffered from multiple drawbacks. The trampoline would prevent direct access to *SIMSAT* during experiments. Stanchions used to support the trampoline would also be cumbersome and potentially interfere with laboratory operations. Furthermore, ensuring the trampoline is taut enough to keep a 300lb object from overly stretching the net would be an extremely difficult task. A hybrid two-net scheme combining the characteristics of both the lion trap and trampoline mechanisms was also rejected for these same reasons.

4.10.6.4 Floor Padding. An easy and relatively inexpensive option considered was the use of thick padding placed on the floor. Athletic-use mats, such as those used for high jump or pole vault landings, are built to safely support the impact of

persons, and thus could potentially support the *SIMSAT* weight. They could also be easily pushed aside to provide access to the system during experimentation, although they would be bulky and somewhat cumbersome. The primary drawback of such a system was the level of shock protection to sensitive and expensive onboard hardware. Significant system damage was still anticipated despite the use of such mats. The mats may also restrict pitch limits for extended payload configurations.

4.10.6.5 Catch Arms. The placement of hydraulic- or pneumatic-actuated arms mounted on the side of the air-bearing pedestal could be used to engage the satellite and prevent it from falling during an emergency situation. This idea is illustrated in Figure 4.35. Upon analysis, this system would have severe drawbacks. Significant hardware construction would be required for the pedestal-mounted arms, which would be needed all around the bearing cup. Activation of such a system would also be a difficult technical challenge. The act of engaging *SIMSAT* with the arms may bounce the satellite anyway, and an unbalanced satellite may topple off the arms despite engagement. In addition, the arms would have performance penalties as the pitch limits of the system would be further constrained.

4.10.6.6 Skullcap. This last proposal appeared to address the fall-protection issue adequately, while offering minimal access interference. The "skullcap" arrangement, shown in Figure 4.36, would involve an articulating arm mounted on the wall of the laboratory, which is stored out of the way when not in use. A metal pole with a padded plate on the end would be attached to the arm. This pole would be lowered over the central sphere of the satellite prior to the start of an experiment. Should the satellite attempt to bounce out of the air-bearing pedestal cup, the skullcap would be positioned to prevent the bearing from moving any appreciable distance. With the addition of a lowering mechanism, the skullcap could be fully lowered onto the bearing (increasing friction) should *SIMSAT* begin to tumble out of control. Because the skullcap is positioned opposite the air-bearing cup, no impingement of pitch limits is made. Drawbacks associated with this design include the need to construct the support structure for the articulating arm, as well as a lowering mechanism for the skullcap itself. The physical positioning of the *SIMSAT*

pedestal made the wall a logical choice for this supporting structure, as ducting in the laboratory ceiling and a lack of rafter reinforcements precluded a ceiling-mounted device.

Based on the analysis of safety alternatives, the skullcap safety mechanism was recommended for implementation. This technically-feasible design provided containment of the central sphere within the air-bearing pedestal cup, while offering limited access restrictions with no performance impediments.

4.10.7 Emergency Shutdown Considerations. Regarding emergency shutdown of the system, several scenarios were considered. A loss of system control due to a physical phenomenon (such as motor seizure, momentum wheel malfunction, or structural failure), loss of power, or controller malfunction would cause limited damage with the addition of the skullcap safety mechanism. The skullcap would prevent catastrophic system damage by preventing the satellite from falling out of the air-bearing cup, but minor damage to the finely-machined central sphere of the satellite may likely occur. Damage to the finely-machined cup would be possible as well. Space Electronics, Inc., stated that repair of the cup and sphere would be possible should significant resurfacing be needed. With the reserve compressor air and the padded skullcap, this damage should not be overly extensive.

Because control law processing occurs onboard the satellite, loss of communications between the ground and satellite should not complicate emergency shutdown. Loss of signal could be recognized, and a predetermined onboard control sequence could be initiated to return the satellite to a preset position. This feature was not designed in the baseline controller model, but its addition would not be difficult should the need for such control logic be identified.

4.10.8 Implementation. With the limited baseline design schedule, it was not possible to begin implementation of the skullcap safety system. Detailed design and fabrication of this system is recommended for follow-on system design. Operation of the *SIMSAT* could still be accomplished without this safety mechanism, but risks of a toppling satellite should be understood and adequately minimized.

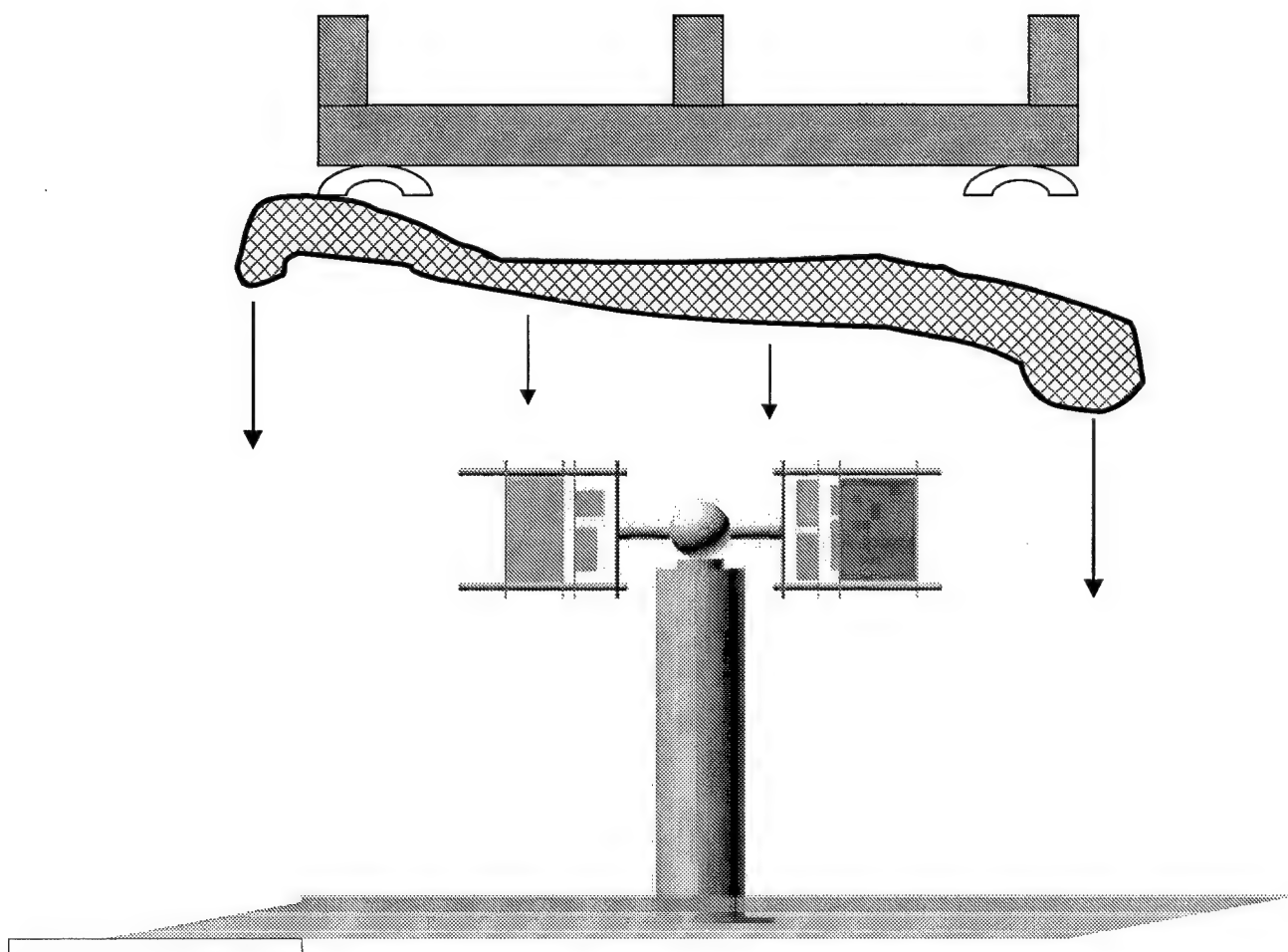


Figure 4.32 The "Cargo Net" Safety System

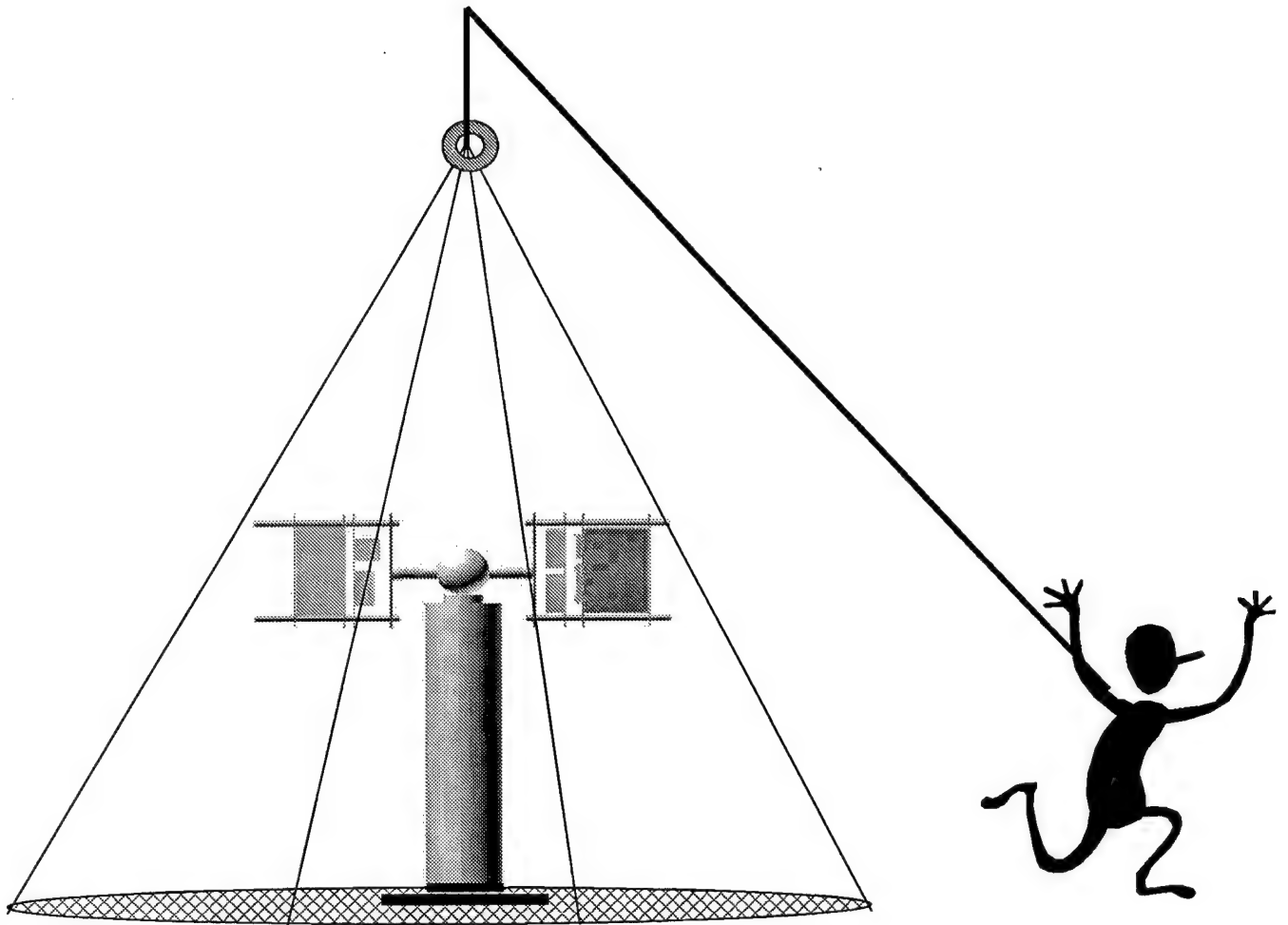


Figure 4.33 The "Lion Trap" Safety System

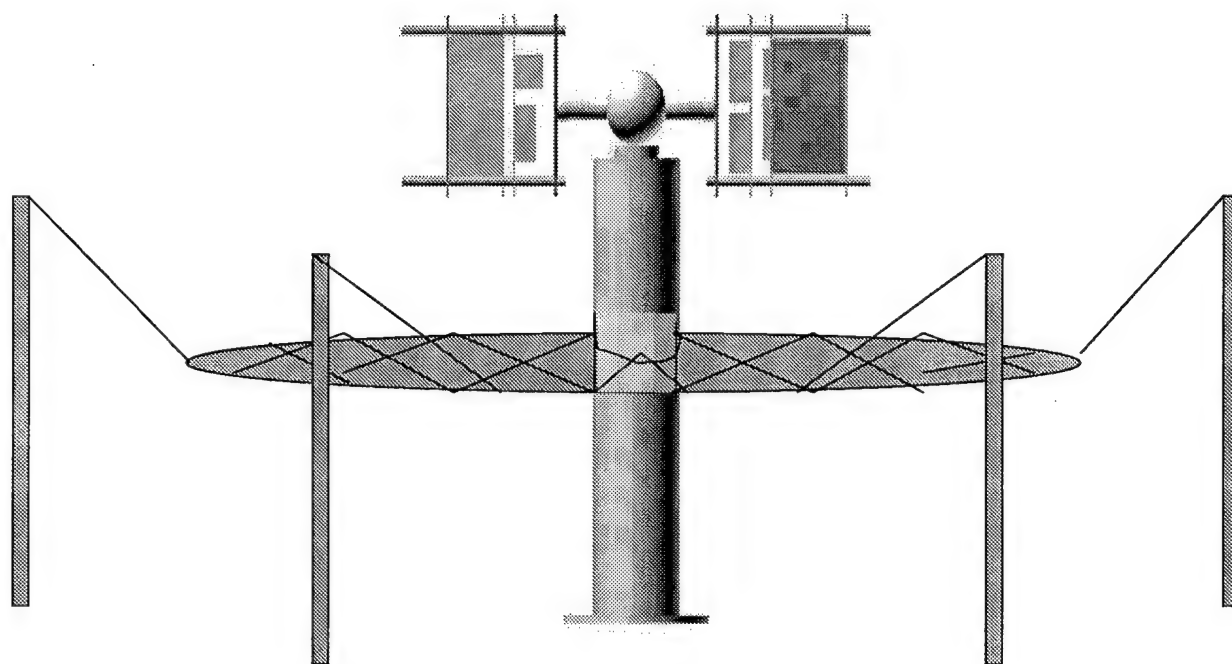


Figure 4.34 The "Trampoline" Safety System

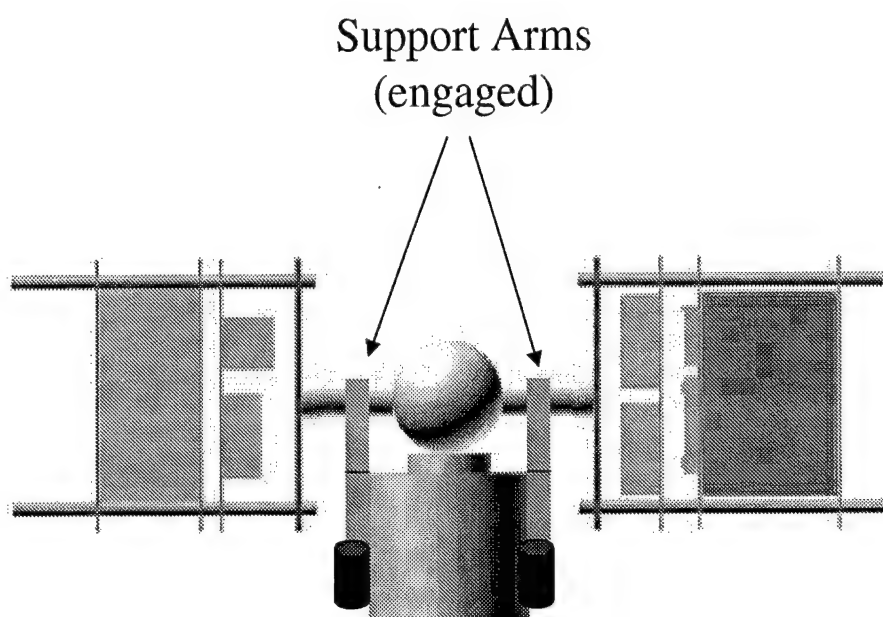


Figure 4.35 The "Catch Arms" Safety System

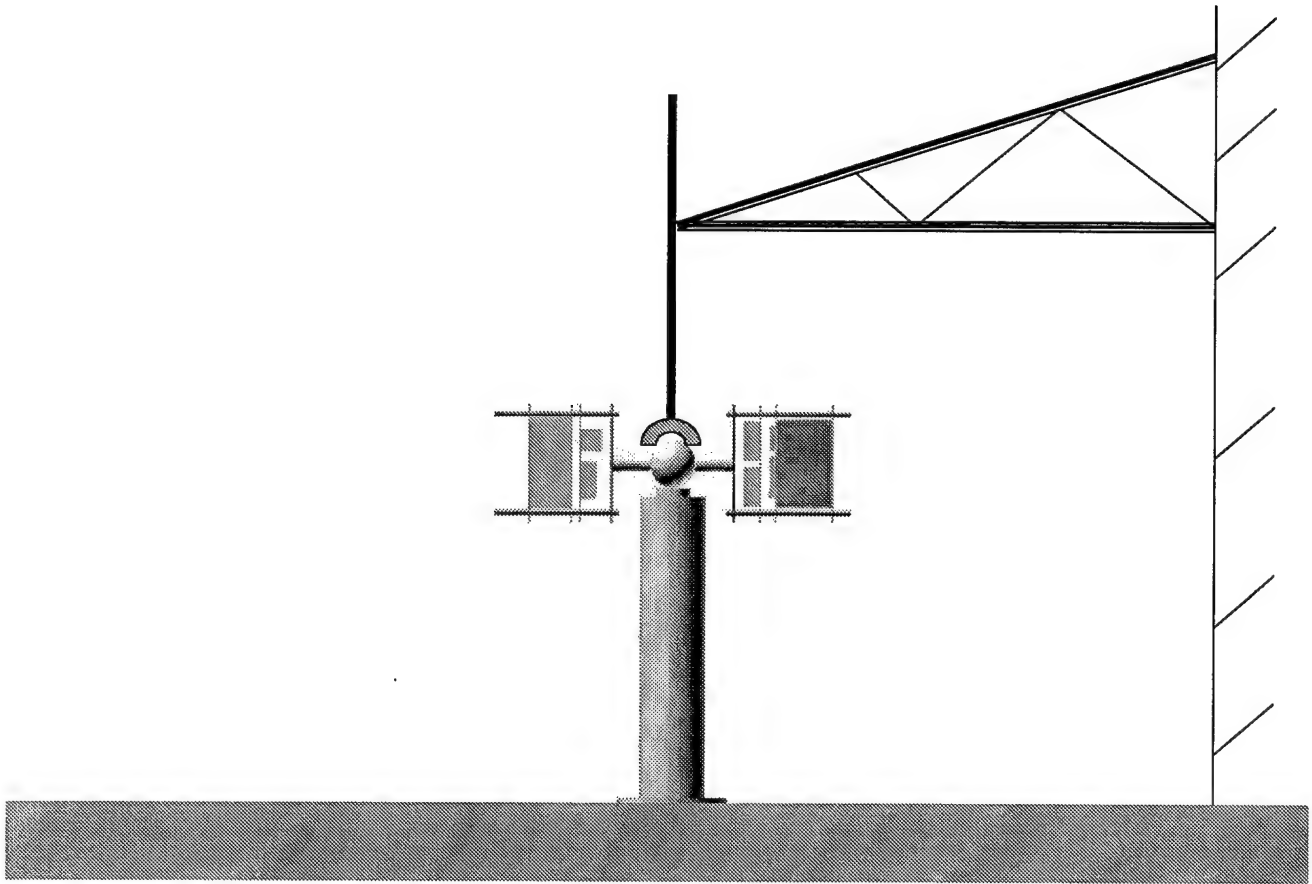


Figure 4.36 The "Skullcap" Safety System

4.11 Thruster Integration

4.11.1 Problem Statement. The following problem statement summarizes the thruster integration subproblem:

Select a feasible thruster alternative for SIMSAT use, and identify the associated integration issues.

4.11.2 Problem Scope. During the Preliminary Design phase, it was decided to use momentum wheels as the primary means of *SIMSAT* attitude control with the ability to add cold-gas thrusters at a later date. This approach fit well with the primary research areas planned for initial *SIMSAT* experiments, while allowing additional capability and flexibility for follow-on work to be added in a timely fashion. Although thrusters would not be present in the baseline design, the basic bus configuration would need to be compatible with future thruster implementation. Therefore, thrusters were actively researched during the Preliminary Design phase to ensure that their implementation would not pose insurmountable integration issues with the primary attitude control system. Discussions with cold-gas thruster manufacturers indicated that the cost of a complete system would be in the neighborhood of \$25,000; therefore, a decision was made to only incorporate thruster compatibility into the baseline design. Implementation would be delayed until that time in the future when sufficient funding became available. To ensure compatibility, a baseline thruster system needed to be investigated, to include thrusters and gas bottles.

4.11.3 Value System Design. In the consideration of thruster system alternatives, the following prioritized evaluation considerations were identified:

- Minimize structural redesign necessary to integrate thrusters, gas bottles, and associated distribution/regulation equipment.
- Minimize weight and inertia penalties.
- Maximize integration ease with respect to signal and power interfaces.
- Minimize system costs.

4.11.4 Thruster Selection. A survey of companies producing cold-gas jet thrusters indicated that the product line developed by Moog, Inc., of East Aurora, NY, would satisfy *SIMSAT* design requirements. Moog is a worldwide supplier of precision fluid and motion control products and systems for aerospace and industrial applications. Founded in 1951, Moog cold-gas jet products have been used on a variety of aerospace vehicles, including GBI/EKV, THAAD, ASAT, and the Shuttle EMU SAFER backpack. For this design, the Model 50-820 cold-gas thruster triad was chosen as the most likely choice for eventual system integration. The Model 50-820 is a member of a family of commercial solenoid cold-gas thruster valves. In particular, the Model 50-820 was designed and qualified for the Pegasus XL launch vehicle attitude control system. The triad configuration is a neat and efficient solution for packing three thrusters into a very small volume, while allowing for three-axis control authority. Additionally, the Model 50-820 minimizes the total number of integration interfaces to other *SIMSAT* subsystems. Physical and performance specifications for the Model 50-820 are listed in Table 4.14 [39]. Figures 4.37 and 4.38 show a schematic and photographic representation of the Model 50-820, respectively.

Table 4.14 Thruster (Moog Model 50-820) Specifications [39]

Operating Pressure	200-2500 psig (13.7-172.4 bar)
Proof Pressure	3750 psig (258.4 bar)
Burst Pressure	6250 psig (431 bar)
Atmospheric Thrust	252N; 1105N (2000 psia tank pressure)
Operating Voltage Range	24-34V DC
Response Time (Open/Close)	< 10ms
Power Consumption	6-12W
Leakage (Internal)	< 10scc/min per seat
Leakage (External)	< 30scc/min for entire module
Cycle Life	> 6000
Weight	0.95lb (0.43kg)
Thermal Capacity (Operating)	0-120 deg. F
Wetted Materials	Aluminum, Stainless Steel, Vespel

4.11.5 Thruster Interfaces. The Model 50-820 uses a MS3476L10-6SN straight-plug connector with backshell strain relief per M85049/52-10 [11]. The inlet port on the manifold is a 3/8" outer diameter tube with a 9/16-18 thread. The port is per

MS33649-06, with the thread listed as 0.5625-18UNJF-3B. Particulate filtration is specified between 10-25 microns.

Although the Model 50-820 was designed to operate using gaseous nitrogen, discussions with Moog engineers indicated that dry air can be successfully used instead. The use of dry filtered air, readily available within the AFIT laboratories, would substantially reduce the cost of operation of the cold-gas thruster subsystem. Discussions with Gas Drying, Inc., manufacturer of the air compressor used by AFIT/ENY, indicated the current unit is capable of achieving 2400 psi pressures and 128 ppm water vapor content [24]. According to Moog engineers, this level of purity should be adequate for use with the Model 50-820 and should pose no problems.

The Model 50-820 was designed to operate at DC voltages between 24-34V. This parameter is consistent with the 28V bus standard used in many aerospace applications. This factor limited, however, the choice of operating voltage available on the main *SIMSAT* electrical bus. Only 24V and 36V main bus voltages were evaluated for use on *SIMSAT* subsequent to the recognition of this limitation, as described in the first iteration of Detailed Design. Additionally, a 24V bus was rated only marginally adequate to support the Model 50-820; an additional voltage source would most likely be needed to ensure reliable and consistent thruster performance. These considerations were evaluated at the system level during the first iteration of the Detailed Design phase.

The thrusters posed no significant signal integration issues at this stage. Once thrusters are purchased and implemented, the required signals could be sent using some of the dSPACE channels allotted to the experimental payload.

4.11.6 Initial Gas Bottle Sizing. To ensure that thrusters could be easily retrofitted to *SIMSAT*, a decision was made to allow for placement of high-pressure gas bottles within the structural envelope of the baseline design. Since gas bottles represent the largest volumetric element of the thruster subsystem, these items must be fully accounted for when considering placement of system components. Additionally, location of the gas bottles relative to the thruster assemblies (located on the exterior of the structure) drives additional considerations such as piping and power cable routing. From the outset, it was

assumed that thrusters would be located on both sides of the air bearing to ensure full three-axis control with single redundancy. To eliminate the need for high-pressure piping routed through the center of the bearing (which is constrained by signal and power cables), a two-bottle architecture was chosen, with one bottle on each side of the *SIMSAT* structure and attached to the respective thruster assembly.

For initial sizing of the gas bottles, a baseline case was developed to estimate how much expelled mass was required to meet performance needs. The required propellant mass for spin-up or spin-down is given by the following formula where W is the required propellant mass (kg), I is the total spin impulse (Ns), g is the acceleration constant (m/s^2), and I_{sp} is the thruster specific impulse (sec):

$$W = I / (g \cdot I_{sp})$$

Using a baseline value for I of 300 Ns (equating to a final spin velocity of 10 rad/s) and an I_{sp} of 50 sec, the expelled mass required to complete a maneuver is 0.6 kg. This mass was compared against the tank capacity of commercially available gas bottles to determine which products might be suitable for this application. Three candidate bottles were found: the Air Products & Chemicals D1- and 4X-series high-pressure bottles, and the SpecAir Specialty Gases Enviro-Cyl Model C-10. Specifications for these three products are listed in Table 4.15, using manufacturer-provided data.

Table 4.15 Gas Bottle Specifications

Alternative	D1-Series	4X-Series	Model C-10
Mass (kg)	7	1.6	1.8
Height (cm) [w/o valve]	41	26	26
Diameter (cm)	18	10	8
Internal Volume (l)	5.9	1.6	1.0
Usable Capacity (kg)	0.69	0.14	0.12
Impulse (Ns)	338	69	59
Bottle Cost (\$)	144	280	92
Regulator Cost (\$)	360	360	110

4.11.7 Gas Bottle Selection. It was quickly determined that the D1 bottle, the only candidate with a usable capacity of greater than 0.6 kg, was too large and heavy for *SIMSAT* integration. Therefore, a decision was made to relax the performance specifications and consider only the 4X and C-10 bottles. Discussions with the decision makers indicated that an angular velocity change capability of 2 rad/s was acceptable for thruster subsystem implementation. Both the 4X and C-10 bottles were capable of meeting this requirement. The use of two gas bottles on *SIMSAT* would allow a total ΔV of 4 rad/s, or the ability to completely spin-up and spin-down 2 rad/s in a single maneuver.

Using the 3D Studio VIZ solid modeling software, both the 4X and C-10 gas bottles were examined for integration issues related to the overall structural design. Bottle placement and fit were checked out relative to other components. Bottles could be adequately positioned outside the main baseline components, minimizing potential plumbing and wiring difficulties. Based on the fact that thrusters would not be implemented during the baseline design phase, the decision makers delayed the choice between the 4X and C-10 bottles until that time when thrusters will be implemented. Minor differences in tank capacity, cost, mass, size, and regulator performance indicated that a further trade study would aid in choosing between the 4X and C-10 bottles at a later date.

4.12 Detailed Design Summary

In this phase, the broad subsystem solution classes of the Preliminary Design phase were narrowed and system-level issues were analyzed in detail. The first iteration of this phase resulted in a detailed system architecture to facilitate the structural design, simulation development, interface identification, and performance estimation. From this architecture, subproblems were addressed using the systems approach to ensure that the important system-level concerns were considered. All subsystem components were selected, and a general integration strategy was formulated. The next lifecycle phase, Final Design, addressed the description and operation of the resulting *SIMSAT* design. Unresolved design issues were documented and future design activities were identified in the Final Design phase.

V. Final Design

5.1 Overview

In this chapter, final *SIMSAT* design specifications are described in detail. Design conclusions are presented, as well as discussion of unresolved design and integration issues. In addition, areas for further research and design are recommended.

Integration, fabrication, and full testing of the *SIMSAT* system were not completed at the time this document went to print. Following the delivery and integration of subsystem components, system assembly and testing will begin. A detailed user's manual providing a more complete description of the system and operational procedures will be created as a stand-alone guide for future reference.

5.2 Subsystem Components

This section describes the major hardware and software components of the *SIMSAT* system for future reference.

5.2.1 Attitude Determination. The Humphrey CF75 Series Axis rate gyro subsystem provides rate sensor capability, including accelerometers, for *SIMSAT* attitude determination functions. The manufacturer-provided gyro characteristics are listed in Table 5.1.

5.2.2 Attitude Control. For satellite attitude control, the *SIMSAT* system uses three momentum wheels, one for each axis, each driven by a dedicated motor and amplifier assembly. *SIMSAT* is also designed for compatibility with cold-gas thruster attitude control systems. The controller onboard the satellite incorporates rate gyro feedback to provide the required control law logic needed to maintain system stability and execute commands for three-axis active control.

5.2.2.1 Momentum Wheels. The momentum wheels were manufactured in-house by the AFIT fabrication shop. Each wheel is comprised of a steel rim

Table 5.1 Humphrey CF75 Characteristics

Parameter	Value
Operating Voltage	28±4V
Operating Current	0.58A
Weight	1.05 kg
Roll Rate Range	±120 deg/sec
Roll Accuracy (Half Range)	1.2 deg/sec
Roll Accuracy (Full Range)	4.8 deg/sec
Pitch/Yaw Rate Range	±40 deg/sec
Pitch/Yaw Accuracy (Half Range)	0.6 deg/sec
Pitch/Yaw Accuracy (Full Range)	2.4 deg/sec

affixed to a thin aluminum disk, with an outside diameter of 8.625". The Animatics BL-3450 brushless DC servo motor and Advanced Motion Control amplifier model BE40A8 provide momentum wheel control. Motor and amp characteristics are listed in Tables 5.2 and 5.3. Figure 5.1 shows a bench test using the momentum wheel attached to the BL-3450 motor, and connected to the amplifier.

Table 5.2 Animatics BL-3450 Motor Characteristics [51]

Parameter	Value
Peak Torque	750 oz-in
Continuous Torque	250 oz-in
Voltage Constant	13.7V/kRPM
No Load Speed	3398 RPM
Torque Constant	18.5 oz-in/Amp
Rotor Inertia	0.025 oz-in-sec ²
Weight	3.27 kg
Number of Poles	4
Number of Slots	24
Length	6.088 in

Table 5.3 Advanced Motion Control Amplifier Characteristics [51]

Parameter	Value
DC Supply Voltage	20-80V
Peak Current	$\pm 40A$
Max. Continuous Current	$\pm 20A$
Switching Frequency	22 ± 15 KHz%
Bandwidth	2.5 KHz

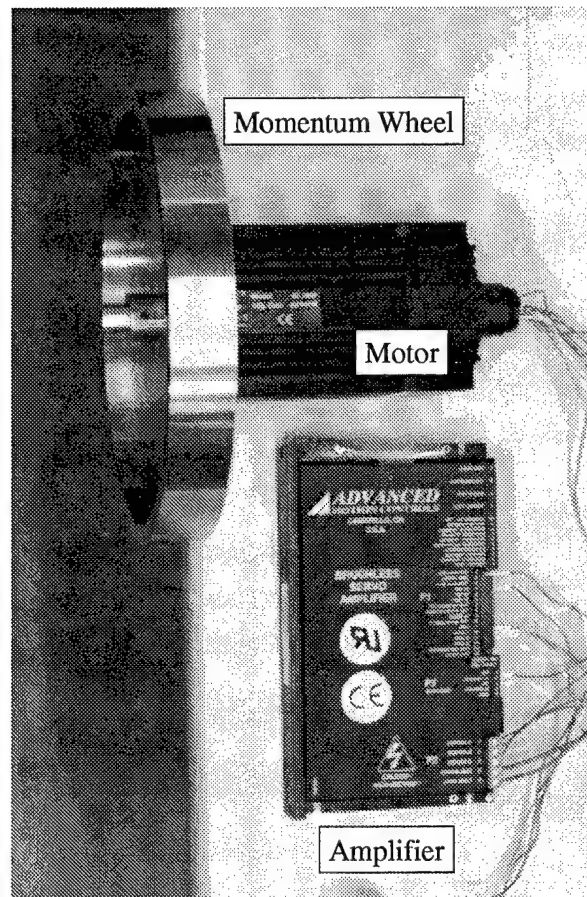


Figure 5.1 Momentum Wheel, Motor, and Amplifier

5.2.2.2 Baseline Command and Control Software. The following SIMULINK files are stored on the ground station PC for modeling and control of the baseline *SIMSAT* system; these files accommodate passive experimental payloads as well.

- *SIMSAT* Block Library (SSMlib.mdl): This backup file contains *SIMSAT* command and control software blocks. It provides a source of existing SIMULINK code blocks for future users, in addition to the application software.
- Simulation Code (*SIMSAT* 1T.mdl): This code includes a plant model based on *SIMSAT* equations of motion. It is designed for simulations of *SIMSAT* dynamics to test new control laws, command and display capabilities, and dSPACE integration. (Refer to Section 4.5, Command and Control Architecture Design, for more information.)
- Real-Time, Onboard Code (*SIMSAT* 1B.mdl): This code is for use during actual *SIMSAT* operations. It contains the same controller and input/output links as the simulation code, but is integrated with the dSPACE hardware on AutoBox. Figure 5.2 illustrates the top-level software architecture of this code.

Payloads utilizing the AutoBox for command and control may require integration into the baseline software architecture. This may necessitate minor changes to the existing code, or major additions and alterations.

Any experiment added to the baseline *SIMSAT*, even passive ones, will change the inertia of the system. Thus, the user is required to enter new inertia values in the Equations of Motion of the baseline system¹. Off-line simulations can then be used to generate any necessary changes to the feedback gains for proper control. These new parameters should be entered into the real-time application of the dSPACE software.

A more complex or active payload may require software modifications in addition to the new inertia values. New SIMULINK code designed for experimental use should also be tested using off-line simulation with an updated software plant model. This activity should occur prior to integration with the actual *SIMSAT* hardware.

¹The *SIMSAT* User's manual provides step-by-step procedures for calculating and inputting new inertia properties based on system configuration.

SIMSAT TOP LEVEL SOFTWARE ARCHITECTURE

NOTE: Remember to check solver options
(in "Simulation, parameters" and/or "Tools, RTW options")

1998-99 Systems Engineering Thesis Team
(baseline version 12FEB99)

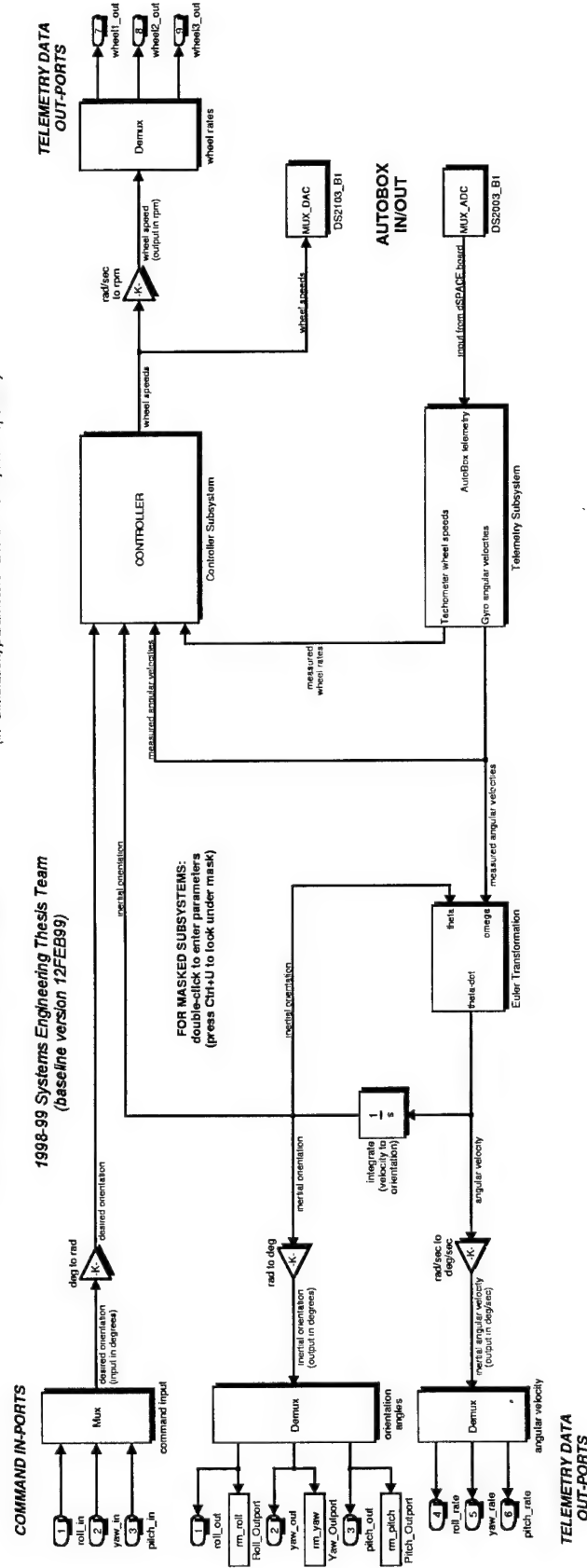


Figure 5.2 Top-Level Software Architecture

5.2.3 Command & Data Handling. The dSPACE control suite provides the command capability, data display and recording, and user interface for the *SIMSAT* system. Use of dSPACE's AutoBox provides onboard control law processing, with wireless communications used for upload of commands and download of telemetry data.

5.2.3.1 AutoBox. AutoBox incorporates 32-input/32-output data channel capability while providing onboard processing. Payload interfaces include 16-input/8-output channels on the primary payload side (AutoBox-side), as well as 8-input/4-output channels on the secondary payload side (momentum wheel-side). These payload interfaces are wired in 4-channel banks that can be selected by the experimenter. The input/output channel interface board is shown in Figure 5.3.

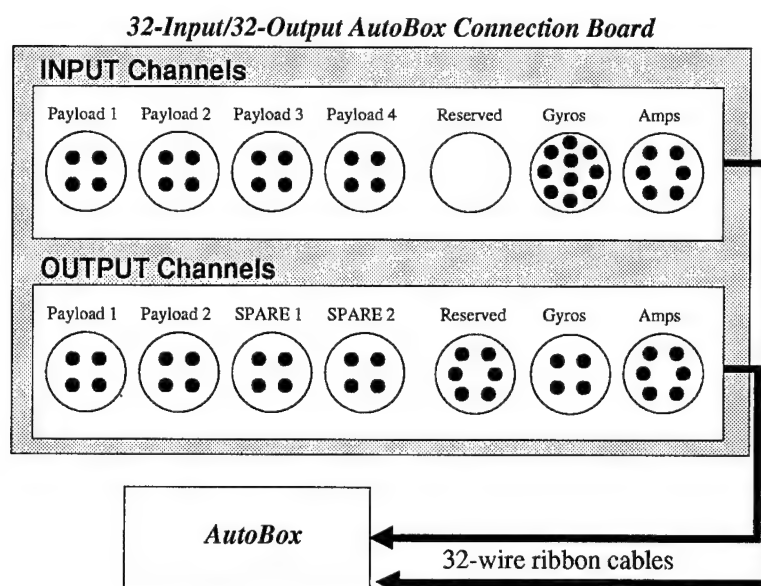


Figure 5.3 Input/Output Channel Interface

5.2.3.2 Command and Control Interface. The COCKPIT ground control display, shown in Figure 5.4, allows command capability using a ground-based PC. The graphical user interface (Grnd-Ctrl.ccs) was designed for use with the baseline system, and passive payloads can be supported without modification. Active control of experiments

from this user interface is possible, but the user must design any additional instruments based on experiment needs. The user interface includes the following instruments²:

- Slide bars (3) for general Roll, Yaw, and Pitch angle control.
- Numeric Inputs (3) for entering the exact Roll, Yaw, and Pitch angle commands.
- Incremental Input instruments (3) for fine control of Roll, Yaw, and Pitch angles.
- Pushbuttons (3) for Roll, Yaw, and Pitch “return to zero” commands.
- Numeric Displays (12) of Roll, Yaw, and Pitch angles (both commanded and measured) and angular velocities, as well as momentum wheel speeds in RPM.
- Gauges (6) providing graphical feedback on Roll, Yaw, and Pitch angular velocities and momentum wheel speeds.
- Alert (1) to indicate Pitch angle reaching limits.

5.2.3.3 Telemetry Display. Figure 5.5 illustrates the TRACE template design used to provide real-time display of motion variable time histories (SSM-TRACE.tpl). As shown, there are three graphing areas; the largest area plots Roll, Yaw, and Pitch angles, and the two smaller plot areas include angular velocities and momentum wheel speeds.

5.2.3.4 3-D Real-Time Animation. REALMOTION provides 3-D animation of real-time *SIMSAT* motion or stored simulations. The geometric model of *SIMSAT* (Simsat.dxf) is linked with the real-time software, providing continual updates of the Roll, Yaw, and Pitch angles. The REALMOTION display is provided in Figure 5.6.

²This user interface can be adjusted to include active payload control variables as necessary.

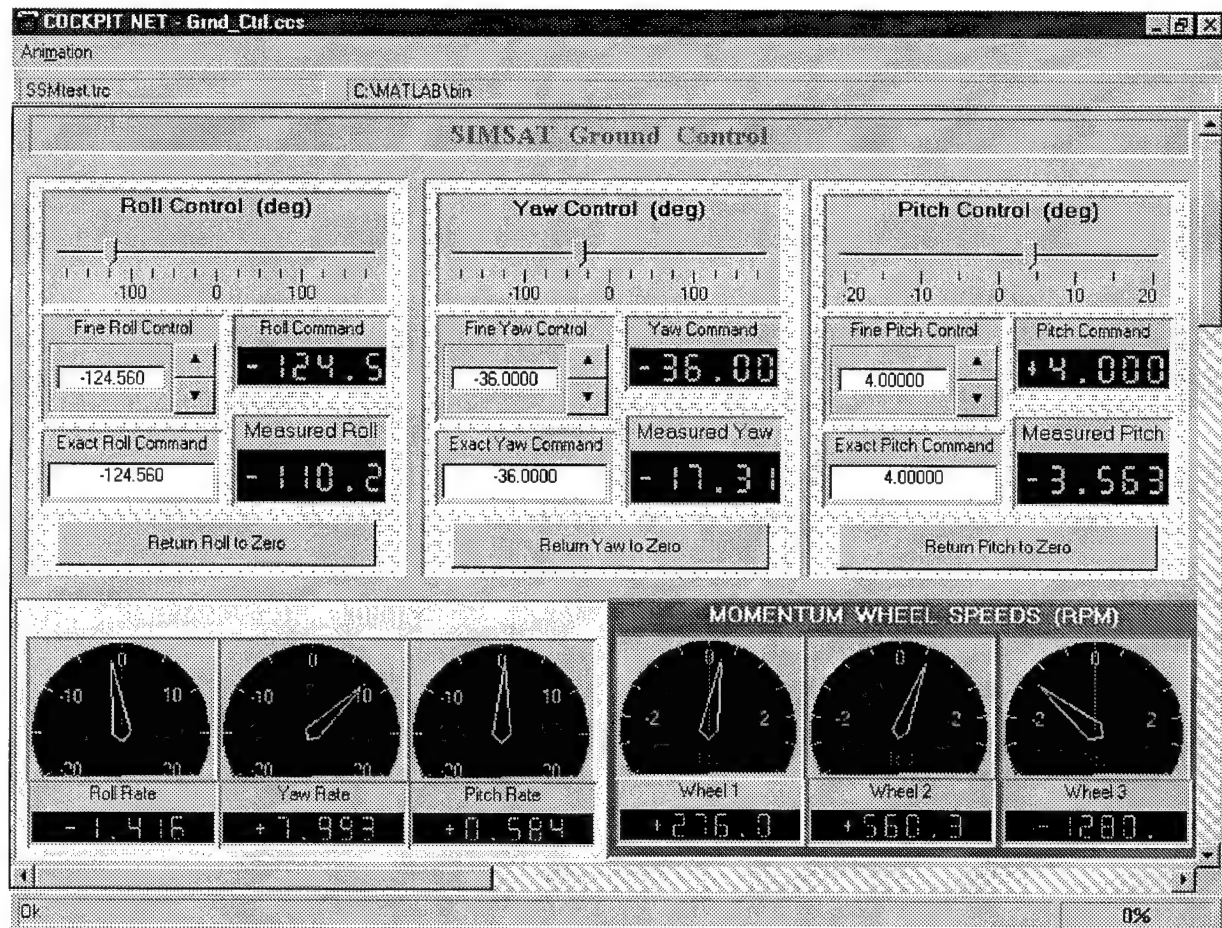


Figure 5.4 COCKPIT Graphical User Interface

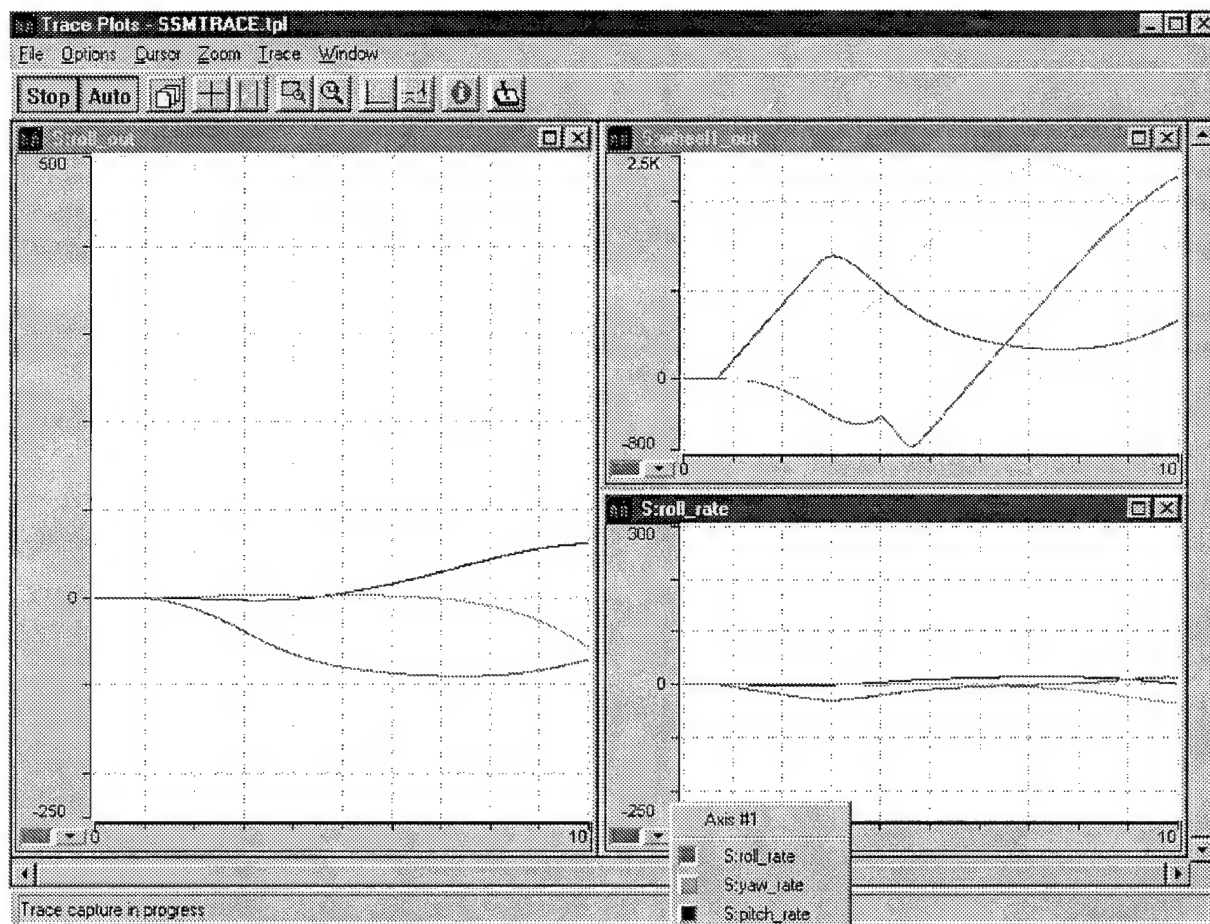


Figure 5.5 TRACE Telemetry Display

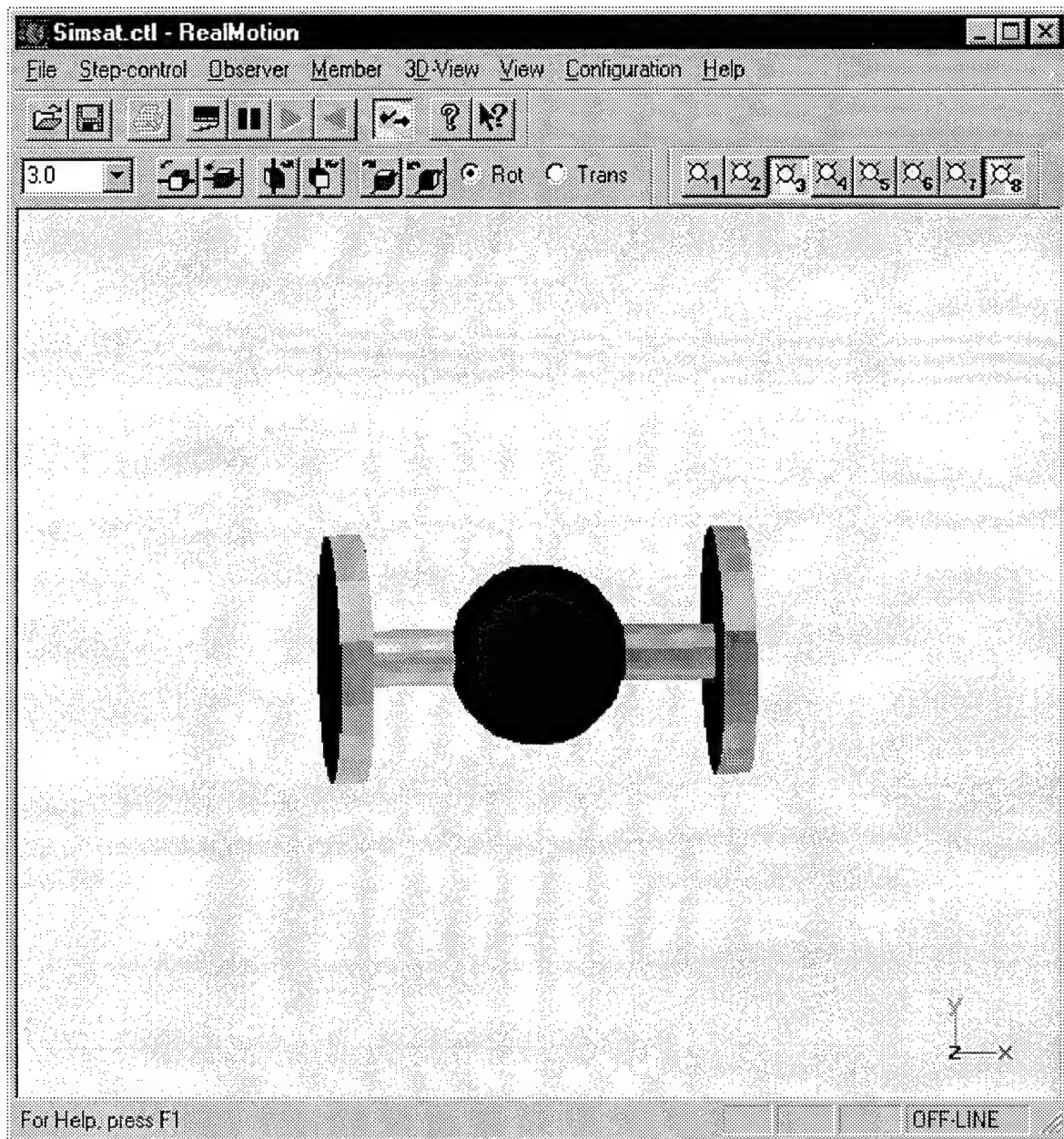


Figure 5.6 REALMOTION 3-D Animation Display

5.2.3.5 Wireless Communications. COCKPIT and TRACE data are transferred to and from the ground using RadioLAN wireless LAN products. The ISA CardLINK Model 101c is connected to the ground station PC, and a DockLINK Model 408 (shown in Figure 5.7) is connected to the AutoBox using the network connection. For the transfer of REALMOTION data, the Digital Wireless Corporation WIT2400 Developer's Kit includes two wireless modems, self-contained battery packs, battery charger, flow control indicators, dipole antennas, RS-232 interface, and configuration software. Purchase of the wireless modem kit will be delayed until successful integration of the wireless LAN system is completed. An interface connector to convert RS-232 to RS-422 protocol is required for modem integration. Black Box Corporation produces a line of converters for this application [6]. Conversation with Black Box technical support indicated that two RS-232 to RS-422 non-powered converters are available: the IC473A (male or female) connector is used for a DB9 connection, and the IC470A (male or female) is used for a DB25 connection [7]. At the time of this writing, the feasibility of the Black Box converters with the AutoBox's RS-422 output port are unknown.

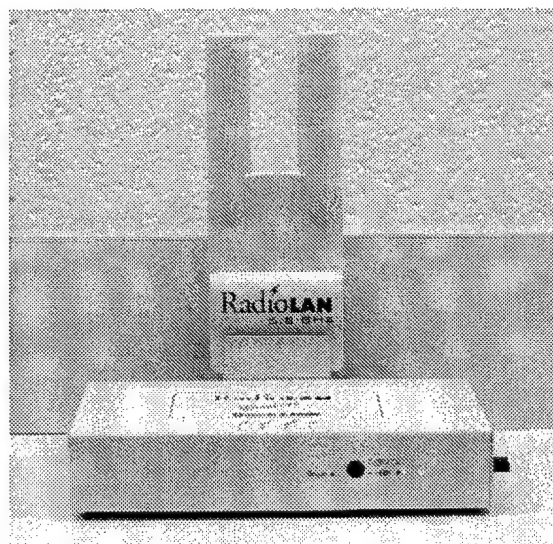


Figure 5.7 Onboard Wireless Communications System

5.2.4 Power System. The *SIMSAT* power subsystem consists of batteries and associated wiring located onboard the satellite. Figure 5.8 shows a schematic of the *SIMSAT* power architecture. Power is provided from three rechargeable Power-Sonic PS-12180 sealed lead-acid batteries, shown in Figure 5.9. The sealed design of the PS-12180 allows for unrestricted operation under all possible *SIMSAT* orientations. Each battery is nominally rated with an 18-Ahr capacity at a DC operating voltage of 12V. The battery case is made of non-conductive polystyrene for high impact resistance. Battery mass is approximately 5.9kg each. Series wiring of the batteries allows for a nominal 36V provided to the momentum wheels. Additionally, 12V, 24V, and 36V bus connections are provided for powering *SIMSAT* components or experimental hardware.

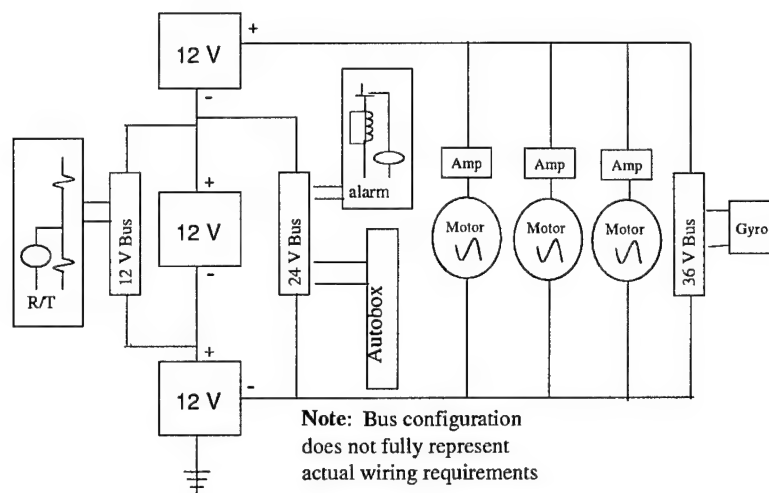


Figure 5.8 System Wiring Diagram

In the event of excessive gas buildup within a battery, a one-way neoprene-rubber relief valve provides a safety mechanism to ensure safe depressurization without case rupture occurring. Vent release pressure is between 2-6 psi. Each battery is mounted within an aluminum enclosure that acts as a mounting interface to the *SIMSAT* truss structure,

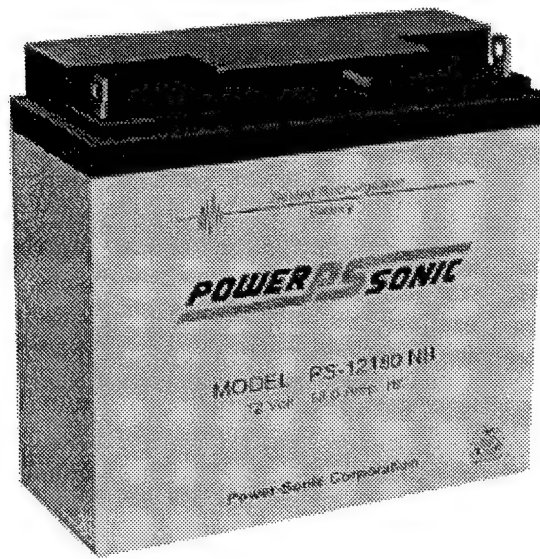


Figure 5.9 Power-Sonic PS-12180 Sealed Lead-Acid Battery

as well as providing additional safety in the event of a battery leak. This arrangement also allows for ease of battery changeout between experiments.

Total power capacity of the baseline *SIMSAT* is 35.1Ahr at the 0.5C (1.3 hr) discharge rate, or 29.7Ahr at the 1.0C (33 min) discharge rate. A total available continuous current of 27A is possible at the 0.5C rate, or 54A at the 1.0C rate. Additional current may be drawn for brief periods of time but is not sustainable and may decrease lifetime battery performance.

Warning of a low power condition is provided by a Macromatic VMP024D voltage monitoring relay wired across two of the three *SIMSAT* batteries. The relay de-energizes when the monitored voltage drops below 23.3V, corresponding to a remaining system battery capacity of approximately 10%.

Wiring for the *SIMSAT* batteries and components is routed through the hollow central sphere to provide connectivity between both sides of the *SIMSAT* truss structure. Wire gauges were selected to ensure an adequate level of protection against overheating. Nominal wire gauges for *SIMSAT* components are shown in Table 5.4.

Table 5.4 Nominal Wire Gauges

Component	Current (A)	Voltage (V)	Power (W)	Minimum Wire Gauge
Autobox	2.5	24	60	18
Motor/Amp 1	20	36	720	12/14
Motor/Amp 2	20	36	720	12/14
Motor/Amp 3	20	36	720	12/14
Receiver/Transmitter	0.5	12	6	27
Gyro	1.78	28	50	18
Thrusters (2)	0.75	32	24	18

With the exception of wiring from the batteries to the amplifiers, all *SIMSAT* components are wired through a 12V, 24V, or 36V bus bar. On the payload side of *SIMSAT* the bus bars are mounted on the reverse side of the gyro/battery/transceiver mounting plate. On the momentum wheel side of *SIMSAT*, the buses are located on the reverse side of the primary battery mounting plate. A multi-strand power connector cable runs from all three payload-side buses to the payload plate. The power connector cable allows for power outputs of up to 60W, 120W, and 180W, for experiments running at 12V, 24V, and 36V, respectively. Payload power connection cables are not provided on the momentum wheel side of the baseline *SIMSAT*; however, this capability can be readily added should the need arise.

5.3 Structural Layout

The *SIMSAT* structure supports individual components and acts as a skeleton for the entire system. The *SIMSAT* structure consists of two box trusses attached to the mounting arms of the central air-bearing assembly. Aluminum and steel are used almost exclusively as construction materials, with Lexan used as a cover surrounding the momentum wheel assembly. Maximum use of standard components and interfaces within the structural design allows for increased modularity and the ability to reconfigure *SIMSAT* to meet changed requirements. Modular design also provides for easy access to items (such as batteries) which must be removed or serviced between experiments. Figures 5.10 and 5.11 illustrate

the final structural design. (All figures in this section follow the structural description ending on page 5-18.)

The baseline *SIMSAT* structure (baseplates, mounting plates and 8 support rods) has a total mass of approximately 37.5 kg. Each side of the *SIMSAT* structure is based upon a box truss construction using standard plates and stringers. Each truss is mounted to the air-bearing with an aluminum 7075-T7 collar (see Figure 5.12). Each cylindrical collar has an outer diameter of 4.875" and a height of 2". A 2" diameter hole is centered on the circular face of the collar to allow for cable routing through the hollow mounting shaft and central sphere. The collar also has a counterbore (3/16" deep and 3" diameter) designed to overlap the air bearing's mounting shaft. This counterbore overlap reduces the shear stress on the collar-to-mounting-shaft attachment screws.

Base plates allow for the attachment of each truss to its respective collar, and mounting plates provide attachment points for individual components. A standard template is used for all plates, which are available in a variety of thicknesses (1/2", 1/4", 3/16", 1/8", and 3/32"). Aircraft-grade aluminum is used in all instances: aluminum 7075-T6 for 1/8" and 3/16" plates, aluminum 7075-T7 for 3/32" plates, and aluminum 2024 for 1/2" and 3/32" plates. The base (innermost) plates are 1/2" thick and are connected to the truss attachment collars; component mounting plates may be thinner to reduce structural weight if load limits are not exceeded.

All plates are 53 cm (20.866") tall by 35 cm (13.78") wide (see Figure 5.13). Four 1" diameter holes are located on the corners of each plate with centers offset 4.4 cm (1.732", vertically and horizontally) from the outer edgeline. These holes allow the mounting plates to slide onto the main steel support rods. Four 10-32 threaded holes (centers located 0.5" in vertically and horizontally from edgeline) provide mounting points for L-bracket attachments. These L-brackets allow for diagonal cross-members to be attached between mounting plates (see Figure 5.14). Diagonal cross-members are not included in the baseline *SIMSAT* design, but can be added to provide additional stiffness if improved vibratory response is required.

The main truss support rods are 60 cm (23.6") long with an outer diameter of 1" and a wall thickness of 0.065". Each of the eight rods is constructed from stainless steel 316 tubing with one end plugged with a metal insert. The plugged end of each rod is placed through the base plate and mated with a connecting bolt to secure the rod in place. This arrangement allows for minimal protrusion on the inside of the base plate, thereby lessening interference with the overall *SIMSAT* pitch envelope.

The mounting plates are fixed to their positions along the support rods through the use of metal clamp-on collars (with a 1" bore hole). Each mounting plate has a total of eight collars (one collar for each side of the four mounting holes) to prevent movement of the mounting plate along the support rod. Mounting plates can be adjusted and secured to different points along the support rods to accommodate equipment changes and/or gross balance requirements. One-piece collars are used primarily for mounting plates not subject to frequent adjustment, while two-piece collars allow for easy take-on/take-off in situations where access is routinely required. Each collar is made from aluminum; a two piece collar weighs 0.04 kg and a one piece collar weighs 0.035 kg (weight includes the cap screws). The cap screws used to tighten the clamp-on collars are manufactured from alloy steel.

The payload plate is the mounting plate furthest from the central sphere located on the AutoBox side of *SIMSAT* (see Figure 5.15). This 1/4" thick mounting plate is identical to a standard mounting plate, with the addition of 212 threaded holes (5/16" diameter) spaced 1" apart (horizontally and vertically) between centers. These holes are referred to collectively as a "pegboard" surface. The pegboard allows the user to attach experimental payloads or balancing weights to the payload plate with a maximum amount of flexibility. Carbon steel blocks of nominal 5 kg and 1 kg masses allow for gross balancing of the *SIMSAT* structure. These blocks can be attached to the pegboard using 5/16" bolts. Experiments can be attached directly to the pegboard with bolts or indirectly using mounting brackets attached to the experiment.

In addition to carbon steel blocks attached to the payload plate, gross *SIMSAT* balancing can be accomplished with 53cm by 35cm steel counterweight plates. Four 2 kg counterweight plates are available and four 5 kg plates are available. These plates are cut from the standard plate template except they have lightening holes to provide the specified

mass. The 2 kg plates are nominally 1/16" thick with a 6.72" diameter hole in the center. The 5 kg plates are nominally 3/16" thick with a 9.9" hole in the center. These plates give the user flexibility to place counterweight near the base plate (closer in towards the central sphere) to reduce inertia penalties.

Fine-tuning of *SIMSAT* balance is accomplished with a counterweight mechanism (see Figure 5.16). The counterweight mechanism can be mounted on either side of *SIMSAT* depending on balancing needs. This mechanism relies upon orthogonal 1/4" stainless steel threaded rods, hollow cylindrical weights (each with a 1/4" hole), and small steel clamp-on collars (1/4" bore). The hollow cylindrical weights slide over the threaded rods and are held in place with the small clamp-on collars. Six 100 gram and five 500 gram hollow weights are available. Hand knobs on the ends of the threaded rods allow the user to make slight adjustments in weight position by turning clockwise or counterclockwise.

Individual components are attached to their respective mounting plates using a variety of structural support mechanisms. The momentum wheels are attached to a mounting plate using a cantilevered support 'shelf' structure (Figure 5.17 shows the shelf assembly from the fabrication shop, with one motor mounted). A safety housing encloses the momentum wheels on all sides; this prevents loose objects from being ejected by rotating parts. The housing consists of a six-sided Lexan box which extends outside of the truss bay in the z-direction (see Figure 5.18). Five sides of the box are attached together and affixed to a separate mounting plate. The sixth side of the box consists of a Lexan sheet mounted to the same plate as the momentum wheels. During *SIMSAT* assembly, the five-sided Lexan box 'slides' over the momentum wheels until a solid press fit is achieved; the final configuration is similar to that of a cake box used to transport baked goods without damage. All Lexan sheets used to construct the box are 0.220" thick. Clearance between the momentum wheels and the interior of the lexan box is approximately 0.5" to 1.0". The cake box configuration allows the user to remove only the exterior mounting plates for access to momentum wheels and motors during maintenance.

Each battery is attached to its respective mounting plate using an aluminum housing which partially encloses the battery on all six sides (see Figure 5.19 and Figure 5.20). Two nylon-tipped bolts are mounted through the backplate; these bolts can be tightened to

press upon the battery contact plate (held on the battery with adhesive) to ensure a snug fit. The removable backplate allows for easy access and replacement of the battery between experiments. The battery housing does not enclose the terminal leads so quick-disconnect wiring connections can be made to the batteries. The battery housing is attached to the mounting plate via four bolts.

The AutoBox is attached to its respective mounting plate using a combination of U- and L-brackets. (see Figure 5.21). Polyurethane padding is inserted between the brackets and the Autobox to provide adequate vibration isolation for electronic components.

An aluminum gyroscope housing provides a support and mounting structure for the Humphrey gyro. To isolate the gyro from vibration, several rubber vibration control mounts and snubbing washers have been purchased. These vibration control mounts and snubbing washers can be used to isolate the gyro housing attachment screws from the mounting plate. The RadioLAN transceiver is attached directly to the mounting plate using integral screw attachments (see Figure 5.22 and Figure 5.23).

SimSat Major Components

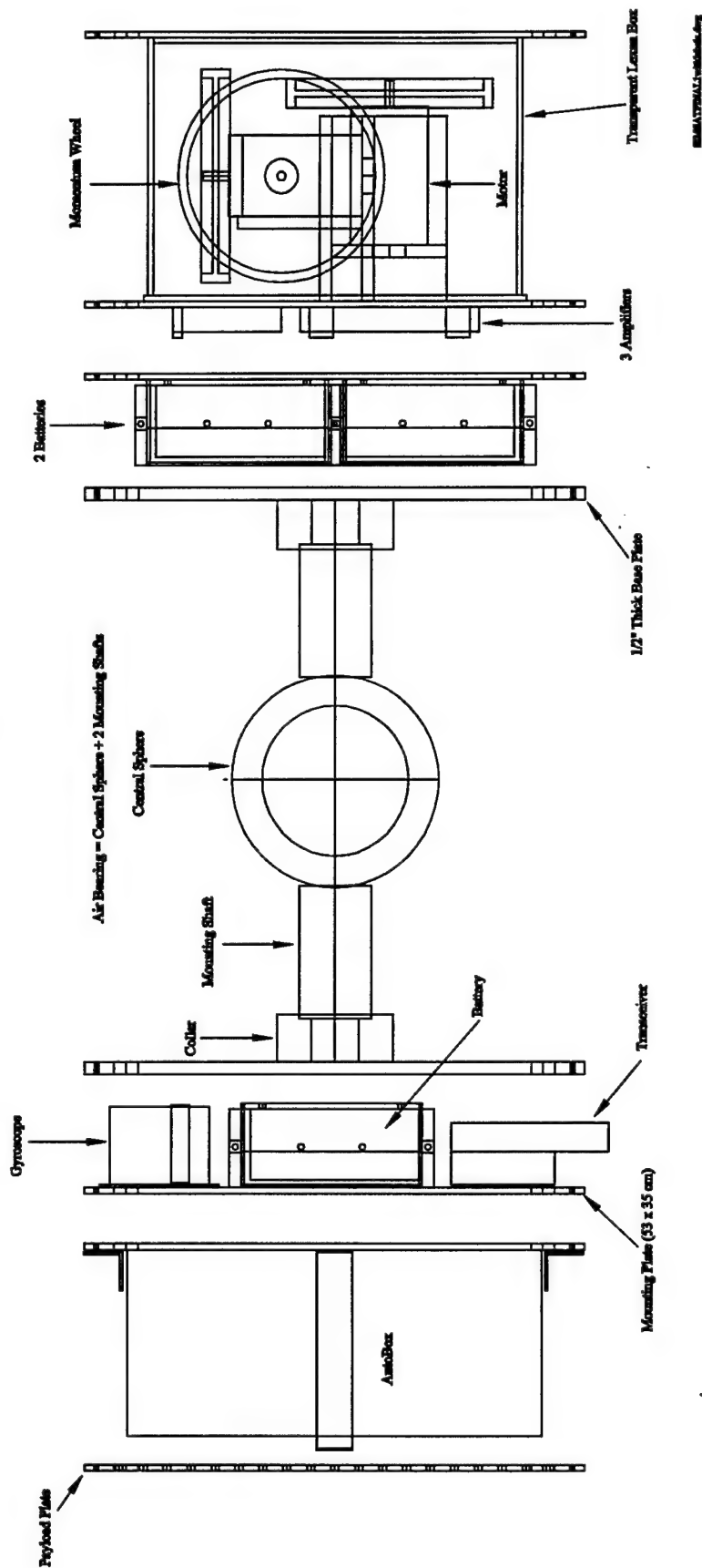


Figure 5.10 Baseline *SIMSAT* Layout without Payload (support rods not shown for clarity)

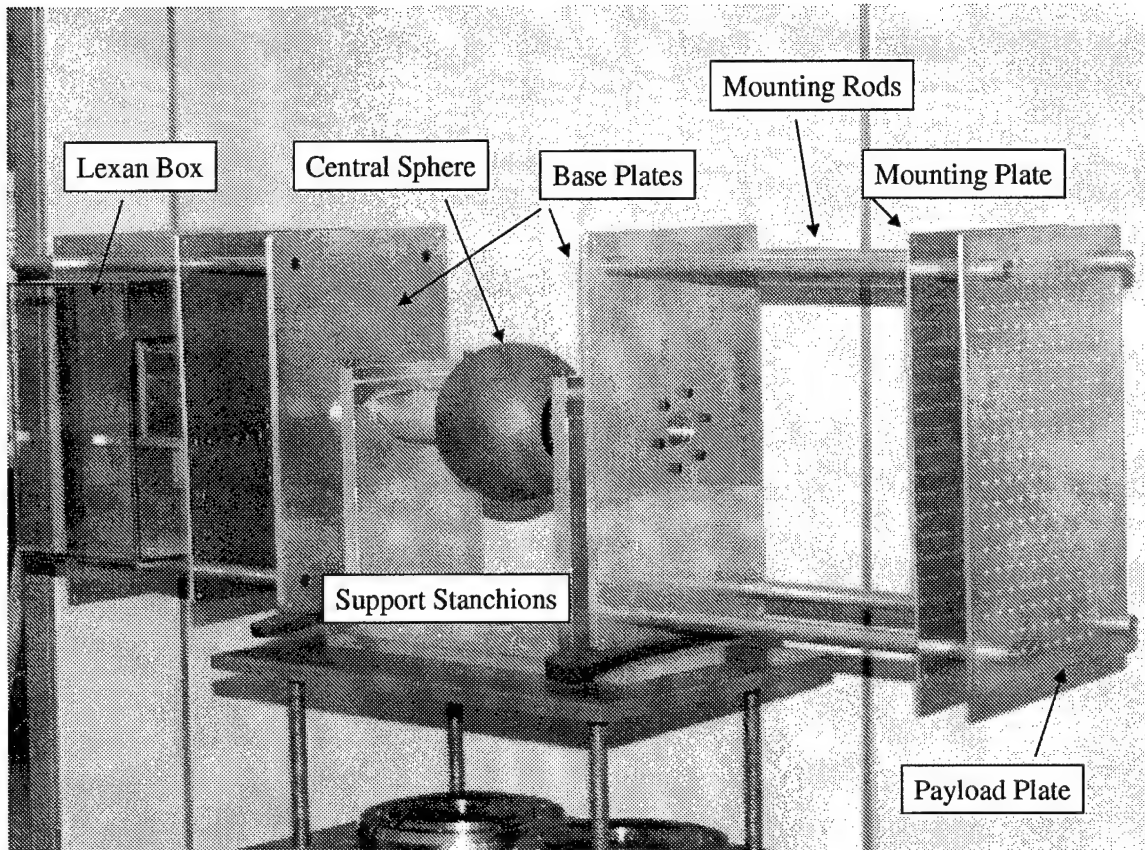
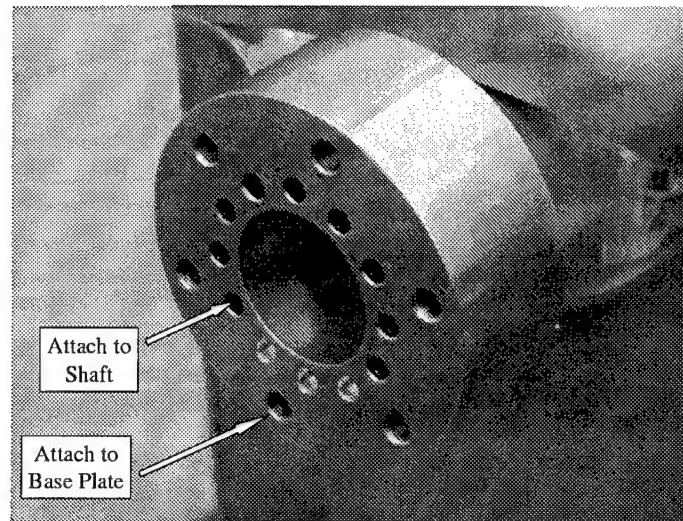
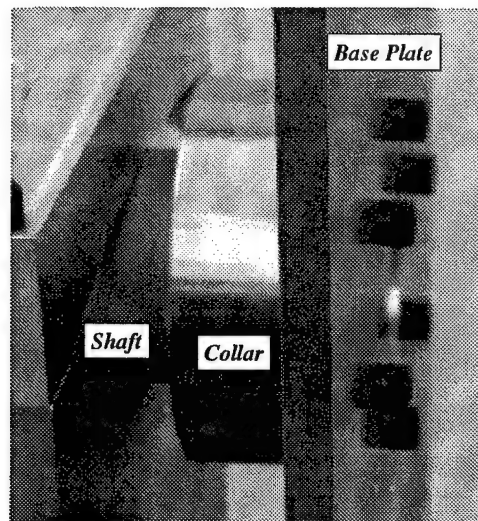


Figure 5.11 Partially-Assembled *SIMSAT* in the Laboratory



(a) Mounting Collars



(b) Collar Attachment

Figure 5.12 Truss Attachment Collars

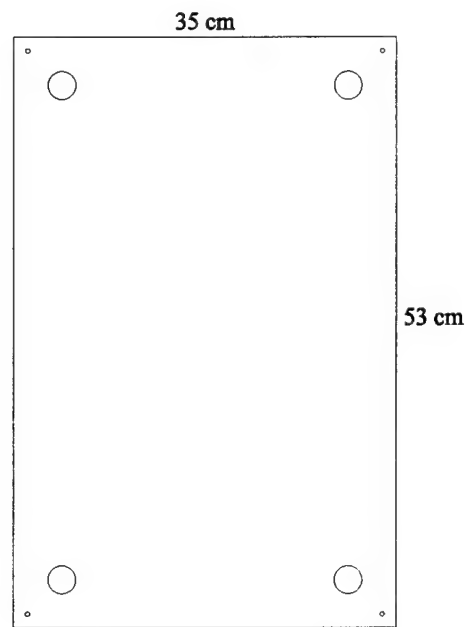


Figure 5.13 Standard Plate

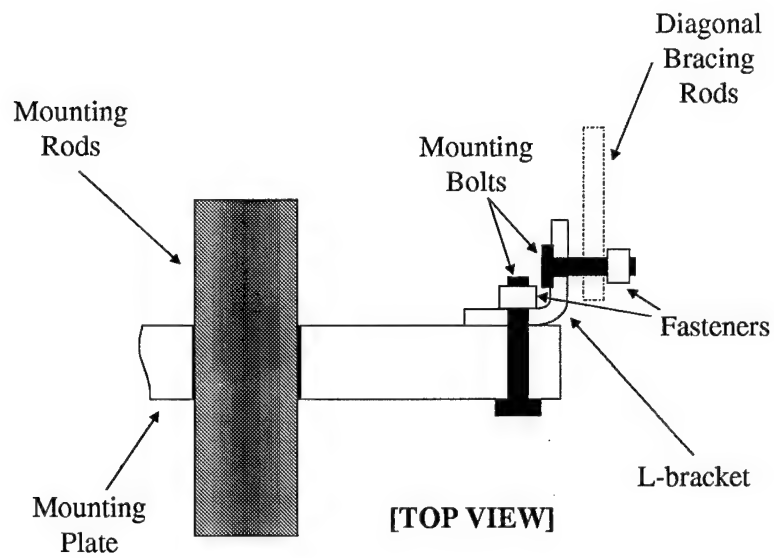


Figure 5.14 Cross Member Attachment Using L-brackets

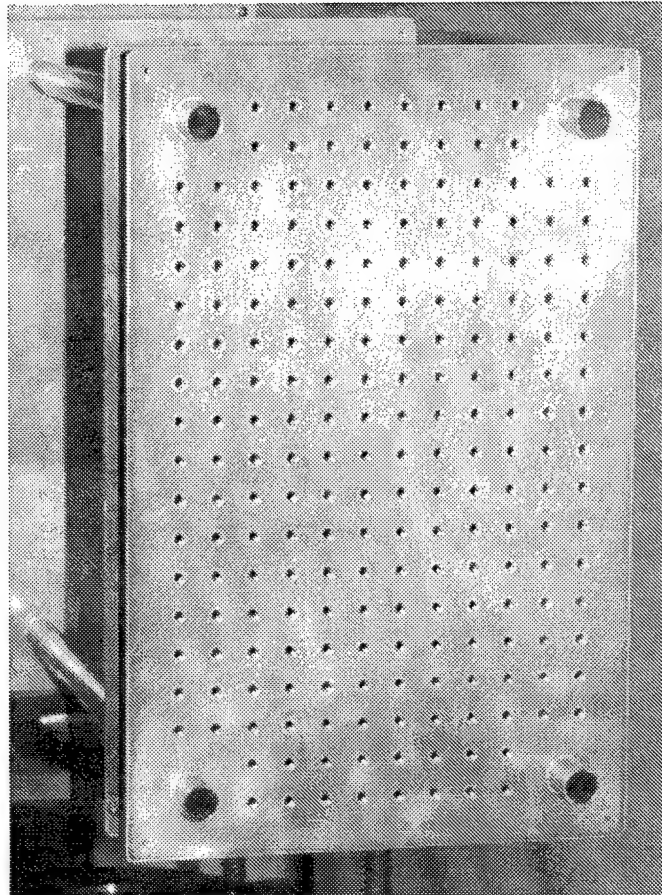


Figure 5.15 Payload Mounting Plate

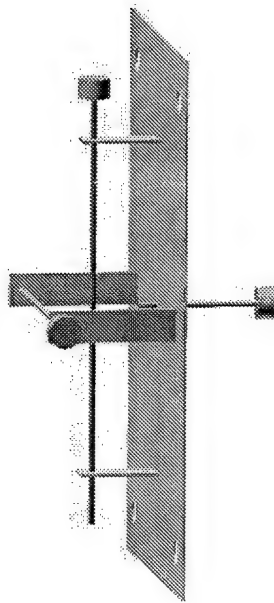


Figure 5.16 Counterweight Mechanism

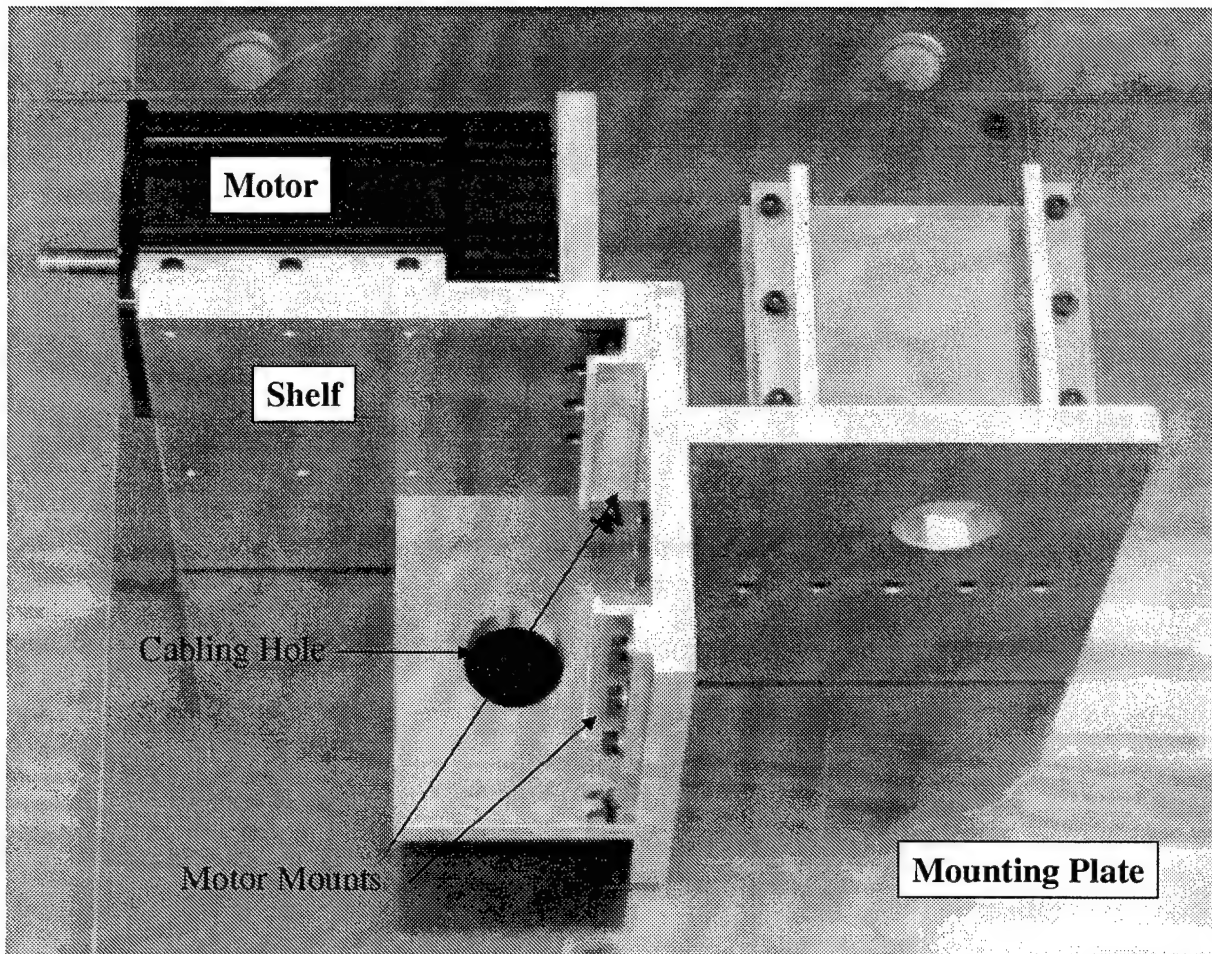


Figure 5.17 Momentum Wheel Shelf Assembly

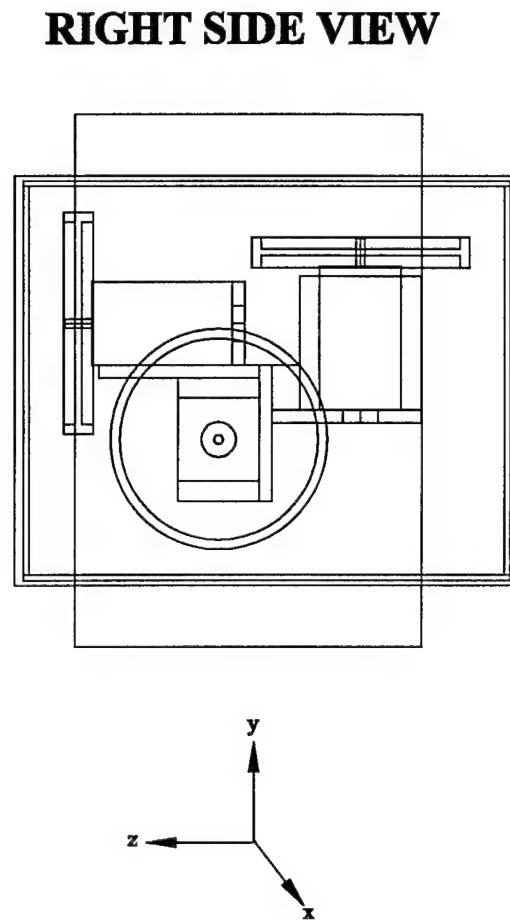
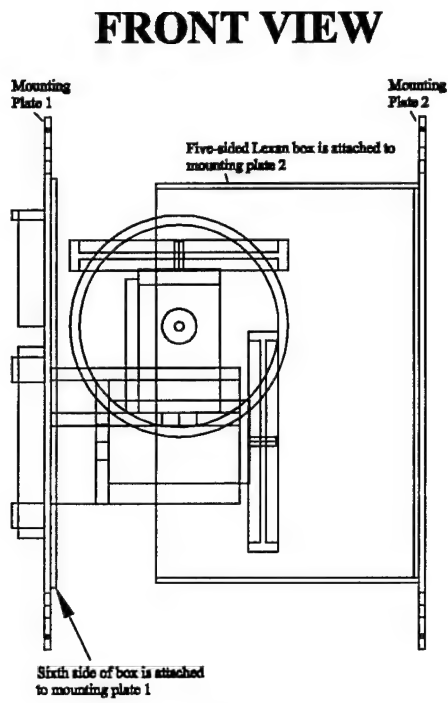


Figure 5.18 Lexan Box

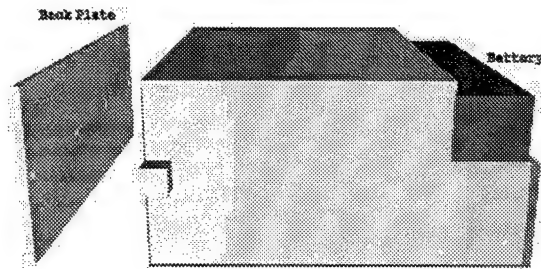


Figure 5.19 Battery Housing

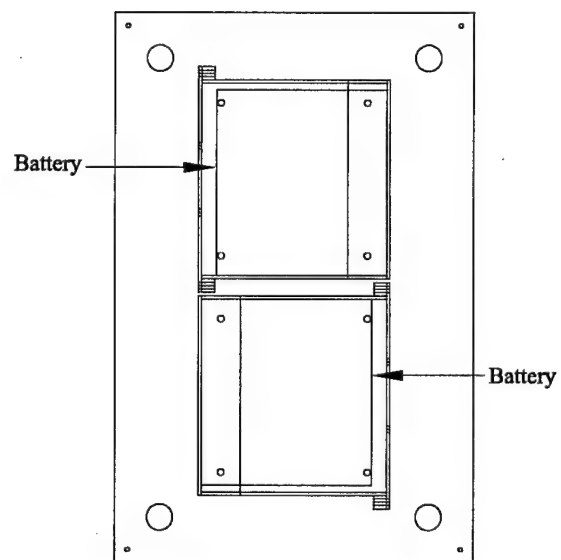


Figure 5.20 Batteries and Battery Housings on Mounting Plate

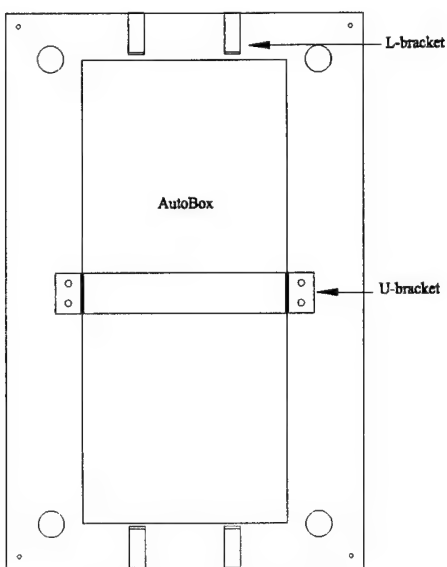


Figure 5.21 Autobox Mounting

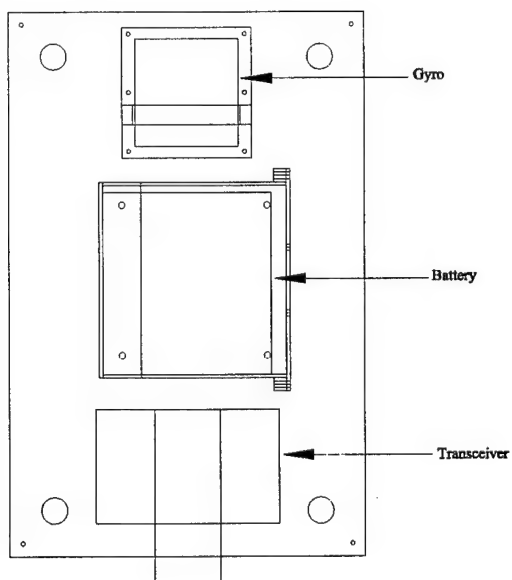


Figure 5.22 Gyroscope, Battery, and Transceiver Mounting

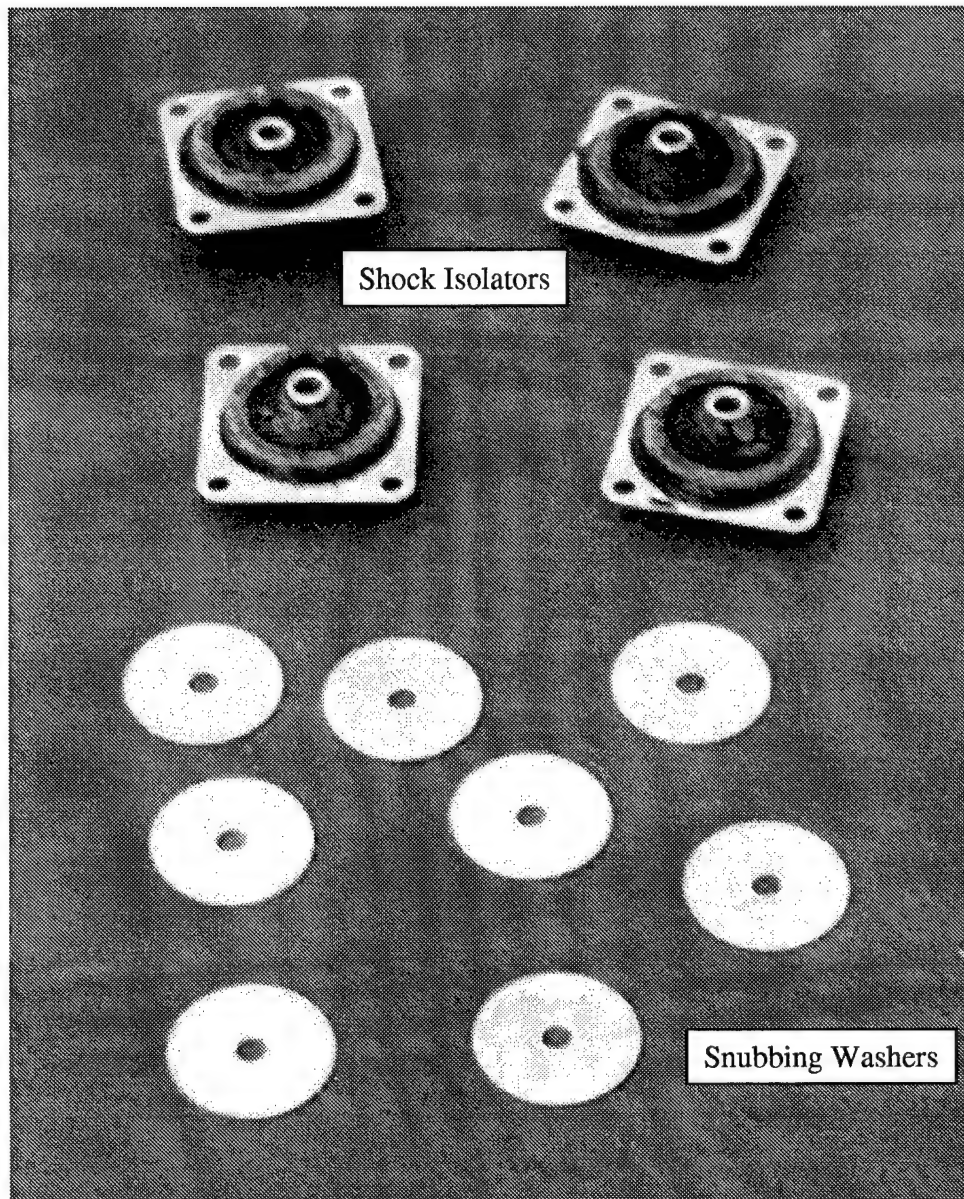


Figure 5.23 Rubber Vibration Control Mounts and Snubbing Washers

5.4 Support Assembly

Between experiments, *SIMSAT* is removed (with a portable hydraulic crane) from the air-bearing pedestal and placed on a stanchion support assembly. This support assembly provides for workbench access when *SIMSAT* is not in use. Support stanchion ‘anti-tip’ collars prevent *SIMSAT* from toppling during removal of heavy components from one side of the *SIMSAT* truss.

5.5 Baseline *SIMSAT* Performance

The final baseline design included 46 components having the following masses and position vectors. The position vectors were measured from the origin (located at the center of the central sphere) to the given component’s center of mass. Table 5.5 lists the properties of each component.

To properly balance the baseline system, a counterweight with the following characteristics was used. This counterweight was also assumed to represent a nominal payload attached to *SIMSAT* (see Figure 5.24).

Mass: 18.927 kg = 41.6 lb

b1 dimension: 5.08 cm (2.0 in)

b2 dimension: 46.6 cm (18.3 in)

b3 dimension: 10.16 cm (4.0 in)

$$\vec{r}_{counterweight} = \begin{bmatrix} -0.7493 \\ -0.0219 \\ 0.0013 \end{bmatrix} \text{ m}$$

Using AutoCAD and MATLAB, the final inertia matrix of the baseline design (including the counterweight) was:

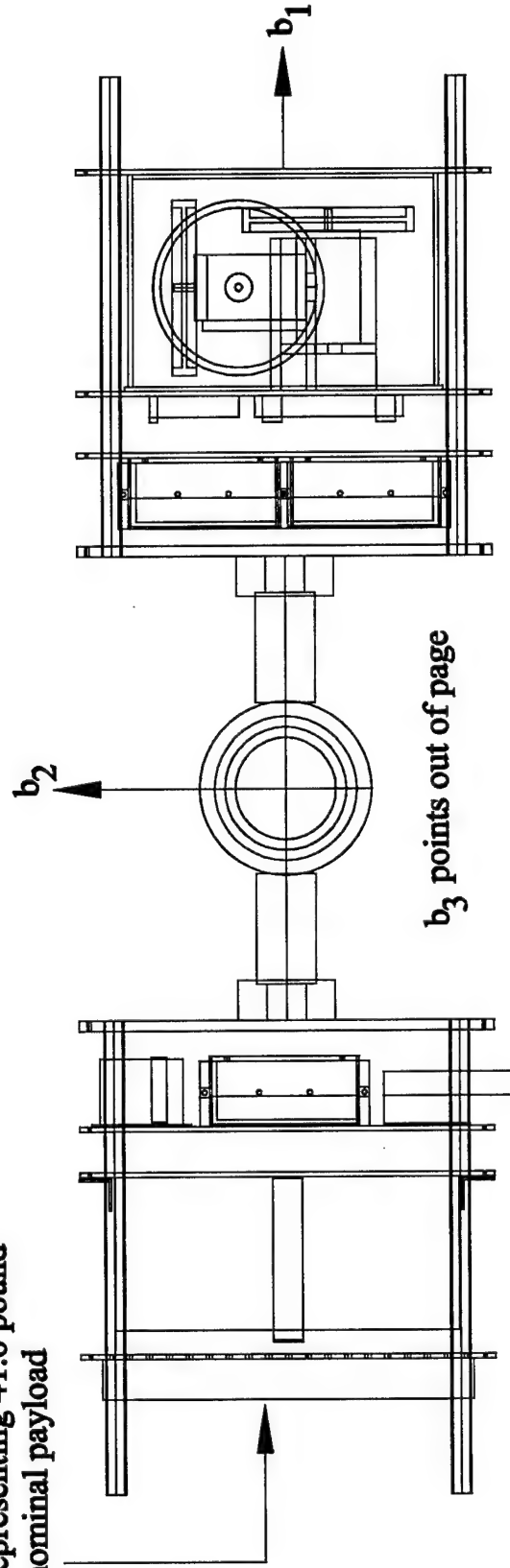
Table 5.5 Baseline Components, Masses, and Positions

Component	Mass		Position Vector (from origin to item's c.g. in cm)
	(kg)	(lb)	
Sphere & mounting shafts	19.3182	42.500	[0, 0, 0]
Mom. wheel side:			
2 Batteries	11.95	26.290	[37.465, 0, 0]
2 Battery housings	2.714	5.971	[38.5651, 0, 0]
3 Amps	1.995	4.389	[48.0608, 0, 0]
3 Motors	9.81	21.582	[62.9051, 1.4268, 0.1284]
Wheel #1	2.06	4.532	[71.35, -5.735, 2.97]
Wheel #2	2.06	4.532	[62.9, 12.715, -11.3]
Wheel #3	2.06	4.532	[62.9, 5.735, 17.1499]
Wheel/Motor shelves	4.127	9.079	[59.1033, -1.3287, -2.2075]
Lexan box	5.741	12.630	[63.3721, 0, -1.7922]
4 Support rods	2.316	5.095	[59.4141, 0, 0]
Base Plate 1	6.596	14.511	[30.0491, 0, 0]
Mounting Plate 1	3.298	7.256	[42.1175, 0, 0]
Mounting Plate 2	3.298	7.256	[49.6825, 0, 0]
Mounting Plate 3	3.298	7.256	[77.4351, 0, 0]
Truss attachment collar 1	1.603	3.527	[26.93, 0, 0]
Total mass mom whl side:	62.926	138.4372	
Autobox side:			
AutoBox	8.6	18.920	[-59, 0, 0]
AutoBox U-bracket	0.164	0.361	[-61.969, 0, 0]
4 AutoBox L-brackets	0.032	0.070	[-50.5731, 0, 0]
Battery #3	5.975	13.145	[-38.1625, 0, 0]
Battery #3 housing	1.357	2.985	[-37.0623, 0.3319, -1.8028]
Gyro	1.05	2.310	[-38.3, 18.6, 0]
Gyro housing	0.178	0.392	[-41.4615, 18.162, 0]
Transceiver/antenna	0.838	1.844	[-39.611, -18.7611, 0]
4 Support rods	2.316	5.095	[-59.4141, 0, 0]
Base Plate 2	6.596	14.511	[-30.0491, 0, 0]
Mounting Plate 4	3.298	7.256	[-43.035, 0, 0]
Mounting Plate 5	3.298	7.256	[-48.9325, 0, 0]
Payload Plate	3.298	7.256	[-72.0675, 0, 0]
Truss attachment collar 2	1.603	3.527	[-26.93, 0, 0]
Counterwt (nominal payload)	18.927	41.639	[-74.925, -2.19, 0.13]
Total mass Abox side:	57.53	126.566	
Total SIMSAT mass:	139.7742	307.503	[0, 0, 0]

Notes:

1. Plates are aluminum 7075 or 2024 and support rods are stainless steel 316--1"OD, 0.065" wall thickness, 60 cm long
2. All plates are 53x35 cm--base plates are 1/2" thick, mounting plates are assumed to be 1/4" thick
(3/16", 1/8" and 3/32" thick mounting plates are also available)
3. Coordinate origin is located at the center of the central sphere

2" x 18.3" x 4" steel block
representing 41.6 pound
nominal payload



SIMSATFINAL17462NOMINALPAYLOAD.dwg

Figure 5.24 Baseline *SIMSAT* Layout with Nominal Payload and Body-Fixed Axes

$$I_{comp} = \begin{bmatrix} 3.1592 & -0.4214 & 0.1161 \\ -0.4214 & 44.0099 & 0.0026 \\ 0.1161 & 0.0026 & 45.3174 \end{bmatrix} \text{ kg m}^2$$

Using this baseline configuration, several system simulations were performed. The results of these simulations are listed in Appendix M.

5.6 Areas Requiring Further Integration

At the time of this writing, major *SIMSAT* structural components were under fabrication by AFIT technical personnel, and initial testing of *SIMSAT* components was ongoing. Full completion of the *SIMSAT* baseline design will not be complete until mid-1999, requiring additional work by AFIT students and technicians. The following areas are listed as known items requiring integration:

- *SIMSAT* structural assembly.
- Physical installation of components onto the *SIMSAT* structure.
- Detailed signal interface between components and the AutoBox.
- Fabrication of signal/power connections, as designed, for experimental payloads.
- Wiring of *SIMSAT* components in accordance with current design drawings.
- Detailed development of *SIMSAT* safety system.
- Development of higher fidelity motor/motor controller transfer function.
- Control software validation using the *SIMSAT* hardware.

5.7 Recommended Future Design Activity

During the course of *SIMSAT* design, additional areas for potential research were recognized but not pursued due to time limitations. The design team's focus on producing a baseline *SIMSAT* configuration excluded several promising concepts from implementation

to reduce overall project risk. These concepts could form the basis for future experimental work.

5.7.1 IPACS. The use of chemical batteries to provide *SIMSAT* power was based partially on the desire to implement a mature power system requiring minimal development. Chemical batteries, however, are heavy in comparison to other potential power sources. Previous AFIT design work examined the potential for an Integrated Power and Attitude Control System (IPACS) combining energy storage and momentum transfer capability into a single system [23]. IPACS holds the potential for future significant reductions in overall subsystem mass required for power and attitude control; the use of *SIMSAT* as a testbed for this research is suggested.

5.7.2 CMGs. As mentioned in previous chapters, the choice of momentum wheels was largely based upon cost limitations. Clearly, the best option for achieving high slew rates is through the use of control moment gyros (CMGs). In the future, it may be possible to remove the momentum wheel package and replace it with a CMG. Additional work will be necessary to modify the existing equations of motion and control laws needed to utilize this new actuation system. However, such a system shows promise in performing realistic slew maneuvers for pointing experiments.

5.7.3 Thrusters. As discussed in depth during Detailed Design, *SIMSAT* was designed for future compatibility with cold-gas jet thruster systems. The Moog Model 50-820 cold-gas thruster triad was used as the baseline for future thruster development. In addition to the possibility of using the Model 50-820, other options may be possible. Near the end of *SIMSAT* development, the design team became aware of a new thruster package developed by the University of Cincinnati for use on a NASA sounding rocket [1]. This design may also prove to be compatible with the baseline *SIMSAT* configuration, and may indicate the opportunity for future collaborative efforts.

5.7.4 MicroAutoBox. During *SIMSAT* development, a new product from dSPACE became commercially available - the MicroAutoBox (shown in Figure 5.25). This product is specifically designed for applications requiring small, powerful processing, such

as the *SIMSAT* design. The MicroAutoBox provides similar processing capability as the AutoBox, but the use of miniaturized cards and tight design allows a much smaller, lighter physical envelope. Unfortunately for the baseline design, this product was not available in time for system consideration. The MicroAutoBox, however, represents a future avenue in the reduction of system weight and inertia, thereby increasing overall performance. Information about this product is listed on the dSPACE website [21].



Figure 5.25 The dSPACE MicroAutoBox [21]

5.7.4.1 ControlDesk. Another new dSPACE product, the ControlDesk experimental software suite, represents an integrated command interface and telemetry display. This package can be considered for future use to replace the individual COCKPIT and TRACE interfaces with one integrated user interface. This would allow both the command and telemetry controls and variables to be viewed simultaneously, without the need to reduce (or minimize) screen windows or use a two-monitor configuration. Experimental software packages are described on dSPACE's website [20].

5.7.5 Dual Spinner. The capability to simulate a dual-spin satellite was a secondary objective for the design project. To perform this function, the momentum wheel assembly would be removed. Two lexan boxes, each containing one momentum wheel, would be aligned along the roll axis on either side of *SIMSAT*. One momentum wheel would provide the necessary torque to spin the vehicle. After the desired spin rate

is achieved the opposite momentum wheel, acting as the platform, would rotate opposite the body at the same angular rate. To an observer, the wheel would appear as though it is not rotating.

5.8 *Conclusions*

Once fully assembled and integrated, the *SIMSAT* design will meet the needs of AFIT in providing a realistic space-platform simulator for experimenters. The design team achieved the top-level goals of developing a baseline satellite simulation tool using the systems engineering approach, weighing cost, schedule, safety, and performance objectives throughout the design process. Following successful integration, *SIMSAT* will provide an in-house, modular, and robust testbed for the following research and educational applications:

- Three-axis stabilization experiments.
- Satellite pointing and tracking.
- Rigid and flexible structure experimentation.
- Pure and dual spinner demonstrations.
- Test and evaluation of various controllers.
- Remote communications and time-delay control.
- Satellite dynamics educational tool.
- Momentum wheel and thruster research and development.
- Computer visualization/user interface development.

It is hoped that *SIMSAT* will spur a new era of space-technology development at AFIT, supporting the Air Force's vision of maintaining preeminence as the world's leading space and air force well into the next century.

Appendix A. Preliminary Design Measurables

A.1 Overview

The measurables from the Preliminary Design objective hierarchy, shown in Figure 3.5, are described in detail in this section. For each measurable, the resolution is defined and the conversion from *raw values* to *scaled scores* is displayed. This conversion allowed each measurable to be judged on the same utility scale, which ranged from 0 (no utility) to 10 (excellent utility). The data points listed under each measurable's value function correspond to the direct inputs given by the decision makers. From these inputs, the curves were fitted to provide mathematical formulas for the conversion of raw data to standardized utility values.

The data in this section correspond to Appendix C of Mr. Hanke's thesis [26]. A decision-making software package, LOGICAL DECISIONS, was used by Mr. Hanke in the generation of value functions based on chief decision maker (CDM) inputs.

The measurables in this appendix are grouped by top-level value (cost, schedule, safety, and performance). Within each value, the measurables are listed alphabetically.

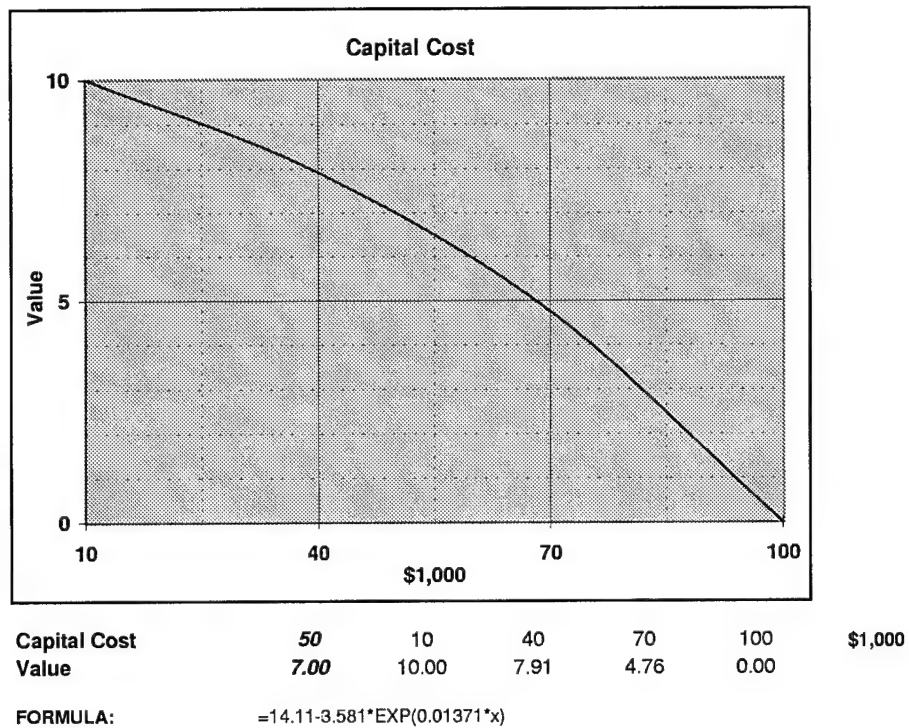


Figure A.1 Capital Cost Value Function

A.2 Cost

A.2.1 Capital Cost. This measure was a continuous “direct” measure reflecting the estimated total cost to purchase and integrate the system. The costs included all the primary subsystem components, support parts, and any labor required for the one-time fabrication of the system. The CDM generated this function by selecting the following value comparison:

$$\text{Value}(\$50,000) = 7$$

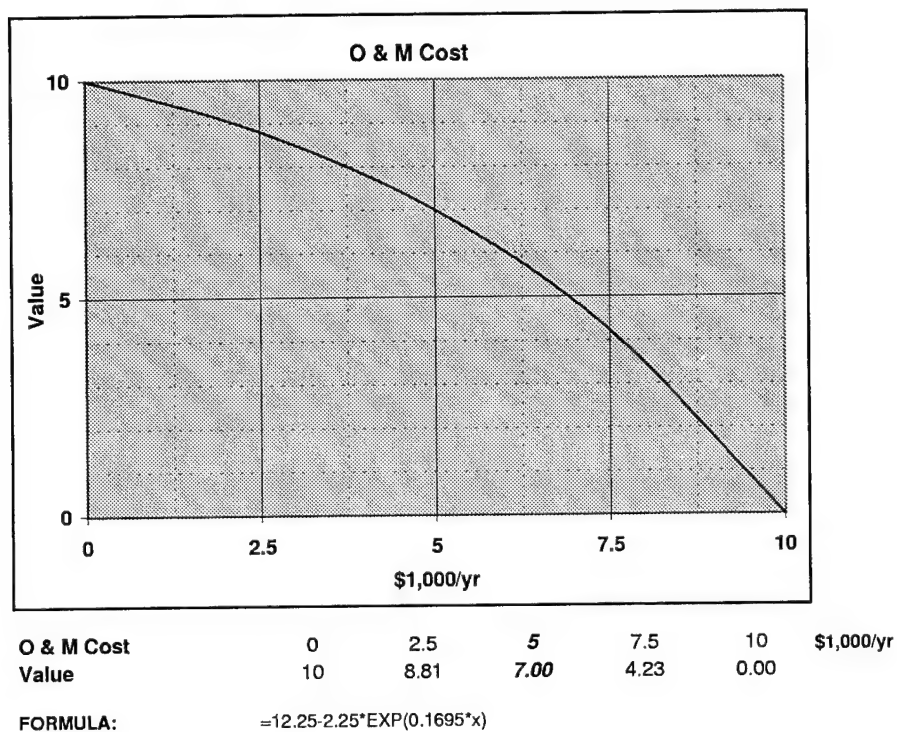


Figure A.2 O&M Cost Value Function

A.2.2 Operations and Maintenance Cost. This measure was a continuous “direct” measure reflecting the estimated yearly cost to operate and maintain the system. The recurring costs included all the consumables, repair parts, and labor required to keep the system running each year. The CDM generated this function by selecting the following value comparison:

$$\text{Value}(\$5,000) = 7$$

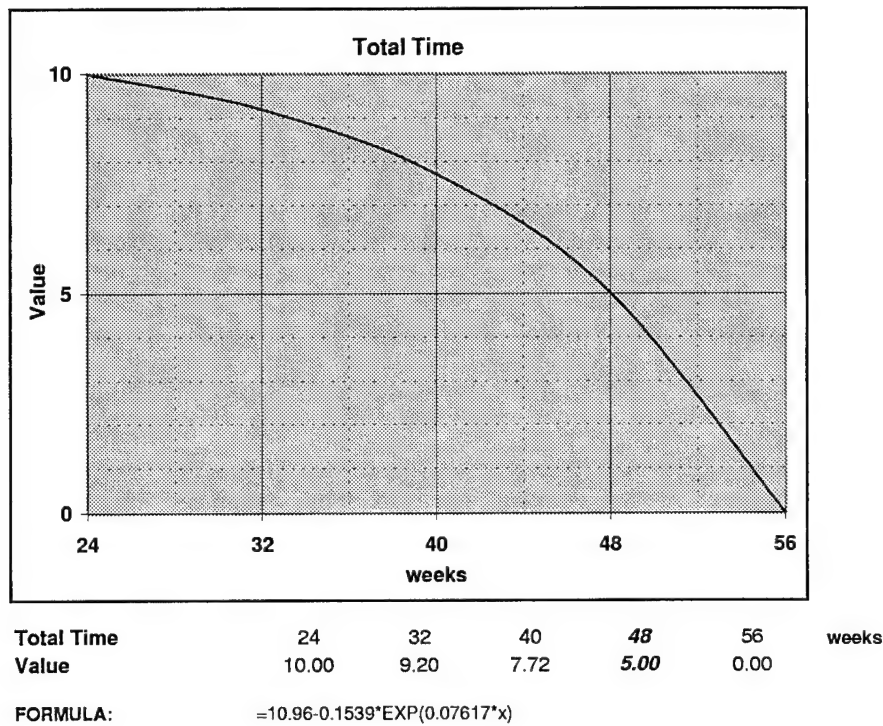


Figure A.3 Total Delivery Weeks Value Function

A.3 Schedule

A.3.1 Total Delivery Weeks. The only measure for the *Schedule* fundamental value is *Total Delivery Weeks*. This measure was a continuous “direct” measure reflecting the summation of the time required to order, produce, deliver, and integrate the entire *SIMSAT* system. The CDM generated this function by selecting the following value comparison:

$$\text{Value}(48 \text{ weeks}) = 5$$

A.4 Safety

The *Safety* measures *Relative Damage Index* and *Relative Injury Index* were based on the table shown in Figure A.4. That table was developed as suggested by MIL-STD-882B [3:7-8, A3-A4], as coordinated with the CDM.

Failure Probability:		Severity of Failure:	Death or System Loss <i>Catastrophic</i>	Severe Injury, Major Damage <i>Critical</i>	Minor Injury, Minor Damage <i>Marginal</i>	Less than Minor Injury/Damage <i>Negligible</i>
0.01	Likely to occur frequently	<i>Freq</i>	1	3	6	10
0.0001 -> 0.01	Occur several times in 5 years	<i>Prob</i>	2	5	9	12
0.00001 -> 0.0001	Likely to occur sometime in 5 years	<i>Occas</i>	4	9	11	15
0.000001 -> 0.00001	May occur sometime in 5 years	<i>Rem</i>	3	12	14	18
< 0.000001	So unlikely can assume may not fail	<i>Improb</i>	10	14	18	20

System Loss means at least 90% of SIMSAT must be replaced

Major Damage means 50-90% of SIMSAT must be replaced

Minor Damage means 25-50% of SIMSAT must be replaced

Less than Minor damage means 0-25% of SIMSAT must be replaced

Severe Injury means at least 1 day of work is missed

Minor Injury means a visit to the hospital is required, but no work is missed

Less than Minor Injury means that, at worst, only minimal first aid is required

Risk Index	Acceptability
1-5	Unacceptable
6-9	Undesirable
10-17	Acceptable with review
18-20	Acceptable as is

Figure A.4 Hazard Index Table

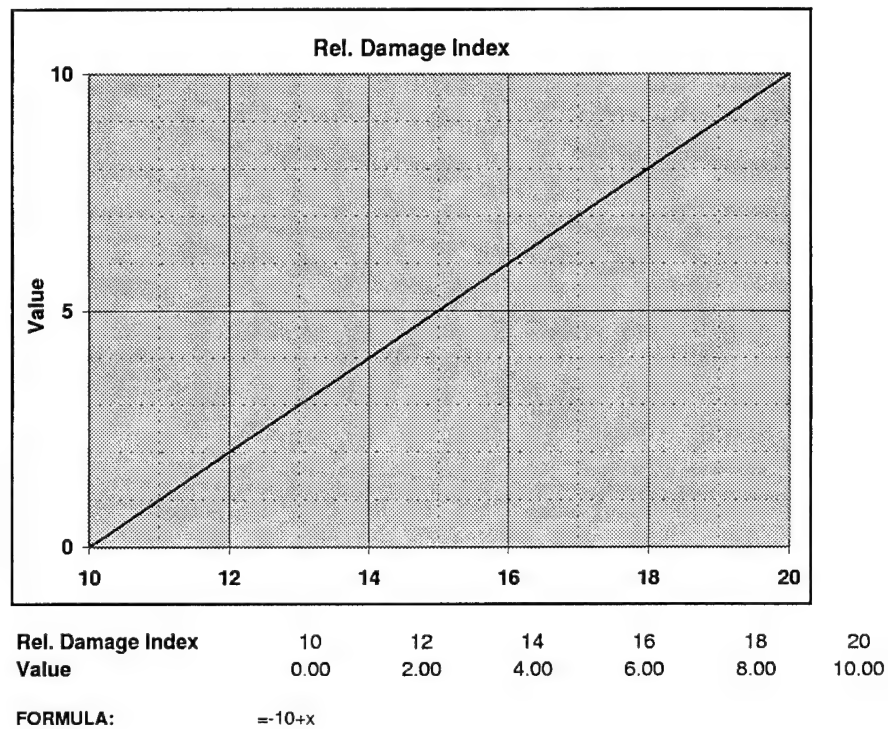


Figure A.5 Relative Damage Index Value Function

A.4.1 Relative Damage Index. See Figure A.4 (page A-5) for definition of this constructed scale, a combination of probability of failure, and severity of that failure.

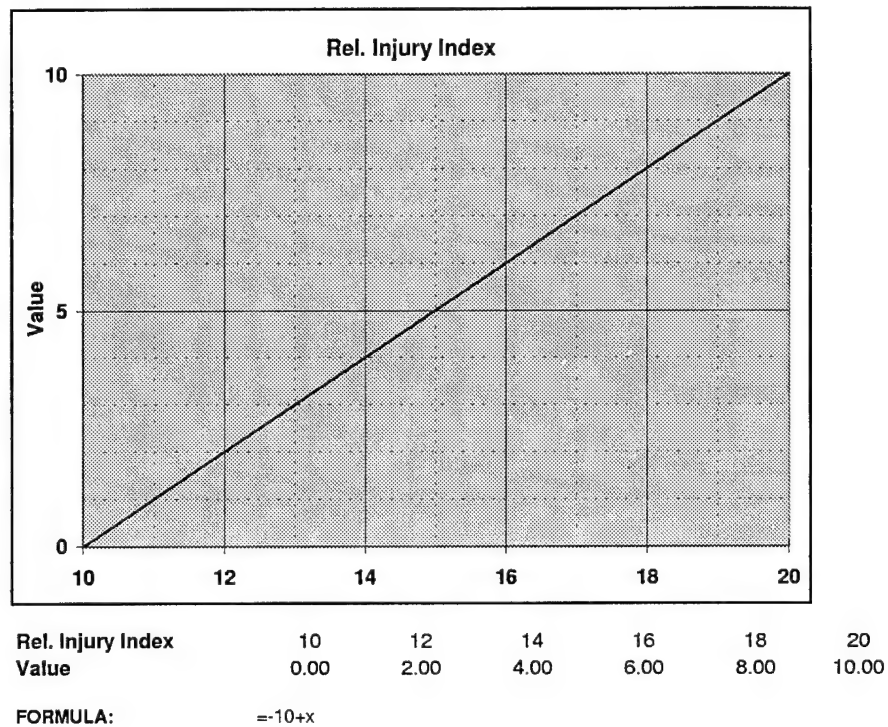


Figure A.6 Relative Injury Index Value Function

A.4.2 Relative Injury Index. See Figure A.4 (page A-5) for definition of this constructed scale, a combination of probability of mishap, and severity of that mishap.

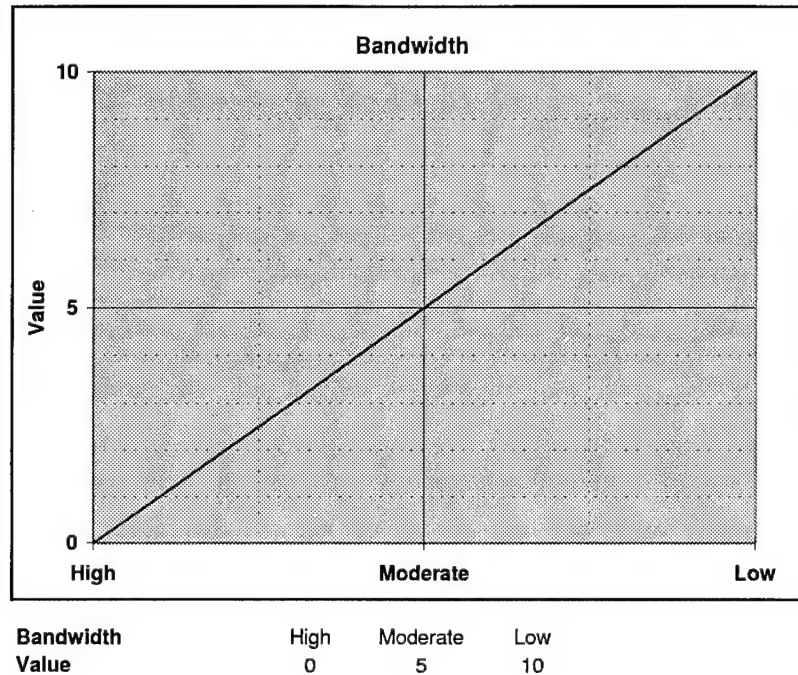


Figure A.7 Bandwidth Requirement Value Function

A.5 Performance

A.5.1 Bandwidth Requirement.

LEVEL	DEFINITION
High	All signals need to be sent
Moderate	Display/Command and ADACS signals need to be sent
Low	Only Display/Command updates need to be sent

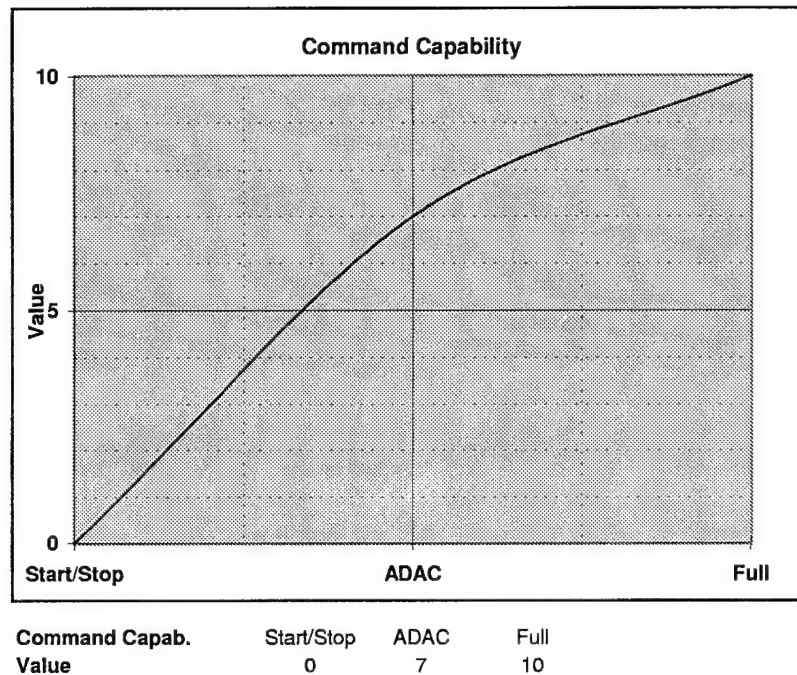


Figure A.8 Command Capability Value Function

A.5.2 Command Capability.

LEVEL	DEFINITION
Start/Stop	Only ground start/stop ground commands
ADAC	Only satellite attitude and direction controlled
Full	ADAC and payload controllable from ground

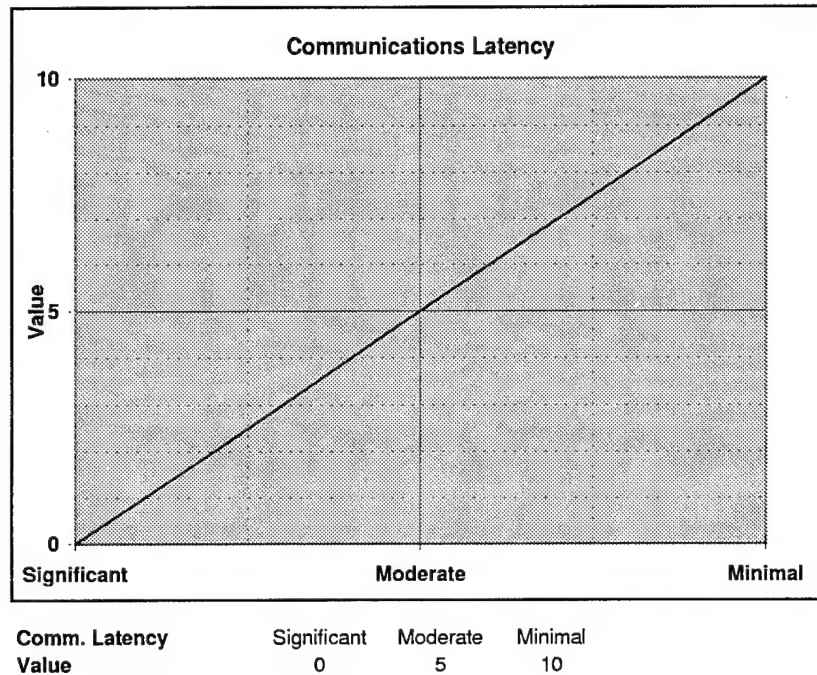


Figure A.9 Communications Latency Value Function

A.5.3 *Communications Latency.*

LEVEL	DEFINITION
Significant	Delay impacts both inner and outer control loops
Moderate	Delay impacts only outer control loop
Minimal	Only delay is between user interface and control loop(s)

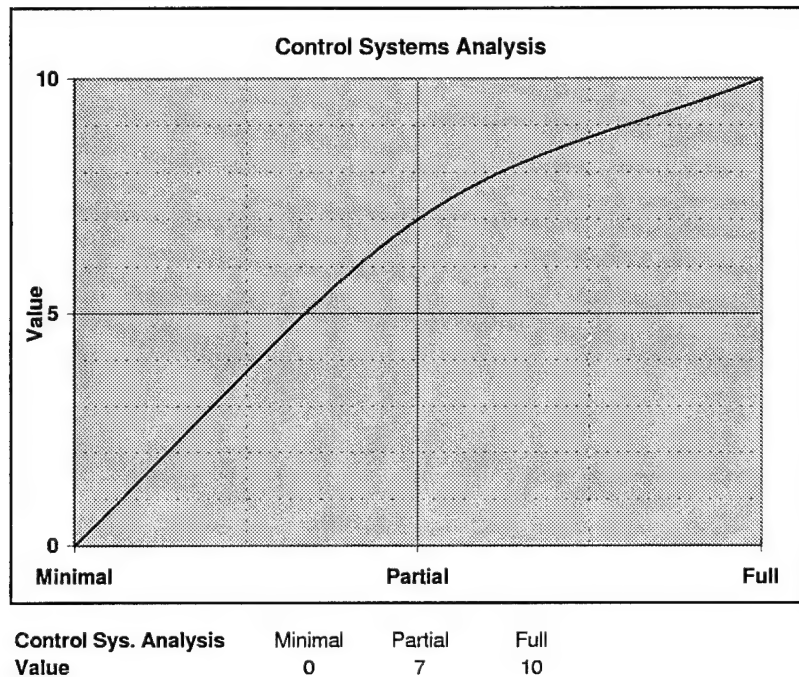


Figure A.10 Control Systems Analysis Value Function

A.5.4 Control Systems Analysis.

LEVEL	DEFINITION
Minimal	<50% of desired system elements defined or the remaining elements are difficult to define
Partial	50-90% of desired system elements defined; simple to define the rest
Full	>90% of desired system elements defined

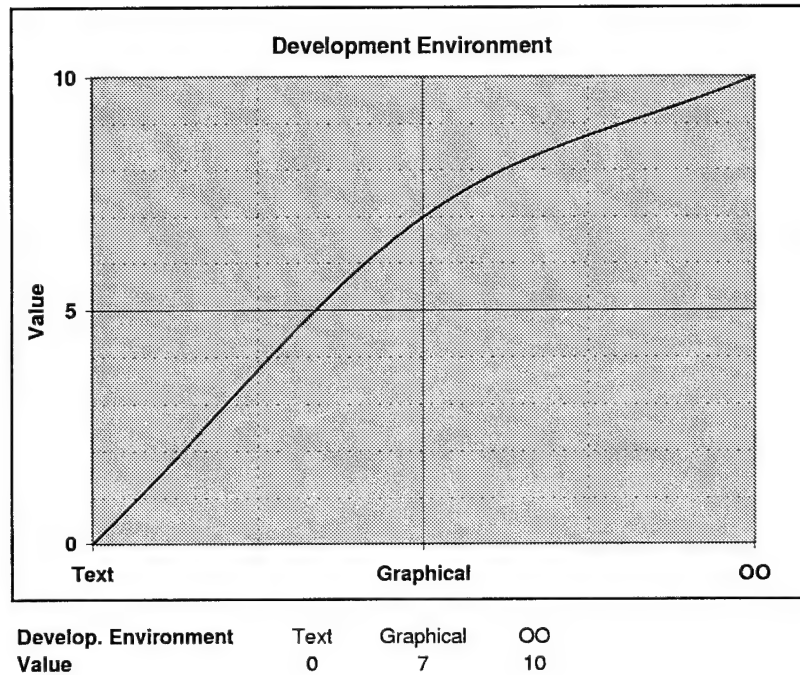


Figure A.11 Development Environment Value Function

A.5.5 Development Environment.

LEVEL	DEFINITION
Text	Time-intensive entry of control laws; prone to errors
Graphical	Not all aspects of control system available as "building blocks" but more user-friendly than <i>Text</i>
Object-Oriented	Graphical; all critical elements available as "building blocks"

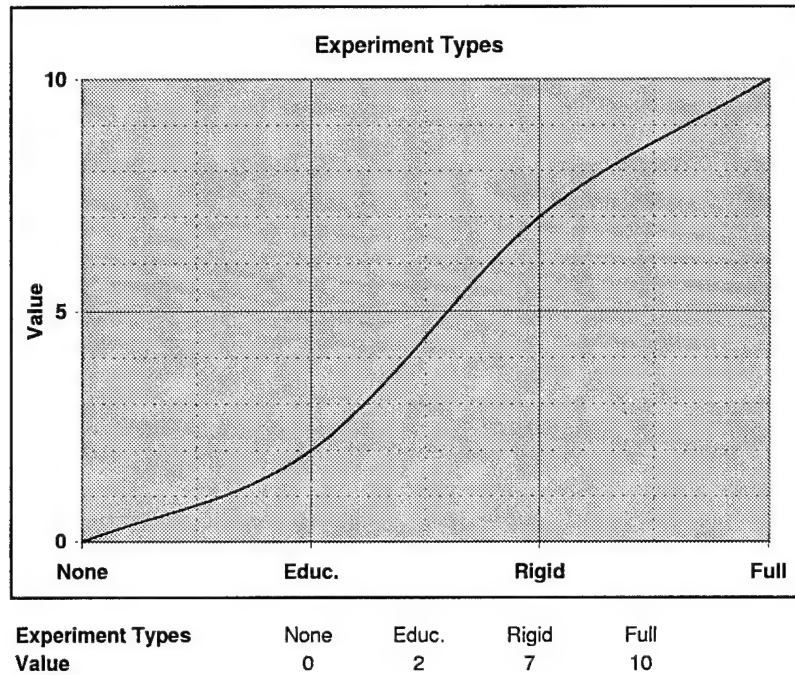


Figure A.12 Experiment Types Value Function

A.5.6 *Experiment Types.*

LEVEL	DEFINITION
None	No experiments possible
Educational	Education/teaching usage only (spinner experiments)
Rigid	Supports spinner and 3-axis rigid experiments
Full	Supports all the desired experiments

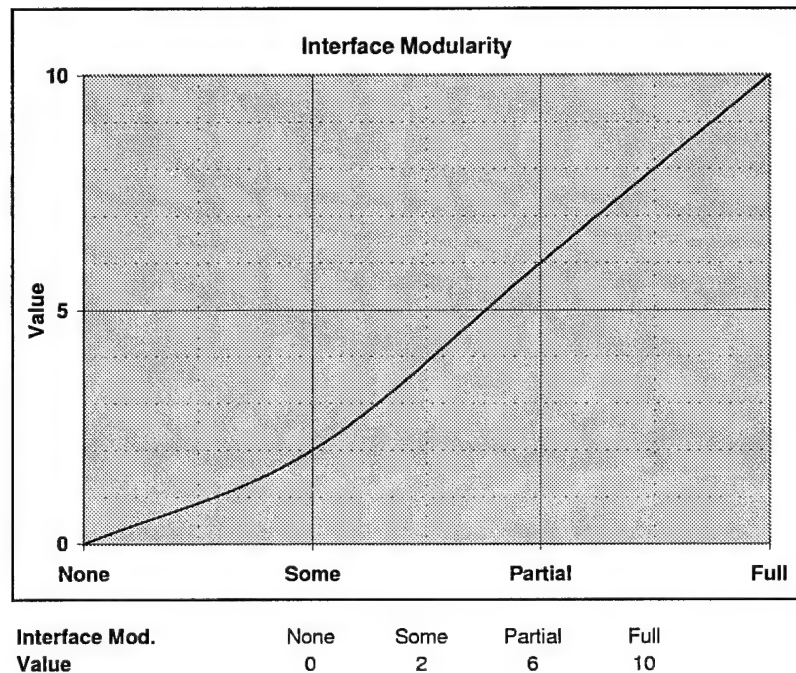


Figure A.13 Interface Modularity Value Function

A.5.7 Interface Modularity.

LEVEL	DEFINITION
None	Only complete subsystems can be replaced with payload parts, not components
Some	10-50% of components/sub-sub-systems can be relocated or substituted with payload parts
Partial	50-75% of components/sub-sub-systems can be relocated or substituted with payload parts
Full	All components/sub-sub-systems can be relocated or substituted with payload parts

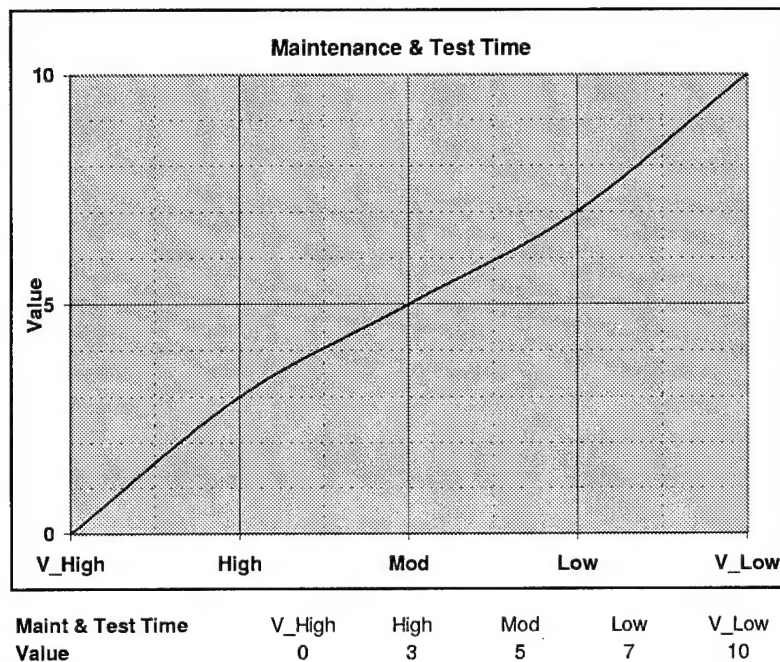


Figure A.14 Maintenance & Test Time Value Function

A.5.8 Maintenance and Test Time.

LEVEL	DEFINITION
Very High	Completely reconfigure to conduct new experiments; requires system validation before test run (> 100 min)
High	Experiment installation and validation requires 76–100 min total time
Mod	Experiment installation and validation requires 36–75 min total time
Low	Experiment installation and validation requires 16–35 min total time
Very Low	Snap-in/snap-out; experiment installation and validation requires 0–15 min total time

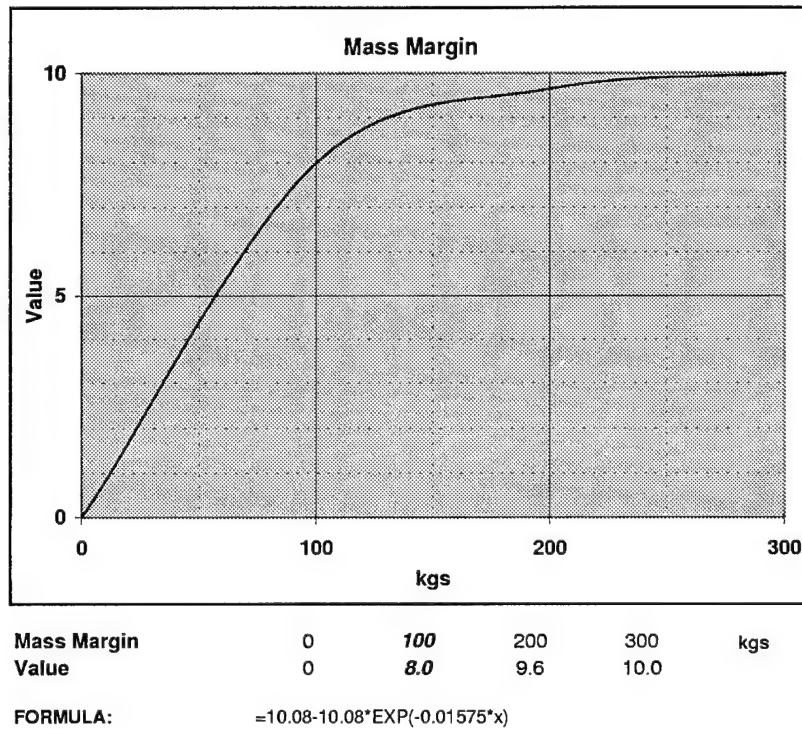


Figure A.15 Mass Margin Value Function

A.5.9 Mass Margin. This measure was a continuous “direct” measure reflecting the estimated mass the air bearing assembly can support after all the required baseline *SIMSAT* components are installed. The CDM generated this function by selecting the following value comparison:

$$\text{Value}(100 \text{ kg}) = 8$$

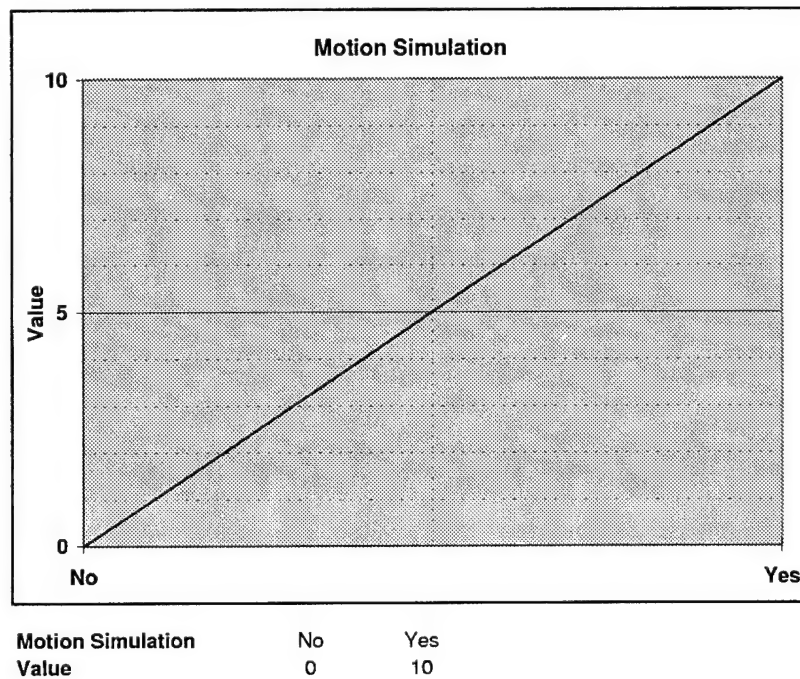


Figure A.16 Motion Simulation Value Function

A.5.10 Motion Simulation. This measure was a binary (yes/no) measure of whether the system could support satellite behavior simulation prior to the execution of an experiment.

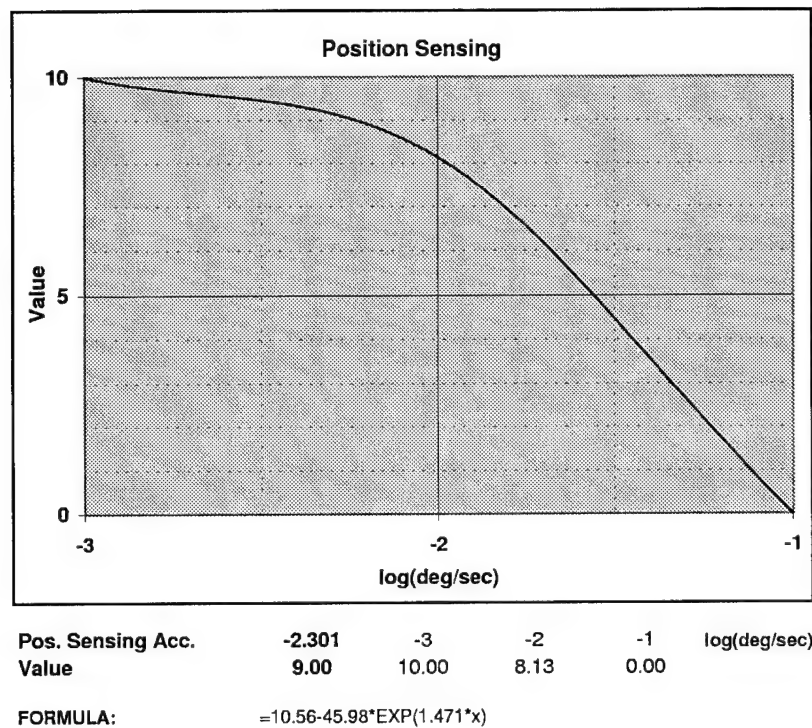


Figure A.17 Rate Sensing Accuracy Value Function

A.5.11 Rate Sensing Accuracy. This measure was a continuous “direct” measure reflecting how accurately *SIMSAT* can sense angular rates. The CDM generated this function by selecting the following value comparison:

$$x = 0.005 \rightarrow \log(x) = -2.301 \dots; \text{Value}(0.005 \text{ deg/sec}) = 9$$

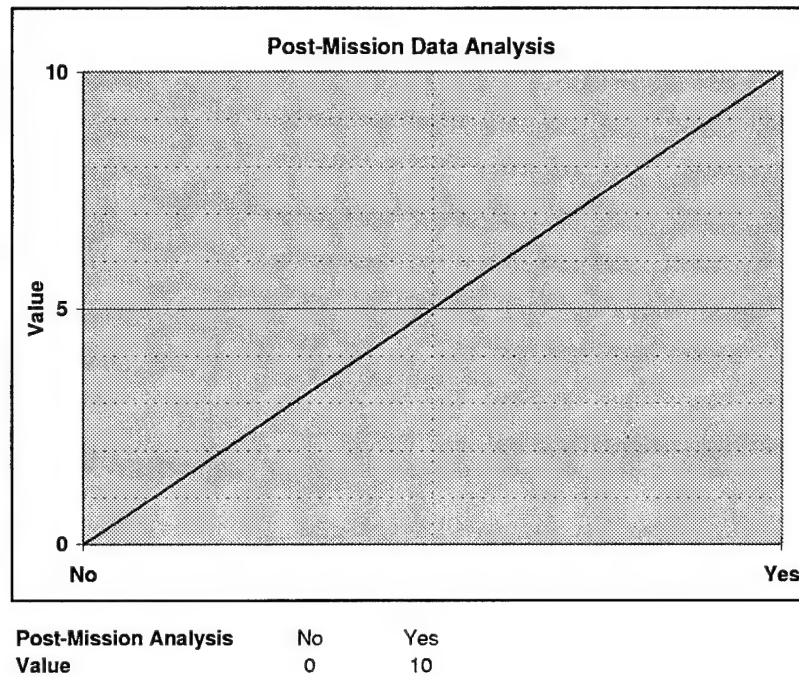


Figure A.18 Post-Mission Data Analysis Value Function

A.5.12 Post-Mission Data Analysis. This measure was a binary (yes/no) measure of the system to support data collection and retrieval capability for post-mission data analysis.

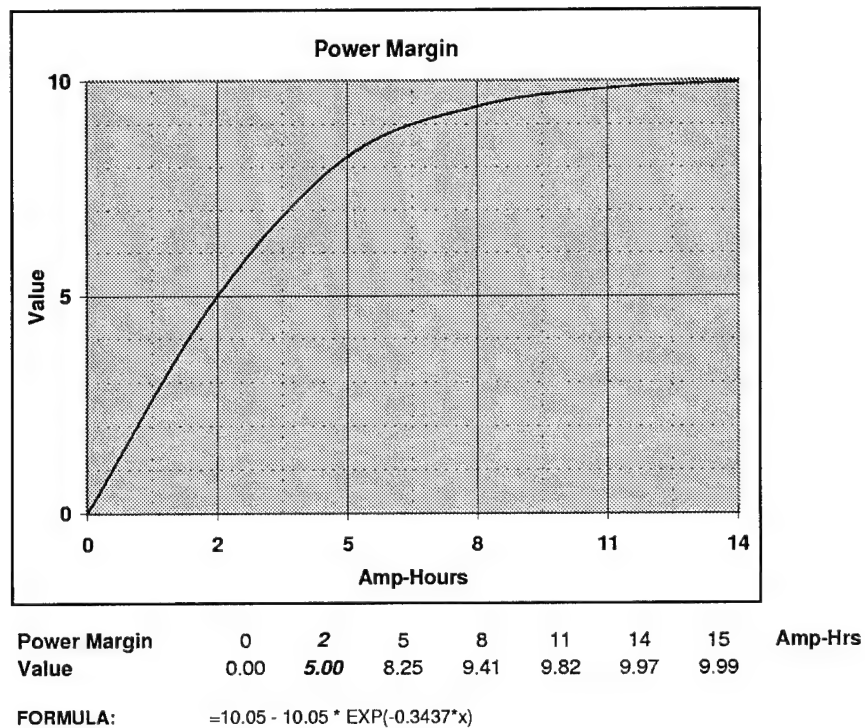


Figure A.19 Power Margin Value Function

A.5.13 Power Margin. This measure was a continuous “direct” measure reflecting the estimated power the battery system can support after all the required baseline *SIMSAT* components are installed (at the nominal system voltage). The CDM generated this function by selecting the following value comparison:

$$\text{Value}(2 \text{ Amp-hrs}) = 5$$

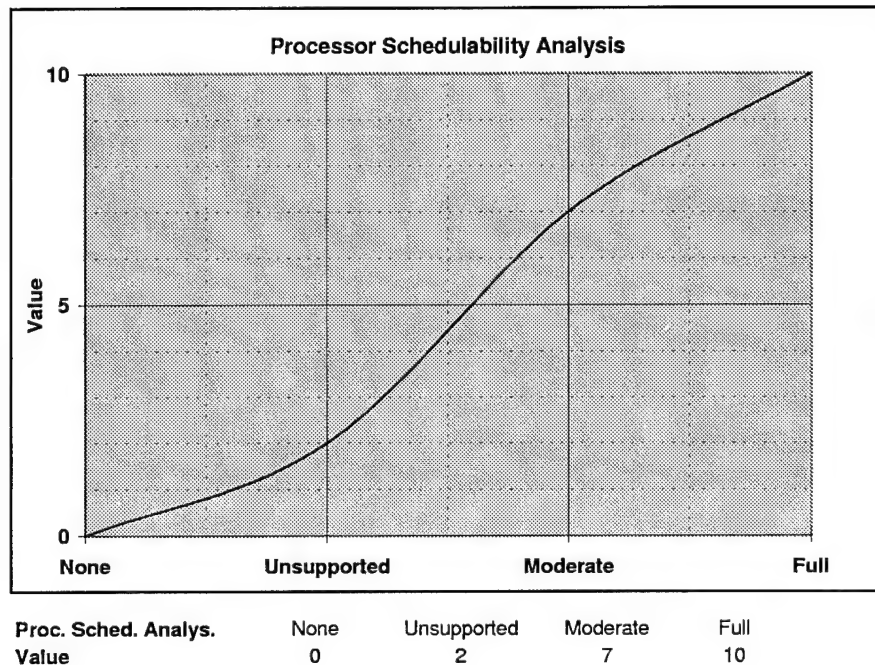


Figure A.20 Processor Schedulability Analysis Value Function

A.5.14 Processor Schedulability Analysis. See Appendix A of Mr. Hanke's thesis [26] for additional rationale on Rate Monotonic Analysis (RMA) as the scheduling technique of choice.

LEVEL	DEFINITION
None	RMA is not supported; insufficient data regarding OS scheduling technique to assess likelihood and impact of missed deadlines
Unsupported	RMA is not supported; but sufficient data regarding OS scheduling technique to assess likelihood and impact of missed deadlines
Moderate	RMA supported at least indirectly; some hand-coding required to fully implement
Full	RMA supported directly in both hardware and software

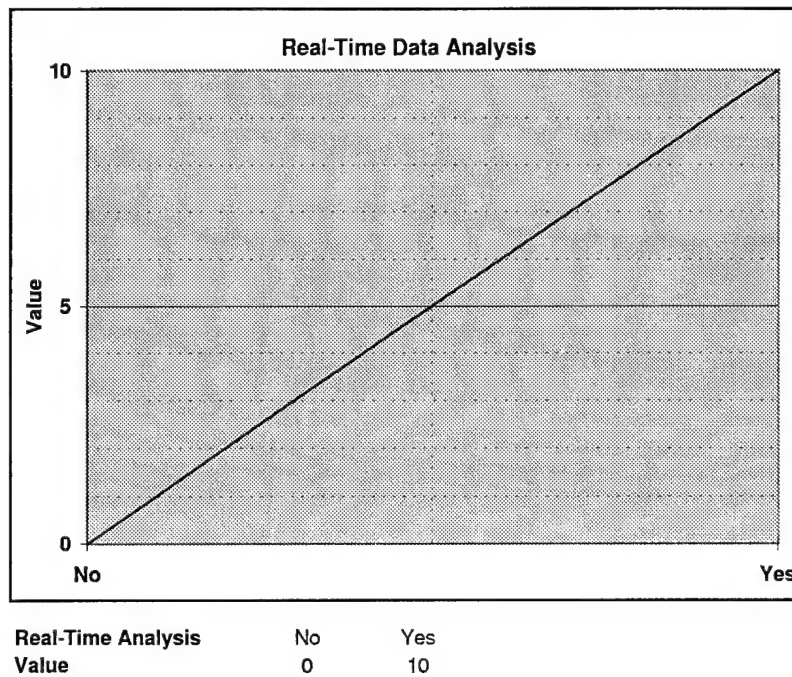


Figure A.21 Real-Time Data Value Function

A.5.15 Real-Time Data. This binary (yes/no) measure indicated the system support for real-time data display.

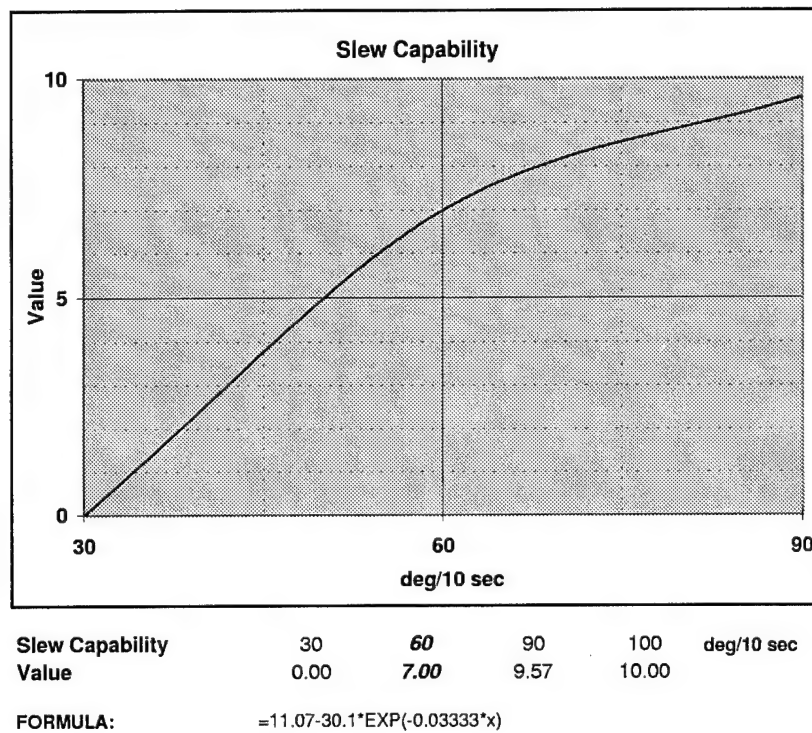
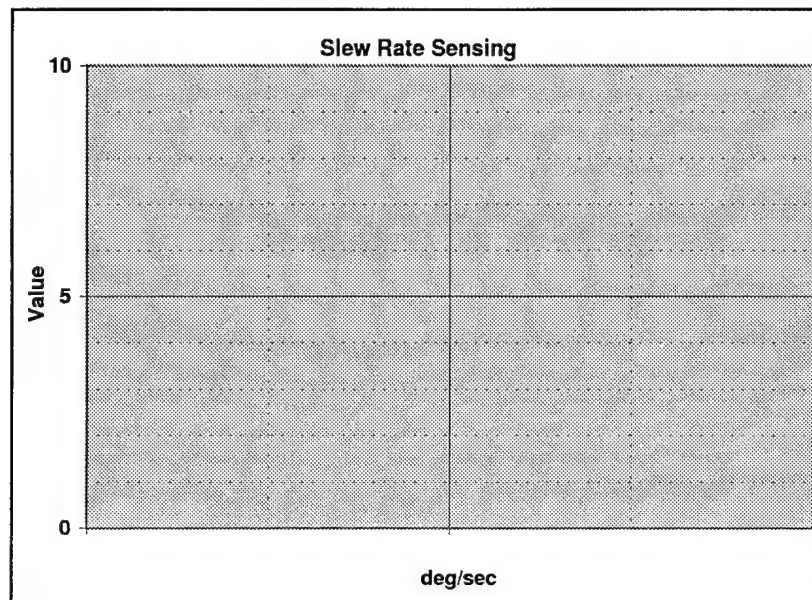


Figure A.22 Slew Capability Value Function

A.5.16 Slew Capability. This measure was a continuous “direct” measure reflecting how far *SIMSAT* can slew in a 10 second timeframe. The CDM generated this function by selecting the following value comparison:

$$\text{Value}(60 \text{ deg in } 10 \text{ sec}) = 7$$



Slew Rate Sensing
Value

deg/sec

FORMULA:

Figure A.23 Slew Rate Sensing Value Function

A.5.17 Slew Rate Sensing. Because the alternatives considered in the Preliminary Design phase did not specifically address the rate gyro subsystem, no alternatives differed in this rate sensing metric since all incorporated a nominal rate gyro subsystem. Thus, the value function for this measurable was determined to be of no consequence at this stage of design. In the Detailed Design phase, *Slew Rate Sensing* was directly addressed.

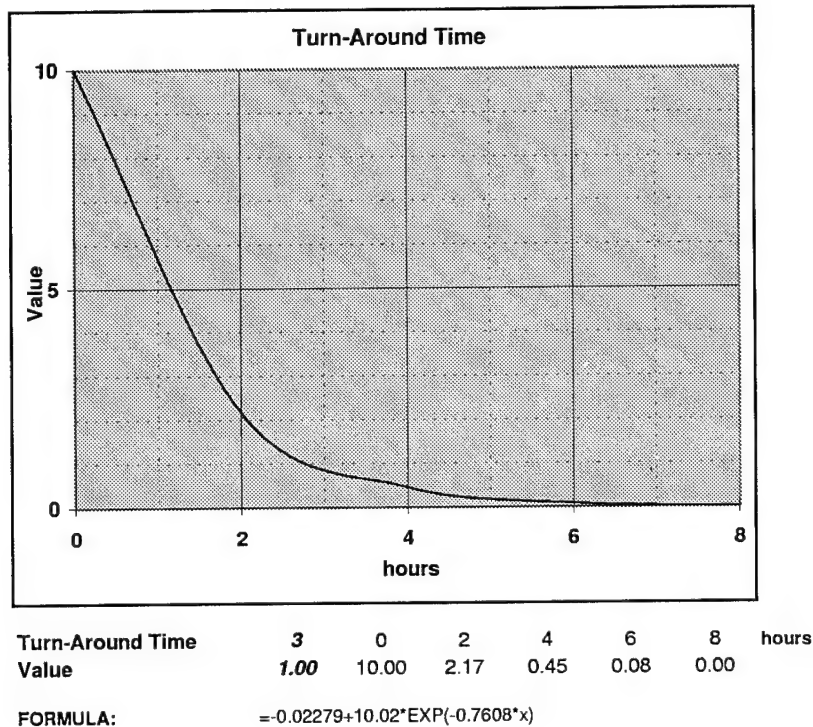


Figure A.24 Turn-Around Time Value Function

A.5.18 Turn-Around Time. This measure was a continuous “direct” measure reflecting the time between experimental runs, assuming no reconfiguration of payload hardware is required. The measure was impacted by both the number of spare batteries available and the recharge cycle time. For example, a single set of batteries that last 4 hours and take 8 hours to recharge would score an 8 and a value of 0 (based upon Figure A.24). Adding another set of 4 hour batteries would score a 4 for a value of 0.45, while 3 sets of batteries would allow the first set to recharge by the time the third ran down, resulting in 0 turn-time for a value of 10. The CDM generated this function by selecting the following value comparison:

$$\text{Value}(3 \text{ hours}) = 1$$

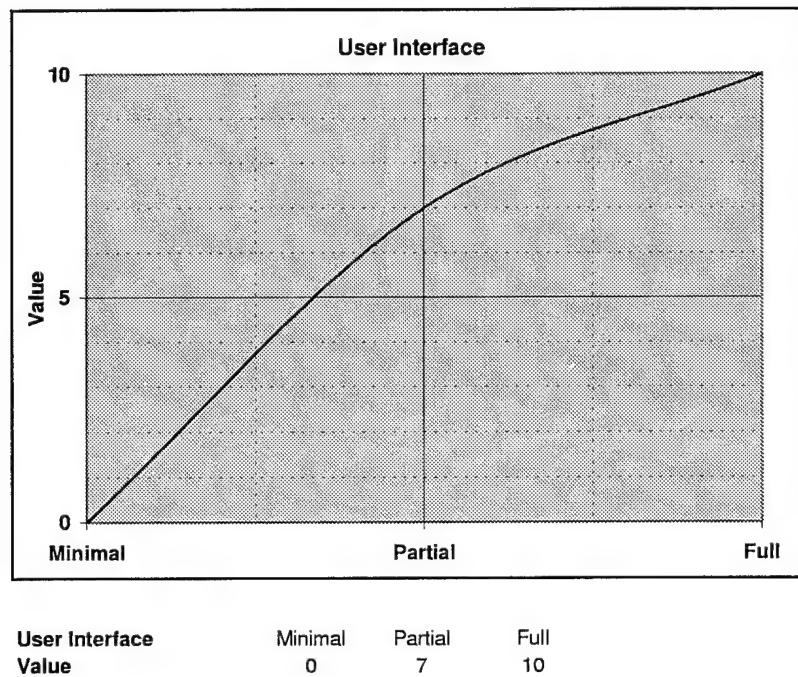


Figure A.25 User Interface Value Function

A.5.19 User Interface.

LEVEL	DEFINITION
Minimal	<50% of controls and displays can be done graphically
Partial	50-90% of controls and displays can be done graphically
Full	>90% of controls and displays can be done graphically

Appendix B. Equations-of-Motion Development

B.1 Overview

This appendix details the equations-of-motion (EOM) development used for the momentum wheel sizing and system modeling of the first Detailed Design iteration. In addition, the EOM modeling served as a basis for the plant model for controller development and satellite simulation.

B.2 Plant Model

The plant model was developed by deriving the equations of motion of the system. As with any formal definition, there was a basic process which was followed. The steps of this process are listed below:

1. List any key assumptions for the system.
2. Define an inertial reference frame.
3. Establish a body-fixed basis and reference point for the system by which all components will be expressed.
4. Identify the relevant forces and moments acting upon the system.
5. Use appropriate fundamental equations to derive the specific system equations of motion.

B.3 Key Assumptions

1. The system behaves as a rigid body. While this is not a completely accurate statement, it simplifies our model by defining a complex system using basic equations of motion. However, it should be understood that *SIMSAT* is not a purely rigid body in reality and will perform as such.

2. The initial system uses three momentum wheels to perform slew maneuvers and maintain pointing accuracy. For the first cut, thrusters were not added to the equations of motion. This decision was made due to the team's inability to purchase thrusters during system creation. While components had been identified for purchase, performance information derived from lab testing was not possible. Therefore, any thruster model developed without accurate information would be useless to include within the system.
3. *SIMSAT* has rotational freedom about the roll and yaw axes. About the pitch axis, there is limited rotational movement (± 15 -30 deg). This limitation is due to the pedestal upon which *SIMSAT* rests. While this limitation did not affect the equations of motion, establishing the degrees of freedom provided clarity to the system design and identified control issues.
4. There are no external torques acting upon *SIMSAT*. This is an engineering approximation. In reality, there are several external torques, such as air drag, which affect the motion of *SIMSAT*. However, there were no estimates for these torques. Therefore, they were ignored until the proper time when these torques were better understood and could be accurately modeled.
5. *SIMSAT*'s origin matches the physical center of *SIMSAT*, which is located at the center of the central sphere.
6. All *SIMSAT* components can be modeled as simple geometric shapes with uniform density. While this does not reflect the true nature of the components, it adequately simplifies the model.
7. The system is assumed to be perfect with no losses due to friction with the air bearing or with other components within the system.

B.4 Inertial Reference Frame, Inertial Basis, and Origin

The inertial reference frame selected for the system was the lab room in which the system is to be contained. Its origin is the point in space upon which the center of the central sphere is located (when placed upon the air bearing pedestal). This point is fixed

with respect to both inertial space and the body of *SIMSAT*. Finally, the basis that defines the inertial reference frame has +x pointing to the right of the page, +y pointing towards the top of the page, and +z pointing out of the page.

With respect to the lab room, the inertial +y axis is pointed directly at the laboratory ceiling. The +x axis points at a pre-defined location, such as a painted mark on the north laboratory wall (or any other convenient wall). With the +x and +y inertial axes defined, the +z inertial axis can be deduced from right-handed orthogonality. For experiments, the body-fixed basis, explained in the next section, will be aligned with the inertial axis system at time $t=0$.

B.5 SIMSAT Body Frame, Body Fixed Basis, and Reference Point

The body frame for *SIMSAT* was defined as the composite structure. Its reference point, the physical center of the body, rests on the origin of the inertial reference frame. Using the document below, the b basis has b1 pointing to the right of the page, b2 pointing towards the top of the page, and b3 pointing out of the page. This orthogonal axis set was used as the common basis by which all components of *SIMSAT* were expressed. It is fixed to the *SIMSAT* body and rotates with the vehicle. With respect to the b basis, the axle of wheel 1 was parallel to the b1 axis, the axle of wheel 2 was parallel to the b2 axis, and the axle of wheel 3 was placed parallel to the b3 axis. Figure B.1 illustrates this arrangement.

In addition to the b basis, each component had its own frame and orthogonal axis set fixed about its own center of mass in accordance with Appendix B in Kramer's text [31]. Each momentum wheel had a specific basis that was used throughout the development of the equations of motion (and subsequent programming codes). Momentum wheel one uses the d basis, momentum wheel two uses the f basis, and momentum wheel 3 uses the h basis. These letters were arbitrarily picked and have no special significance.

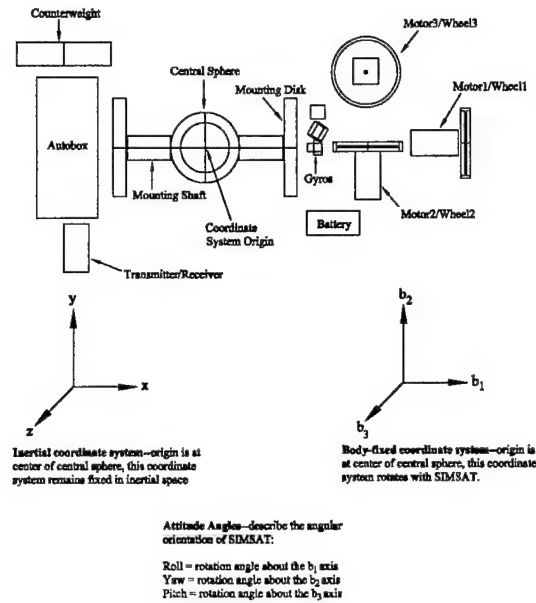


Figure B.1 *SIMSAT* with Axes

B.6 Identify Relevant Forces and Moments

As stated in the list of assumptions, there were no external forces modeled within the system. The resultant force due to gravity acts in a downward direction at the center of mass of *SIMSAT*. The resultant upward force generated by the air bearing effectively negates this gravitational force.

There are only four rotations which affect the angular momentum of *SIMSAT*. First, there is the rotation of *SIMSAT* about the inertial origin. The remaining three rotations are due to each momentum wheel having its own rotation with respect to its center of mass.

B.7 Fundamental Equations

To develop the proper equations of motion, the first step was identifying which fundamental laws to use. No translational movement was anticipated due to the design characteristics. Therefore, rotational motion was the only concern when modeling the system.

Following the general theory of kinematics for a rigid body, the vector relationship shown below was used as the starting point:

$$M^o = \dot{H}^o \quad (B.1)$$

This equation states the force moment, M^o , about a given point (o denotes the origin) equals the time rate of change of the angular momentum of a system, \dot{H}^o . [31:56]

The angular momentum, H , of a body is a product of its inertia matrix and the angular velocity vector with which it rotates about a defined point in space.

$$H = I\omega \quad (B.2)$$

In the design, the total angular momentum of the system is comprised of four components. The first segment, *SIMSAT*'s body, rotates about the origin. The remaining three components are due to the rotations of the momentum wheels.

$$H = H_{SIMSAT} + H_{w1} + H_{w2} + H_{w3} \quad (B.3)$$

The four components can be expressed, in terms of the b frame, as:

$$H_{SIMSAT} = {}^b I_{comp}^c {}^b \omega_s^{b,i} \quad (B.4)$$

$$H_{w1} = {}^b J_{w1}^c {}^b \omega_s^{b,i} + C^{bdd} J_{w1}^{w1d} \omega_{w1}^{w1,b} \quad (B.5)$$

$$H_{w2} = {}^b J_{w2}^c {}^b \omega_s^{b,i} + C^{bff} J_{w2}^{w2f} \omega_{w2}^{w2,b} \quad (B.6)$$

$$H_{w3} = {}^b J_{w3}^c {}^b \omega_s^{b,i} + C^{bhh} J_{w3}^{w3h} \omega_{w3}^{w3,b} \quad (B.7)$$

${}^bI_{comp}^c$ represents the inertia matrix of *SIMSAT* defined about the origin in the b basis. *SIMSAT*'s angular velocity vector, ${}^b\omega_s^{b,i}$, relates the motion of the *SIMSAT* body with respect to inertial space. The different inertia matrices of the three momentum wheels are expressed in two different fashions. First, they are defined with respect to *SIMSAT*'s physical center using the b basis, shown as ${}^bJ_{wi}^c$. Also, they are written with respect to their own centers of mass using their specific bases (d, f, and h), shown as ${}^{(d,f,h)}J_{wi}^{wi}$. The angular velocity vector for each momentum wheel, ${}^{(d,f,h)}\omega_{wi}^{wi,b}$, is expressed as its relative motion with respect to *SIMSAT*'s body using the proper basis (d, f, or h, depending on the wheel). Finally, the C matrices represent necessary transformation matrices to express the different angular momentum components in a common basis, the b basis.

Having these expressions for the angular momentum of the system, the next logical step was calculating \dot{H} to find the torque equation. Since the angular momentum is a vector quantity, it was necessary to use the vector derivative form:

$$T = \dot{H} = \frac{d}{dt}H + {}^b\omega_s^{b,i} \times H \quad (B.8)$$

Since the system has no external torques, T disappears to yield

$$\frac{d}{dt}H + {}^b\omega_s^{b,i} \times H = 0 \quad (B.9)$$

Following several steps, the final expression to be used as the plant model is

$$\begin{aligned} {}^b\dot{\omega}_s^{b,i} = & [{}^bI_s^c - {}^bJ_{\omega_1}^c - {}^bJ_{\omega_2}^c - {}^bJ_{\omega_3}^c]^{-1} * [C^{bdd}J_{\omega_1}^{wi}d\dot{\omega}_1^{\omega_1,b} + C^{bff}J_{\omega_2}^{wi}f\dot{\omega}_2^{\omega_2,b} + C^{bhh}J_{\omega_3}^{wi}h\dot{\omega}_3^{\omega_3,b} \\ & + {}^b\omega_s^{b,i} \times {}^bI_s^c {}^b\omega_s^{b,i} + {}^b\omega_s^{b,i} \times {}^bJ_{\omega_1}^c {}^b\omega_s^{b,i} + {}^b\omega_s^{b,i} \times C^{bdd}J_{\omega_1}^{wi}d\omega_1^{\omega_1,b} + {}^b\omega_s^{b,i} \times {}^bJ_{\omega_1}^c {}^b\omega_s^{b,i} \\ & + {}^b\omega_s^{b,i} \times C^{bff}J_{\omega_2}^{wi}f\omega_2^{\omega_2,b} + {}^b\omega_s^{b,i} \times {}^bJ_{\omega_2}^c {}^b\omega_s^{b,i} + {}^b\omega_s^{b,i} \times C^{bhh}J_{\omega_3}^{wi}h\omega_3^{\omega_3,b}] \quad (B.10) \end{aligned}$$

This expression relates the motion of *SIMSAT* to the motion of the three momentum wheels. Using this system of equations, along with a motor model which related output motor torque as a function of motor speed, a variable step Runge-Kutta numerical integration technique was used to calculate *SIMSAT*'s angular velocities.

However, direct numerical integration could not be used to calculate *SIMSAT*'s angular position since the equations of motion were derived for the body fixed basis. Since this axis system rotates with *SIMSAT*, orientation information could not be obtained using this basis. In order to correctly express angular position as a function of *SIMSAT*'s angular velocity with respect to the inertial reference frame, Euler rotations were employed. The following equation shows the relationship between the attitude angle, θ , and the angular velocity, ${}^b\omega_s^{b,i}$, of a given body using a transformation matrix C_{rot} .

$$\theta = C_{rot} * {}^b\omega_s^{b,i} \quad (B.11)$$

To specify the proper rotations, the first step was defining the roll, yaw, and pitch axes with respect to the b basis. The b1 axis was defined as the roll axis. About this axis, *SIMSAT* had full rotational freedom. The b2 axis corresponded to the yaw axis. As with the previous case, *SIMSAT* had full rotational freedom about the b2 axis. The pitch axis, defined as the b3 axis, had a limitation of ± 25 degrees due to the presence of the air bearing pedestal.

Next, the correct sequence of rotations had to be selected. For any given change in orientation, there are twelve possible rotation sequences which can be used [28:28]. However, due to the possible points of singularity for a defined sequence, the order of rotations about the roll, yaw, and pitch axes must be chosen carefully.

To avoid the singularity, the roll-pitch-yaw (1-3-2) rotation sequence was chosen. The composite transformation matrix assumed the form [28:28]:

$$C_{rot} = \begin{bmatrix} 1 & -\cos(\theta_{roll})\tan(\theta_{pitch}) & \sin(\theta_{roll})\tan(\theta_{pitch}) \\ 0 & \frac{\cos(\theta_{roll})}{\cos(\theta_{pitch})} & \frac{-\sin(\theta_{roll})}{\cos(\theta_{pitch})} \\ 0 & \sin(\theta_{roll}) & \cos(\theta_{roll}) \end{bmatrix}$$

By choosing this sequence, the terms in the denominator can only be zero if the pitch angle is 90 degrees. As stated before, the pitch angle is limited to ± 25 degrees. Therefore, a singularity never occurs and the orientation angles can be calculated.

To calculate or measure the quantities represented by the different variables, several steps occur. While the angular velocity components are simply measured quantities from the gyro or the wheel motor, computing the inertia matrices for the *SIMSAT* body and the momentum wheels required several mathematical manipulations. The process listed below was used to find the *SIMSAT* inertia matrix, known as I_{comp} in the MATLAB code. As part of the intermediate steps, the inertia matrices for the momentum wheels in various forms were also calculated.

1. Use simple geometric bodies to approximate *SIMSAT*'s components.
2. Orientation of each object has to be rotated using transformation matrices.
3. *SIMSAT*'s center of mass is adjusted, using counterweights, to be co-located with *SIMSAT*'s physical center resting on the origin.
4. Using the parallel axis theorem, the component inertia matrices are expressed about *SIMSAT*'s center of mass.

The first step, modeling the components as simple geometric bodies with uniform densities, simplified the problem to a manageable level. The *SIMSAT* vehicle is comprised of 19 components. Connectors, such as bolts and clamps, were not modeled due to the realization that the model exists as an approximation of the actual *SIMSAT* body and is not perfect. As a compromise, the masses of these connectors were added to the components with which they were associated. It was understood that the inertia of these components would not be captured. Additionally, the wiring between components was neglected. Table B.1 includes the breakout of components and what shape they were modeled as. MATLAB was used to calculate the inertia matrix.

Once the proper shapes were selected, the next step involved orienting each component on the *SIMSAT* vehicle. Initially, all components were aligned with the u_1 axis pointing to the right, the u_2 axis pointing up, and the u_3 axis pointing out of the page.

Table B.1 *SIMSAT* Components

Component	Qty	Geometric Shape
Autobox	1	Rectangular Parallelepiped
Mounting Disk	2	Rectangular Parallelepiped
Battery	1	Rectangular Parallelepiped
Mounting Shafts	2	Right Circ. Cylinder
Central Sphere	1	Sphere
Counterweight Mechanism	1	Right Circ. Cylinder
Gyro	4	Rectangular Parallelepiped
Momentum Wheel	3	Right Circ. Cylinder
Motor	3	Rectangular Parallelepiped
Transmitter/Receiver	1	Rectangular Parallelepiped

The choice of a *u* basis was consistent with Kramer [31:Appendix D] to represent the component's own axes. Please refer to Figure B.2 for the geometric shapes and their axes.

In order to express *SIMSAT*'s components in a common basis (the *b* basis), transformation matrices were developed for each component. This method provided additional flexibility when determining location and orientation of each item. The other alternative, fixing a component's dimensions to match the orientation with respect to the *b* basis, proved more difficult when changing the mechanism's alignment.

Each transformation matrix used a 1-2-3 rotation sequence. While most components were only subject to one rotation of 90 degrees, the full capability of the three rotation sequence was used to increase flexibility during the detailed design phase.

$$Rot_a = \begin{bmatrix} c(\theta_2)c(\theta_3) & c(\theta_1)s(\theta_3) + s(\theta_1)s(\theta_2)c(\theta_3) & s(\theta_1)s(\theta_3) - c(\theta_1)s(\theta_2) \\ -c(\theta_2)s(\theta_3) & c(\theta_1)c(\theta_3) - s(\theta_1)s(\theta_2)s(\theta_3) & s(\theta_1)c(\theta_3) + c(\theta_1)s(\theta_2) \\ s(\theta_2) & -s(\theta_1)c(\theta_2) & c(\theta_1)c(\theta_2) \end{bmatrix}$$

Mathematically, to change from one basis to another, a given matrix needs to be multiplied by both the rotation matrix and the rotation matrix's transpose. This ensures multiplication by the equivalent of an identity matrix to maintain the values within the original matrix.

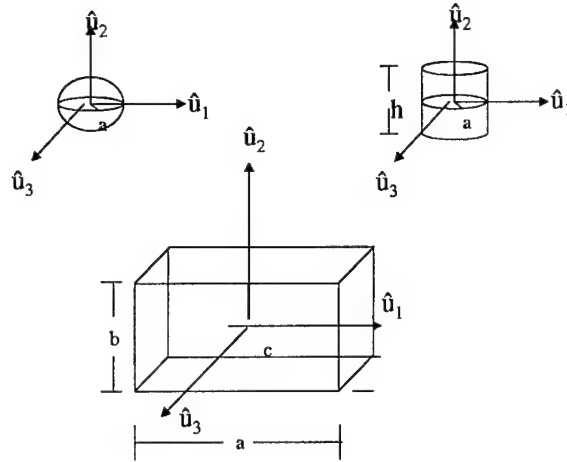


Figure B.2 Geometric Shapes

$$I_{battb} = C^{ub} * I_{battu} * C^{ubT} \quad (B.12)$$

For the nominal design, the rotations listed in Table B.2 were used for the different components.

Following the rotations, the next phase was locating the composite center of mass for the *SIMSAT* body. The goal was aligning the composite center of mass as close to the origin as possible through the use of weight plates and the counterweight mechanism.

The first step involved calculating the mass difference between the two sides. Weight plates were added to the lighter side until the system was balanced. In order to place the weight plates properly to adjust the center of mass to the origin, the following technique was used. (Please refer to Figure B.3 throughout this discussion).

Within the confines of the design problem, the position vector of each component was measured from the physical center of *SIMSAT* (which rests at the origin). The center of mass of *SIMSAT*, point c, represents a point which will most likely be located away

Table B.2 Component Rotation Angles

Component	Theta 1	Theta 2	Theta 3
Autobox	90	0	0
Battery	0	90	90
Mounting Shaft 1	0	0	90
Mounting Shaft 2	0	0	-90
Central Sphere	0	0	0
Gyro 1	0	0	90
Gyro 2	0	0	0
Gyro 3	-90	0	0
Gyro 4	45	45	45
Momentum Wheel 1	0	0	90
Momentum Wheel 2	0	0	0
Momentum Wheel 3	-90	0	0
Motor 1	0	0	90
Motor 2	0	0	0
Motor 3	-90	0	0
Transmitter/Receiver	0	0	90

from the origin. The distance between these two points represents the delta which the counterweight was designed to remove.

In general, the position vector of the center of mass can be expressed as

$${}^o r^c = \frac{\sum_{i=1}^n m_i {}^o r_{pi}}{m} \quad (\text{B.13})$$

where ${}^o r^c$ represents the position of the center of mass with respect to the origin. The summation includes all components of *SIMSAT*. The mass in the denominator denotes the total mass of the system.

To solve for the position vector of the counterweight, the equation was rewritten as:

$${}^o r^c = \frac{\sum_{i=1}^n [m_i {}^o r_{pi}] + m_{cw} {}^o r_{cw}}{m} \quad (\text{B.14})$$

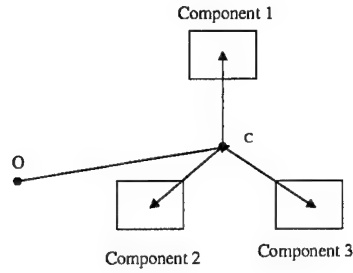


Figure B.3 Center of Mass for Multiple Components

The goal at this point was to eliminate the distance between the center of mass and the origin. Therefore, ${}^o r^c$ equals the zero vector. To do this, the expression in the numerator must equal zero.

$$\sum_{i=1}^n [m_i * {}^o r_{pi}] + m_{cw} * {}^o r_{cw} = 0 \quad (\text{B.15})$$

It follows that

$${}^o r_{cw} = \frac{-\sum_{i=1}^n [m_i * {}^o r_{pi}]}{m_{cw}} \quad (\text{B.16})$$

At this stage, the center of mass was coincident with both the origin and physical center of *SIMSAT*.

Finally, the composite inertia matrix was calculated. Despite being in a common basis, the different components had to be expressed about a common reference point, the origin. To do this, the parallel axis theorem [56:109] was used.

$$I_{origin_i} = I_{com_i} + m_{com_i} * \begin{bmatrix} \Delta y^2 + \Delta z^2 & -\Delta y \Delta x & -\Delta z \Delta x \\ -\Delta x \Delta y & \Delta x^2 + \Delta z^2 & -\Delta z \Delta y \\ -\Delta x \Delta z & -\Delta y \Delta z & \Delta x^2 + \Delta y^2 \end{bmatrix}$$

I_{com_i} represents the inertia matrix of a given component with respect to its center of mass. The mass of the component is represented by m_{com_i} . Within the matrix, the Δx , Δy , and Δz values are the distances between the component's center of mass and *SIMSAT*'s origin. I_{origin_i} represents the inertia matrix of the component about the origin. Once the inertia matrices were adjusted to be expressed with respect to the origin, they were simply added together. The final expression was I_{comp} , the inertia of the *SIMSAT* body, including all components. The values within this matrix were considered constant throughout a given experiment.

$$I_{comp} = \sum_{i=1}^n [I_{origin_i}] \quad (B.17)$$

Appendix C. Momentum Wheel Sizing

C.1 Momentum Wheel Development

Once the *SIMSAT* equations of motion had been developed and coded into a MATLAB computer program, the team focused on momentum wheel design. Momentum wheel development was clearly a system driver, and early resolution of wheel issues was critical for the subsequent development of other subsystems.

C.1.1 Location of Components. To analyze the effects of various wheel designs on *SIMSAT* motion, a nominal "best guess" configuration for *SIMSAT* was selected. Although the final appearance of *SIMSAT* was not yet known, the salient characteristics of competing wheel designs could still be compared. Figure C.1 and Table C.1 show a listing of individual components, masses, dimensions, and position vectors from the inertial origin (the center of the central sphere) to the center of gravity (c.g.) of each component. At this point in the design, only the masses and dimensions of the battery, AutoBox, model helicopter (Horizon) gyroscopes, SmartMotor, central sphere, mounting shafts, and mounting disks were known. The mass and dimensions of the transmitter/receiver were estimated from vendor catalogs, and the parameters of the momentum wheels were left as design variables.

The counterweight was a notional object used to balance *SIMSAT* in the MATLAB computer simulation. The counterweight was modeled as a right circular cylinder with 15 cm radius and 7 cm height. The mass of the counterweight was calculated as the mass difference between the positive 'b₁' side components (3 motors, 3 momentum wheels, 4 gyros, 1 battery) and the negative 'b₁' side components (Autobox and transmitter/receiver). The center of mass of the counterweight was placed at a position vector that balanced *SIMSAT* (i.e., the overall system center-of-gravity was located at [0, 0, 0] of the body coordinate system at time t=0). Mathematically, the counterweight's position vector was calculated from:

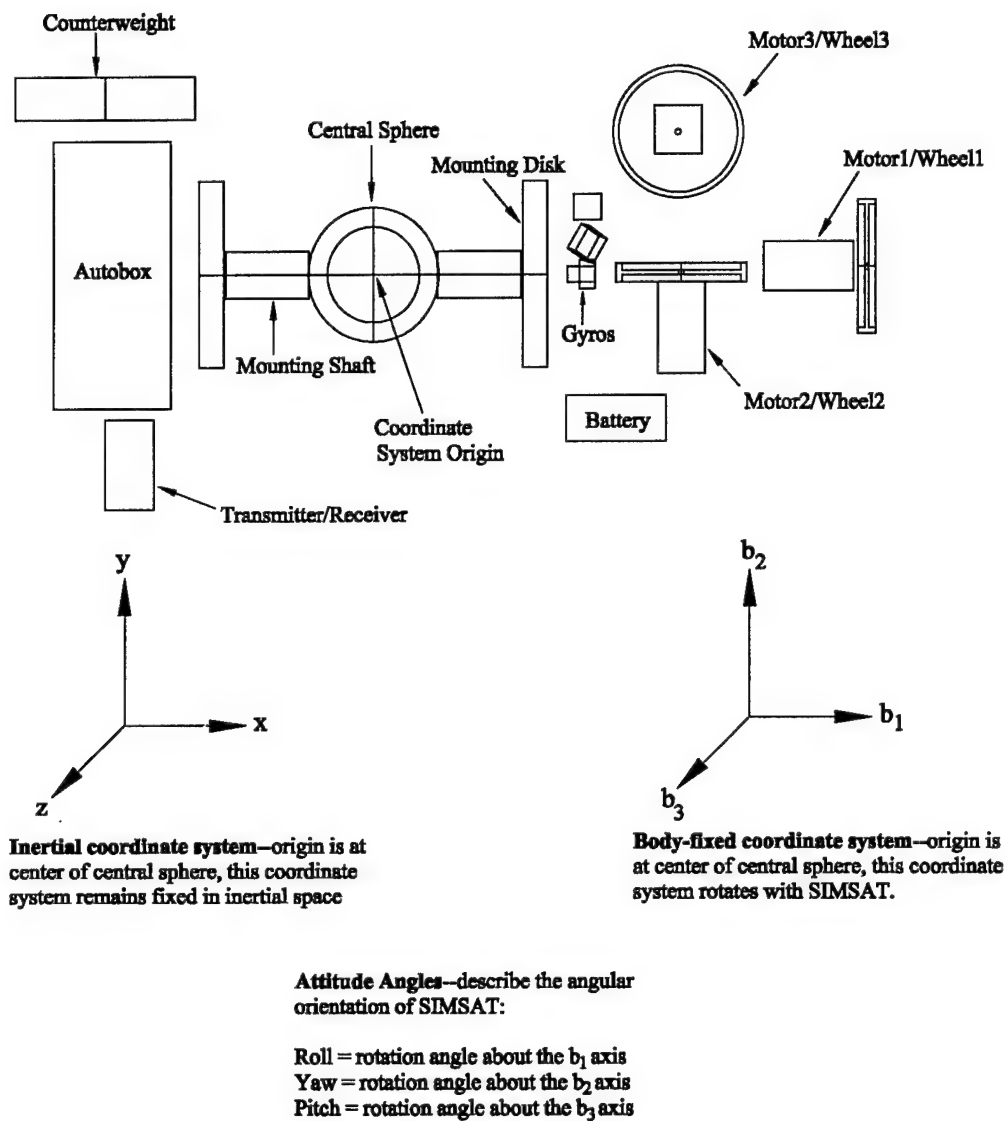


Figure C.1 Nominal Configuration Used for Momentum Wheel Design

Table C.1 Nominal Configuration Component Properties

Nominal SIMSAT Components used for Momentum Wheel Design

Item	Mass (kg)	Dimensions (cm)	Position Vector (from origin to item's c.g. in cm)
Sphere	7.6	radius = 11	[0, 0, 0]
Mt. Shaft 1	0.855	radius = 4, height = 13	[17.5, 0, 0]
Mt. Shaft 2	0.855	radius = 4, height = 13	[-17.5, 0, 0]
Mt. Disk 1	4.845	radius = 15, height = 5.1	[26.55, 0, 0]
Mt. Disk 2	4.845	radius = 15, height = 5.1	[-26.55, 0, 0]
Motor 1	3.635	15*8*8	[50.1, 0, 0]
Motor 2	3.635	8*15*8	[43.6, 0, 25.5]
Motor 3	3.635	8*8*15	[41.6, 23.5, 0]
Wheel1	Design Variable	Design Variables	[71.1, 0, 0]
Wheel2	Design Variable	Design Variables	[43.6, 0, 46.5]
Wheel3	Design Variable	Design Variables	[41.6, 44.5, 0]
Battery	20	16.7*7.6*18.1	[37.9, -23.35, 0]
Gyro 1	0.05	2.65*4.65*4.25	[36, 0, -11]
Gyro 2	0.05	4.65*2.65*4.25	[35, 0, 2]
Gyro 3	0.05	4.65*4.25*2.65	[36, 11, 0]
Gyro 4	0.05	same as gyro 2 but rotated 45° about each 'b' axis	[36, 5, 5]
Autobox	8.6	19.5*44*20	[-43.85, 0, -25]
Xmit/Rec	2.2	8.2*15*5.2	[-36.7, -35.8, 0]
Counterwt	Varies to balance SimSat	radius = 15, height = 7	Varies to balance SimSat

Notes:

1. Dimensions are given as length in b_1 direction * width in b_2 direction * depth in b_3 direction
2. Position vectors are in the body reference frame [b_1 vector component, b_2 vector component, b_3 vector component]
3. Coordinate origin is at center of central sphere

$$\vec{r}_{comp} = \frac{\sum_{i=1}^{19} m_i \vec{r}_i}{\sum_{i=1}^{19} m_i} \quad (C.1)$$

where

\vec{r}_{comp} = position vector from the origin to the composite center of mass of the system

m_i = mass of the i th component

\vec{r}_i = position vector from the origin to the c.g. of the i th component

For a balanced system, $\vec{r}_{comp} = [0, 0, 0]$. Solving for \vec{r}_{cw} to balance the system:

$$\vec{r}_{cw} = \frac{-\sum_{i=1}^{18} m_i \vec{r}_i}{m_{cw}} \quad (C.2)$$

where

\vec{r}_{cw} = position vector from the origin to the c.g. of the counterweight

m_{cw} = mass of the counterweight

C.1.2 Estimating Motor Torque. The torque characteristics of the 3450 series SmartMotor needed to be estimated before computer simulation of *SIMSAT* motion could begin. The manufacturer of the SmartMotor, Animatics Corporation, supplied a Torque vs. Motor speed graph that displays peak and continuous performance at 48V (see Figure C.2). Although the 3450 motor is capable of operating up to the peak torque curve, the operating duration in this region is limited. Sustained operation at peak torque heavily taxes the motor and is inefficient because significant motor power is lost as heat.

For a fast *SIMSAT* slewing (yaw) maneuver, it was conservatively assumed the motor would be operated at its maximum continuous torque capability. For incorporation into a MATLAB simulation, the manufacturer's maximum continuous torque curve was approximated with an exponential curvefit. At this point in the *SIMSAT* design process, a 24V and a 36V electrical bus were still being considered as possible options. Therefore, the manufacturer's torque curve needed to be scaled down from 48V to 36V and 24V for performance analysis. If it is assumed that power input to the motor is roughly equal to

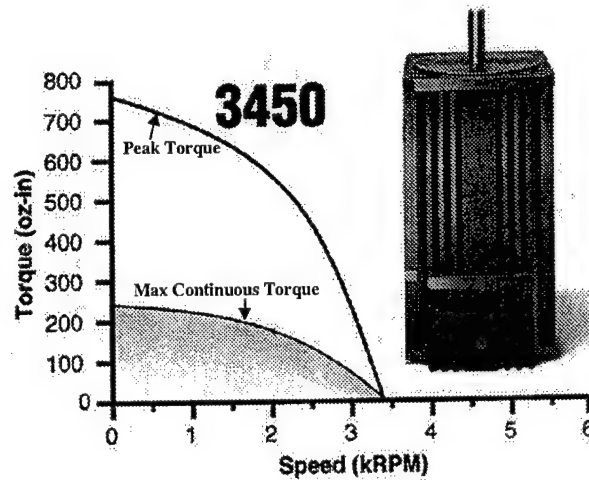


Figure C.2 Animatics SmartMotor Torque vs. Motor Speed Curves

power output of the motor, then a 36V torque curve (with amperage held constant) is a 75% scaling of the 48V curve, similarly, a 24V curve is a 50% scaling.

The manufacturer's 48V torque curve was approximated with:

$$T(\omega) = 250 - e^{0.00162\omega}$$

where

T = Torque (in ounce-inches)

ω = motor speed (in revolutions per minute)

After converting from English units to metric units, a 36V torque curve was mathematically approximated with:

$$T(\omega) = 0.007061 * (188 - e^{0.0193942\omega})$$

where

T = Torque (in Newton-meters)

ω = motor speed (in radians/second)

A 24V torque curve was approximated with:

$$T(\omega) = .007061 * (125 - e^{0.0271251\omega})$$

See Figure C.3, Figure C.4, and Figure C.5 for graphs of $T(\omega)$:

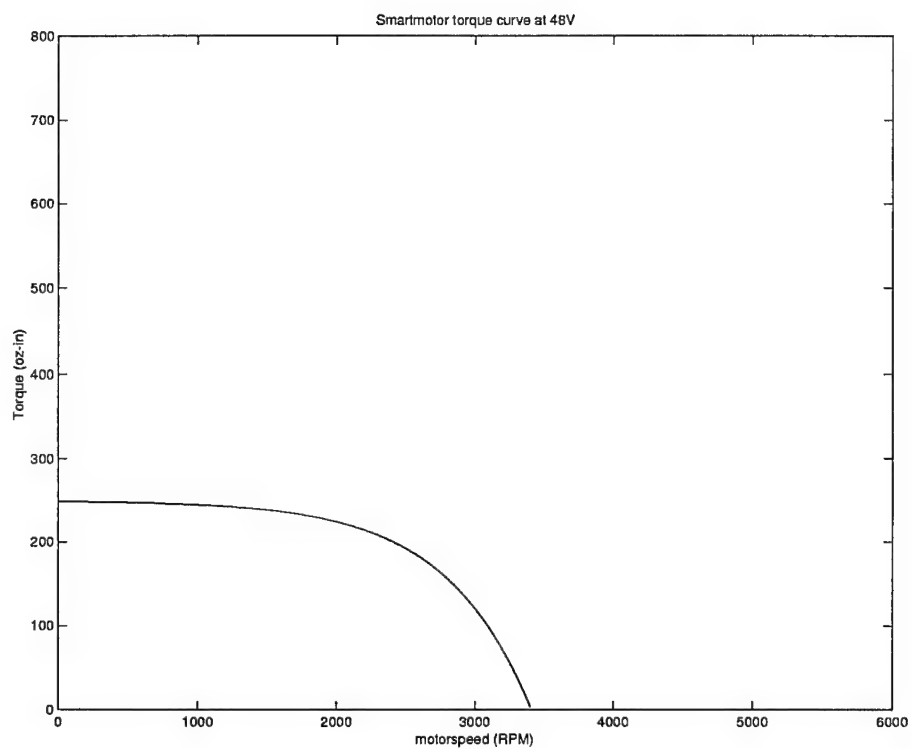


Figure C.3 48V Torque vs. Motor Speed Curve

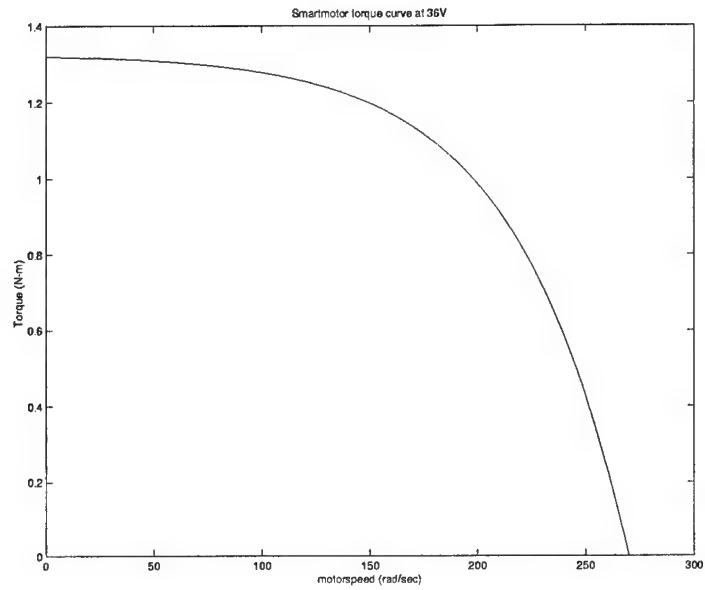


Figure C.4 36V Torque vs. Motor Speed Curve

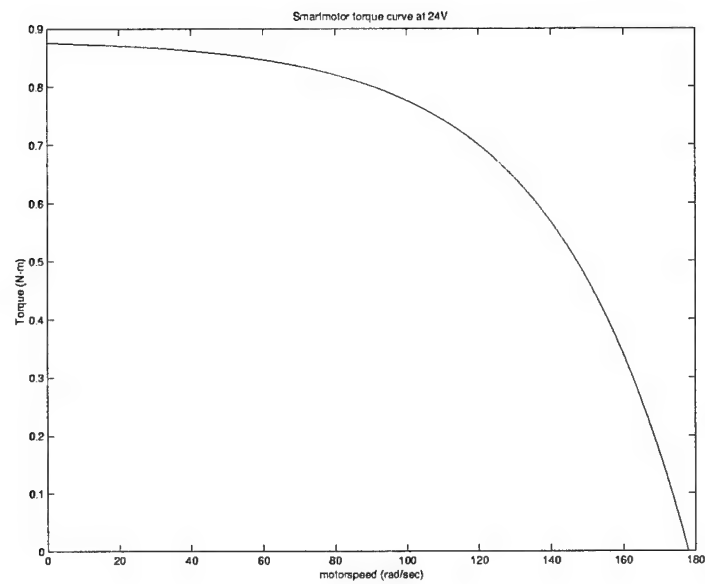


Figure C.5 24V Torque vs. Motor Speed Curve

C.1.3 Design Groundrules. Before analysis of different momentum wheel designs could begin, a performance criterion was needed to assess competing designs. Discussions with the *SIMSAT* customers revealed that maximizing slew (yaw) rate for a 10 second maneuver was an important goal. For an initial design and to simplify analysis, the customers also stated that orienting three momentum wheels orthogonal to each other was an acceptable way of providing motion input to *SIMSAT*.

Theoretically, a non-orthogonal arrangement of momentum wheels (i.e., using more than three wheels or not orienting three wheels orthogonal to each other) could possibly improve motion performance. However, a non-orthogonal arrangement complicates the analysis of attitude control and dynamics, and an untraditional momentum wheel orientation could create structural mounting challenges. Also, optimization of one subsystem can penalize the overall system. For instance, the time spent optimizing the momentum wheel arrangement could have created a schedule delay for the final design of the entire *SIMSAT* system.

Orthogonal momentum wheels still did not change the coupled inertia properties of *SIMSAT*. The different masses and shapes of *SIMSAT*'s components made the overall system an asymmetric body with products of inertia (off-diagonal terms) in its inertia matrix. These products of inertia created a coupling effect so that when a torque was applied to one axis, motion resulted in the other two axes as well. However, MATLAB simulations using the nominal *SIMSAT* configuration revealed that a one axis input torque resulted in motion primarily about that same axis. For instance, a motor #2 input torque about an axis parallel to the b_2 axis (see Figure ??) caused significant *SIMSAT* yaw motion (in the direction opposite than the input torque). Because of the inertia coupling, roll and pitch motion also occurred, but to a lesser degree than the yaw motion.

Since the *SIMSAT* roll axis (' b_1 ' axis in Figure ??) had the smallest moment of inertia, the idea of making wheel #1 smaller and lighter than the other two wheels was considered. If a high roll rate was not important to a customer, a lower performance roll axis momentum wheel might be acceptable. However, the customers' desire was to make all three momentum wheels identical.

C.1.4 Initial Wheel Analysis. With the design ground-rules established, momentum wheels of different sizes, shapes, and metal composition were analyzed via MATLAB computer simulation. Aluminum and steel designs were compared because both metals were readily available and could be easily machined by the AFIT fabrication shop.

To compare the 10 second yaw performance of various wheel designs, a simulated open-loop “bang-bang” control input was assumed. The yaw axis SmartMotor (modeled using the $T(\omega)$ equations describe earlier) applied a maximum continuous positive torque to one momentum wheel for the first five seconds, and a maximum continuous negative torque to the same wheel for the last five seconds. As a result, this simulated momentum wheel was accelerated for the first five seconds and decelerated for seconds 5 through 10. The intended effect of this simulated maneuver was to have *SIMSAT* start at rest at time $t = 0$ seconds, yaw, and end at rest at time $t = 10$ seconds.

For a real-world open-loop “bang-bang” scenario, input-shaping of the current (amperes) supplied to the motor would need to occur. This input-shaping would force the motor to accelerate along its maximum continuous torque curve for the first five seconds and then decelerate along this curve for the last five seconds. Although this open-loop approach would probably never be used to control the real-world *SIMSAT*, such an approach was conducive to computer simulation for momentum wheel sizing.

To simplify momentum wheel analysis, the roll and pitch axis motors (motors #1 and #3) received zero torque during the computer simulations. Even though the roll and pitch wheels remained motionless, *SIMSAT* still displayed some roll and pitch motion because of the inertia coupling effects explained earlier.

The first set of computer simulations compared aluminum and steel solid disk wheels. The radius and thickness of the solid disks were varied to determine the effect on *SIMSAT* yaw performance. Table C.2 summarize these solid disk designs. The terminology and assumptions used in Table C.2 are defined as follows:

- Motor1/Wheel1 – oriented parallel to the roll axis, used to provide torque input primarily to the roll axis.

Table C.2 Aluminum and Steel Solid Disk Wheels

Momentum Wheel Analysis (with all three wheels identical size)
for Wheel #2
Solid Disk

Aluminum (density = 2.8 g/cc)

radius (inches)	radius (cm)	thickness (inches)	thickness (cm)	Wheel mass		CW mass (kg)	Max wheel speed (rad/sec)	Yaw rate at 5 sec (rad/sec)	Yaw angle at 10 sec (rad)	Slew rate 10 sec avg (deg/sec)
8	20.32	1	2.54	9.23	20.306	47.98	35	0.17	0.8565	4.91
6	15.24	1	2.54	5.19	11.418	35.87	110	0.23	1.1941	6.84
4	10.16	1	2.54	2.31	5.082	27.22	270	0.16	1.2056	6.91
3	7.62	1	2.54	1.3	2.86	24.2	saturates	0.06	0.36	2.06
8	20.32	2	5.08	18.45	40.59	75.66	17	0.12	0.5263	3.02
6	15.24	2	5.08	10.38	22.836	51.44	55	0.16	0.8	4.58
4	10.16	2	5.08	4.61	10.142	34.14	240	0.22	1.2069	6.92
3	7.62	2	5.08	2.59	5.698	28.09	270	0.1	0.8232	4.72
4	10.16	3	7.62	6.92	15.224	41.06	175	0.19	1.0141	5.81
2	5.08	3	7.62	1.73	3.806	25.49	saturates	0.03	0.19	1.09

Steel (density = 7.85 g/cc)

radius (inches)	radius (cm)	thickness (inches)	thickness (cm)	Wheel mass		CW mass (kg)	Max wheel speed (rad/sec)	Yaw rate at 5 sec (rad/sec)	Yaw angle at 10 sec (rad)	Slew rate 10 sec avg (deg/sec)
8	20.32	1	2.54	25.86	56.892	97.9	10	0.08	0.4027	2.31
6	15.24	1	2.54	14.55	32.01	63.95	40	0.13	0.6345	3.64
4	10.16	1	2.54	6.47	14.234	39.7	90	0.21	1.05	6.02
3	7.62	1	2.54	3.64	8.008	31.22	270	0.12	0.9382	5.38
2	5.08	1	2.54	1.62	3.564	25.15	saturates	0.03	0.19	1.09
4	10.16	2	5.08	12.93	28.446	59.1	100	0.13	0.6919	3.96
3	7.62	2	5.08	7.27	15.994	41.13	250	0.17	0.9262	5.31
2	5.08	2	5.08	3.233	7.1126	30	saturates	0.05	0.34	1.95
2	5.08	3	7.62	4.85	10.67	34.85	270	0.06	0.5207	2.98
2	5.08	4	10.16	6.47	14.234	39.7	270	0.07	0.595	3.41

- Notes:
1. Initial conditions: all three momentum wheels at rest, SimSat at rest, all euler angles zero
 2. Positive b₁ side - motors, momentum wheels, battery, 4 gyros
 3. Negative b₁ side - Autobox, xmit/receiver, counterweight
 4. Max allowable wheel speed = 270 rad/sec (2600 rpm)
 5. Simulation run for 10 seconds
 6. Max **continuous** torque curve applied to motor #2 for first 5 seconds, torque reversed to motor #2 for seconds 5 through 10 (motors #1 & #3 motionless)
 7. Effect of a wheel axle is ignored
 8. **36 volts** (simulated) applied to motor #2

- Motor2/Wheel2 – oriented parallel to the yaw axis, used to provide torque input primarily to the yaw axis.
- Motor3/Wheel3 – oriented parallel to the pitch axis, used to provide torque input primarily to the pitch axis.
- CW mass – counterweight mass necessary to balance *SIMSAT* in the simulation.
- Saturation – when a simulated momentum wheel exceeds the maximum speed capability of the SmartMotor in a 10 second maneuver. Wheels that are too small or light lack inertia storage capability and tend to saturate.
- Yaw Rate at 5 Seconds – the maximum instantaneous yaw rate; occurs at the $t = 5$ second point in the maneuver, measured in radians/second.
- Yaw Angle at 10 Seconds – the final *SIMSAT* yaw angle after a 10 second maneuver from rest (starting with zero yaw angle), measured in radians.
- 10 Second Average Slew Rate – the primary criterion used to compare momentum wheel designs, defined as the final *SIMSAT* yaw angle (in degrees) divided by 10 seconds.
- Since a wheel axle's inertia is small in relation to the entire wheel, all wheels were modeled without axles.

From Table C.2, it can be seen that aluminum designs, in general, give higher yaw performance than steel designs. Because of the distance of the momentum wheel from the *SIMSAT* origin, a dense object, such as a solid steel disk, creates more of a system inertia penalty than an object of lesser density. However, solid steel wheels are less likely to saturate than their aluminum counterparts. The higher density of steel gives it more inertia storage capability than aluminum. Since wheel inertia properties are dictated by mass and area, aluminum and steel designs with small radii and/or thicknesses also tended to saturate.

Figure C.6 shows a solid disk wheel (as well as the other wheel shapes that were analyzed).

MATLAB output graphs from a typical simulation (solid aluminum disk wheel with 6" radius and 1" thick) are shown in Figure C.7, Figure C.8 and Figure C.9.

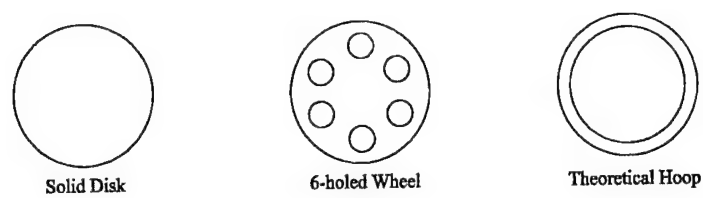


Figure C.6 Momentum Wheel Shapes

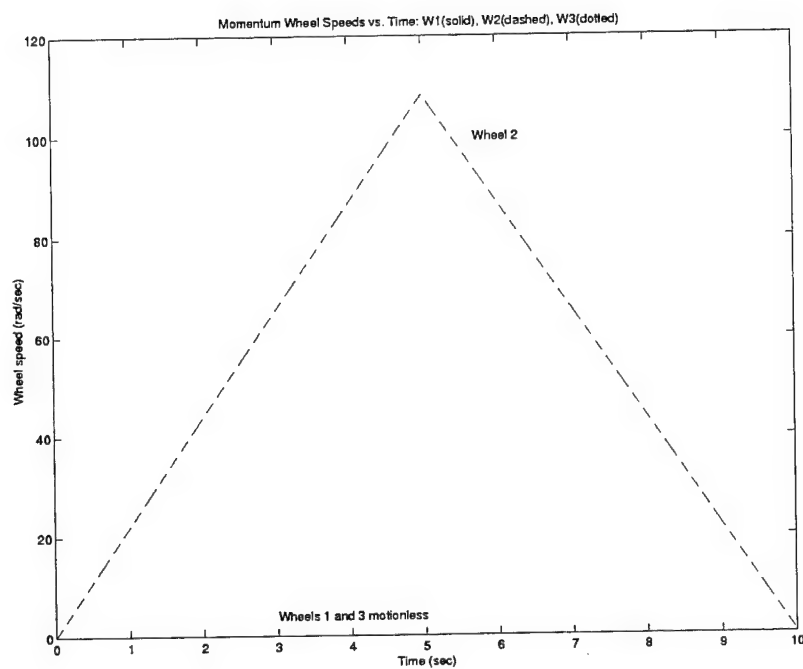


Figure C.7 Momentum Wheel Speeds

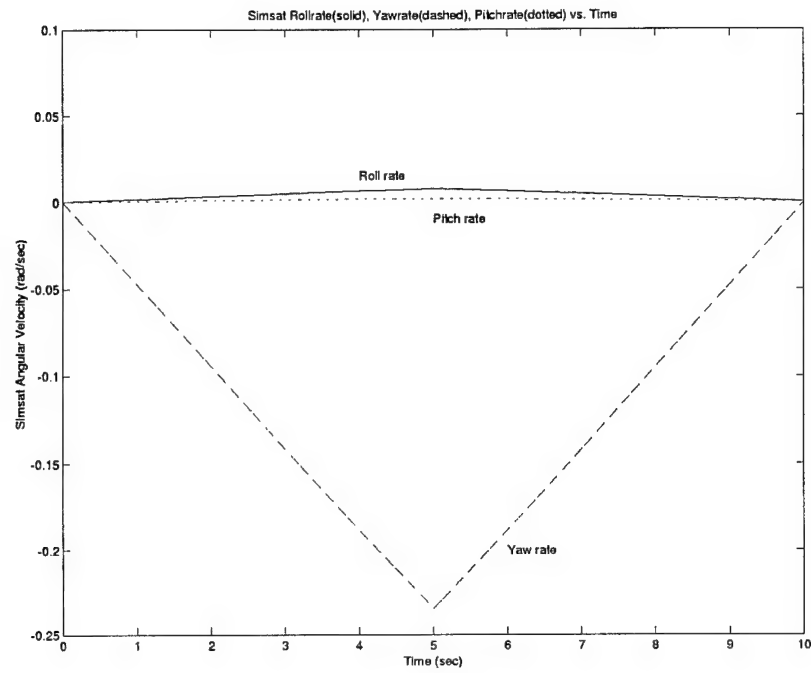


Figure C.8 *SIMSAT* Angular Velocities

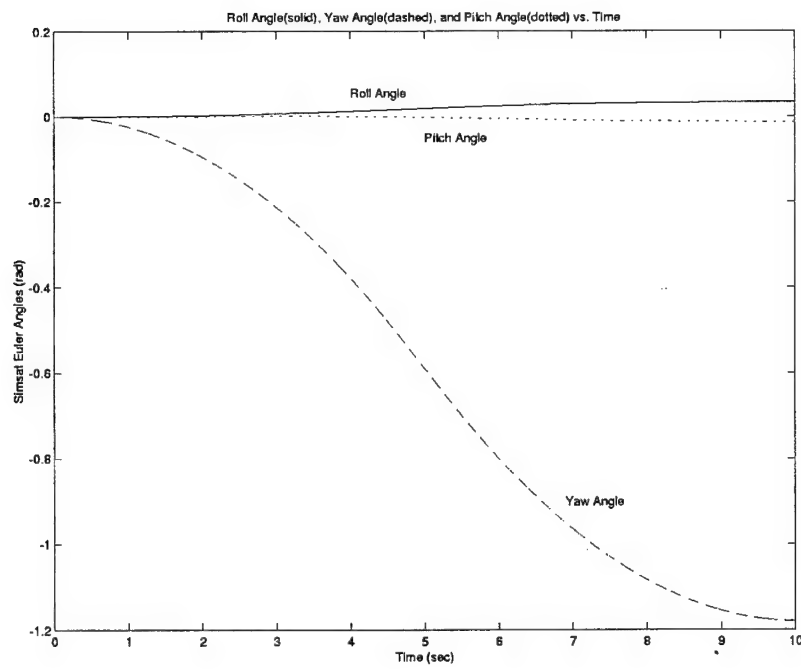


Figure C.9 *SIMSAT* Euler Angles

To simulate a “wheel-and-spoke” configuration, aluminum and steel disks with six holes were also examined (see Table C.3). Because mass was removed from the solid wheel face, the six-holed wheels performed better than their solid disk counterparts. With few exceptions, the aluminum designs outperformed the steel designs.

“Theoretical” hoop-shaped momentum wheels were also analyzed. Although a pure hoop without spokes is not physically feasible, the inertia properties of a hoop warranted study. As seen in Table C.4, hoop-shaped wheels, in general, had better yaw performance than solid disks or six-holed wheels. Since the moment of inertia of a wheel is dependent upon the square of its radius, locating most of a wheel’s mass near its circumference (rather than near its center) is beneficial.

After the attractive inertia properties of the hoop shape were identified, a more detailed analysis of aluminum vs. steel began. First, hoop width (width = outer radius - inner radius) and thickness were held constant, but the outer radius of the hoop was allowed to vary. The objective was to find the dimensions of an aluminum hoop that possessed the same moment of inertia as a steel hoop. From Table C.5, it can be seen that aluminum hoops outperformed steel hoops with the same inertia. However, the aluminum wheels were much larger than their steel counterparts. This is noteworthy because trying to integrate three large momentum wheels onto *SIMSAT* could present other difficulties (such as structural mounting).

Next, the outer radius, moment of inertia, and thickness of aluminum and steel hoops were held constant, but the steel hoop width was allowed to vary. Table C.6 summarizes this analysis. This table demonstrates that a steel hoop with a thin width outperforms an aluminum hoop of larger width. Designing an aluminum hoop with a thin width, however, is not a preferred solution because this wheel causes the motor to saturate in a 10 second maneuver. A saturated motor cannot provide any torque to *SIMSAT*.

C.1.5 Detailed Wheel Design. From the preceding analysis, it was evident that a wheel design imitating a hoop shape, possessing a large outer radius, and using a thin rim would maximize *SIMSAT* yaw performance. Before proceeding further,

Table C.3 Aluminum and Steel Wheels with Six Holes

Momentum Wheel Analysis (with all three wheels identical size)
for Wheel #2
Wheel with 6 holes

Aluminum (density = 2.8 g/cc)

Outer radius (inches)	Hoop width (inches)	Wheel thickness (inches)	Hole radius (inches)	Outer radius (cm)	Wheel thickness (cm)	Hole radius (cm)	Whl mass (kg)	Whl mass (lb)	Max wheel speed (rad/sec)	Yaw rate at 5 sec (rad/sec)	Yaw angle at 10 sec (rad)	Slew rate 10 sec avg (deg/sec)
5	1	0.75	1.25	12.7	1.905	3.175	1.6892	3.71624	265	0.25	1.5682	8.99
4.5	1	0.75	1.125	11.43	1.905	2.8575	1.3683	3.01026	270	0.17	1.3241	7.59
4	1	0.75	0.875	10.16	1.905	2.2225	1.2331	2.71282	270	0.12	0.9973	5.71
5	1	1	1.25	12.7	2.54	3.175	2.2523	4.95506	250	0.27	1.5805	9.06
4.5	1	1	1.125	11.43	2.54	2.8575	1.8244	4.01368	270	0.22	1.4578	8.35
4	1	1	0.875	10.16	2.54	2.2225	1.6442	3.61724	270	0.15	1.1701	6.70
5	1	1.25	1.25	12.7	3.175	3.175	2.8154	6.19388	220	0.3	1.5157	8.68
4.5	1	1.25	1.125	11.43	3.175	2.8575	2.2805	5.0171	260	0.25	1.4984	8.59
4	1	1.25	0.875	10.16	3.175	2.2225	2.0552	4.52144	270	0.17	1.2741	7.30

Steel (density = 7.85 g/cc)

Outer radius (inches)	Hoop width (inches)	Wheel thickness (inches)	Hole radius (inches)	Outer radius (cm)	Wheel thickness (cm)	Hole radius (cm)	Whl mass (kg)	Whl mass (lb)	Max wheel speed (rad/sec)	Yaw rate at 5 sec (rad/sec)	Yaw angle at 10 sec (rad)	Slew rate 10 sec avg (deg/sec)
5	1	0.75	1.25	12.7	1.905	3.175	4.7359	10.41898	140	0.24	1.246	7.14
4.5	1	0.75	1.125	11.43	1.905	2.8575	3.8361	8.43942	200	0.26	1.3523	7.75
4	1	0.75	0.875	10.16	1.905	2.2225	3.4572	7.60584	255	0.23	1.3318	7.63
5	1	1	1.25	12.7	2.54	3.175	6.3145	13.8919	105	0.22	1.0778	6.18
4.5	1	1	1.125	11.43	2.54	2.8575	5.1148	11.25256	155	0.23	1.197	6.86
4	1	1	0.875	10.16	2.54	2.2225	4.6096	10.14112	220	0.23	1.2312	7.05
5	1	1.25	1.25	12.7	3.175	3.175	7.8932	17.36504	85	0.18	0.9498	5.44
4.5	1	1.25	1.125	11.43	3.175	2.8575	6.3935	14.0657	125	0.22	1.0692	6.13
4	1	1.25	0.875	10.16	3.175	2.2225	5.762	12.6764	185	0.22	1.1189	6.41

- Notes:
1. Initial conditions: all three momentum wheels at rest, SimSat at rest, all euler angles zero
 2. Positive b₁ side - motors, momentum wheels, battery, 4 gyros
 3. Negative b₁ side - Autobox, xmit/receiver, counterweight
 4. Max allowable wheel speed = 270 rad/sec (2600 rpm)
 5. Simulation run for 10 seconds
 6. Max continuous torque curve applied to motor #2 for first 5 seconds, torque reversed to motor #2 for seconds 5 through 10 (motors #1 & #3 motionless)
 7. Effect of a wheel axle is ignored
 8. 36 volts (simulated) applied to motor #2

Table C.4 Theoretical Aluminum and Steel Hoop Wheels

Momentum Wheel Analysis (with all three wheels identical size)
for Wheel #2
Hoop Shape

Aluminum (density = 2.8 g/cc)

Outer radius (inches)	Inner radius (inches)	width (inches)	height (inches)	Outer radius (cm)	Inner radius (cm)	height (cm)	Wht mass (kg)	Wht mass (lb)	Max wheel speed (rad/sec)	Yaw rate at 5 sec (rad/sec)	Yaw angle at 10 sec (rad)	Slew rate 10 sec avg (deg/sec)
8	7	1	1	20.32	17.78	2.54	2.16	4.752	85	0.34	1.7016	9.75
6	5	1	1	15.24	12.7	2.54	1.59	3.498	200	0.35	1.8348	10.51
4	3	1	1	10.16	7.62	2.54	1.009	2.2198	270	0.14	1.1325	6.49
2	1	1	1	5.08	2.54	2.54	0.432	0.9504	saturates	0.01	0.1	0.57
8	7	1	2	20.32	17.78	5.08	4.32	9.504	40	0.25	1.2903	7.39
6	5	1	2	15.24	12.7	5.08	3.17	6.974	105	0.3	1.4883	8.53
4	3	1	2	10.16	7.62	5.08	2.02	4.444	265	0.23	1.4876	8.52
2	1	1	2	5.08	2.54	5.08	0.865	1.903	saturates	0.02	0.12	0.69
4	3	1	3	10.16	7.62	7.62	3.03	6.666	235	0.27	1.4534	8.33
2	1	1	3	5.08	2.54	7.62	1.3	2.86	saturates	0.04	0.19	1.09
2	1	1	4	5.08	2.54	10.16	1.73	3.806	saturates	0.04	0.25	1.43
8	6	2	1	20.32	15.24	2.54	4.04	8.888	50	0.26	1.3362	7.66
6	4	2	1	15.24	10.16	2.54	2.88	6.336	135	0.31	1.5419	8.83
4	2	2	1	10.16	5.08	2.54	1.73	3.806	270	0.17	1.2614	7.23
8	6	2	2	20.32	15.24	5.08	8.07	17.754	25	0.18	0.921	5.28
6	4	2	2	15.24	10.16	5.08	5.77	12.694	70	0.23	1.1296	6.47
4	2	2	2	10.16	5.08	5.08	3.46	7.612	245	0.24	1.3558	7.77
4	2	2	3	10.16	5.08	7.62	5.19	11.418	190	0.23	1.1789	6.75

Steel (density = 7.85 g/cc)

Outer radius (inches)	Inner radius (inches)	width (inches)	height (inches)	Outer radius (cm)	Inner radius (cm)	height (cm)	Wht mass (kg)	Wht mass (lb)	Max wheel speed (rad/sec)	Yaw rate at 5 sec (rad/sec)	Yaw angle at 10 sec (rad)	Slew rate 10 sec avg (deg/sec)
8	7	1	1	20.32	17.78	2.54	6.06	13.332	30	0.22	1.0845	6.21
6	5	1	1	15.24	12.7	2.54	4.45	9.79	75	0.26	1.2856	7.37
4	3	1	1	10.16	7.62	2.54	2.83	6.226	245	0.27	1.474	8.45
2	1	1	1	5.08	2.54	2.54	1.21	2.662	saturates	0.03	0.19	1.09
8	7	1	2	20.32	17.78	5.08	12.12	26.664	15	0.14	0.7029	4.03
6	5	1	2	15.24	12.7	5.08	8.89	19.558	40	0.17	0.8773	5.03
4	3	1	2	10.16	7.62	5.08	5.66	12.452	140	0.23	1.1394	6.53
2	1	1	2	5.08	2.54	5.08	2.43	5.346	saturates	0.05	0.34	1.95
4	3	1	3	10.16	7.62	7.62	8.49	18.678	95	0.18	0.9092	5.21
2	1	1	3	5.08	2.54	7.62	3.64	8.008	saturates	0.07	0.55	3.15
2	1	1	4	5.08	2.54	10.16	4.85	10.67	270	0.08	0.655	3.75
8	6	2	1	20.32	15.24	2.54	11.32	24.904	18	0.15	0.7404	4.24
6	4	2	1	15.24	10.16	2.54	8.08	17.776	50	0.18	0.9326	5.34
4	2	2	1	10.16	5.08	2.54	4.85	10.67	200	0.23	1.2146	6.96
8	6	2	2	20.32	15.24	5.08	22.63	49.786	10	0.09	0.4419	2.53
6	4	2	2	15.24	10.16	5.08	16.17	35.574	25	0.12	0.5841	3.35
4	2	2	2	10.16	5.08	5.08	9.7	21.34	105	0.17	0.837	4.80
4	2	2	3	10.16	5.08	7.62	14.55	32.01	70	0.13	0.6369	3.65

- Notes:
1. Initial conditions: all three momentum wheels at rest, SimSat at rest, all euler angles zero
 2. Positive b, side - motors, momentum wheels, battery, 4 gyros
 3. Negative b, side - Autobox, xmit/receiver, counterweight
 4. Max allowable wheel speed = 270 rad/sec (2600 rpm)
 5. Simulation run for 10 seconds
 6. Max continuous torque curve applied to motor #2 for first 5 seconds, torque reversed to motor #2 for seconds 5 through 10 (motors #1 & #3 motionless)
 7. Effect of a wheel axle is ignored
 8. 36 volts (simulated) applied to motor #2

Table C.5 Aluminum vs. Steel Hoops-Inertia Held Constant

Momentum Wheel Analysis (with all three wheels identical size)
for Wheel #2
Hoop Shape-HOLDING INERTIA CONSTANT

Aluminum (density = 2.8 g/cc)

Outer radius (inches)	Inner radius (inches)	Hoop width (inches)	Hoop thickness (inches)	Outer radius (cm)	Inner radius (cm)	Hoop thickness (cm)	I(2,2) term (N-m-sec ²)	Wht mass (kg)	Max wheel speed (rad/sec)	Yaw rate at 5 sec (rad/sec)	Yaw angle at 10 sec (rad)	Slew rate 10 sec avg (deg/sec)
6	5	1	1	15.24	12.7	2.54	0.031	1.59	200	0.35	1.8348	10.51
4	3	1	1	10.16	7.62	2.54	0.008	1.009	270	0.14	1.1325	6.49
4	3	1	2	10.16	7.62	5.08	0.016	2.02	265	0.23	1.4876	8.52

Steel (density = 7.85 g/cc)

Outer radius (inches)	Inner radius (inches)	Hoop width (inches)	Hoop thickness (inches)	Outer radius (cm)	Inner radius (cm)	Hoop thickness (cm)	I(2,2) term (N-m-sec ²)	Wht mass (kg)	Max wheel speed (rad/sec)	Yaw rate at 5 sec (rad/sec)	Yaw angle at 10 sec (rad)	Slew rate 10 sec avg (deg/sec)
4.384488	3.384488	1	1	11.1366	8.5966	2.54	0.031	3.1397	200	0.29	1.5009	8.60
2.952008	1.952008	1	1	7.4981	4.9581	2.54	0.008	1.9619	270	0.12	1.0056	5.76
2.952008	1.952008	1	2	7.4981	4.9581	5.08	0.016	3.9637	265	0.18	1.1548	6.62

- Notes:
1. Initial conditions: all three momentum wheels at rest, SimSat at rest, all euler angles zero
 2. Positive b, side - motors, momentum wheels, battery, 4 gyros
 3. Negative b, side - Autobox, xmit/receiver, counterweight
 4. Max allowable wheel speed = 270 rad/sec (2600 rpm)
 5. Simulation run for 10 seconds
 6. Max continuous torque curve applied to motor #2 for first 5 seconds, torque reversed to motor #2 for seconds 5 through 10 (motors #1 & #3 motionless)
 7. Effect of a wheel axle is ignored
 8. 36 volts (simulated) applied to motor #2

Table C.6 Aluminum vs. Steel Hoops-Width Variation of Steel Hoop

Momentum Wheel Analysis (with all three wheels identical size)
for Wheel #2
Hoop Shape-HOLDING INERTIA AND OUTER RADIUS CONSTANT

Aluminum (density = 2.8 g/cc)

Outer radius (inches)	Inner radius (inches)	Hoop width (inches)	Hoop thickness (inches)	Outer radius (cm)	Inner radius (cm)	Hoop thickness (cm)	I(2,2) term (N-m-sec ²)	Wht mass (kg)	Max wheel speed (rad/sec)	Yaw rate at 5 sec (rad/sec)	Yaw angle at 10 sec (rad)	Slew rate 10 sec avg (deg/sec)
6	5	1	1	15.24	12.7	2.54	0.031	1.59	200	0.35	1.8348	10.51
4	3	1	1	10.16	7.62	2.54	0.008	1.009	270	0.14	1.1325	6.49
4	3	1	2	10.16	7.62	5.08	0.016	2.02	265	0.23	1.4876	8.52

Steel (density = 7.85 g/cc)

Outer radius (inches)	Inner radius (inches)	Hoop width (inches)	Hoop thickness (inches)	Outer radius (cm)	Inner radius (cm)	Hoop thickness (cm)	I(2,2) term (N-m-sec ²)	Wht mass (kg)	Max wheel speed (rad/sec)	Yaw rate at 5 sec (rad/sec)	Yaw angle at 10 sec (rad)	Slew rate 10 sec avg (deg/sec)
6	5.701417	0.298583	1	15.24	14.4816	2.54	0.031	1.4119	200	0.41	2.0609	11.81
4	3.730051	0.269949	1	10.16	9.47433	2.54	0.008	0.8433	270	0.16	1.2864	7.37
4	3.730051	0.269949	2	10.16	9.47433	5.08	0.016	1.6866	265	0.27	1.6645	9.54

- Notes:
1. Initial conditions: all three momentum wheels at rest, SimSat at rest, all euler angles zero
 2. Positive b, side - motors, momentum wheels, battery, 4 gyros
 3. Negative b, side - Autobox, xmit/receiver, counterweight
 4. Max allowable wheel speed = 270 rad/sec (2600 rpm)
 5. Simulation run for 10 seconds
 6. Max continuous torque curve applied to motor #2 for first 5 seconds, torque reversed to motor #2 for seconds 5 through 10 (motors #1 & #3 motionless)
 7. Effect of a wheel axle is ignored
 8. 36 volts (simulated) applied to motor #2

a quick "back-of-the-envelope" wheel structural analysis was performed. A wheel with excellent inertia properties could still break apart when spinning at high speeds.

Considering only hoop stress, the bursting velocity of a momentum wheel is approximated by [40:338]:

$$V = \sqrt{10s}$$

where

V = bursting velocity of outside circumference of rim in feet per second

s = tensile strength of the rim material in pounds per square inch

If the wheel rim is conservatively assumed to be ASTM-A36 carbon steel (which has one of the lowest steel tensile strengths), $s = 36,000$ psi and $V = 600$ ft/sec = 15,279 rpm. This burst velocity is well above the maximum SmartMotor speed rating of 3400 rpm (at 48V).

Another general formula which takes into account material properties, construction, rim thickness, and joint efficiencies is given by [40:341]:

$$N = (C \cdot A \cdot M \cdot E \cdot K) / D$$

where

N = maximum rated operating speed in revolutions per minute

$C = 1.0$ for wheels driven by a constant speed electric motor

$= 0.90$ for wheels driven by variable speed motors

$A = 0.90$ for 4 arms or spokes

$= 1.00$ for 6 arms of spokes

$= 1.08$ for 8 arms or spokes

$= 1.50$ for disc type

$M = 1.00$ for cast iron of 20,000 psi tensile strength, or unknown

$= 1.12$ for cast iron of 25,000 psi tensile strength

$= 1.22$ for cast iron of 30,000 psi tensile strength

$= 1.32$ for cast iron of 35,000 psi tensile strength

- = 2.20 for nodular iron of 60,000 psi tensile strength
- = 2.45 for cast steel of 60,000 psi tensile strength
- = 2.75 for plate or forged steel of 60,000 psi tensile strength

E = joint efficiency

- = 1.0 for solid rim
- = 0.85 for link or prison joints
- = 0.75 for split rim-bolted joint at arms
- = 0.70 for split rim-bolted joint between arms

K = 1355 for rim thickness equal to 1% of outside diameter

- = 1650 for rim thickness equal to 2% of outside diameter
- = 1840 for rim thickness equal to 3% of outside diameter
- = 1960 for rim thickness equal to 4% of outside diameter
- = 2040 for rim thickness equal to 5% of outside diameter
- = 2140 for rim thickness equal to 7% of outside diameter
- = 2225 for rim thickness equal to 10% of outside diameter
- = 2310 for rim thickness equal to 15% of outside diameter
- = 2340 for rim thickness equal to 20% of outside diameter

D = outside diameter of rim in feet

Assuming a momentum wheel with a continuous disk for “spokes”, cast steel solid rim, outside diameter of 9”, and a rim thickness of 1”:

$$N = (.90 * 1.5 * 2.45 * 1.0 * 2225)/0.75$$

$$N = 9812 \text{ rpm (safely exceeds the 3400 rpm capability of the SmartMotor)}$$

After completing this “rough” structural analysis, detailed design of the wheels continued. To determine the wheel dimensions that maximized yaw performance, a MATLAB constrained optimization approach was used:

Objective (cost) function was: Maximize the *SIMSAT* yaw angle at $t = 10$ seconds. (By default, this also maximizes the *SIMSAT* 10-second-average slew rate). This yaw angle was calculated from a MATLAB simulation of the equations of motion and the SmartMotor torque curves described earlier.

The constraints were:

1) Steel hoop with a width $\geq 3/8''$ (width = outer radius - inner radius)

-This constraint was used to prevent the optimization routine from returning an infinitely small hoop width (the smaller the hoop width, the better the yaw performance). This width was intuitively chosen so there was enough metal available for strength and "spoke" attachment purposes.

2) Solid aluminum disk for "spokes", aluminum disk is $\geq 1/4''$ thick.

Note: Outer radius of the aluminum disk is equal to the inner radius of the hoop. Also, the effect of a wheel axle hole was ignored for the optimization routine.

-A solid aluminum disk arrangement was chosen because it would be easier to fabricate and be stronger than spokes. The $1/4''$ disk thickness would allow enough metal for attachment of an axle but would be thin enough to still approximate a theoretical hoop. Although a theoretical hoop has massless spokes, a thin aluminum disk would be a good compromise. Aircraft grade aluminum has excellent strength and only 35% the density of steel.

3) Thickness (depth) of the steel hoop $\geq 0.2''$

-This constraint was imposed to prevent the optimization routine from returning a hoop that was too thin to fabricate.

4) Outer radius of the steel hoop $\leq 6''$

-This constraint was imposed to prevent the optimization routine from returning a wheel too large to reasonably integrate onto *SIMSAT*. However, this constraint was removed for certain computer runs.

The design variables were:

-Outer radius of the steel hoop

-Thickness (depth) of the steel hoop

After mathematically formulating the constrained optimization problem, the MATLAB code was constructed. The MATLAB *SIMSAT* motion simulation was implemented within a MATLAB optimization driver program. The first computer run returned a wheel design with a hoop outer radius of 6" (not surprisingly, on the edge of the constraint boundary). The computer program was then run with a 4.5" and a 4" constraint on the outer hoop radius. The program was also run for the 36V case with no constraint placed on the hoop outer radius. Finally, the process was repeated using an aluminum disk and an aluminum hoop with the same constraints. The results of the optimization for the steel hoop and aluminum hoop wheels are summarized in Table C.7. Results in this table are shown for motor voltages of 36V and 24V.

Table C.7 Steel and Aluminum Wheel Optimization at 36V and 24V

Optimized Disk/Hoop Shape at 36V												
Aluminum Hoop												
Outer radius (cm)	Hoop width (cm)	Hoop thickness (cm)	Disk thickness (cm)	Outer radius (inches)	Hoop width (inches)	Hoop thickness (inches)	Disk thickness (inches)	Wht mass (kg)	Max wheel speed (rad/sec)	Yaw rate at 5 sec (rad/sec)	Yaw angle at 10 sec (rad)	Slew rate 10 sec avg (deg/sec)
*15.8729	0.9525	0.508	0.635	6.249	0.375	0.2	0.25	1.6695	238	0.36	1.8803	10.77
11.43	0.9525	3.3325	0.635	4.5	0.375	1.312008	0.25	1.9531	258	0.29	1.6904	9.69
10.16	0.9525	5.0589	0.635	4	0.375	1.991693	0.25	2.2184	262	0.27	1.5815	9.06
Steel Hoop												
Outer radius (cm)	Hoop width (cm)	Hoop thickness (cm)	Disk thickness (cm)	Outer radius (inches)	Hoop width (inches)	Hoop thickness (inches)	Disk thickness (inches)	Wht mass (kg)	Max wheel speed (rad/sec)	Yaw rate at 5 sec (rad/sec)	Yaw angle at 10 sec (rad)	Slew rate 10 sec avg (deg/sec)
*14.2625	0.9525	0.508	0.635	5.615	0.375	0.2	0.25	1.7943	237	0.35	1.8334	10.50
11.43	0.9525	1.1893	0.635	4.5	0.375	0.468	0.25	1.9538	258	0.29	1.6906	9.69
10.16	0.9525	1.8065	0.635	4	0.375	0.711	0.25	2.2203	262	0.27	1.582	9.06
Optimized Disk/Hoop Shape at 24V												
Aluminum Hoop												
Outer radius (cm)	Hoop width (cm)	Hoop thickness (cm)	Disk thickness (cm)	Outer radius (inches)	Hoop width (inches)	Hoop thickness (inches)	Disk thickness (inches)	Wht mass (kg)	Max wheel speed (rad/sec)	Yaw rate at 5 sec (rad/sec)	Yaw angle at 10 sec (rad)	Slew rate 10 sec avg (deg/sec)
15.24	0.9525	0.6993	0.635	6	0.375	0.275315	0.25	1.6433	160	0.23	1.2246	7.02
Steel Hoop												
Outer radius (cm)	Hoop width (cm)	Hoop thickness (cm)	Disk thickness (cm)	Outer radius (inches)	Hoop width (inches)	Hoop thickness (inches)	Disk thickness (inches)	Wht mass (kg)	Max wheel speed (rad/sec)	Yaw rate at 5 sec (rad/sec)	Yaw angle at 10 sec (rad)	Slew rate 10 sec avg (deg/sec)
11.43	0.9525	1.1889	0.635	4.5	0.375	0.468	0.25	1.9534	170	0.19	1.1139	6.38
10.16	0.9525	1.7925	0.635	4	0.375	0.706	0.25	2.2076	172	0.18	1.0438	5.98

- Notes:
- * Unconstrained outer radius
 - 1. Initial conditions: all three momentum wheels at rest, SimSat at rest, all euler angles zero
 - 2. Positive b1 side - motors, momentum wheels, battery, 4 gyros
 - 3. Negative b1 side - Autobox, xmit/receiver, counterweight
 - 4. Max allowable wheel speed = 270 rad/sec (2600 rpm)
 - 5. Simulation run for 10 seconds
 - 6. Max continuous torque curve applied to motor #2 for first 5 seconds, torque reversed to motor #2 for seconds 5 through 10 (motors #1 & #3 motionless)
 - 7. Effect of a wheel axle is ignored
 - 8. 36 or 24 volts (simulated) applied to motor #2

For smaller diameter wheels (8" and 9" diameter), the aluminum and steel hoops have the same performance, but the aluminum hoops are much thicker. If no constraint is placed on the outer radius, a 12.5" diameter aluminum hoop wheel at 36V yields the best performance.

C.1.6 Final Momentum Wheel Design Alternatives. With yaw performance numbers in hand, six momentum wheel design alternatives were carried forward to be evaluated at the overall system level. Three wheel alternatives for a 24V bus configuration would be evaluated, and three wheel alternatives for a 36V bus would be evaluated. Even though an infinite number of wheel alternatives existed, limiting the number of alternatives to six was considered to be tractable in a system-level evaluation matrix. Table C.8 shows the three wheel alternatives for a 36V bus and the three wheel alternatives for a 24V bus. Figure C.10 also illustrates these alternatives.

Table C.8 Final Wheel Alternatives for 36V and 24V Bus

Momentum Wheel Alternatives for 36 Volt Bus

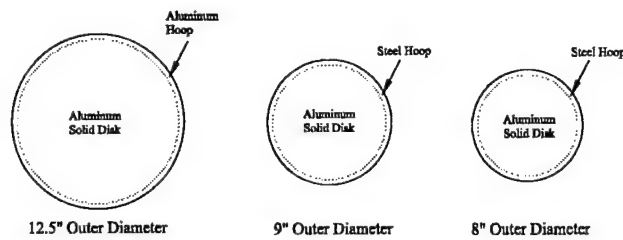
Aluminum Hoop													
Outer radius (cm)	Hoop width (cm)	Hoop thickness (cm)	Disk thickness (cm)	Outer radius (inches)	Hoop width (inches)	Hoop thickness (inches)	Disk thickness (inches)	Wht mass (kg)	Max wheel speed (rad/sec)	Yaw rate at 5 sec (rad/sec)	Yaw angle at 10 sec (rad)	Slew rate 10 sec avg (deg/sec)	
15.8729	0.9525	0.508	0.635	6.249	0.375	0.2	0.25	1.6695	238	0.36	1.8803	10.77	

Steel Hoop													
Outer radius (cm)	Hoop width (cm)	Hoop thickness (cm)	Disk thickness (cm)	Outer radius (inches)	Hoop width (inches)	Hoop thickness (inches)	Disk thickness (inches)	Wht mass (kg)	Max wheel speed (rad/sec)	Yaw rate at 5 sec (rad/sec)	Yaw angle at 10 sec (rad)	Slew rate 10 sec avg (deg/sec)	
11.43	0.9525	1.1893	0.635	4.5	0.375	0.468	0.25	1.9538	258	0.29	1.6906	9.69	
10.16	0.9525	1.8065	0.635	4	0.375	0.711	0.25	2.2203	262	0.27	1.582	9.06	

Momentum Wheel Alternatives for 24 Volt Bus

Aluminum Hoop												
Outer radius (cm)	Hoop width (cm)	Hoop thickness (cm)	Disk thickness (cm)	Outer radius (inches)	Hoop width (inches)	Hoop thickness (inches)	Disk thickness (inches)	Wht mass (kg)	Max wheel speed (rad/sec)	Yaw rate at 5 sec (rad/sec)	Yaw angle at 10 sec (rad)	Slew rate 10 sec avg (deg/sec)
15.24	0.9525	0.6993	0.635	6	0.375	0.275315	0.25	1.6433	160	0.23	1.2246	7.02

Steel Hoop												
Outer radius (cm)	Hoop width (cm)	Hoop thickness (cm)	Disk thickness (cm)	Outer radius (inches)	Hoop width (inches)	Hoop thickness (inches)	Disk thickness (inches)	Wht mass (kg)	Max wheel speed (rad/sec)	Yaw rate at 5 sec (rad/sec)	Yaw angle at 10 sec (rad)	Slew rate 10 sec avg (deg/sec)
11.43	0.9525	1.1889	0.635	4.5	0.375	0.468	0.25	1.9534	170	0.19	1.1139	6.38
10.16	0.9525	1.7925	0.635	4	0.375	0.706	0.25	2.2076	172	0.18	1.0438	5.98



Notes:
 -All hoop widths are 3/8" (width is measured in plane of page)
 -All inner aluminum disks are 1/4" thick, disks are centered with reference to hoop thickness
 -See Table for hoop thicknesses (varies for 24V or 36V bus voltage)
 -Thickness is measured into/out of page

Figure C.10 Sizes of Final Wheel Alternatives

Reasons for choosing the three different outer diameters were as follows:

1) 12.5" outer diameter (for 36V case, 12" outer diameter for the 24V case) aluminum hoop wheel with inner aluminum disk

-This was the best yaw performance alternative from a wheel subsystem perspective. However, the placement of three large-sized momentum wheels on *SIMSAT* could create system-level integration challenges.

2) 9" outer diameter steel hoop wheel with inner aluminum disk

-A medium yaw performance wheel that had a medium size. A steel hoop was chosen because it offers the same performance and weight as a 9" diameter aluminum hoop, but a steel hoop is thinner. A thinner hoop allows a tighter packaging arrangement for three wheels.

3) 8" outer diameter steel hoop wheel with inner aluminum disk-

-A low yaw performance wheel that had a small size. Its size may allow easier integration onboard *SIMSAT*.

These wheel alternatives effectively captured performance (low, medium, and high) vs. size (large, medium, and small). System-level evaluation of the momentum wheel alternatives could now begin.

Appendix D. Gyro Range and Accuracy Analysis

D.1 Overview

This appendix presents the methodology and data used to specify the Humphrey CF75 rate gyro range required for the *SIMSAT* application. Determination of gyro accuracy is included as part of this analysis, as well. The first part of the discussion explains how estimates for maximum roll, pitch, and yaw rates were determined. The second section shows our analysis. The last section covers what choices were made.

D.2 Rate Determination

The following Mathcad 7 document was used in determining the estimated slew rates for *SIMSAT* with thrusters. At this point in the design process, it was desirable to select the gyro ranges to account for the possibility of thrusters being added to the baseline design.

Thruster slew rate calculations:

For our system, we are going to use two tri-axial thruster systems on either wing of Simsat. Here is what we know about the thrusters and the two air tanks we have chosen:

$$F := 25.35 \text{ N}$$

$$\Delta t_{\min} := .005 \text{ s}$$

$$m_{4x} := .14 \text{ kg}$$

$$m_{c10} := .12 \text{ kg}$$

Using SMAD and Chobotov, the best equation for determining slew rate based on the thrust of a system is:

$$\dot{\theta}(F, L, \Delta t, I) := \frac{(F \cdot L \cdot \Delta t)}{I}$$

F ~ Thrust (in N)

L ~ Moment arm for thruster (in m)

Dt ~ Impulse duration (in sec)

I ~ Moment of Inertia (in kg·m²)

L := 1 m for pitch and yaw axes. This is an estimate at the moment (no pun intended).

L_{roll} := .05 m due to the Tri-axial thruster, we will pay a penalty for the roll qdot.

For the moments of inertia, our latest estimates are (from using our inertia4.m):

$$I_{\text{roll}} := 4.5 \text{ kg} \cdot \text{m}^2$$

$$I_{\text{pitch}} := 17.2 \text{ kg} \cdot \text{m}^2$$

$$I_{\text{yaw}} := 15.8 \text{ kg} \cdot \text{m}^2$$

To find Dt , we first need to solve for the mass flow rate, \dot{m} . We used a generic I_{sp} value from SMAD of 50s for cold gas jet thrusters. SMAD had a vacuum I_{sp} range of 50s to 75s. We are attempting to be conservative with 50s since we are not operating in a vacuum.

$$I_{sp} := 50 \text{ s} \quad \dot{m} := \frac{F}{I_{sp} \cdot g}$$

$$\dot{m} = 0.052 \frac{\text{kg}}{\text{s}}$$

$$\Delta t_{4x} := \frac{m_{4x}}{\dot{m}} \quad \Delta t_{c10} := \frac{m_{c10}}{\dot{m}}$$

$$\Delta t_{4x} = 2.708 \text{ s} \quad \Delta t_{c10} = 2.321 \text{ s}$$

These values represent a single burn with durations of 2.71 seconds and 2.321 seconds. A smarter way would be using x amount of shorter pulses instead of one big pulse. However, for our initial estimates for max angular rate, it will work.

So, for a max angular velocity due to a single burn (pure spinner), we get:

$$\text{Roll} \quad \dot{\theta}(F, L_{\text{roll}}, \Delta t_{4x}, I_{\text{roll}}) = 43.702 \frac{\text{deg}}{\text{s}}$$

$$\dot{\theta}(F, L_{\text{roll}}, \Delta t_{c10}, I_{\text{roll}}) = 37.459 \frac{\text{deg}}{\text{s}}$$

We are paying a severe penalty for having such a small moment arm for the roll axis. We may need to consider using a separate thruster for the roll axis mounted further from the roll axis.

$$\text{Pitch} \quad \dot{\theta}(F, L, \Delta t_{4x}, I_{\text{pitch}}) = 228.672 \frac{\text{deg}}{\text{s}}$$

$$\dot{\theta}(F, L, \Delta t_{c10}, I_{\text{pitch}}) = 196.005 \frac{\text{deg}}{\text{s}}$$

$$\text{Yaw} \quad \dot{\theta}(F, L, \Delta t_{4x}, I_{\text{yaw}}) = 248.934 \frac{\text{deg}}{\text{s}}$$

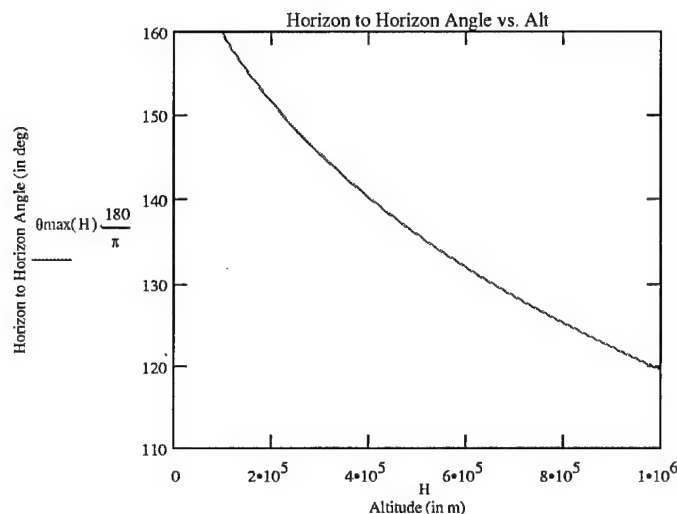
$$\dot{\theta}(F, L, \Delta t_{c10}, I_{\text{yaw}}) = 213.372 \frac{\text{deg}}{\text{s}}$$

As you can see from this Mathcad document and the Excel spreadsheet, we will need to trade the value of a higher slew rate versus the value of position accuracy using the VSD. Nudge proposed the idea of using the Horizon gyros for the educational experiments (pure spin, dual spin) and using the Humphrey gyro for the three axis experiments. This would allow you to sense the high rates (up to 720 deg/sec) for the spin experiments while not being concerned about the position accuracy.

Here is a quick estimate for your maneuver in a certain amount of time. Let's begin with a disclaimer stating this method assumes a fixed amount of thrust for any duration (not gonna happen). I supposed we had a LEO satellite at given altitude (below 1000km). The maximum angle slew from horizon to horizon with respect to the earth is:

$$r := 6378 \text{ km} \quad H := 100 \text{ km}, 120 \text{ km}, 1000 \text{ km}$$

$$\theta_{\max}(H) := 2 \cdot \arcsin\left(\frac{r}{r+H}\right) \quad \theta_{\max}(100 \text{ km}) = 159.839 \cdot \text{deg}$$



$$\Delta t := .94 \text{ s}$$

$$(2 \cdot \dot{\theta}(F, L, \Delta t, I_{\text{yaw}}) \cdot \Delta t) = 162.454 \cdot \text{deg}$$

$$\dot{\theta}(F, L, \Delta t, I_{\text{yaw}}) = 86.411 \frac{\text{deg}}{\text{s}}$$

So according to our numbers, if we lived in a perfect world, we could slew our satellite 162 degrees in 1.88 seconds. This would give us a rate of 86.411 deg/s. We can scale this back and say we would need an 80 deg/s slew rate sensing capability for thruster assist maneuvers. Using the Excel spreadsheet, this gives us the following accuracies:

$$\delta\text{HalfRange} := 0.8 \frac{\text{deg}}{\text{s}}$$

$$\delta\text{HalfToFullRange} := 3.2 \frac{\text{deg}}{\text{s}}$$

I am assuming the yaw axis is the only axis of interest. Otherwise, we would want to use momentum wheels for a three-axis situation.

D.3 Range and Accuracy Analysis

To select the best gyro for the *SIMSAT* design, a comparison of rate ranges was performed using utility analysis. The two measurables chosen were sensing range and accuracy to discriminate between alternatives. For each axis, utility scores were calculated for both range and accuracy for the different choices. Then, using the weighting factors within the system level VSD, a final utility score was calculated. For Tables D.1 and D.2, it is necessary to describe each column and its formula (if applicable).

Range - Sensing Range of the Gyro in a given axis (deg/s)

Accuracy - Sensing Accuracy of the gyro in a given axis (deg/s)

Range Utility - Utility based on minimum range requirements of a given axis and the maximum capability of 200 deg/s (unitless)

Formula: $0.006429 * (Range) - 0.2858$

Accuracy Utility - Utility based on 0.0 as a maximum accuracy and 4.4 as a minimum accuracy

Formula: $-0.204545 * (Accuracy) + 1$

RPM - Revolutions Per Minute (in RPMs)

Final Utility - Utility composed of the range and the accuracy with respect to the VSD measurable weighting

Formula: $0.5 * 0.4 * 0.4 * (0.4 * Range) * (0.2 * Accuracy)$

Utility - Utility composed of the range and the accuracy without the measurable weighting

Formula: $(0.4 * Range) * (0.2 * Accuracy)$

Roll Axis (Maximum Rate without thrusters is 57.3 deg)

Range: 60-200 deg/s is acceptable. Anything below 60 deg/s will not meet the max rate and will score a zero.

Accuracy: 1.2 to 4.4 deg/s using the range above.

From 60 deg/s to 110 deg/s range, the gyro is operating in the half-to-full range mode. However, from 120 deg/s to 200 deg/s, the gyros are always running in the half range mode. Therefore, the accuracy of the gyro improves from 4.4 deg/s to 1.2 deg/s.

Table D.1 Roll Range Utility

Range	Accuracy	Range Utility	Accuracy Utility	RPM	Final Utility	Utility
20	0.8	0.000	0.000	3.33	0.0000	0.0000
30	1.2	0.000	0.000	5.00	0.0000	0.0000
40	1.6	0.000	0.000	6.67	0.0000	0.0000
50	2.0	0.000	0.000	8.33	0.0000	0.0000
60	2.4	0.100	0.509	10.00	0.0003	0.0041
70	2.8	0.164	0.427	11.67	0.0004	0.0056
80	3.2	0.229	0.345	13.33	0.0005	0.0063
90	3.6	0.293	0.264	15.00	0.0005	0.0062
100	4.0	0.357	0.182	16.66	0.0004	0.0052
110	4.4	0.421	0.100	18.33	0.0003	0.0034
120	1.2	0.486	0.755	20.00	0.0023	0.0293
130	1.3	0.550	0.734	21.66	0.0026	0.0323
140	1.4	0.614	0.714	23.33	0.0028	0.0351
150	1.5	0.679	0.693	25.00	0.0030	0.0376
160	1.6	0.743	0.673	26.66	0.0032	0.0400
170	1.7	0.807	0.652	28.33	0.0034	0.0421
180	1.8	0.871	0.632	30.00	0.0035	0.0440
190	1.9	0.936	0.611	31.66	0.0037	0.0458
200	2.0	1.000	0.591	33.33	0.0038	0.0473

Pitch/Yaw Axis (Maximum Rate with thrusters is around 80 deg/s)

Range: 80-200 deg/s is acceptable. Anything below 80 deg/s will not meet the max rate and score a zero. Anything above 160 deg/s will score a 1.

Accuracy: 1.6-6.0 deg/s using the ranges above.

From 80 deg/s to 150 deg/s range, the gyro is operating in the half-to-full range mode. However, from 160 deg/s to 200 deg/s, the gyros are always running in the half range mode. Therefore, the accuracy of the gyro improves from 6.0 deg/s to 1.6 deg/s.

Table D.2 Pitch/Yaw Range Utility

Range	Accuracy	Range Utility	Accuracy Utility	RPM	Final Utility	Utility
20	0.8	0.000	0.000	3.33	0.0000	0.0000
30	1.2	0.000	0.000	5.00	0.0000	0.0000
40	1.6	0.000	0.000	6.67	0.0000	0.0000
50	2.0	0.000	0.000	8.33	0.0000	0.0000
60	2.4	0.000	0.000	10.00	0.0000	0.0000
70	2.8	0.000	0.000	11.67	0.0000	0.0000
80	3.2	0.100	0.520	13.33	0.0003	0.0042
90	3.6	0.213	0.460	15.00	0.0006	0.0078
100	4.0	0.325	0.400	16.66	0.0008	0.0104
110	4.4	0.438	0.340	18.33	0.0010	0.0119
120	4.8	0.550	0.280	20.00	0.0010	0.0123
130	5.2	0.663	0.220	21.66	0.0009	0.0117
140	5.6	0.775	0.160	23.33	0.0008	0.0099
150	6.0	0.888	0.100	25.00	0.0006	0.0071
160	1.6	1.000	0.760	26.66	0.0049	0.0608
170	1.7	1.000	0.745	28.33	0.0048	0.0596
180	1.8	1.000	0.730	30.00	0.0047	0.0584
190	1.9	1.000	0.715	31.66	0.0046	0.0572
200	2.0	1.000	0.700	33.33	0.0045	0.0560

D.4 Design Decisions

Using the utility figures, the best choice for each axis was a 200 deg/s roll rate range and a 160 deg/s pitch/yaw rate range. However, this utility analysis was strongly based upon the range being twice as important as accuracy within the VSD. However, after reviewing the figures with the chief decision maker, the decision was made to place greater importance on the accuracy of the system. Therefore, the chief decision making authority requested a roll rate range of 120 deg/s and pitch/yaw rate ranges of ± 40 deg/s.

Appendix E. Gyro Calibration Curves

E.1 Overview

This section contains all the manufacturer's information on the Humphrey CF75 Gyro. Regression analysis using Excel was performed to create a best-fit curve. The formulas developed in this section were used to convert incoming gyro signals to rate and acceleration inputs within the SIMULINK code.

E.2 Pitch Axis Regression

Best Fit Curve Formula: $PitchRate = 16.01418821 * OutputVoltage - 40.13635991$

Table E.1 Pitch Axis Gyro Regression Analysis

Output Voltage	Truth	Pitch Rate	Delta
0.006	-40	-40.04027478	0.040274781
0.008	-40	-40.0082464	0.008246404
0.508	-32	-32.0011523	0.001152299
0.510	-32	-31.96912392	-0.030876077
1.010	-24	-23.96202982	-0.037970182
1.012	-24	-23.93000144	-0.069998559
1.504	-16	-16.05102084	0.051020842
1.511	-16	-15.93892152	-0.061078475
2.006	-8	-8.011898361	0.011898361
2.009	-8	-7.963855796	-0.036144204
2.505	0	-0.020818444	0.020818444
2.507	0	0.011209932	-0.011209932
3.001	8	7.922218908	0.077781092
3.005	8	7.986275661	0.013724339
3.506	16	16.00938395	-0.009383954
3.509	16	16.05742652	-0.057426519
4.009	24	24.06452062	-0.064520624
4.012	24	24.11256319	-0.112563189
4.506	32	32.02357216	-0.023572164
4.509	32	32.07161473	-0.071614729
5.014	40	40.15877977	-0.158779775
5.016	40	40.19080815	-0.190808151

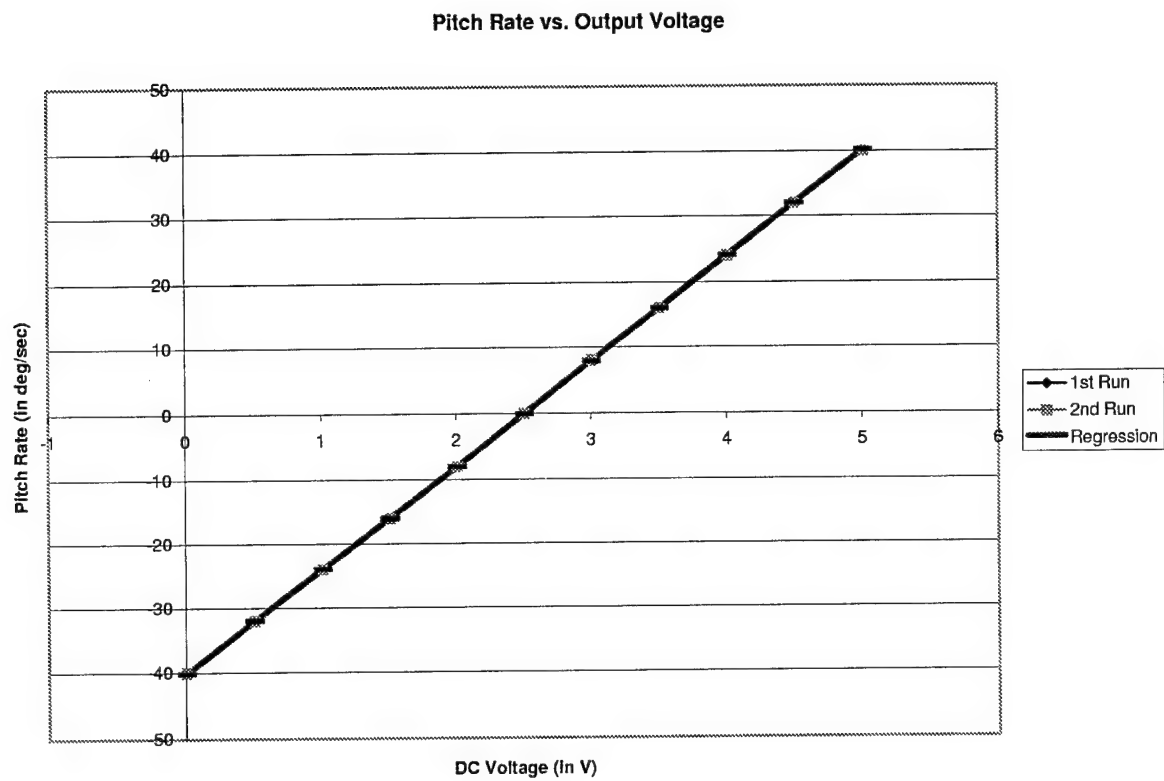


Figure E.1 Pitch Rate vs. Output Voltage

E.3 Roll Axis Regression

Best Fit Curve Formula: $RollRate = 47.67069299 * OutputVoltage - 119.2577727$

Table E.2 Roll Axis Gyro Regression Analysis

Output Voltage	Truth	Roll Rate	Delta
-0.015	-120	-119.9728331	-0.027166905
-0.012	-120	-119.829821	-0.170178984
0.490	-96	-95.89913313	-0.100866865
0.492	-96	-95.80379175	-0.196208251
0.990	-72	-72.06378664	0.06378664
0.992	-72	-71.96844525	-0.031554746
1.495	-48	-47.99008668	-0.00991332
1.498	-48	-47.8470746	-0.152925399
1.996	-24	-24.10706949	0.107069492
1.998	-24	-24.01172811	0.011728106
2.500	0	-0.081040225	0.081040225
2.502	0	0.014301161	-0.014301161
3.002	24	23.84964766	0.150352344
3.005	24	23.99265973	0.007340265
3.509	48	48.018689	-0.018689002
3.512	48	48.16170108	-0.161701081
4.011	72	71.94937688	0.050623117
4.015	72	72.14005965	-0.140059655
4.511	96	95.78472338	0.215276622
4.513	96	95.88006476	0.119935236
5.010	120	119.5723992	0.42760082
5.012	120	119.6677406	0.332259434

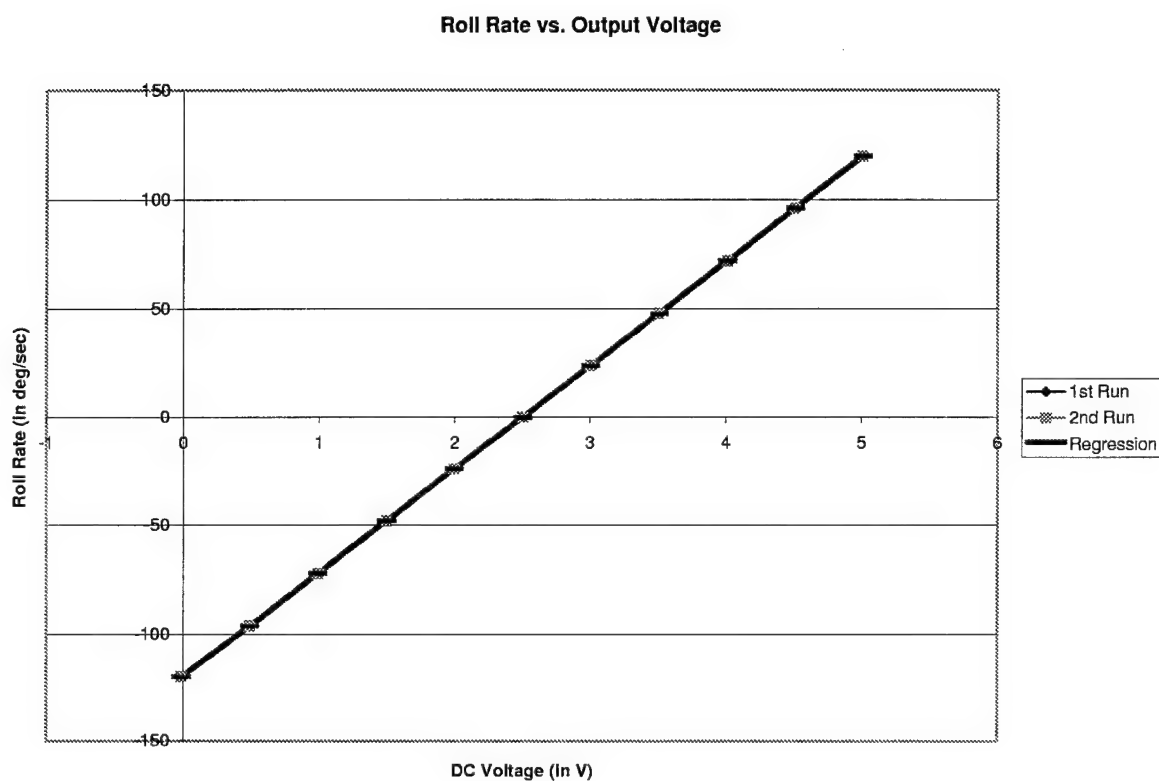


Figure E.2 Roll Rate vs. Output Voltage

E.4 Yaw Axis Regression

Best Fit Curve Formula: $YawRate = 16.07699608 * OutputVoltage - 40.28734448$

Table E.3 Yaw Axis Gyro Regression Analysis

Output Voltage	Truth	Yaw Rate	Delta
0.017	-40	-40.01403555	0.014035547
0.019	-40	-39.98188155	-0.018118446
0.509	-32	-32.10415348	0.104153475
0.512	-32	-32.05592249	0.055922487
1.010	-24	-24.04957844	0.049578439
1.012	-24	-24.01742445	0.017424447
1.508	-16	-16.04323439	0.043234391
1.509	-16	-16.0271574	0.027157395
2.008	-8	-8.004736351	0.004736351
2.013	-8	-7.924351371	-0.075648629
2.507	0	0.017684693	-0.017684693
2.509	0	0.049838685	-0.049838685
3.001	8	7.959720756	0.040279244
3.002	8	7.975797752	0.024202248
3.500	16	15.9821418	0.0178582
3.502	16	16.01429579	-0.014295792
4.000	24	24.02063984	-0.02063984
4.003	24	24.06887083	-0.068870828
4.508	32	32.18775385	-0.187753849
4.511	32	32.23598484	-0.235984837
5.012	40	40.29055987	-0.290559873
5.014	40	40.32271387	-0.322713865

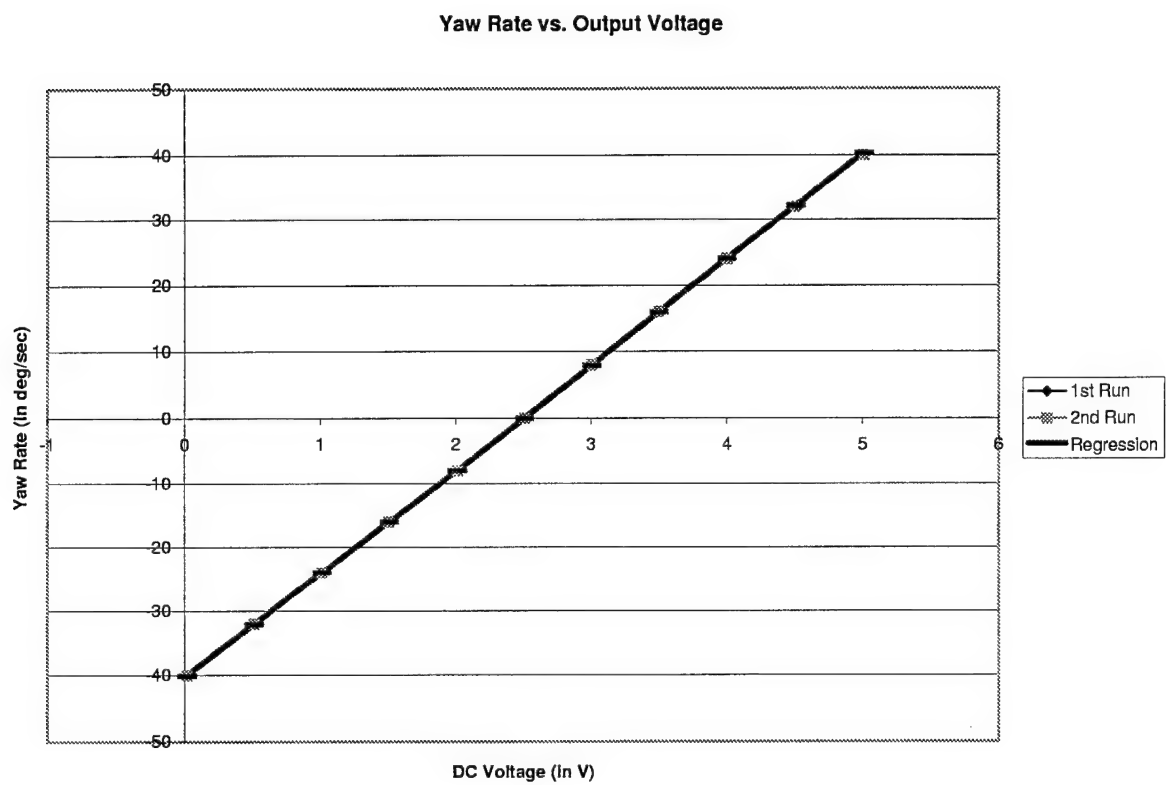


Figure E.3 Yaw Rate vs. Output Voltage

E.5 Fore/Aft Acceleration Regression

Best Fit Curve Formula: $Acceleration = 1.985948707 * OutputVoltage - 4.967038257$

Table E.4 Fore/Aft Acceleration Regression Analysis

Output Voltage	Truth	Measured Gs	Delta
0.005	-5	-4.957108513	-0.042891487
0.005	-5	-4.957108513	-0.042891487
0.455	-4	-4.063431595	0.063431595
0.481	-4	-4.011796929	0.011796929
0.956	-3	-3.068471293	0.068471293
1.012	-3	-2.957258166	-0.042741834
1.457	-2	-2.073510991	0.073510991
1.517	-2	-1.954354068	-0.045645932
1.958	-1	-1.078550689	0.078550689
2.048	-1	-0.899815305	-0.100184695
2.464	0	-0.073660643	0.073660643
2.494	0	-0.014082182	0.014082182
2.985	1	0.961018633	0.038981367
3.055	1	1.100035043	-0.100035043
3.500	2	1.983782218	0.016217783
3.551	2	2.085065602	-0.085065602
3.996	3	2.968812776	0.031187224
4.056	3	3.087969699	-0.087969699
4.512	4	3.993562309	0.006437691
4.542	4	4.05314077	-0.05314077
4.987	5	4.936887945	0.063112055
4.988	5	4.938873894	0.061126106

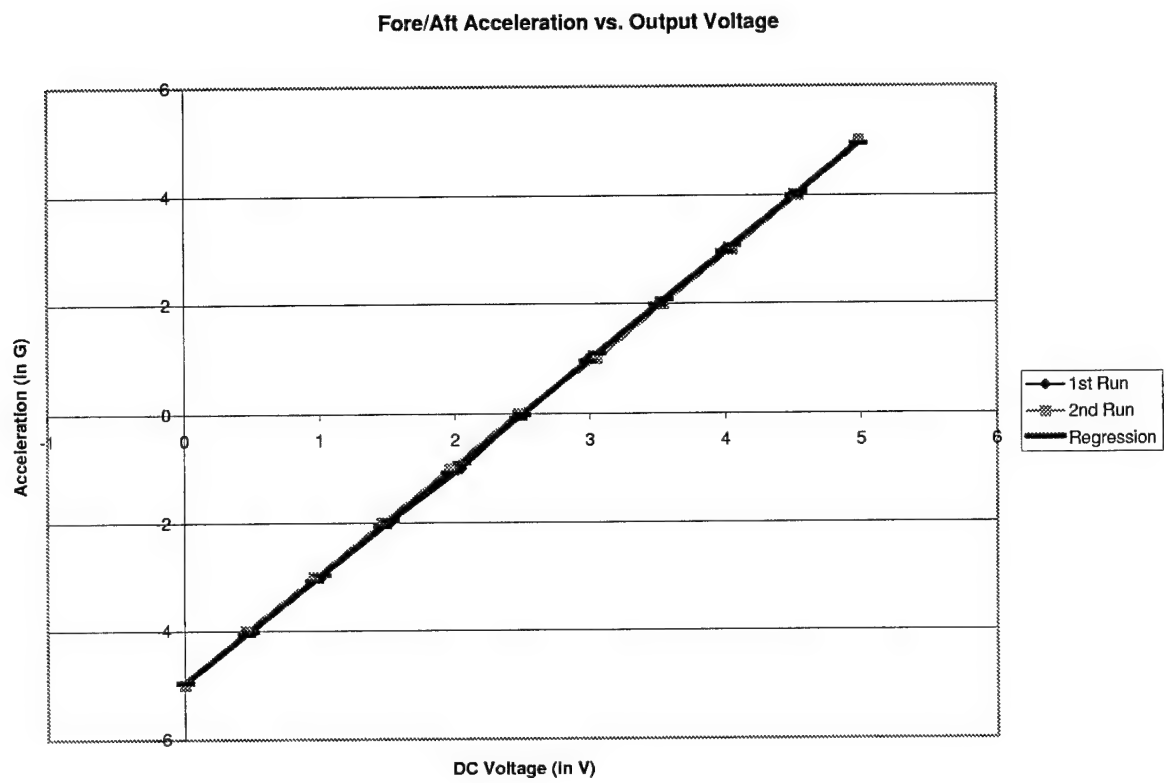


Figure E.4 Fore/Aft Acceleration vs. Output Voltage

E.6 Lateral Acceleration Regression

Best Fit Curve Formula: $Acceleration = 2.004813213 * OutputVoltage - 5.001917838$

Table E.5 Lateral Acceleration Regression Analysis

Output Voltage	Truth	Measured Gs	Delta
0.005	-5	-4.991893772	-0.008106228
0.005	-5	-4.991893772	-0.008106228
0.481	-4	-4.037602683	0.037602683
0.511	-4	-3.977458286	-0.022541714
0.981	-3	-3.035196076	0.035196076
1.012	-3	-2.973046866	-0.026953134
1.457	-2	-2.080904987	0.080904987
1.537	-2	-1.92051993	-0.07948007
1.978	-1	-1.036397303	0.036397303
2.033	-1	-0.926132576	-0.073867424
2.464	0	-0.062058081	0.062058081
2.489	0	-0.011937751	0.011937751
2.975	1	0.962401471	0.037598529
3.035	1	1.082690263	-0.082690263
3.470	2	1.954784011	0.045215989
3.521	2	2.057029485	-0.057029485
3.976	3	2.969219497	0.030780503
4.011	3	3.039387959	-0.039387959
4.477	4	3.973630917	0.026369083
4.507	4	4.033775313	-0.033775313
4.982	5	4.986061589	0.013938411
4.982	5	4.986061589	0.013938411

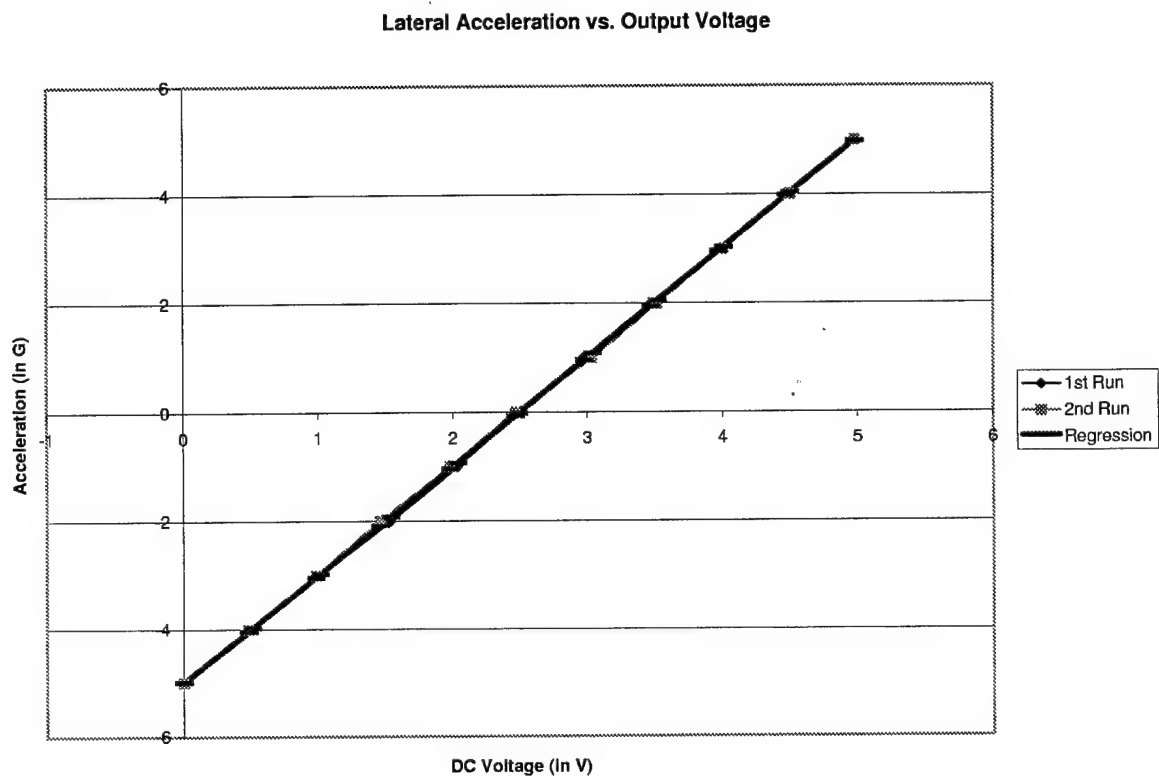


Figure E.5 Lateral Acceleration vs. Output Voltage

E.7 Vertical Acceleration Regression

Best Fit Curve Formula: $Acceleration = 1.990529233 * OutputVoltage - 4.975418296$

Table E.6 Vertical Acceleration Regression Analysis

Output Voltage	Truth	Measured Gs	Delta
0.005	-5	-4.96546565	-0.03453435
0.005	-5	-4.96546565	-0.03453435
0.486	-4	-4.008021089	0.008021089
0.521	-4	-3.938352566	-0.061647434
0.946	-3	-3.092377642	0.092377642
0.991	-3	-3.002803826	0.002803826
1.452	-2	-2.08516985	0.08516985
1.507	-2	-1.975690742	-0.024309258
1.948	-1	-1.09786735	0.09786735
2.043	-1	-0.908767073	-0.091232927
2.459	0	-0.080706912	0.080706912
2.504	0	0.008866903	-0.008866903
2.985	1	0.966311465	0.033688535
3.050	1	1.095695865	-0.095695865
3.490	2	1.971528727	0.028471273
3.546	2	2.082998364	-0.082998364
3.986	3	2.958831227	0.041168773
4.041	3	3.068310335	-0.068310335
4.502	4	3.985944311	0.014055689
4.527	4	4.035707542	-0.035707542
4.998	5	4.973246811	0.026753189
4.998	5	4.973246811	0.026753189

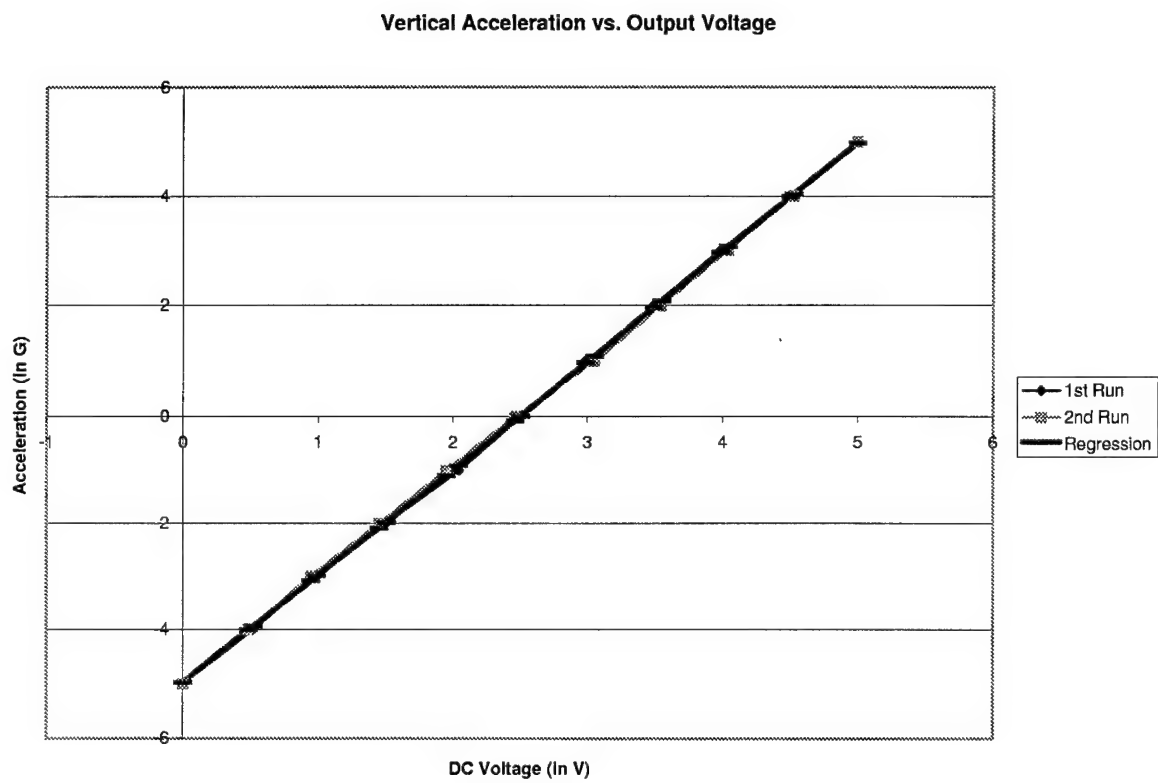


Figure E.6 Vertical Acceleration vs. Output Voltage

Appendix F. Detailed Design Raw Values & Scoring

F.1 Overview

The first iteration of Detailed Design evaluated 60 system alternatives. This appendix presents the raw data for each objective measurable of this design iteration. In addition, the complete ranking of system alternatives is shown, based on the raw values, utility conversions, and weighting factors.

F.2 Objective Measurables Raw Data

The raw data values used in the evaluation of each objective measurable are shown in Tables F.1 and F.2.

F.3 System Scoring

The 60 system alternatives considered in the first iteration of Detailed Design are sorted by system score in Table F.3.

Table F.1 Detailed Design Raw Values

SYSTEM ALTERNATIVES				Capital Cost			Slew Rate	Rate Sensing	Comparative			CDH Compatibility/	Slew
MOTOR	WHEEL	GYRO	BATTERY	(\$)			Sensing	Accuracy	Volume (cubic in)			Interface	Capability
TYPE	SIZE	OPTION	OPTION	Motors	Batteries	TOTAL	(deg/sec)	(L/M.H)	Wheel Boxes	Batteries	TOTAL	(L.M.H)	(deg/s; 10s avg)
Dumb	12.5"	Humphrey	3-batt-18	5325	188	5513	20	High	492	421	913	High	10.77
Dumb	12.5"	Humphrey	3-batt-12	5325	140	5465	20	High	492	255	747	High	10.77
Dumb	12.5"	Humphrey	3-batt-10	5325	131	5456	20	High	492	265	757	High	10.77
Dumb	12.5"	Humphrey	2-batt-18	5325	126	5451	20	High	492	280	772	High	7.00
Dumb	12.5"	Humphrey	2-batt-12	5325	94	5419	20	High	492	170	662	High	7.00
Dumb	12.5"	Horizon	3-batt-18	5325	188	5513	720	Low	492	421	913	High	10.77
Dumb	12.5"	Horizon	3-batt-12	5325	140	5465	720	Low	492	255	747	High	10.77
Dumb	12.5"	Horizon	3-batt-10	5325	131	5456	720	Low	492	265	757	High	10.77
Dumb	12.5"	Horizon	2-batt-18	5325	126	5451	720	Low	492	280	772	High	7.00
Dumb	12.5"	Horizon	2-batt-12	5325	94	5419	720	Low	492	170	662	High	7.00
Dumb	9"	Humphrey	3-batt-18	5325	188	5513	20	High	320	421	741	High	9.69
Dumb	9"	Humphrey	3-batt-12	5325	140	5465	20	High	320	255	575	High	9.69
Dumb	9"	Humphrey	3-batt-10	5325	131	5456	20	High	320	265	585	High	9.69
Dumb	9"	Humphrey	2-batt-18	5325	126	5451	20	High	320	280	600	High	6.38
Dumb	9"	Humphrey	2-batt-12	5325	94	5419	20	High	320	170	490	High	6.38
Dumb	9"	Horizon	3-batt-18	5325	188	5513	720	Low	320	421	741	High	9.69
Dumb	9"	Horizon	3-batt-12	5325	140	5465	720	Low	320	255	575	High	9.69
Dumb	9"	Horizon	3-batt-10	5325	131	5456	720	Low	320	265	585	High	9.69
Dumb	9"	Horizon	2-batt-18	5325	126	5451	720	Low	320	280	600	High	6.38
Dumb	9"	Horizon	2-batt-12	5325	94	5419	720	Low	320	170	490	High	6.38
Dumb	8"	Humphrey	3-batt-18	5325	188	5513	20	High	300	421	721	High	9.06
Dumb	8"	Humphrey	3-batt-12	5325	140	5465	20	High	300	255	555	High	9.06
Dumb	8"	Humphrey	3-batt-10	5325	131	5456	20	High	300	265	565	High	9.06
Dumb	8"	Humphrey	2-batt-18	5325	126	5451	20	High	300	280	580	High	5.98
Dumb	8"	Humphrey	2-batt-12	5325	94	5419	20	High	300	170	470	High	5.98
Dumb	8"	Horizon	3-batt-18	5325	188	5513	720	Low	300	421	721	High	9.06
Dumb	8"	Horizon	3-batt-12	5325	140	5465	720	Low	300	255	555	High	9.06
Dumb	8"	Horizon	3-batt-10	5325	131	5456	720	Low	300	265	565	High	9.06
Dumb	8"	Horizon	2-batt-18	5325	126	5451	720	Low	300	280	580	High	5.98
Dumb	8"	Horizon	2-batt-12	5325	94	5419	720	Low	300	170	470	High	5.98
Smart	12.5"	Humphrey	3-batt-18	6850	188	7038	20	High	492	421	913	Low	10.77
Smart	12.5"	Humphrey	3-batt-12	6850	140	6990	20	High	492	255	747	Low	10.77
Smart	12.5"	Humphrey	3-batt-10	6850	131	6981	20	High	492	265	757	Low	10.77
Smart	12.5"	Humphrey	2-batt-18	6850	126	6976	20	High	492	280	772	Low	7.00
Smart	12.5"	Humphrey	2-batt-12	6850	94	6944	20	High	492	170	662	Low	7.00
Smart	12.5"	Horizon	3-batt-18	6850	188	7038	720	Low	492	421	913	Low	10.77
Smart	12.5"	Horizon	3-batt-12	6850	140	6990	720	Low	492	255	747	Low	10.77
Smart	12.5"	Horizon	3-batt-10	6850	131	6981	720	Low	492	265	757	Low	10.77
Smart	12.5"	Horizon	2-batt-18	6850	126	6976	720	Low	492	280	772	Low	7.00
Smart	12.5"	Horizon	2-batt-12	6850	94	6944	720	Low	492	170	662	Low	7.00
Smart	9"	Humphrey	3-batt-18	6850	188	7038	20	High	320	421	741	Low	9.69
Smart	9"	Humphrey	3-batt-12	6850	140	6990	20	High	320	255	575	Low	9.69
Smart	9"	Humphrey	3-batt-10	6850	131	6981	20	High	320	265	585	Low	9.69
Smart	9"	Humphrey	2-batt-18	6850	126	6976	20	High	320	280	600	Low	6.38
Smart	9"	Humphrey	2-batt-12	6850	94	6944	20	High	320	170	490	Low	6.38
Smart	9"	Horizon	3-batt-18	6850	188	7038	720	Low	320	421	741	Low	9.69
Smart	9"	Horizon	3-batt-12	6850	140	6990	720	Low	320	255	575	Low	9.69
Smart	9"	Horizon	3-batt-10	6850	131	6981	720	Low	320	265	585	Low	9.69
Smart	9"	Horizon	2-batt-18	6850	126	6976	720	Low	320	280	600	Low	6.38
Smart	9"	Horizon	2-batt-12	6850	94	6944	720	Low	320	170	490	Low	6.38
Smart	8"	Humphrey	3-batt-18	6850	188	7038	20	High	300	421	721	Low	9.06
Smart	8"	Humphrey	3-batt-12	6850	140	6990	20	High	300	255	555	Low	9.06
Smart	8"	Humphrey	3-batt-10	6850	131	6981	20	High	300	265	565	Low	9.06
Smart	8"	Humphrey	2-batt-18	6850	126	6976	20	High	300	280	580	Low	5.98
Smart	8"	Humphrey	2-batt-12	6850	94	6944	20	High	300	170	470	Low	5.98
Smart	8"	Horizon	3-batt-18	6850	188	7038	720	Low	300	421	721	Low	9.06
Smart	8"	Horizon	3-batt-12	6850	140	6990	720	Low	300	255	555	Low	9.06
Smart	8"	Horizon	3-batt-10	6850	131	6981	720	Low	300	265	565	Low	9.06
Smart	8"	Horizon	2-batt-18	6850	126	6976	720	Low	300	280	580	Low	5.98
Smart	8"	Horizon	2-batt-12	6850	94	6944	720	Low	300	170	470	Low	5.98

Table F.2 Detailed Design Raw Values (continued)

SYSTEM ALTERNATIVES				Mass Margin										Power Margin										30V Baseline
				(kg under maximum of 130kg)										(Available Watts)										Bus Avail.
MOTOR	WHEEL	GYRO	BATTERY	Motors	Wheels	Gyro	Autoblox	Comm	Thrusters	Batteries	Spare	TOTAL	Motors	Wheels	Gyro	Autoblox	Comm	Thrusters	Batteries	TOTAL	(yes/no)			
TYPE	SIZE	OPTION	OPTION																					
Dumb	12.5"	Humphrey	3-batt-18	10	11	1	10	2	7	18	30%	59	-360	N/A	-25	-65	-0.1	-12	972	509	Yes			
Dumb	12.5"	Humphrey	3-batt-12	10	11	1	10	2	7	13	30%	66	-360	N/A	-25	-65	-0.1	-12	648	185	Yes			
Dumb	12.5"	Humphrey	3-batt-10	10	11	1	10	2	7	13	30%	66	-360	N/A	-25	-65	-0.1	-12	540	77	Yes			
Dumb	12.5"	Humphrey	2-batt-18	10	11	1	10	2	7	12	30%	67	-162	N/A	-25	-65	-0.1	-12	432	167	No			
Dumb	12.5"	Humphrey	2-batt-12	10	11	1	10	2	7	9	30%	71	-162	N/A	-25	-65	-0.1	-12	288	23	No			
Dumb	12.5"	Horizon	3-batt-18	10	11	1	10	2	7	18	30%	59	-360	N/A	0	-65	-0.1	-12	972	534	Yes			
Dumb	12.5"	Horizon	3-batt-12	10	11	1	10	2	7	13	30%	66	-360	N/A	0	-65	-0.1	-12	648	210	Yes			
Dumb	12.5"	Horizon	3-batt-10	10	11	1	10	2	7	13	30%	66	-360	N/A	0	-65	-0.1	-12	540	102	Yes			
Dumb	12.5"	Horizon	2-batt-18	10	11	1	10	2	7	12	30%	67	-162	N/A	0	-65	-0.1	-12	432	192	No			
Dumb	12.5"	Horizon	2-batt-12	10	11	1	10	2	7	9	30%	71	-162	N/A	0	-65	-0.1	-12	288	48	No			
Dumb	9"	Humphrey	3-batt-18	10	9.5	1	10	2	7	18	30%	61	-360	N/A	-25	-65	-0.1	-12	972	509	Yes			
Dumb	9"	Humphrey	3-batt-12	10	9.5	1	10	2	7	13	30%	68	-360	N/A	-25	-65	-0.1	-12	648	185	Yes			
Dumb	9"	Humphrey	3-batt-10	10	9.5	1	10	2	7	13	30%	68	-360	N/A	-25	-65	-0.1	-12	540	77	Yes			
Dumb	9"	Humphrey	2-batt-18	10	9.5	1	10	2	7	12	30%	69	-162	N/A	-25	-65	-0.1	-12	432	167	No			
Dumb	9"	Humphrey	2-batt-12	10	9.5	1	10	2	7	9	30%	73	-162	N/A	-25	-65	-0.1	-12	288	23	No			
Dumb	9"	Horizon	3-batt-18	10	9.5	1	10	2	7	18	30%	61	-360	N/A	0	-65	-0.1	-12	972	534	Yes			
Dumb	9"	Horizon	3-batt-12	10	9.5	1	10	2	7	13	30%	68	-360	N/A	0	-65	-0.1	-12	648	210	Yes			
Dumb	9"	Horizon	3-batt-10	10	9.5	1	10	2	7	13	30%	68	-360	N/A	0	-65	-0.1	-12	540	102	Yes			
Dumb	9"	Horizon	2-batt-18	10	9.5	1	10	2	7	12	30%	69	-162	N/A	0	-65	-0.1	-12	432	192	No			
Dumb	9"	Horizon	2-batt-12	10	9.5	1	10	2	7	9	30%	73	-162	N/A	0	-65	-0.1	-12	288	48	No			
Dumb	8"	Humphrey	3-batt-18	10	10	1	10	2	7	18	30%	61	-360	N/A	-25	-65	-0.1	-12	972	509	Yes			
Dumb	8"	Humphrey	3-batt-12	10	10	1	10	2	7	13	30%	67	-360	N/A	-25	-65	-0.1	-12	648	185	Yes			
Dumb	8"	Humphrey	3-batt-10	10	10	1	10	2	7	13	30%	67	-360	N/A	-25	-65	-0.1	-12	540	77	Yes			
Dumb	8"	Humphrey	2-batt-18	10	10	1	10	2	7	12	30%	68	-162	N/A	-25	-65	-0.1	-12	432	167	No			
Dumb	8"	Humphrey	2-batt-12	10	10	1	10	2	7	9	30%	72	-162	N/A	-25	-65	-0.1	-12	288	23	No			
Dumb	8"	Horizon	3-batt-18	10	10	1	10	2	7	18	30%	61	-360	N/A	0	-65	-0.1	-12	972	534	Yes			
Dumb	8"	Horizon	3-batt-12	10	10	1	10	2	7	13	30%	67	-360	N/A	0	-65	-0.1	-12	648	210	Yes			
Dumb	8"	Horizon	3-batt-10	10	10	1	10	2	7	13	30%	67	-360	N/A	0	-65	-0.1	-12	540	102	Yes			
Dumb	8"	Horizon	2-batt-18	10	10	1	10	2	7	12	30%	68	-162	N/A	0	-65	-0.1	-12	432	192	No			
Dumb	8"	Horizon	2-batt-12	10	10	1	10	2	7	9	30%	72	-162	N/A	0	-65	-0.1	-12	288	48	No			
Smart	12.5"	Humphrey	3-batt-18	8	11	1	10	2	7	18	30%	62	-360	N/A	-25	-65	-0.1	-12	972	509	Yes			
Smart	12.5"	Humphrey	3-batt-12	8	11	1	10	2	7	13	30%	68	-360	N/A	-25	-65	-0.1	-12	648	185	Yes			
Smart	12.5"	Humphrey	3-batt-10	8	11	1	10	2	7	13	30%	68	-360	N/A	-25	-65	-0.1	-12	540	77	Yes			
Smart	12.5"	Humphrey	2-batt-18	8	11	1	10	2	7	12	30%	70	-162	N/A	-25	-65	-0.1	-12	432	167	No			
Smart	12.5"	Humphrey	2-batt-12	8	11	1	10	2	7	9	30%	74	-162	N/A	-25	-65	-0.1	-12	288	23	No			
Smart	12.5"	Horizon	3-batt-18	8	11	1	10	2	7	18	30%	62	-360	N/A	0	-65	-0.1	-12	972	534	Yes			
Smart	12.5"	Horizon	3-batt-12	8	11	1	10	2	7	13	30%	68	-360	N/A	0	-65	-0.1	-12	648	210	Yes			
Smart	12.5"	Horizon	3-batt-10	8	11	1	10	2	7	13	30%	68	-360	N/A	0	-65	-0.1	-12	540	102	Yes			
Smart	12.5"	Horizon	2-batt-18	8	11	1	10	2	7	12	30%	70	-162	N/A	0	-65	-0.1	-12	432	192	No			
Smart	12.5"	Horizon	2-batt-12	8	11	1	10	2	7	9	30%	74	-162	N/A	0	-65	-0.1	-12	288	48	No			
Smart	9"	Humphrey	3-batt-18	8	9.5	1	10	2	7	18	30%	64	-360	N/A	-25	-65	-0.1	-12	972	509	Yes			
Smart	9"	Humphrey	3-batt-12	8	9.5	1	10	2	7	13	30%	70	-360	N/A	-25	-65	-0.1	-12	648	185	Yes			
Smart	9"	Humphrey	3-batt-10	8	9.5	1	10	2	7	13	30%	70	-360	N/A	-25	-65	-0.1	-12	540	77	Yes			
Smart	9"	Humphrey	2-batt-18	8	9.5	1	10	2	7	12	30%	72	-162	N/A	-25	-65	-0.1	-12	432	167	No			
Smart	9"	Humphrey	2-batt-12	8	9.5	1	10	2	7	9	30%	76	-162	N/A	-25	-65	-0.1	-12	288	23	No			
Smart	9"	Horizon	3-batt-18	8	9.5	1	10	2	7	18	30%	64	-360	N/A	0	-65	-0.1	-12	972	534	Yes			
Smart	9"	Horizon	3-batt-12	8	9.5	1	10	2	7	13	30%	70	-360	N/A	0	-65	-0.1	-12	648	210	Yes			
Smart	9"	Horizon	3-batt-10	8	9.5	1	10	2	7	13	30%	70	-360	N/A	0	-65	-0.1	-12	540	102	Yes			
Smart	9"	Horizon	2-batt-18	8	9.5	1	10	2	7	12	30%	72	-162	N/A	0	-65	-0.1	-12	432	192	No			
Smart	9"	Horizon	2-batt-12	8	9.5	1	10	2	7	9	30%	76	-162	N/A	0	-65	-0.1	-12	288	48	No			
Smart	8"	Humphrey	3-batt-18	8	10	1	10	2	7	18	30%	63	-360	N/A	-25	-65	-0.1	-12	972	509	Yes			
Smart	8"	Humphrey	3-batt-12	8	10	1	10	2	7	13	30%	70	-360	N/A	-25	-65	-0.1	-12	648	185	Yes			
Smart	8"	Humphrey	3-batt-10	8	10	1	10	2	7	13	30%	70	-360	N/A	-25	-65	-0.1	-12	540	77	Yes			
Smart	8"	Humphrey	2-batt-18	8	10	1	10	2	7	12	30%	71	-162	N/A	-25	-65	-0.1	-12	432	167	No			
Smart	8"	Humphrey	2-batt-12	8	10	1	10	2	7	9	30%	75	-162	N/A	-25	-65	-0.1	-12	288	23	No			
Smart	8"	Horizon	3-batt-18	8	10	1	10	2	7	18	30%	63	-360	N/A	0	-65	-0.1	-12	972	534	Yes			
Smart	8"	Horizon	3-batt-12	8	10	1	10	2	7	13	30%	70	-360	N/A	0	-65	-0.1	-12	648	210	Yes			
Smart	8"	Horizon	3-batt-10	8	10	1	10	2	7	13	30%	70	-360	N/A	0	-65	-0.1	-12	540	102	Yes			
Smart	8"	Horizon	2-batt-18	8	10	1	10	2	7	12	30%	71	-162	N/A	0	-65	-0.1	-12	432	192	No			
Smart	8"	Horizon	2-batt-12	8	10	1	10	2	7	9	30%	75	-162	N/A	0	-65	-0.1	-12	288	48	No			

Table F.3 System Scoring and Ranking

SYSTEM ALTERNATIVE				SYSTEM SCORE
MOTORS	MOM. WHEELS	GYRO	BATT SYS.	(x 10000)
Dumb	9" wheel	Humphrey	3-batt-18Ahr	233.74
Dumb	9" wheel	Horizon	3-batt-18Ahr	233.18
Dumb	8" wheel	Humphrey	3-batt-18Ahr	232.75
Dumb	8" wheel	Horizon	3-batt-18Ahr	232.19
Dumb	12.5" wheel	Humphrey	3-batt-18Ahr	224.69
Dumb	12.5" wheel	Horizon	3-batt-18Ahr	224.13
Dumb	9" wheel	Humphrey	3-batt-12Ahr	202.58
Dumb	9" wheel	Horizon	3-batt-12Ahr	202.02
Dumb	8" wheel	Humphrey	3-batt-12Ahr	199.73
Dumb	8" wheel	Horizon	3-batt-12Ahr	199.17
Dumb	9" wheel	Humphrey	2-batt-18Ahr	191.45
Dumb	12.5" wheel	Humphrey	3-batt-12Ahr	191.43
Dumb	9" wheel	Horizon	2-batt-18Ahr	190.89
Dumb	12.5" wheel	Horizon	3-batt-12Ahr	190.87
Dumb	8" wheel	Humphrey	2-batt-18Ahr	188.60
Dumb	8" wheel	Horizon	2-batt-18Ahr	188.04
Dumb	9" wheel	Humphrey	3-batt-10Ahr	185.02
Dumb	9" wheel	Horizon	3-batt-10Ahr	184.46
Dumb	8" wheel	Humphrey	3-batt-10Ahr	182.17
Dumb	8" wheel	Horizon	3-batt-10Ahr	181.61
Dumb	12.5" wheel	Humphrey	2-batt-18Ahr	181.29
Dumb	12.5" wheel	Horizon	2-batt-18Ahr	180.73
Smart	9" wheel	Humphrey	3-batt-18Ahr	179.77
Dumb	9" wheel	Humphrey	2-batt-12Ahr	179.76
Smart	9" wheel	Horizon	3-batt-18Ahr	179.22
Dumb	9" wheel	Horizon	2-batt-12Ahr	179.20
Smart	8" wheel	Humphrey	3-batt-18Ahr	176.92
Dumb	8" wheel	Humphrey	2-batt-12Ahr	176.91
Smart	8" wheel	Horizon	3-batt-18Ahr	176.36
Dumb	8" wheel	Horizon	2-batt-12Ahr	176.35
Dumb	12.5" wheel	Humphrey	3-batt-10Ahr	173.87
Dumb	12.5" wheel	Horizon	3-batt-10Ahr	173.31
Smart	12.5" wheel	Humphrey	3-batt-18Ahr	170.73
Smart	12.5" wheel	Horizon	3-batt-18Ahr	170.17
Dumb	12.5" wheel	Humphrey	2-batt-12Ahr	169.59
Dumb	12.5" wheel	Horizon	2-batt-12Ahr	169.04
Smart	9" wheel	Humphrey	3-batt-12Ahr	146.76
Smart	9" wheel	Horizon	3-batt-12Ahr	146.20
Smart	8" wheel	Humphrey	3-batt-12Ahr	145.77
Smart	8" wheel	Horizon	3-batt-12Ahr	145.21
Smart	9" wheel	Humphrey	2-batt-18Ahr	137.49
Smart	9" wheel	Horizon	2-batt-18Ahr	136.93
Smart	12.5" wheel	Humphrey	3-batt-12Ahr	135.60
Smart	12.5" wheel	Horizon	3-batt-12Ahr	135.05
Smart	8" wheel	Humphrey	2-batt-18Ahr	134.63
Smart	8" wheel	Horizon	2-batt-18Ahr	134.08
Smart	9" wheel	Humphrey	3-batt-10Ahr	129.20
Smart	9" wheel	Horizon	3-batt-10Ahr	128.64
Smart	8" wheel	Humphrey	3-batt-10Ahr	128.21
Smart	8" wheel	Horizon	3-batt-10Ahr	127.65
Smart	12.5" wheel	Humphrey	2-batt-18Ahr	127.32
Smart	12.5" wheel	Horizon	2-batt-18Ahr	126.76
Smart	9" wheel	Humphrey	2-batt-12Ahr	125.79
Smart	9" wheel	Horizon	2-batt-12Ahr	125.24
Smart	8" wheel	Humphrey	2-batt-12Ahr	122.94
Smart	8" wheel	Horizon	2-batt-12Ahr	122.39
Smart	12.5" wheel	Humphrey	3-batt-10Ahr	118.05
Smart	12.5" wheel	Horizon	3-batt-10Ahr	117.49
Smart	12.5" wheel	Humphrey	2-batt-12Ahr	115.63
Smart	12.5" wheel	Horizon	2-batt-12Ahr	115.07

Appendix G. Initial Controller Design

G.1 Overview

This appendix contains the controller gains and MATLAB output graphs for the various *SIMSAT* maneuvers described in Chapter IV, Section 4.5 (Command and Control Architecture). These maneuvers are NOT performed sequentially; the *SIMSAT* state vector is set to zero before each maneuver. This appendix only represents the initial controller design for an early iteration of *SIMSAT*; this appendix does not represent the controller used for the final *SIMSAT* design.

G.2 Gain Settings Development

The following pages list the input gain matrices used in the controller design. For each set of input gains, system output performance is illustrated using the MATLAB simulation. Successive iterations were used to determine an adequate set of gains to accomodate the various *SIMSAT* operating modes. These gains can be adjusted by the user in actual system operation as necessary.

Table G.1 Options 1 and 2 - Gains

Initial Closed-Loop Controller Design

Option #1 (Target Mode)

Manvr #	Command (degrees)	Gain Matrix K_1			Gain Matrix K_2			Gain Matrix K_4		
1	Roll = -30	100	0	0	-50	0	0	1	0	0
	Yaw = -50	0	200	0	0	-50	0	0	1	0
	Pitch = -10	0	0	1000	0	0	-10	0	0	1
2	Roll = 5	1000	0	0	-10	0	0	1	0	0
	Yaw = 5	0	1000	0	0	-50	0	0	1	0
	Pitch = 5	0	0	1000	0	0	-10	0	0	1
3	Roll = 0	3000	0	0	-10	0	0	1	0	0
	Yaw = 10	0	1000	0	0	-50	0	0	1	0
	Pitch = 0	0	0	1000	0	0	-10	0	0	1
4	Roll = 0	3000	0	0	-10	0	0	1	0	0
	Yaw = 90	0	300	0	0	-50	0	0	1	0
	Pitch = 0	0	0	1000	0	0	-10	0	0	1
5	Roll = 30	100	0	0	-50	0	0	1	0	0
	Yaw = 50	0	200	0	0	-50	0	0	1	0
	Pitch = 10	0	0	1000	0	0	-10	0	0	1

$$K_3 = 0.0585$$

Option #2 (Target Mode with Roll Rate)

Manvr #	Command (RPM/degrees)	Gain Matrix K_1			Gain Matrix K_2			Gain Matrix K_4		
1	RollRate = 1	0	0	0	1	0	0	20000	0	0
	Yaw = 10	0	1500	0	0	-50	0	0	1	0
	Pitch = -5	0	0	1500	0	0	-10	0	0	1
2	RollRate = 9	0	0	0	1	0	0	40	0	0
	Yaw = 30	0	500	0	0	-50	0	0	1	0
	Pitch = 5	0	0	1500	0	0	-10	0	0	1
3	RollRate = -5	0	0	0	1	0	0	40	0	0
	Yaw = 20	0	1000	0	0	-50	0	0	1	0
	Pitch = 10	0	0	1000	0	0	-10	0	0	1

$$K_3 = 0.0585$$

Note: 1 RPM = 6 deg/sec

Table G.2 Options 3 and 4 - Gains

Initial Closed-Loop Controller Design

Option #3 (Roll Spin Mode)

Manvr #	Command (RPM)	Gain Matrix K_1			Gain Matrix K_2			Gain Matrix K_4		
1	RollRate = 1	0	0	0	1	0	0	20000	0	0
		0	1500	0	0	-50	0	0	1	0
		0	0	1500	0	0	-10	0	0	1
2	RollRate = 9	0	0	0	1	0	0	20000	0	0
		0	1500	0	0	-50	0	0	1	0
		0	0	1500	0	0	-10	0	0	1
3	RollRate = -5	0	0	0	1	0	0	20000	0	0
		0	1500	0	0	-50	0	0	1	0
		0	0	1500	0	0	-10	0	0	1

$$K_3 = 0.0585$$

Option #4 (Yaw Spin Mode)

Manvr #	Command (RPM)	Gain Matrix K_1			Gain Matrix K_2			Gain Matrix K_4		
1	YawRate= 1	2000	0	0	-50	0	0	1	0	0
		0	0	0	0	1	0	0	200000	0
		0	0	1000	0	0	-10	0	0	1
2	YawRate= 2	2000	0	0	-50	0	0	1	0	0
		0	0	0	0	1	0	0	200000	0
		0	0	1000	0	0	-10	0	0	1
3	YawRate= 2.6	2000	0	0	-50	0	0	1	0	0
		0	0	0	0	1	0	0	200000	0
		0	0	1000	0	0	-10	0	0	1
4	YawRate= -1	2000	0	0	-50	0	0	1	0	0
		0	0	0	0	1	0	0	200000	0
		0	0	1000	0	0	-10	0	0	1
5	YawRate= -2	2000	0	0	-50	0	0	1	0	0
		0	0	0	0	1	0	0	200000	0
		0	0	1000	0	0	-10	0	0	1
6	YawRate= -2.6	2000	0	0	-50	0	0	1	0	0
		0	0	0	0	1	0	0	200000	0
		0	0	1000	0	0	-10	0	0	1

$$K_3 = 0.0585$$

Note: 1 RPM = 6 deg/sec

Table G.3 Option 5 - Gains

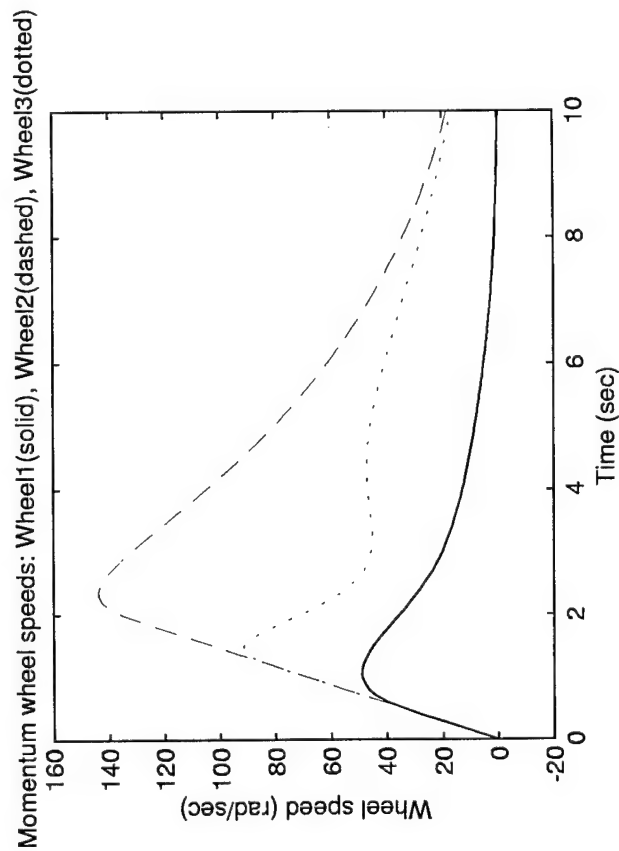
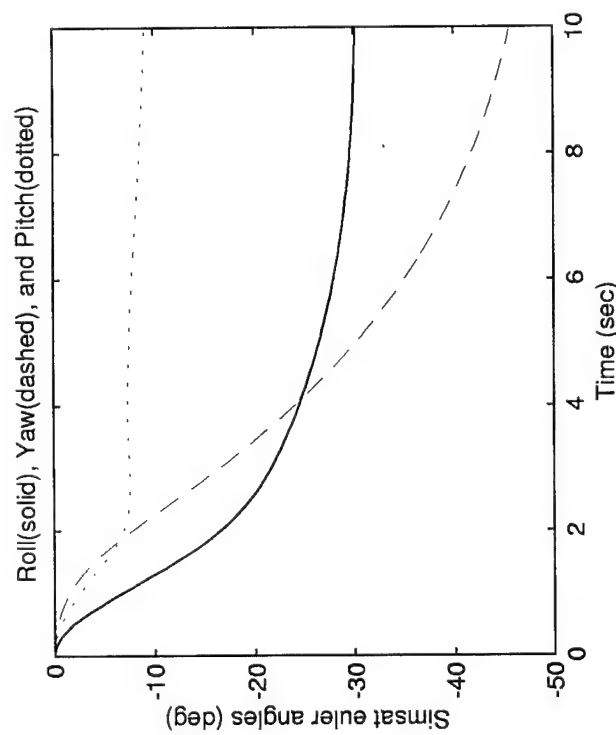
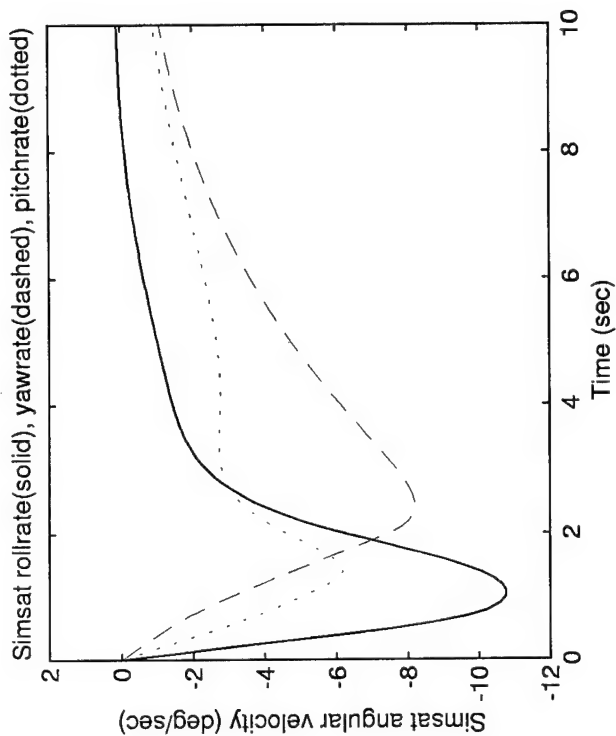
Initial Closed-Loop Controller Design

Option #5 (Wheel RPM Mode)

Manvr #	Command (RPM)	Gain Matrix K_1			Gain Matrix K_2			Gain Matrix K_4		
1	Wheel 1 = 50	0	0	0	0	0	0	1	0	0
	Wheel 2 = 20	0	0	0	0	0	0	0	1	0
	Wheel 3 = 10	0	0	0	0	0	0	0	0	1
2	Wheel 1 = 100	0	0	0	0	0	0	1	0	0
	Wheel 2 = 0	0	0	0	0	0	0	0	1	0
	Wheel 3 = 0	0	0	0	0	0	0	0	0	1
3	Wheel 1 = 0	0	0	0	0	0	0	1	0	0
	Wheel 2 = 100	0	0	0	0	0	0	0	1	0
	Wheel 3 = 0	0	0	0	0	0	0	0	0	1
4	Wheel 1 = 0	0	0	0	0	0	0	1	0	0
	Wheel 2 = 0	0	0	0	0	0	0	0	1	0
	Wheel 3 = 100	0	0	0	0	0	0	0	0	1

$$K_3 = 0.0585$$

Note: 1 RPM = 0.1047198 rad/sec



Option 1 (Target Mode)
Maneuver #
1

Figure G.1 Option 1 (Target Mode) - Maneuver 1

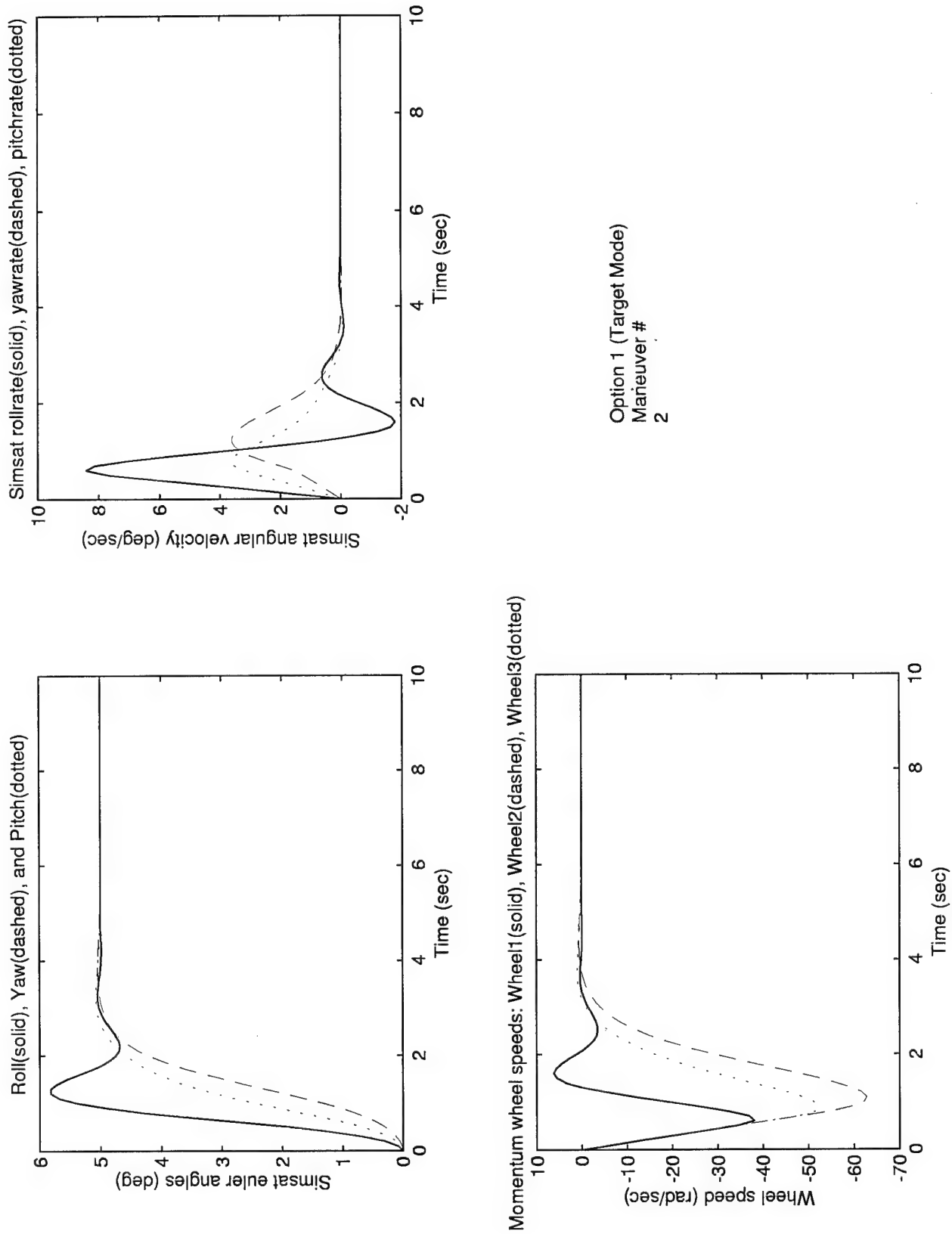
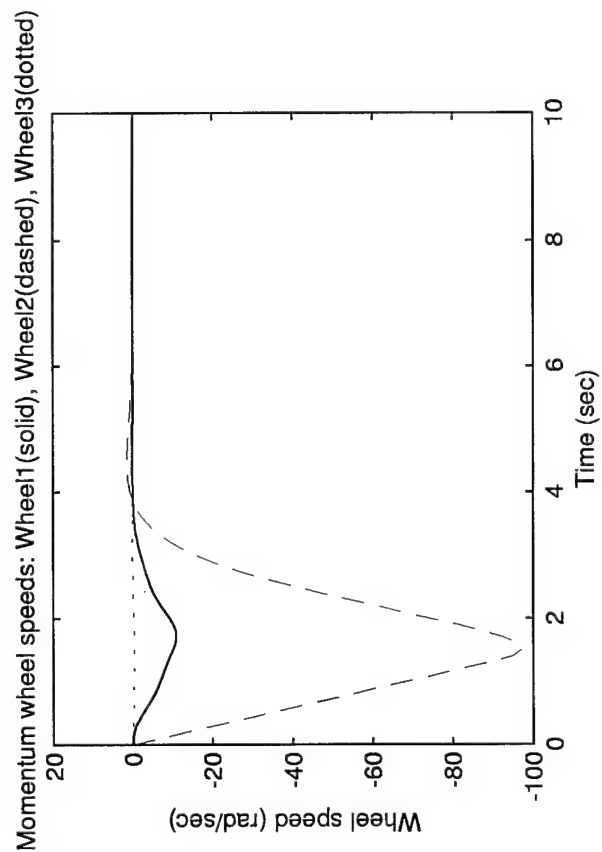
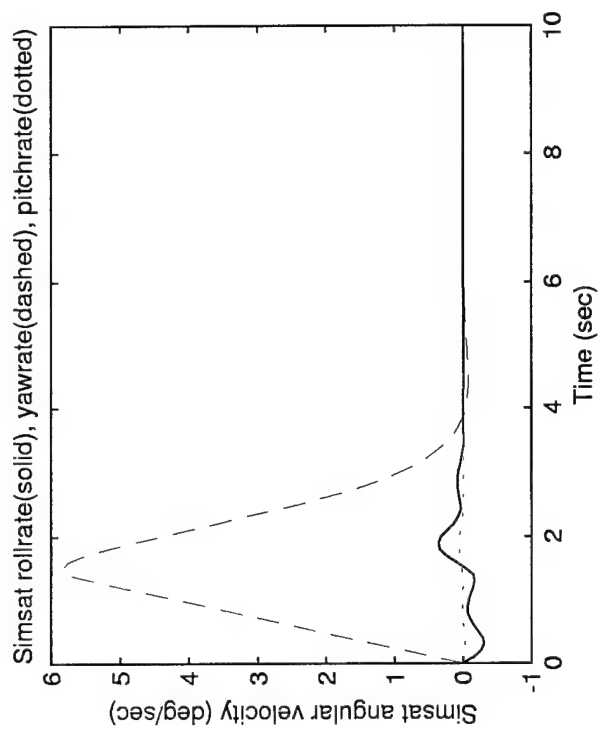
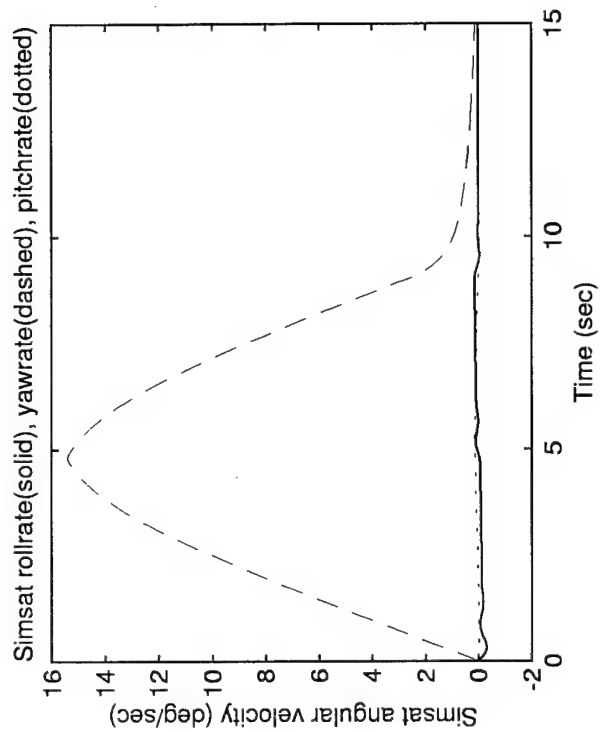


Figure G.2 Option 1 (Target Mode) - Maneuver 2



Option 1 (Target Mode)
Maneuver #
3

Figure G.3 Option 1 (Target Mode) - Maneuver 3



Option 1 (Target Mode)
Maneuver #
4

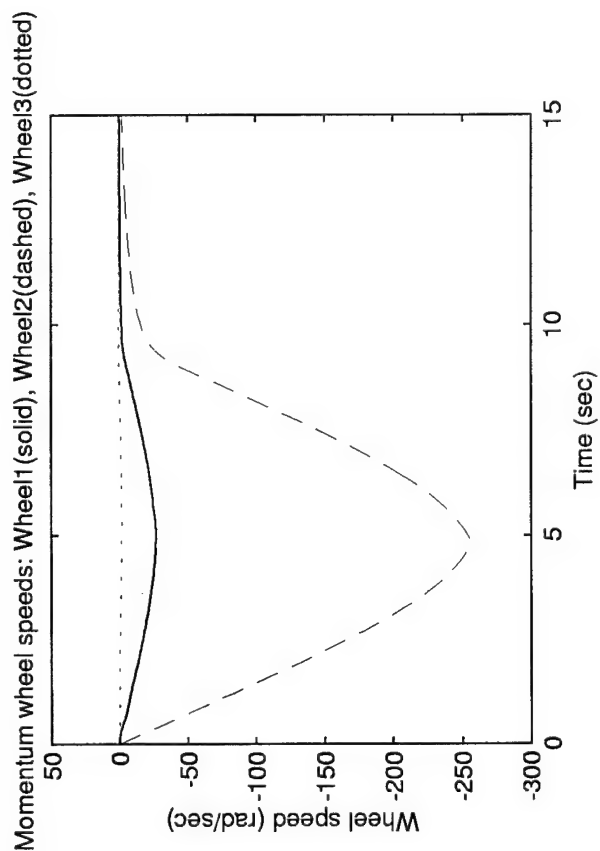
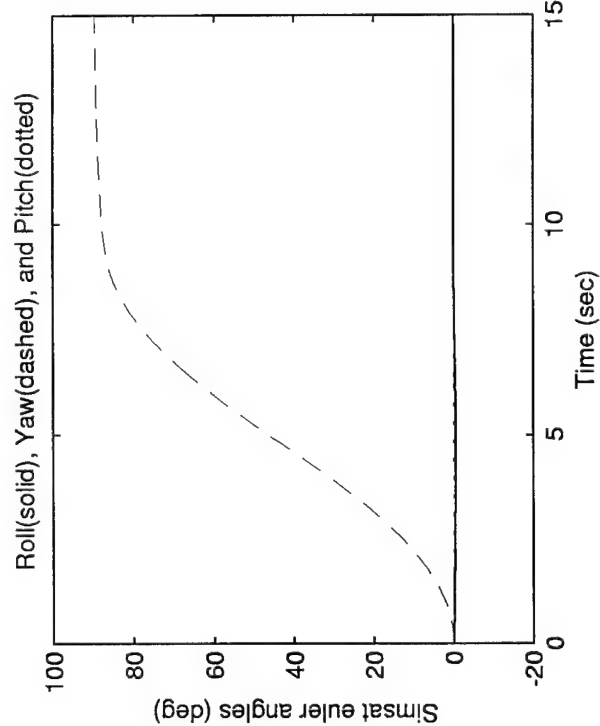
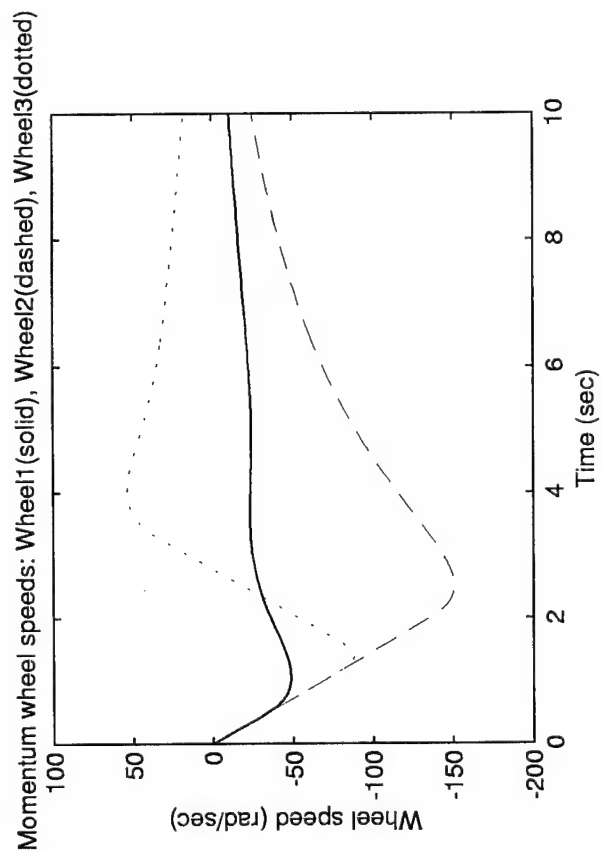
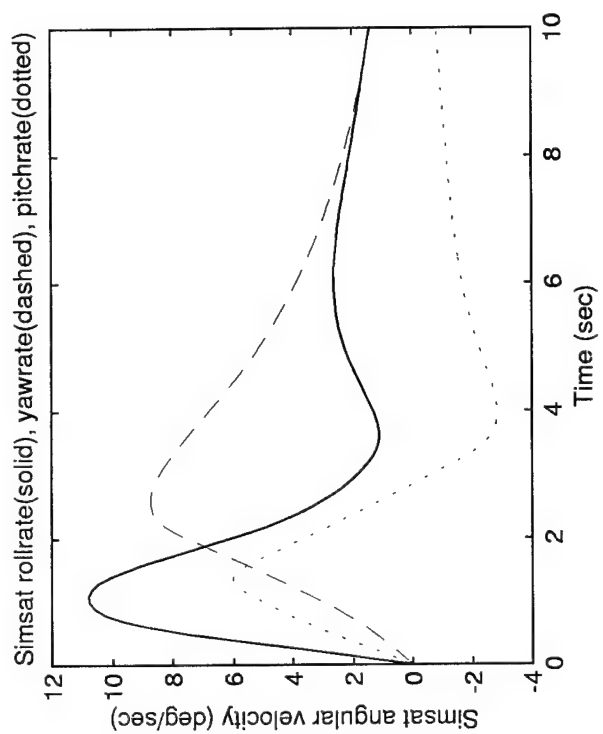
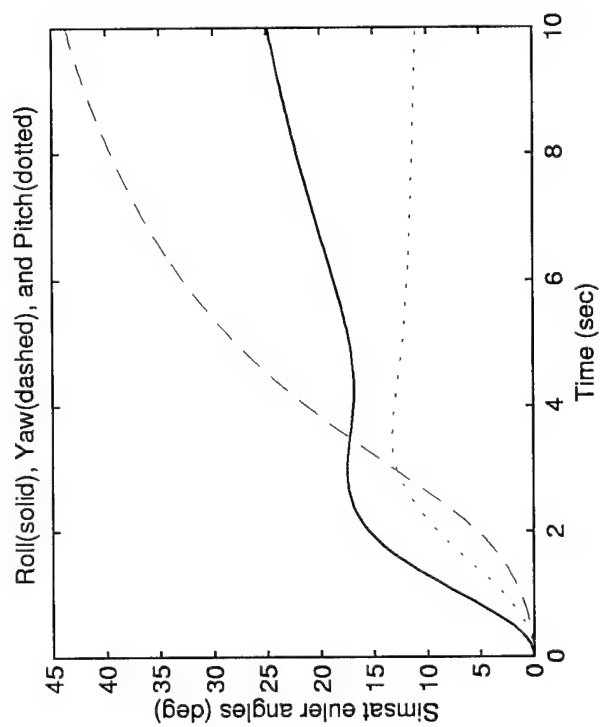
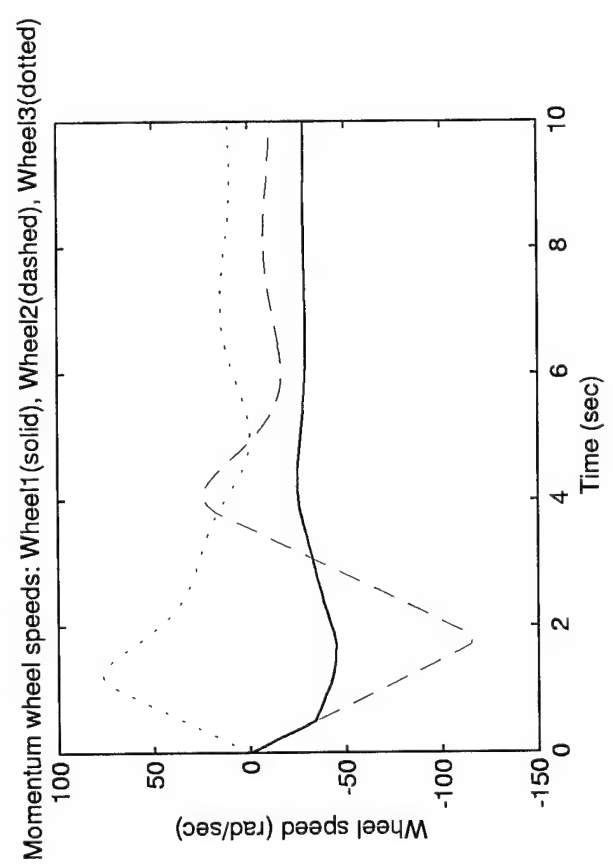
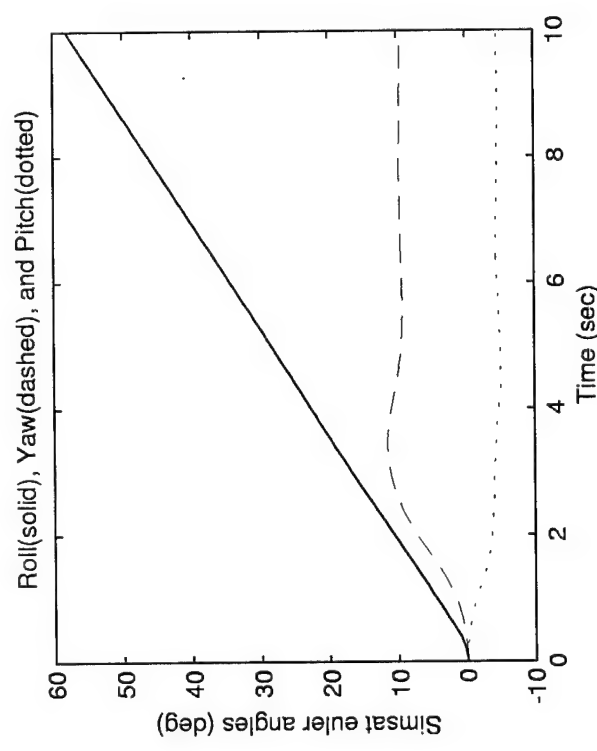
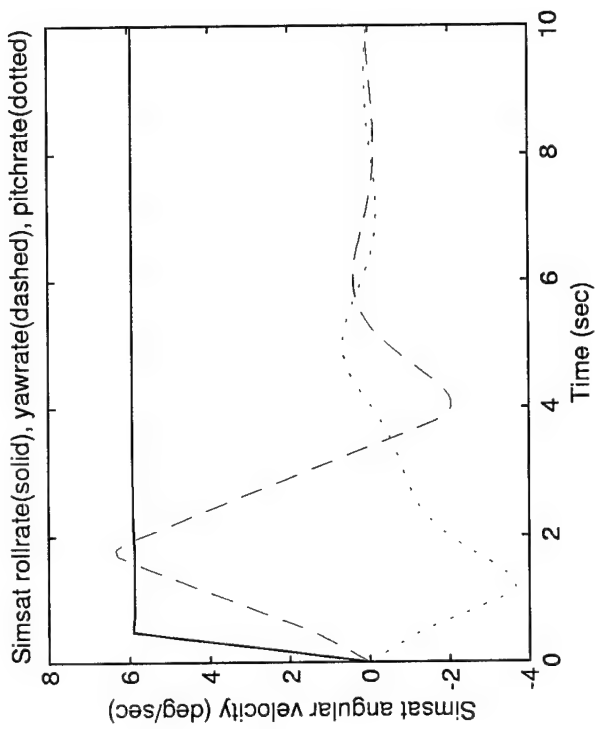


Figure G.4 Option 1 (Target Mode) - Maneuver 4



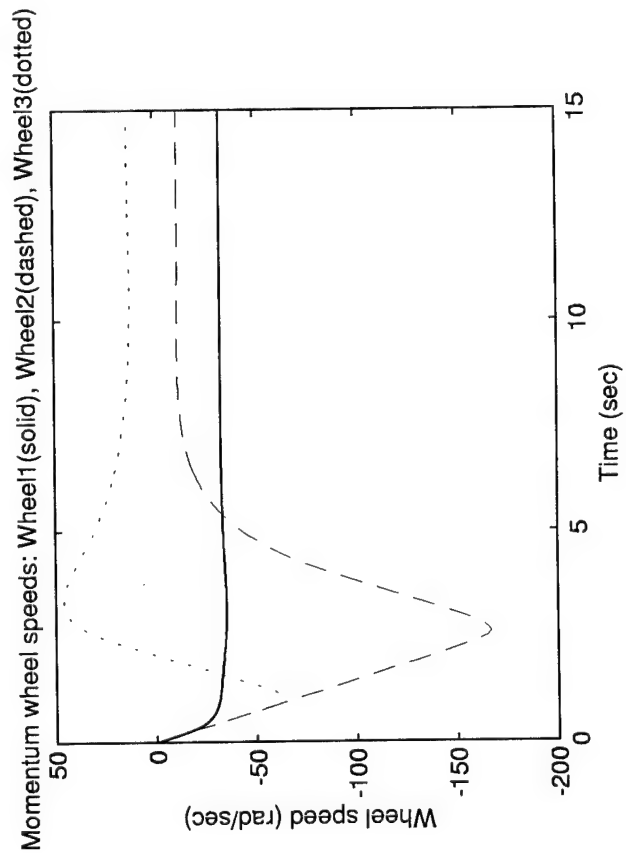
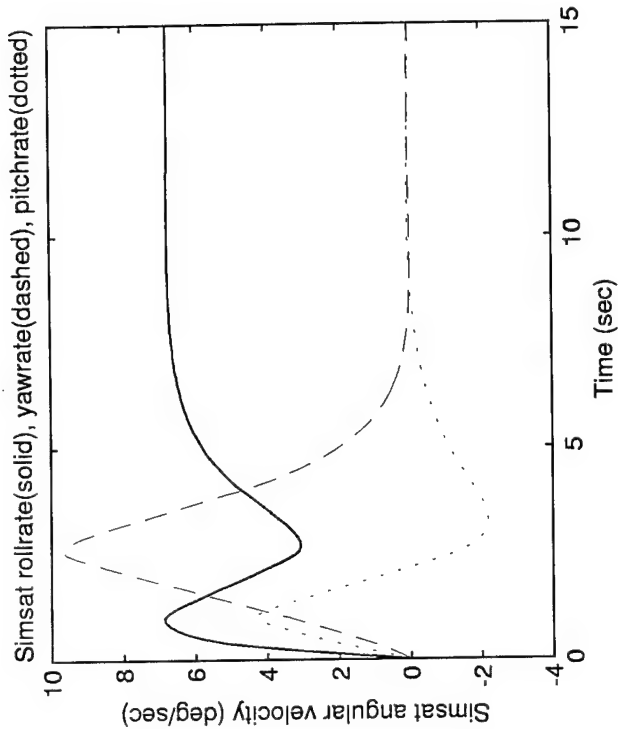
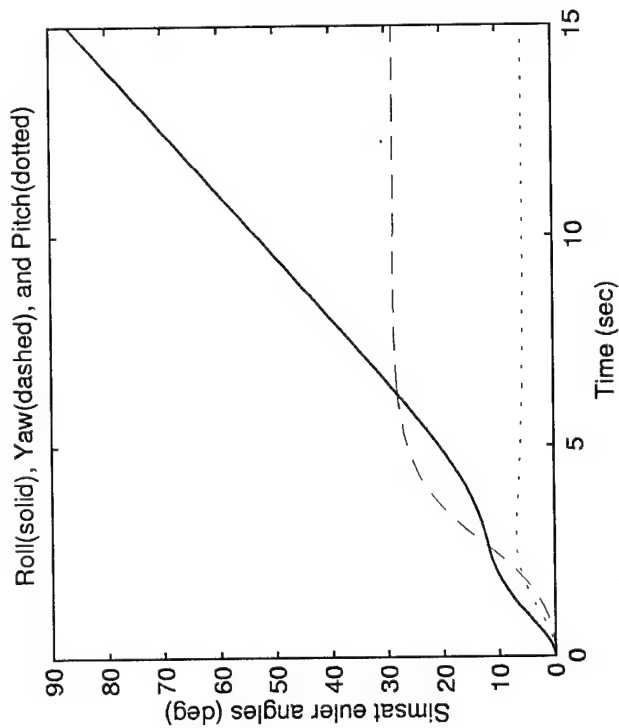
Option 1 (Target Mode)
Maneuver #
5

Figure G.5 Option 1 (Target Mode) - Maneuver 5



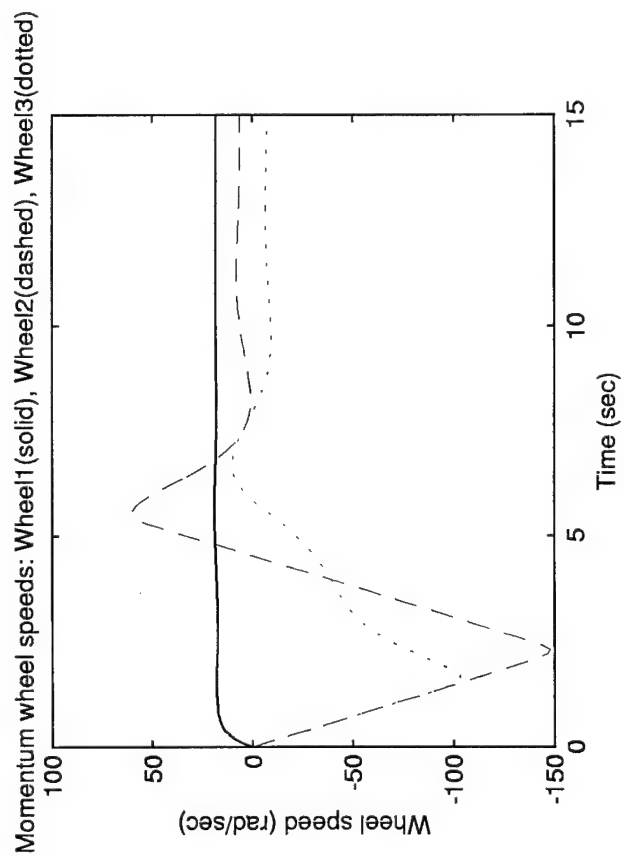
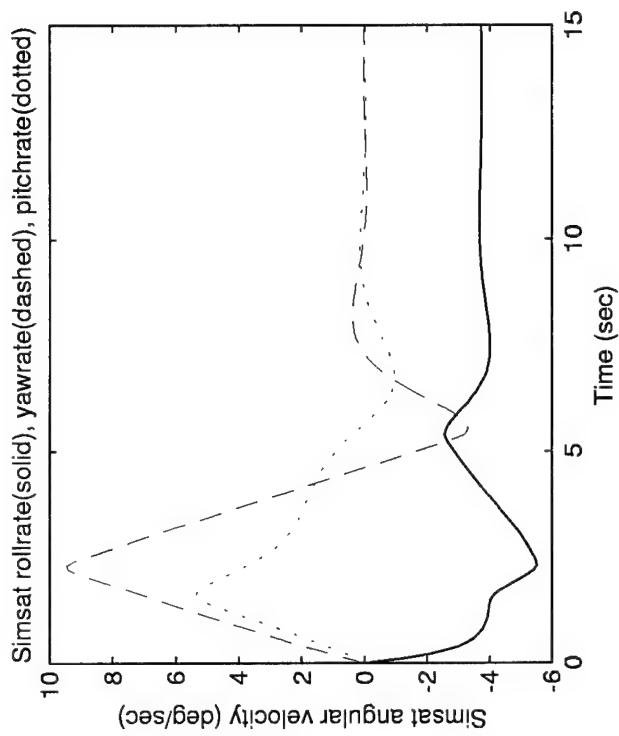
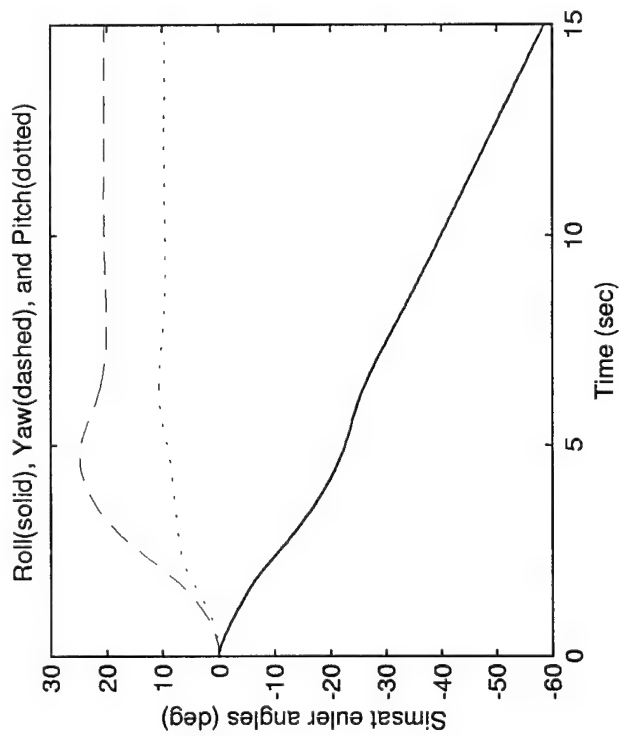
Option 2 (Target Mode with Roll Rate)
Maneuver #
1

Figure G.6 Option 2 (Target Mode with Roll Rate) - Maneuver 1



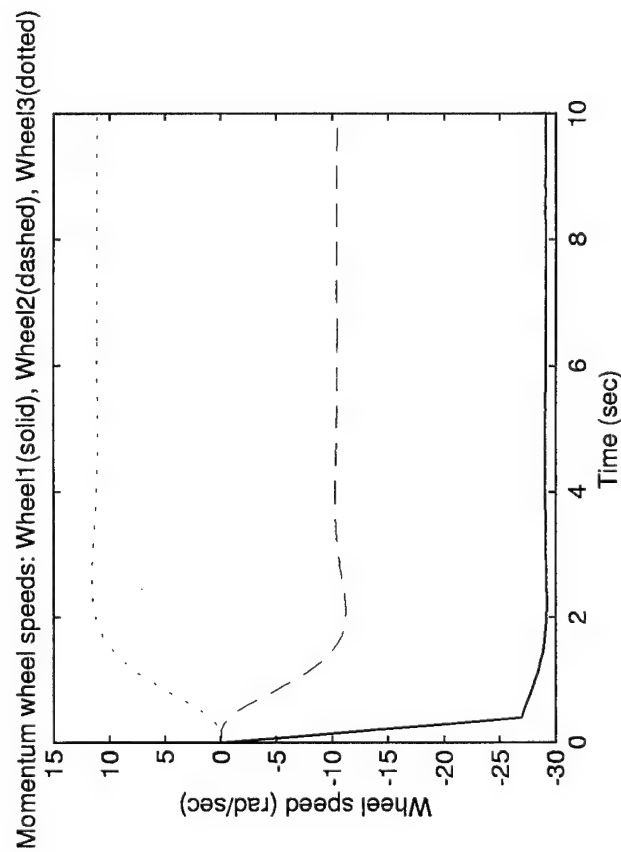
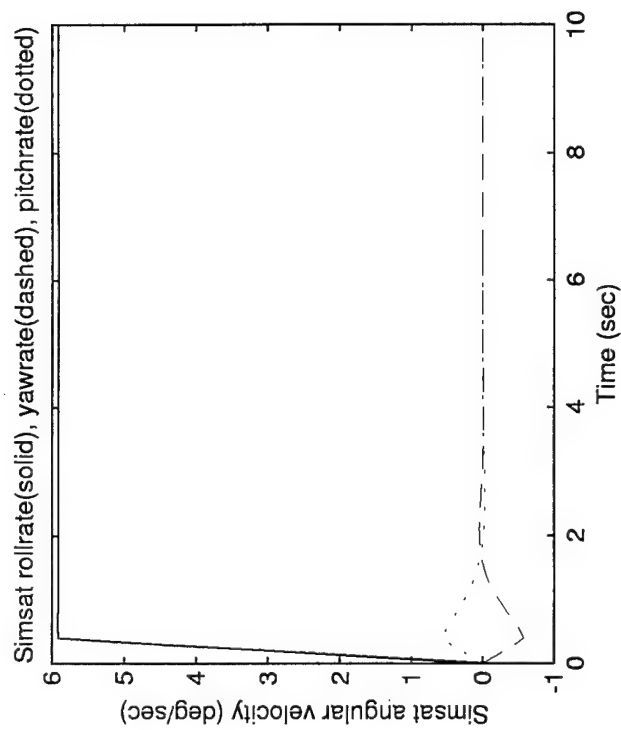
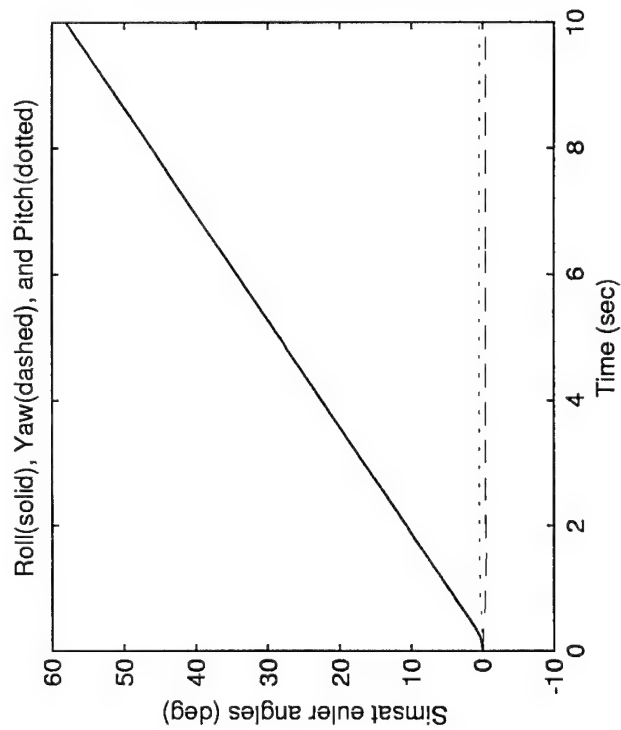
Option 2 (Target Mode with Roll Rate)
Maneuver #
2

Figure G.7 Option 2 (Target Mode with Roll Rate) - Maneuver 2



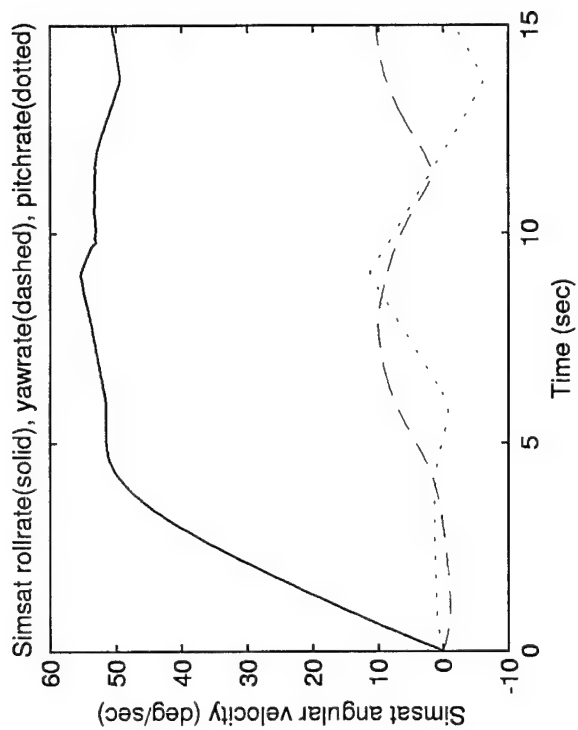
Option 2 (Target Mode with Roll Rate)
Maneuver #
3

Figure G.8 Option 2 (Target Mode with Roll Rate) - Maneuver 3



Option 3 (Roll Spin Mode)
Maneuver #
1

Figure G.9 Option 3 (Roll Spin Mode) - Maneuver 1



Option 3 (Roll Spin Mode)
Maneuver #
2

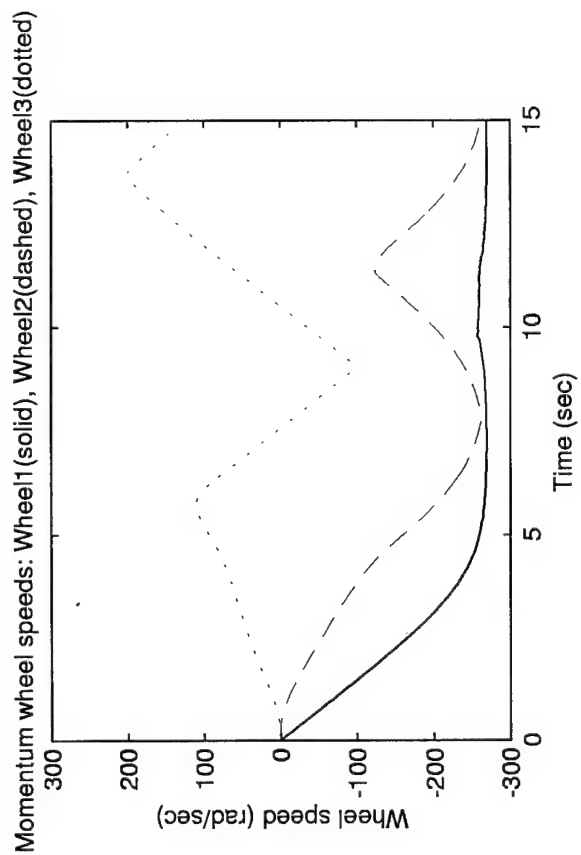
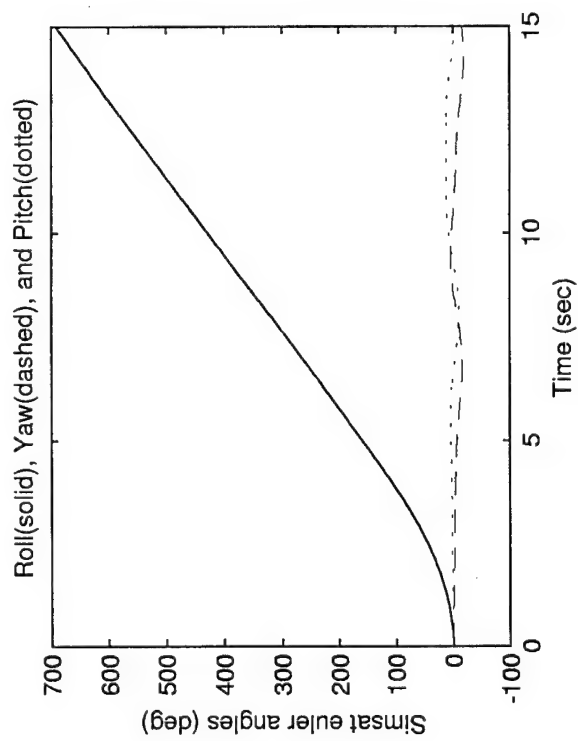
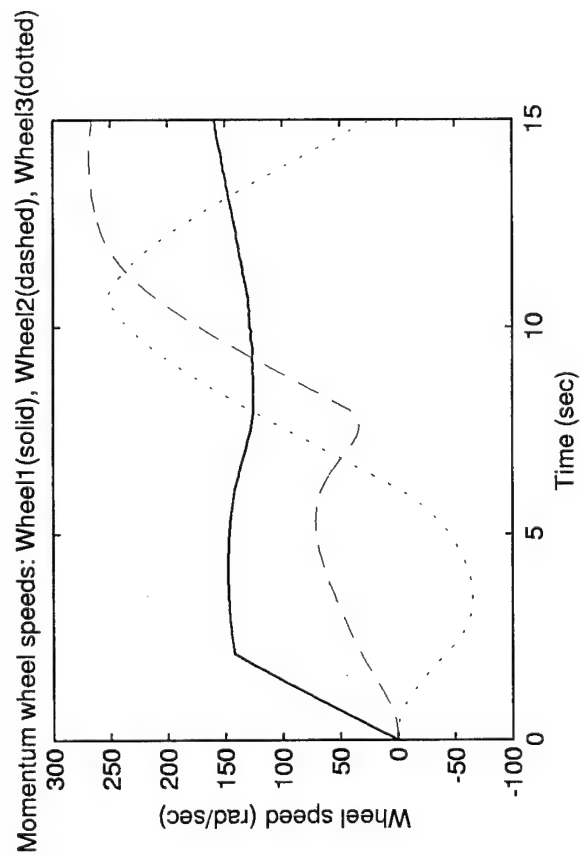
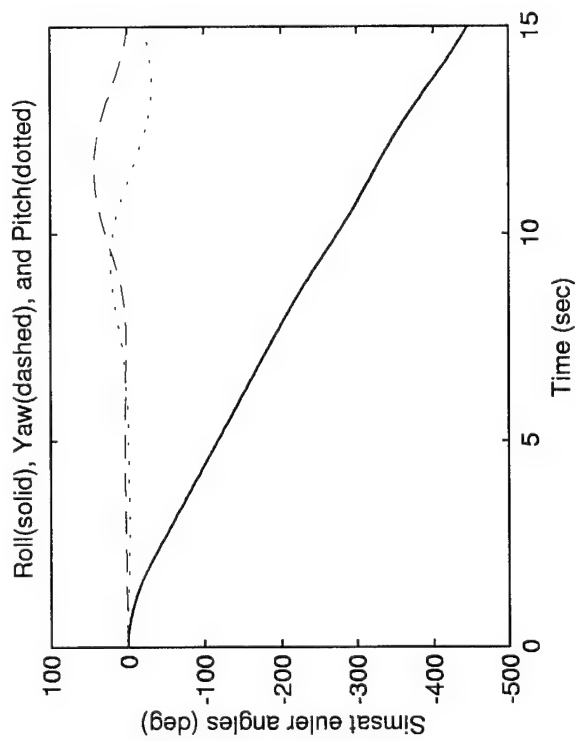
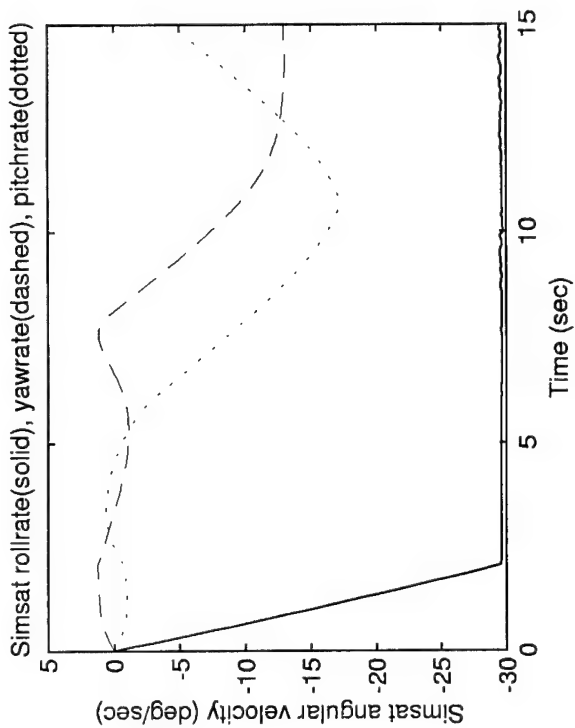
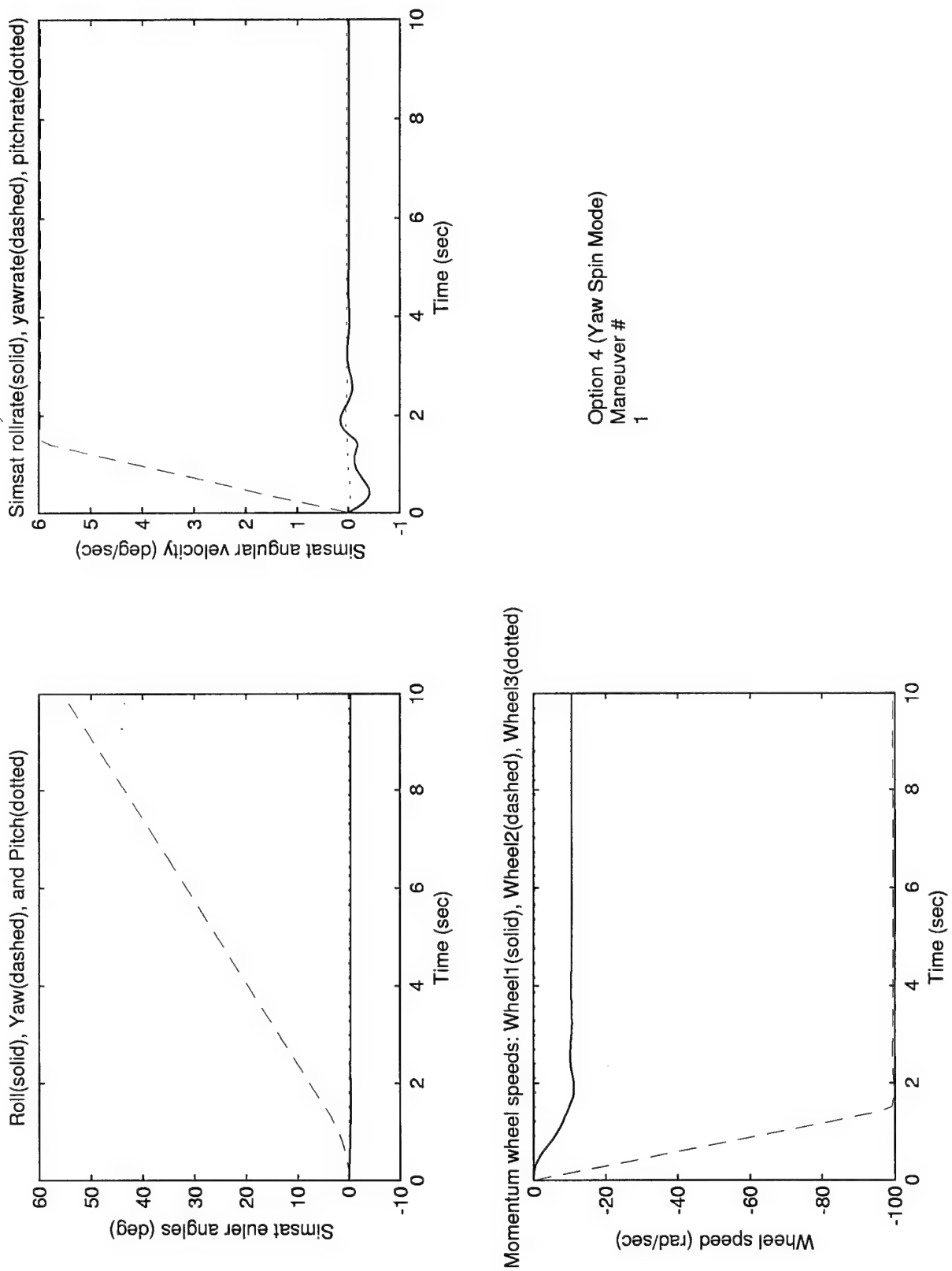


Figure G.10 Option 3 (Roll Spin Mode) - Maneuver 2



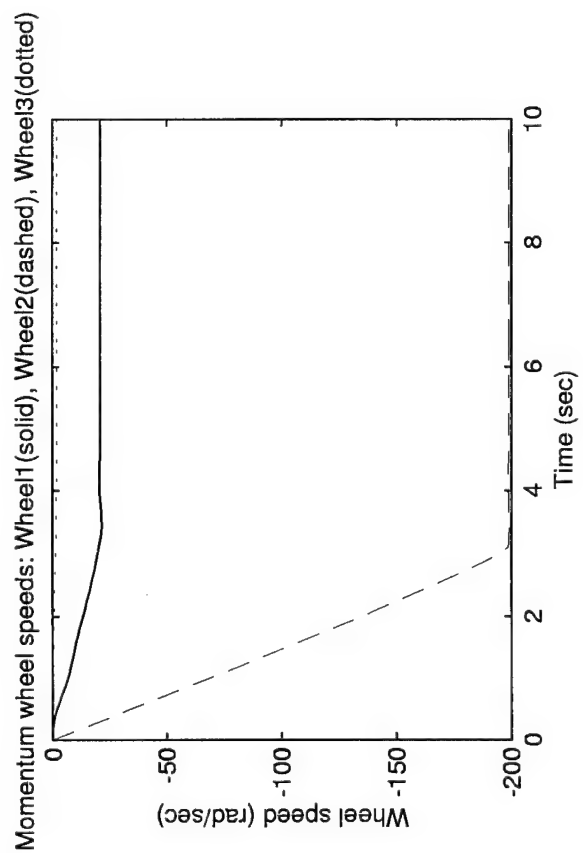
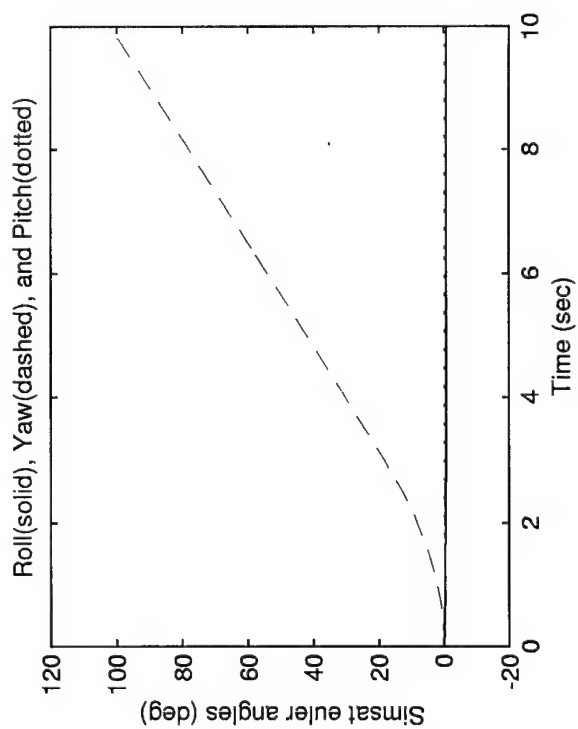
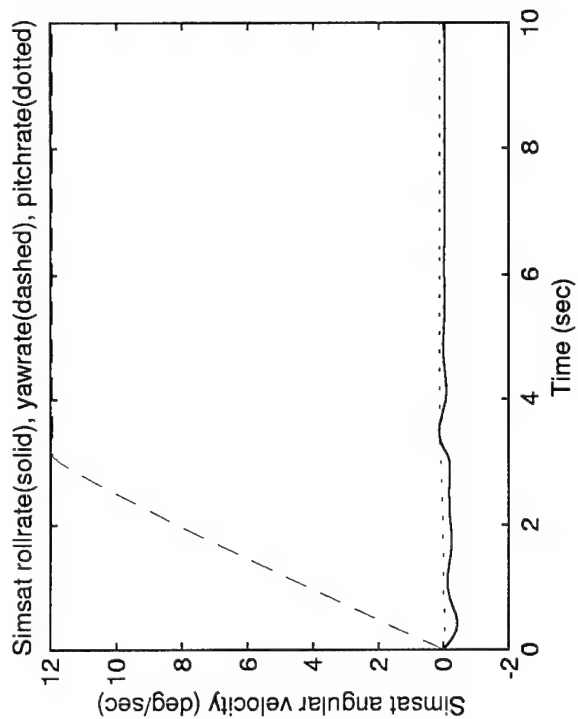
Option 3 (Roll Spin Mode)
Maneuver #
3

Figure G.11 Option 3 (Roll Spin Mode) - Maneuver 3



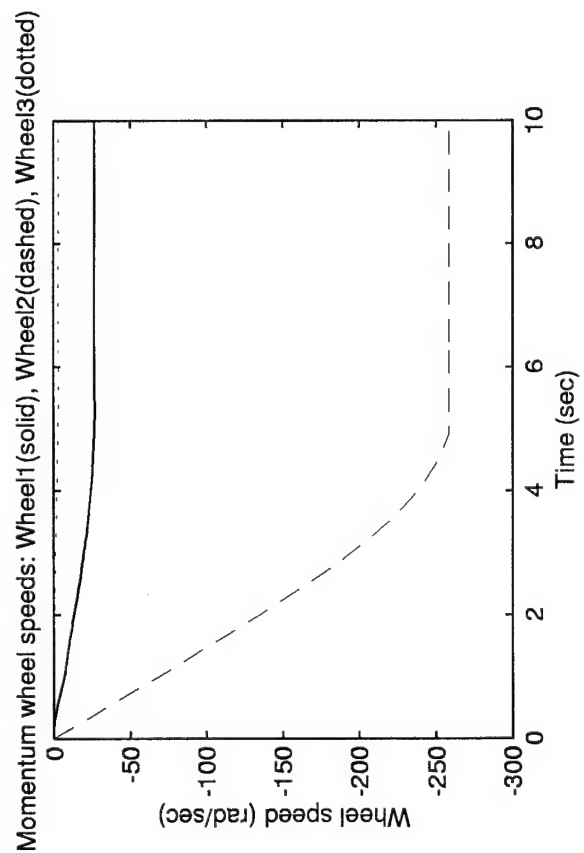
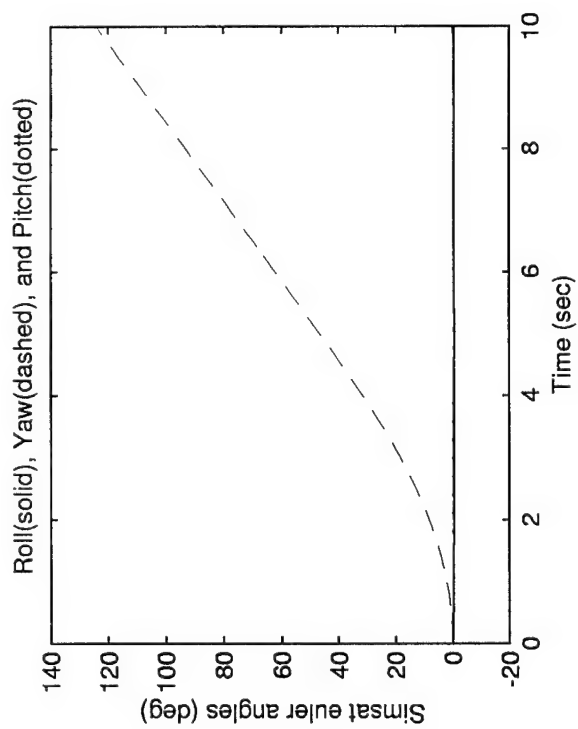
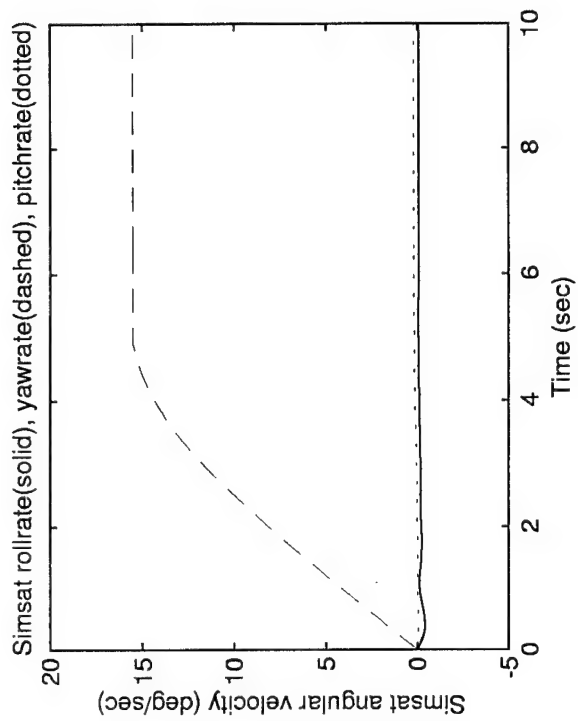
Option 4 (Yaw Spin Mode)
Maneuver #
1

Figure G.12 Option 4 (Yaw Spin Mode) - Maneuver 1



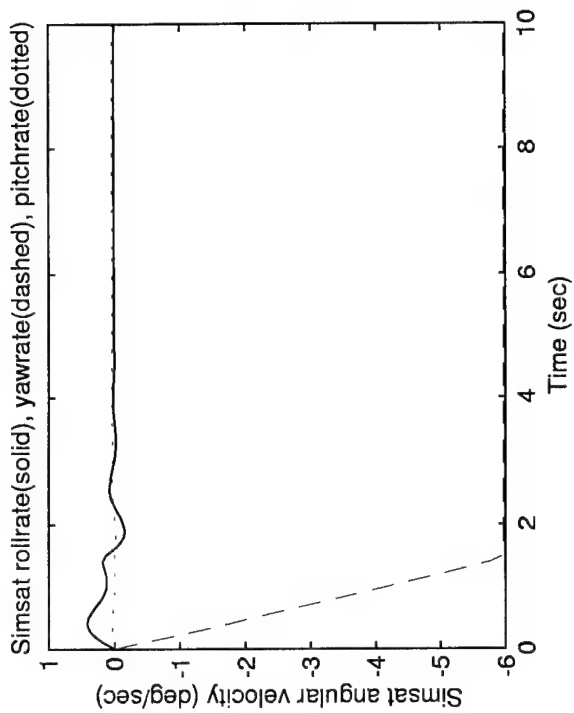
Option 4 (Yaw Spin Mode)
Maneuver #
2

Figure G.13 Option 4 (Yaw Spin Mode) - Maneuver 2



Option 4 (Yaw Spin Mode)
Maneuver #
3

Figure G.14 Option 4 (Yaw Spin Mode) - Maneuver 3



Option 4 (Yaw Spin Mode)
Maneuver #
4

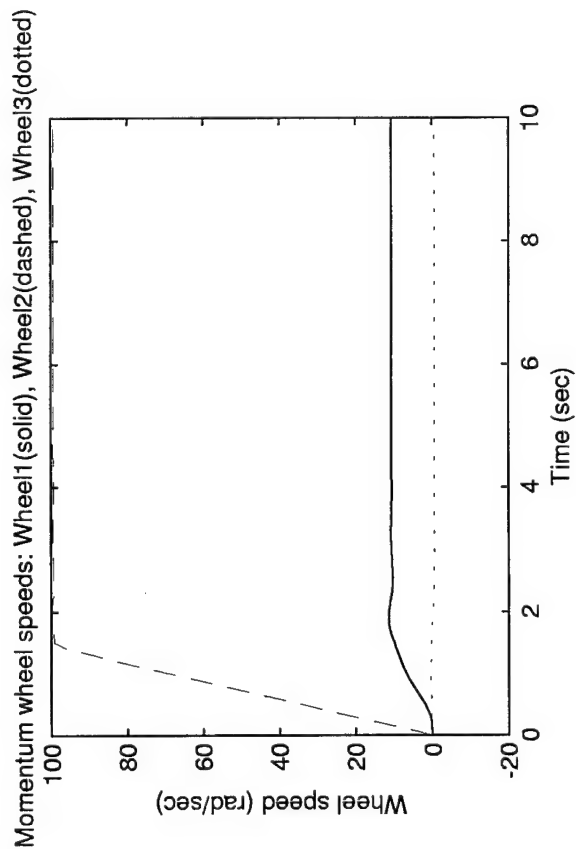
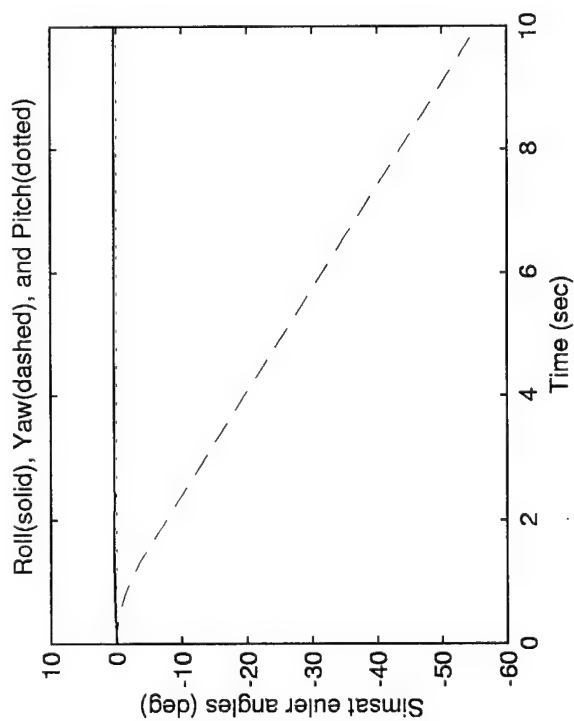
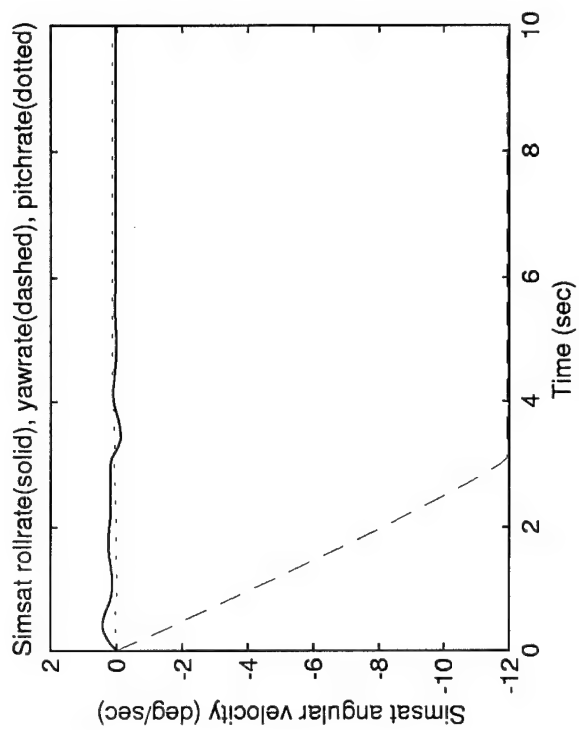


Figure G.15 Option 4 (Yaw Spin Mode) - Maneuver 4



Option 4 (Yaw Spin Mode)
Maneuver #
5

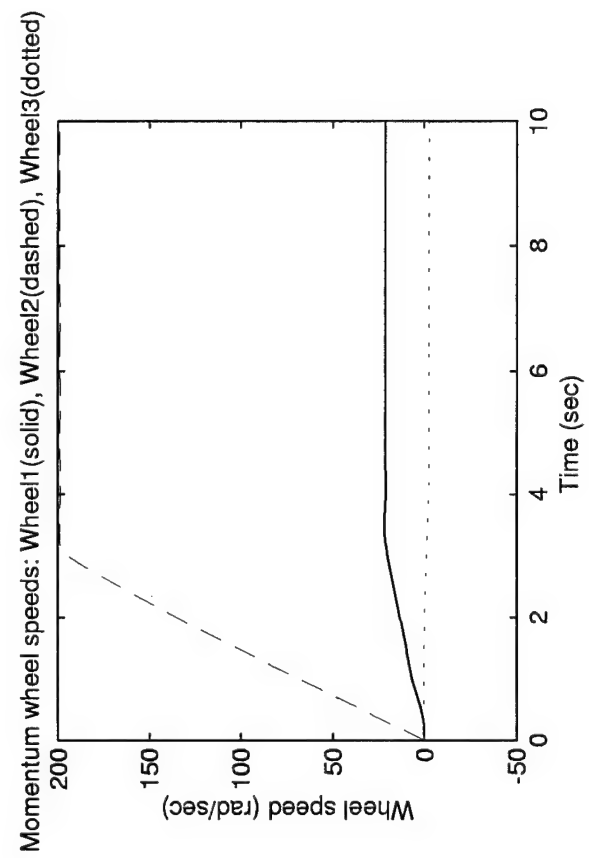
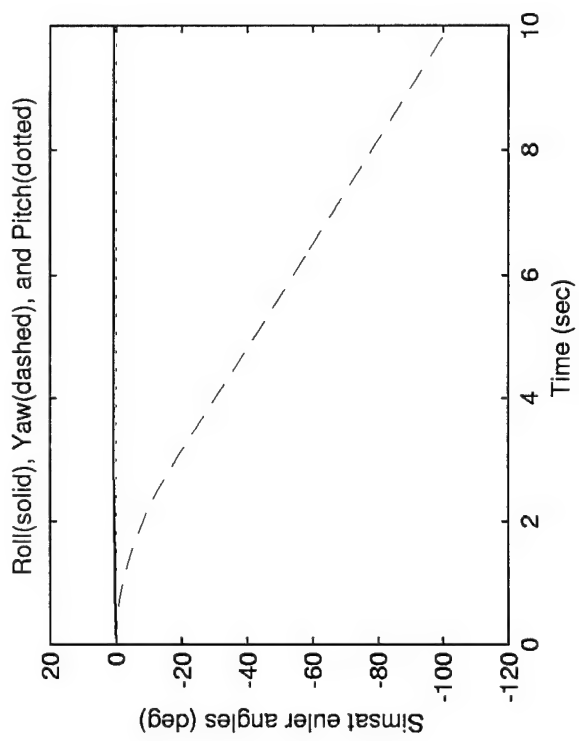
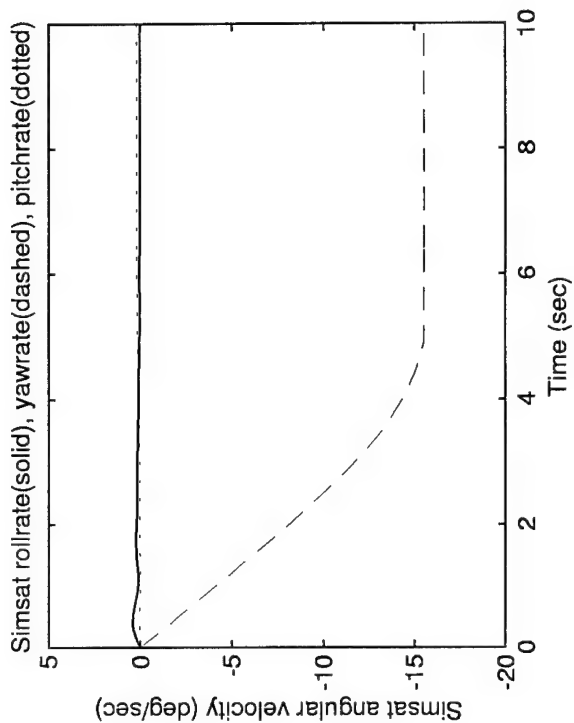


Figure G.16 Option 4 (Yaw Spin Mode) - Maneuver 5



Option 4 (Yaw Spin Mode)
Maneuver #
6

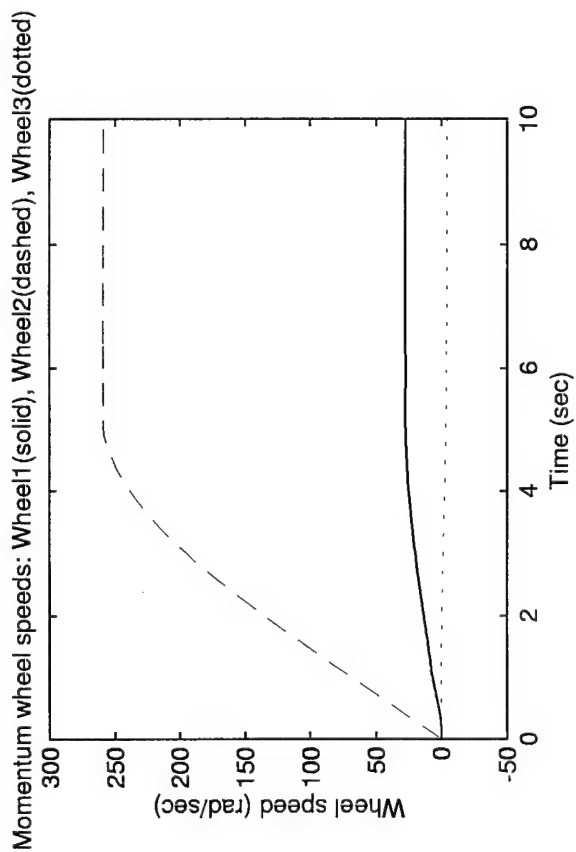
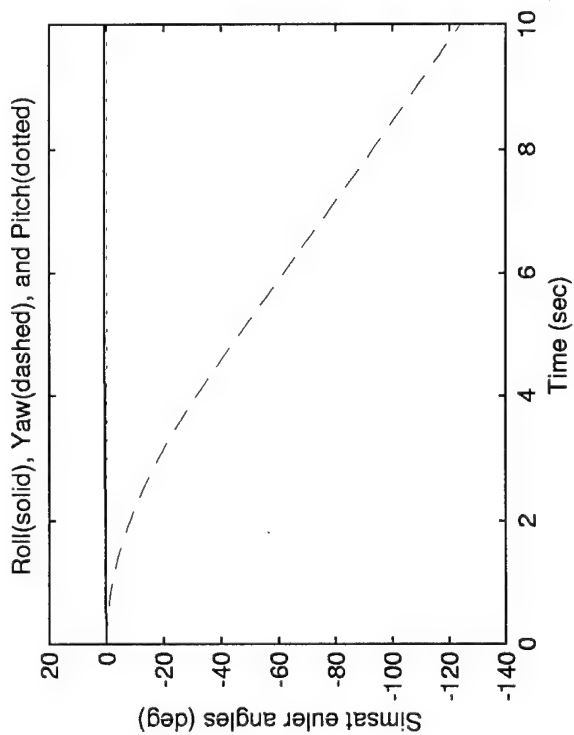
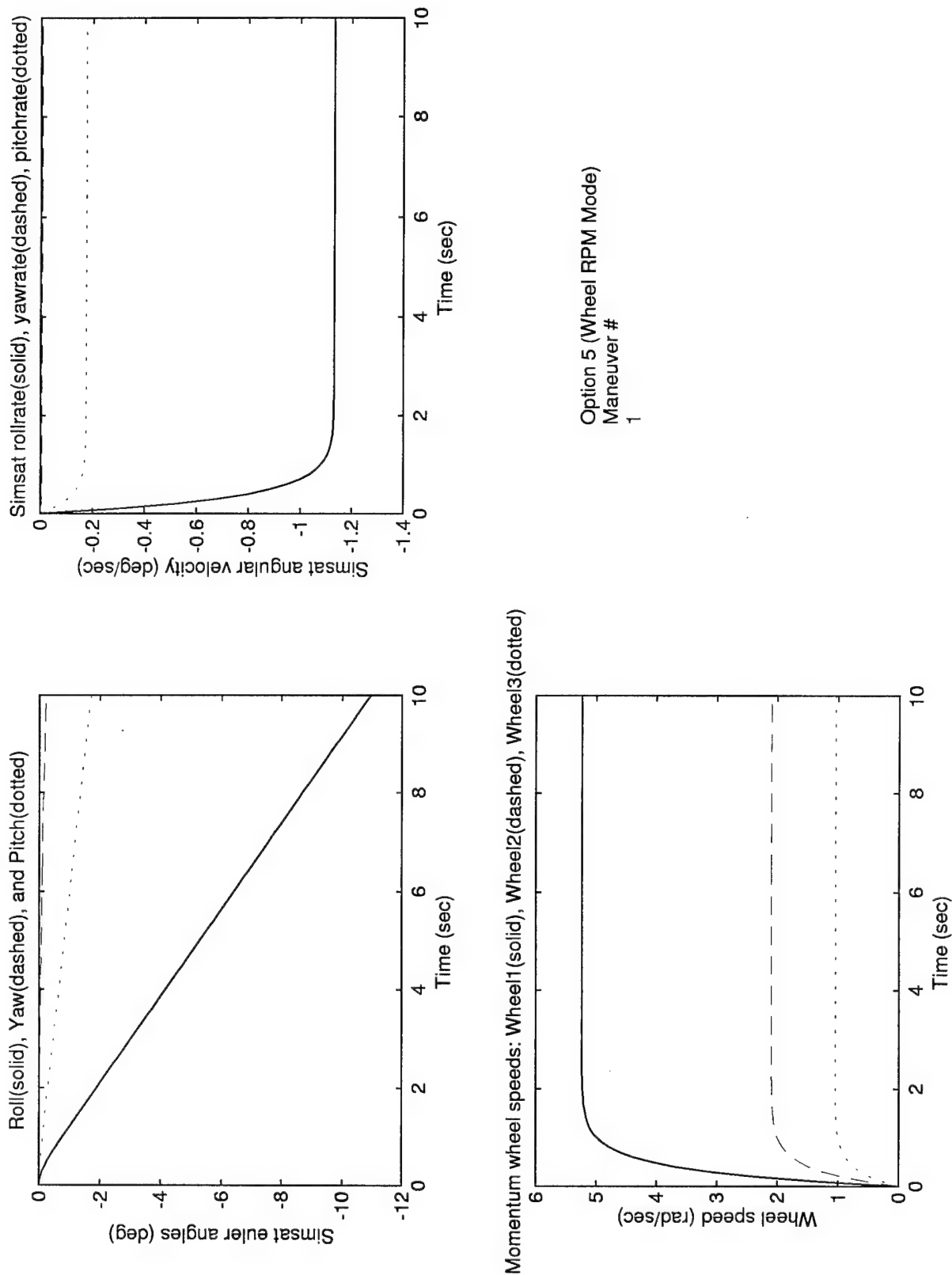
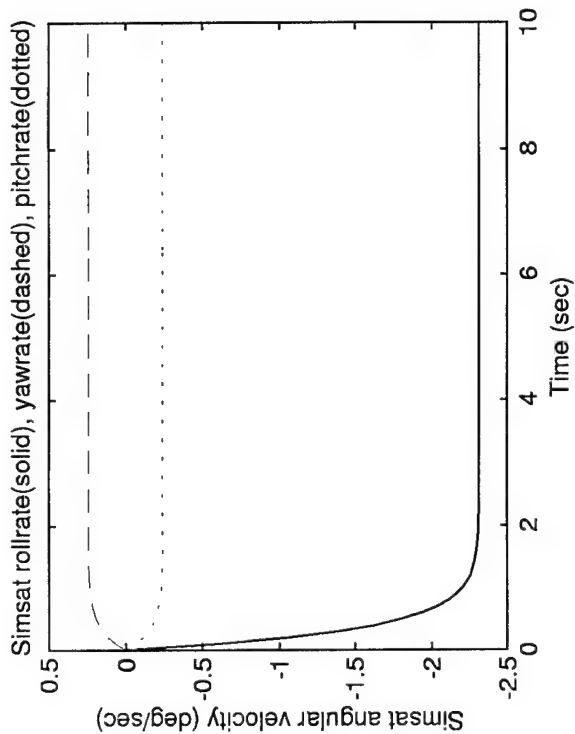


Figure G.17 Option 4 (Yaw Spin Mode) - Maneuver 6



Option 5 (Wheel RPM Mode)
 Maneuver #
 1

Figure G.18 Option 5 (Wheel RPM Mode) - Maneuver 1



Option 5 (Wheel RPM Mode)
Maneuver #
2

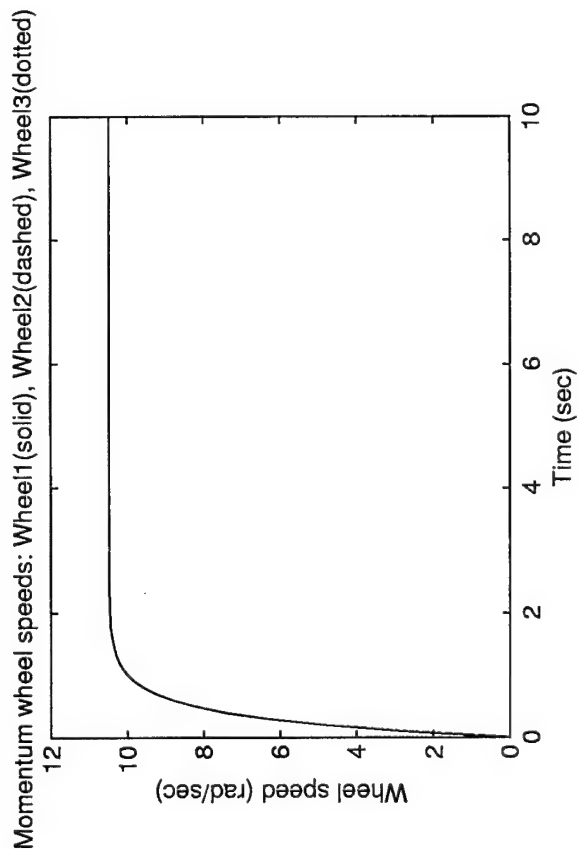
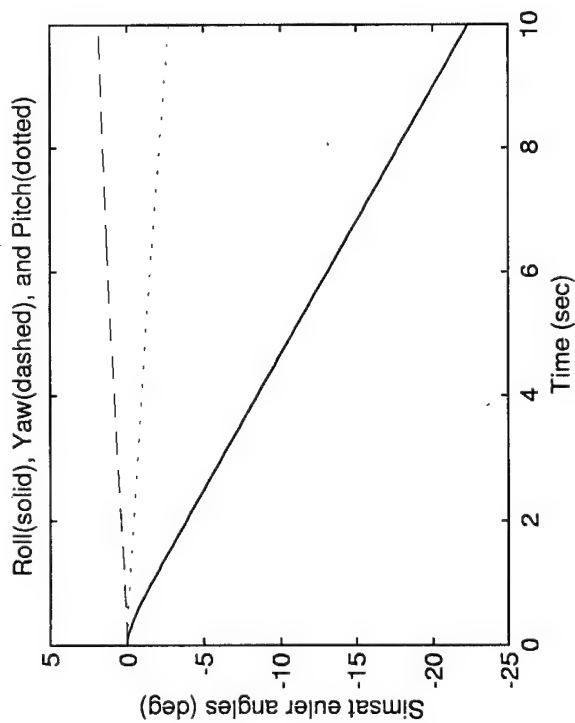
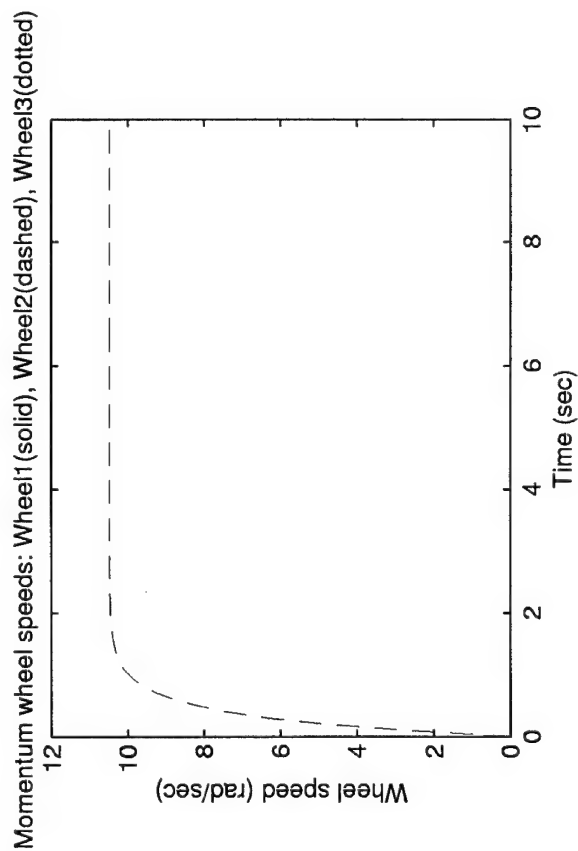
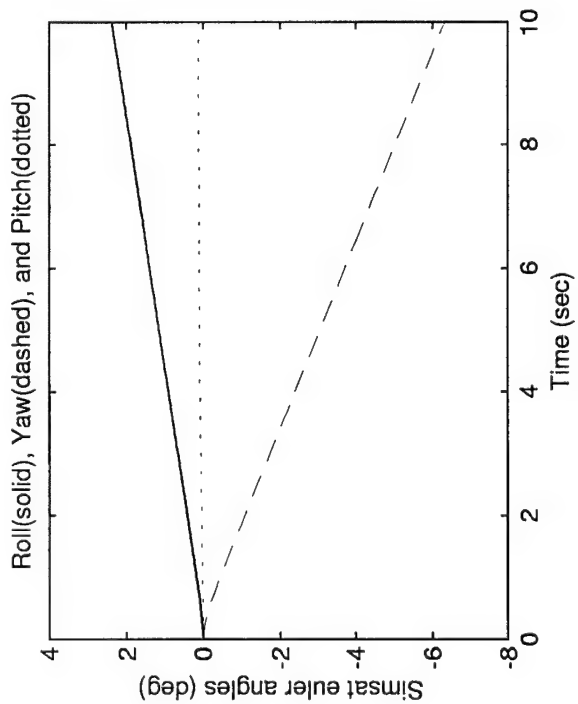
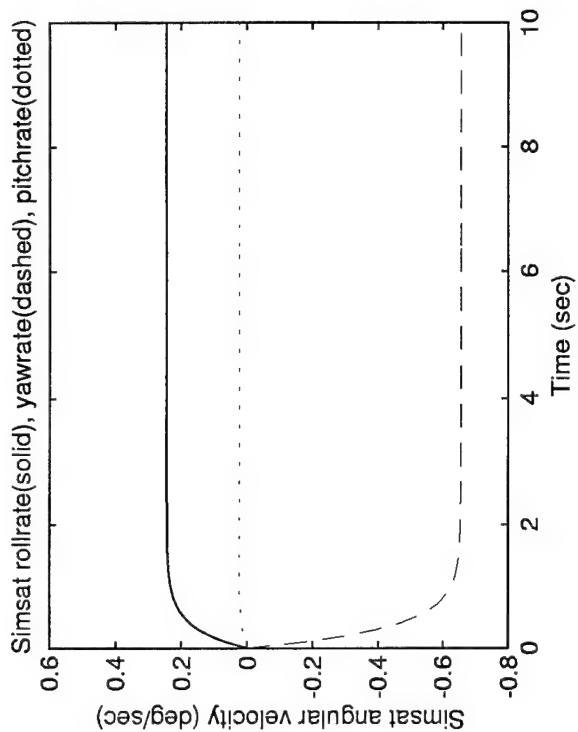


Figure G.19 Option 5 (Wheel RPM Mode) - Maneuver 2



Option 5 (Wheel RPM Mode)
Maneuver #
3

Figure G.20 Option 5 (Wheel RPM Mode) - Maneuver 3

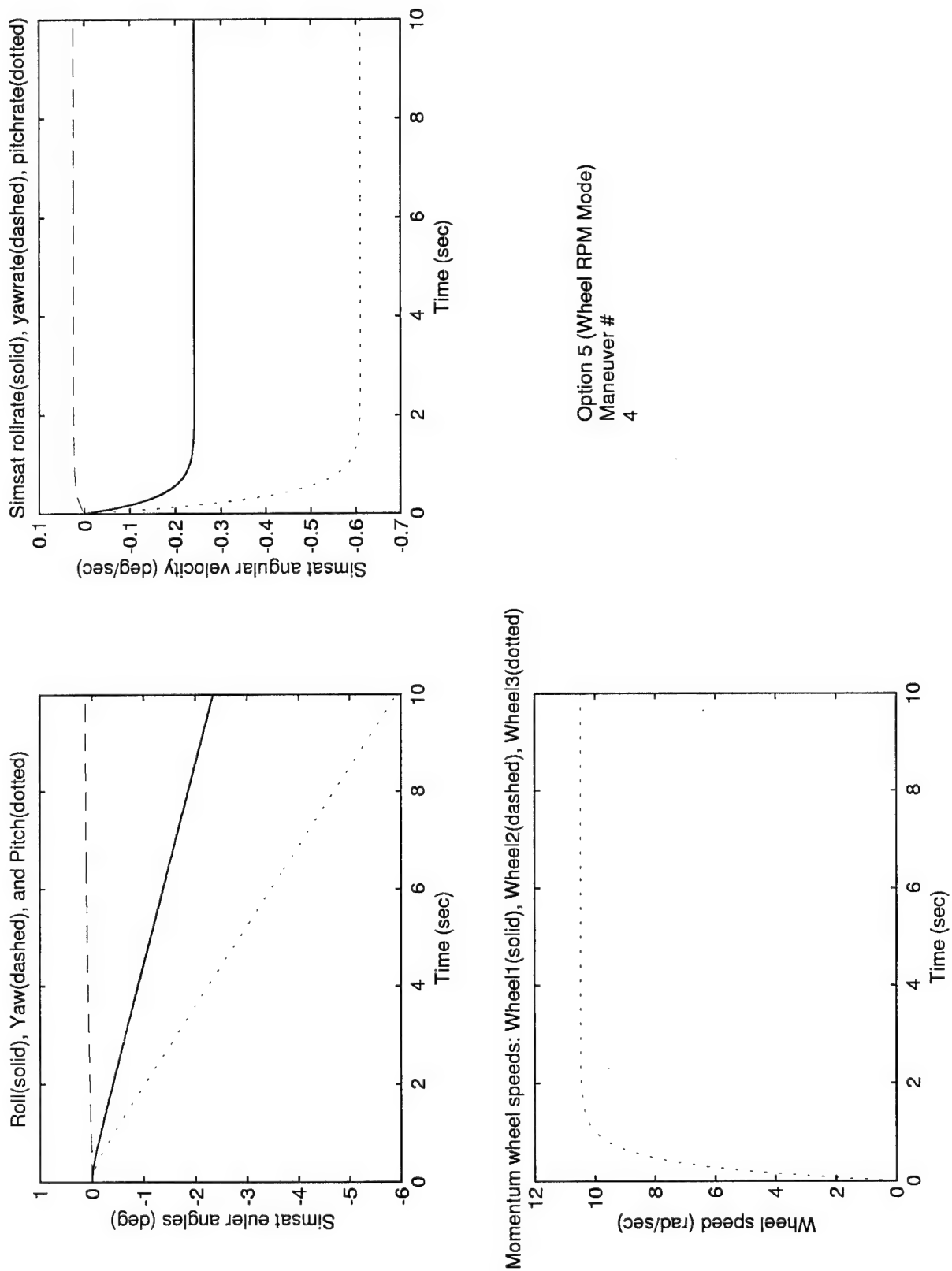


Figure G.21 Option 5 (Wheel RPM Mode) - Maneuver 4

Appendix H. Model Transfer Procedures

H.1 Overview

This appendix describes the procedures required to compile and download a SIMULINK model from the ground station PC to the AutoBox.

H.2 Model Compilation and Transfer Procedures.

After creating a SIMULINK model, it should be tested to ensure correct coding before beginning the compilation procedure. Run the model within the SIMULINK environment by selecting "Start" from the "Simulation" menu, or clicking on the "play" icon. Once the coding errors have been debugged within SIMULINK, continue with the following process:

1. Power up the AutoBox. (A double-beep will sound after a few seconds.)
2. From the "dSPACE Files" window, select "Connect to Autobox." (If there was not a double-beep following the previous step, it should sound after completing this step. Otherwise, check all power and data connections and start over.)
3. From the "dSPACE Files" window, select "Ping AutoBox." A DOS window will briefly appear indicating three to four replies from the AutoBox. If no replies are received (i.e., "request timed out"), repeat the previous step. Otherwise, check all power and data connections and start over.
4. Start SIMULINK (using either the "dSPACE Library" or "Simulink" icons in the "dSPACE Files" window).
 - (a) Open the desired SIMULINK model (*.mdl).
 - (b) From within SIMULINK, select "RTW Build" from the "Tools" menu, or press (Ctrl+B), to begin the compilation process (if the RTW Options have already been set correctly). Otherwise:
 - i. Select "RTW Options..." from the "Tools" menu (or select "Parameters..." from the "Simulation" menu).

- ii. Check the options on the “Solver” tab. dSPACE requires a fixed-step solver for real-time applications. (A fixed step size of 0.001, using ode4 or ode5, is recommended.)
 - iii. If using TRACE and/or COCKPIT applications, the options on the “Workspace I/O” tab can be ignored.
 - iv. Select the “RTW” tab and ensure all entries are correct:
 - Code generation, System target file: rti1003.tlc
 - Build options, Template makefile: rti1003n.tmf
 - Build options, Make command: make-rti board=autobox
 - v. Once the above options are set correctly, select “Build” from the “RTW” tab.
5. The Real Time Workshop (RTW) and Real Time Interface (RTI) will then begin the process of compiling the SIMULINK model into C-code, generating the associated files, and downloading to AutoBox.
- The first time a SIMULINK model is compiled a dialog box stating “Error executing build command: Error using rtw-c” will appear. Within the MATLAB Command Window, the messages shown in Figure H.1 will appear (for a SIMULINK model named “example”).
6. After the above error occurs, open the indicated *.stp file within a text editor. Change the text from “AutoBox” to “DS1003” and save the *.stp file with the same name.
7. Rebuild the model following the same process in Step 4(b) above. The messages shown in Figure H.2 will appear in the MATLAB Command Window indicating a successful download. (To avoid the above error from occurring with future changes of the SIMULINK model use the same filename.)

```

*** Starting RTI build procedure with RTI1003 3.1 (28-Apr-1998)

### Starting RTW build procedure for model: example
### Invoking Target Language Compiler on example.rtw
tlc -r example.rtw c:\dsp_cit\matlab\rti1003\tlc\rti1003.tlc -O. -
Ic:\dsp_cit\matlab\rti1003\tlc -IC:\MATLAB\rtw\c\tlc -aInlineParameters=0
### Creating project marker file: rtw_proj.tmw
### Creating example.mk from rti1003n.tmf
### Building example: dsmake -f example.mk board=autobox

BUILDING PROGRAM (single timer task mode)

Initial SimState: default (defined in srtframe.c)

[srtframe.c]
[example.c]
[rt_sim.c]
[ode4.c]

LINKING PROGRAM ...

LOADING PROGRAM ...

MON40NET - DS1003 Processor Board Monitor, Vs 5.4 - 32, (C) 1997 by dSPACE GmbH

DS1003 - autobox - I/O [0318H] - 64 KB at [0D0000H]
1024 KW local RAM (bank0), 0 KW local RAM (bank1), 256 KW global RAM

Searching DS1003 peripherals ...
Loading system setup ...

Loading setup example.stp ...
Error reading setup file example.stp.

Error loading setup.

DSP not started.

OPUS MAKE: Shell line exit status 1 (ignored)

DOWNLOAD ABORTED

```

Figure H.1 Error Messages
H-3

```

*** Starting RTI build procedure with RTI1003 3.1 (28-Apr-1998)

### Starting RTW build procedure for model: example
### Invoking Target Language Compiler on example.rtw
tlc -r example.rtw c:\dsp_cit\matlab\rti1003\tlc\rti1003.tlc -O. -
Ic:\dsp_cit\matlab\rti1003\tlc -IC:\MATLAB\rtw\c\tlc -aInlineParameters=0
### example.mk which is generated from rti1003n.tmf is up to date
### Building example: dsmake -f example.mk board=autobox

BUILDING PROGRAM (single timer task mode)

Initial SimState: default (defined in srtframe.c)

[srtframe.c]
[example.c]
[rt_sim.c]
[ode4.c]

LINKING PROGRAM ...

LOADING PROGRAM ...

MON40NET - DS1003 Processor Board Monitor, Vs 5.4 - 32, (C) 1997 by dSPACE GmbH

DS1003 - autobox - I/O [0318H] - 64 KB at [0D0000H]
1024 KW local RAM (bank0), 0 KW local RAM (bank1), 256 KW global RAM

Searching DS1003 peripherals ...
Loading system setup ...

Loading setup example.stp ...
Loading object module example.obj ...

DSP started ...

DOWNLOAD SUCCEEDED

### Successful completion of RTW build procedure for model: example

*** Finished RTI build procedure for model example

```

Figure H.2 Successful Download Messages

8. With a successful download, the above process is not required to reload the compiled model after a power-down. After restarting AutoBox, follow these steps:

- (a) From the "dSPACE Files" window, select "Monitor" to run the MON40NET program. A DOS window will appear with "DSP is RESET" followed by several options. Select "Load object module" by typing a 1 at the prompt.
- (b) At the prompt "Enter the filename of object module (without suffix)" type the name of the *.obj file (for the compiled model) with its full path and press enter.
- (c) Select "Restart DSP" by typing a 2 at the prompt. "DSP is RUNNING" will appear above the menu, indicating that the program is now running on AutoBox.

Appendix I. Designing the User Interface

I.1 Overview

This appendix describes the procedures required to link SIMULINK variables with TRACE and COCKPIT applications. The following sections outline the process of implementing the user-interface software once a properly working SIMULINK model is successfully compiled and downloaded to the AutoBox.

I.2 TRACE.

1. From the "dSPACE Files" window, select the "Trace" icon. (If the PC is not currently communicating with the operating AutoBox, an error message will display. This can be ignored for design purposes, but the simulation program must be running on the AutoBox and communicating with the ground station PC to receive real-time updates of plotting data.)
2. Two windows will open: the "TRACE Net Control Panel," containing the tools for linking the command and control variables with TRACE plots, and the "Trace Plots" window, containing the graphing area.
3. The last TRACE files used in both windows will automatically open by default. The "File" menu on the Control Panel can be used to open other previously created files. To create a new TRACE set-up, follow these steps:
 - (a) Select "Load Trace File..." from the "File" menu or click on the first icon on the Control Panel toolbar.
 - (b) Find the TRACE file (*.trc) corresponding to the compiled real-time or simulation program that will be running on AutoBox and open it. This *.trc filename should appear below the menu toolbars, followed by the path to the folder containing this file and all the other files created by the compilation process.

- (c) Once the TRACE file is loaded, two Control Panel windows will display the tree structure of the corresponding simulation code. The small window simply shows the entire structure, while the large center window zooms in on the tree to allow access to the model structure.
- (d) Click within the large tree structure window at the center of the Control Panel and find the “Model Root” block. Select this block to display a list of simulation variables on the right side of the Control Panel. The variable names are preceded by one of the following letters:
- L = labeled signal
 - B = block output
 - S = input of signal sink
 - P = block parameter
- (e) From this variable list, select the desired signal to plot in the graphing display. Output blocks in the original SIMULINK code correspond to variables preceded by an “S,” so ensure the variables chosen for TRACE display have an “S” in front of the variable name.
- (f) After clicking on the desired signal variable, a graphing window for this variable should appear on the plotting screen. With a signal to plot, a TRACE “template” file can be created to store the desired graphing options for the user interface.
- (g) Return to the Control Panel and select the other signals to plot. If it is desired to plot multiple signals on a single graph, initially only select one variable per plot to establish the graphing window. Once all signals have been selected (or one variable of a multiple signal plot), arrange the graphing windows as desired within the TRACE plots screen.
- (h) General graphing features can be selected under the “Options” menu of the plotting screen. For example, a grid can be placed on the graph and “Scaling of Axes...” can be used to set upper and lower bounds of the graph or choose “Floating” to automatically rescale based on the current data capture.

- (i) To plot multiple signals on one graph, select "Reference..." under the "Options" menu of the plotting screen. This process is similar to the initial signal selection from the Control Panel. Use the "tree" window to find the "model root." Within the list of variables on the right, the initial signal selection will have a block marking it. Simply select any other variables to plot on the same graph and return to the plotting screen. A small box at the lower left of the current graph can be selected to show the signals to be plotted, and their corresponding line colors.
 - (j) After completing the process of selecting the desired signals to plot, and designing the TRACE Plots window to the user's preference, ensure the template is saved under the "File" menu.
 - (k) Once the desired TRACE file (*.trc) and template (*.tpl) are open within the TRACE environment, check the rest of the TRACE options on the Control Panel. The interval length of real-time data capture can be selected in the lower left of the Control Panel. This allows near instantaneous variable updates, however a length of 10 seconds is recommended to provide frequent updates, but with more data displayed at a time. Upon finishing the set-up of the TRACE environment the settings must be saved by selecting "Save Experiment..." from the Control Panel "File" menu. The current TRACE file, template, and settings will automatically display the next time TRACE is started unless a new experiment is opened.
4. Before beginning a simulation or real-time application, check to make sure the desired TRACE files are being used. The *.trc file corresponding to the program running on AutoBox should be shown below the Control Panel toolbar, along with the proper directory path. The current template will be listed at the top of the TRACE Plots screen. The loaded experiment file (*.exp) will be listed at the bottom of both screens.
 5. When all the above steps have been successfully completed, TRACE is ready to display telemetry. If the simulation or real-time application is running on AutoBox, and communication links are working, selecting "Start" in the TRACE windows will begin

data capture and plotting. Selecting "Auto" (next to "Start" in the plotting window and below "Start" on the Control Panel) allows automatic updating of plots according to the defined interval length. If "Auto" is not selected, the user must manually select when to conduct a data capture. To stop TRACE telemetry monitoring, simply select "Stop."

6. Following a telemetry monitoring session, TRACE plot data can be saved to a MATLAB *.mat file using the "Save Current Capture..." option on the "File" menu of the Control Panel. This *.mat file is then available to graph the results in MATLAB at a later time, according to user needs.

I.3 COCKPIT.

1. From the "dSPACE Files" window, select the "Cockpit" icon. (If the PC is not currently communicating with the operating AutoBox, an error message will display. This can be ignored for design purposes, but the simulation program must be running on the AutoBox and communicating with the ground station PC to use COCKPIT for command and control.)
2. The "COCKPIT Net" window will open. At the top are the menu and toolbar for designing the graphical user interface. The area below the menus is available for positioning input and output control and display instruments.
3. Use the "File" menu to open a previously created file. Otherwise, follow these steps to create a new COCKPIT display:
 - (a) Select "Load Trace File..." from the "File" menu or click on the corresponding toolbar icon.
 - (b) Find the TRACE file (*.trc) corresponding to the compiled real-time or simulation program that will be running on AutoBox and open it. This *.trc filename should appear below the menu toolbars, followed by the path to the folder containing this file and all the other files created by the compilation process.

- (c) Once the TRACE file is loaded, design of ground controls can begin. Under the "Options" menu a "Quick Control" toolbox can be selected for display, in addition to the standard toolbar, or COCKPIT instruments can be accessed from the "Control" menu.
 - (d) Select a control instrument in one of the ways listed above. Once a specific control is selected, it can be placed anywhere in the empty window and sized as desired. This instrument will continue to be drawn until another type is selected.
 - (e) Double-click on an instrument placed in the design area to open its parameter dialog box. The application program's tree structure will be displayed, just as on the TRACE Control Panel.
 - (f) Click within the large tree structure and select the "Model Root" block.
 - (g) From the variable list on the right, select the desired variable to link to the control instrument. Input blocks in the original SIMULINK code correspond to variables preceded by a "B," so ensure a variable chosen for sending commands has a "B" in front of the variable name. Just as in TRACE, use a variable preceded by an "S" for a display instrument.
 - (h) Depending on the type of control instrument selected, other parameter entries are made. For example, the initial value (origin) of a variable and its maximum and minimum commanded values can be set. These parameter choices will be reflected in a graphical instrument upon returning to the main window.
 - (i) Once all instruments have been selected (ensure parameters are properly defined), arrange them as desired for the user interface.
 - (j) The method of obtaining initial values when starting a simulation can be defined using the "Setup" menu.
 - (k) Save the COCKPIT instrument layout as a *.ccs file, which allows it to be reloaded in the future.
4. Before beginning a simulation or real-time application, check to make sure the desired TRACE files are being used. The *.trc file corresponding to the program running

on AutoBox should be shown below the menu and toolbar, along with the proper directory path. The loaded instrument set-up file (*.ccs) will be listed at the top of the window.

5. When all the above steps are complete, the COCKPIT user interface is ready for operation. If the simulation or real-time application is running on AutoBox, and communication links are working, select "Start" on the toolbar or from the "Animation" menu.

Appendix J. Design and Operation of REALMOTION Interface

J.1 Overview

This appendix describes the design and operation of the REALMOTION 3-D animation tool. REALMOTION is a dSPACE software product allowing visualization of *SIMSAT* motion real-time, as well as post-mission (or simulated from data). A separate PC is required to run the REALMOTION software.

J.2 Software Links.

The design process included modifying C-code generated by the dSPACE compilation of SIMULINK, creating a geometric model, and developing its associated scene control file. The operation of REALMOTION required locating the DSP card to load the necessary simulation files, and starting the 3-D animation by opening REALMOTION. The following steps outline how the SIMULINK-designed code was modified for use with REALMOTION.

1. The header file `rmproto.h` was included in the application C-code.
2. The snapshot buffer was defined according to the variables of the software. This block of code is necessary to ensure REALMOTION preserves enough memory.
3. The snapshot function is used to "freeze" model variables by storing them consistently into the snapshot buffer.
4. The transformation function calculates the translation vectors and the rotation matrix for each of the model members. The "frozen" snapshot buffer data are copied to local variables from which the motion data of the members are derived.
5. The `rm-init-interface` call is the main initialization function of REALMOTION. The parameters for this section of code include the number of members, the name of the transformation function, the name of the snapshot function, and the size of the snapshot buffer.

6. The `rm-set-member-name` is an optional call used to store legible names for each member together with the motion data in order to easily identify the motion data structures in REALMOTION.
7. The `snapshot` call is used to call the `rm-snapshot` macro from within the model's real-time section.
8. The `rm-service-realmotion` call is used to call the `rm-service-realmotion` macro from within the background task.

The above steps can be reaccomplished with each new version of software architecture. However, since REALMOTION is simply displaying the change in orientation variables, which will always be available, a one-time file modification can be made. Adding the above code segments to the *.usr file will allow new versions of command and control software to be created, without having to add the above code every time.

J.3 Scene Control.

Example code segments of a REALMOTION Scene Control File affecting all animations:

```
RAMSIZE = 800000
```

```
NFRAMES = 1500
```

```
STARTFRAME = 1
```

```
STEPFRAME = 1
```

```
RESULT = ORIENTATION, %ONLINE
```

```
GPOLYGON = TRUE
```

```
BACKGROUND = 1, 1, 0.705
```

General data for all windows:

RAMSIZE = 800000 sets the memory allocation (limit=2,000,000 bytes).

NFRAMES = 1500 gives the total number of displayed frames (max=1500).

STARTFRAME = 1 establishes the first frame to display.

STEPFRAME = 1 defines the step size of the frame counter.

RESULT = ORIENTATION, %ONLINE indicates that real-time motion data retrieval will be used during the animation, rather than an off-line data file. The result filename (ORIENTATION) links the motion data with the geometric model components.

Window dependent data:

GPOLYGON = TRUE displays all components of the geometric model as polygons.

BACKGROUND = 1, 1, 0.705 sets the background color, in terms of amount red, green, and blue (from 0 to 1 each), i.e. this background is a light yellow.

Example of code to define a graphical *.dxf file "member" (a SIMSAT component):

MEMBER = ARM1, SIMSAT.DXF, 1

FORMAT = DXF

MAPPING = TRUE

MOTIONRESULT = ORIENTATION, 1

RGB = 1, 1, 0

WIRE = TRUE

MEMBER = ARM1, SIMSAT.DXF, 1 defines the name of the graphical object (ARM1), the *.dxf file to use (SIMSAT.DXF), and the object's number (if more than one).

FORMAT = DXF is the format of the geometry file.

MAPPING = TRUE allows use of automatic centering and distance adaptation.

MOTIONRESULT = ORIENTATION, 1 names the file for motion result data (orientation.mdf).

RGB = 1, 1, 0 assigns the color of the object (red, green, and blue) based on the intensity (0-1), i.e. this member is yellow.

WIRE = TRUE indicates a wire model representation.

(The above code segment is repeated for the other SIMSAT members, with appropriate modifications. For example, different colors can be assigned to members on opposite sides to allow easier identification of a side during animation. Each member should also be given a short, descriptive name. The name will appear in the Member List of the display window's "Member" menu. This can be used to select a member and modify its attributes directly from the display window, without changing the default scene control file.)

Example of code to define an "Observer" perspective:

```
OBSERVER = REMOTE-PILOT, FIXED, INERTIAL
ACENTER = TRUE
DISTANCE = 1
ROFFSET = 90, 0, 0
VIEWRoffset = 1, 1, 1
VIEWToffset = 1, 1, 1
ZOOM = 1.5
```

OBSERVER = REMOTE-PILOT, FIXED, INERTIAL names the observer (remote-pilot) and sets the reference frame fixed in inertial space.

ACENTER = TRUE sets automatic centering for all members, preventing them from being moved with the mouse.

DISTANCE = 1 represents a distance scaling factor (greater than 1 increases the distance, less than 1 decreases the distance), i.e. DISTANCE = 2 halves the picture size.

ROFFSET = 90, 0, 0 provides the basic rotation (pivoting of observer) around the axes, i.e. this observer is rotated about the x-axis to provide a side-view of the object.

VIEWRoffset = 1, 1, 1 is the pivoting angle of the scene.

VIEWToffset = 1, 1, 1 is the translation of the scene.

ZOOM = 1.5 is a zoom angle factor (greater than 1 increases the zoom angle, less than 1 decreases the zoom angle), i.e. ZOOM = 2 halves the picture size.

(Up to eleven different "observers" can be defined. The point-of-view for observing can then be chosen from the "Observer" menu of the display window.)

Using one of the following sets of steps accesses the REALMOTION DSP card, loads the necessary files, and gets the animation running.

1. Change the active path to the directory containing the dSPACE and REALMOTION files for the desired application.
2. Type "mon40 *name-of-file* -B RealMot".
3. Start the REALMOTION application by selecting "REALMOTION" from the "dSPACE Files" window.
4. Load the desired scene control file (i.e., Simsat.ctl).

Equivalent process:

1. Select the "Monitor" icon in the "dSPACE Files" window.
2. From the MON40 menu, select [1] Load object module.
3. Type desired path and filename.
4. The MON40 menu should reappear. If not, check to make sure that the desired file and directory exist, and retry the previous steps.
5. Select [2] Restart DSP.
6. Start REALMOTION.
7. Load the desired scene control file (i.e. Simsat.ctl).

Animation should begin automatically.

Appendix K. Final Structural Design

K.1 Overview

This appendix describes the detailed design of the *SIMSAT* structure. Using the AutoCAD and 3D Studio VIZ software packages, structural evolution progressed from initial concepts and sketches to detailed drawings suitable for system fabrication. The figures at the end of this appendix are copies of the design drawings submitted to the AFIT Fabrication Shop.

The following pages describe in detail the structural elements of the *SIMSAT* design. Rationale for these design decisions is also presented.

K.2 Structural Design

The *SIMSAT* structure supports individual components and acts as a skeleton for the entire system. The *SIMSAT* structure consists of two box trusses attached to the mounting arms of the central air-bearing assembly. Aluminum and steel are used almost exclusively as construction materials, with lexan used as a cover surrounding the momentum wheel assembly. Maximum use of standard components and interfaces within the structural design allows for increased modularity and the ability to reconfigure *SIMSAT* to meet changed requirements. Modular design also provides for easy access to items (such as batteries) which must be removed or serviced between experiments.

The baseline *SIMSAT* structure (baseplates, mounting plates and 8 support rods) has a total mass of approximately 37.5 kg. This mass represents an upper limit and does not reflect the effect of follow-on efforts to reduce structural mass through the use of thinner mounting plates, lightening holes, or better-optimized structural members.

Each side of the *SIMSAT* structure is based upon a box truss construction using standard plates and stringers. Each truss is mounted to the air-bearing with an aluminum 7075-T7 collar. Each cylindrical collar has an outer diameter of 4.875" and a height of 2". A 2" diameter hole with 3/16" deep counterbore (3" diameter) is centered on the circular

face of the collar to allow for cable routing through the hollow mounting shafts and central sphere.

Base plates allow for the attachment of each truss to its respective collar, and mounting plates provide attachment points for individual components. A standard template is used for all plates, which are available in a variety of thicknesses ($1/2''$, $1/4''$, $3/16''$, $1/8''$, and $3/32''$). Aircraft-grade aluminum is used in all instances: aluminum 7075-T6 for $1/8''$ and $3/16''$ plates, aluminum 7075-T7 for $3/32''$ plates, and aluminum 2024 for $1/2''$ and $3/32''$ plates. The base (innermost) plates are $1/2''$ thick and are connected to the truss attachment collars; component mounting plates may be thinner to reduce structural weight if load limits are not exceeded.

All plates are 53 cm (20.866") tall by 35 cm (13.78") wide. The 53 cm height and 35 cm width of the plates were chosen for several reasons:

- To allow room for mounting the Autobox to a plate in a vertical direction.
- To provide adequate height to mount the five-sided lexan box to a plate and still have the box clear the momentum wheels.
- To provide adequate room to mount three motor amplifiers (controllers) on one side of a plate.
- To provide space to mount two batteries on one side of a plate.
- To make all plates a standard size so the *SIMSAT* truss is symmetrical.

Four $1''$ diameter holes are located on the corners of each plate with centers offset 4.4 cm ($1.732''$, vertically and horizontally) from the outer edgeline. These holes allow the mounting plates to slide onto the main steel support rods. Four 10-32 threaded holes (centers located $0.5''$ in vertically and horizontally from edgeline) provide mounting points for L-bracket attachments. These L-brackets allow for diagonal cross-members to be attached between mounting plates. Diagonal cross-members are not included in the baseline *SIMSAT* design, but can be added to provide additional stiffness if improved vibratory response is required.

The main truss support rods are 60 cm (23.6") long with an outer diameter of 1" and a wall thickness of 0.065". Each of the eight rods is constructed from stainless steel 316 tubing with one end plugged with a metal insert. The plugged end of each rod is placed through the base plate and mated with a connecting bolt to secure the rod in place. This arrangement allows for minimal protrusion on the inside of the base plate, thereby lessening interference with the overall *SIMSAT* pitch envelope.

Since bending deflection of a rod is dependent upon its inertia, a hollow tube (with its mass concentrated near its outer diameter) has a better stiffness to weight ratio than a solid rod. The 60 cm length of the rods offers support for the baseline components and provides 8 to 10 cm of excess length for possible future components. Rods with 1" outer diameter and 0.065" wall thickness were chosen in part because these dimensions were a standard tube size available in vendor catalogs. The CADRE analysis discussed earlier showed these rods to have adequate strength and vibratory stiffness.

The mounting plates are fixed to their positions along the support rods through the use of metal clamp-on collars (with a 1" bore hole). Each mounting plate has a total of eight collars (one collar for each side of the four mounting holes) to prevent movement of the mounting plate along the support rod. Mounting plates can be adjusted and secured to different points along the support rods to accommodate equipment changes and/or gross balance requirements.¹ One-piece collars are used primarily for mounting plates not subject to frequent adjustment, while two-piece collars allow for easy take-on/take-off in situations where access is routinely required. Each collar is made from aluminum; a two piece collar weighs 0.04 kg and a one piece collar weighs 0.035 kg (weight includes the cap screws). The cap screws used to tighten the clamp-on collars are manufactured from alloy steel.

The payload plate is the mounting plate furthest from the central sphere located on the AutoBox side of *SIMSAT*. This 1/4" thick mounting plate is identical to a standard mounting plate, with the addition of 212 threaded holes (5/16" diameter) spaced 1" apart

¹The current location of mounting plates in the *SIMSAT* baseline includes cabling space to meet nominal wire bend requirements. These estimates are conservative and may allow for closer spacing of plates following actual hardware integration.

(horizontally and vertically) between centers. These holes are referred to collectively as a 'pegboard' surface. The pegboard allows the user to attach experimental payloads or balancing weights along the payload plate with a maximum amount of flexibility. Carbon steel blocks of nominal 5 kg and 1 kg masses allow for gross balancing of the *SIMSAT* structure. These blocks can be attached to the pegboard using 5/16" bolts. Experiments can be attached directly to the pegboard with bolts or indirectly using mounting brackets attached to the experiment.

In addition to carbon steel blocks attached to the payload plate, gross *SIMSAT* balancing can be accomplished with 53cm by 35cm steel counterweight plates. Four 2 kg counterweight plates are available and four 5 kg plates are available. These plates are cut from the standard plate template except they have lightening holes to provide the specified mass. The 2 kg plates are nominally 1/16" thick with a 6.72" diameter hole in the center. The 5 kg plates are nominally 3/16" thick with a 9.9" hole in the center. These plates give the user flexibility to place counterweight near to the base plate (closer in towards the central sphere) to reduce inertia penalties. Since inertia varies with the square of distance, placing dense counterweight plates near the central sphere results in a lower moment of inertia (and better yaw performance) than placing light objects at a further distance from the sphere.

Fine-tuning of *SIMSAT* balance is accomplished with a counterweight mechanism. The counterweight mechanism can be mounted on either side of *SIMSAT* depending on balancing needs. This mechanism relies upon orthogonal 1/4" stainless steel threaded rods, hollow cylindrical weights (each with a 1/4" hole), and small steel clamp-on collars (1/4" bore). The hollow cylindrical weights slide over the threaded rods and are held in place with the small clamp-on collars. Six 100 gram and five 500 gram hollow weights are available. Hand knobs on the ends of the threaded rods allow the user to make slight adjustments in weight position by turning clockwise or counterclockwise.

Individual components are attached to their respective mounting plates using a variety of structural support mechanisms. The momentum wheels are attached to a mounting plate using a cantilevered support 'shelf' structure. To prevent debris (such as a loose screw) from being ejected by the rotating wheels, the momentum wheels are enclosed in

a safety housing. This housing consists of a five-sided lexan box which extends outside of the truss bay in the z-direction. One side of the box is attached to a mounting plate (not the momentum wheel mounting plate) and the other side is free. The sixth side of the box consists of a lexan sheet mounted to the same plate as the momentum wheels. During *SIMSAT* assembly, the five-sided lexan box 'slides' over the momentum wheels until a solid press fit is achieved; the final configuration is similar to that of a cake box used to transport baked goods without damage. All lexan sheets used to construct the box are 0.220" thick. Clearance between the momentum wheels and the interior of the lexan box is approximately 0.5" to 1.0". The cake box configuration allows the user to remove only the exterior mounting plates for access to momentum wheels and motors during maintenance.

Each battery is attached to its respective mounting plate using an aluminum housing which partially encloses the battery on all six sides. Two nylon-tipped bolts are mounted through the backplate; these bolts can be tightened to press upon the battery contact plate (held on the battery with adhesive) to ensure a snug fit. The removable backplate allows for easy access and replacement of the battery between experiments. The battery housing does not enclose the terminal leads so quick-disconnect wiring connections can be made to the batteries. The battery housing is attached to the mounting plate via four bolts.

The AutoBox is attached to its respective mounting plate using a combination of U- and L-brackets. Polyurethane padding is inserted between the brackets and the Autobox to provide adequate vibration isolation for electronic components.

An aluminum gyroscope housing provides a support and mounting structure for the Humphrey gyro. The RadioLAN transceiver is attached directly to the mounting plate using integral screw attachments.

K.3 Structure Summary

Overall, the *SIMSAT* structural design emphasizes modularity and ease of reconfiguration, while attempting to minimize structural mass and complexity.

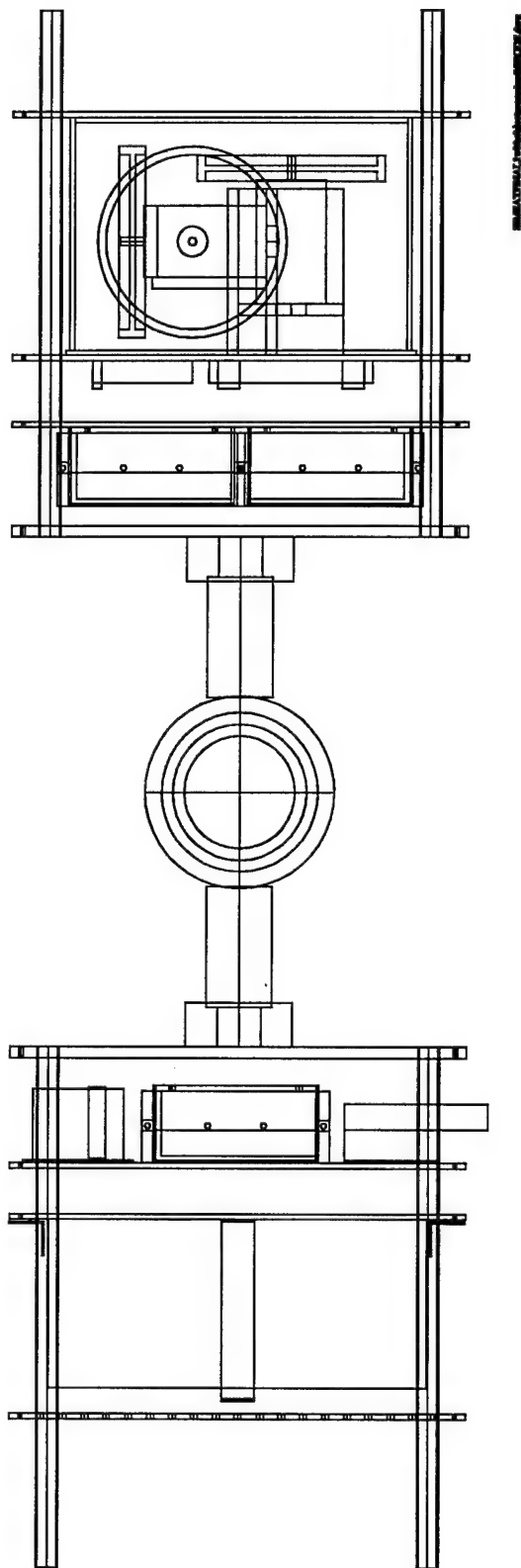
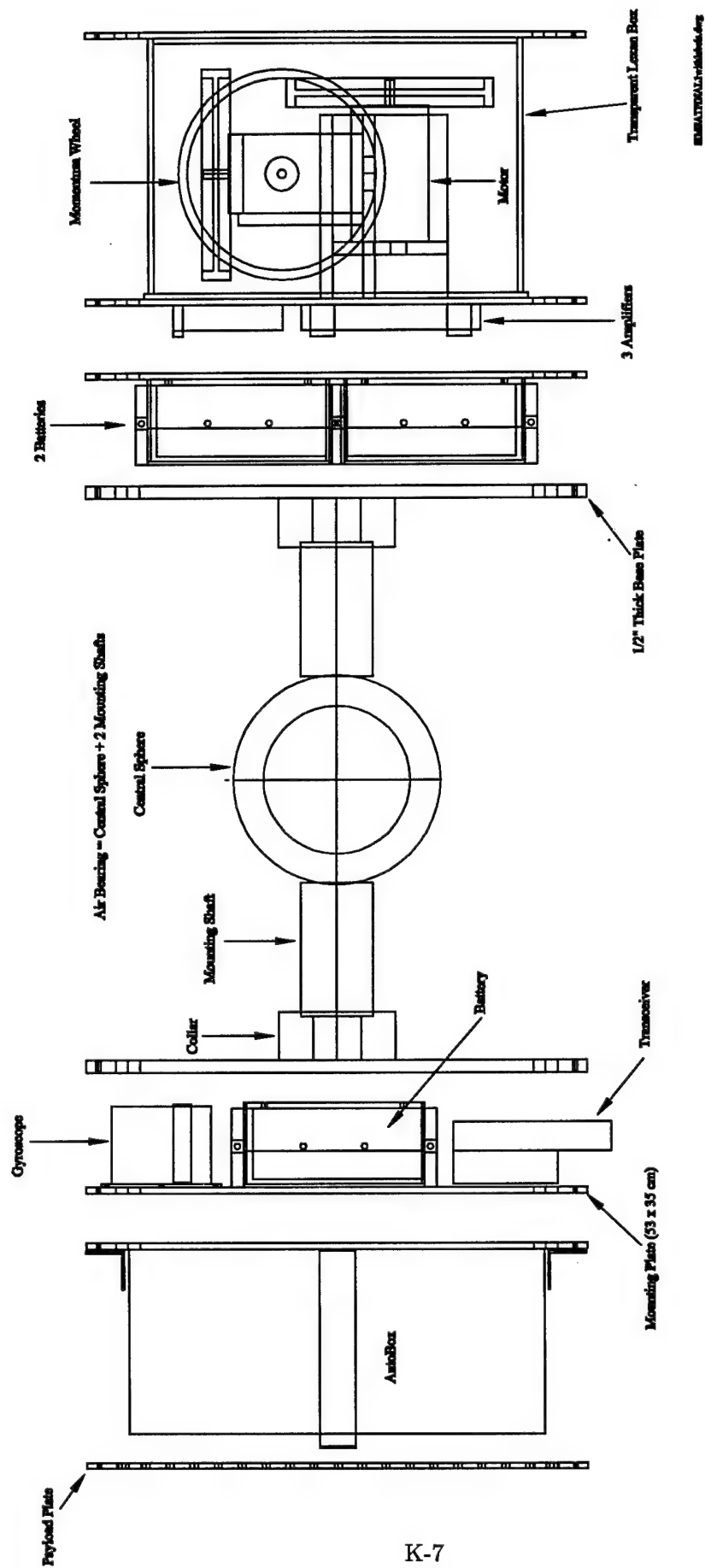


Figure K.1 SIMSAT with Support Rods

SimSat Major Components



K-7

Figure K.2 Baseline *SIMSAT* Layout (support rods not shown for clarity)

Aluminum 7075-T7 Collar



Figure K.3 Truss Attachment Collar - Front View

Aluminum 7075-T7 Collars

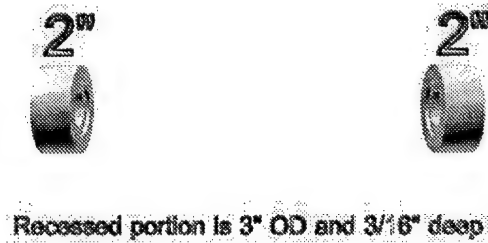


Figure K.4 Truss Attachment Collars - Side View

Payload/Dummy Mass Mounting Plate

- Aluminum plate is 1/4" thick
- 4 large holes should allow 1" OD stainless steel rods to pass through
- 212 small holes should be threaded to fit a 5/16" bolt, small hole centers are 1" apart horizontally and vertically
- All dimensions shown are in inches

Corners are slightly rounded
to eliminate sharp points

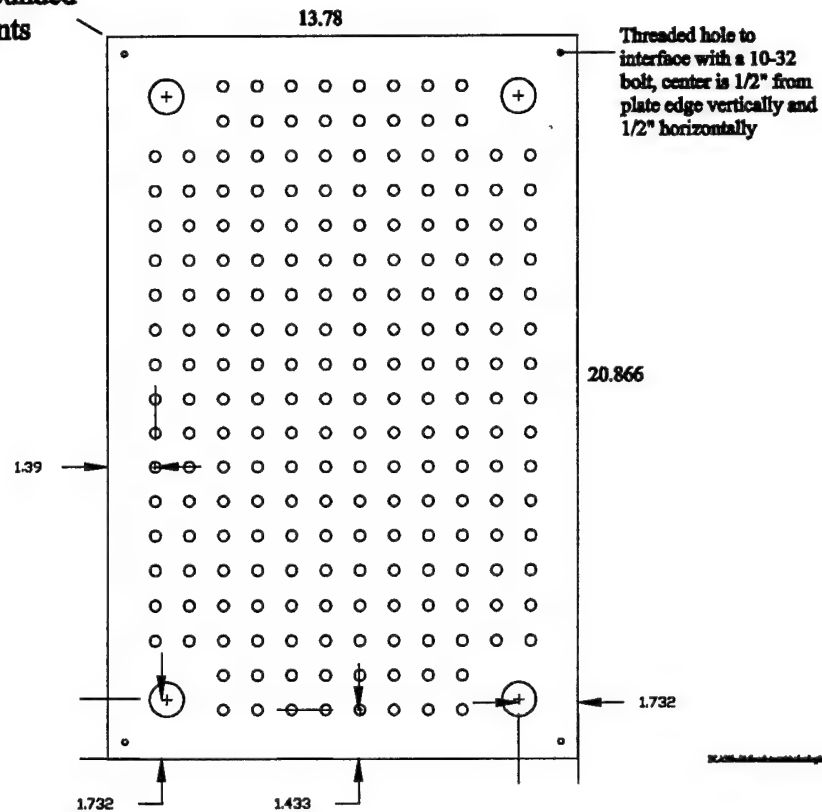


Figure K.5 Payload Mounting Plate
K-9

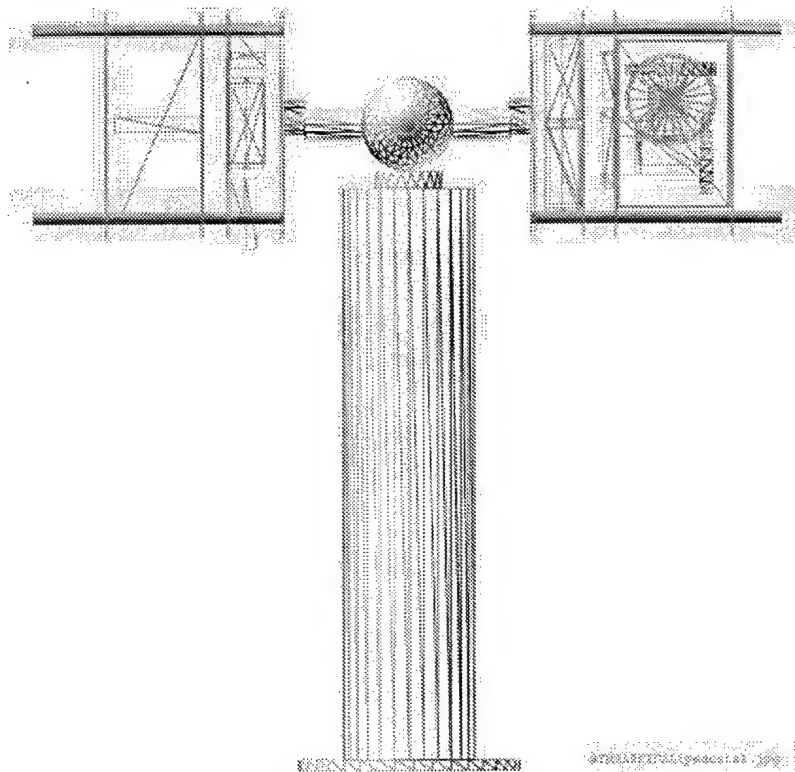


Figure K.6 *SIMSAT* on Pedestal - Wireframe View

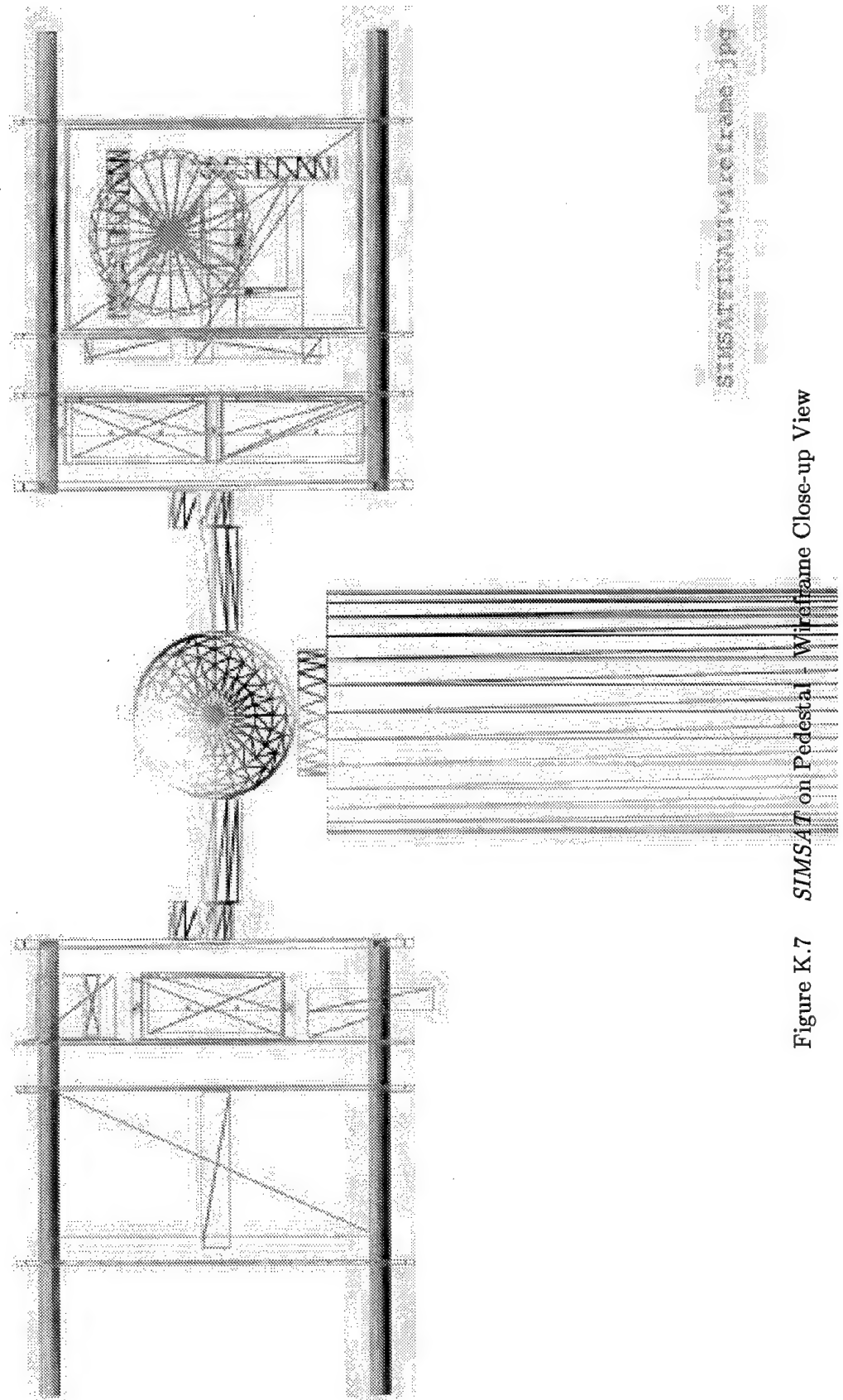


Figure K.7 SIMSAT on Pedestal - Wireframe Close-up View

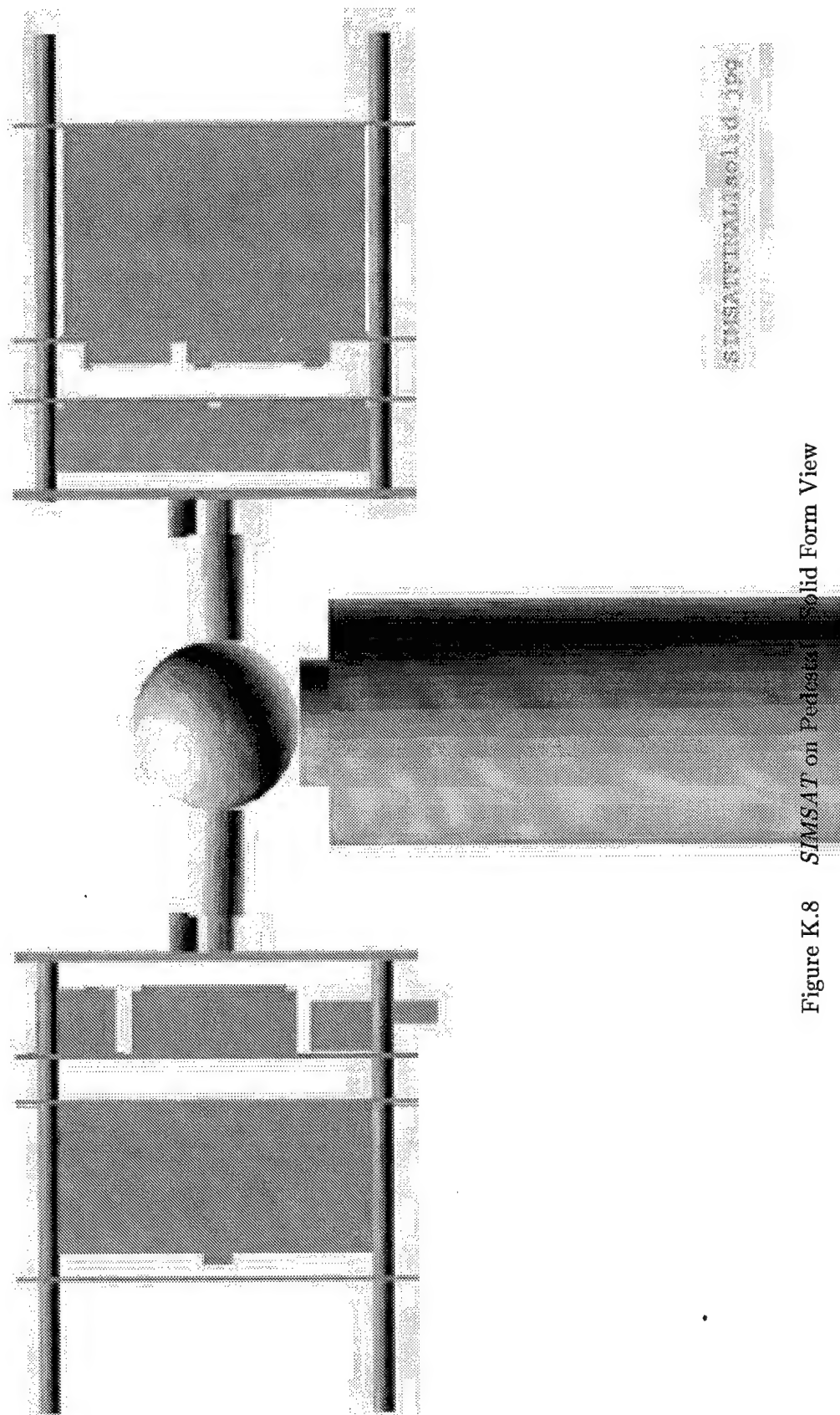


Figure K.8 *SIMSAT* on Pedestal Solid Form View

Aluminum Plate Template

- 4 large holes should allow 1" outer diameter Stainless Steel-316 tubes (with 0.065" wall thickness) to pass through
- 4 small holes are for L-bracket attachment for cross-members
- All dimensions shown are in inches

Corners on all plates
are slightly rounded to
eliminate sharp points

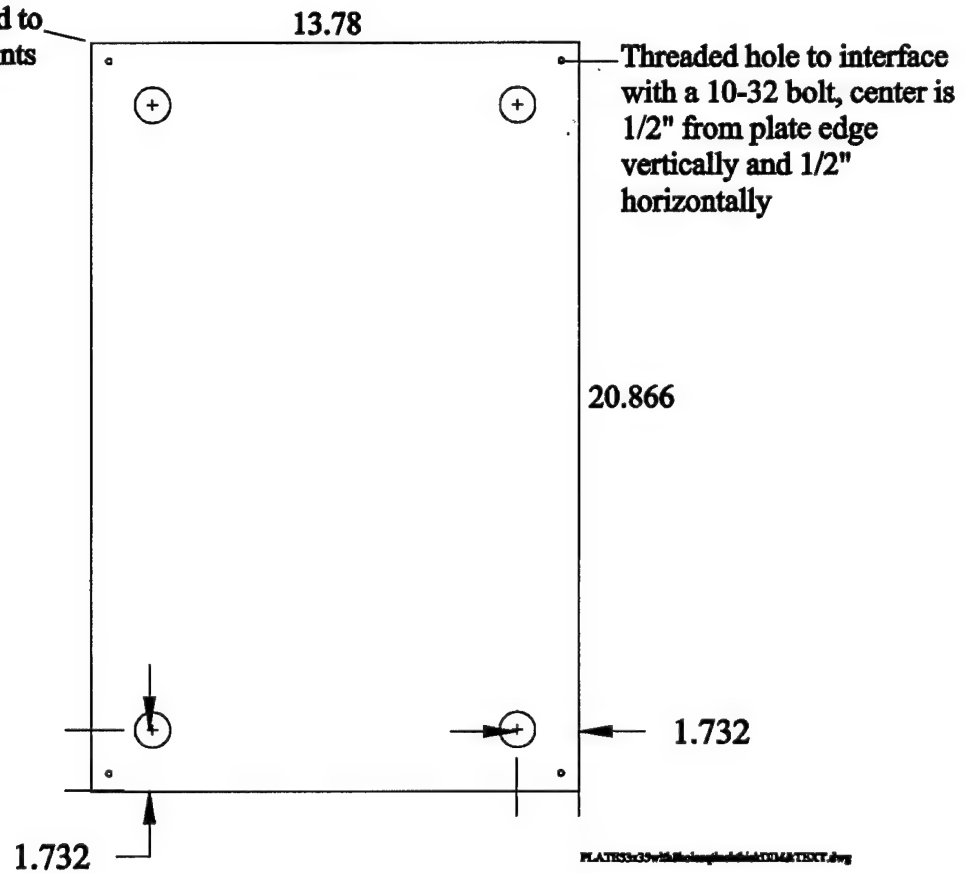


Figure K.9 Standard Mounting Plate Template

Two Battery Mounting Plate Template

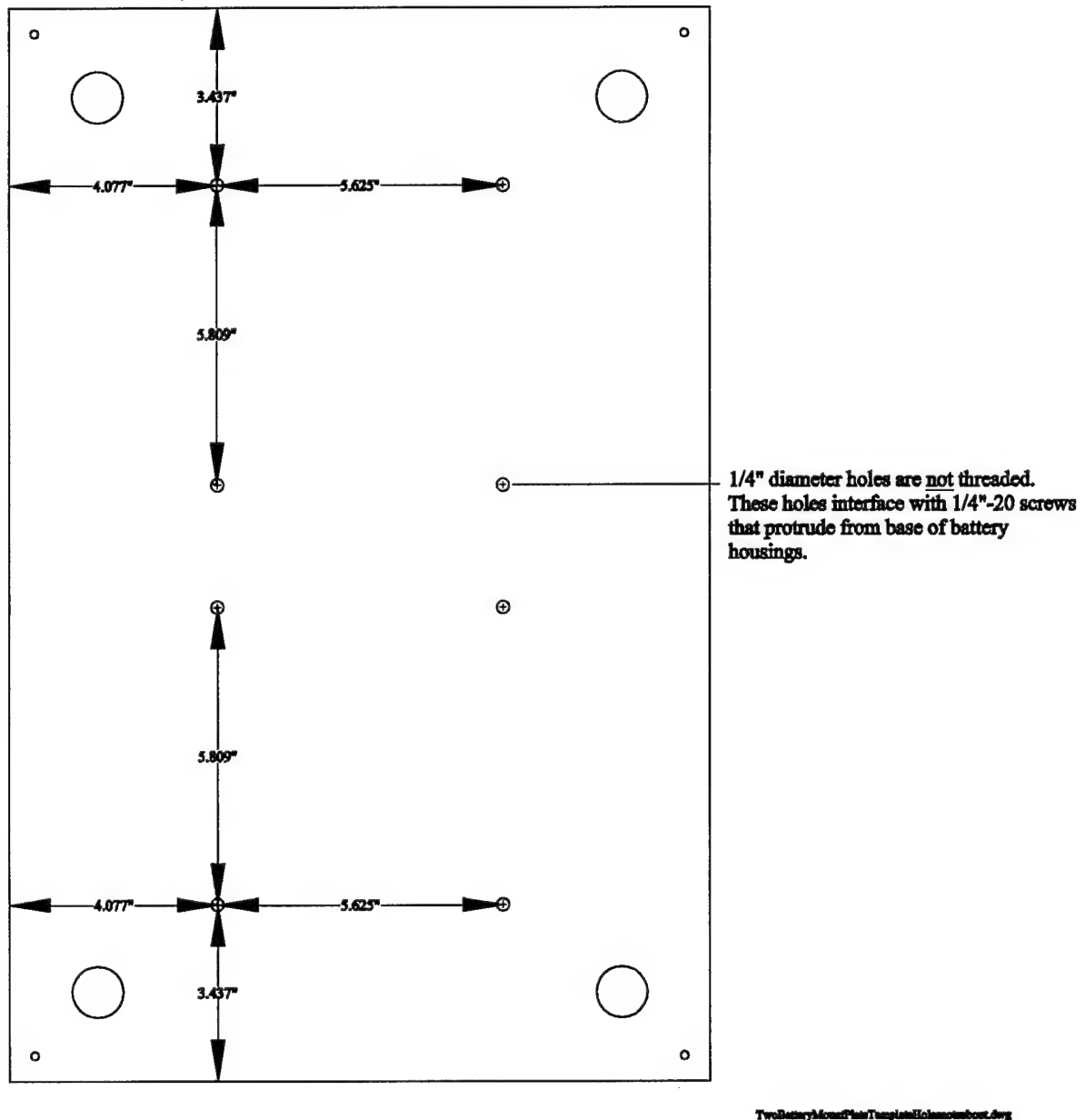
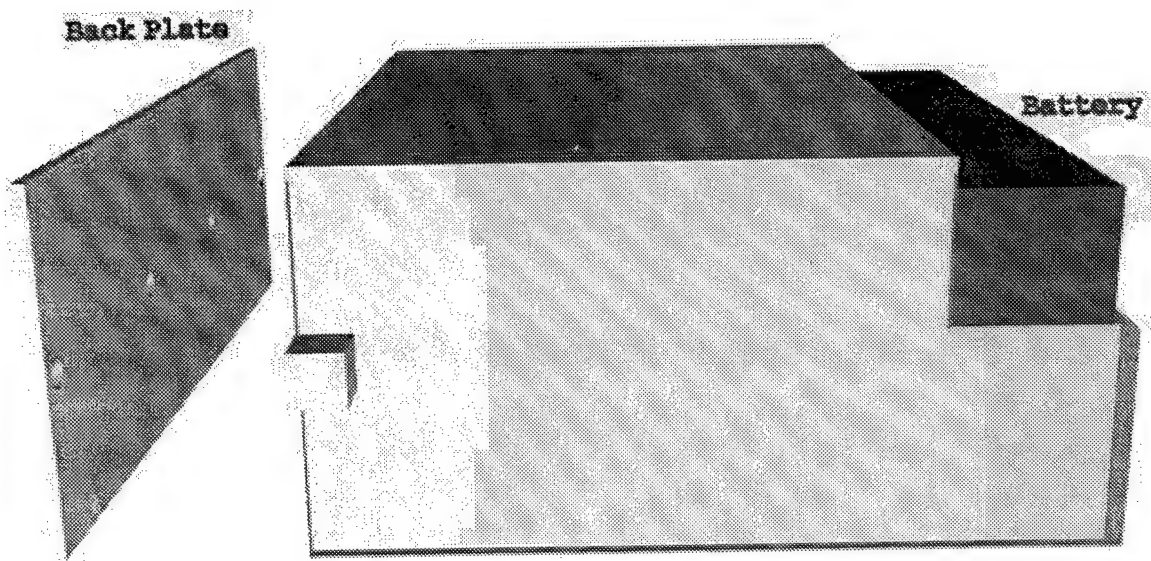


Figure K.10 Two-Battery Mounting Plate Template
K-14

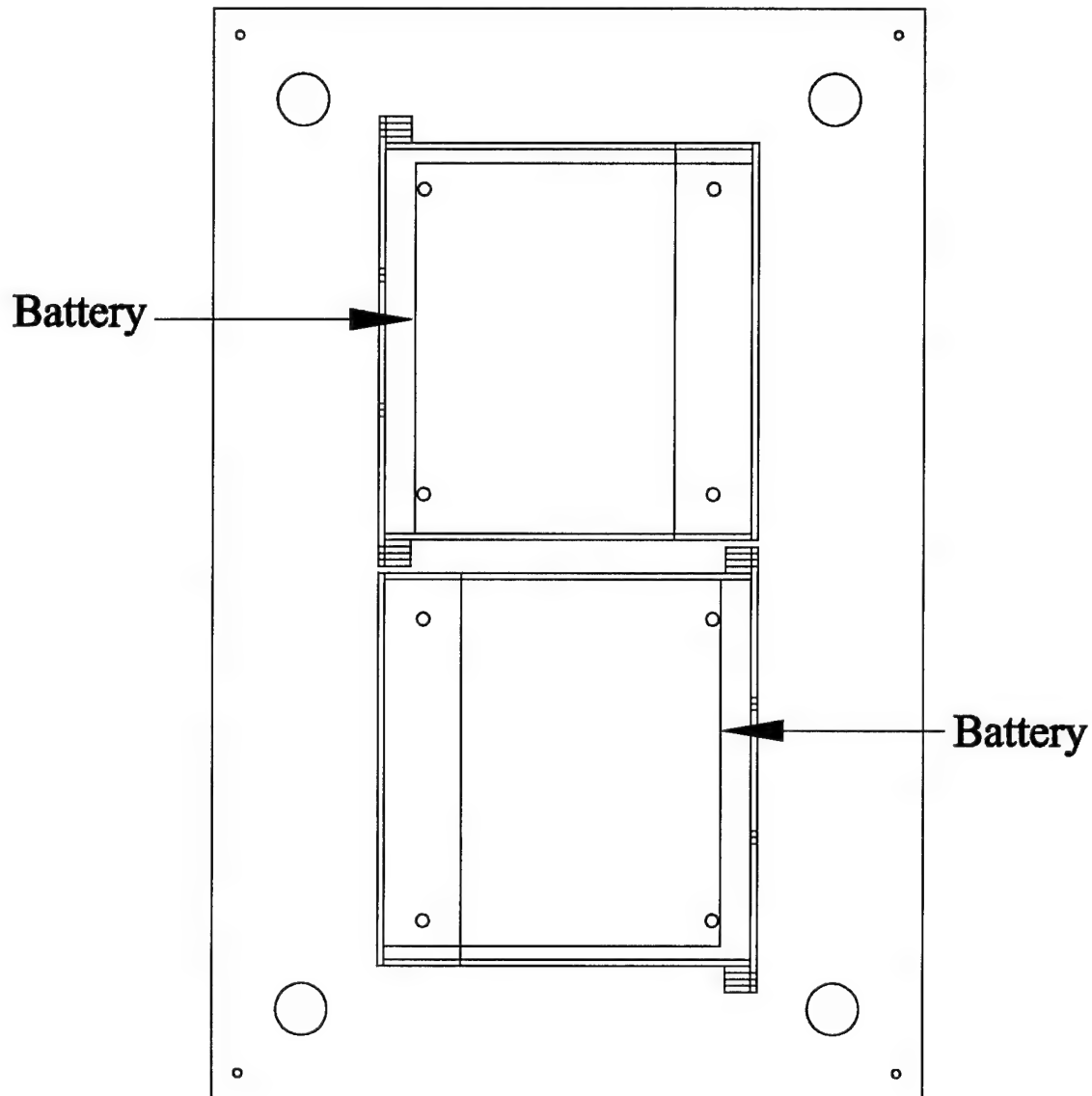
Aluminum Housing for Battery



batteryhousing - 154

Figure K.11 Battery Housing - 3D View
K-15

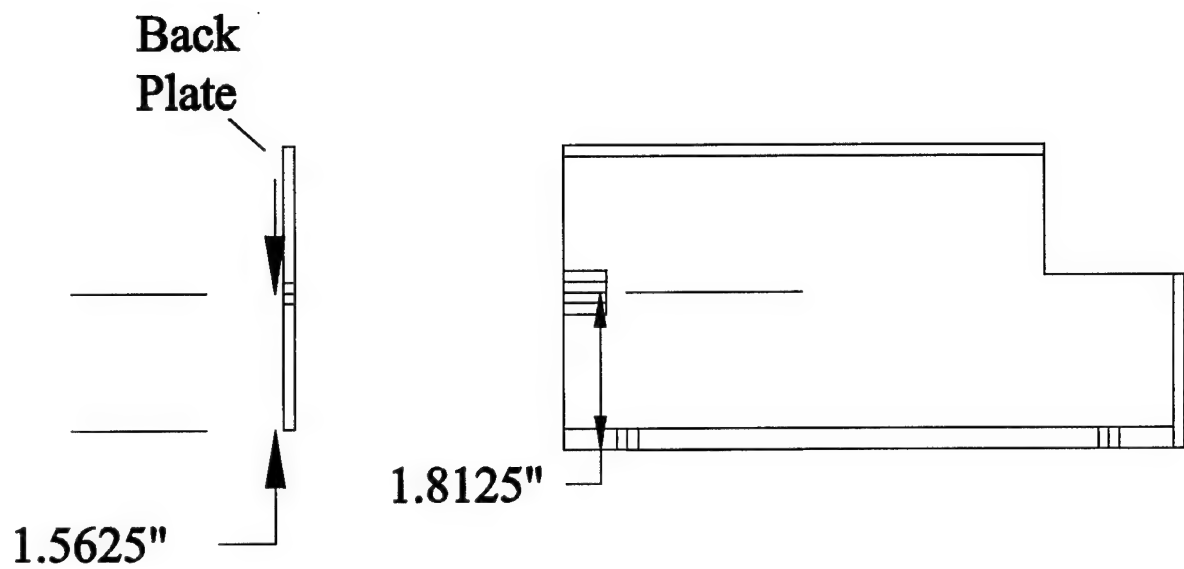
Batteries & Battery Housings on Mounting Plate



batteryhousingPLATEWITHBATTERYmounted against the plateEOLBNOTSUBOUTMPLATE.dwg

Figure K.12 Battery Mounting
K-16

Battery Housing--Side View



BATTERYMTsideviewHOLESOUT.dwg

Figure K.13 Battery Housing - Side View
K-17

Battery Housing Pieces

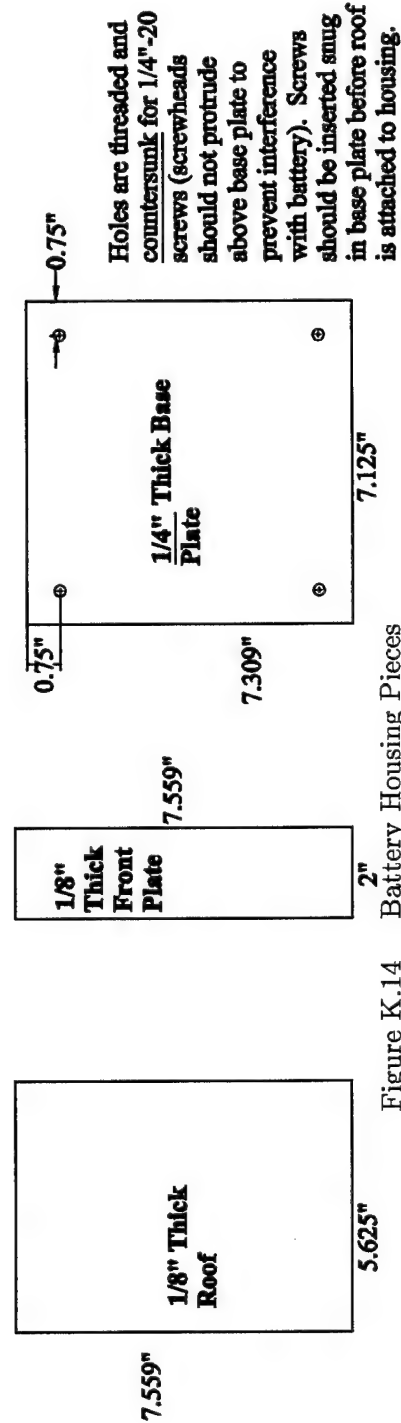
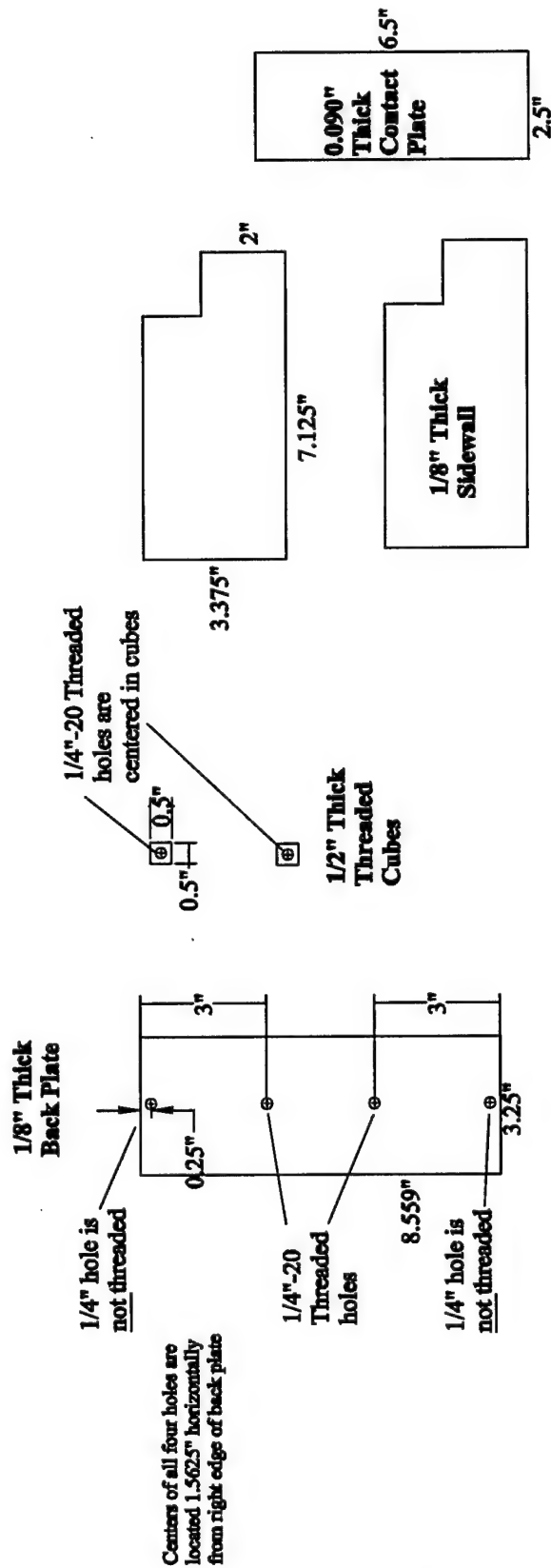


Figure K.14 Battery Housing Pieces

Find big hole diameter of steel plates that gives a particular mass
dimensions in cm

w := 35

l := 53

t := 0.15875 (using 1/16" thick plate)

rsmall := 1.27 (using four 1 inch diameter holes for stainless steel rods)

rtiny := 0.2413 (using four 0.19 inch diameter holes for 10-32 screws for stiffening member L-bracket)

δsteel := 7.85 g/cm³

Initial Guess

rbig := 5

Given

$$2000 = \delta_{\text{steel}} \cdot \left[w \cdot l \cdot t - (r_{\text{big}}^2 \cdot \pi \cdot t) - 4 \cdot (r_{\text{small}}^2 \cdot \pi \cdot t) - 4 \cdot (r_{\text{tiny}}^2 \cdot \pi \cdot t) \right]$$

x := Find(rbig)

x = 8.539696350203382 2 kg steel plate hole radius in cm

$$\left(\frac{x}{2.54} \right) \cdot 2 = 6.72417 \quad \text{2 kg steel 1/16" plate hole DIAMETER} = 6.72417 \text{ inches}$$

w := 35

l := 53

t := 0.47625 (using 3/16" thick plate)

rsmall := 1.27 (using 1 inch diameter holes for stainless steel rods)

rtiny := 0.2413 (using four 0.19 inch diameter holes for 10-32 screws for stiffening member L-bracket)

δsteel := 7.85 g/cm³

Initial Guess

rbig := 1

cwplatethickness4.mcd

Given

$$5000 = \delta_{\text{steel}} \cdot [w \cdot l \cdot t - (r_{\text{big}}^2 \cdot \pi \cdot t) - 4 \cdot (r_{\text{small}}^2 \cdot \pi \cdot t) - 4 \cdot (r_{\text{tiny}}^2 \cdot \pi \cdot t)]$$

$x := \text{Find}(r_{\text{big}})$

$x = 12.57253889023823$ 5 kg steel plate hole radius in cm

$$\left(\frac{x}{2.54}\right) \cdot 2 = 9.89964 \quad \text{5 kg steel 3/16" plate hole DIAMETER} = 9.89964 \text{ inches}$$

$t := .635$ (using 1/4" thick STEEL plate)

$\delta_{\text{steel}} := 7.85$ g/cm³

Initial Guess

$r_{\text{big}} := 10$

Given

$$5000 = \delta_{\text{steel}} \cdot [w \cdot l \cdot t - (r_{\text{big}}^2 \cdot \pi \cdot t) - 4 \cdot (r_{\text{small}}^2 \cdot \pi \cdot t) - 4 \cdot (r_{\text{tiny}}^2 \cdot \pi \cdot t)]$$

$y := \text{Find}(r_{\text{big}})$

$y = 16.26335250302494$

$$\left(\frac{y}{2.54}\right) \cdot 2 = 12.80579 \quad \text{5 kg steel 1/4" plate hole DIAMETER} = 12.80579 \text{ inches}$$

Find dimensions for Carbon Steel 1018 rectangles that attach as weight to payload plate:

$$h := 5.08 \text{ cm (2")}$$

$$w := 10.16 \text{ cm (4")}$$

$$\delta_{\text{steel1018}} := 7.87 \text{ g/cm}^3$$

$$l := \frac{(5000)}{\delta_{\text{steel1018}} \cdot h \cdot w}$$

$$l = 12.30943 \text{ cm} \quad \text{length}_{\text{inches}} := \frac{1}{2.54}$$

$$\text{length}_{\text{inches}} = 4.846$$

$$\text{5 kg steel block dimensions} = 2" \times 4" \times 4.846"$$

$$h := 5.08 \text{ cm (2")}$$

$$w := 10.16 \text{ cm (4")}$$

$$\delta_{\text{steel1018}} := 7.87 \text{ g/cm}^3$$

$$l := \frac{(1000)}{\delta_{\text{steel1018}} \cdot h \cdot w}$$

$$l = 2.46189 \text{ cm} \quad \text{length}_{\text{inches}} := \frac{1}{2.54}$$

$$\text{length}_{\text{inches}} = 0.969$$

$$\text{1 kg steel block dimensions} = 2" \times 4" \times 0.969"$$

Find dimensions for hollow steel cylinders for counterweight mechanism rods:

$$\delta_{\text{steel}} := 7.85 \text{ g/cm}^3$$

$$r_{\text{hole}} := .3175 \text{ cm} \quad (\text{hole fits } 1/4" \text{ diameter threaded rods})$$

$$r_{\text{outer}} := 1.5875 \text{ cm} \quad (1.25" \text{ outer diameter steel cylinder})$$

Initial Guess

$$\text{length} := 1$$

Given

$$100 = \delta_{\text{steel}} \cdot (r_{\text{outer}}^2 \cdot \pi \cdot \text{length} - r_{\text{hole}}^2 \cdot \pi \cdot \text{length})$$

$$x := \text{Find}(\text{length})$$

$$x = 1.67603 \text{ cm}$$

$$\left(\frac{x}{2.54} \right) = 0.65985 \quad \boxed{100 \text{ gram steel weight cylinder length} = 0.65985 \text{ inches}}$$

$$\delta_{\text{steel}} := 7.85 \text{ g/cm}^3$$

$$r_{\text{hole}} := .3175 \text{ cm} \quad (\text{hole fits } 1/4" \text{ diameter threaded rods})$$

$$r_{\text{outer}} := 1.5875 \text{ cm} \quad (1.25" \text{ outer diameter steel cylinder})$$

Initial Guess

$$\text{length} := 1$$

Given

$$500 = \delta_{\text{steel}} \cdot (r_{\text{outer}}^2 \cdot \pi \cdot \text{length} - r_{\text{hole}}^2 \cdot \pi \cdot \text{length})$$

$$x := \text{Find}(\text{length})$$

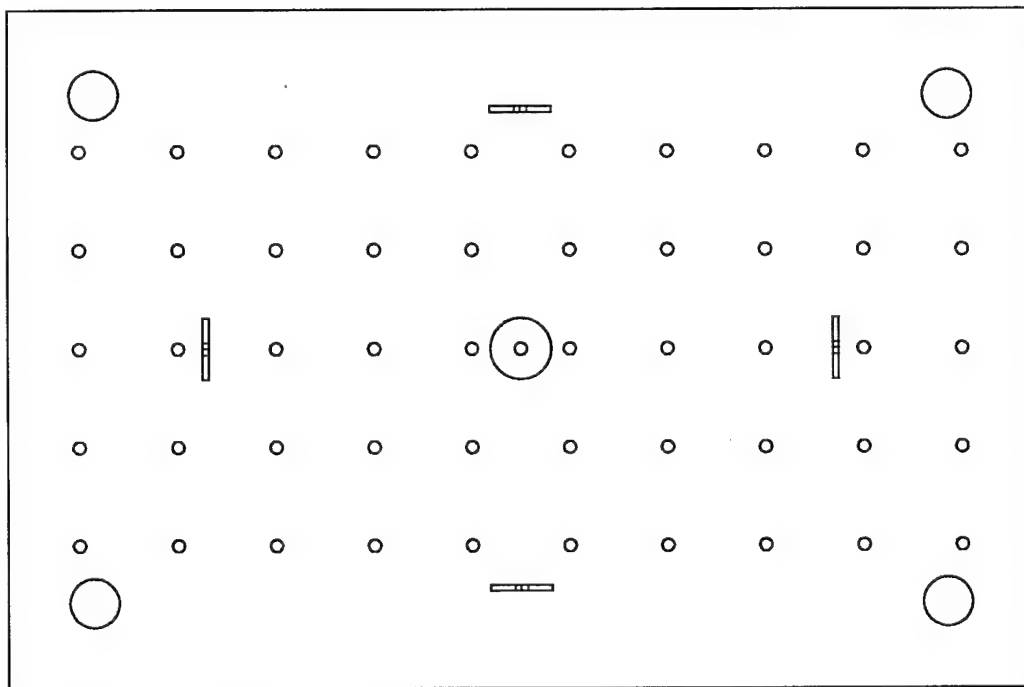
$$x = 8.38015 \text{ cm}$$

$$\left(\frac{x}{2.54} \right) = 3.29927 \quad \boxed{500 \text{ gram steel weight cylinder length} = 3.29927 \text{ inches}}$$

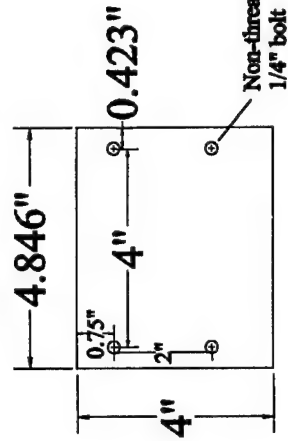
For counterweight, Simsat needs:

- four 2 kg steel plates
- four 5 kg steel plates
- four 1 kg carbon steel-1018 blocks 2" x 4" x 0.969" with 5/16" holes
- four 5 kg carbon steel-1018 blocks 2" x 4" x 4.846" with 5/16" holes
- four 1 kg carbon steel-1018 blocks 2" x 4" x 0.969" with 1/4" holes
- one 5 kg carbon steel-1018 block 2" x 4" x 4.846" with 1/4" holes
- six 100 gram steel hollow cylinders 1.25" OD, 0.25" diameter hole, 0.65985" long
- five 500 gram steel hollow cylinders 1.25" OD, 0.25" diameter hole, 3.299" long

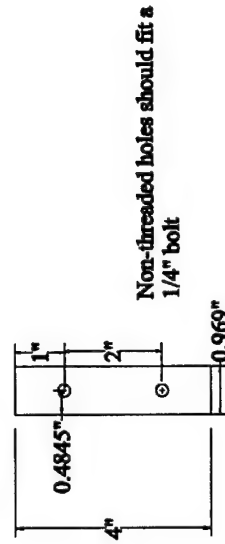
Counter-Weight Mechanism Pegboard



5 kg carbon steel-1018 block, quantity = 1
Depth = 2"



1 kg carbon steel-1018 block, quantity = 4
Depth = 2"



100 gram steel hollow cylinder
1.25" OD, 0.25" diameter non-threaded hole,
0.63985" long
quantity = 6



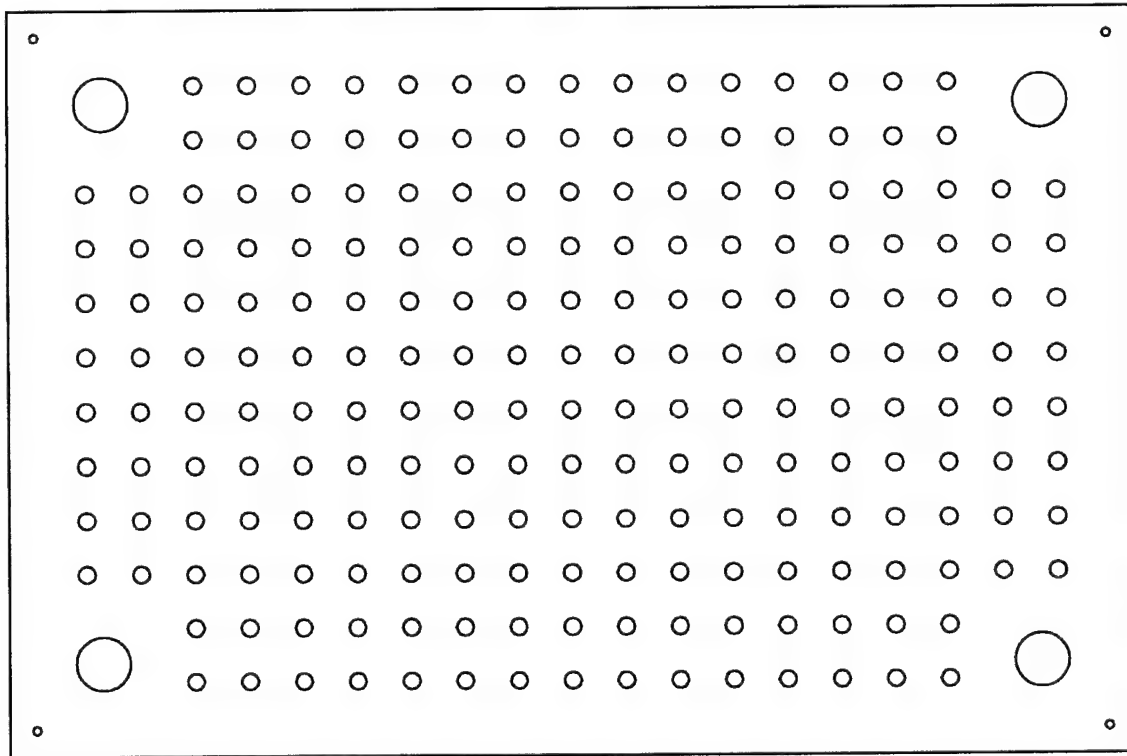
500 gram steel hollow cylinder
1.25" OD, 0.25" diameter non-threaded hole,
3.299" long
quantity = 5



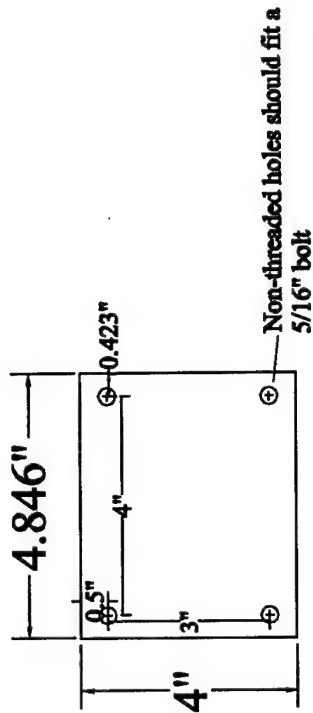
Figure K.16 Counterweight Fine-Tuning Mechanism with Weights

c:\mechanism\PECEBOARD\Detailbooks.dwg

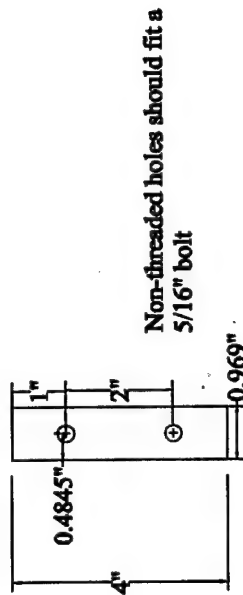
Payload Mounting Plate



5 kg carbon steel-1018 block, quantity = 4
Depth = 2"



1 kg carbon steel-1018 block, quantity = 4
Depth = 2"



PayloadPlatewithsteelblocks.dwg

Figure K.17 Payload Plate with Weights

Counter-Weight Mechanism with
1/4"-20 Threaded Rods and Turn Knobs

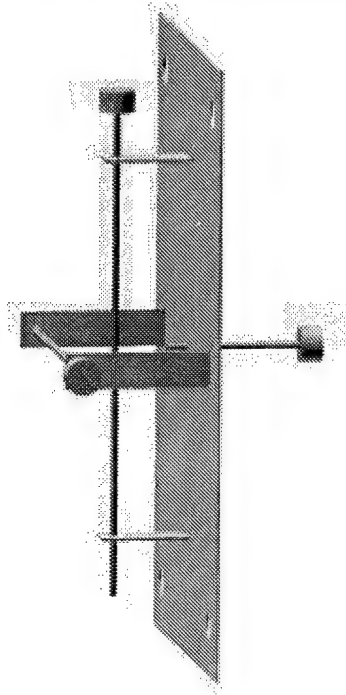


Figure K.18 Counterweight Fine-Tuning Balance Mechanism - Side view
K-26

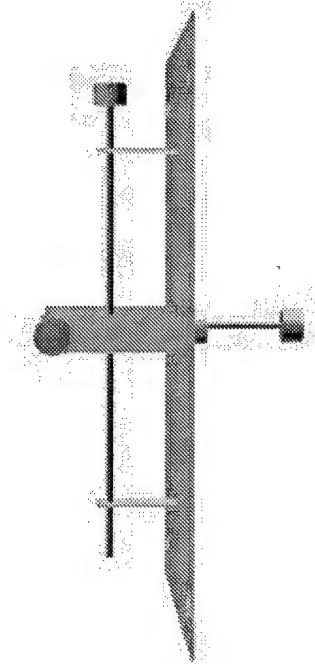
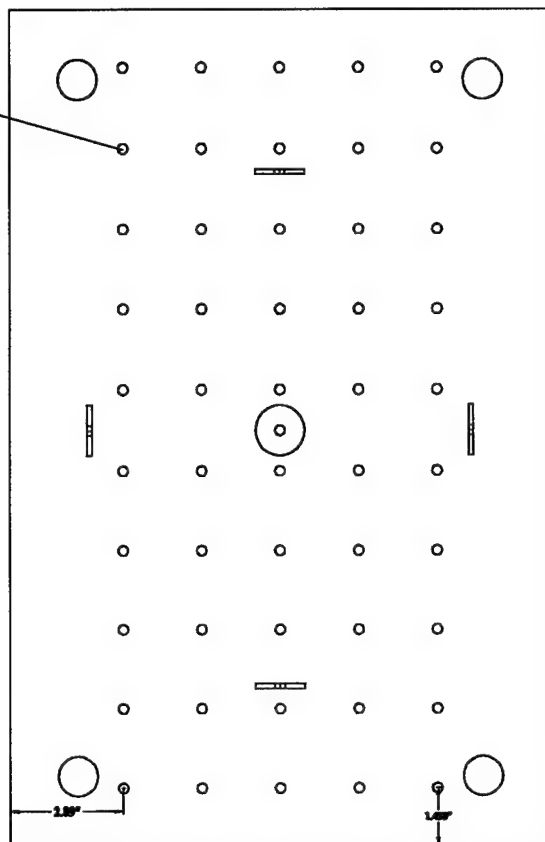


Figure K.19 Counterweight Fine-Tuning Balance Mechanism - Perspective View
K-27

Counter-Weight Mechanism—Pegboard Design

50 small holes are threaded 1/4"-20.
Small hole centers are 2" apart
vertically and horizontally

Corners are slightly
rounded to eliminate sharp
points



Mass (approx) = 2.93 lbs

www.mechanismPEGBOARDMAHOLESCOUT.dwg

Figure K.20 Counterweight Fine-Tuning Mechanism - Pegboard Design

Counter-Weight Mechanism—Right Side View

* indicates 1/4"-20 Threaded hole. Other holes are not threaded

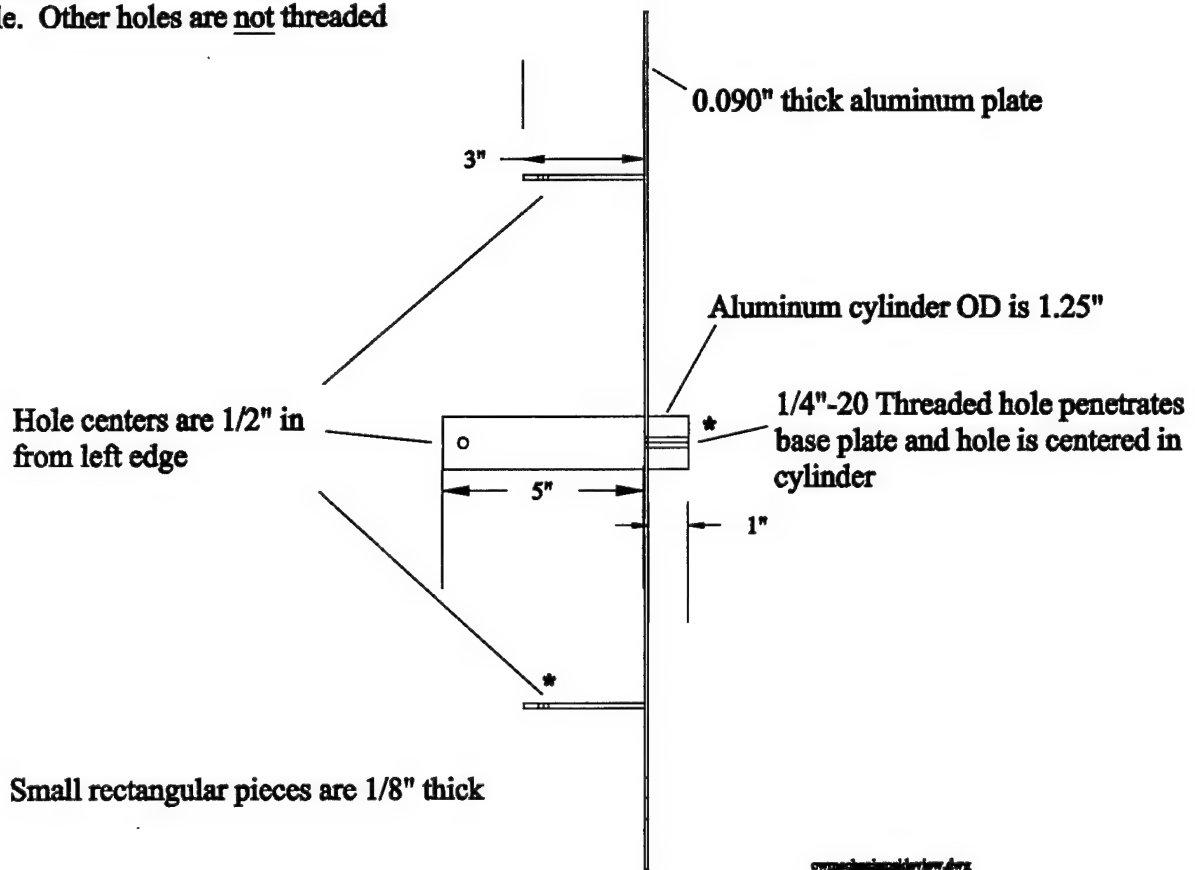


Figure K.21 Counterweight Mechanism with Dimensions - Right Side View

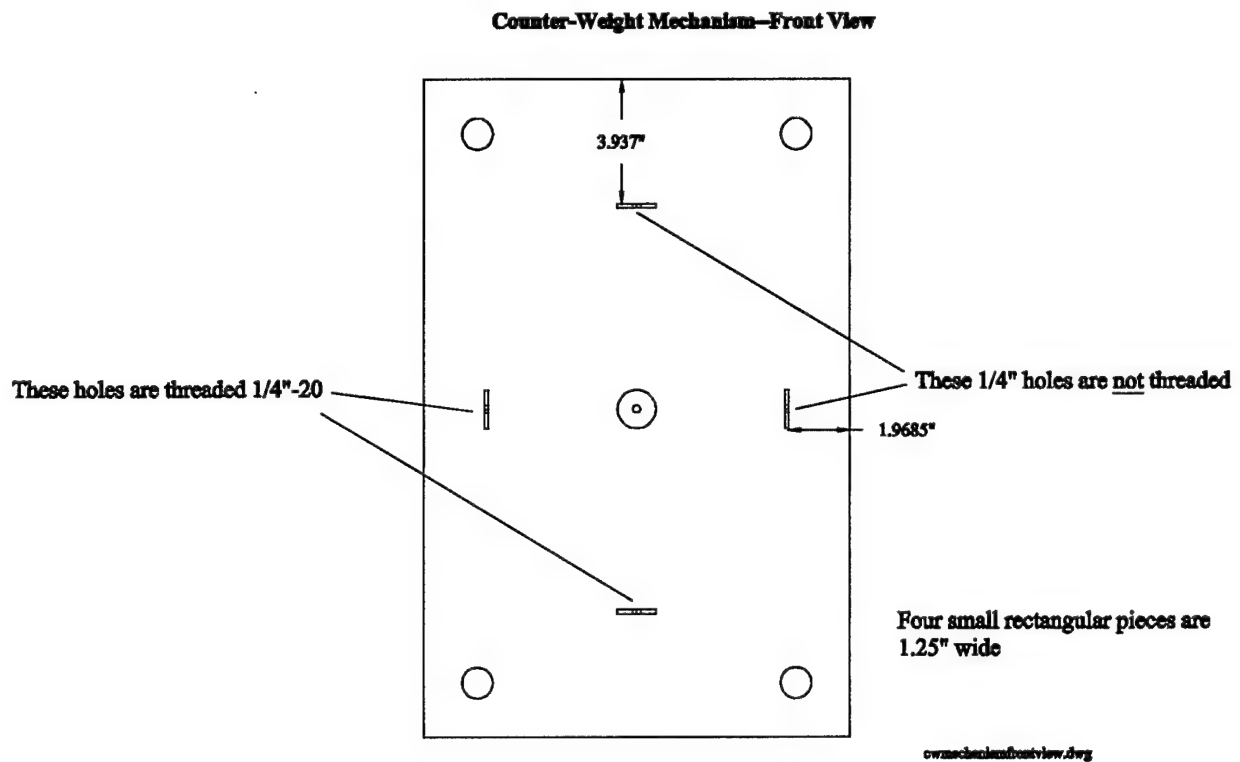
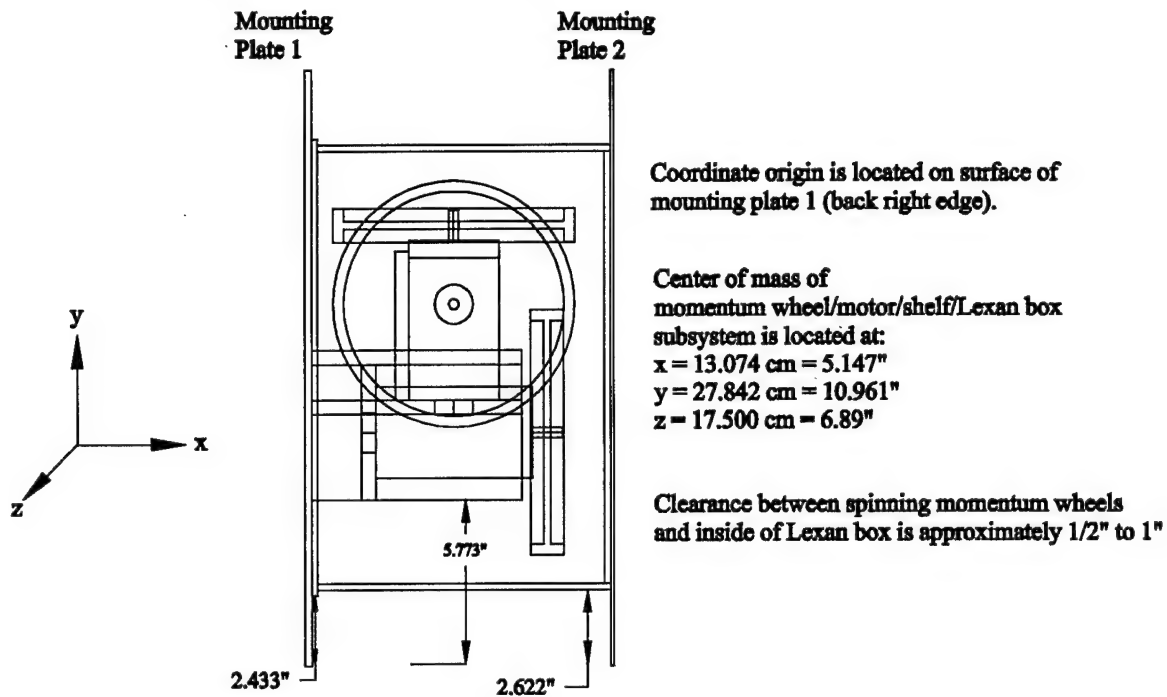


Figure K.22 Counterweight Mechanism with Dimensions (Pegboard Not Shown)

FRONT VIEW—Momentum Wheel Bay Subsystem centered between stainless steel rods along "y" axis



RIGHT SIDE VIEW

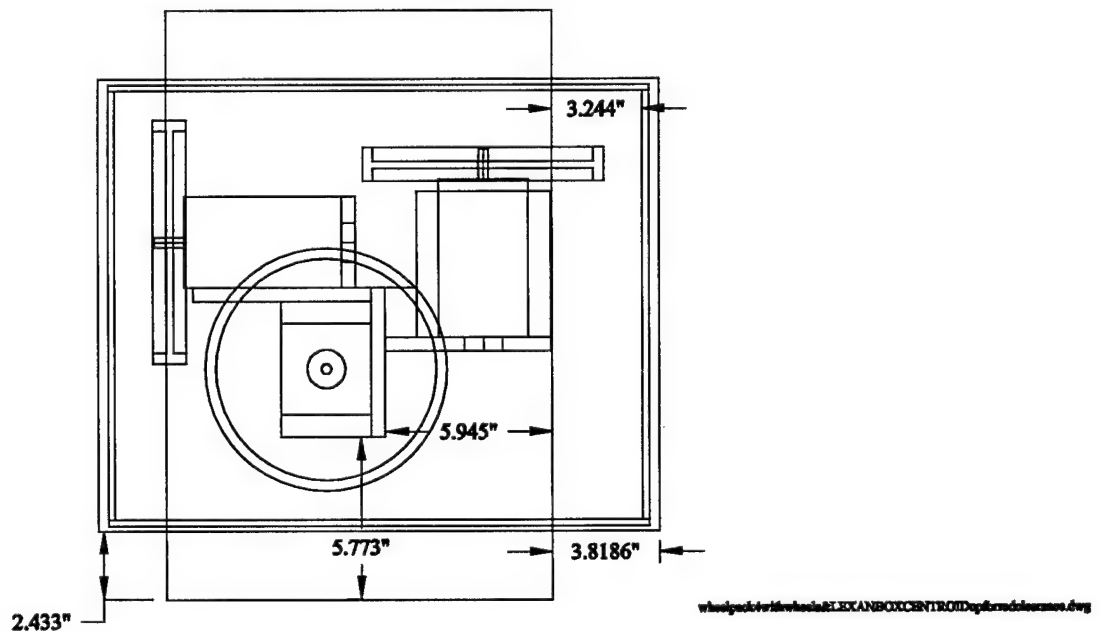
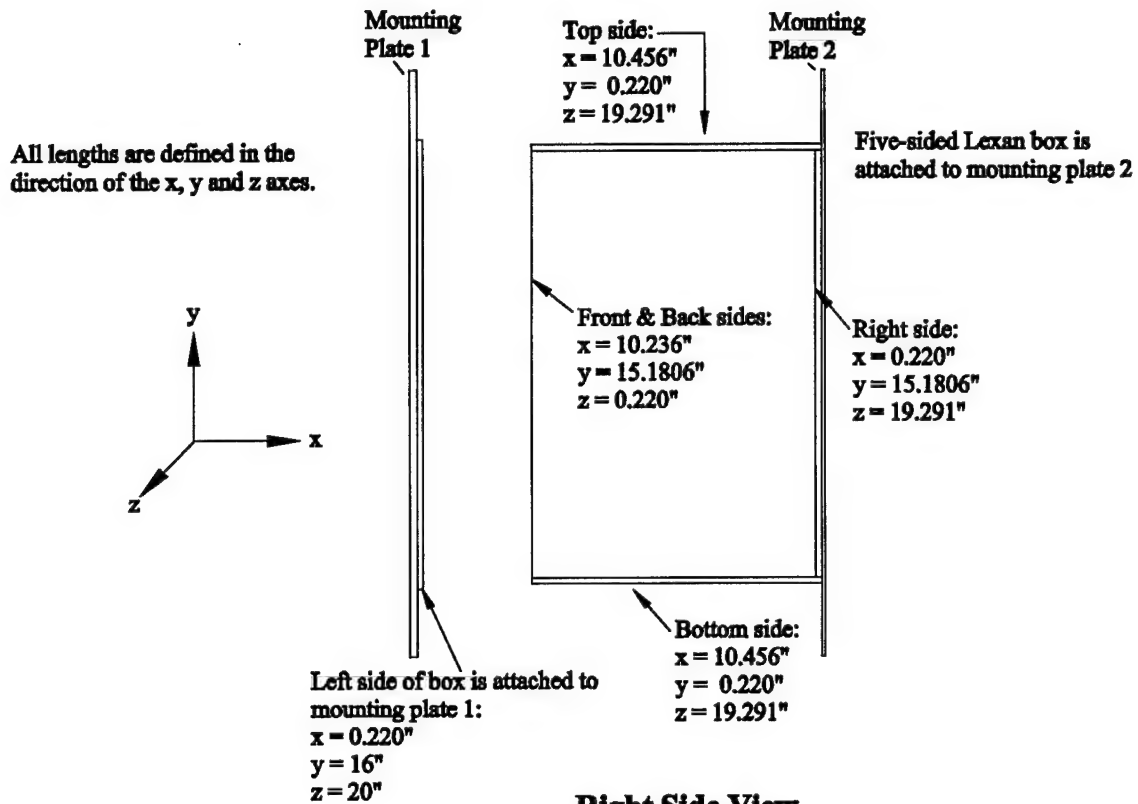
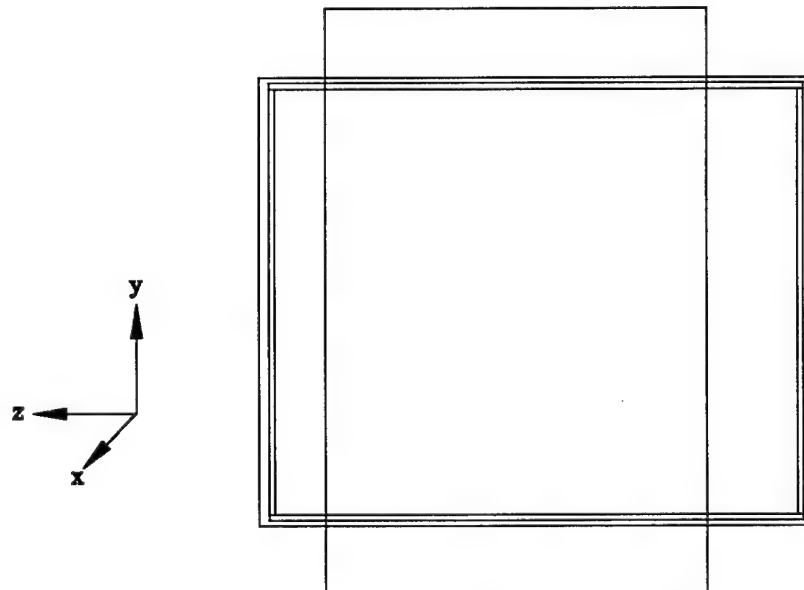


Figure K.23 Momentum Wheel Bay (Amplifiers Not Shown)

LEXAN SAFETY BOX—Front View



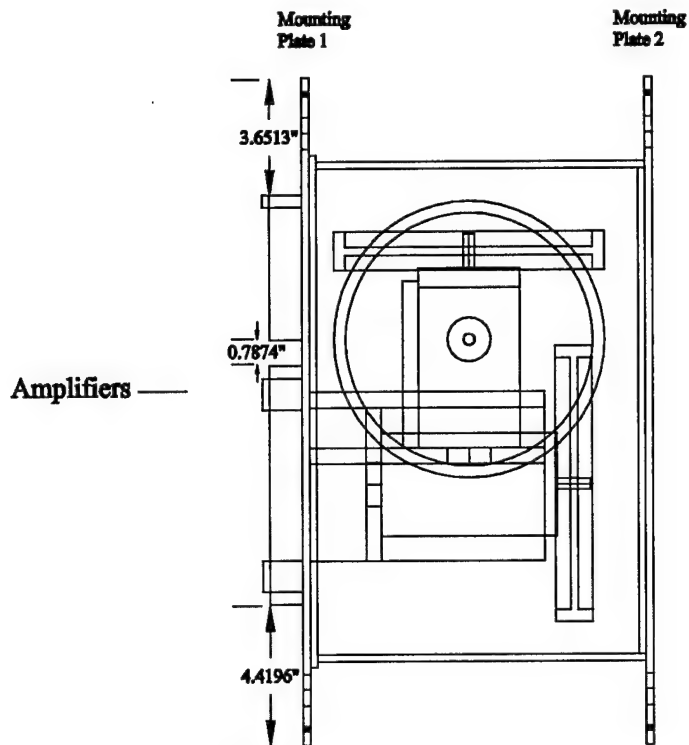
Right Side View



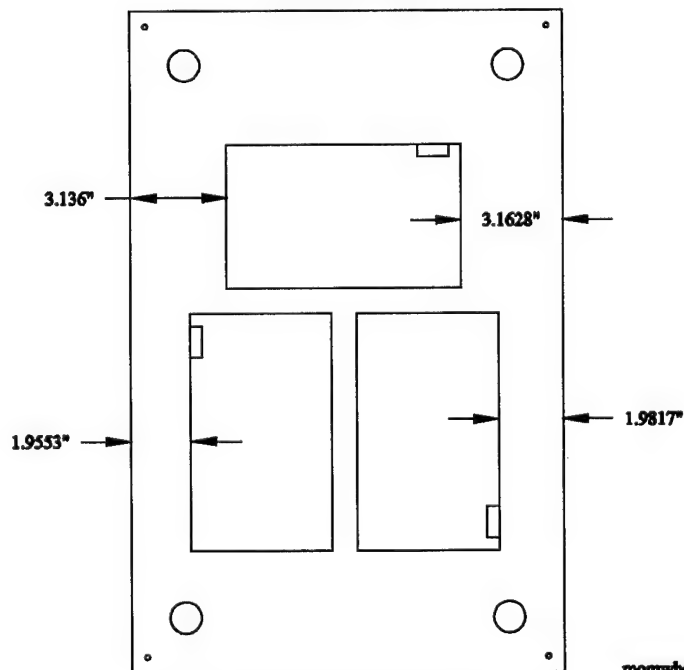
LEXANSAFETYBOXFINAL.dwg

Figure K.24 Lexan Box (Momentum Wheels and Motors Not Shown)

Amplifier Mounting—Front View



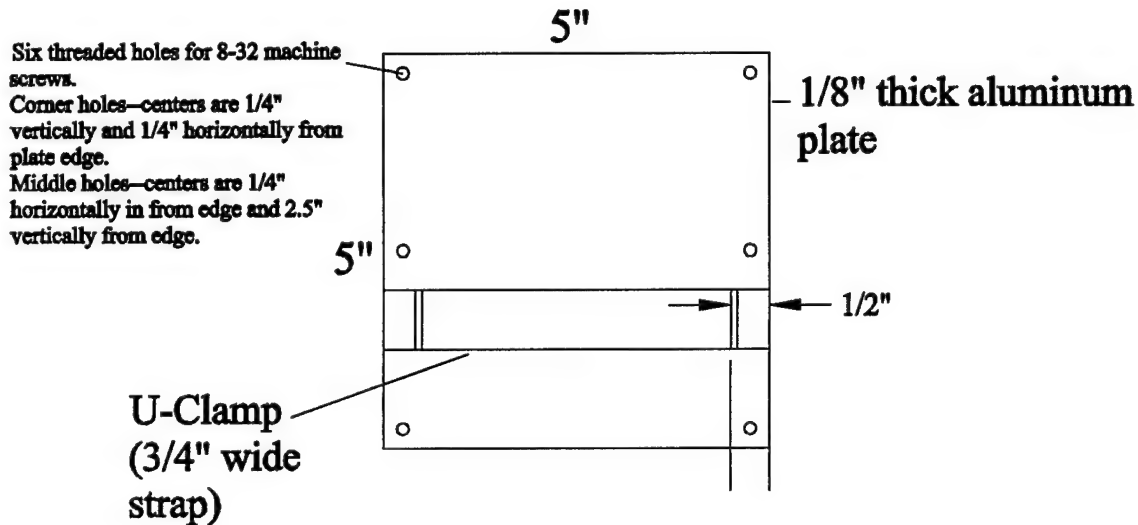
Left Side View



momwheelbaywithamplifiers.dwg

Figure K.25 Amplifier Arrangement
K-33

Gyro Housing--Top View

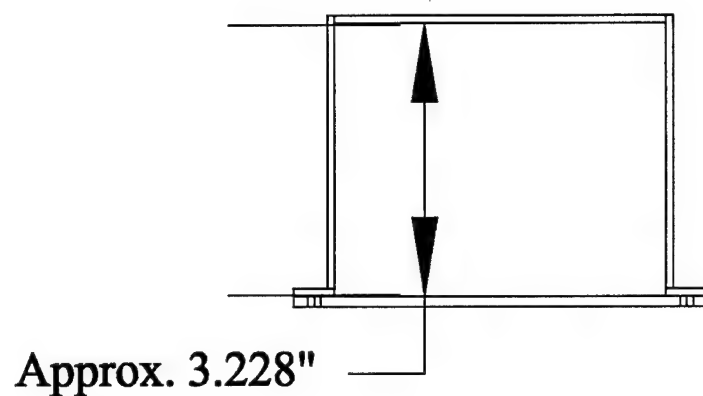


Removable U-Clamp is attached to plate (and to top of gyro) by appropriate means with no (or slight) protrusion out bottom of plate

gyrohousingwC-CLAMPwtext&dim.dwg

Figure K.26 Gyroscope Housing for Attachment to Mounting Plate - Front View

Gyro Housing--Side View



gyrohousingwC-CLAMPwtext&dimSIDEVIEW.dwg

Figure K.27 Gyroscope Housing - Side View

Gyroscope, Battery, and Transceiver Mounting

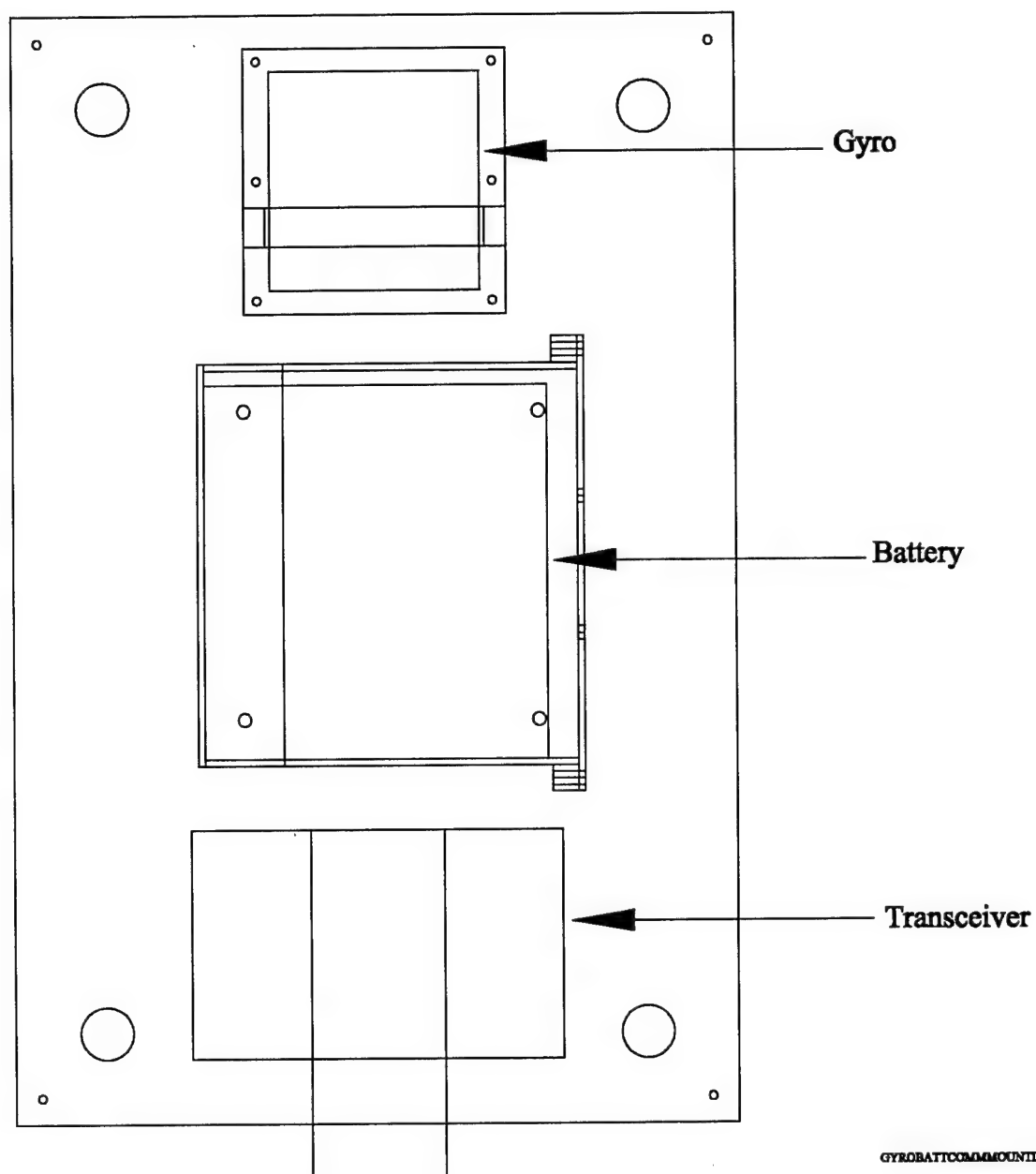
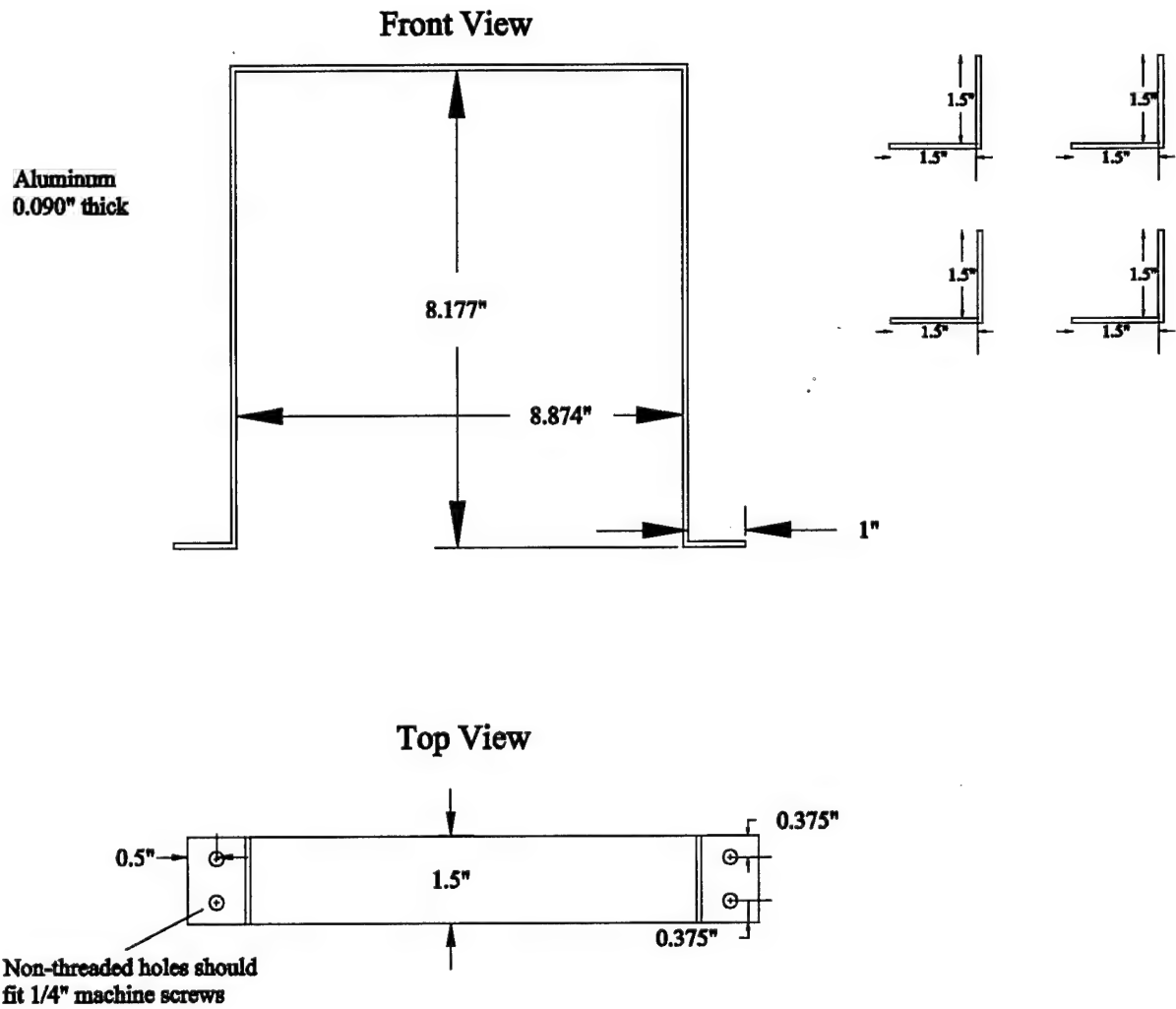


Figure K.28 Gyro, Battery, and Transceiver Mounting

AUTOBOX U-CLAMP & FOUR L-BRACKETS



U-clamp provides 1/2" clearance around AutoBox

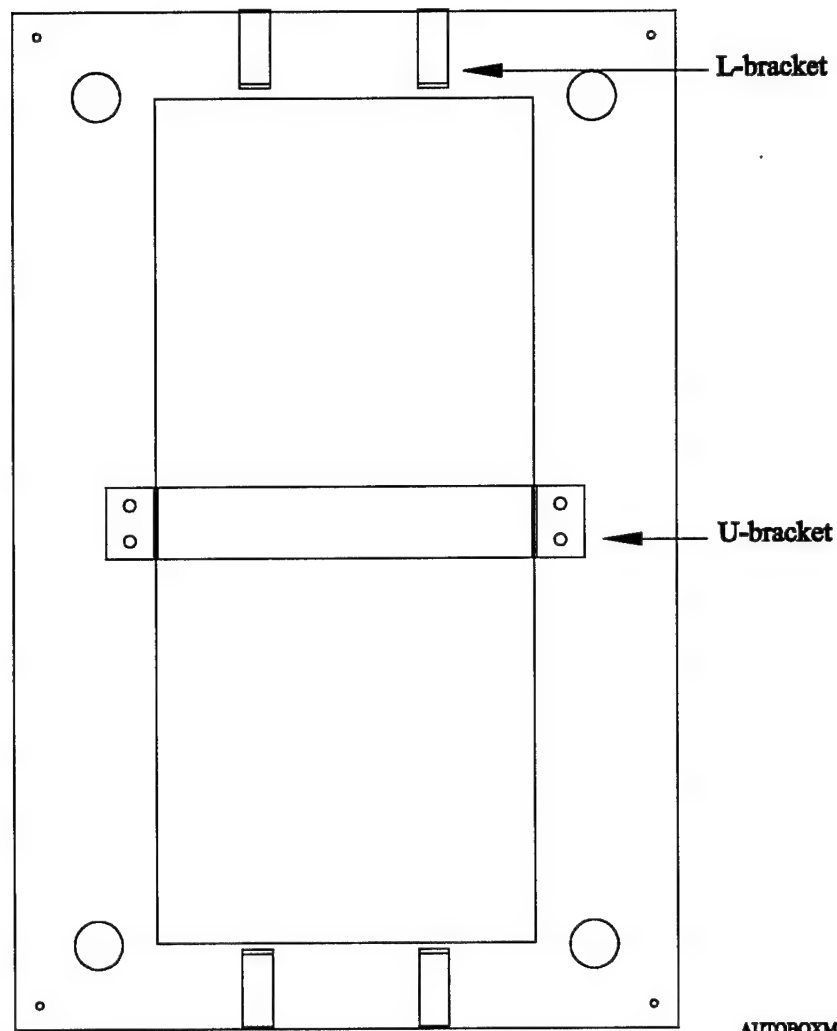
UBRACKETLBRACKESBzAUTOBOX.dwg

Figure K.29 AutoBox U-clamp and Restraint L-brackets
K-37

Autobox Mounting

Polyurethane padding
should be inserted
between
U-bracket/Lbrackets
and the Autobox to
isolate the Autobox
from vibrations.

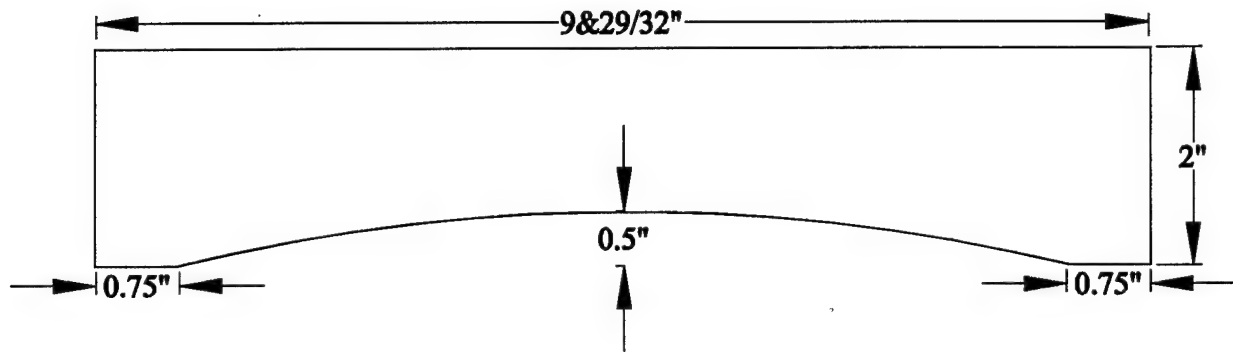
AutoBox is
centered on
mounting plate.



AUTOBOXMOUNTING.dwg

Figure K.30 AutoBox Mounting
K-38

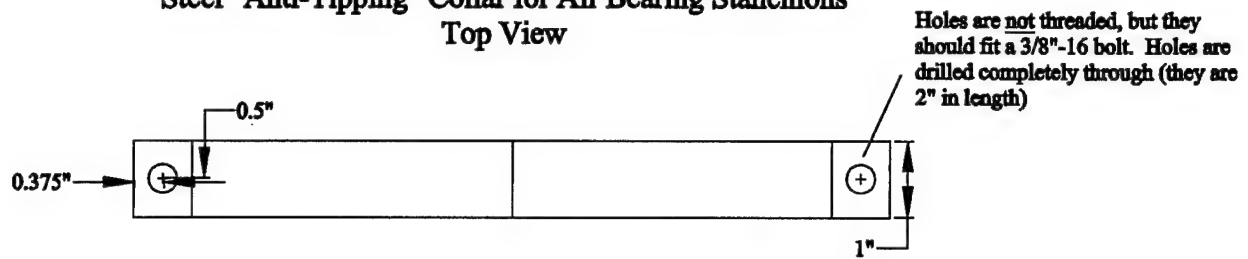
Steel "Anti-Tipping" Collar for Air Bearing Stanchions
Side View



ANTITIPSTRIP.dwg

Figure K.31 Stanchion Restraint Collars - Side View
K-39

Steel "Anti-Tipping" Collar for Air Bearing Stanchions Top View



Air Bearing Stanchion Holes (not shown) should be threaded to accept a 3/8"-16 bolt with at least 3/4" penetration.

ANITIPSTRIPtopview.dwg

Figure K.32 Stanchion Restraint Collars - Top View
K-40

Appendix L. Finite-Element Modeling

L.1 Overview

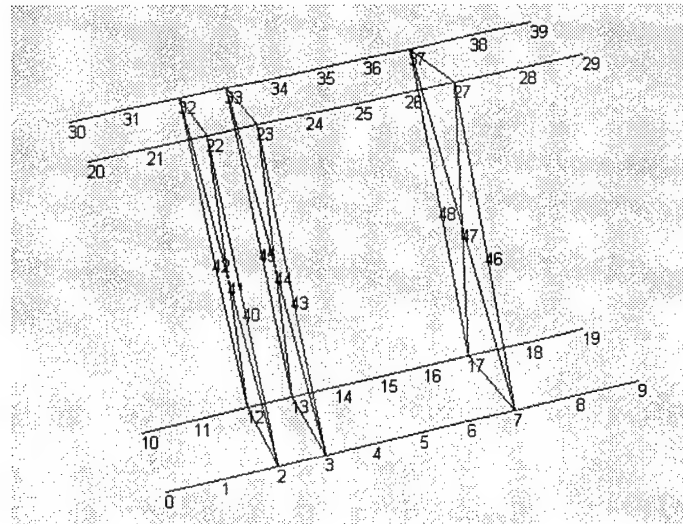
The inputs for each finite-element model are listed in this appendix in MKS units. Inputs include the nodal coordinates, loads, material properties, and element masses and inertias. Moreover, the static deflections are listed, with deflections designated for each node as computed by the *CADRE* software.

L.2 CADRE Models

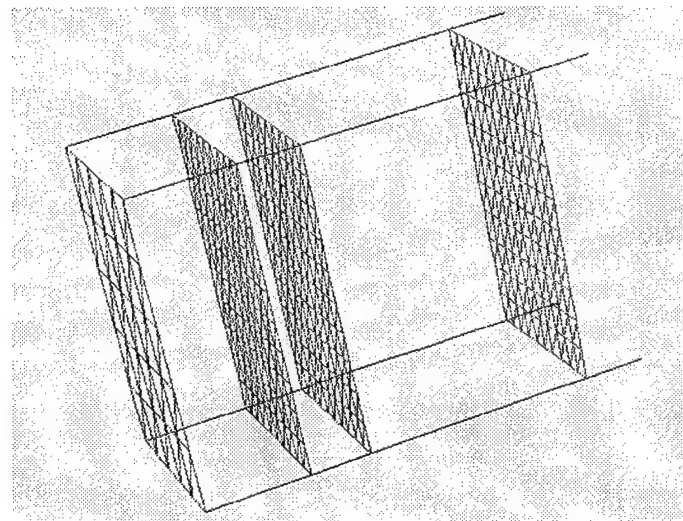
The payload-side model included the AutoBox, rate gyros, battery, communications equipment, an 18kg dummy payload, and structures. This model is shown in Figure L.1. The momentum wheel-side model included the momentum wheel assembly (to include three momentum wheels with motors, shelving structure, and lexan enclosure), two batteries, three motor amps, and structures. The inputs and displacement results of the *CADRE* models are listed at the end of this appendix.

L.3 CADRE Pro Model

The momentum wheel-side structure was also modeled using the *CADRE Pro* software. This model allowed the construction and analysis of 2-D plates, also shown in Figure L.1. The same nodal loading parameters were used in the *CADRE Pro* model as in the *CADRE* model, with updated material specifications.



(a) Payload-Side *CADRE* Model



(b) Wheel-Side *CADRE Pro* Model

Figure L.1 Finite-Element Models

Table L.1 Payload-Side Nodal Coordinates

Basic Data:			
Structural Nodes	49		
Reference Nodes	2		
Number of elements	66		
Properties per Element	4		
Number of bounds	49		
Number of Mass Nodes	49		
Nodal Coordinates:			
Ident	X	Y	Z
0	0000.0000	0000.0000	0000.0000
1	0000.0700	0000.0000	0000.0000
2	0000.1400	0000.0000	0000.0000
3	0000.2000	0000.0000	0000.0000
4	0000.2600	0000.0000	0000.0000
5	0000.3200	0000.0000	0000.0000
6	0000.3800	0000.0000	0000.0000
7	0000.4400	0000.0000	0000.0000
8	0000.5200	0000.0000	0000.0000
9	0000.6000	0000.0000	0000.0000
10	0000.0000	0000.0000	-0000.2400
11	0000.0700	0000.0000	-0000.2400
12	0000.1400	0000.0000	-0000.2400
13	0000.2000	0000.0000	-0000.2400
14	0000.2600	0000.0000	-0000.2400
15	0000.3200	0000.0000	-0000.2400
16	0000.3800	0000.0000	-0000.2400
17	0000.4400	0000.0000	-0000.2400
18	0000.5200	0000.0000	-0000.2400
19	0000.6000	0000.0000	-0000.2400
20	0000.0000	0000.4400	0000.0000
21	0000.0700	0000.4400	0000.0000
22	0000.1400	0000.4400	0000.0000
23	0000.2000	0000.4400	0000.0000
24	0000.2600	0000.4400	0000.0000
25	0000.3200	0000.4400	0000.0000
26	0000.3800	0000.4400	0000.0000
27	0000.4400	0000.4400	0000.0000
28	0000.5200	0000.4400	0000.0000
29	0000.6000	0000.4400	0000.0000
30	0000.0000	0000.4400	-0000.2400
31	0000.0700	0000.4400	-0000.2400
32	0000.1400	0000.4400	-0000.2400
33	0000.2000	0000.4400	-0000.2400
34	0000.2600	0000.4400	-0000.2400
35	0000.3200	0000.4400	-0000.2400
36	0000.3800	0000.4400	-0000.2400
37	0000.4400	0000.4400	-0000.2400
38	0000.5200	0000.4400	-0000.2400
39	0000.6000	0000.4400	-0000.2400
40	0000.1400	0000.2200	0000.0000
41	0000.1400	0000.2200	-0000.1200
42	0000.1400	0000.2200	-0000.2400
43	0000.2000	0000.2200	0000.0000
44	0000.2000	0000.2200	-0000.1200
45	0000.2000	0000.2200	-0000.2400
46	0000.4400	0000.2200	0000.0000
47	0000.4400	0000.2200	-0000.1200
48	0000.4400	0000.2200	-0000.2400
49	0000.0000	0000.2200	0000.0000
50	0000.0000	0000.2200	-0000.2400

Table L.2 Payload-Side Element Specifications

Element Definition Data: (Properties)

Ident	Type	AE	EIy	EIz	JG
0000.0001	S	2.253E+07	1.751E+03	1.751E+03	1.301E+03
0001.0002	S	2.253E+07	1.751E+03	1.751E+03	1.301E+03
0002.0003	S	2.253E+07	1.751E+03	1.751E+03	1.301E+03
0003.0004	S	2.253E+07	1.751E+03	1.751E+03	1.301E+03
0004.0005	S	2.253E+07	1.751E+03	1.751E+03	1.301E+03
0005.0006	S	2.253E+07	1.751E+03	1.751E+03	1.301E+03
0006.0007	S	2.253E+07	1.751E+03	1.751E+03	1.301E+03
0007.0008	S	2.253E+07	1.751E+03	1.751E+03	1.301E+03
0008.0009	S	2.253E+07	1.751E+03	1.751E+03	1.301E+03
0010.0011	S	2.253E+07	1.751E+03	1.751E+03	1.301E+03
0011.0012	S	2.253E+07	1.751E+03	1.751E+03	1.301E+03
0012.0013	S	2.253E+07	1.751E+03	1.751E+03	1.301E+03
0013.0014	S	2.253E+07	1.751E+03	1.751E+03	1.301E+03
0014.0015	S	2.253E+07	1.751E+03	1.751E+03	1.301E+03
0015.0016	S	2.253E+07	1.751E+03	1.751E+03	1.301E+03
0016.0017	S	2.253E+07	1.751E+03	1.751E+03	1.301E+03
0017.0018	S	2.253E+07	1.751E+03	1.751E+03	1.301E+03
0018.0019	S	2.253E+07	1.751E+03	1.751E+03	1.301E+03
0020.0021	S	2.253E+07	1.751E+03	1.751E+03	1.301E+03
0021.0022	S	2.253E+07	1.751E+03	1.751E+03	1.301E+03
0022.0023	S	2.253E+07	1.751E+03	1.751E+03	1.301E+03
0023.0024	S	2.253E+07	1.751E+03	1.751E+03	1.301E+03
0024.0025	S	2.253E+07	1.751E+03	1.751E+03	1.301E+03
0025.0026	S	2.253E+07	1.751E+03	1.751E+03	1.301E+03
0026.0027	S	2.253E+07	1.751E+03	1.751E+03	1.301E+03
0027.0028	S	2.253E+07	1.751E+03	1.751E+03	1.301E+03
0028.0029	S	2.253E+07	1.751E+03	1.751E+03	1.301E+03
0030.0031	S	2.253E+07	1.751E+03	1.751E+03	1.301E+03
0031.0032	S	2.253E+07	1.751E+03	1.751E+03	1.301E+03
0032.0033	S	2.253E+07	1.751E+03	1.751E+03	1.301E+03
0033.0034	S	2.253E+07	1.751E+03	1.751E+03	1.301E+03
0034.0035	S	2.253E+07	1.751E+03	1.751E+03	1.301E+03
0035.0036	S	2.253E+07	1.751E+03	1.751E+03	1.301E+03
0036.0037	S	2.253E+07	1.751E+03	1.751E+03	1.301E+03
0037.0038	S	2.253E+07	1.751E+03	1.751E+03	1.301E+03
0038.0039	S	2.253E+07	1.751E+03	1.751E+03	1.301E+03
0002.0012	S	1.374E+06	2.148E+00	2.148E+00	1.615E+00
0003.0013	S	1.374E+06	2.148E+00	2.148E+00	1.615E+00
0007.0017	S	1.374E+06	2.148E+00	2.148E+00	1.615E+00
0002.0040	S	1.374E+06	2.148E+00	2.148E+00	1.615E+00
0003.0043	S	1.374E+06	2.148E+00	2.148E+00	1.615E+00
0007.0046	S	1.374E+06	2.148E+00	2.148E+00	1.615E+00
0022.0032	S	1.374E+06	2.148E+00	2.148E+00	1.615E+00
0023.0033	S	1.374E+06	2.148E+00	2.148E+00	1.615E+00
0027.0037	S	1.374E+06	2.148E+00	2.148E+00	1.615E+00
0040.0022	S	1.374E+06	2.148E+00	2.148E+00	1.615E+00
0043.0023	S	1.374E+06	2.148E+00	2.148E+00	1.615E+00
0046.0027	S	1.374E+06	2.148E+00	2.148E+00	1.615E+00
0032.0042	S	1.374E+06	2.148E+00	2.148E+00	1.615E+00
0042.0012	S	1.374E+06	2.148E+00	2.148E+00	1.615E+00
0033.0045	S	1.374E+06	2.148E+00	2.148E+00	1.615E+00
0045.0013	S	1.374E+06	2.148E+00	2.148E+00	1.615E+00
0037.0048	S	1.374E+06	2.148E+00	2.148E+00	1.615E+00
0048.0017	S	1.374E+06	2.148E+00	2.148E+00	1.615E+00
0002.0041	S	1.374E+06	2.148E+00	2.148E+00	1.615E+00
0012.0041	S	1.374E+06	2.148E+00	2.148E+00	1.615E+00
0022.0041	S	1.374E+06	2.148E+00	2.148E+00	1.615E+00
0032.0041	S	1.374E+06	2.148E+00	2.148E+00	1.615E+00
0003.0044	S	1.374E+06	2.148E+00	2.148E+00	1.615E+00
0013.0044	S	1.374E+06	2.148E+00	2.148E+00	1.615E+00
0023.0044	S	1.374E+06	2.148E+00	2.148E+00	1.615E+00
0033.0044	S	1.374E+06	2.148E+00	2.148E+00	1.615E+00
0007.0047	S	1.374E+06	2.148E+00	2.148E+00	1.615E+00
0017.0047	S	1.374E+06	2.148E+00	2.148E+00	1.615E+00
0027.0047	S	1.374E+06	2.148E+00	2.148E+00	1.615E+00
0037.0047	S	1.374E+06	2.148E+00	2.148E+00	1.615E+00

Table L.3 Payload-Side Nodal Mass Properties

Mass Properties:

Node	Mass	Ix	Iy	Iz	Xcg	Ycg	Zcg	DOF
0	1.000E-01	0.000E+00	0.000E+00	0.000E+00	0.000E+00	0.000E+00	0.000E+00	010000
1	1.000E-01	0.000E+00	0.000E+00	0.000E+00	7.000E-02	0.000E+00	0.000E+00	010000
2	4.500E-01	0.000E+00	0.000E+00	0.000E+00	1.400E-01	0.000E+00	0.000E+00	010000
3	4.500E-01	0.000E+00	0.000E+00	0.000E+00	2.000E-01	0.000E+00	0.000E+00	010000
4	1.000E-01	0.000E+00	0.000E+00	0.000E+00	2.600E-01	0.000E+00	0.000E+00	010000
5	1.000E-01	0.000E+00	0.000E+00	0.000E+00	3.200E-01	0.000E+00	0.000E+00	010000
6	1.000E-01	0.000E+00	0.000E+00	0.000E+00	3.800E-01	0.000E+00	0.000E+00	010000
7	4.500E-01	0.000E+00	0.000E+00	0.000E+00	4.400E-01	0.000E+00	0.000E+00	010000
8	1.000E-01	0.000E+00	0.000E+00	0.000E+00	5.200E-01	0.000E+00	0.000E+00	010000
9	1.000E-01	0.000E+00	0.000E+00	0.000E+00	6.000E-01	0.000E+00	0.000E+00	010000
10	1.000E-01	0.000E+00	0.000E+00	0.000E+00	0.000E+00	0.000E+00	-2.400E-01	010000
11	1.000E-01	0.000E+00	0.000E+00	0.000E+00	7.000E-02	0.000E+00	-2.400E-01	010000
12	4.500E-01	0.000E+00	0.000E+00	0.000E+00	1.400E-01	0.000E+00	-2.400E-01	010000
13	4.500E-01	0.000E+00	0.000E+00	0.000E+00	2.000E-01	0.000E+00	-2.400E-01	010000
14	1.000E-01	0.000E+00	0.000E+00	0.000E+00	2.600E-01	0.000E+00	-2.400E-01	010000
15	1.000E-01	0.000E+00	0.000E+00	0.000E+00	3.200E-01	0.000E+00	-2.400E-01	010000
16	1.000E-01	0.000E+00	0.000E+00	0.000E+00	3.800E-01	0.000E+00	-2.400E-01	010000
17	4.500E-01	0.000E+00	0.000E+00	0.000E+00	4.400E-01	0.000E+00	-2.400E-01	010000
18	1.000E-01	0.000E+00	0.000E+00	0.000E+00	5.200E-01	0.000E+00	-2.400E-01	010000
19	1.000E-01	0.000E+00	0.000E+00	0.000E+00	6.000E-01	0.000E+00	-2.400E-01	010000
20	1.000E-01	0.000E+00	0.000E+00	0.000E+00	0.000E+00	4.400E-01	0.000E+00	010000
21	1.000E-01	0.000E+00	0.000E+00	0.000E+00	7.000E-02	4.400E-01	0.000E+00	010000
22	4.500E-01	0.000E+00	0.000E+00	0.000E+00	1.400E-01	4.400E-01	0.000E+00	010000
23	4.500E-01	0.000E+00	0.000E+00	0.000E+00	2.000E-01	4.400E-01	0.000E+00	010000
24	1.000E-01	0.000E+00	0.000E+00	0.000E+00	2.600E-01	4.400E-01	0.000E+00	010000
25	1.000E-01	0.000E+00	0.000E+00	0.000E+00	3.200E-01	4.400E-01	0.000E+00	010000
26	1.000E-01	0.000E+00	0.000E+00	0.000E+00	3.800E-01	4.400E-01	0.000E+00	010000
27	4.500E-01	0.000E+00	0.000E+00	0.000E+00	4.400E-01	4.400E-01	0.000E+00	010000
28	1.000E-01	0.000E+00	0.000E+00	0.000E+00	5.200E-01	4.400E-01	0.000E+00	010000
29	1.000E-01	0.000E+00	0.000E+00	0.000E+00	6.000E-01	4.400E-01	0.000E+00	010000
30	1.000E-01	0.000E+00	0.000E+00	0.000E+00	0.000E+00	4.400E-01	-2.400E-01	010000
31	1.000E-01	0.000E+00	0.000E+00	0.000E+00	7.000E-02	4.400E-01	-2.400E-01	010000
32	4.500E-01	0.000E+00	0.000E+00	0.000E+00	1.400E-01	4.400E-01	-2.400E-01	010000
33	4.500E-01	0.000E+00	0.000E+00	0.000E+00	2.000E-01	4.400E-01	-2.400E-01	010000
34	1.000E-01	0.000E+00	0.000E+00	0.000E+00	2.600E-01	4.400E-01	-2.400E-01	010000
35	1.000E-01	0.000E+00	0.000E+00	0.000E+00	3.200E-01	4.400E-01	-2.400E-01	010000
36	1.000E-01	0.000E+00	0.000E+00	0.000E+00	3.800E-01	4.400E-01	-2.400E-01	010000
37	4.500E-01	0.000E+00	0.000E+00	0.000E+00	4.400E-01	4.400E-01	-2.400E-01	010000
38	1.000E-01	0.000E+00	0.000E+00	0.000E+00	5.200E-01	4.400E-01	-2.400E-01	010000
39	1.000E-01	0.000E+00	0.000E+00	0.000E+00	6.000E-01	4.400E-01	-2.400E-01	010000
40	3.500E-01	0.000E+00	0.000E+00	0.000E+00	1.400E-01	2.200E-01	0.000E+00	010000
42	3.500E-01	0.000E+00	0.000E+00	0.000E+00	1.400E-01	2.200E-01	-2.400E-01	010000
41	1.200E+01	0.000E+00	0.000E+00	0.000E+00	1.000E-01	2.200E-01	-1.200E-01	010000
43	3.500E-01	0.000E+00	0.000E+00	0.000E+00	2.000E-01	2.200E-01	0.000E+00	010000
45	3.500E-01	0.000E+00	0.000E+00	0.000E+00	2.000E-01	2.200E-01	-2.400E-01	010000
44	1.000E+01	0.000E+00	0.000E+00	0.000E+00	3.100E-01	2.200E-01	-1.200E-01	010000
46	3.500E-01	0.000E+00	0.000E+00	0.000E+00	4.400E-01	2.200E-01	0.000E+00	010000
48	3.500E-01	0.000E+00	0.000E+00	0.000E+00	4.400E-01	2.200E-01	-2.400E-01	010000
47	1.800E+01	0.000E+00	0.000E+00	0.000E+00	5.600E-01	2.200E-01	-1.200E-01	010000

Table L.4 Payload-Side Displacements

Nodal Displacements:						
Node	X	Y	Z	Rx	Ry	Rz
000.000	0.000E+00	0.000E+00	0.000E+00	0.000E+00	0.000E+00	0.000E+00
001.000	6.212E-09	4.571E-05	-3.595E-07	2.051E-07	8.649E-06	1.248E-03
002.000	1.242E-08	1.666E-04	-9.837E-07	4.102E-07	7.563E-06	2.148E-03
003.000	1.639E-08	3.125E-04	-1.334E-06	5.387E-07	4.677E-06	2.685E-03
004.000	1.866E-08	4.860E-04	-1.598E-06	6.199E-07	4.093E-06	3.079E-03
005.000	2.092E-08	6.797E-04	-1.824E-06	7.010E-07	3.412E-06	3.359E-03
006.000	2.319E-08	8.868E-04	-2.005E-06	7.822E-07	2.632E-06	3.526E-03
007.000	2.546E-08	1.101E-03	-2.138E-06	8.634E-07	1.754E-06	3.582E-03
008.000	2.546E-08	1.388E-03	-2.278E-06	8.634E-07	1.754E-06	3.590E-03
009.000	2.546E-08	1.675E-03	-2.418E-06	8.634E-07	1.754E-06	3.592E-03
010.000	0.000E+00	0.000E+00	0.000E+00	0.000E+00	0.000E+00	0.000E+00
011.000	6.212E-09	4.571E-05	3.595E-07	-2.051E-07	-8.649E-06	1.248E-03
012.000	1.242E-08	1.666E-04	9.837E-07	-4.102E-07	-7.563E-06	2.148E-03
013.000	1.639E-08	3.125E-04	1.334E-06	-5.387E-07	-4.677E-06	2.685E-03
014.000	1.866E-08	4.860E-04	1.598E-06	-6.199E-07	-4.093E-06	3.079E-03
015.000	2.092E-08	6.797E-04	1.824E-06	-7.010E-07	-3.412E-06	3.359E-03
016.000	2.319E-08	8.868E-04	2.005E-06	-7.822E-07	-2.632E-06	3.526E-03
017.000	2.546E-08	1.101E-03	2.138E-06	-8.634E-07	-1.754E-06	3.582E-03
018.000	2.546E-08	1.388E-03	2.278E-06	-8.634E-07	-1.754E-06	3.590E-03
019.000	2.546E-08	1.675E-03	2.418E-06	-8.634E-07	-1.754E-06	3.592E-03
020.000	0.000E+00	0.000E+00	0.000E+00	0.000E+00	0.000E+00	0.000E+00
021.000	-6.212E-09	4.571E-05	3.595E-07	2.051E-07	-8.649E-06	1.248E-03
022.000	-1.242E-08	1.666E-04	9.837E-07	4.102E-07	-7.563E-06	2.148E-03
023.000	-1.639E-08	3.125E-04	1.334E-06	5.387E-07	-4.677E-06	2.685E-03
024.000	-1.866E-08	4.860E-04	1.598E-06	6.199E-07	-4.093E-06	3.079E-03
025.000	-2.092E-08	6.797E-04	1.824E-06	7.010E-07	-3.412E-06	3.359E-03
026.000	-2.319E-08	8.868E-04	2.005E-06	7.822E-07	-2.632E-06	3.526E-03
027.000	-2.546E-08	1.101E-03	2.138E-06	8.634E-07	-1.754E-06	3.582E-03
028.000	-2.546E-08	1.388E-03	2.278E-06	8.634E-07	-1.754E-06	3.590E-03
029.000	-2.546E-08	1.675E-03	2.418E-06	8.634E-07	-1.754E-06	3.592E-03
030.000	0.000E+00	0.000E+00	0.000E+00	0.000E+00	0.000E+00	0.000E+00
031.000	-6.212E-09	4.571E-05	-3.595E-07	-2.051E-07	8.649E-06	1.248E-03
032.000	-1.242E-08	1.666E-04	-9.837E-07	-4.102E-07	7.563E-06	2.148E-03
033.000	-1.639E-08	3.125E-04	-1.334E-06	-5.387E-07	4.677E-06	2.685E-03
034.000	-1.866E-08	4.860E-04	-1.598E-06	-6.199E-07	4.093E-06	3.079E-03
035.000	-2.092E-08	6.797E-04	-1.824E-06	-7.010E-07	3.412E-06	3.359E-03
036.000	-2.319E-08	8.868E-04	-2.005E-06	-7.822E-07	2.632E-06	3.526E-03
037.000	-2.546E-08	1.101E-03	-2.138E-06	-8.634E-07	1.754E-06	3.582E-03
038.000	-2.546E-08	1.388E-03	-2.278E-06	-8.634E-07	1.754E-06	3.590E-03
039.000	-2.546E-08	1.675E-03	-2.418E-06	-8.634E-07	1.754E-06	3.592E-03
040.000	-5.765E-21	1.669E-04	2.226E-19	6.502E-06	-2.774E-18	-1.074E-03
041.000	4.044E-20	1.742E-04	2.091E-19	-1.787E-16	-2.243E-19	-9.060E-04
042.000	-1.578E-22	1.669E-04	1.965E-19	-6.502E-06	-3.143E-18	-1.074E-03
043.000	4.479E-20	3.128E-04	3.993E-19	8.829E-06	-3.473E-18	-1.342E-03
044.000	-3.797E-22	3.191E-04	3.611E-19	-3.545E-16	-2.268E-19	-1.131E-03
045.000	-4.442E-20	3.128E-04	4.297E-19	-8.829E-06	-4.018E-18	-1.342E-03
046.000	-9.634E-20	1.101E-03	1.680E-18	1.414E-05	-4.718E-18	-1.791E-03
047.000	-2.492E-20	1.112E-03	1.684E-18	-1.451E-15	-2.816E-19	-1.507E-03
048.000	-1.066E-20	1.101E-03	1.518E-18	-1.414E-05	-5.687E-18	-1.791E-03

Table L.5 Wheel-Side Nodal Coordinates

Basic Data:
 Structural Nodes 49
 Reference Nodes 0
 Number of elements 66
 Properties per Element 4
 Number of bounds 49
 Number of Loaded Nodes 49

Nodal Coordinates:

Ident	X	Y	Z
0	0000.0000	0000.0000	0000.0000
1	0000.0700	0000.0000	0000.0000
2	0000.1400	0000.0000	0000.0000
3	0000.2200	0000.0000	0000.0000
4	0000.2800	0000.0000	0000.0000
5	0000.3400	0000.0000	0000.0000
6	0000.4000	0000.0000	0000.0000
7	0000.4600	0000.0000	0000.0000
8	0000.5200	0000.0000	0000.0000
9	0000.6000	0000.0000	0000.0000
10	0000.0000	0000.0000	-0000.2400
11	0000.0700	0000.0000	-0000.2400
12	0000.1400	0000.0000	-0000.2400
13	0000.2200	0000.0000	-0000.2400
14	0000.2800	0000.0000	-0000.2400
15	0000.3400	0000.0000	-0000.2400
16	0000.4000	0000.0000	-0000.2400
17	0000.4600	0000.0000	-0000.2400
18	0000.5200	0000.0000	-0000.2400
19	0000.6000	0000.0000	-0000.2400
20	0000.0000	0000.4400	0000.0000
21	0000.0700	0000.4400	0000.0000
22	0000.1400	0000.4400	0000.0000
23	0000.2200	0000.4400	0000.0000
24	0000.2800	0000.4400	0000.0000
25	0000.3400	0000.4400	0000.0000
26	0000.4000	0000.4400	0000.0000
27	0000.4600	0000.4400	0000.0000
28	0000.5200	0000.4400	0000.0000
29	0000.6000	0000.4400	0000.0000
30	0000.0000	0000.4400	-0000.2400
31	0000.0700	0000.4400	-0000.2400
32	0000.1400	0000.4400	-0000.2400
33	0000.2200	0000.4400	-0000.2400
34	0000.2800	0000.4400	-0000.2400
35	0000.3400	0000.4400	-0000.2400
36	0000.4000	0000.4400	-0000.2400
37	0000.4600	0000.4400	-0000.2400
38	0000.5200	0000.4400	-0000.2400
39	0000.6000	0000.4400	-0000.2400
40	0000.1400	0000.2200	0000.0000
41	0000.1400	0000.2200	-0000.1200
42	0000.1400	0000.2200	-0000.2400
43	0000.2200	0000.2200	0000.0000
44	0000.2200	0000.2200	-0000.1200
45	0000.2200	0000.2200	-0000.2400
46	0000.5200	0000.2200	0000.0000
47	0000.5200	0000.2200	-0000.1200
48	0000.5200	0000.2200	-0000.2400

Table L.6 Wheel-Side Element Specifications

Element Definition Data: (Properties)

Ident	Type	AE	EIy	EIz	JG
0000.0001	S	2.253E+07	1.751E+03	1.751E+03	1.301E+03
0001.0002	S	2.253E+07	1.751E+03	1.751E+03	1.301E+03
0002.0003	S	2.253E+07	1.751E+03	1.751E+03	1.301E+03
0003.0004	S	2.253E+07	1.751E+03	1.751E+03	1.301E+03
0004.0005	S	2.253E+07	1.751E+03	1.751E+03	1.301E+03
0005.0006	S	2.253E+07	1.751E+03	1.751E+03	1.301E+03
0006.0007	S	2.253E+07	1.751E+03	1.751E+03	1.301E+03
0007.0008	S	2.253E+07	1.751E+03	1.751E+03	1.301E+03
0008.0009	S	2.253E+07	1.751E+03	1.751E+03	1.301E+03
0010.0011	S	2.253E+07	1.751E+03	1.751E+03	1.301E+03
0011.0012	S	2.253E+07	1.751E+03	1.751E+03	1.301E+03
0012.0013	S	2.253E+07	1.751E+03	1.751E+03	1.301E+03
0013.0014	S	2.253E+07	1.751E+03	1.751E+03	1.301E+03
0014.0015	S	2.253E+07	1.751E+03	1.751E+03	1.301E+03
0015.0016	S	2.253E+07	1.751E+03	1.751E+03	1.301E+03
0016.0017	S	2.253E+07	1.751E+03	1.751E+03	1.301E+03
0017.0018	S	2.253E+07	1.751E+03	1.751E+03	1.301E+03
0018.0019	S	2.253E+07	1.751E+03	1.751E+03	1.301E+03
0020.0021	S	2.253E+07	1.751E+03	1.751E+03	1.301E+03
0021.0022	S	2.253E+07	1.751E+03	1.751E+03	1.301E+03
0022.0023	S	2.253E+07	1.751E+03	1.751E+03	1.301E+03
0023.0024	S	2.253E+07	1.751E+03	1.751E+03	1.301E+03
0024.0025	S	2.253E+07	1.751E+03	1.751E+03	1.301E+03
0025.0026	S	2.253E+07	1.751E+03	1.751E+03	1.301E+03
0026.0027	S	2.253E+07	1.751E+03	1.751E+03	1.301E+03
0027.0028	S	2.253E+07	1.751E+03	1.751E+03	1.301E+03
0028.0029	S	2.253E+07	1.751E+03	1.751E+03	1.301E+03
0030.0031	S	2.253E+07	1.751E+03	1.751E+03	1.301E+03
0031.0032	S	2.253E+07	1.751E+03	1.751E+03	1.301E+03
0032.0033	S	2.253E+07	1.751E+03	1.751E+03	1.301E+03
0033.0034	S	2.253E+07	1.751E+03	1.751E+03	1.301E+03
0034.0035	S	2.253E+07	1.751E+03	1.751E+03	1.301E+03
0035.0036	S	2.253E+07	1.751E+03	1.751E+03	1.301E+03
0036.0037	S	2.253E+07	1.751E+03	1.751E+03	1.301E+03
0037.0038	S	2.253E+07	1.751E+03	1.751E+03	1.301E+03
0038.0039	S	2.253E+07	1.751E+03	1.751E+03	1.301E+03
0002.0012	S	1.374E+06	2.148E+00	2.148E+00	1.615E+00
0003.0013	S	1.374E+06	2.148E+00	2.148E+00	1.615E+00
0008.0018	S	1.374E+06	2.148E+00	2.148E+00	1.615E+00
0002.0040	S	1.374E+06	2.148E+00	2.148E+00	1.615E+00
0003.0043	S	1.374E+06	2.148E+00	2.148E+00	1.615E+00
0008.0046	S	1.374E+06	2.148E+00	2.148E+00	1.615E+00
0022.0032	S	1.374E+06	2.148E+00	2.148E+00	1.615E+00
0023.0033	S	1.374E+06	2.148E+00	2.148E+00	1.615E+00
0028.0038	S	1.374E+06	2.148E+00	2.148E+00	1.615E+00
0040.0022	S	1.374E+06	2.148E+00	2.148E+00	1.615E+00
0043.0023	S	1.374E+06	2.148E+00	2.148E+00	1.615E+00
0046.0028	S	1.374E+06	2.148E+00	2.148E+00	1.615E+00
0032.0042	S	1.374E+06	2.148E+00	2.148E+00	1.615E+00
0042.0012	S	1.374E+06	2.148E+00	2.148E+00	1.615E+00
0033.0045	S	1.374E+06	2.148E+00	2.148E+00	1.615E+00
0045.0013	S	1.374E+06	2.148E+00	2.148E+00	1.615E+00
0038.0048	S	1.374E+06	2.148E+00	2.148E+00	1.615E+00
0048.0018	S	1.374E+06	2.148E+00	2.148E+00	1.615E+00
0002.0041	S	1.374E+06	2.148E+00	2.148E+00	1.615E+00
0012.0041	S	1.374E+06	2.148E+00	2.148E+00	1.615E+00
0022.0041	S	1.374E+06	2.148E+00	2.148E+00	1.615E+00
0032.0041	S	1.374E+06	2.148E+00	2.148E+00	1.615E+00
0003.0044	S	1.374E+06	2.148E+00	2.148E+00	1.615E+00
0013.0044	S	1.374E+06	2.148E+00	2.148E+00	1.615E+00
0023.0044	S	1.374E+06	2.148E+00	2.148E+00	1.615E+00
0033.0044	S	1.374E+06	2.148E+00	2.148E+00	1.615E+00
0008.0047	S	1.374E+06	2.148E+00	2.148E+00	1.615E+00
0018.0047	S	1.374E+06	2.148E+00	2.148E+00	1.615E+00
0028.0047	S	1.374E+06	2.148E+00	2.148E+00	1.615E+00
0038.0047	S	1.374E+06	2.148E+00	2.148E+00	1.615E+00

Table L.7 Wheel-Side External Loading

External Nodal Loads:

[illegible]

Table L.8 Wheel-Side Displacements

Nodal Displacements:						
Node	X	Y	Z	Rx	Ry	Rz
000.000	0.000E+00	0.000E+00	0.000E+00	0.000E+00	0.000E+00	0.000E+00
001.000	6.212E-09	4.571E-05	-3.595E-07	2.051E-07	8.649E-06	1.248E-03
002.000	1.242E-08	1.666E-04	-9.837E-07	4.102E-07	7.563E-06	2.148E-03
003.000	1.639E-08	3.125E-04	-1.334E-06	5.387E-07	4.677E-06	2.685E-03
004.000	1.866E-08	4.860E-04	-1.598E-06	6.199E-07	4.093E-06	3.079E-03
005.000	2.092E-08	6.797E-04	-1.824E-06	7.010E-07	3.412E-06	3.359E-03
006.000	2.319E-08	8.868E-04	-2.005E-06	7.822E-07	2.632E-06	3.526E-03
007.000	2.546E-08	1.101E-03	-2.138E-06	8.634E-07	1.754E-06	3.582E-03
008.000	2.546E-08	1.388E-03	-2.278E-06	8.634E-07	1.754E-06	3.590E-03
009.000	2.546E-08	1.675E-03	-2.418E-06	8.634E-07	1.754E-06	3.592E-03
010.000	0.000E+00	0.000E+00	0.000E+00	0.000E+00	0.000E+00	0.000E+00
011.000	6.212E-09	4.571E-05	3.595E-07	-2.051E-07	-8.649E-06	1.248E-03
012.000	1.242E-08	1.666E-04	9.837E-07	-4.102E-07	-7.563E-06	2.148E-03
013.000	1.639E-08	3.125E-04	1.334E-06	-5.387E-07	-4.677E-06	2.685E-03
014.000	1.866E-08	4.860E-04	1.598E-06	-6.199E-07	-4.093E-06	3.079E-03
015.000	2.092E-08	6.797E-04	1.824E-06	-7.010E-07	-3.412E-06	3.359E-03
016.000	2.319E-08	8.868E-04	2.005E-06	-7.822E-07	-2.632E-06	3.526E-03
017.000	2.546E-08	1.101E-03	2.138E-06	-8.634E-07	-1.754E-06	3.582E-03
018.000	2.546E-08	1.388E-03	2.278E-06	-8.634E-07	-1.754E-06	3.590E-03
019.000	2.546E-08	1.675E-03	2.418E-06	-8.634E-07	-1.754E-06	3.592E-03
020.000	0.000E+00	0.000E+00	0.000E+00	0.000E+00	0.000E+00	0.000E+00
021.000	-6.212E-09	4.571E-05	3.595E-07	2.051E-07	-8.649E-06	1.248E-03
022.000	-1.242E-08	1.666E-04	9.837E-07	4.102E-07	-7.563E-06	2.148E-03
023.000	-1.639E-08	3.125E-04	1.334E-06	5.387E-07	-4.677E-06	2.685E-03
024.000	-1.866E-08	4.860E-04	1.598E-06	6.199E-07	-4.093E-06	3.079E-03
025.000	-2.092E-08	6.797E-04	1.824E-06	7.010E-07	-3.412E-06	3.359E-03
026.000	-2.319E-08	8.868E-04	2.005E-06	7.822E-07	-2.632E-06	3.526E-03
027.000	-2.546E-08	1.101E-03	2.138E-06	8.634E-07	-1.754E-06	3.582E-03
028.000	-2.546E-08	1.388E-03	2.278E-06	8.634E-07	-1.754E-06	3.590E-03
029.000	-2.546E-08	1.675E-03	2.418E-06	8.634E-07	-1.754E-06	3.592E-03
030.000	0.000E+00	0.000E+00	0.000E+00	0.000E+00	0.000E+00	0.000E+00
031.000	-6.212E-09	4.571E-05	-3.595E-07	-2.051E-07	8.649E-06	1.248E-03
032.000	-1.242E-08	1.666E-04	-9.837E-07	-4.102E-07	7.563E-06	2.148E-03
033.000	-1.639E-08	3.125E-04	-1.334E-06	-5.387E-07	4.677E-06	2.685E-03
034.000	-1.866E-08	4.860E-04	-1.598E-06	-6.199E-07	4.093E-06	3.079E-03
035.000	-2.092E-08	6.797E-04	-1.824E-06	-7.010E-07	3.412E-06	3.359E-03
036.000	-2.319E-08	8.868E-04	-2.005E-06	-7.822E-07	2.632E-06	3.526E-03
037.000	-2.546E-08	1.101E-03	-2.138E-06	-8.634E-07	1.754E-06	3.582E-03
038.000	-2.546E-08	1.388E-03	-2.278E-06	-8.634E-07	1.754E-06	3.590E-03
039.000	-2.546E-08	1.675E-03	-2.418E-06	-8.634E-07	1.754E-06	3.592E-03
040.000	-5.765E-21	1.669E-04	2.226E-19	6.502E-06	-2.774E-18	-1.074E-03
041.000	4.044E-20	1.742E-04	2.091E-19	-1.787E-16	-2.243E-19	-9.060E-04
042.000	-1.578E-22	1.669E-04	1.965E-19	-6.502E-06	-3.143E-18	-1.074E-03
043.000	4.479E-20	3.128E-04	3.993E-19	8.829E-06	-3.473E-18	-1.342E-03
044.000	-3.797E-22	3.191E-04	3.611E-19	-3.545E-16	-2.268E-19	-1.131E-03
045.000	-4.442E-20	3.128E-04	4.297E-19	-8.829E-06	-4.018E-18	-1.342E-03
046.000	-9.634E-20	1.101E-03	1.680E-18	1.414E-05	-4.718E-18	-1.791E-03
047.000	-2.492E-20	1.112E-03	1.684E-18	-1.451E-15	-2.816E-19	-1.507E-03
048.000	-1.066E-20	1.101E-03	1.518E-18	-1.414E-05	-5.687E-18	-1.791E-03

Appendix M. Final Controller Design

M.1 Overview

This appendix contains the controller gains and MATLAB output graphs for various maneuvers of the baseline *SIMSAT* design shown in Figure 5.24. These maneuvers are NOT performed sequentially; the *SIMSAT* state vector is set to zero before each maneuver.

M.2 Gain Settings Development

The following pages list the input gain matrices used in the final controller design. For each set of input gains, system output performance is illustrated using the MATLAB simulation graphs. Successive iterations were used to determine gain sets to accommodate the various *SIMSAT* operating modes. These gains can be adjusted by the user in actual system operation as necessary.

Table M.1 Options 1 and 2 - Gains

Final Closed-Loop Controller Design

Option #1 (Target Mode)

Manvr #	Command (degrees)	Gain Matrix K_1			Gain Matrix K_2			Gain Matrix K_4		
1	Roll = 0	1000	0	0	-10	0	0	1	0	0
	Yaw = 90	0	350	0	0	-50	0	0	1	0
	Pitch = 0	0	0	1000	0	0	-10	0	0	1
2	Roll = 90	200	0	0	-10	0	0	1	0	0
	Yaw = 0	0	500	0	0	-50	0	0	1	0
	Pitch = 0	0	0	500	0	0	-10	0	0	1
3	Roll = 0	1000	0	0	-10	0	0	1	0	0
	Yaw = 0	0	1000	0	0	-50	0	0	1	0
	Pitch = 20	0	0	600	0	0	-10	0	0	1
4	Roll = -30	100	0	0	-50	0	0	1	0	0
	Yaw = -50	0	400	0	0	-50	0	0	1	0
	Pitch = -10	0	0	1000	0	0	-10	0	0	1
5	Roll = 30	100	0	0	-50	0	0	1	0	0
	Yaw = 50	0	400	0	0	-50	0	0	1	0
	Pitch = 10	0	0	1000	0	0	-10	0	0	1

Option #2 (Target Mode with Roll Rate)

Manvr #	Command (RPM/degrees)	Gain Matrix K_1			Gain Matrix K_2			Gain Matrix K_4		
1	RollRate = 1	0	0	0	1	0	0	20000	0	0
	Yaw = 10	0	1500	0	0	-50	0	0	1	0
	Pitch = -5	0	0	1500	0	0	-10	0	0	1
2	RollRate = 9	0	0	0	1	0	0	40	0	0
	Yaw = 30	0	500	0	0	-50	0	0	1	0
	Pitch = 5	0	0	1500	0	0	-10	0	0	1

$$K_3 = 0.0585$$

Note: 1 RPM = 6 deg/sec

Table M.2 Options 3 and 4 - Gains

Final Closed-Loop Controller Design

Option #3 (Roll Spin Mode)

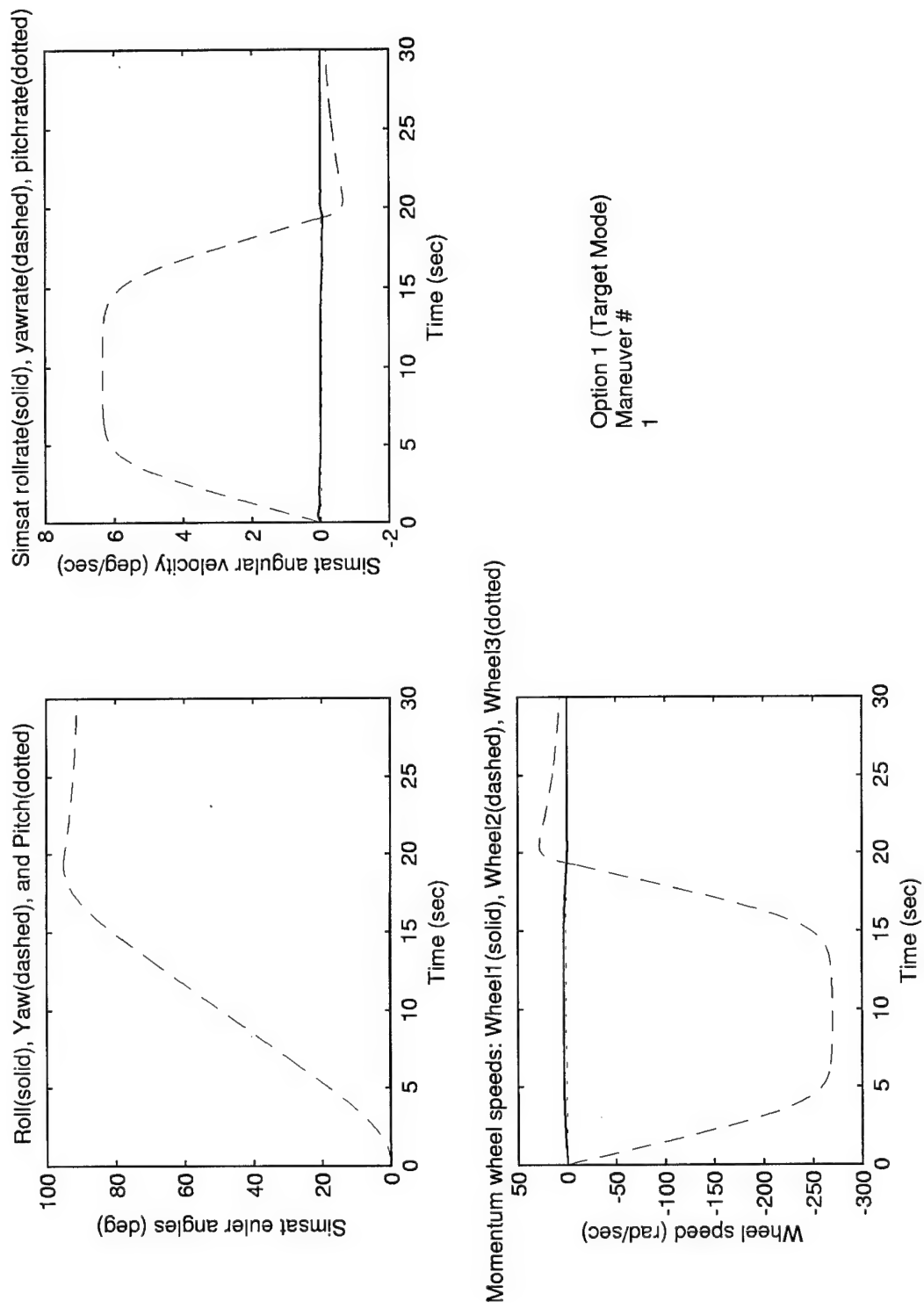
Manvr #	Command (RPM)	Gain Matrix K_1			Gain Matrix K_2			Gain Matrix K_4		
1	RollRate = 12	0	0	0	1	0	0	30000	0	0
		0	1500	0	0	-50	0	0	1	0
		0	0	1500	0	0	-10	0	0	1
2	RollRate = 1	0	0	0	1	0	0	30000	0	0
		0	1500	0	0	-50	0	0	1	0
		0	0	1500	0	0	-10	0	0	1
3	RollRate = -5	0	0	0	1	0	0	30000	0	0
		0	1500	0	0	-50	0	0	1	0
		0	0	1500	0	0	-10	0	0	1

Option #4 (Yaw Spin Mode)

Manvr #	Command (RPM)	Gain Matrix K_1			Gain Matrix K_2			Gain Matrix K_4		
1	YawRate= 1	2000	0	0	-50	0	0	1	0	0
		0	0	0	0	1	0	0	200000	0
		0	0	1000	0	0	-10	0	0	1
2	YawRate= -1	2000	0	0	-50	0	0	1	0	0
		0	0	0	0	1	0	0	200000	0
		0	0	1000	0	0	-10	0	0	1

$$K_3 = 0.0585$$

Note: 1 RPM = 6 deg/sec



Option 1 (Target Mode)
Maneuver #
1

Figure M.1 Option 1 (Target Mode) - Maneuver 1

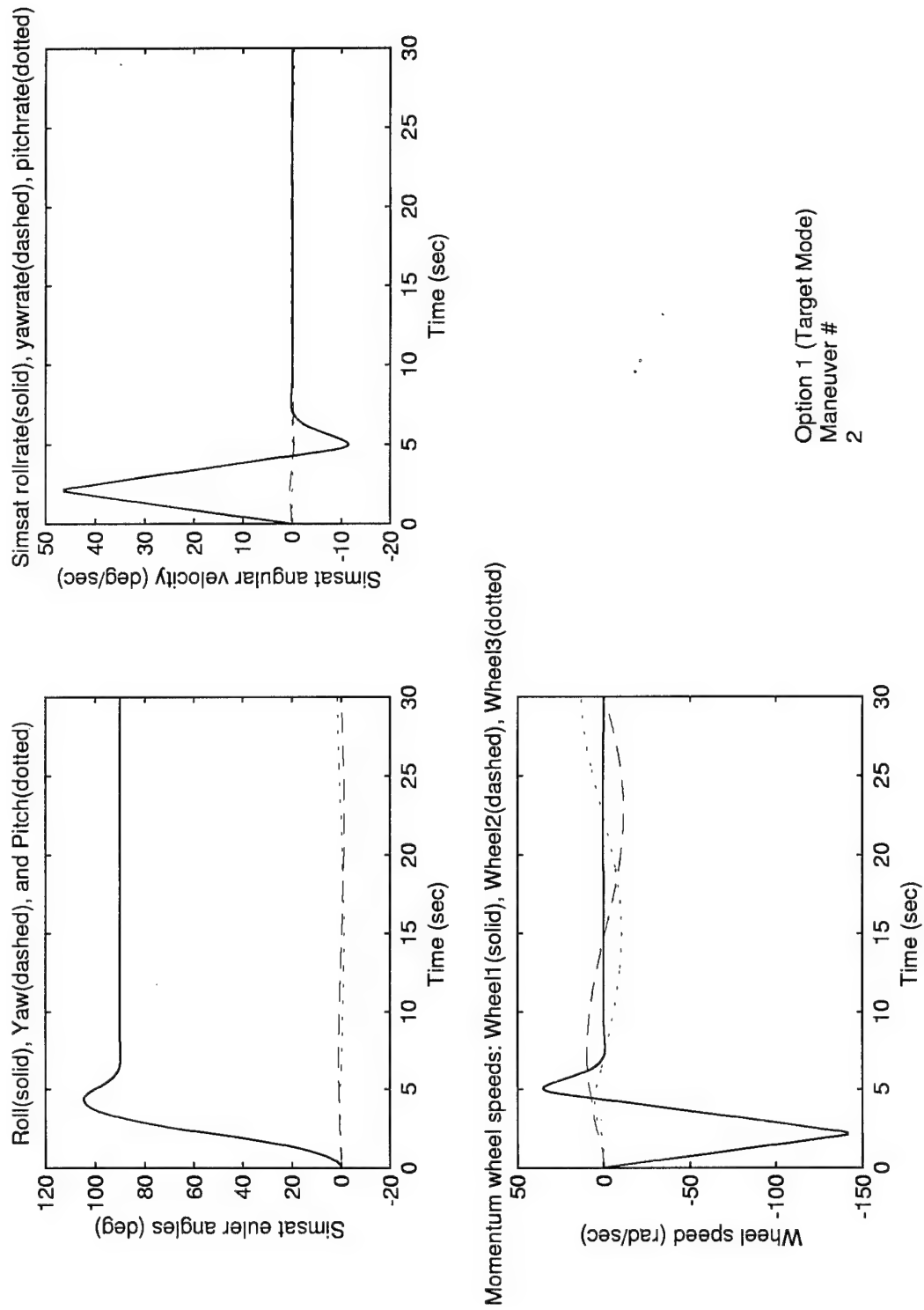


Figure M.2 Option 1 (Target Mode) - Maneuver 2

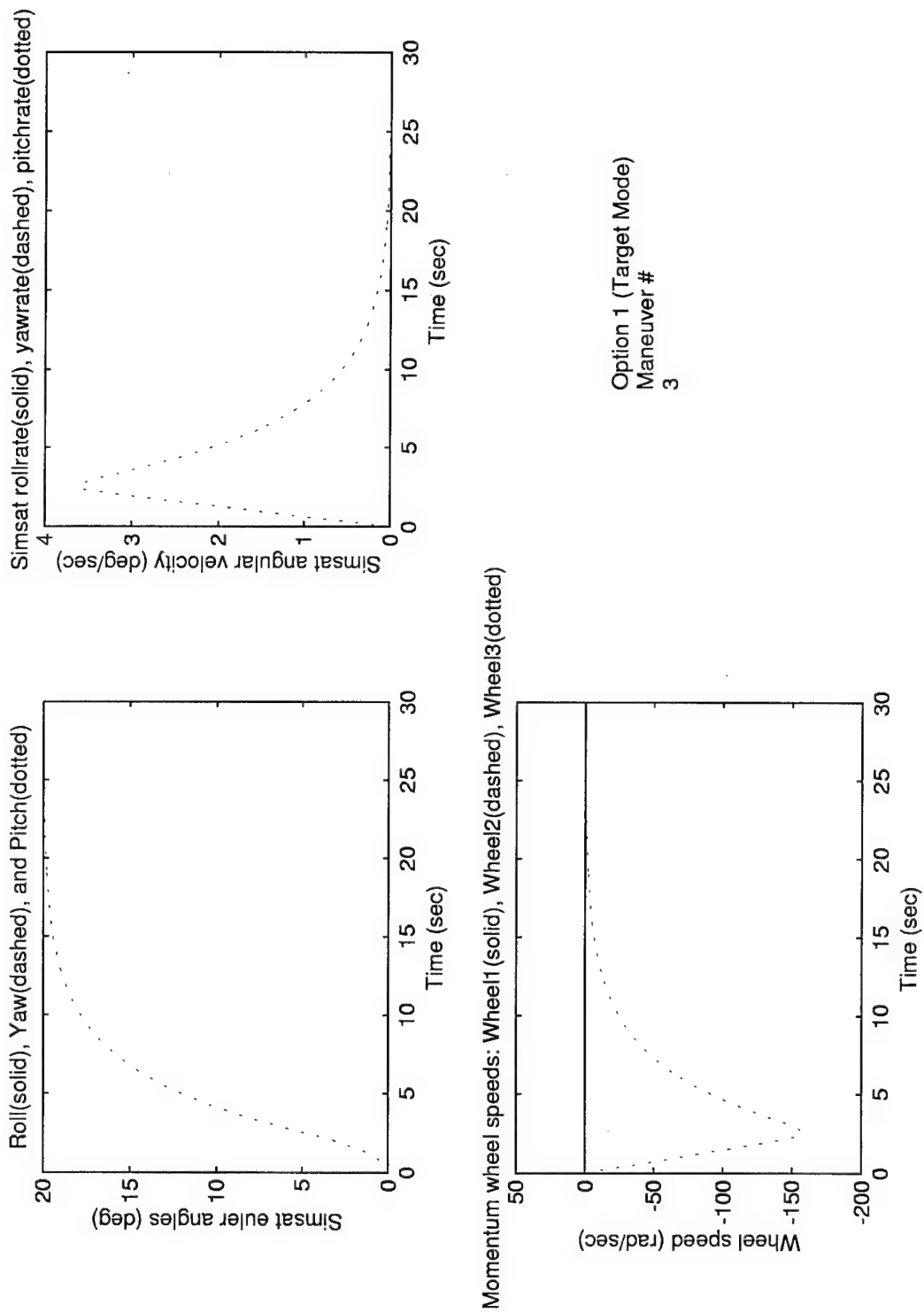
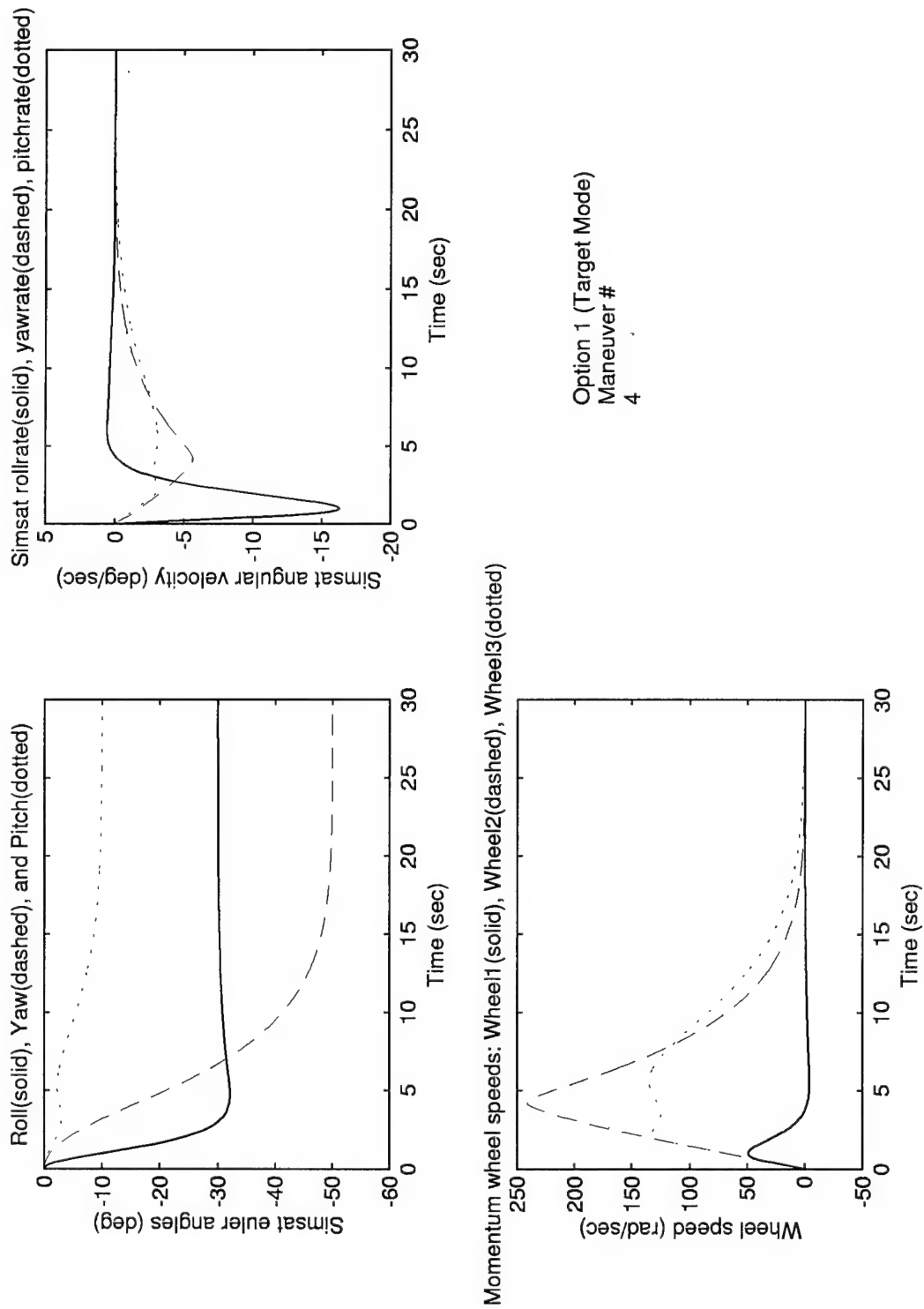


Figure M.3 Option 1 (Target Mode) - Maneuver 3



Option 1 (Target Mode)
Maneuver #
4

Figure M.4 Option 1 (Target Mode) - Maneuver 4

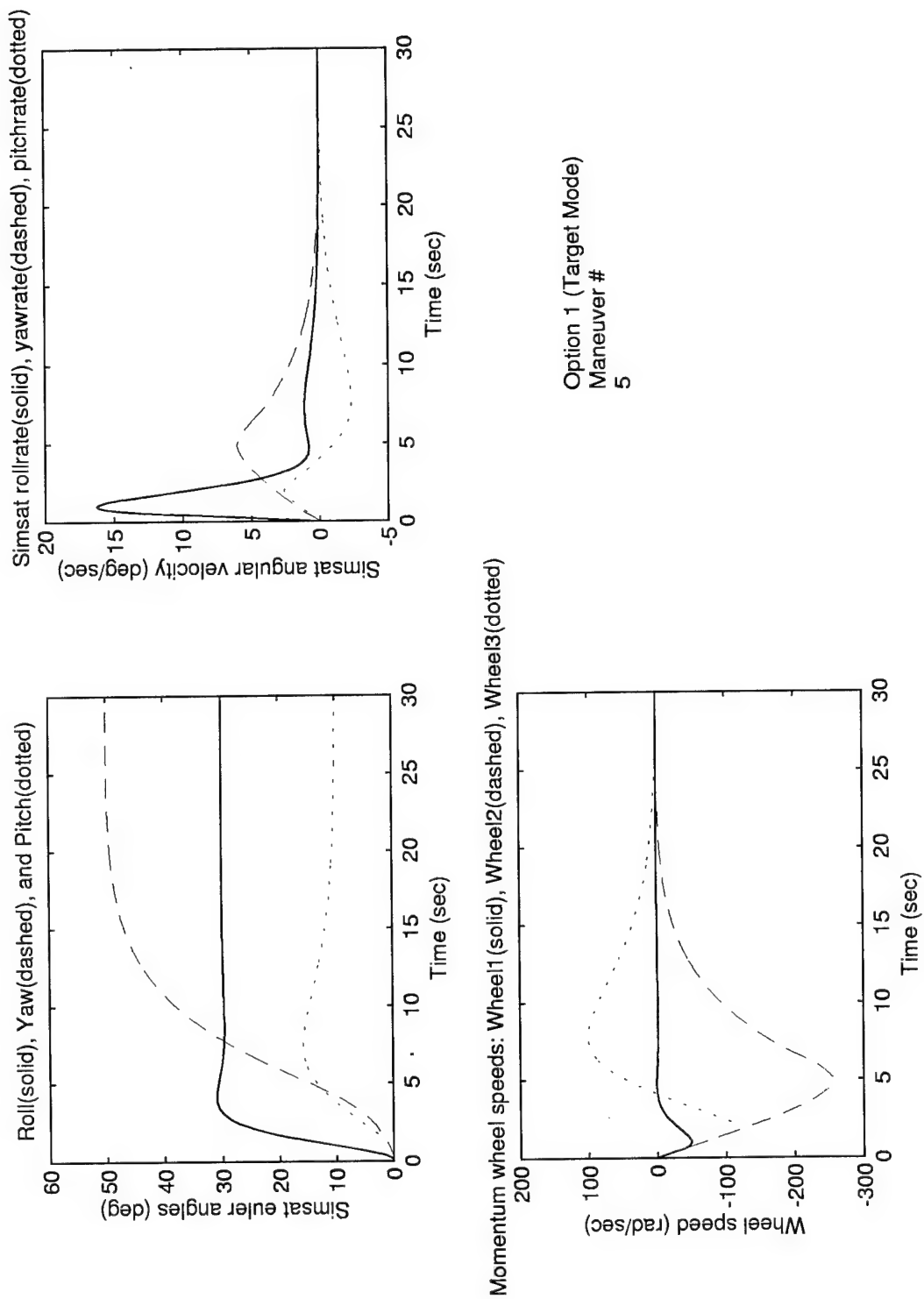
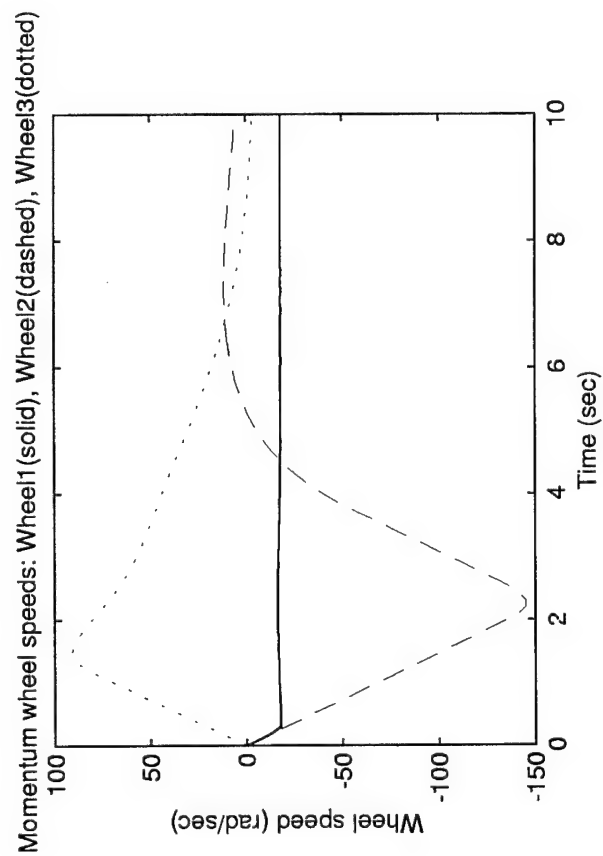
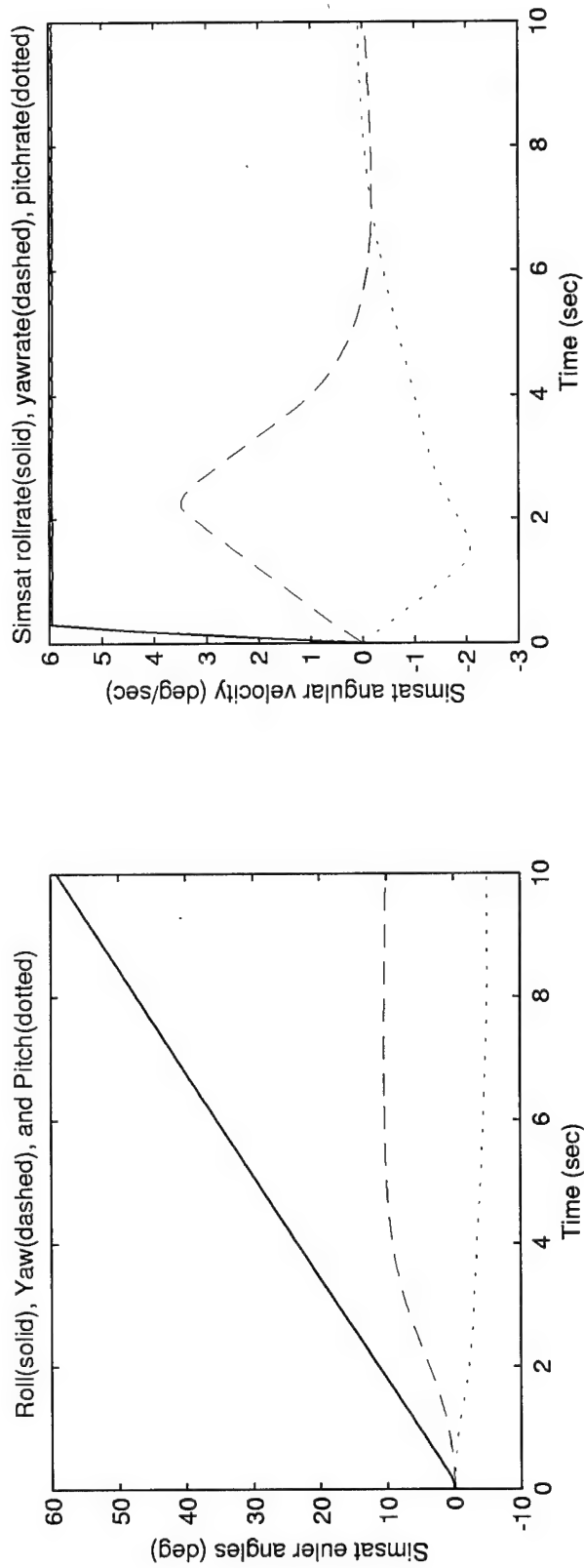
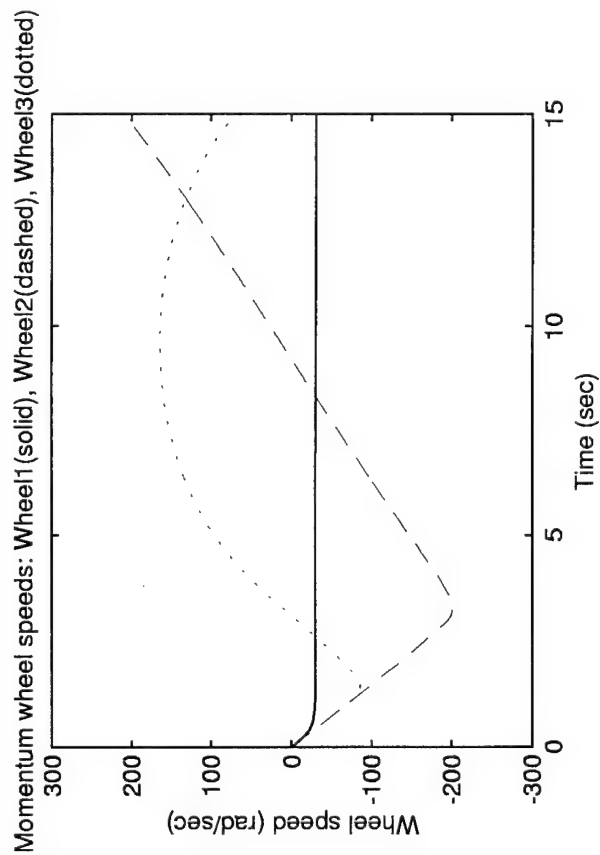
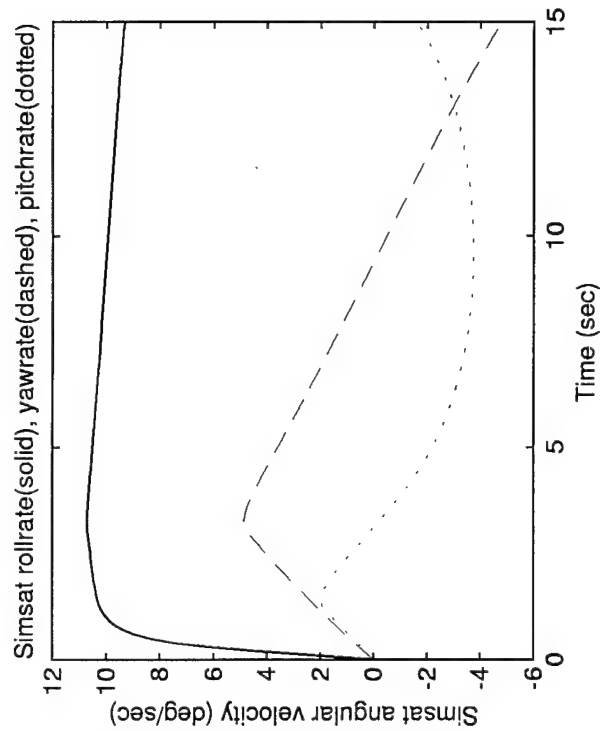
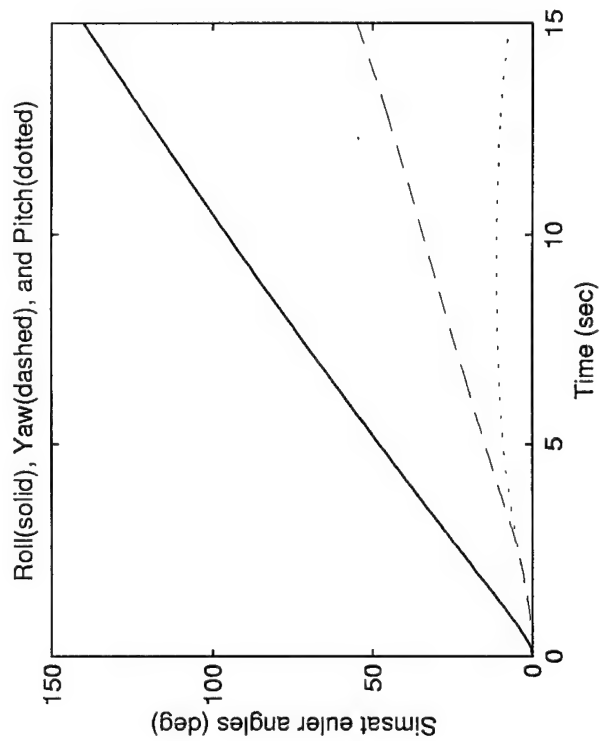


Figure M.5 Option 1 (Target Mode) - Maneuver 5



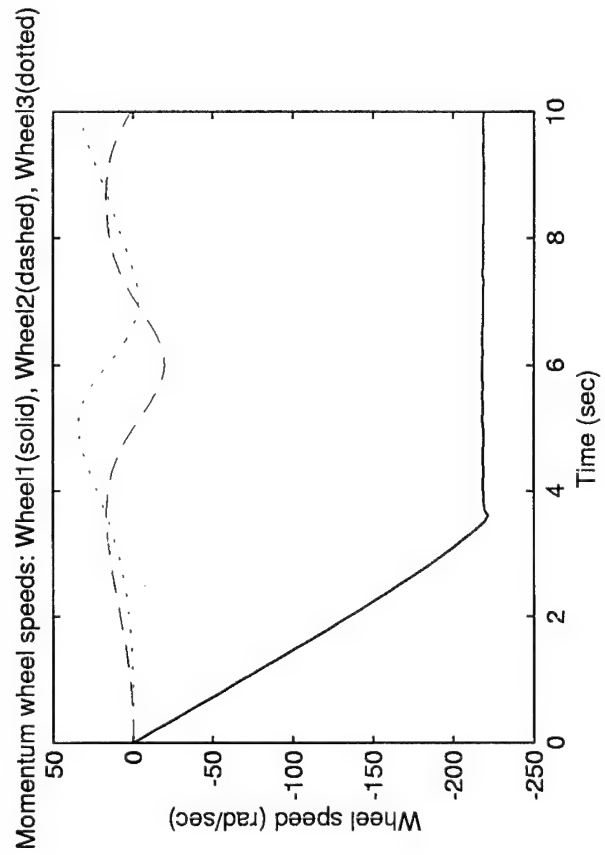
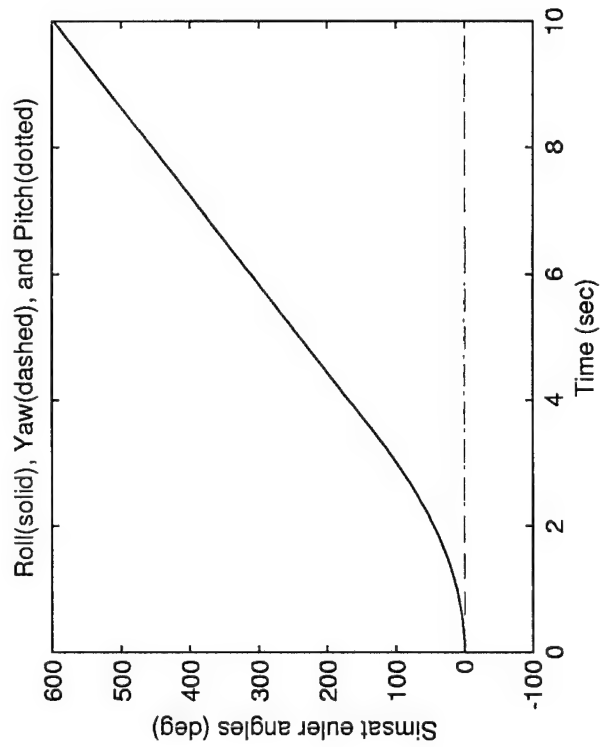
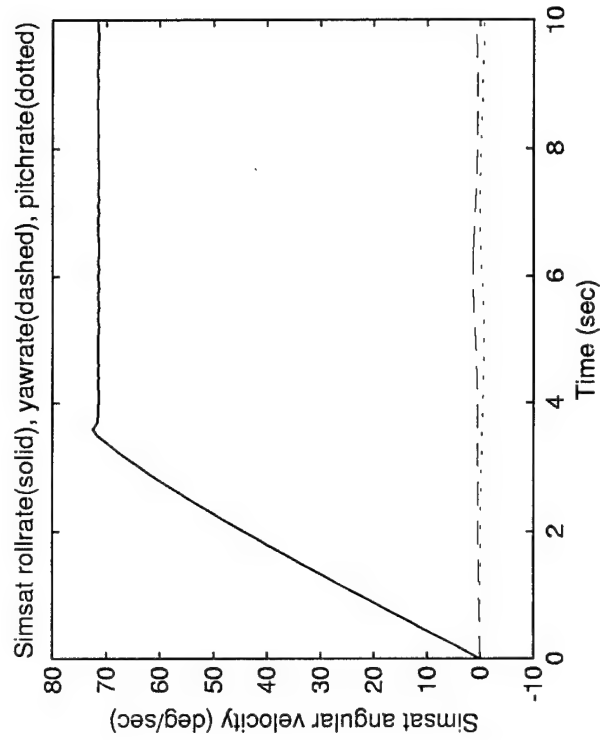
Option 2 (Target Mode with Roll Rate)
Maneuver #
1

Figure M.6 Option 2 (Target Mode with Roll Rate) - Maneuver 1



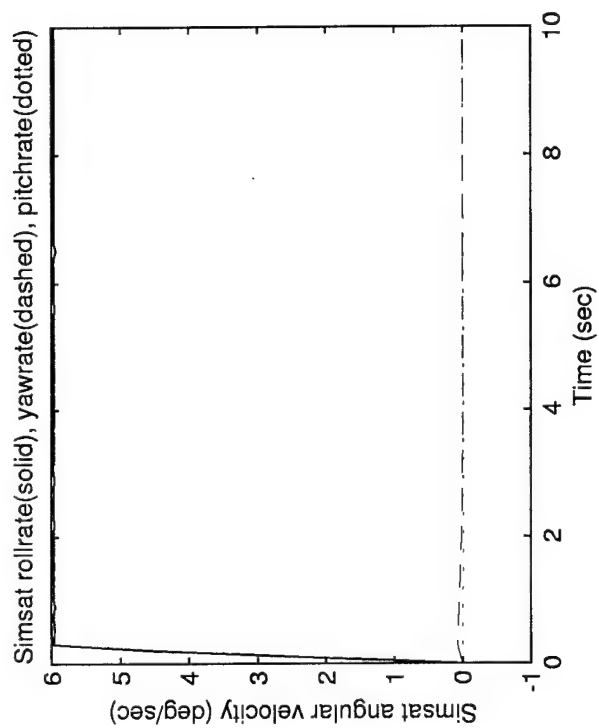
Option 2 (Target Mode with Roll Rate)
Maneuver #
2

Figure M.7 Option 2 (Target Mode with Roll Rate) - Maneuver 2



Option 3 (Roll Spin Mode)
Maneuver #
1

Figure M.8 Option 3 (Roll Spin Mode) - Maneuver 1



Option 3 (Roll Spin Mode)
Maneuver #
2

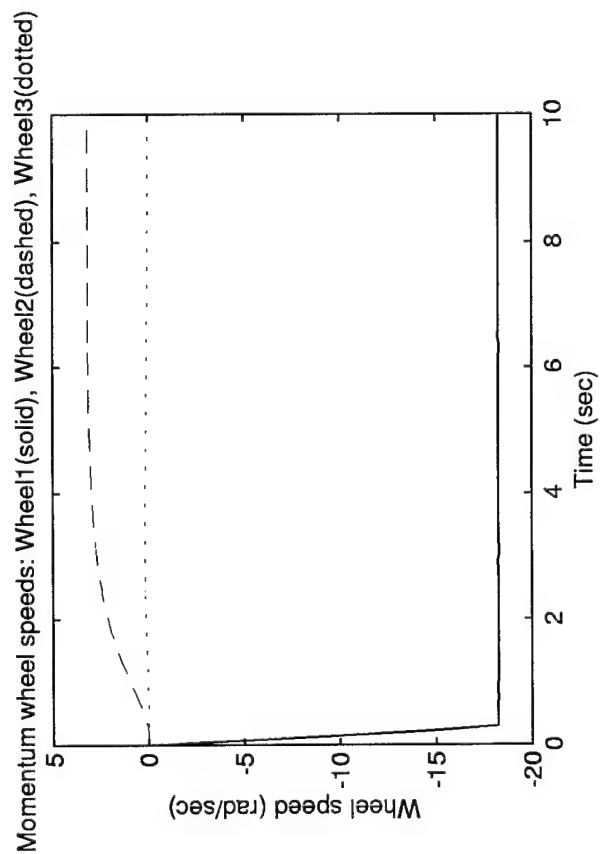
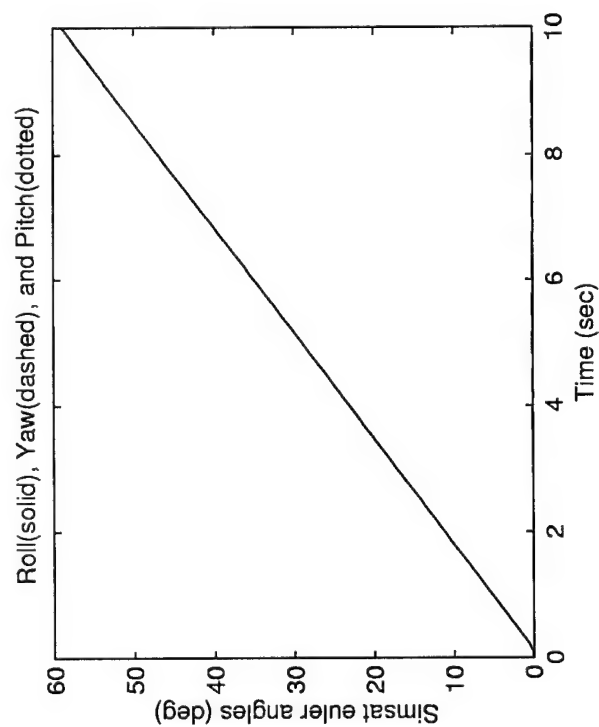
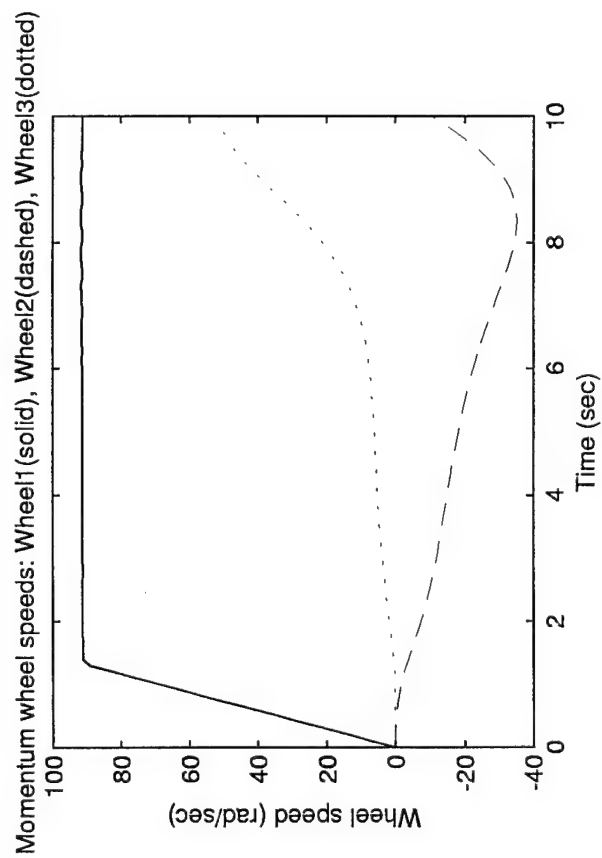
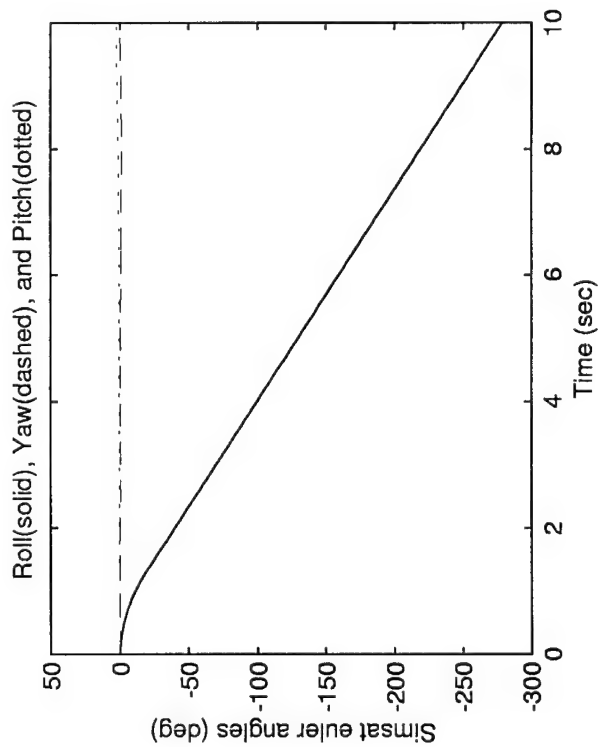
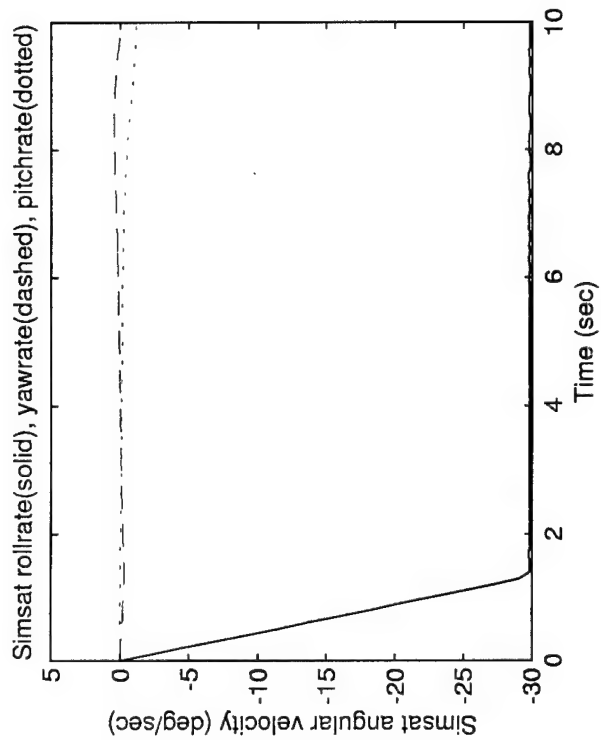
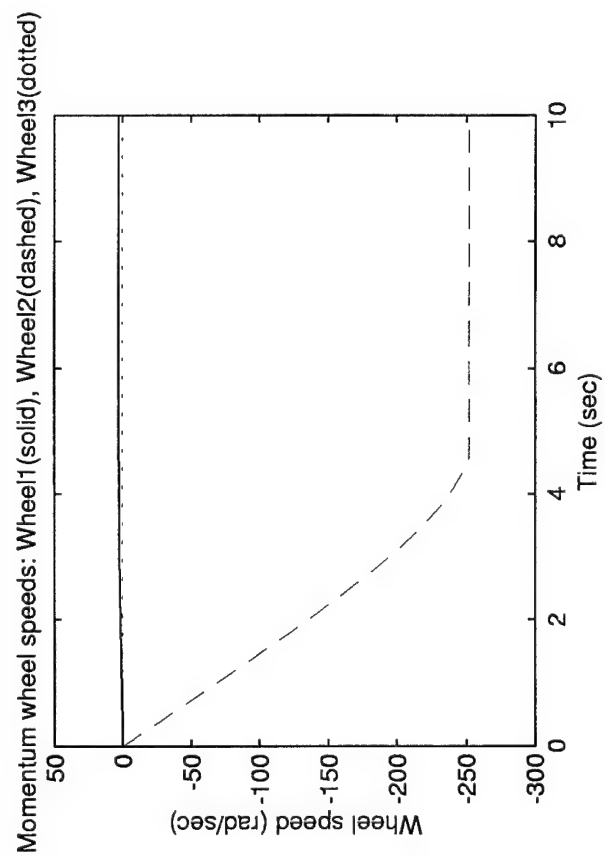
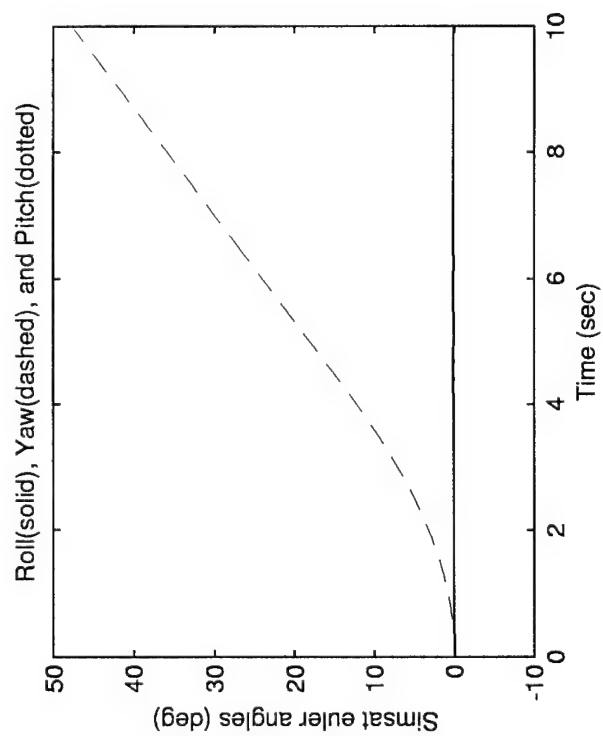
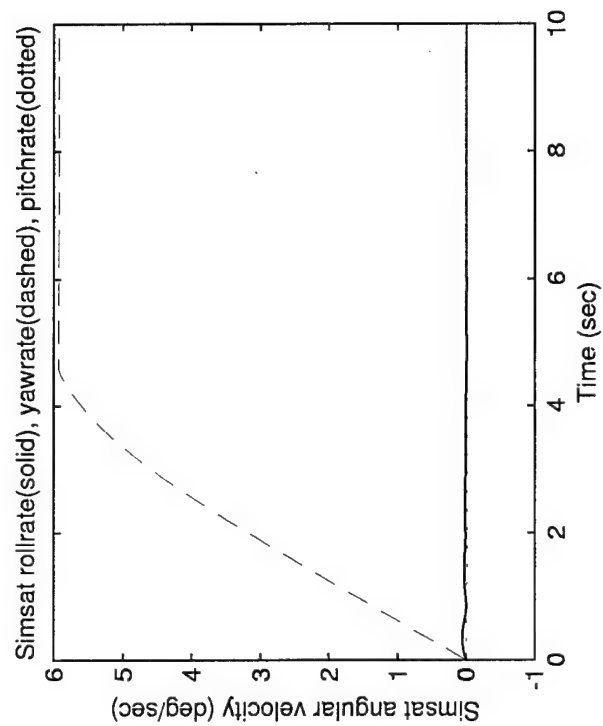


Figure M.9 Option 3 (Roll Spin Mode) - Maneuver 2



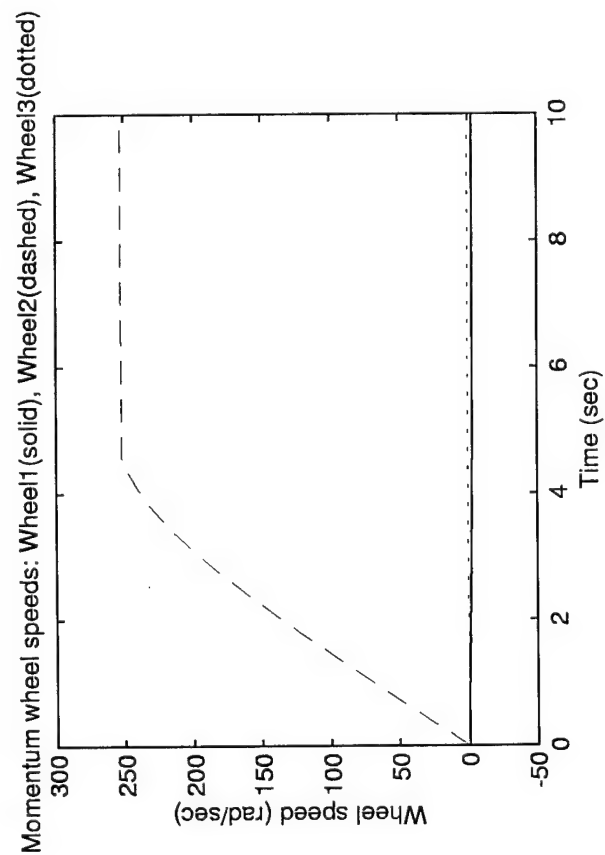
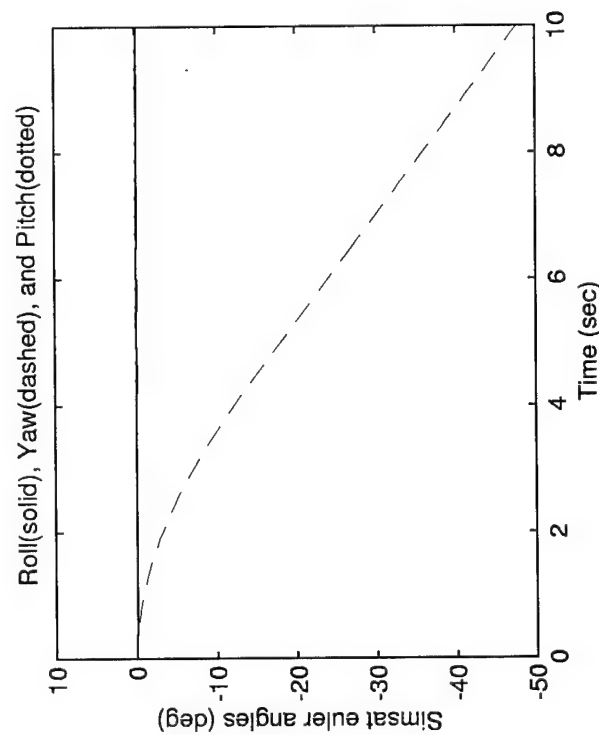
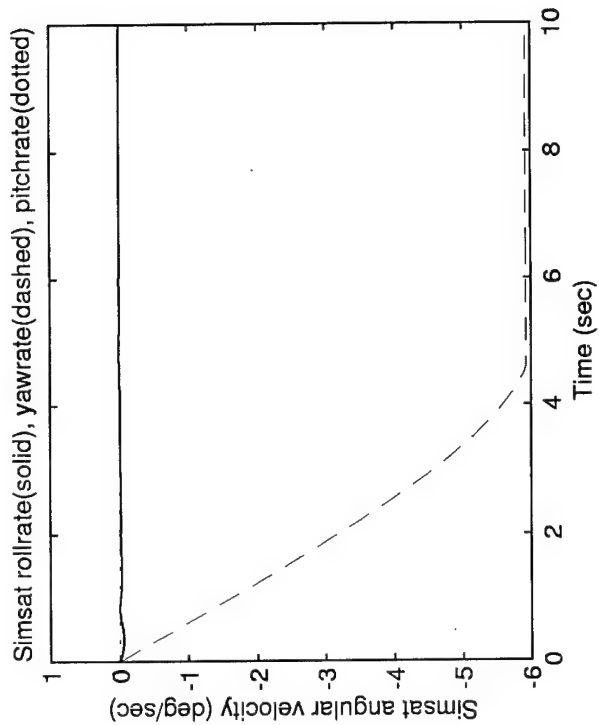
Option 3 (Roll Spin Mode)
Maneuver #
3

Figure M.10 Option 3 (Roll Spin Mode) - Maneuver 3



Option 4 (Yaw Spin Mode)
Maneuver #
1

Figure M.11 Option 4 (Yaw Spin Mode) - Maneuver 1



Option 4 (Yaw Spin Mode)
Maneuver #
2

Figure M.12 Option 4 (Yaw Spin Mode) - Maneuver 2

Bibliography

1. Agnes, Greg. Personal Communications.
2. Aironet Wireless Communications, Inc., 3875 Embassy Parkway, Akron, OH 44333. Phone (800)247-6638. *Aironet Website*. <http://www.aironet.com>.
3. Air Force Material Command, U.S. Air Force. *System Safety, MIL-STD-882B*, 1984.
4. Aydin Vector Division, Aydin Corporation. "Aydin Vector Product Catalog,". P.O. Box 328, Newtown, PA 18940-0328. Phone (215)968-4271.
5. Beam, Walter R. *Systems Engineering: Architecture and Design*. McGraw-Hill, 1990.
6. Black Box Corporation, 1000 Park Drive, Lawrence, PA 15055-1018. Phone (724)746-5500. *Black Box Online*. <http://www.blackbox.com>.
7. Black Box, Technical Support. Personal Communications, March 1999. email tech-sup@bboxtech.net.
8. Blanchard, Benjamin S. *System Engineering Management*. John Wiley and Sons, 1991.
9. CADRE, "CADRE Analytic Home Page." <http://www.cadreanalytic.com>.
10. Carr, Clifford C. *American Electrician's Handbook*. McGraw-Hill, 1961.
11. Chaves, Marc. Personal FAX Memo.
12. Davis, Beth. "Wider, Wireless LANs," *InformationWeek, Issue 699* p. 103 7 September, 1998.
13. Defense Acquisition Deskbook Joint Program Office, 2275 D Street, Bldg 16, WPAFB OH 45433-7233. *Defense Acquisition Handbook (CD-ROM)*. <http://www.deskbook.osd.mil>.
14. Digital Wireless Corporation. *Digital Wireless Corporation Wireless Modems*. <http://www.digital-wireless.com>.
15. dSPACE, Inc., Technologiepark 25, D 33100 Paderborn, Germany. *3-D Animation Tool (RealMotion)* (Reference and user's guide (v. 1.0) Edition), 1996.
16. dSPACE, Inc., Technologiepark 25, D 33100 Paderborn, Germany. *COCKPIT Instrument Panel* (Reference and user's guide (v. 3.3) Edition), 1996.
17. dSPACE, Inc., Technologiepark 25, D 33100 Paderborn, Germany. *Real-Time TRACE Module* (Reference and user's guide (v. 3.1) Edition), 1996.
18. dSPACE, Inc., Technologiepark 25, D 33100 Paderborn, Germany. *Real-Time Interface to Simulink 2 (RTI1003)* (User's guide (v. 3.2) Edition), 1997.
19. dSPACE, Inc., Technologiepark 25, D 3310 Paderborn, Germany. *Solutions for Control: Catalogue 1997*, 1997.

20. dSPACE, Inc., Technologiepark 25, D 33100 Paderborn, Germany. *dSPACE Experiment Software*. <http://www.dspace.de/en/Products/Experisw.htm>.
21. dSPACE, Inc., Technologiepark 25, D 33100 Paderborn, Germany. *dSPACE In-Vehicle Systems*. <http://www.dspace.de/en/Products/invehicl.htm>.
22. Eisner, Howard. *Computer-Aided Systems Engineering*. Prentice Hall, 1988.
23. Fischer, Steven A., et. al. *Satellite Integrated Power and Attitude Control System Design Study*. MS thesis, Air Force Institute of Technology, 1997. GSE-97D and GSO-97D Systems Engineering Design Study Team.
24. Gas Drying, Inc. Personal Communications.
25. Hall, Andrew D. "Three Dimensional Morphology of Systems Engineering," *IEEE Transactions on Systems Science and Cybernetics*, vol. SSC-5 no. 2, pp. 156-160 1969.
26. Hanke, Michael P. *Design of the Computer Subsystem for the AFIT Simulation Satellite (SIMSAT)*. MS thesis, Air Force Institute of Technology, 1998.
27. Howard, Bill. "New Dimensions for Wireless LANs," *PC Magazine*, p. 97 1 September, 1998.
28. Hughes, Peter C. *Spacecraft Attitude Dynamics*. John Wiley Sons, Inc., 1986.
29. INCOSE, International Council on Systems Engineering, "Definition of Systems Engineering." <http://www.incose.org/whatis.html>, 1996.
30. Jung, Bongjin and Wayne P. Burleson. "Performance Optimization of Wireless Local Area Networks Through VLSI Data Compression," *Wireless Networks*, pp. 27-39 1998.
31. Kramer, Stuart C., Lt. Col. *Vector Dynamics*. Air Force Institute of Technology, 1997.
32. Kramer, Stuart (LtCol) and Greg (Capt) Agnes. Initial Meeting, March 1998.
33. Larson, Wiley J. and Wertz James R., editors. *Space Mission Analysis and Design* (Second Edition). Microcosm, Inc., and Kluwer Academic Publishers, 1993.
34. Linden, David, editor. *Handbook of Batteries and Fuel Cells*. McGraw-Hill, 1984.
35. Mathworks, Inc., 24 Prime Park Way, Natick, MA 01760. *SIMULINK: Dynamic System Simulator for MATLAB* (User's guide (v. 2) Edition), 1996.
36. Mathworks, Inc., 24 Prime Park Way, Natick, MA 01760. *MATLAB Target Language Compiler* (Reference guide (v. 1) Edition), 1997.
37. Mathworks, Inc., 24 Prime Park Way, Natick, MA 01760. *Real-Time Workshop* (User's guide (v. 2) Edition), 1997.
38. Meredith, Dale D., et. al. *Design and Planning of Engineering Systems*. Prentice Hall, 1985.
39. Moog, Inc. "Moog Space Products Division Catalog," . P.O. Box 18, East Aurora, NY 14052-0018.

40. Oberg, Erik, Franklin D. Jones and Holbrook L. Horton. *Machinery's Handbook, A Reference Book for the Mechanical Engineer, Draftsman, Toolmaker and Machinist* (21st Edition). Industrial Press Inc., 1980.
41. Oriental Motor Company. *Oriental Motor General Catalog*, 1993.
42. Ottawa Amateur Radio Club. *Wireless LAN/MAN Modem Product Directory*. <http://hydra.carleton.ca>.
43. Power-Sonic. *Power-Sonic Sealed Lead-Acid Batteries Technical Handbook*, June 1998. <http://www.power-sonic.com>.
44. RadioLAN. *Wireless DockLINK Model 408 User Guide*, 1998.
45. RadioLAN, 455 DeGuine Drive, Sunnyvale, CA 94086. Phone (408)616-6300. *Radi-oLAN website*. <http://www.radiolan.com>.
46. Rechtin, Eberhardt. *Systems Architecting: Creating and Building Complex Systems*. Prentice Hall, 1991.
47. Redmill, Keith. Personal Communications, October 1998.
48. Reilly, Norman B. *Successful Systems Engineering for Engineers and Managers*. Van Nostrand Reinhold, 1993.
49. Sage, Andrew P. *Methodology for Large-Scale Systems*. McGraw-Hill, 1977.
50. Sage, Andrew P. *Systems Engineering*. Wiley Series in Systems Engineering, John Wiley and Sons, 1992.
51. Servo Systems Company, 115 Main Road, Montville, NJ 07045-0097. *Servo Systems Company Catalog (1999-2000)*.
52. Sonik Technologies Corporation. *Sonik's SkyLine Series of Wireless Modems*. <http://www.sonik.com/modem.html>.
53. Space Electronics, Inc., 81 Fuller Way, Berlin, CT 06037-1540. *Tri-Axis Gas Bearing Model 2630 Instruction Manual*, 1997.
54. United States Air Force. *Global Engagement: A Vision of the 21st Century Air Force*, 1996.
55. Wainwright, Lewis F. *Aircraft Electrical Practice*. Odhams Press Limited, 1961.
56. Wiesel, William E. *Spaceflight Dynamics*. McGraw-Hill Series in Aeronautical and Aerospace Engineering, McGraw-Hill, 1997.
57. "Networking Kits," *PC Magazine*, pp. 220-226 1 September, 1998.

Vita

VITA-1

Captain James E. Colebank was born in February 1970 in McKeesport, PA. He graduated from Lake Havasu High School, Lake Havasu City, AZ, in 1988 and began his undergraduate studies at the United States Air Force Academy (USAFA) later the same year. In May 1992, he graduated from USAFA with academic distinction earning a B.S. degree in Astronautical Engineering. Upon graduation, he received his Regular Commission as a Second Lieutenant in the USAF.

In July 1992, he began his first assignment as a Titan Booster Mechanical Engineer with the 6595th Aerospace Test Group, Vandenberg AFB, CA. After supporting two Titan IV booster launches, he became a Titan Satellite Launch Engineer in June 1993. In this position, he served on the team that launched the Clementine lunar exploration satellite on a Titan II booster in January 1994. He also was a team member for the launch of the DARPASAT and Step Mission 0 spacecraft on the nation's first Taurus booster in March 1994. Later that year, he supported two Titan IV launches at Cape Canaveral AS, FL.

In February 1995 he became a Satellite Operations Controller with the newly formed 4th Space Launch Squadron (AFSPC). After being certified Mission Ready in this position, he led a 250 person crew during satellite countdown operations for the launch of a Titan IV in December 1995. In 1996, he supported two Titan IV launches to include the first publicly acknowledged launch of a National Reconnaissance Office (NRO) satellite. In 1997, he became the Mission Ready Assistant Launch Director for the launch of a Defense Meteorological Satellite Program (DMSP) spacecraft on a Titan II booster.

In August 1997, he entered the School of Engineering, Air Force Institute of Technology, as Section Leader for Systems Engineering Class 99M. His follow-on assignment is to the F-15/F-16 Propulsion System Program Office at Wright Patterson AFB, OH.

Captain Colebank's awards include the Air Force Association (AFA) Best Space Operations Crew in the USAF Award for 1995 and the Vandenberg AFA, Robert H. Goddard Chapter, Engineer of the Year Award for 1996.

Captain Robert D. Jones was born on 16 September 1971 in Williams AFB, Phoenix, AZ. He graduated from Rogers High School, Newport, RI, in 1989 and began his undergraduate studies at the United States Air Force Academy (USAFA) later the same year. In 1993, he graduated from USAFA with an B.S. degree from the Department of Physics (Space Physics). Upon graduation, he received his Regular Commission as a Second Lieutenant in the USAF.

He began Undergraduate Space Training (UST) with the 392nd Space and Missile Training Squadron (AETC), Vandenberg AFB, CA, in August 1993, graduating in November 1993 as a member of the first UST class formed at Vandenberg. Upon arrival at the 3rd Space Operations Squadron (AFSPC), located at Falcon AFB, CO, he began his first assignment as a MILSTAR Satellite Crew Commander. He also served as MILSTAR Staff Instructor and Chief of Pass Plan development. In December 1996, he was transferred to the 4th Space Operations Squadron (AFSPC) as a SGLS Satellite Engineering Officer following a reorganization of the MILSTAR program under the 50th Space Wing.

In August 1997, he entered the School of Engineering, Air Force Institute of Technology, as Assistant Section Leader for Graduate Space Operations Class 99M. His follow-on assignment is to Headquarters Air Force Space Command at Peterson AFB, CO.

First Lieutenant Donald R. Mannebach was born on 25 September 1972 in Salina, KS. In 1991, he graduated from Colby High School (KS) and began undergraduate studies at the United States Air Force Academy (USAFA). In 1995, he graduated from USAFA with a B.S. degree in Space Operations from the Department of Astronautics, and was commissioned as a Second Lieutenant in the USAF. He graduated in the top 15% of his class, and was awarded the Top Graduate in the Space Operations Major.

He was a Distinguished Graduate from Undergraduate Space and Missile Training with the 392nd Space and Missile Training Squadron (AETC), Vandenberg AFB, CA, in November 1995. His first assignment was as a Ballistic Missile Early Warning Site (BMEWS) Crew Commander at the 13th Space Warning Squadron (AFSPC), Clear Air Station, AK, from January 1996 to July 1997. During this assignment he served as a Crew Commander Instructor and the Additional Duty Intelligence Officer. He was selected as the 13th SWS crew commander competing in the 1997 AFSPC Guardian Challenge competition.

He began his Master's degree in Graduate Space Operations Class 99M at the School of Engineering, Air Force Institute of Technology, in August 1997.

Captain George R. Nagy was born on 24 May 1970 in Bethlehem, PA. He graduated from Southern Lehigh High School, Center Valley, PA, in 1988 and began his undergraduate studies at the Massachusetts Institute of Technology (MIT) later the same year. In 1992, he graduated from MIT with an S.B. degree from the Department of Aeronautics and Astronautics (Course XVI). Upon graduation he was commissioned a Second Lieutenant in the USAF, having completed a four-year scholarship awarded through the Reserve Officer Training Corps.

He began Undergraduate Missile Training (UMT) with the 4315th Combat Crew Training Squadron (ACC), Vandenberg AFB, CA, in April 1993. He graduated UMT in July 1993 as a member of Class CDB-170, the first mission-ready class formed under the newly-organized 392nd Training Squadron (AETC). Upon arrival at the 91st Missile Wing (AFSPC), Minot AFB, ND, he was certified combat-ready in the Minuteman III weapon system in October 1993.

He was assigned to the 741st Missile Squadron (AFSPC) from August 1993 until September 1995, serving in a variety of positions including Deputy Missile Combat Crew Commander, Instructor/Evaluator Deputy Missile Combat Crew Commander, Missile Combat Crew Commander, and Squadron Weapons Safety Officer.

In October 1995, he was selected for the newly-reorganized 91st Operations Group (AFSPC) Standardization/Evaluation Division, where he served as a Missile Combat Crew Commander Evaluator, Operations Group Technical Order Distribution Officer, and Evaluation Scriptwriter. In 1996 he was awarded a Master of Science degree in Space Studies from the University of North Dakota under the Missile Crewmember Education Program.

In January 1997 he became Section Chief for the Training Scripts section of the 91st Operations Support Squadron (AFSPC). He attended Squadron Officer School at Maxwell AFB, AL, from February 1997 to April 1997 as a member of SOS Class 97C. In August 1997, he entered the School of Engineering, Air Force Institute of Technology, as Section Leader for Graduate Space Operations Class 99M. His follow-on assignment is to the 17th Test Squadron (AFSPC) at Schriever AFB, CO.

Captain Randall D. Pollak was born on 30 April 1972 in Harvey, IL. Following graduation from Homewood-Flossmoor High School, Flossmoor, IL, he attended the University of Illinois at Urbana-Champaign. In May 1994, he received the Master Designer award as the top designer in the 1994 Aircraft Design Project, sponsored by the Department of Aeronautical and Astronautical Engineering and McDonnell-Douglas Aircraft. In addition, his design team received the top design award. He graduated with Highest Honors having earned a Bachelor of Science degree in Aeronautical and Astronautical Engineering. As the Outstanding Graduate of Officer Training School class 95-01, he received his commission as a Second Lieutenant in November 1994 and was nominated for a Regular Commission.

Next assigned to Barksdale AFB, LA, he was a member of the 49th Test Squadron of the 53d Wing (ACC). During that assignment, he served as the Lead Engineer and Airborne Lead Engineer for the operational test and evaluation of the Advanced Cruise Missile, Air-Launched Cruise Missile, and Conventional Air-Launched Cruise Missile. Since August 1997, he has attended the Air Force Institute of Technology as a graduate student in the Systems Engineering program. In April 1999, he will begin his next assignment at the Air Force Operational Test and Evaluation Center, Kirtland AFB, NM.

REPORT DOCUMENTATION PAGE			Form Approved OMB No. 0704-0188	
Public reporting burden for this collection of information is estimated to average 1 hour per response, including the time for reviewing instructions, searching existing data sources, gathering and maintaining the data needed, and completing and reviewing the collection of information. Send comments regarding this burden estimate or any other aspect of this collection of information, including suggestions for reducing this burden, to Washington Headquarters Services, Directorate for Information Operations and Reports, 1215 Jefferson Davis Highway, Suite 1204, Arlington, VA 22202-4302, and to the Office of Management and Budget, Paperwork Reduction Project (0704-0188), Washington, DC 20503.				
1. AGENCY USE ONLY (Leave blank)		2. REPORT DATE March 1999		3. REPORT TYPE AND DATES COVERED Master's Thesis
4. TITLE AND SUBTITLE SIMSAT: A SATELLITE SYSTEM SIMULATOR AND EXPERIMENTAL TEST BED FOR AIR FORCE RESEARCH				5. FUNDING NUMBERS
6. AUTHOR(S) James E. Colebank, Capt; R. Dan Jones, Capt; Donald M. Mannebach, 1st Lt; George R. Nagy, Capt; Randall D. Pollak, Capt				
7. PERFORMING ORGANIZATION NAME(S) AND ADDRESS(ES) Air Force Institute of Technology 2950 P Street Wright-Patterson AFB, OH 45433-7765				8. PERFORMING ORGANIZATION REPORT NUMBER AFIT/GSE/GSO/ENY/99M-1
9. SPONSORING/MONITORING AGENCY NAME(S) AND ADDRESS(ES) Lt Col Stuart C. Kramer, AFIT/ENY Capt Gregory S. Agnes, AFIT/ENY Air Force Institute of Technology 2950 P Street Wright-Patterson AFB, OH 45433-7765 (937) 255-3636 (DSN 785-3636) x4578				10. SPONSORING/MONITORING AGENCY REPORT NUMBER
11. SUPPLEMENTARY NOTES Advisors: Lt Col Stuart C. Kramer, AFIT/ENY, (937) 255-3636 (DSN 785-3636) x4578 Stuart.Kramer@afit.af.mil Capt Gregory S. Agnes, AFIT/ENY, (937) 255-3636 (DSN 785-3636) x4317 Gregory.Agnes@afit.af.mil				
12a. DISTRIBUTION AVAILABILITY STATEMENT Approved for public release; distribution unlimited				12b. DISTRIBUTION CODE A
13. ABSTRACT (Maximum 200 words) SIMSAT (the SIMulation SATellite) is an AFIT-sponsored program to develop a laboratory-based physical satellite simulator. SIMSAT supports experimentation in areas of attitude control, precision pointing, and vibration suppression. SIMSAT development began with the purchase of a three-axis gas bearing which simulates a torque-free space environment. SIMSAT subsystems provide power, attitude control, telemetry, and structural support to experimental payloads. Project challenges included integration of attitude control software/hardware, high-output power storage devices, remote communications, high-frequency data collection, structural design, and computer display outputs.				
14. SUBJECT TERMS Systems Engineering; Space Operations; Satellite Simulator; Momentum Wheels; Satellite Attitude Dynamics; Control; Pointing; Vibration Suppression				15. NUMBER OF PAGES 494
				16. PRICE CODE
17. SECURITY CLASSIFICATION OF REPORT UNCLASSIFIED		18. SECURITY CLASSIFICATION OF THIS PAGE UNCLASSIFIED		19. SECURITY CLASSIFICATION OF ABSTRACT UNCLASSIFIED
				20. LIMITATION OF ABSTRACT UL